Taxonomy and ecology of the planktonic diatom family Chaetocerotaceae (Bacillariophyta) from the Adriatic sea

Bosak, Sunčica

University of Zagreb

FACULTY OF SCIENCE
DEPARTMENT OF GEOLOGY
INTERDISCIPLINARY DOCTORAL STUDY IN OCEANOLOGY

Sunčica Bosak

TAXONOMY AND ECOLOGY OF THE PLANKTONIC DIATOM FAMILY CHAETOCEROTACEAE (BACILLARIOPHYTA) FROM THE ADRIATIC SEA

DOCTORAL THESIS

Zagreb, 2013

University of Zagreb

PRIRODOSLOVNO-MATEMATIČKI FAKULTET
GEOLOŠKI ODSJEK
INTERDISCIPLINARNI DOKTORSKI STUDIJ IZ OCEANOLOGIJE

Sunčica Bosak

TAKSONOMIJA I EKOLOGIJA PLANKTONSKIH DIJATOMEJA IZ PORODICE CHAETOCEROTACEAE (BACILLARIOPHYTA) U JADRANSKOM MORU

DOKTORSKI RAD

Zagreb, 2013

University of Zagreb

FACULTY OF SCIENCE
DEPARTMENT OF GEOLOGY
INTERDISCIPLINARY DOCTORAL STUDY IN OCEANOLOGY

Sunčica Bosak

TAXONOMY AND ECOLOGY OF THE PLANKTONIC DIATOM FAMILY CHAETOCEROTACEAE (BACILLARIOPHYTA) FROM THE ADRIATIC SEA

DOCTORAL THESIS

Supervisors:

Dr. Diana Sarno

Prof. Damir Viličić

Zagreb, 2013

University of Zagreb

PRIRODOSLOVNO-MATEMATIČKI FAKULTET
GEOLOŠKI ODSJEK
INTERDISCIPLINARNI DOKTORSKI STUDIJ IZ OCEANOLOGIJE

Sunčica Bosak

TAKSONOMIJA I EKOLOGIJA PLANKTONSKIH DIJATOMEJA IZ PORODICE CHAETOCEROTACEAE (BACILLARIOPHYTA) U JADRANSKOM MORU

DOKTORSKI RAD

Mentori:

Dr. Diana Sarno

Prof. dr. sc. Damir Viličić

Zagreb, 2013

This doctoral thesis was made in the Division of Biology, Faculty of Science, University of Zagreb under the supervision of Prof. Damir Viličić and in one part in Stazione Zoologica Anton Dohrn in Naples, Italy under the supervision of Diana Sarno.

The doctoral thesis was made within the University interdisciplinary doctoral study in Oceanology at the Department of Geology, Faculty of Science, University of Zagreb.

The presented research was mainly funded by the Ministry of Science, Education and Sport of the Republic of Croatia Project No. 119-1191189-1228 and partially by the two transnational access projects (BIOMARDI and NOTCH) funded by the European Community – Research Infrastructure Action under the FP7 ‘‘Capacities’’ Specific Programme (Ref. ASSEMBLE grant agreement no. 227799).

ACKNOWLEDGEMENTS

... to my Croatian supervisor and my boss, Prof. Damir Viličić, for all the support and for listening to my sometimes impossible ideas and proposals. I am grateful especially for introducing me to this beautiful diatom family, and teaching me all the basics of science research

...to my Neapolitan supervisor, Diana Sarno, for enormous amount of patience, incredible advices, help and support in both professional and private moments in my life

... to Zrinka, Kore, Maja, my lab colleagues and great friends, for all the support I got on a daily basis but especially for all that they taught me about statistics and counting

... to my fellow colleague Pero for being a good friend who makes me laugh each day and has an excellent taste in music ☺

... to my dearest friends from SZN, especially to my most precious ones: Cioccio and Swaraj - my favourite italo-indian nerd duo, for endless chats and laughs that we shared but most of all for being true and honest friends ☺*. To Deepak, my fellow diatom researcher, for all help in molecular lab work. To Krzysiu, Filip, Eleonora, Sandra, Isabella, Vasco, Laura E. and Laura V., Gauri and all other PhD and Postdocs that I have met and shared incredible moments of scientific breakthroughs, but also fun aperitivos, coffee times and excursions in and around Naples.*
... to Marina Montresor for embracing me in the LEEP lab
... to electron microscopy SZN support team, Giovanna Benvenuto and Franco Iamunno, for their patience and help in my long hours spent at TEM & SEM, due to them I got a huge collection of beautiful high quality images
You all certainly made me feel like me second home in SZN, I could never dreamed that I could feel so welcome and comfortable somewhere else than home. An enormous grazie per tutti...

...to Tina and Vedran, everything started with Kotor chinchillas and beers, thank you for all the friendship and scientific conversations and especially to Tina for including me in the RV001 field research which was full of funny and exciting sampling moments.

... To Luka for all samples, isolations, culturing work in the lab and beautiful micrographs but above all for a great friendship and support. I am very lucky that I have found someone who shares my passion for phytoplankton taxonomy ☺*.*

... to Dario and Cedric for including me in their Cotutelle project and providing me the samples from Krka Estuary

... to all people from CIM Rovinj, IRB Zagreb, Institute Institute forMarine and Coastal Research in Dubrovnik and many others with whom I shared many sampling trips and who helped me in so many ways...

... to Galja, Vesna; Amela from IRB Zagreb, for their collaboration on the AFM cell jacket paper during which we shared great and exciting moments of this excellent scientific discovery

... to all of my friends who provided some of the samples of opportunity, especially to Fani and Duje

... to Vilim for all the patience, love and support

...to all the bands that play music which inspired me and helped me in various situations in my life.

Without music, life would be a mistake...

...above all, I am grateful to my loving mother who was always there for me

TABLE OF CONTENTS

CHAPTER 3 RESULTS

TEMELJNA DOKUMENTACIJSKA KARTICA

Sveučilište u Zagrebu
Prirodoslovno-matematički fakultet
Geološki odsjek
Interdisciplinarni doktorski studij Oceanologije

Doktorska disertacija

TAKSONOMIJA I EKOLOGIJA PLANKTONSKIH DIJATOMEJA IZ PORODICE CHAETOCEROTACEAE (BACILLARIOPHYTA) U JADRANSKOM MORU

SUNČICA BOSAK

Sveučilište u Zagrebu, Prirodoslovno-matematički fakultet, Biološki odsjek,
Rooseveltov trg 6, 10 000 Zagreb, Hrvatska

Kozmopolitska porodica dijatomeja Chaetocerotaceae je brojna u morskom fitoplanktonu obalnih područja te obuhvaća oko 170 vrsta svrstanih u dva roda *Chaetoceros* i *Bacteriastrum*. U Jadranu skupina je vrlo raznolika i ekološki značajna te zastupljena s oko 50 vrsta čija je identifikacija često problematična. Morfologija vrsta je određena analizirajući materijal izoliranih kultura stanica i uzoraka planktona prikupljenih na terenu, na 8 lokacija duž istočnojadranske obale u razdoblju 2006 – 2012. Sve svojte su analizirane pomoću svjetlosne, skenirajuće i transmisijske elektronske mikroskopije te vrsta *Bacteriastrum jadranum* dodatno s mikroskopom atomskih sila (AFM). Ekološki odnosi su istraženi: 1) na jednoj postaji (RV001) u obalnom području sjevernog Jadrana (2008 – 2009, svaka dva tjedna) 2) u području ušća rijeke Krke (dva puta dnevno, tijekom šest dana u srpnju 2010). Određeno je 49 morfološki različitih svojti od kojih 6 pripadaju rodu *Bacteriastrum* a 43 rodu *Chaetoceros*, s 41 vrsta, dva varijeteta dvije uvjetno identificirane svojte i četiri nepoznata morfotipa. Tri nadopunjene dijagnoze su predložene za vrste: *Chaetoceros vixvisibilis*, *Bacteriastrum jadranum* i *B. mediterraneum*. Pet vrsta je zabilježeno po prvi put u Jadranu. Razjašnjena je prethodna pogrešna identifikacija kod *Bacteriastrum furcatum/B. delicatulum, Chaetoceros contortus/C. compressus, C. decipiens/C. lorenzianus* and *C. lauderi/C. teres.* Analiza je pokazala da je samo prva vrsta iz svakog navedenog para prisutna u analiziranom materijalu. Procijenjena je taksonomska važnost pojedinih morfoloških obilježja s posebnim naglaskom na morfologiju mirujućih spora, ornamentaciju valve i strukturu seta. Razlikuje se 9 različitih tipova struktura seta kod vrsta podroda *Chaetoceros* i isto toliko kod *Hyalochaete.* Kod vrste *Bacteriastrum jadranum* otkriven je i opisan jedinstven i novi način formiranja kolonija kod planktonskih morskih dijatomeja, gdje stanice nisu povezane pomoću fuzije silikatnih struktura nego pomoću optički transparentnog organskog matriksa. Rezultati molekularne filogenetske analize odvojila su *Bacteriastrum furcatum* i *B. hyalinum* u jednu grupu te *B. jadranum* i *B. mediterraneum* u drugu. U odnosu na ostale vrste *Bacteriastrum* vrste se grupiraju unutar roda *Chaetoceros*, ali za drastične taksonomske promjene potrebna su daljnja istraživanja. Multivarijantna analiza sezonske dinamike i ekoloških odnosa pokazala je da su vrste skupine Chaetocerotaceae stalno prisutne u fitoplanktonu a sukcesivno se izmjenjuju tijekom godine. Sukcesijski obrazac se može djelomično objasniti okolišnim parametrima, sa temperaturom, silikatima, salinitetom i fosfatima. Opisi vrsta dijatomeja će olakšati buduću ispravnu identifikaciju u planktonskim uzorcima što će u budućnosti pridonijeti boljoj biogeografskoj rezoluciji i ekološkoj interpretaciji u pelagijalu.

(256 stranica, 88 slika, 23 tablice, 4 priloga, 276 literaturnih navoda, izvornik na engleskom jeziku)

Rad je pohranjen u Središnjoj geološkoj knjižnici, Horvatovac 102a, Zagreb, Hrvatska te u Nacionalnoj i sveučilišnoj knjižnici, Hrvatske bratske zajednice 4, Zagreb.

Ključne riječi: morski fitoplankton, dijatomeje, morfologija, taksonomija, sukcesija, Jadransko more

Mentori: Prof. dr. sc. Damir Viličić,
Dr. sc. Diana Sarno, zn. sur.

Ocjenitelji: Prof. dr. sc. Nenad Jasprica
Doc. dr. sc. Zrinka Ljubešić
Dr. sc.. Živana Ninčević Gladan, znanstvena savjetnica

Rad prihvaćen: 11. listopada 2013.

BASIC DOCUMENTATION CARD

University of Zagreb
Faculty of Science
Department of Geology
Interdisciplinary Doctoral Study in Oceanology

Doctoral Thesis

TAXONOMY AND ECOLOGY OF THE PLANKTONIC DIATOM FAMILY CHAETOCEROTACEAE (BACILLARIOPHYTA) FROM THE ADRIATIC SEA

SUNČICA BOSAK

University of Zagreb, Faculty of Science, Division of Biology,
Rooseveltov trg 6, 10 000 Zagreb, Croatia

The cosmopolitan diatom family Chaetocerotaceae abounds in the phytoplankton of coastal regions, comprising ca. 170 species, belonging to two genera, *Chaetoceros* and *Bacteriastrum.* In the Adriatic Sea the group is ecologically important represented with ca. 50 species whose identification is often problematic. The species morphology was assessed by analysing the material from cultured strains and the field plankton samples collected at 8 locations along the eastern Adriatic coast from 2006 to 2012. All taxa were studied with light, scanning and transmission electron microscopy. Ecological relationships were investigated: (i) in the coastal area of northern Adriatic (biweekly in 2008 – 2009) (ii) in Krka River estuary (twice a day during six days in July 2010). 49 morphologically distinct taxa were recorded, of which six were affiliated with the genus *Bacteriastrum* and 43 with genus *Chaetoceros* with 41 species, two varieties, two tentatively identified and four unknown morphotypes. Five taxa have been reported for the first time for the Adriatic and three emended diagnoses were proposed for *Chaetoceros vixvisibilis*, *Bacteriastrum jadranum* and *B. mediterraneum*. The morphological analysis helped to clear previously common misidentifications of species *Bacteriastrum delicatulum/B. furcatum, Chaetoceros contortus/C. compressus, C. decipiens/C. lorenzianus* and *C. lauderi/C. teres* where that in all observed material only first species from the given pair could be identified. The individual morphological characters were classified according to their identification significance with the particular emphasis on comparison and establishing species-specific traits such as resting spore morphology, ultrastructure of the setae and valves. We distinguished 9 different setae structural types in the subgenus *Chaetoceros* and the same number in the subgenus *Hyalochaete*. A novel and unique type of colony formation in planktonic marine diatoms was discovered and characterized with the atomic force microscopy (AFM) for *Bacteriastrum jadranum* which forms colonies by enclosing the cells within the organic network (cell jacket). The phylogenetic analysis of 28S rDNA separated *Bacteriastrum furcatum* and *B. hyalinum* in one clade and *B. jadranum* and *B. mediterraneum* in the other one. In relation to other *Chaetoceros* species results imply that that *Bacteriastrum* species form a lineage within the genus *Chaetoceros*, but for the drastic changes in the taxonomy there is still a need for a more thorough investigation. The multivariate analysis of seasonal dynamics and ecological relationships showed the permanent presence of chaetocerotacean species in the phytoplankton with with a change in dominance and clear annual succession. The pattern can be partially explained by the environmental parameters, with the temperature, silicate, salinity and phosphate as most important factors driving the community succession.

(256 pages, 88 figures, 23 tables, 4 appendices, 276 references, original in English language)

Thesis is deposited in the Central Geological Library, Horvatovac 102a, Zagreb, Croatia and National and University Library, Hrvatske bratske zajednice 4, Zagreb, Croatia

Keywords: marine phytoplankton, diatoms, morphology, taxonomy, succession, Adriatic

Supervisors: Damir Viličić, Full Professor
Diana Sarno, Research Scientist

Reviewers: Nenad Jasprica, Associate Professor
Zrinka Ljubešić, Assistant Professor
Živana Ninčević Gladan, Senior Research Scientist

Thesis accepted: October 11th 2013

PROŠIRENI SAŽETAK

Dijatomeje (Bacillariophyta) su jednostanične eukariotske mikroalge široko rasprostranjene u kopnenim vodama i u moru. Dominiraju brojnošću i biomasom u većini obalnih ekosustava te se smatra da su zaslužne za oko 1/5 ukupne globalne primarne proizvodnje. Stanice dijatomeja posjeduju jedinstven tip periplasta građenog od amorfnog silicija i organskog materijala koji se naziva frustula. Oblikovanje i dizajn silikatne komponente je pod strogom genetičkom kontrolom stanica zbog čega se identifikacija i klasifikacija pojedinih vrsta temelji na određivanju oblika i specifičnosti struktura periplasta. Kozmopolitska porodica Chaetocerotaceae, koja pripada skupini bi/multipolarnih centrica (Mediophyceae), je jedna od vrstama najbogatijih i morfološki najraznolikijih skupina morskih planktonskih dijatomeja koja ima značajnu ulogu u neritičkim hranidbenim mrežama te u ciklusu ugljika i silicija. Karakteristično obilježje porodice su sete, dugi i šuplji silikatni izdanci koji izlaze s rubnog dijela frustule. Nekoliko vrsta je solitarno, no češće se susjedne stanice povezuju pomoću seta tvoreći prekrasne kolonije u obliku lanaca. Mnoge vrste stvaraju specifične mirujuće spore koje su često prisutne u fosilnim zapisima. Skupina broji oko 170 vrsta svrstanih u dva roda: (i) *Chaetoceros* Ehrenberg čije stanice imaju dvije sete po valvi i *Bacteriastrum* Shadbolt s brojnim (6- 20) setama. Identifikacija svojti iz oba roda je često problematična zbog velike intraspecijske varijabilnosti i pojave prijelaznih oblika. U Jadranskom moru porodica je vrlo raznolika i zastupljena s oko 50 različitih vrsta. Do sada je istraživanje vrsta bilo ograničeno na općenita istraživanja sezonske dinamike i prostorne distribucije morskog fitoplanktona te je premalo pozornosti posvećeno vrstama iz ove porodice iako su ove dijatomeje vrlo značajne i često razvijaju guste populacije u Jadranu. Stoga je cilj ovog istraživanja detaljan pregled morfologije i taksonomije vrsta porodice Chaeocerotaceae pronađenih duž istočne obale Jadranskog mora te njihova prostorna distribucija, sezonska dinamika i ekološki odnosi.

Morfologija vrsta je analizirana u kulturama stanica izoliranih u laboratoriju i u uzorcima prikupljenim na terenu, na osam lokacija duž istočne obale Jadrana (Limski kanal, obalno područje Rovinja, Velebit i Paški kanal, uvala Telašćica, estuarij rijeke Krke, otok Mljet, Bokokotorski zaljev, obalno more Albanije), u razdoblju 2006-2012 godine. Sve svojte su proučavane sa svjetlosnim, skenirajućim i transmisijskim elektronskim mikroskopom (SEM, TEM) te vrsta *Bacteriastrum jadranum* dodatno s mikroskopom atomskih sila (AFM). Molekularno-filogenteski su analizirana (28S rDNA sekvence) četiri soja roda *Bacteriastrum* i jedan soj vrste *Chaetoceros affinis*. Ekološki odnosi su analizirani u dva istraživanja 1) na jednoj postaji (RV001) u obalnom području sjevernog Jadrana (uzorci za plankton i prateće biološke i ekološke parametre sakupljani su svaka dva tjedna tijekom jedne godine od jeseni 2008 do jeseni 2009) 2) u području ušća rijeke Krke uzorci su uzimani dva puta dnevno, na jednoj postaji (Martinska) u razdoblju od šest dana u srpnju 2010.

Rezultati su podijeljeni u tri glavna potpoglavlja. U prvom dijelu, opisi vrsta su dani za 49 morfološki različite svojte, uključujući i 25 svojti identificiranih iz 48 kultivirana soja. Opisi vrsta

uključuju popis literature, česte sinonime, morfometrijske podatke. Zasebno su prikazani rezultati dobiveni svjetlosnom i elektronskom mikroskopijom. Svaki opis je popraćen s istaknutim prepoznatljivim značajkama i komentarom o sličnim vrstama. Tekst je praćen odgovarajućim visokokvalitetnim mikrofotografijama što uvelike olakšava identifikaciju vrsta. Svojte su navedene abecednim redom u rodu *Bacteriastrum* (6 svojti) i unutar svake od podroda *Chaetoceros* koji uključuju 10 vrsta *Chaetoceros* (*Phaeoceros*), 32 vrste podroda *Hyalochaete* i jednu podroda *Bacteriastroides*. Popis obuhvaća 41 vrstu, dva varijeteta, dvije uvjetno identificirane svojte i četiri nepoznata morfotipa identificirana kao *Chaetoceros* sp. "A", "B", "C" i "D". Tri nadopunjene dijagnoze s dodatnim morfološkim i/ili molekularnim informacijama su predložene za vrste koje su prvotno opisane iz Jadrana: *Chaetoceros vixvisibilis*, *Bacteriastrum jadranum* i *B. mediterraneum*. Većina jadranskih vrsta roda *Bacteriastrum* i *Chaetoceros* može se prepoznati po obilježjima koja su vidljiva svjetlosnim mikroskopom ali se vrste mogu identificirati i elektronskim mikroskopom jer posjeduju neke specifične ultrastrukturne detalje koji do sad nisu bili zabilježeni u literaturi. Na temelju dobivenih podataka iz terenskih uzoraka i kultura procijenjena je taksonomska važnost pojedinih morfoloških obilježja. Obilježja koja se koriste za identifikaciju vrsta podijeljena su u tri skupine: manje važna, umjereno važna i jako važna. Jedne od najvažnijih značajki su: morfologija mirujućih spora, ornamentacija i dizajn valve i struktura seta. Utvrđeno je da možemo razlikovati 9 različitih strukturnih tipova kod podroda *Chaetoceros* (*Phaeoceros*), 9 tipa s četiri dodatna podtipa kod podroda *Hyalochaete*, vrsta *C. bacteriastroides* pripada posebnom tipu i kod roda *Bacteriastrum* možemo razlikovati tri tipa. Također, u sklopu disertacije, kod vrste *Bacteriastrum jadranum* otkriven je i opisan jedinstven način formiranja kolonija koji do sada nije bio poznat kod planktonskih morskih dijatomeja, gdje stanice nisu povezane mehanički pomoću fuzije različitih silikatnih struktura već uklapanjem stanica u optički transparentni organski matriks („cell jacket“). Rezultati molekularne filogenetske analize 28S (LSU) sekvence iz četiri soja roda *Bacteriastrum* odvojila su *B. furcatum* i *B. hyalinum* u jednu grupu te *B. jadranum* i *B. mediterraneum* u drugu. U odnosu na ostale vrste *Bacteriastrum* vrste se grupiraju unutar roda *Chaetoceros*, ali za drastične taksonomske promjene potrebno je temeljitije istraživanje koja bi obuhvatilo veći broj sojeva i uključilo veći broj molekularnih markera.

U drugom dijelu rezultata, dan je popis vrsta iz porodice Chaetocerotaceae identificiranih u osam područja (na 31 postaji) duž čitave obale Jadrana. Pet svojti je po prvi zabilježeno u Jadranu: *Chaetoceros pseudodichaeta*, *C. bacteriastroides*, *C. neocompactus*, *C. circinalis* i *C. salsugineus*. Morfološki slične vrste koje su do sada određivane kao *Bacteriastrum furcatum/B. delicatulum, C. contortus/C. compressus, C. lorenzianus/C. decipiens* te *C. lauderi/C. teres* zapravo pripadaju vrstama *B. furcatum, C. contortus, C. decipiens* i *C. lauderi*.

U trećem dijelu utvrđeno je da i *Bacteriastrum* i *Chaetoceros* vrste čine dominantne dijatomeje u istočnom obalnom području Jadrana, prisutne su tijekom cijele godine, a sukcesivno se izmjenjuju tijekom godine. Većina vrsta se razvija se samo jednom u godini. Od 36 zabilježenih vrsta, 10 može biti dominantno u zajednici. U jesenskom maksimumu se vrsta *C. contortus* izmjenjuje s vrstom *C. vixvisibilis* što upućuje na kombinaciju različitih životnih strategija. Proljetni maksimum je izostao, umjesto njega je ljeto 2009 bilo obilježeno širenjem slatke vode od rijeke Po do istočne obale što je uzrokovalo monospecifični cvat vrste *Chaetoceros vixvisibilis* što je dovedeno u vezu s povećanom dostupnošću fosfata. Multivarijatna analiza pokazala je sukcesiju vrsta s pet različitih skupina. U jesen 2008, vrste *C. contortus* i *C. vixvisibilis* su bile najznačajnije, ali i *B. mediterraneum* i *C. socialis*. Zimsko radoblje 2008/2009 karakterizirano je vrstama *C. danicus, C. eibenii, B. hyalinum* i malim *C.* cf. *wighamii*. Rano proljeće 2009 obilježeno je s malim jednostaničnim vrstama *C. tenuissimus, C. throndsenii* var. *throndsenia* i *Chaetoceros* sp . "B", *C. simplex*. U kasno proljeće primijećen je intenzivan razvoj različitih zajednica sličnim jesenskim s dodatkom vrsta *C. curvisetus, C. danicus* i *Bacteriastrum furcatum*. U srpnju 2009 zabilježena je monospecifična cvatnja *C. vixvisibilis* dok je u jesen 2009 dominirala raznolika zajednica sastavljena od vrsta *C. decipiens* i *C. affinis* s *B. jadranum, C. tortissimus, C. anastomosans*, *C. lauderi*. Sukcesija se može djelomično objasniti djelovanjem temperature, silikata, saliniteta i fosfata.

Točni i potpuni opisi vrsta dijatomeja prikupljeni u ovom istraživanju će olakšati buduću ispravnu identifikaciju u planktonskim uzorcima i poboljšati taksonomijsku rezoluciju ovog važnog roda na lokalnoj, tako i globalnoj razini. To će u budućnosti pridonijeti podacima o globalnoj biogeografskoj rasprostranjenosti, kao i doprinijeti poboljšanju kvalitete podataka o ekologiji fitoplanktona.

SUMMARY

Diatoms represent one of the principal groups of eukaryotic microoorganisms in the modern marine phytoplankton assemblages. They are one of the most species-rich and dominant groups of microalgae, responsible for about $1/5^{th}$ of global primary production. The cosmopolitan family Chaetocerotaceae, a member of bi/multipolar centrics (Mediophyceae), abounds in the phytoplankton of coastal regions, thus playing a significant role in the neritic food webs and carbon/silica cycle. The group comprises ca. 170 species, belonging to two genera, *Chaetoceros* Ehrenberg and *Bacteriastrum* Shadbolt. The hallmarks of the family are setae, characteristic long and hollow silicate spine-like projections protruding from the valve surface. The identification of the taxa from both genera is often problematic due to the large intraspecific morphological variability and occurrence of intermediate forms and species have been frequently misidentified. In the Adriatic Sea the group is highly diverse, represented with ca. 50 species. Thus far the seasonal dynamics and spatial distribution of *Bacteriastrum* and *Chaetoceros* species have been analysed in the frame of different ecological studies. Overall, a little attention has been paid to the species from this family although these diatoms are ecologically important in the area as they represent a constitutive component of the phytoplankton and often develop dense populations. Therefore, the aim of this study was to give a detailed overview of the morphology and taxonomy of chaetocerotacean species found along the eastern Adriatic coast and with the improved taxonomic resolution contribute to the information on their spatial distribution, seasonal dynamics and ecological relationships.

The species morphology was assessed by analysing the material from cultured strains and the field plankton samples collected at eight locations along the eastern Adriatic coast: Lim Bay, coastal area of Rovinj, Velebit and Pag Channel system, Telašćica Bay, Krka estuary, the island of Mljet, Boka Kotorska Bay and the Albanian coastal zone. The samples were obtained from various studies from the period 2006-2012. All taxa were studied with light, scanning and transmission electron microscopy (SEM, TEM) and *Bacteriastrum jadranum* additionally with atomic force microscopy (AFM). Separately, 28S (LSU) sequences from four *Bacteriastrum* strains and one strain of *Chaetoceros affinis* were analysed. For the ecological part of the study, two field studies were conducted. First, in the coastal area of northern Adriatic (at station RV001) samples for plankton and accompanying biological and environmental parameters were taken every two weeks from autumn 2008 to autumn 2009. Second, in the Krka River estuary samples were taken twice a day at one station (Martinska) during six days in the July of 2010.

The Results are divided in three main subchapters. In the first part, the species descriptions were provided for 49 morphologically distinct taxa, including 25 taxa identified from 48 cultivated strains. The descriptions include bibliography, synonyms, morphometric data and observations obtained with light and electron microscopy. Each description is accompanied with the emphasized distinctive features and comments on the similar species. The text is accompanied with appropriate excellent

quality micrographs which greatly facilitate the species identification. The taxa are listed alphabetically within *Bacteriastrum* (six taxa) and each of *Chaetoceros* generic subdivision (subgenera) which includes 10, 32 and one species from *Chaetoceros* (*Phaeoceros*), *Hyalochaete* and *Bacteriastroides*, respectively. The list encompasses 41 species, two varieties, two tentatively identified taxa and four unknown morphotypes designated as *Chaetoceros* sp. "A", "B", "C" and "D". The emended diagnoses based on new morphological and/or molecular information on 3 species which had been originally described from Adriatic Sea, *Chaetoceros vixvisibilis, Bacteriastrum jadranum* and *B. mediterraneum*, are provided. The majority of Adriatic chaetocerotacean species can be identified by the characters visible with light microscopy, but the species could be further recognized in electron microscope due to some species-specific ultrastructural features. According to the importance in species identification we classified the individual morphological characters into 3 groups: not important, moderately important and very important. One of the most important features for identification were found to be morphology of the resting spores, the ornamentation pattern of the valve and structural design of the setae. We distinguished 9 different structural types in *Chaetoceros* (*Phaeoceros*) species, 9 types with four additional subtypes for the subgenus *Hyalochaete, C. bacteriastroides* belong to the separate type and in genus *Bacteriastrum* we found 3 types. Within this dissertation, the unique and novel colony formation for planktonic marine diatoms was revealed and described in species *Bacteriastrum jadranum* which forms chain colonies by enclosing the cells within an optically transparent organic matrix called a cell jacket. The results from molecular phylogenetic analysis of 28S (LSU) sequences from four *Bacteriastrum* strains placed together *B. furcatum* and *B. hyalinum* in one clade and *B. jadranum* and *B. mediterraneum* in the other one. In relation to other *Chaetoceros* species results imply that that *Bacteriastrum* species form a lineage within the genus *Chaetoceros*, but for the drastic changes in the taxonomy there is still a need for a more thorough investigation which would encompass a larger number of strains and include larger number of molecular markers.

In the second part of results, the checklist of the species from the family Chaetocerotaceae is provided along the Adriatic Sea. Five taxa have been reported for the first time for the Adriatic Sea: *Chaetoceros pseudodichaeta, C. bacteriastroides, C. neocompactus, C. circinalis* and *C. salsugineus*. The morphological analysis helped to clear previously common misidentifications in the dominant Adriatic species in cases of *Bacteriastrum furcatum/B. delicatulum, Chaetoceros contortus/C. compressus, C. decipiens/C. lorenzianus* and *C. lauderi/C. teres*. The analysis showed that in all analysed material only first species from the given pair could be identified.

In the third part of results the focus is on the succession and ecological relationships. It was established that both *Bacteriastrum* and *Chaetoceros* species were among dominant diatoms in the eastern coastal Adriatic Sea, with a change in dominance and clear annual succession pattern. Most of species showed only one peak in their abundance. From 36 recorded species, 10 are found to be dominant. In the autumn bloom the *C. contortus* alternated with *C. vixvisibilis* indicating the

combination of different life-strategies with former species population developing from low number of cells present in the plankton and being followed by spore germination from the sediment of the later species. Vernal bloom was lacking, and instead summer 2009 was characterized with a spreading of freshwater from river Po up to the eastern coast triggering the monospecific *Chaetoceros vixvisibilis* bloom which corresponds to an increased availability of phosphate. The multivariate analysis which included only chaetocerotacean taxa showed the succession of the species composition pointing out five distinct groups. In the autumn 2008, blooms of *C. contortus* and *C. vixvisibilis* were most significant, but also *B. mediterraneum* and *C. socialis* were abundant. In winter 2008/2009 *C. danicus*, *C. eibenii*, *B. hyalinum* but also small chain-forming species *C.* cf. *wighamii*. Early spring 2009 was characterised with small single celled *C. tenuissimus*, *C. throndsenii* var. *throndsenia* and *Chaetoceros* sp. "B", *C. simplex*. In late spring intensive development of diverse community similar to autumn one was observed with addition of *C. curvisetus*, *C. danicus* and *Bacteriastrum furcatum*. In July 2009 monospecific bloom of *C. vixvisibilis* was observed while in autumn 2009 a diverse community composed of *C. decipiens* and *C. affinis* with *B. jadranum, C. tortissimus, C. anastomosans, C. lauderi* was recorded. The succession pattern can be partially explained by the environmental parameters, with the temperature, silicate, salinity and phosphate as most important factors driving the community succession.

The accurate and complete diatom taxa descriptions obtained in this study will facilitate future correct species identification and improve the taxonomic resolution of this important family on the local as well as global level which will in long term add information to the global biogeographical species distribution as well as contribute to the improvement of quality of the data on phytoplankton ecology in the future studies.

CHAPTER 1

INTRODUCTION

"...There is grandeur in this view of life, with its several powers, having been originally breathed into a few forms or into one; and that, whilst this planet has gone cycling on according to the fixed law of gravity, from so simple a beginning endless forms most beautiful and most wonderful have been, and are being, evolved."

Charles Robert Darwin (1809–1882) from "The origin of species"

1.1 A brief diatom biology

Diatoms are photosynthetic unicellular microalgae with the unique morphological and life-cycle features. Despite a number of studies to examine their phylogeny, using one or several genes, the evolutionary relationships of diatoms to other groups are still unclear and there are still huge gaps in our knowledge. They are currently recognized as the separate group Diatomea Durtmortier 1821 (= Bacillariophyta Haeckel 1878) placed among the clade of heterokont protists Stramenopiles within the eukaryotic super-group Sar (Adl et al., 2012). The word "diatom" is a combination of two Greek words: *δια-* (dia-) and *τεμνειν* (temnein) = *diatemnein*, meaning "cut in half; split into two" and it perfectly reflects their distinctive character: the cells are encased within the compound cell wall composed of two slightly unequal parts that fit together as the lid on the box. However, the origin of the name actually derives from the observations of the zig-zag shaped diatom colonies by a french naturalist Augustin Pyrame De Candolle in 1805 reflecting the clefts between cells in the filament and not the split within the single cell (Edgar, 2013).

1.1.1 The silica cell wall - frustule

The hallmark of the diatom cell is the frustule, an unique mineralized cell wall built of a amorphous hydrated silica ($SiO_2 \times nH_2O$) and organic material (proteins, polysaccharides). The frustule is elaborately structured on the nano- to micro-scale displaying beautiful, highly regular and ornate patterns. The two overlapping parts of the frustule are called thecae, and as they are unequal in size we distinguish "epitheca" – upper/larger part and "hypotheca"- bottom/smaller part, with each of them composed of a valve and a series of hoop-like or segmental girdle bands (also called the cingular bands). The first girdle band adjacent to the valve is called valvocopula while other bands are reffered to as copulae and the connecting band between two thecae is reffered to as pleura (Fig. 1.1.).

Assembly of new silicate components of the frustule takes place in the silica deposition vesicles (SDV). Dissolved silicic acid is actively taken up from environment and concentrated in the cytoplasm where the silicic acid transport (SIT) proteins bind the silica and transport it to the SDV. Other classes of peptides, including silaffins, silacidins, and long chain polyamines (LCPA) are produced in the endoplasmic reticulum and transported into the SDV where they form a matrix onto which the supersaturated silica precipitates in an amorphous form (Kröger and Poulsen, 2008). The design of silicate component is

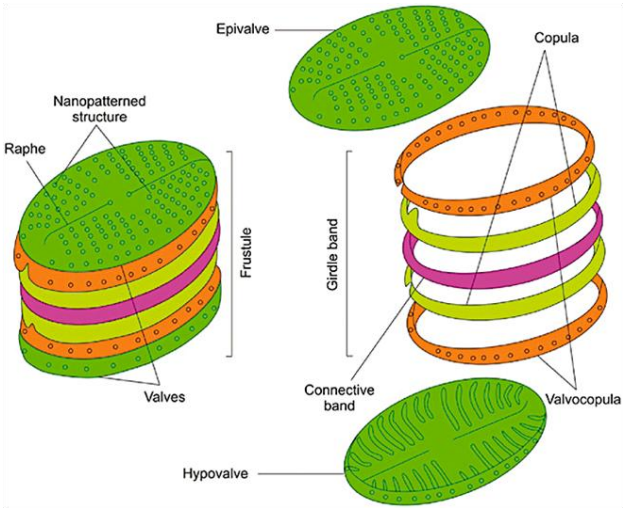

Figure 1.1. Shematic overview of the structure of a diatom frustule. Valves are in green while the bands forming the girdle region are represented by orange, yellow and pink rings (from Francius et al., 2008).

under strict control of the cell genetics and due to this fact the species identification and taxonomy is based on the determination of the shape and structural specificities of the frustule (Round et al., 1990). The diatom frustules are usually perforated by diverse types of pores and often ornamented with ridges, various processes or spines protruding from the valve surface. The extraordinary complexity of the frustule architecture and the fact that these nano-patterns are faithfully inherited through mitotic division have attracted the scientists from various areas of the industry and applied science (Bradbury, 2004). The diatom structural, mechanical, genomic, optical and photonic properties and the silica biomineralization process, may have their application in nanotechnology leading to the nanofabrication and engineering of new materials and devices based on diatom silica (Gordon et al., 2009).

1.1.2 The diatom metabolism and origin of plastids

Beneath the diatom frustule is the protoplast consisting of a large vacuole, a diploid nucleus and a variable number of plastids. The diatom chloroplasts characteristically contain photosynthetic pigments chlorophyll *a* and *c*, and accessory pigments fucoxanthin, diadinoxanthin, diatoxanthin and betacarotene. The fucoxanthin is responsible for golden-brown or brown-green colour of the diatom cells. Diatoms as one of the members of heterokont class of algae have plastids surrounded by four membranes which is an indication of their complex evolutionary origin. Common to all photosynthetic eukaryotes was a primary endosymbiosis event where a heterotrophic eukaryote enslaved or was invaded by a cyanobacterium. Most of the cyanobacterial genes were transferred to the nucleus as the cyanobacterium evolved into the chloroplast (Gould et al., 2008). The ancestral phototrophic eukaryote resulting from primary endosymbiosis gave rise to the glaucophytes, red algae, green algae and plants. The evolutionary story is probably more complex as the comparative analyses with the Chlamydiae, a group of intracellular bacteria that today exist only as pathogens or symbionts, showed the presence of some chlamydial genes in both plants and red algae, but not in cyanobacteria, suggests that a chlamydial endosymbiont also tagged along during the early stages of the primary endosymbiosis (Becker et al., 2008).

A secondary endosymbiosis later occurred between a different heterotrophic eukaryote and a red alga. The red algal endosymbiont was the progenitor of the plastids found in Stramenopiles, a group that except diatoms includes also various brown and golden-brown flagellated microalgae, brown macroalgae and plant parasites (Adl et al., 2012). To the further complexity of the specific history of diatom lineage adds the study of Moustafa et al. (2009) which showed that the most symbiont-derived genes in the diatom genome have a green algal origin and only a small minority derive from red alga. This indicates that they first possessed a green algal endosymbiont which was only later replaced by a contemporary red plastid.

Diatom genomes contain abundant numbers (up to 5%) of genes derived from bacteria of various classes (Armbrust et al., 2004, Bowler et al., 2008) and this complex mixture of genes results in a

unique combination of metabolic processes, which combine both plant- and animal-like characteristics and provide novel possibilities for perception of environmental signals. Some bacterial genes replaced homologous genes found in other phototrophs, whereas others provided new metabolic functions to the diatoms. The example is the finding of a complete urea cycle in diatom metabolism which was previously thought to be restricted to organisms that consume complex organic nitrogen compounds and excrete nitrogenous waste (Armbrust et al., 2004, Bowler et al., 2008). Diatoms also combine an animal-like ability to generate chemical energy from the breakdown of fat with a plant-like ability to generate metabolic intermediates from the breakdown, a combination that probably allows diatoms to survive long periods of darkness, as occurs at the poles, and resume division and growth when they return to the light (Armbrust et al., 2004).

The storage products in diatoms are known to be chrysolaminaran, a β-1,3-linked glucan, which is stored in special vacuoles, and oil. The metabolic potential of diatoms in accumulation of lipids along with their inherently high growth rates and good performance in large-scale cultures makes them a desirable organism for the microalgal biofuel research and production (Hildebrand et al., 2012).

1.1.3 Diatom life cycle

Diatoms are almost unique among microalgae in having a diplontic life cycle (Mann, 1993) where the vegetative cells that undergo growth are diploid (2N), and the only haploid (N) cells are the gametes. Typically, the diatom life cycle (Figure 1.2.) comprises two principal phases: a prolonged vegetative phase, up to several years, during which the cells divide mitotically, and a comparatively short phase that includes sexual reproduction (gametogenesis and fertilization, occupying several hours) and then a complex developmental process leading to the formation of new vegetative cells (many hours to a week or more) (Chepurnov et al., 2004). Their unique frustule structure of two overlapping thecae and the division pattern in which new cell wall components are formed within the parental cell, cause diatoms to gradually reduce their cell size in the course of the mitotic part of the life cycle (MacDonald-Pfitzer rule) and after the cell size reaches the minimum viable threshold they die (Round et al., 1990). At a critical (upper) size threshold which is the size of the cells first capable of sexual size restitution, they can engage in sexual reproduction as this is the common way for most of the diatoms to restore the original cell size (Kaczmarska et al., 2013).

In addition to being in the right cell size window and in the active growth phase of the population the environmental factors and chemical interactions between cells regulate the sexual part of the life cycle (Chepurnov et al., 2004, Scalco, 2012). Gametogenesis occurs by meiosis and the cell walls of gametangia are discarded. The gametes fuse to form a peculiar zygote called the auxospore within which the initial cell is produced. The auxospore lacks the rigid siliceous wall and it starts expanding by the formation of the perizonium, a cell wall consisting of bands made of organic matrix in which usually some silica particles are incorporated. In some diatoms, e.g. *Skeletonema costatum*, there is an alternative process to reconstitute cell size called vegetative cell enlargement. This implies a complete release of a vegetative cell protoplast from its frustule, its subsequent expansion, and the formation of the new bigger valves (Round et al., 1990, Kaczmarska et al., 2013). However, the sexual reproduction is firmly integrated into the life cycle of diatoms because periodical sexual events are vital for the majority of species to re-establish the initial cell size and to avoid becoming too small for survival (D'Alelio et al., 2010). As genetic recombination is also achieved through sexual reproduction, the obligatory nature of sex in their life cycle may be linked with their evolutionary and ecological success.

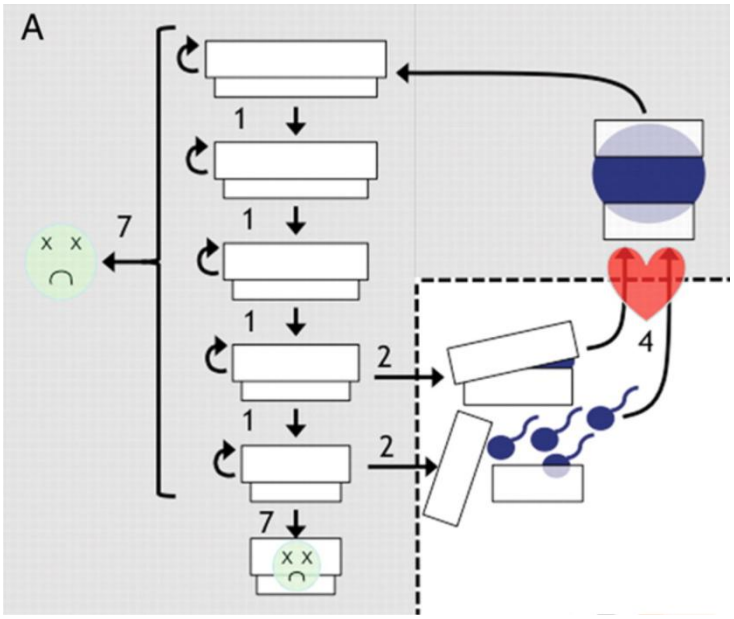

Figure 1.2. Schematic drawings illustrating the life cycle of the diplontic centric diatom. The grey shading delimits diploid stages. (1) vegetative division results in size reduction as each cell produces one cell of the same size and one daughter cell of a smaller size than its parent; (2) the cell can undergo meiosis; 4) the gamete can find a compatible partner (syngamy, shown by the 'heart"); (7) the cell death may occur, either due to external cues or to failure to restore cell size.(from von Dassow and Montresor, 2011).

The life cycle of many diatom species also includes the formation of resting stages, either as resting cells, which are morphologically similar to vegetative cells but physiologically and cytologically modified (Sicko-Goad et al., 1989, Kuwata et al., 1993, Kaczmarska et al., 2013), or as resting spores, specialized cells morphologically different from vegetative ones in having a thick and heavily silicified wall (Hargraves, 1976). Resting stage cells have the ability to tolerate unfavourable conditions, such as darkness, nutrient depletion, and temperature changes, allowing the population to survive until more favourable conditions return. Furthermore, diatom resting spores in sediment also play an important role in providing a seed population for subsequent blooms in the water column (French III and Hargraves, 1986). They are commonly formed within the vegetative phase of the diatom's life history as a result of two subsequent mitotic divisions during which modified highly-silicified valves are produced. However, there are two known exceptions in marine planktonic species:

Leptocylindrus danicus (French III and Hargraves, 1986) and *Chaetoceros eibenii* (von Stosch et al., 1973) in which the resting spore is the product of sexual reproduction because it is formed directly from the auxospore.

1.2 Diatom diversity

Diatoms are widely distributed and highly abundant in all aquatic habitats from the tropics to the polar regions, occurring in the plankton and benthos of both marine and fresh waters, and in terrestrial environments, such as damp soils and moist surfaces of rocks and plants (Round et al., 1990). The diversity of diatoms is estimated to range between 10 000 and 200 000 extant species (Mann and Droop, 1996) most of which are not properly identified as such (Kooistra and Medlin, 2007). Arguably most diatom diversity is not planktonic, but benthic or epiphytic and it is assumed that approximately 5 000 to 10 000 species are from marine phytoplankton (Sournia et al., 1991). These estimated numbers are generally based on the morphological descriptions and the exact number is difficult to obtain as there are multiple synonyms, varieties and insufficiently characterized species in the literature along with the continuous descriptions of newly discovered taxa. In addition, in recent years it was revealed that within morphologically well circumscribed marine planktonic species, previously regarded as cosmopolitan, there is a considerable hidden and cryptic diversity with variations in reproductive, molecular, physiological, and ecological characteristics (Amato et al., 2007, Kooistra et al., 2008, Nanjappa, 2012).

Traditionally, diatoms are categorized into two major groups: “centrics” and “pennates”. The principal differences are the structural plan of the valve and the mode of sexual reproduction (oogamy versus morphological isogamy). Centric diatoms (Coscinodiscophytina) possess radially organized valves with ribs radiating from a central region or ring, whereas pennates (Bacillariophytina) have elongated valves with ribs oriented perpendicular to a midrib (called a sternum), like in a feather (Round et al., 1990). The molecular data show the centrics as a whole to be paraphyletic (Medlin and Kaczmarska, 2004) and currently recognized major groups are: the radial centrics (Coscinodiscophyceae), the bi/multipolar centrics (Mediophyceae), the araphid pennates (Fragillariophyceae), and the raphid pennates (Bacillariophyceae) (Figure 1.3.). However, exact phylogenetic and taxonomic relationships between these groups are currently unclear (Adl et al., 2012).

Fossil records and molecular clock indicate that diatoms have a relative young evolutionary history, having originated not earlier than the Mesozoic. The radial centrics as the most primitive lineage first appeared in the early Jurassic (ca. 190 millions of years before present), multipolar centrics in the Early Cretaceous, pennates in the Late Cretaceous and the youngest are the group of raphid pennates which appeared in Paleocene, in the Paleogene period ca. 55 millions years B.P.. The diatoms apparently traversed the K/T boundary relatively unscathed and show from then onwards an increasing diversity (Kooistra et al., 2007, Not et al., 2012).

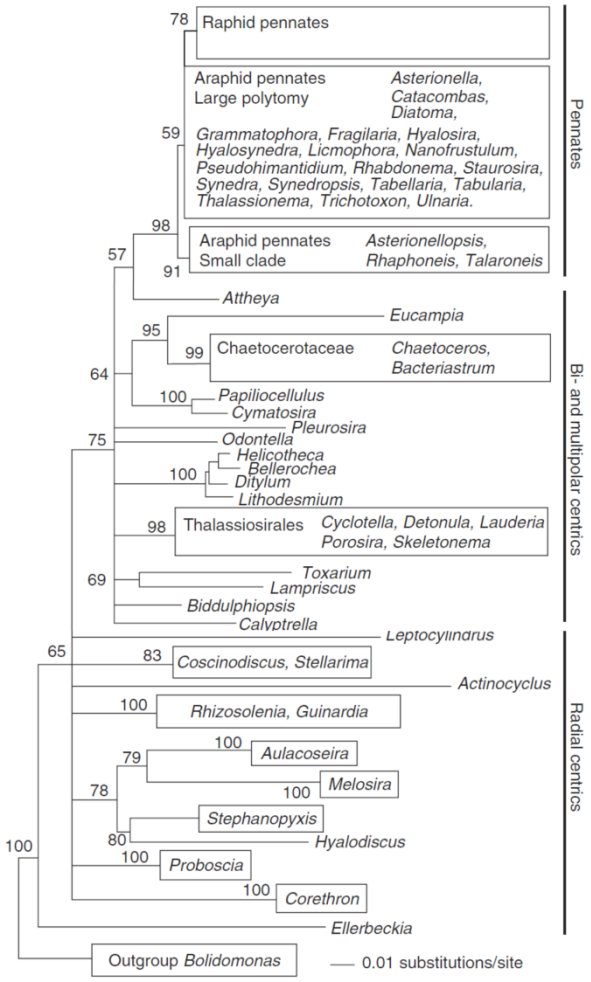

Figure 1.3. Phylogenetic tree of diatoms based on SSU rRNA (from Kooistra et al., 2007).

1.3 Marine planktonic diatoms: general characteristics and importance

Diatoms represent one of the principal groups of eukaryotic microoorganisms in the modern marine phytoplankton assemblages together with dinoflagellates and prymnesiophytes. They have a considerate global ecological significance as it is estimated that they account for approximately 25% of total global annual primary production (Mann, 1999). They play a very important part in global cycling of many elements, but particularly carbon and silica. Unlike much of the carbon generated by terrestrial ecosystems, the organic carbon produced by diatoms is consumed rapidly and it serves as a base for marine food webs. The diatoms are dominating in terms of biomass and abundance in majority of the coastal ecosystems and its members form intense spring blooms in coastal temperate and high latitude environments after the day-length increases and inorganic nutrients become available in the photic zone following the seasonal vertical mixing of the water column. Diatoms thrive particularly well in the non-stratified conditions in the water column. As their cells are non-motile they avoid the nutrient depletion in the proximity of the cells by sinking and positively exploiting the action of turbulence. In accordance, the large range in size and shape of diatom species occurring

simultaneously during blooms can be considered as adaptations to the different scales of turbulence present in the marine environment (Margalef, 1978). Diatoms have a essential role in sustaining fisheries, as the major producers of 'new' phytoplankton biomass, sustained by fluxes of nutrients from deeper waters as opposed to nutrients recycled via the 'microbial loop' (Falkowski et al., 1998). In the open ocean, a relatively large proportion of diatom organic matter sinks rapidly from the surface, becoming food for deep-water organisms. A small fraction of this sinking organic matter escapes consumption and settles on the sea floor, where it is sequestered over geological timescales in sediments and rocks and contributes to nascent petroleum reserves thus constituting a key component of the biological carbon pump (Hildebrand et al., 2012). Diatoms are also the major sources of biogenic silica, transforming dissolved orthosilicic acid into the hydrated amorphous silica of their frustules; the silica is dissolved from the rocks into the rivers and the sea and it is taken mostly by diatoms and, when they die is either dissolved again or buried on the sea floor in form of siliceous ooze.

Marine planktonic diatoms mostly belong to the centric and bi- and multipolar centric lineages but there are also a few important pennate genera. The size of diatom cells ranges from very small of a few micrometers as in the picoplanktonic species e.g. *Minutocellus* spp. to large cells of the genera *Rhizosolenia* or *Thalassiotrix* which can reach up to hundreds of micrometers. Although diatoms are unicellular organisms, in many species sibling cells adhere to each other to create various types of colonies by a variety of means: (i) interlocking/fusion of different types of siliceous structures (e.g. processes, spines) or (ii) using extracellular polymeric substances (EPS) in form of mucilage or chitin threads (Round et al., 1990). Different forms of colonial lifestyle in diatoms are considered as species evolutionary adaptations to diverse ecological and physiological requirements. The general shape of the colony and the method of cells linkage are often recognized as particularly important diagnostic characters for recognising the diatom taxonomic affiliation (Fryxell, 1978, Fryxell and Medlin, 1981).

Important planktonic representatives of radial centrics are *Corethron, Coscinodiscus* and *Melosira* which usually possess a ring of labiate processes (rimoportulae) around their valve mantle forming tubes that may enable secretion of organic material. However, this character is lacking in some centric genera such as *Leptocylindrus* and *Rhizosolenia.* The bi- and multipolar centrics also show a radial organization of ribs, but their cell form is usually elongate, triangular or star-like. Rimoportulae, if present, are located on the central area of valves. Many species possess apical pore fields at their valve poles with densely packed pores. Mucilage is extruded through these pores, enabling the chain formation such as in the genus *Eucampia.* There are genera which appear radial, but they only secondarily acquired this feature such as *Lauderia*, *Porosira*, *Skeletonema* and *Thalassiosira*. They possess specialized tube-like processes, so-called strutted processes (fultoportulae), through which chitin filaments are extruded linking cells into chains or simply extending to the surrounding medium. In genera *Chaetoceros* and *Bacteriastrum*, colonial species usually form inseparable chains by fusion of the silica between setae of the adjacent cells. The both

groups of pennates have elongated shape with the raphid pennates possessing a raphe – a slit-shaped process and araphid pennates having apical pore fields and apical labiate processes. The raphe enables raphid pennates which are usually found in benthic habitats to move actively over the substratum. However, in the very important planktonic genus *Pseudo-nitzschia*, cells use their raphe to enable them to slide along each other and to assume a position in which they are just attached at their valve apices, forming chains in this way. The araphid pennates are also typically benthic, but there are also several lineages that are found in plankton, including *Asterionella*, *Asterionellopsis*, *Lioloma* and *Thalassionema* forming zig-zag or star-like colonies (Not et al., 2012).

1.4 The planktonic diatom family Chaetocerotaceae: general features, taxonomy and morphology

The family Chaetocerotaceae Ralfs in Pritchard 1861 is one of the largest, most diverse and widespread groups among planktonic diatoms in marine environment with several species reported from inland waters. In the current classification system the family is placed in the order Chaetocerotales Round et Crawford, class Mediophyceae (Jousé et Proshkina-Lavrenko) Medlin et Kaczmarska within the subdivision Bacillariophytina Medlin et Kacmarzscka (Adl et al., 2012). The family has been regarded previously by some authors as belonging to suborder Biddulphioideae (Hustedt, 1930) and by others to Rhizosoleniineae under the name Chaetoceraceae Smith (Simonsen, 1972) but it was also suggested that the family occupies an isolated position as the exact relationship to other diatoms was found to be quite controversial (Evensen and Hasle, 1975). Therefore, the classification system of Round et al. (1990) placed it within the order Chaetocerotales which together with Leptocylindrales Round et Crawford comprises the subclass Chaetocerotophycidae Round et Crawford. According to the same classification the Chaetocerotales included two more monotypic diatom families: (i) Acanthocerataceae Crawford with one genus *Acanthoceros* Honigmann encompassing one freshwater species *A. magdeburgense* Honigmann and (ii) Attheyaceae Round et Crawford with the genus *Attheya* West. Nevertheless, relationships within Chaetocerotales remain uncertain and especially the position of the *Attheya* species is under debate. The two marine benthic species *Attheya armata* (West) Crawford and *A. septentrionalis* (Østrup) Crawford were considered by Round et al (1990) as members of the genus *Gonioceros* H. Peragallo et M. Peragallo which was placed within the family Chaetocerotaceae. However, the genus was excluded from the family and its species transferred to *Attheya* by Crawford et al. (1994) on the basis of the morphological features, more precisely the differences in the structure and the formation of the valve projections which in these species are named horns. Moreover, the recent phylogenetic studies (Rampen et al., 2009, Sorhannus and Fox, 2012) showed that the: *Attheya. longicornis* Crawford et Gardner and *A. septentrionalis* constitute a separate lineage within the diatoms and are related more closely to the pennates than to any of the species of the Chaetocerotophycidae group.

The family Chaetocerotaceae is currently comprised of only two genera: *Chaetoceros* Ehrenberg and *Bacteriastrum* Shadbolt. The hallmarks of the family are setae, characteristic long and hollow silicate spine-like projections protruding from the valve surface. The main distinctions between members of these two genera are the valve shape and the number of setae per valve. *Bacteriastrum* species are showing multipolar/radial symmetry with numerous (6-20) setae regularly arranged around the circular valve margin as opposed to *Chaetoceros* species having bipolar/bilateral symmetry with elliptically shaped valves each adorned with usually two setae (Round et al., 1990). Nevertheless, within the genus *Chaetoceros* there are exceptions as some solitary forms have reduced number of setae to just one (Aké Castillo et al., 2004). Moreover, the species *Chaetoceros bacteriastroides* Karsten the single member of the subgenus Bacteriostroidea is considered as the link between the two genera due to the presence of six setae per bilaterally symmetric intercalary valve of which only two are large and robust, and the rest are small strongly spirally undulated forms (Hernández-Becerril, 1993).

Besides these two extant genera, there are also fossil representatives, the genera described solely on the basis of resting spores, so called "spore genera". These species may belong to the extinct taxa which were similar to *Chaetoceros* species and are affiliated to the genera such as *Dicladia* Ehrenberg, *Syndendrium* Ehrenberg ,*Liradiscus* Greville, *Monocladia* Suto, *Peripteropsis* Suto, *Truncatulus* Suto (Suto, 2006, Ishii et al., 2011). However, the majority of them are now considered to be synonyms of *Chaetoceros* (VanLandingham, 1968). The weakly silicified vegetative cells of *Chaetoceros* and *Bacteriastrum* species rarely remain preserved in a fossil record therefore little is known about their evolutionary history. Historically, the classification systems included subdivisions within both genera (Gran, 1900, Ostenfeld, 1903, Pavillard, 1925) but they were developed on presumed overall morphological similarity rather than reflecting the phylogenetic relations. Recent studies revised evolutionary relationships among species of Chaetocerotaceae considering morphological characteristics (Rines and Theriot, 2003) and combination of morphological and molecular information (Kooistra et al., 2010). These results indicate that the origin of the family is polyphyletic with very complicated phylogenetic interrelationships and that there are many inconsistencies in the traditional classification system, however for its change more additional investigations are essential.

1.4.1 Genus *Chaetoceros*

The bi(multi)polar centric diatom genus *Chaetoceros* Ehrenberg is together with the genus *Thalassiosira* considered to be one of the marine planktonic diatom genera with highest species diversity and widest distribution. The group is often the subject of taxonomical and ecological investigations due to the extraordinary morphological diversity and complexity of the species. Many taxa are cosmopolitan and several are euryhaline and eurythermal (Hustedt, 1930, Rines and Hargraves, 1988, Jensen and Moestrup, 1998). The genus is primarily marine but a few species occur at very low salinities in estuaries and freshwater lakes e.g. *Chaetoceros muelleri* Lemmermann and *C.*

amanita Cleve-Euler (Kaczmarska et al., 1985). Members of the genus occupy both neritic and oceanic environments where at times they constitute a large portion of the phytoplankton in terms of both abundance and biomass. The genus *Chaetoceros* usually blooms in coastal ecosystems of temperate and polar seas in the autumn and early spring period where it can simultaneously appear up to 15-20 different species of which typically one to three species dominate. The bloom may be established rapidly and it may vanish again in only a few days but also it can last for several weeks and during this period a succession of species usually takes place (Jensen and Moestrup, 1998, Rines and Hargraves, 1988). The important role in bloom formation can have the formation of resting stages as approximately one-third of the *Chaetoceros* species are reported to be capable of producing resting spores (Hargraves, 1976). The spore formation occurs during the blooms or at their end, and these spores are resuspended during subsequent upwelling events and reinoculated in the water column (Pitcher, 1990). However, the clear cut evidence that a timing of spore germination might act as an inoculum for the bloom is still lacking. There are some indications that a photoperiod may act as a trigger for their germination (Eilertsen 1995).

The genus exhibits the largest species diversity in warm tropical seas (Hernández-Becerril, 1996). Some interesting associations can be found within the genus, such as the apparently symbiotic relationships of *C. dadayi* Pavillard and *C. tetrastichon* Cleve with the tintinid *Eutintinus* sp. and *C. coarctatus* Lauder with ciliate *Vorticella* sp. (Hernández-Becerril, 1996). In addition, it is observed that *Chaetoceros* setae often serve as a host to variety of epiphytic organisms e.g. *Pseudo-nitschia* linea and *P. americana* (Lundholm et al., 2002) or they can serve as a suitable environment for development of *Phaeocystis globosa* colonies (Rousseau et al., 2007). A few species with large and robust setae such as *C. convolutus* Castracane and *C. concavicornis* Manguin may mechanically harm fish gills or species such as *C. socialis* Lauder, *C. wighamii* Brightwell and *C. debilis* Cleve may occlude the gills by producing large quantities of mucilaginous material and in this way causing fish death (Smayda, 2006).

1.4.1.1 Historical background and taxonomic relationships

The understanding of taxonomic history of *Chaetoceros* starts with a description of two species: *Chaetoceros dichaeta* and *C. tetrachaeta* and the establishment of the new genus by Ehrenberg (1844), from Antarctic material collected during the Captain Ross expedition to the South Pole (1841–1843). From these two species, *C. dichaeta* is described as a type species of the genus as it is frequently recorded among the dominant planktonic diatoms of the Southern Ocean (Assmy et al., 2008) while *C. tetrachaeta* is not well known and by VanLandingham (1968) is regarded as a taxonomic name not recommended to use. Further studies by Brightwell (1856) provided an emended description of the genus and included two new species *C. wighamii* and *C. peruvianus*. The name *Chaetoceros* originates from two Greek words: χαιτη (caith), a feminine noun meaning hair and κεραϲ (ceras), a neuter noun meaning horn which is reflecting the hallmark of the genus, the setae. However, when the Ehrenberg

selected the name whose origin ends with the neuter noun, he created the confusion in later design of the species epithets because various authors throughout history have treated this genus neuter although it should be masculine. Moreover, the names of the same species have been published with different endings, and hence in VanLandingham (1968) there is a list of equaly valid nomenclatural synonyms. The extensive discussion on the history of the problem of correct gender in *Chaetoceros* has been provided in Rines and Hargraves (1988) together with the extensive list of species names with recommended spelling and it is concluded that the name should be properly considered masculine.

Since the Ehrenberg's original description of the type species, approximatelly 400 species has been described as members of the genus (Hasle and Syvertsen, 1997). According to VanLandigham catalogue (1968) the number of species is 177, including one fossil species, 4 species described only from spores, 5 freshwater species and 36 forms and varieties. Nevertheless, the number of valid species in reality is hard to estimate due to the numerous inadequate type descriptions and illustrations and to the large number of synonyms existing in the literature of which probably just one-third to one-half represent different taxa (VanLandingham, 1968, Rines and Hargraves, 1988).

The traditional classification within the genus *Chaetoceros* is quite controversial because it was apparently based on presumed overall similarity in morphological characters and it shows many inconsistencies in infrageneric structuring (Rines and Hargraves, 1988). It was suggested that the genus is paraphyletic as the established groups do not truly reflect the phylogenetic relationships between species (Rines and Theriot, 2003, Kooistra et al., 2010). The first classification system was developed by Gran (1897) who divided the genus *Chaetoceros* into two subgenera: *Phaeoceros* and *Hyalochaete.* The subgenus epithet *Phaeoceros* was replaced by Hendey (1964) with *Chaetoceros*, because the subgenus that includes the type species of the genus (*C. dichaeta*) has to keep the epithet of the genus, following the rules of the International Code of Botanical Nomenclature. Hernández-Becerril (1993) has proposed a third monotypic subgenus, *Bacteriastroidea,* to accommodate the species *C. bacteriastroides*. According to Hernández-Becerril (1996) the following key features are important for each subgenus:

1. *Chaetoceros* (*Phaeoceros*) – heavily silicified, robust forms; valves perforated with poroids, with thickenings or costae; at least one process on each valve, central or positioned to one side of the valve; tubular, circular, oval, or slit-like; one pair of setae per valve; setae thick and strong, containing chloroplasts, polygonal in cross-section, ornamented with spines, the setae sides areolated by rows of poroids or striae and costae pattern; resting spores known in only one species (*C. eibenii*).

2. *Hyalochaete* – less robust forms, many delicate and fragile, not thickly silicified; the valve face having an annulus from which a pattern of weak or strong costae radiates and rows of poroids run in between the costae; at least one process is present only on terminal valves, being central or eccentric, circular, slit-like or a flattened hollow with a true labiates structure inside; one pair of setae per valve; setae thin and fragile, lacking chloroplasts, generally circular in cross-section, in few cases polygonal,

with short spines running straight or in a spiral, the sides perforated by rows of poroids also running straight or in a spiral; resting spores present in the majority of the species.

3. *Bacteriastroidea* – fairly robust species; three pairs of setae per valve (two pairs reduced), lacking chloroplasts; slit-like central process present only on terminal valves; resting spores unknown.

Ostenfeld (1903) divided the two original subgenera into 16 sections based on the characters such as number of chloroplasts, form of valve, girdle and setae as well as the structure of the resting spore. With subsequent merging of some sections and recent addition of others by Hernandez-Becerril (1991a, 1996, 1998) the present classification divides the three subgenres into 22 sections, 6 in *Phaeoceros* and 16 in *Hyalochaete* (Table 1.1.). However, due to the inconsistency of species assignment to sections (Rines and Hargraves, 1988), doubtful morphological characters defining each section with little/no information on the fine structure included (Evensen and Hasle, 1975, Jensen and Moestrup, 1998) and lacking the support of the results of the phylogenetic molecular analyses (Kooistra et al., 2010) it is necessary to re-establish the new infrageneric clasification consistent with the natural similarities between species. Therefore, in this thesis, the use of sections is avoided and it is mentioned here purely for historical purposes.

Table 1.1. Subgenera and sections of genus *Chaetoceros*

Genus *Chaetoceros* Ehrenberg 1844
Subgenus *Chaetoceros* Hendey (1964) (*Phaeoceros* Gran (1897))
Section Atlantica Ostenfeld 1903
Section Borealia Ostenfeld 1903
Section Peruviana Hernández-Becerril 1996
Section Coarctata Hernández-Becerril 1991
Section Rostrata Hernández-Becerril 1998
Section Tetrastichona Hernández-Becerril 1998
Subgenus *Hyalochaete* Gran 1897
Section Dicladia (Ehrenberg) Gran 1905
Section Cylindrica Ostenfeld 1903
Section Compressa Ostenfeld 1903
Section Protuberantia Ostenfeld 1903
Section Constricta Gran 1897
Section Stenocincta Ostenfeld 1903
Section Laciniosa Ostenfeld 1903
Section Diadema Ostenfeld 1903
Section Diversa Ostenfeld 1903
Section Brevicatenata Gran 1908
Section Curviseta (Ostenfeld) Gran 1903
Section Anastomosantia Ostenfeld 1903
Section Furcillata Ostenfeld 1903
Section Socialia Ostenfeld 1903
Section Simplicia Ostenfeld 1903
Section Conspicua Hernández-Becerril 1993
Subgenus *Bacteriastroidea* Hernández-Becerril 1993

1.4.1.2 Morphology and species identification

Chaetoceros species are bipolar centric diatoms, usually colonial forming inseparable chains with only a few solitary representatives. The cells are cylindrically shaped containing one, two or more chloroplasts. When viewed from side (girdle view), they appear rectangular and from valve view most of them are elliptical but also circular. The cells can be precisely defined and described with three axes (Figure 1.4.): pervalvar axis (cell length), apical axis (cell width in wide girdle view), transapical axis (cell width in narrow girdle view); and three planes of symmetry: valvar plane, apical plane and transapical plane. Each frustule possesses four setae, two per each valve with some solitary species having reduced number of setae to just one per valve. The cells are joined in chains in various manners all of them including fusion/interlinking of the setae or different siliceous structures of the frustule such as fusion of valve edges and setae, holding of setae, presence of prehensors and fusion of linking spines. The terms used to describe the morphology of *Chaetoceros* cells are shown in the Figure 1.4. and the definition and the description of the terms is available in the Glossary in the Appendix I of this thesis.

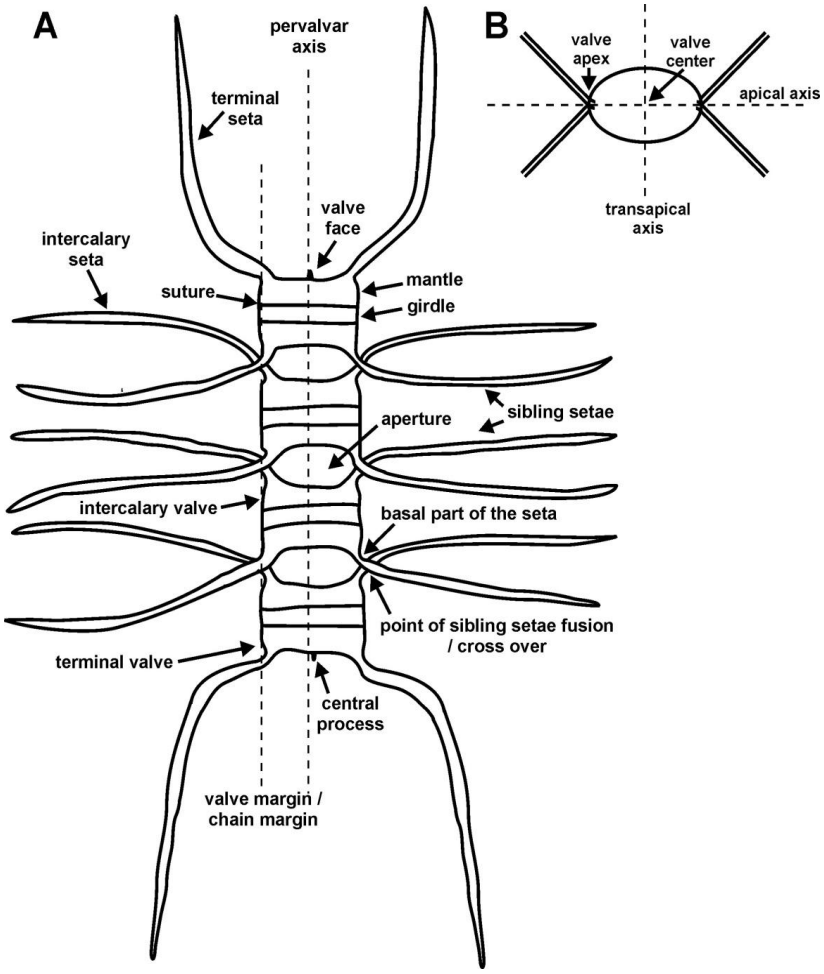

Figure 1.4. A) Chain of *Chaetoceros* in broad girdle view with indicated terminology used for the description. **B)** *Chaetoceros* cell in valve view. (adapted from Jensen and Moestrup, 1998).

The species identification in *Chaetoceros* genus is rather difficult as it can be expected from the genus so large and ubiquitus, and it is additionally complicated by a wide range of morphological variability within species (e.g. *C. affinis*) and frequent presence of intermediate forms such as in *C. decipiens/C. lorenzianus* complex (Jensen and Moestrup, 1998).

The identification on the species level is essentially based on the determination of morphological characters visible by light microscopy (Cupp, 1943, Hasle and Syvertsen, 1997) such as morphology of the colonies, shape of cells, chloroplasts (number and size, presence/absence in setae), thickness

and direction of the setae, point of setae crossing, shape and size of the aperture, resting spore morphology and position within the cell. However, some of the ultrastructural characters observable only by electron microscopy such as the setae pattern, the structure of the valves, location, number and shape of rimoportulae are also considered significant and important in morphological studies (Evensen and Hasle 1975).

The morphology of *Chaetoceros* species is extremely variable therefore one need to be careful when referring to species descriptions. The ratio of the apical to pervalvar axis of both vegetative cells and resting spores changes with the aging of the population, with each subsequent generation the cells becoming narrower and longer. Therefore, the overall appearance of the colony can be very different depending on the growth phase. The ratio of valve mantle height to girdle height is variable, depending on the mitotic stage, and recently formed setae may have a different appearance from the older ones being shorter and differently curved. In addition to colonies, many species have single celled forms and this present further identification problems because none of the colony features can be used for the species identification. These have often been given a separate varietal form status, but they may simply represent a stage in the life cycle of the population (eg. post-auxospore initial cell of the colony (Rines and Hargraves, 1988).

1.4.1.3 Life cycle

The observations on the life cycle of *Chaetoceros* species have been well documented in several species e.g. *C. dichaeta* (Assmy et al., 2008), *C. eibenii* Grunow in Van Heurck and *C. dydimus* Ehrenberg (von Stosch et al., 1973). The size reduction due to the subsequent vegetative divisions in *Chaetoceros* results in the cell apical axis reducing more than the pervalvar axis therefore the cells become relatively more elongated in the girdle view with age. The maximum cell size is restored by sexual reproduction which is oogamy, which means that a non-motile oogonium (female gametangium) is fertilized by a small uni-flagellate motile sperm cell. All investigated species are found to be monoecious (homothallic), that means that the sexual reproduction can occur within a single strain, though for *C. dydimus* it was observed that most of the sexualized colonies are either completely male or contain vegetative and female cells (von Stosch et al., 1973). The zygote protrudes through a gap in girdle band forming a lateral auxospore and may remain attached to the mother cell for some period. The zygote is surrounded by a proximal primary wall, which is organic and often covered by siliceous scales, and by a distal secondary wall (perizonium) that is constituted by a system of silica rings, in *C. dydimus* series of bands arranged in a fan shape (von Stosch et al., 1973) and in *C. dichaeta* concentric rings (Assmy et al., 2008). The initial cell is formed within the auxospore envelope, which is ruptured during these last events and thus liberates the new enlarged cell.

A large number of *Chaetoceros* species, mostly belonging to the subgenus *Hyalochaete* with only *C. eibenii* from subgenus *Chaetoceros*, are forming species-specific resting spores which are often present in the fossil record (Suto, 2006). The spores are formed endogenously, generally centrally

positioned or in some cases, laterally within the mother cell. Each spore has two valves, primary and a secondary valve. The surface of the resting spores may be smooth or ornamented with various spines or processes (Ishii et al., 2011). In C. *eibenii* the peculiar case occurs where the initial cell within the auxospore obligatory develops into the resting spore and this does not occur otherwise during the vegetative phase of the life cycle (von Stosch et al., 1973).

1.4.2 Genus *Bacteriastrum*

The exclusively marine multipolar centric diatom genus *Bacteriastrum* Shadbolt is ubiquitous in the tropical and temperate environments worldwide. Although frequently found in pelagic microalgal assemblages, it seems that *Bacteriastrum* species rarely achieve dominance. However, there are reports of high abundances of *B. furcatum* in the Gulf of Mexico (Fryxell, 1978) and regular development of *B. hyalinum* blooms during summer period in the Northern Sea (Kraberg et al., 2010, Hoppenrath et al., 2009).

1.4.2.1 Historical background and taxonomic relationships

The genus *Bacteriastrum* was established by Shadbolt (1854) to accommodate new three species: *Bacteriastrum furcatum, B. curvatum* and *B. nodulosum* described on the basis of the observations of single cells or single valves from natural material collected in Port Natal [current name Durban], South Africa, Indian Ocean. The name *Bacteriastrum* originates from Greek words: βακτηρια (bacteria), meaning stick and *astron* (*αστρον*), a star and it describes the regular arrangement of the numerous setae around the valve margin, clearly distinctive in the samples that he examined. The observations of *Bacteriastrum* whole chain colonies from the samples collected in Hong Kong were made by Lauder (Lauder, 1864) who described *B. hyalinum* and *B. varians* and suggested that Shadbolt's three species could be in fact intercalary and terminal cells of colonies of the same species. The century later, Boalch (1974, 1975) officially designated *B. furcatum* Shadbolt as the type species of the genus and the lectotype material for this species and for Lauder's two species as well. Several diatomists working with marine planktonic material have treated at least few species in their works (see Ikari, 1927) but it was Pavillard (1916, 1924, 1925) who provided the first and most comprehensive overview of the whole genus. In addition to the descriptions of four new species from the Mediterranean Sea: *B. mediterraneum, B. biconicum, B. elegans* and *B. comosum* he introduced both the plane of bifurcation of intercalary setae and the shape and orientation of the terminal setae as the characters of main taxonomic importance. Based on the latter feature he divided the genus into two sections: *Isomorpha* (isopolar) and *Sagittata* (heteropolar) respectively characterized by having the terminal setae morphologically similar or different from those of the posterior terminal valve (Pavillard, 1925). These diagnostic characters identified by Pavillard are still considered significant and followed in taxonomic literature (Cupp, 1943, Hasle and Syvertsen, 1997) therefore for the accurate species identification it is necessary to observe the complete chain colony. However, some of the previous observations often included broken colonies or cleaned material that has dissociated into individual

valves hence these records frequently led to many incomplete species descriptions and subsequent taxonomic confusions. The original vague descriptions of *Bacteriastrum* species resulted in many synonyms for the type species in the literature. Hustedt (1930) and Pavillard (1924, 1925) considered *B. furcatum* and *B. curvatum* as synonyms of *B. delicatulum*. VanLandigham (1968) considered *B. furcatum* as a synonym of both *B. varians* and *B. delicatulum* and Boalch (1975) placed both *B. nodulosum* and *B. curvatum* in synonymy with *B. furcatum*. However, if these names are all assumed to refer to one species, *B. furcatum* has the priority, even it is not possible to prove it from the original Shadbolt material (Boalch, 1974). Moreover, *B. delicatulum* Cleve and *B. varians* Lauder are currently considered as distinct valid species (Sarno et al., 1997) but the exact taxonomic differences between them and their relationship with *B. furcatum* still needs careful re-investigation.

The number of valid *Bacteriastrum* species is controversial due to the existence of multiple synonyms, varieties and insufficiently characterized species. For instance, Catalogue of Diatom Names (Fourtanier and Kociolek, 2011) enumerates total of 44 taxa described in the genus so far. According to VanLandigham (1968) there are 13 validly published species and 3 varieties, including *B. solitarium* Mangin which was later shown to be an initial cell of *B. hyalinum* by Drebes (1967). Furthermore, he did not consider *B. furcatum* and *B. minus* Karsten (Karsten, 1907, Reinecke, 1969) to be valid taxonomic entities as well. The genus currently encompasses 16 species due to the recent addition of two new members: *B. parallelum* Sarno, Zingone et Marino (Sarno et al., 1997) and *B. jadranum* Godrijan, Maric et Pfannkuchen (Godrijan et al., 2012, Bosak et al., 2012a). Although ultrastructural information on the basis of cultivated and natural material has been provided in these papers as well as in several other studies [*B. furcatum* (Fryxell, 1978, Sarno et al., 1997); *B. hyalinum* (Okuno, 1962, Round et al., 1990, Kooistra et al., 2010)], a comprehensive analysis of the fine morphological features and phenotypic plasticity of the *Bacteriastrum* taxa is still lacking.

The molecular analyses have been performed for *B. hyalinum* for which are available partial gene sequences for RNA polymerase alpha subunit (rpoA) (Sorhannus and Fox, 2012) and 16S rRNA (Rampen et al., 2009) of the chloroplast, 5.8 S rRNA and ITS2 (Moniz and Kaczmarska, 2010) and LSU rRNA (Kooistra et al., 2010) and for *B. jadranum* 18S rRNA partial sequence(Godrijan et al., 2012). The molecular phylogenetic analysis of the Chaetocerotaceae family by Kooistra et al. (2010) based on the LSU sequences included two available strains of *B. hyalinum*, suggests that *Bacteriastrum* species form a lineage within the genus *Chaetoceros* and that the traditional delineation between these two genera is not supported. Moreover, this conclusion is further corroborated with the results of the cladistic analysis performed on a series of defined morphological characters found within this diatom family (Rines and Theriot, 2003, Kooistra et al., 2010). From this point of view, the inclusion of additional species in the phylogenetic analyses would be considered as a step forward to the clarification of the taxonomical status of the *Bacteriastrum* genus.

1.4.2.2 Morphology and species identification

Bacteriastrum species are multipolar centric diatoms, usually colonial with only one solitary species. The cells are cylindrical with circular base containing many small chloroplasts. The cells can be precisely defined and described with two axes (Figure 1.5.): apical axis (cell width) and pervalvar axis (cell length) and two planes of symmetry: valvar plane and apical (pervalvar) plane. In the majority of the colonial species the cells are bound into chains by the fusion of the numerous setae that are regularly arranged around the valve margin. Setae of two cells are fused for a certain distance beyond the base and farther out branching again having bifurcated appearance. Terminal setae are not fused and differently curved than the intercalary ones.

Species identification of *Bacteriastrum* species has been mainly based on the characters visible by light microscope and not on ultrastructural details observable with electron microscopy (Sarno et al., 1996). The members of the genus share with the *Chaetoceros* species (subgenus *Hyalochaete*) the ultrastructural characteristics of the frustule with regard to the structure of the valves and setae as well as the presence of a central process on the terminal valve (Evensen and Hasle, 1975) and available EM observations of the fine structure indicate that there is no significant differences between the taxa (Sarno et al., 1996).

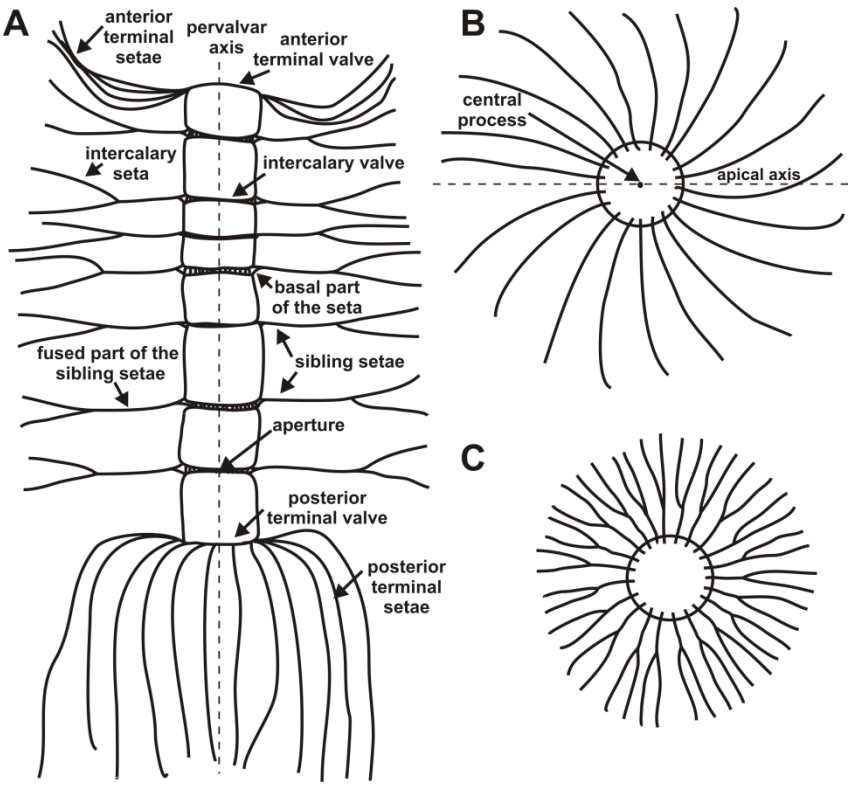

Figure 1.5. A) Chain of *Bacteriastrum* in girdle view with indicated terminology used for the description; B) *Bacteriastrum* terminal valve in valve view; C) *Bacteriastrum* intercalary valve in valve view

The morphological features such as the mode of cell linkage, the distance between cells, the plane of bifurcation of intercalary setae and the shape and orientation of the terminal setae are the most informative for the delineation of species. The terms used to describe the *Bacteriastrum* cell morphology are indicated in the Figure 1.5. and their definition is available in the Glossary in the Appendix I of this thesis.

1.4.2.3 Life cycle

The information on the life cycle features are fragmentary for majority of the *Bacteriastrum* taxa. The life history of a single species, *B. hyalinum* (Figure 1.4.) has been described by Drebes (1972) from cultivated material and includes the resting spore formation and oogamous sexual reproduction. The formation of the resting spore starts with the slight elongation of the cell and with the moving of centrally located nucleus to one valve. Mitosis follows accompanied by an onesided spontaneous plasmolysis. Firstly, the primary valve of the prospective resting spore is secreted on the exposed surface of the protoplast followed by the secretion of the secondary valve. Subsequently one of the two daughter nuclei degenerates. Both spore valves are developed acytokinetically (nuclear division without cytokinesis) and endogenously (inside the mother cell). *B. hyalinum*, typically for all centric diatoms, is a homothallic species which means that the gametes of opposite mating type (+) and (-) are produced in the same clonal culture.

The mode of sexual reproduction is oogamy and that means that in the female gametangium one non-motile large macro- gametes (egg cells) is formed and within the (-) male gametangium (spermatogonium) numerous small uni-flagellate motile gametes (sperm cells) are produced. The transition of the vegetative cells into sexual cells was observed in old cultures of high cell density when the cells decreased to a diameter below 33 µm. After fertilization the zygote leaves oogonial cell wall through a girdle aperture and inflates to an auxospore laterally positioned on the empty oogonium. The thin auxospore membrane detaches from the protoplast and becomes substituted by a second more robust and silicified membrane, perizonium, which is in the upper part composed of several concentric bands slightly roofing one another. Within the auxospore the formation of the initial cell takes place. Chemotaxis and recognition phenomena are presumably involved in the fertilization process but the basis of these remains uninvestigated (Round et al., 1990).

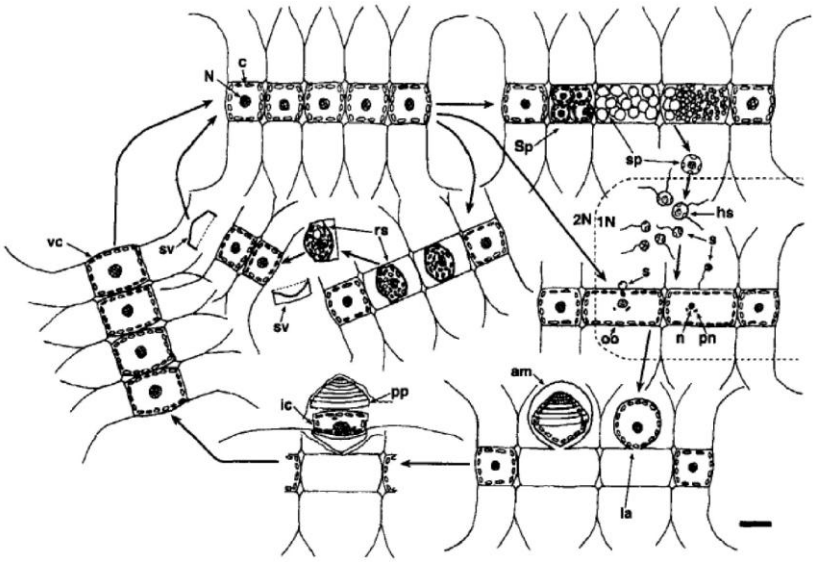

Figure 1.6. *Bacteriastrum hyalinum* life history – oogamy and resting spore formation. am-auxospore membrane; c-chloroplast; hs-hologenous spore formation; ic-initial cell; la-lateral auxospore; N-diploid nucleus; n-haploid nucleus; oo-oogonium; pn-pycnotic nucleus; pp-properizonium; rs-resting spore; s-sperm; sp-spermatogonium; Sp-spermatogonial filament; sv-spore valve; vc-vegetative cells; 2N-diploid portion of life cycle; 1N- haploid portion of life cycle (from Edlund and Stoermer, 1997).

1.5 The previous investigations of the family C*haetocerotaceae* in the Adriatic Sea

Morphology of the Adriatic species from the family Chaetocerotaceae has not been previously thoroughly investigated, and the information on their ecology is only available from the general studies on seasonal dynamics and spatial distribution of phytoplankton in particular areas. In the eastern part of the Adriatic Sea 56 members of the family has been recorded from which 49 species from the genus *Chaetoceros* and 7 species from the genus *Bacteriastrum* (Viličić et al., 2002). Checklist in the western coast of the Adriatic Sea includes total of 90 taxa from the family of which 78 from genus *Chaetoceros* and 12 of genus *Bacteriastrum* with subspecies, forms, variations and synonyms included (Cabrini et al., 2010). Ecological investigations of phytoplankton in the northern part of the Adriatic Sea recorded 4 species from the genus *Bacteriastrum* and 32 from the genus *Chaetoceros* of which species *C. socialis*, *C. vixvisibilis*, *C. curvisetus*, *C. decipiens* and *C. affinis* are identified as dominant in microphytoplankton in the period from 2002 to 2007 (Viličić et al., 2009a). Revelante and Gilmartin (1976) in their investigation of the phytoplankton succession during 1972 and 1973 in the northern Adriatic recorded *C. curvisetus* as one of the dominant species during winter and *C. affinis* and *B. delicatulum* in late winter period. During spring *C. compressus* was recognized as a dominant species, and in summer of the first investigated year *C. diversus* dominated while during the following year *C. curvisetus*. Another report on the phytoplankton species succession in the western coast of the northern Adriatic in the period 1990-1999 (Bernardi Aubry et al., 2004) identifies as dominant species in spring *C. socialis* and *C. curvisetus* in the end of autumn. In coastal area of central Adriatic , study in Krka estuary (Cetinić et al., 2006) identifies *C. socialis* as dominant species in spring period and in summer *C. compressus*, *C. danicus*, *C. affinis*, *C. decipiens* and solitary species *C. simplex*. In Zrmanja estuary *B. delicatulum*, *C. curvisetus* and *C. decipiens* are dominant in winter, *C. vixvisibilis* in spring and *C. subtilis* in autumn (Burić et al., 2007). In open waters of the middle Adriatic, study by Totti et al. (2000) lists 4 *Bacteriastrum* species and 10 *Chaetoceros* species which are considered to be among dominant diatoms in the the deep chlorophyll maximum. In phytoplankton from the southern Adriatic the species *B. delicatulum*, *C. convolutus*, *C. curvisetus*, *C. danicus*, *C. decipiens*, *C. lauderi* are recorded as dominant and *C. vixvisibilis*, *C. compressus* and *C. affinis* as a significant component of the spring bloom (Viličić et al. 1995). In the study from Ston Bay, *C. affinis* was recorded in late March, *C. socialis* late April and *Chaetoceros* spp. characteristic for late May (Čalić et al., 2013). In majority of the previous studies in the Adriatic Sea many *Chaetoceros* and *Bacteriastrum* cells were considered as a supraspecific group which was frequently dominant in the microphytoplankton, however we do not know their exact species composition as they are not identified on the species level.

1.6 Aims of the study

The main objective of this thesis was to obtain a better understanding of the taxonomy, spatial distribution and ecology of planktonic diatoms from the genera *Bacteriastrum* and *Chaetoceros* in the Adriatic Sea. Species belonging to these genera are ecologically important as they represent a constitutive component of the phytoplankton in the area, often developing dense populations. However, the previous investigations specifically focused on these taxa are extremely scarce.

The specific aims of the thesis are:

(1) To provide detailed taxonomic descriptions of the general morphology and ultrastructure of the species from the family Chaetocerotaceae accompanied with the adequate photographical illustrations.

(2) To determine the useful taxonomic characters for the identification of the Adriatic morphotypes for the first time using strains isolated in the laboratory cultures.

(3) To evaluate the importance of the delineating characters and to complement a set of proposals for the terminology used in the *Chaetoceros* and *Bacteriastrum* descriptions.

(4) Contribute to the better understanding of taxonomic relationships within the family by including molecular and phylogenetic analyses of particular species, with the emphasis on the members of the *Bacteriastrum* genus.

(5) With developed precise identification tools to establish accurate and precise *Chaetoceros* and *Bacteriastrum* taxonomic list and to determine the species spatial distribution along the eastern coast of the Adriatic Sea.

(6) To describe and interpret seasonal dynamics and species succession on the fine temporal scale.

The long term objective of this thesis is to facilitate correct species identification of the marine planktonic diatoms on the local as well as global level which will provide the basis for future studies on biogeographical diatom distribution. Also, better understanding of phytoplankton ecology involves the improvement of taxonomic resolution but it is often too much time/effort consuming for usual monitoring activities so the data obtained within this research will also serve to improve the quality of ecological data in the future.

CHAPTER 2

MATERIAL AND METHODS

"Now, the invention of the scientific method and science is, I'm sure we'll all agree, the most powerful intellectual idea, the most powerful framework for thinking and investigating and understanding and challenging the world around us that there is..."

Douglas Adams (1951 – 2001)

2.1 Study area: the Adriatic Sea

The Adriatic Sea is the northernmost basin of the Mediterranean Sea, with length of 800 km, width of 200–250 km and the average depth of 252 m. It covers approximately the surface area of 138 600 km^2 and has a volume of 35 000 km^3. According to bathymetry and latitude it may be divided into three parts: (i) the shallow northern Adriatic basin with a maximum depth of 50 m, (ii) the central/middle Adriatic basin with depressions up to 280 m and (iii) the southern Adriatic basin characterized by a deep, the South Adriatic Pit, at its centre, reaching a depth of 1230 m. The bottom of the Pit rises to a 780-m deep sill in the 75-km wide Strait of Otranto, where the Adriatic is connected to the Ionian Sea and rest of the Mediterranean. The average temperature of the Adriatic Sea ranges between 22 and 24 °C in summer and from 12 to 14 °C in winter, while the salinity generally varies between 38 and 39 (Cushman-Roisin et al., 2001).

The general circulation of the Adriatic Sea is basin-wide cyclonic, with re-circulation cells embedded in basin-wide flows found in the lower northern, central and southern sub-basins (Poulain, 2001). This pattern is due to the prevailing conditions in thermohaline features (freshwater influx, wind forces) as well as in the geomorphology of the various parts of the basin. Unlike the Mediterranean, the Adriatic is generally a dilution basin, exporting relatively fresh water while receiving more saline and warmer water. The eastern Adriatic region is exposed to the northwesterly inflowing East Adriatic Current (EAC) which brings highly saline and low-nutrient waters from the Ionian and Levantine Seas along its pathway (Gačić et al., 2001). The low-nutrient karstic rivers discharging along the eastern coast do not contribute significantly to the nutrient budget of the eastern Adriatic Sea therefore the whole eastern Adriatic coastal area can be described as oligotrophic (Viličić et al., 2008). On the other hand, the northwestern Adriatic coast receives large amounts of high-nutrient freshwater from

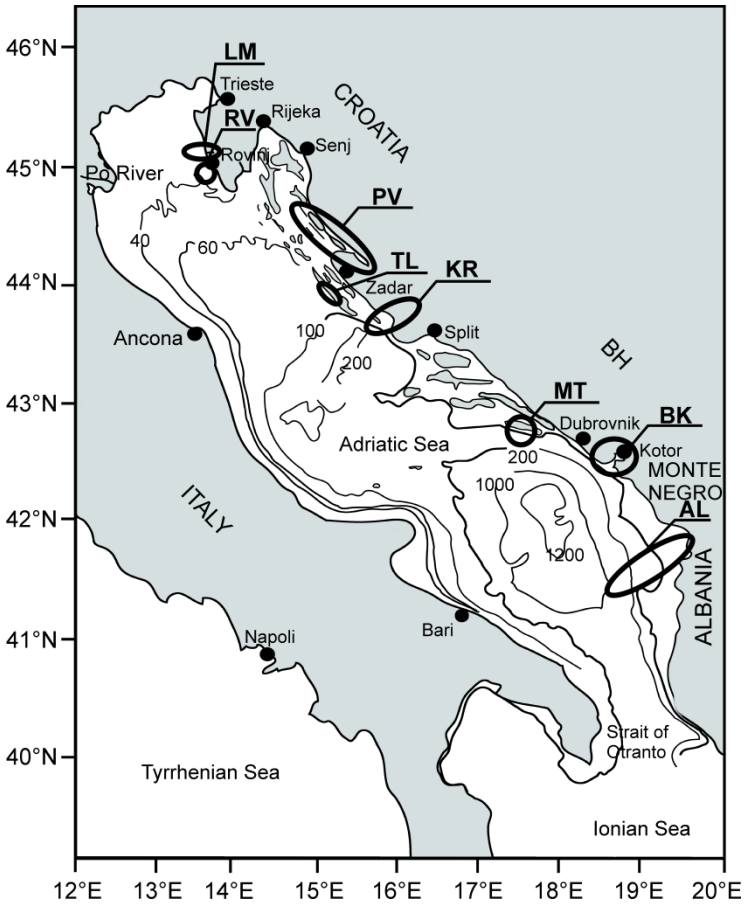

Figure 2.1. Map of the Adriatic Sea showing the investigated locations along the eastern coast. The approximate extent of sampling areas from which the samples were obtained is noted by the ellipses. LM- Lim Bay; RV- coastal area in front of the city of Rovinj; PV- Pag and Velebit Channel system including Novigrad Sea; TL- Telašćica Bay; KR- Krka River estuary; MT- island of Mljet; BK- Boka Kotorska Bay; AL- Albanian coastal zone.

the Po River, which flows out from the northern Adriatic to become the south-easterly outflowing Western Adriatic Current (WAC). These hydrographical features combine to make the Adriatic Sea quite heterogeneous marine system with the across-shelf and longitudinal trophic gradient resulting in the asymmetric distribution of the phytoplankton composition, abundance and biomass (Polimene et al., 2007).

The field material for this study was collected from eight main different locations along the eastern Adriatic coast between parallels 41° N and 46° N (Figure 2.1.) with additional sites where live net samples were taken for the isolation of some of the cultured strains – the so-called "samples of opportunity" (Table 2.3.). The employed approach has a goal to encompass the most of the diversity of the marine environments found in the eastern Adriatic coastal region ranging from human impacted, shallow and nutrient-enriched (e.g. river mouths, bays) to extremely oligotrophic and pristine areas (offshore location, outer side of the islands), including one freshwater shallow lake (Vransko lake).

2.1.1 Northern Adriatic: Rovinj, Lim Bay, Pag and Velebit Channel system

The northern Adriatic is a dynamic system where the stratification/mixing regime and the trophic state is mainly influenced by the Po River freshwater discharge, coupled with the meteorological forcing factors (north-eastern Bora wind) and the inflow of the salty, oligotrophic water brought by EAC (Socal et al., 2008). The circulation within the basin is rather complex, exhibiting small-scale spatial structures, high temporal variability and dynamics of largely thermohaline origin. The mean geostrophic circulation pattern is a cyclonic flow connecting the EAC and WAC in which spatially more elaborate and transient smaller-scale circulation patterns are embedded (Poulain, 2001). The north-eastern coastal area is mostly oligotrophic due to the EAC influence (Artegiani et al., 1997). A cyclonic gyre is one of the more permanent features of the basin, and during episodes of weaker EAC influence, the northern Adriatic becomes more isolated from the central part and the riverine freshwater influence on the eastern coast becomes more prominent. Episodes of strong Bora wind may provoke a double-gyre system (mostly in winter): a cyclonic gyre in the Gulf of Trieste, an anticyclonic gyre off western Istria as well as the formation of the Istrian Coastal Counter Current which transfers water enriched with nutrients from the Po River close to the Istrian coast (Supić et al., 2000). Moreover, during stable vertical stratification, characteristic for the summer period, a branch of the Po River plume can spread in the surface layer eastward reaching coastal north-eastern part of Adriatic Sea and bring nutrients as well decrease the salinity in the upper part and contributing to the stability of the water column (Viličić et al., 2013).

2.1.1.1 Lim Bay

Lim Bay is a narrow embayment, 11 km long and 0.5 km wide, located on the west side of the Istrian peninsula in the northeastern Adriatic Sea. Because of its geomorphologic value it is designated as a Special Marine Reserve. The maximum depth is about 33 m in the outer part while the inner part is about 17 m deep. It is a semi-enclosed embayment without any strong freshwater source; however,

many characteristic karstic effluents and a number of underwater freshwater springs, especially in the inner part, contribute to influence the higher productivity of the Bay (Bosak et al., 2009). The freshwater inflow becomes important during heavy rainfall period usually in January/February and October/November. Another important influence on the trophic state of the bay has the oligotrophic water inflow coming from the open sea according to tidal regime changes. Comparison of the physico-chemical and biological properties between Lim Bay and other similar locations in the middle Adriatic Sea have indicated moderate eutrophication with a rather high anthropogenic influence in Lim Bay (Bosak et al., 2009, Šilović et al., 2012b).

2.1.1.2 Pag and Velebit Channel system

Velebit Channel, the longest channel in the northern part of the eastern Adriatic, and adjacent Pag Channel form a 40 km long and 4-14 km wide system extending parallel to the coast between the island of Pag and the mainland. The system communicates with the open sea through the Kvarnerić strait, and in the southern end it is connected with Zrmanja River estuary through Novigrad Sea. Hydrographic characteristics of the area are defined by Zrmanja River inflow and numerous freshwater springs („vruljas“), which transport freshwater from mainland through karstic underground channels. The effect of river and „vruljas“ inflow is especially important during rainy season, from October to December and the period of snow melting from March to May. Bora wind is another phenomenon that highly influences hydrography of this area (Orlić et al., 2000). It reaches speed of 40 m/s, being the strongest wind in the eastern Adriatic coast. The influence of karstic Zrmanja River is the strongest in Novigrad Sea area and it reaches almost the middle part of the Velebit Channel. Despite of the freshwater influence, the area has very low nutrient levels and it is considered extremely oligotrophic (Šupraha et al., 2011).

2.1.2 Central Adriatic: Telašćica Bay and Krka estuary

2.1.2.1 Telašcica Bay

Telašćica Bay is situated in the southeastern part of the island of Dugi otok in the central part of the eastern Adriatic. It is retracted into the land about 8 km and on its south side is the widest part of about 1.6 km, That part of the bay which is turned towards the south-east, is open towards the neighbouring Kornati islands. The bay itself is very indented with 25 bays, capes and 5 islands having the total coast length of 68.78 km. Thanks to its position it is protected from the blows of the north-eastern Bora wind from the mainland and the south wind from the open sea. Owing to well-indented coastline and specific and diverse plant and animal life, this area is protected by the law and proclaimed as the Nature Park of the Republic of Croatia. This marine area is considered to be mainly oligotrophic, especially in the outer part. However, in the inner part of the Bay, the nutrient levels are increased probably due to the anthropogenic influence mainly from the touristic activities (Ljubešić, personal communication).

2.1.2.2. Krka estuary

The estuary of the karstic river Krka is a saltwedge, highly stratified estuary located in the central part of the eastern Adriatic coast. The estuary is 23.5 km long, starting below waterfalls (Skradinski buk) and ends at the mouth of the Šibenik channel. It is relatively narrow except for two wider parts: Prokljan lake and Šibenik harbour. Along the estuary water column is permanently stratified because of a sheltered geography and a low tidal range (20–50 cm). The density structure in the water column comes mainly through salinity difference, while the temperature difference may be neglected. The sharp halocline is characterised by a salinity gradient greater than 1%/cm (Legović et al., 1991). In the upper reach of the estuary, decomposing freshwater phytoplankton, which develops in Visovac Lake, situated above the waterfalls, is the main nutrient source (Cetinić et al., 2006). The Krka river is one of the most pristine European rivers, characterized by low concentrations of nutrients and extremely low input of terrigeneous material (Svensen et al., 2007). The town of Šibenik, located in the estuary's lower reach, is the only source of direct anthropogenic eutrophication (Cetinić et al., 2006).

2.1.3 Southern Adriatic: Mljet, Boka Kotorska Bay, Albanian coastal zone

2.1.3.1 The island of Mljet

The island of Mljet is an offshore south Adriatic island that extends in a northwestern-southeastern direction. The 8-10 km wide Mljet Canal separates it from the mainland. The island is directly exposed and influenced by to the inflowing low-nutrient waters of EAC and the area is considered to be generally oligotrophic (Benović et al., 2000)

2.1.3.2 Boka Kotorska Bay

The Boka Kotorska Bay is the largest bay of the Adriatic Sea, located on its south-eastern coast. It is often described as 'Europe's southernmost fjord' because of the steep and high slopes that surround it, but it is in fact a drowned river valley. The total surface area is 87.3 km^2 with a maximum depth of 60 m. The Bay area can be divided into four, smaller, interconnected bays (Herceg Novi Bay, Tivat Bay, Risan Bay and Kotor Bay). The freshwater influx from five small rivers, numerous streams and karstic submarine springs greatly affects the hydrological and chemical properties of the water column (Milanović, 2007). Previous studies have shown that the annual rainfall pattern has a significant influence on nutrient-loading seasonality in the area (Krivokapić et al., 2009), since the Bay is surrounded by the high (above 1800 m) steep limestone mountains of the Dinaric Alps, which have one of the highest levels of precipitation (4584 mm per year) in Europe. The small rivers entering Boka Kotorska Bay are not seriously impacted by humans, and the source of organic matter is primarily from in situ biological production (Campanelli et al., 2009). The human impact on eutrophication in the area is still generally considered less than that from natural sources, but anthropogenic influences from urbanization and tourism have become more evident in recent years.

2.1.3.3 The Albanian coastal zone

The Albanian coastal zone represents a narrow shelf smoothly sloping into the Southern Adriatic Pit. The circulation is greatly influenced by inflowing EAC which consists of two distinct water masses: the Ionian Surface Water (ISW) close to the surface and the Levantine Intermediate Water (LIW) at intermediate depths (Poulain and Cushman-Roisin, 2001). In the southern Adriatic, the EAC is also influenced by the strong freshwater inflow by seven Albanian rivers (Buna, Drini, Semani, Vijose, Erzen, Ishem, Mati), with an average discharge of 1.308 $m^3 s^{-1}$ or 4.1×10^4 $km^3 year^{-1}$ (Cullaj et al., 2005), which tend to push the EAC flow further offshore (Zavatarelli et al., 2002). However, the EAC flow is still oriented to the northwest, because the bathymetry mostly prevents cross-shore variations. In winter, when southeasterly winds prevail and Adriatic waters are denser than Ionian, the ISW extend well into the central part of the Adriatic basin, keeping the Adriatic Surface Waters (ASW) close to the western shores. The situation reverses in summer, when oceanographic and meteorological conditions favour lateral expansion of the ASW, pushing the ISW closer to the eastern shores. The intrusion of warm and saline LIW usually occurs in the intermediate layer, at depths between 100 and 600 m, with the core from 200 to 400 m (Socal et al., 1999). In spite of the apparent significant riverine influence, the whole area of the Albanian coastal zone is generally considered to be highly oligotrophic (Saracino and Rubino, 2006).

2.2 Field sampling design

The marine plankton field samples examined in this research and used for the spatial distribution study were collected as a part of eight scientific and monitoring projects conducted along the eastern coast of the Adriatic Sea in which the author of this thesis has actively participated at different seasons in the period from 2006 to 2012. The details of each particular study sampling design are presented in Table 2.1. This research encompasses altogether 31 stations distributed at eight different locations ranging from coastal to the offshore sites (see Chapter 2.1.). The geographical locations and stations average depth are listed in Table 2.2.

Table 2.1. The sampling design at the investigated locations

Study location	Location ID	Sampling period	sampling frequency	No net samples
Lim Bay	LM	March 2006 - November 2011	bimonthly	117
Rovinj	RV	September 2008 - October 2009	every two weeks	25
Pag and Velebit Channel	PV	July 2007 - October 2008	seasonally	24
Telašćica Bay	TL	July 2011 - August 2012	seasonally	24
Krka*	KR	April 2010 - February 2011	seasonally	16
Mljet	MT	August 2011 - November 2011	monthly	4
Boka Kotorska Bay	BK	April 2008 - March 2009	seasonally	12
Albanian coastal zone	AL	May 2009	once	6

* At station M (Martinska) additional sampling was performed two time daily once in 10 15 and second at 16 15 h during 6 days (from 19 to 24 July 2010). No net sample was obtained within this particular study.

The floristic composition of the diatom family Chaetocerotaceae was assessed primarily through net sampling as this approach gives a good overview of the less abundant chain-forming microphytoplankton taxa. It also provides sufficient amount of material for the examination of the samples with electron microscope. Moreover, when it was possible, especially in Telašćica Bay and Krka estuary, the species were brought into culture. The culturing procedure enables the growth of a single species in sufficient numbers facilitating the examination of morphological characters often difficult to observe in field samples, such as overall aspect of the chain colony or resting spores. Although the sampling strategy cannot be exhaustive enough to encompass and describe the true diversity of this family in eastern Adriatic as for example, the molecular identification of the majority of taxa is lacking; the collected data have nevertheless provided us with some new insights.

Table 2.2. Geographical characteristics of the sampling stations.

Location name	Location ID	Station ID	Latitude (N)	Longitude E	Depth (m)
Lim Bay	LM	LIM1	45°07'55"	13°37'10"	32
Lim Bay	LM	LIM2	45°07'51"	13°41'10"	27
Lim Bay	LM	LIM3	45°08'07"	13°43'00"	18
Rovinj	RV	RV001	45°04'48"	13°36'36"	29
Pag Channel	PV	P1	44°39'17"	14°52'34"	85
Pag Channel	PV	P2	44°42'03"	14°46'13"	80
Pag Channel	PV	P3	44°43'07"	14°42'17"	85
Velebit Channel	PV	V1	44°15'42"	15°28'00"	27
Velebit Channel	PV	V2	44°26'21"	15°09'39"	70
Velebit Channel	PV	V3	44°31'43"	15°02'50"	70
Velebit Channel	PV	V4	44°36'25"	14°56'47"	75
Novigrad Sea	PV	N1	44°11'48"	15°33'36"	24
Telašćica Bay	TL	T0	43°50'96"	15°12'37"	85
Telašćica Bay	TL	T1	43°52'01"	15°12'14"	55
Telašćica Bay	TL	T2	43°53'39"	15°11'24"	60
Telašćica Bay	TL	T3	43°53'97"	15°09'51"	34
Krka estuary	KR	C1	43°41'20"	15°49'43"	30
Krka estuary	KR	E5	43°43'15"	15°51'09"	27
Krka estuary	KR	M	43°44'09"	15°52'37"	9
Krka estuary	KR	E4a	43°44'12"	15°53'05"	38
Krka estuary	KR	E3	43°47'24"	15°51'51"	24
Mljet	MT	G	42°45'45"	17°23'14"	50
Boka Kotorska Bay	BK	BK1	42°2 6'12"	18°45'41"	18
Boka Kotorska Bay	BK	BK2	42°28'03"	18°44'52"	30
Boka Kotorska Bay	BK	BK3	42°29'04"	18°41'45"	30
Albanian coastal zone	AL	A50	41°42'07"	19°22'04"	50
Albanian coastal zone	AL	A150	41°34'02"	19°02'04"	100
Albanian coastal zone	AL	A200	41°32'03"	18°56'06"	200
Albanian coastal zone	AL	A300	41°30'04"	18°51'09"	300
Albanian coastal zone	AL	A900	41°25'07"	18°38'01"	900
Albanian coastal zone	AL	A1000	41°25'05"	18°33'03"	1000

2.3 Field methods

Qualitative phytoplankton sampling

In all surveys the plankton material for the diatom morphological analyses was collected by plankton net vertically hauled in the euphotic layer of the water column (mostly in the upper 20m, depending on the average water depth on the particular station). The net mesh size used in all surveys was 20 μm except of 53 μm and 5 μm mesh which was used in surveys conducted in Mljet and Albanian coastal zone, respectively. The number of net samples per each study site is provided in Table 2.1.. A total of 228 qualitative net samples was obtained and preserved with glutaraldehyde (1% final concentration) or hexamine-neutralized formaldehyde (1.4 % final concentration).

An environmental dataset (temperature, salinity, nutrient concentrations) was gathered in all aforementioned surveys (Chapter 2.2.) as well as the data on phytoplankton abundances and biomass (Chl *a* concentration, carbon content). The descriptions of the methods used and the presentation of these particular biological and environmental results are available either as part of published papers or at the request to the author of this Ph.D. thesis and listed in Table 2.3.. However, as the aim of this part of the thesis is to gather the information on the Chaetocerotaceae species morphology and their spatial distribution providing the updated taxonomic lists of the particular areas, the details on the data sampling and processing procedures will not be described here. The exception is the detailed description of the methods used in the samplings undertaken at stations RV001 and M which is provided below (Chapters 2.3.1. and 2.3.2) due to presentation of the available biological and environmental data in this thesis and their use in the ecological analyses of *Chaetoceros* and *Bacteriastrum* species in these areas.

Table 2.3. The published reports of studies conducted in each of investigated sites where detailed methods and selected results on environmental and biological parameters for the investigated period are available.

Study location	Location ID	Source
Lim Bay	LM	Bosak et al.(2009), Ljubešić et al.(2011), Šilović et al.(2012b)
Rovinj	RV	Šilović et al.(2012a)
Pag and Velebit Channel	PV	Viličić et al. (2007),Viličić et al. (2009b), Šupraha et al. (2011)
Telašćica Bay	TL	Polović (2013)
Krka*	KR	Šupraha (2012)
Mljet	MT	Lucić (pers. comm.)
Boka Kotorska Bay	BK	Krivokapić et al. (2011), Bosak et al.(2012b),
Albanian coastal zone	AL	Viličić et al. (2011), Šilović et al. (2011)

2.3.1 Northeastern Adriatic coastal zone (station RV001)

Seawater samples were collected by the Niskin sampler (5L) from five depths (0, 5, 10, 20, and 27 m) at coastal station RV001, one nautical mile from the shore of Rovinj, the city in northeastern Adriatic Sea. The sampling was performed every 2 weeks between 28. September 2008 and October 2009. Physical, chemical and chlorophyll a (Chl *a)* data were collected by the staff of Centre for the

Marine Research, Institute Ruđer Bošković, Rovinj, Croatia and kindly provided for all analysis of this Ph.D. thesis.

2.3.1.1 Physico-chemical parameters and chlorophyll a

Temperature and salinity profiles were obtained with a CTD SBE 25 Sealogger probe *in situ*, while samples for nutrient and Chl *a* concentration were collected in polycarbonate bottles and processed in the laboratory. Subsamples for the determination of dissolved nutrient concentrations such as nitrate- NO_3^-, nitrite – NO_2^-, ammonium-NH_4^+, ortophosphate-PO_4^- and silicate- SiO_4^+ were analyzed immediately after collection according to (Ivančić and Degobbis, 1984, Parsons et al., 1984).

Subsamples (0.5 L) for the total Chl *a* were filtered directly onto GF/F filters (0.7 µm). The subsamples (0.5 L) for the size-fractionated Chl *a* (0.5 L) were prefiltered (i) through 20 µm net directly to GF/F filters and (ii) through 3 µm polycarbonate Nucleopore filters to GF/F filters. A filtration vacuum of <2 cm Hg was used for all filtration steps. Filters were frozen (-20 °C) and analyzed with Turner TD-700 fluorimeter following the procedure after Parsons et al. (1984). The micro Chl *a* fraction was obtained by subtracting the values obtained by (i) from total Chl *a*. The nano Chl *a* fraction was obtained from the values obtained by (i). The pico Chl *a* fraction values were obtained by subtracting (ii) from values obtained by (i).

2.3.1.2 Phytoplankton abundances

A total number of 125 samples (200 mL) for the phytoplankton cell counts were preserved with pseudo- Lugol's solution (0.4% final concentration) according to Verity et al. (2007). The pseudo-Lugol's solution was prepared from mixing equal volumes of solutions (A) and (B) where (A) 30 g KI and 19.5 g I_2 in 500 mL of deionized water and (B) 135 mL of deionized water, 315 mL of absolute alcohol, 35 mL of 25% glutaraldehyde and 15 mL of glacial acetic acid.

Cells were identified and counted using a Zeiss Axiovert 200 (Carl Zeiss, Oberkochen, Germany) inverted microscope operating with phase contrast and brightfield optics. The variable volume (10 or 50 mL) of sub-samples depending on the cell density was sedimented in Utermöhl combined plate counting chambers (HydroBios, Kiel, Germany) and analysed after > 24 h (Utermöhl, 1958, Lund et al., 1958). For cells smaller than 20 µm (nanophytoplankton) which were relatively abundant, the half of transect (i.e. 1/2 diameter of counting chamber) along the counting chamber bottom was examined at 400x magnification. Individual cells with either maximum linear dimension (MLD) or equivalent spherical diameter (ESD) larger than 20 µm (microphytoplankton) and colony-forming diatom species in which chain length exceeds 20 µm were counted along two transects at 200x magnification. Very abundant species were counted on a variable number (5-20) of random chosen fields at either 200x or at 400x magnification depending on their size. In addition, the bottom half of the chamber was also examined at a magnification of 100x, to obtain a more correct evaluation of less abundant microphytoplankton taxa. The minimum concentration of microphytoplankton cells that can be detected by this method is 20 cells L^{-1}. Phytoplankton cells were divided in the principal groups of

diatoms, dinoflagellates, coccolithophores and flagellates. The identification was made at species level as far as possible in light microscopy at 1000x magnification or by detailed examination with electron microscopy (procedure described in Chapter 2.4.). Microalgae that could not be identified to specific or generic level were assigned to suprageneric groups by size (e.g. cryptophytes 5-20 µm, coccolithophores >10 µm, etc). Identifications were performed referring to general references of phytoplankton taxonomy (Cupp, 1943, Tomas, 1997, Bérard-Therriault et al., 1999, Hoppenrath et al., 2009, Kraberg et al., 2010). The special literature dealing with the Chaetocerotaceae taxa which was used for their identification is listed in Chapter 2.5.. Species descriptions were often checked in peer-reviewed publications and relevant websites (e.g. www.algaebase.org) were consulted for up to date systematic classification.

2.3.1.3 Phytoplankton biomasses

The cells of all taxa recorded while counting on the inverted microscope (Zeiss AxioVert 200) were photographed using a Zeiss MRc digital camera and their linear measurements obtained after processing and image analysis using digital system AxioVision 4.8.2. Cell sizes were determined on measuring more than ten specimens for rare species and on more than 50 specimens for abundant species with calculating averaged values of cell dimensions. The cells were attributed to nano- (2-20 µm) and microphytoplankton (>20 µm) size classes (Sieburth et al., 1978) according either to their maximum cellular linear dimension (MLD) or the equivalent spherical diameter (ESD) (Appendix III of this thesis). In the case of the colony forming diatom taxa (e.g. *Skeletonema marinoi, Chaetoceros diversus*), the chain length was considered instead of the single cell dimensions which was smaller than 20 µm and species was attributed to the larger size class. Phytoplankton cell biovolumes were calculated by approximating cell shapes (in some cases different parts of the cells e.g. setae) of each species assigning them to geometric bodies and applying standard formulae (Hillebrand et al., 1999). Cell volumes were calculated for 180 photosynthetic and 14 heterotrophic taxa and supra-specific groups out of a total of 204 taxa identified in this study (Appendix III). A distinction between photosynthetic and non-photosynthetic species was made using the information available in the literature (Hoppenrath et al., 2009). Small, unidentified nanoplankton flagellates and dinoflagellates were always included, despite the probable presence of heterotrophic species. The phytoplankton carbon content was calculated from mean cell biovolumes using the conversion formulae introduced by Menden Deuer and Lessard (2000).

2.3.1.4 Graphical and statistical data analyses

All data were processed and graphical presentations created using the software packages Microsoft Office Excel 2007 and 2010, Golden Software Grapher 8.0. and Ocean Data View 4.5.6 (Schlitzer, 2011). Basic descriptive statistics and Pearson correlation coefficients between selected parameters were calculated using statistical software Statistica 10 (StatSoft). For statistical multivariate analyses (PCA-Principal Component Analysis; MDS – Multidimensional Scaling, Cluster

Analysis, BIO-ENV procedure, CAP -Canonical Analysis of Principal coordinates) and the graphical presentations of selected analyses statistical software PRIMER 6 v.6.1.11. & PERMANOVA+ v.1.0.1. (Clarke and Gorley, 2006) was used. For all multivariate statistical procedures, the data from samples collected at different depths were integrated and averaged for each sampling date, and transformed using log (x+1) overall transformation. The analyses on physio chemical parameters were performed on resemblance matrices created using Euclidean distances and the anaylses on species abundances on matrices created using Bray-Curtis similarities (Clarke and R.M., 2001).

2.3.2 Krka River estuary (station Martinska –M)

Seawater samples were directly collected in bottles with a total volume of 1 L, by scuba diving from six depths (0.5m, 1.3 m, 1.9 m, 2.6 m, 3.5 m, 8m) at the coastal station M near the the scientific marine station "Martinska" of Ruđer Bošković Institute, located in front of Šibenik town (Table 2.2.). The sampling was performed from 19 to 24 July 2010 at two times daily at 10 15 and 16 15 hours.

Physico-chemical data and samples for the analysis of phytoplankton pigments and abundances were collected by the staff of the laboratory for Physical Chemistry of Traces, Division for Marine and Environmental Research, Institute Ruđer Bošković, Zagreb, Croatia and kindly provided for all analysis of this Ph.D. thesis.

2.3.2.1 Physico-chemical parameters

The temperature was measured *in situ* by scuba diving using HOBO data loggers and the salinity was measured *ex situ* in each obtained subsample by Hach Lange – multiprobe HQ40D. Unfortunatelly, no nutrient data is available from this study.

2.3.2.2 Phytoplankton abundances

The 200 mL of samples were collected and preserved with formalin (1.4 % final concentration). The counting procedure was as described in paragraph 2.3.1.a.

2.3.2.3 Phytoplankton biomasses

The procedure was as decribed in paragraph 2.3.2.c. Cell volumes were calculated for 137 photosynthetic taxa and groups out of a total of 148 taxa identified in this study. In Appendix IV are listed measurements of taxa additionaly identified in this part of study, or with different values than in Appendix III

2.3.2.4 Phytoplankton biomarker pigments

The phytoplankton pigments (chlorophyll *a*, fucoxanthin) were measured by High Performance Liquid Cromatography (HPLC). The sample (0.5 L) was filtered onto GF/F Whatman glass-fibre filters (0.7 μm), which were immediately frozen in liquid nitrogen and stored at -80 °C until analysis. The extraction was done in 4 mL of cold 90% acetone using sonication, and then centrifuged to clarify the extract. Pigments were separated by reversed phase HPLC (Barlow et al., 1997). Extracts were mixed (1:1 v/v) with 1 M ammonium acetate and injected into an HPLC system incorporating a 3 mm

Thermo Hypersil column MOS2, C-8, 120 A pore size, 150 x 4.6 mm (Thermo Hypersil-Keystone). Pigments were separated at a flow rate of 1 mL min^{-1} using a linear gradient program in duration of 40 mins. Solvent A consisted of 70:30 (v/v) methanol: 1 M ammonium acetate and solvent B was 100% methanol. Chlorophyll and carotenoids were detected by absorbance at 440 nm (Spectra System, Model UV 2000). Qualitative and quantitative analyses of individual pigments were performed by external standard calibration using authentic pigment standards (VKI, Denmark).

2.3.2.5 Graphical and statistical data analyses

For data processing and graphical analyses the software packages Microsoft Office Excel 2007 and 2010, Golden Software Grapher 8.0. Basic descriptive statistics and Pearson correlation coefficients between selected parameters were calculated using statistical software Statistica 10 (StatSoft).

2.4 Laboratory methods

2.4.1 Isolation of strains and culture conditions

A total of 48 laboratory cultures were obtained during the course of this study of which four strains belonged to genus *Bacteriastrum* and 44 strains to genus *Chaetoceros*. The information on strain designation, species identity and origin including the dates of their isolation are provided in the Table 2.4.. Strains were identified using taxonomic literature reported in the Chapter 2.5.

The culturing media used were based on f/2 marine enrichment medium (Guillard, 1975). The media were prepared either using the Guillard's (F/2) Marine Enrichment Basal Salt Mixture or Guillard's (F/2) Marine Water Enrichment Solution, both enriched with silicate but the first mixture lacking vitamins. The oligotrophic seawater of salinity 38 used for the media preparation was collected at the stations C1 and T0 (location in Table 2.2.), sterilized using filtration on 0.2 μm Nucleopore filters and the media were prepared according to the manufacturer (Sigma - Aldrich Co.) instructions.

Clonal cultures were established by isolation of individual chains or single cells picked either from live plankton samples or from enrichment cultures. The live samples were collected by 20 μm mesh net on stations C1 and T0 and on various localities ("samples of opportunity) along the eastern coast of the Adriatic Sea from November 2010 to January 2013 (Table 2.4.). Enrichment cultures were established by incubating the small amount (5-10 mL) of net sample in f/2 medium for 2 - 7 days in the culture conditions described below. The chains/cells were isolated using Pasteur micropipettes and an inverted Zeiss Axiovert 200 or Olympus CKX41 (Olympus, Tokyo, Japan) light microscope both equipped with bright-field optics and phase contrast. The cells were first placed in sterile plastic 90-mm Petri dish filled with ca. 10 ml f/2 medium and observed each day during the first week for growth and conditions of the cells. When the cell density was high enough the established cultures were transferred to 70 ml BD Falcon polystyrene cell culture flasks (model 353082; BD Biosciences, Le Pont De Claix, France) filled with 30 – 40 ml of f/2 medium. For isolation of strain BA1 slightly

modified procedure was used: the isolated chains were first placed in a 4-well Nunclon Multidish plate (Nunc A/S, Roskilde Denmark) filled with 1mL f/2 culture medium diluted for 50% with filter-sterilized seawater and subsequently transferred to 50-ml glass Erlenmeyer conical flasks with 30 ml f/2 culture medium.

The strains were maintained in growth culture chamber under cool white (40 W) fluorescent light (30 µmol photons m^{-2} s^{-1}) at a room temperature of 20°C in a 16 h: 8 h light/dark cycle and sub-cultured every 1-2 weeks depending on the cell growth. The cultures were examined frequently under the light microscope during 3-6 weeks. The material for morphological studies was obtained in the exponential growth phase of each strain within maximum of 2 months from its establishment due to the cell deformations resulting from miniaturization often observed in the older cultures. Selected strains were incubated at low light intensity (5 µmol photons m^{-2} s^{-1}) under nutrient limited conditions (in filter-sterilized seawater) to induce resting stage formation. However, this was not achieved but instead the resting spores formed spontaneously in the older (>5-6 weeks) cultures. The glutaraldehyde preserved culture material (1-2% final concentration) and permanent slides from selected strains are available on request to the author of this Ph.D. thesis.

2.4.2 Morphological analyses

The cultured strains and plankton net field samples were examined in detail in light microscopy (LM), scanning electron microscopy (SEM) and transmission electron microscopy (TEM). The LM observations were made on the live material when it was possible, but also on the fixed samples and permanent slides. This resulted in large collection of high quality images of the general morphology and ultrastructural details of Chaetocerotacean taxa and it provided the necessary basis for the morphometric measurements and morphological descriptions. Images were processed with Adobe Photoshop software only to adjust the optimal brigtness/contrast and color. The figures were assembled in plates using CorelDraw x3 software.

The unique features of the colony formation in species *Bacteriastrum jadranum* were additionally investigated with atomic force microscopy (AFM).

All available material was subjected to cleaning treatment in order to remove the organic matter from diatom frustules. The strains of strongly silicified species and all field samples were first desalinized by rinsing with distilled water, treated with strong acids (1:1:4; sample:H_2SO_4:HNO_3), boiled for a few seconds and then washed again with distilled water. The gentler Simonsen's cleaning method (Simonsen, 1974, Hasle, 1978) was used for the cultured strains having lightly silicified frustules (e.g. PMFBA1, PMFW2). The samples were first rinsed with distilled water, then the equal amount of saturated $KMnO_4$ (or diluted 50%) for oxidation of organic matter was added and left for 24 hours. The next day an equal amount of conc. HCl was added, gently heated over a flame and then rinsed again with distilled water.

Permanent slides were prepared by drying cleaned and non-cleaned (only rinsed with water) material on coverslips and mounting in Naphrax following (Hasle, 1978).

2.4.2.1 Light microscopy

For LM observations, we used an inverted Zeiss Axiovert 200, a Zeiss Axiophot (Carl Zeiss, Oberkochen, Germany), and a Olympus BX1 (Olympus, Tokyo, Japan) microscope, all of them equipped with a bright-field (BF) optics, phase contrast (PC) and Nomarski differential interference contrast (DIC). The Axiophot microscope was also equipped with an ultraviolet mercury lamp for epifluorescence illumination. Light micrographs were taken using a Zeiss AxioCam MRc and Artray digital cameras and processed with an AxioVision 4.8.2. digital image processing software or DP70 Digital Camera System operating with DP Controller and DP Manager software, respectively.

For observations of *Bacteriastrum jadranum* cell jacket, two stains were applied to examine their reactions with the extracellular polymeric substances embedding the cell colonies. Alcian Blue is a cationic dye that stains acid mucopolysaccharides and glycosaminoglycans, and it is commonly used in staining transparent exopolymeric substances in the marine environment (Ramus, 1977). Amino acid specific dye Coomasie Brilliant Blue -250 was used for detection of proteins (Long and Azam, 1996, Alldredge et al., 1993). Alcian Blue was also used in experiments with the cultured material of *Chaetoceros anastomosans* for the detection of EPS surrounding the chains. A drop of dye was added directly to the small amount of sample either from glutaraldehyde fixed net sample and laboratory cultures on the glass slides and microscopically observed.

2.4.2.2 Electron microscopy

For SEM observations, the cleaned material was filtered and air dried on 3-µm Nucleopore polycarbonate filters (Nucleopore, Pleasanton, CA). For observation of whole cells and chains, particular field samples (e.g. from Albania survey) were rinsed with water, concentrated and air- dried on the filters. For examination of *B. jadranum* organic cell jacket network, the glutaraldehyde fixed net samples from August 2009, station RV001, were directly filtered on two separate polycarbonate filters and rinsed with distilled water. One sample was air-dried and the other sample was dehydrated in a series of ethanol solutions (25, 35, 50, 75, 80, 90%) prepared with distilled water and absolute ethanol, finishing with three rinses of 100% ethanol. For the drying method, the hexamethyldisilazane (HMDS) treatment was used (Bray et al., 1993). The sample was rinsed in a series of 100% ethanol: HMDS solutions (3:1, 1:1, 1:3), finishing with three changes of 100% HMDS. The sample was treated for a minimum of 5 min at each step, allowing the last HMDS rinse to evaporate slowly at room temperature.

All prepared Nucleopore filters were mounted on stubs, sputter coated with gold or platinum and examined using SEM JEOL JSM-6500F (JEOL-USA Inc., Peabody, MA, USA) or Mira II FE LMU (Tescan, Brno, Chech republic).

TEM observations were made by deposition of cleaned and rinsed material on Formvar/carbon coated 200 mesh nickel grids and examined using a LEO 912AB TEM (LEO, Oberkochen, Germany).

2.4.2.3 Atomic force microscopy

To resolve the fine structure of the *Bacteriastrum jadranum* cell jacket, we introduced the use of atomic force microscopy (AFM), which uses a sharp probe to image the topography of surfaces at a lateral resolution greater than 1 nm and a vertical resolution of 0.01 nm under ambient conditions (Higgins and Wetherbee, 2011). The AFM experiments were performed using drop deposition method modified for marine samples (Pletikapić et al., 2011a, Mišić Radić et al., 2011). A 5-µL volume of the PMFBA1 cell culture was pipetted directly onto freshly cleaved mica. Mica slides were placed in enclosed Petri dish for approximately 30–45 min. Samples were then rinsed three times for 30 s in ultrapure water and placed in enclosed Petri dish to evaporate excess water from the mica. All measurements were performed in air at room temperature and 50–60% relative humidity, which leaves the samples with a small hydration layer, helping to maintain the original structures.

AFM imaging was performed using a Multimode AFM with a Nanoscope IIIa controller (Bruker, Billerica USA) with a vertical engagement (JV) 125-µm scanner. Contact mode was used throughout the study. Imaging was performed using standard silicon-nitride tips (NP-20, Bruker, nom. freq. 56 KHz, nom. spring constant of 0.32 N/m) and extra sharpened silicon nitride tips (MSNL, Bruker, tip radius nom. 2 nm, nom. freq. 4–10 KHz, nom. spring constant of 0.01 N/m) for high-resolution imaging. The force was kept at the lowest possible value to minimise the forces of interaction between the tip and the surface. Continuous scans were performed over the same region (10 times, slow scan: 1 Hz, 512 samples), and the structures were not altered. The linear scanning rate was optimised between 1.5 and 2 Hz with scan resolution of 512 samples per line. Processing and analysis of images was carried out using NanoScope^{TM} software (Digital Instruments, version V614r1). All images presented are raw data except for the first order two-dimensional flattening. Analysis of pore size was performed by automatic pore detection and pore surface measurements using Image J software.

AFM experiments were performed at two quite different scales: 50–100 µm with a vertical scale of 100–1000 nm to identify cell colony and 1–10 µm with a vertical scale of only 5–20 nm to resolve the ultrastructure of overlaid polysaccharide network. All images were acquired in contact mode under ambient conditions using mica as the substrate.

Table 2.4. The information on the 48 Chaetocerotacean cultured strains examined in this study. NA-Northern Adriatic, CA – Central Adriatic, SA, Southern Adriatic.

Species	strain	isolation site	isolation date
Bacteriastrum furcatum	PMFBA4	43° 10' N, 16° 34' E, Stari Grad Bay, SA	10.05.2011.
B. hyalinum	PMFBA2	44° 28' N, 14° 54' E, Maun Channel, NA	28.02.2011.
B. mediterraneum	PMFBA3	44° 06' N, 15° 13' E, Zadar Channel, NA	28.04.2011.
B. jadranum	PMFBA1	44° 28' N, 14° 54' E, Maun Channel, NA	17.11.2010.
Chaetoceros affinis	PMFC1	44° 28' N, 14° 54' E, Maun Channel, NA	17.11.2010.
C. affinis	PMFC2	43° 41' N, 15° 49' E, Zlarin, st. C1, CA	22.02.2011.
C. affinis	PMFC5	43° 10' N, 16° 34' E, Stari Grad Bay, SA	10.05.2011.
C. affinis	PMFE1	43° 30' N, 16° 23' E, Split, SA	28.01.2011.
C. amanita	PMFM1	43° 51' N, 15° 37' E, Vransko jezero, CA	26.04.2011.
C. anastomosans	PMFAN1	44° 28' N, 14° 54' E, Maun Channel, NA	17.11.2010.
C. anastomosans	PMFAN2	45° 00' N, 14° 37' E, Punat Bay, NA	04.12.2011.
C. brevis	PMFBR1	43° 51' N, 15° 12' E, Telašćica, st. T0, CA	22.03.2012.
C. brevis	PMFBR2	44° 28' N, 14° 54' E, Maun Channel, NA	09.04.2012.
C. circinalis	PMFG4	42° 39' N, 18° 04' E, Dubrovnik, SA	02.05.2011.
C. contortus	PMFCO1	43° 51' N, 15° 12' E, Telašćica, st. T0, CA	01.03.2012.
C. contortus	PMFCO2	44° 28' N, 14° 54' E, Maun Channel, NA	21.03.2012.
C. costatus	PMFB2	43° 41' N, 15° 49' E, Zlarin, st. C1, CA	04.02.2011.
C. costatus	PMFB6	43° 41' N, 15° 49' E, Zlarin, st. C1, CA	18.11.2010.
C. costatus	PMFB7	43° 31' N, 16° 27' E, Vranjic Bay, CA	08.10.2012.
C. costatus	PMFB8	43° 31' N, 16° 27' E, Čiovo, SA	09.01.2013.
C. curvisetus	PMFD2	43° 41' N, 15° 49' E, Zlarin, st. C1, CA	04.02.2011.
C. curvisetus	PMFD6	43° 41' N, 15° 49' E, Zlarin, st. C1, CA	18.11.2010.
C. curvisetus	PMFD7	43° 51' N, 15° 12' E, Telašćica, st. T0, CA	12.10.2011.
C. curvisetus	PMFD8	43° 51' N, 15° 12' E, Telašćica, st. T0, CA	01.03.2012.
C. danicus	PMFDA1	44° 28' N, 14° 54' E, Maun Channel, NA	21.03.2012.
C. decipiens	PMFDE1	43° 51' N, 15° 12' E, Telašćica, st. T0, CA	12.10.2011.
C. decipiens	PMFDE2	43° 41' N, 15° 53' E, Solaris, CA	21.09.2012.
C. decipiens	PMFDE3	43° 31' N, 16° 27' E, Vranjic Bay, SA	08.10.2012.
C. decipiens	PMFE4	42° 39' N, 18° 04' E, Dubrovnik, SA	02.05.2011.
C. diversus	PMFDIV1	44° 28' N, 14° 54' E, Maun Channel, NA	21.03.2012.
C. eibenii	PMFH1	44° 28' N, 14° 54' E, Maun Channel, NA	01.01.2013.
C. lauderi	PMFL1	43° 51' N, 15° 12' E, Telašćica, st. T0, CA	12.10.2011.
C. pseudodichaeta	PMFED1	43° 51' N, 15° 12' E, Telašćica, st. T0, CA	01.03.2012.
C. rostratus	PMFR1	45° 00' N, 14° 37' E, Punat Bay, NA	04.12.2011.
C. rostratus	PMFR2	43° 51' N, 15° 12' E, Telašćica, st. T0, CA	12.10.2011.
C. rostratus	PMFR3	43° 51' N, 15° 12' E, Telašćica, st. T0, CA	22.03.2012.
C. rostratus	PMFR4	43° 31' N, 16° 27' E, Vranjic Bay, SA	08.10.2012.
C. salsugineus	PMFW1	43° 51' N, 15° 12' E, Telašćica, T0 CA	12.10.2011.
C. socialis	PMFA1	43° 51' N, 15° 12' E, Telašćica, st. T0, CA	01.03.2012.
C. socialis	PMFA2	43° 41' N, 15° 49' E, Zlarin, st. C1, CA	04.02.2011.
C. socialis	PMFA3	45° 00' N, 14° 37' E, Punat Bay, NA	04.12.2011.
C. socialis	PMFA6	43° 41' N, 15° 49' E, Zlarin, st. C1, CA	09.06.2010.
C. socialis	PMFA7	44° 51' N, 13° 48' E, Pula, NA	17.11.2012.
Chaetoceros sp. "A"	PMFS2	43° 31' N, 16° 27' E, Vranjic Bay, SA	08.10.2012.
C. tenuissimus	PMFF1	42° 39' N, 18° 04' E, Dubrovnik, SA	02.05.2011.
C. tenuissimus	PMFF2	43° 31' N, 16° 27' E, Vranjic Bay, SA	08.10.2012.
C. tortissimus	PMFT1	43° 51' N, 15° 12' E, Telašćica, st. T0, CA	12.10.2011.
C. cf. wighamii	PMFW2	43° 41' N, 15° 53' E, Solaris, CA	21.09.2012.

2.4.3 Molecular analyses

Extraction of the total DNA, PCR amplification and sequencing of the hypervariable D1-D3 region of the nuclear-encoded large subunit ribosomal RNA gene region (LSU rDNA gene) were carried out according to Orsini et al. (2002), Sarno et al. (2005) and Kooistra et al. (2010).

2.4.3.1 DNA extraction

The total DNA was extracted from selected strains (Table 2.4.) using the following protocol. The cells from 30 mL culture were harvested during exponential growth phase by two centrifugation steps, first at 2 000 *g* for 15 min at 4 °C and the second at 10 000 *g* for 15 min at 4 °C. The cell pellets were then resuspended in 500 µl CTAB extraction buffer (2% CTAB- Hexadecyltrimethylammonium bromide, 200 mM Tris HCL pH 8.0, 1.4 M NaCl, 50 mM EDTA, 2.5% PVP, 0.2% β-mercaptoethanol) containing 2 µl of RNase (10 mg μl^{-1}, Roche, Italy). The mixture was incubated at 65 °C in a water bath for 45 min, vortexing every 15 min to allow efficient disruption of cells and release of cell contents. After incubation, the tubes were put on ice for 10 mins. To each tube 500 µl of chloroform: isoamyl alcohol (24:1) solution was added and mixed well by inverting the tubes. This precipitates the cell debris leaving DNA and other soluble molecules in the supernatant. The supernatant (500 µl) was collected in new tubes after centrifuging at 10 000 *g* for 10 min at room temperature. To the collected supernatant 400 µl ice-cold isopropanol was added to precipitate DNA and left at -20 °C for at least one hour. The DNA pellet was collected by centrifugation at 10 000 *g* for 30 min at room temperature. Obtained pellet was washed with 400 µl of 75% ethanol to remove salts and centrifuged again for 15 mins at 10 000 *g*. Residual ethanol was removed by drying the DNA pellet in a vacuum drier for 8 mins at 60 °C, or left in a fume hood. The clean dry DNA pellet was resuspended in 0.1x TE buffer (1x TE buffer**:** 10 mM Tris-HCl, 1 mM EDTA) and stored at -20 °C.

Table 2.5. Strains used in the phylogenetic analyses

Species	Strain designation	GenBank accession number (LSU)
Bacteriastrum furcatum	PMF BA4	KC914887
B. hyalinum	PMF BA2	KC914886
B. jadranum	PMF BA1	KC914885
B. mediterraneum	PMF BA3	KC914888
Chaetoceros affinis	PMF E1	KC914884

2.4.3.2 PCR amplification

The marker region nuclear large subunit (LSU or 28S) of rDNA of ca. 750 bp was amplified using the primers D1R (forward: 5'- ACC CGC TGA ATT TAA GCA TA -3') and D2R (reverse: 5'- TGA AAA GGA CTT TGA AAA GA-3'). The Polymerase Chain Reaction (PCR) was carried out using an initial denaturating step of 4 min at 94°C, followed by 35 cycles of denaturation step at 94 °C for 30 sec, annealing step at 55 °C for 1 min and extension step at 72°C for 1 min, then a step of final extension 10 min at 72 °C and a final hold of 15 min at 10 °C. The PCR products were purified using a QIAquick gel extraction kit (Qiagen, Milan, Italy) according to the manufacturer's instructions.

2.4.3.3 Sequencing, and phylogenetic analyses

Purified PCR products were analysed on an automated Capillary Electrophoresis Sequencer ''3730 DNA Analyzer'' (Applied Biosystems, CA, U.S.A.). Sequencing primers were the same as those utilized for amplification. The obtained sequences were aligned, along with sequences from Kooistra et al. (2010), using Bioedit v. 7.1.3 then adjusted by eyeball in the sequence alignment editor Se-Al version 2.0a11 (Rambaut, 1996-2002). Maximum likelihood (ML) tree was constructed utilizing PAUP* (Phylogenetic Analyses Using Parsimony; version 4.0 and other methods) (Swofford, 1998). The Akaike information criterion including optimal base substitution model and values for base composition and gamma shape parameter were included from Kooistra et al. (2010). ML tree was obtained by heuristic search and bootstrap values associated to internodes was based on 1000 bootstrap replicates.

2.5 Taxonomical references

The cultured strains and specimens from field samples were mainly identified using general taxonomical references for the marine plankton diatoms (Hustedt, 1930, Cupp, 1943, Hasle and Syvertsen, 1997, Bérard-Therriault et al., 1999). Specifically for *Bacteriastrum* spp. the additional literature used was Ikari (1927). For *Chaetoceros* spp. the main taxonomical literature sources included: (Rines and Hargraves, 1988, Hernández-Becerril, 1996, Jensen and Moestrup, 1998, Shevchenko et al., 2006, Sunesen et al., 2008, Kooistra et al., 2010, Ikari, 1926, Ikari, 1928, Hernández-Becerril and Flores Granados, 1998). Particular species descriptions were regularly verified in peer-reviewed publications and the consulted publication listed in the bibliography part of each description.

The general diatom terminology used for the morphological descriptions followed proposals recommended by Anonymous (1975), Ross et al. (1979), Round et al. (1990), Hasle and Syvertsen (1997) and Kaczmarska et al. (2013). The specific terminology for *Chaetoceros* followed Evensen and Hasle (1975) and Kooistra et al. (2010) for the descriptions of ultrastructural features and for the general morphological characteristics Brunel (1966, 1972), Rines & Hargraves (1988), Hernández-Becerril (1996) Jensen and Moestrup (1998), and Kooistra et al. (2010). The glossary of the common terms used in the species descriptions is given in Appendix I of the thesis.

The morphological species descriptions are based on the Ph.D. thesis author original observations. The morphometric data were included from the literature in order to compare it with the values obtained within this study. A detailed list of synonyms for each described taxon is not included; however, some frequently found synonyms for each species have been provided following the names mostly provided by VanLandingham (1968) or according to the updated and more recent studies.

In the taxonomical part of this PhD thesis the taxa are listed alphabetically within the *Bacteriastrum* genera and each of the *Chaetoceros* generic subdivision (subgenera). The use of sections discussed in the introduction has been avoided following the practice of Rines and Hargraves (1988), Jensen and Moestrup (1998) and Kooistra et al. (2010), in spite of the examples in some other literature sources as in Hernadez Becerril (1996), Shevchenko (2006), Sunesen (2008). The subdivisions within the both genera are considered provisional as more ultrastructural and molecular information is becoming available (Kooistra et al., 2010).

CHAPTER 3

RESULTS

"Taxonomy is described sometimes as a science and sometimes as an art, but really it's a battleground."

Bill Bryson (1951 –) from "A Short History of Nearly Everything"

3.1 Genera and species descriptions

A total number of 49 morphologically distinct taxa belonging to the family Chaetocerotaceae were recognized in the material from the Adriatic Sea (Table 3.1.) including 25 taxa identified from 48 monoclonal strains isolated in the cultures. 43 morphotypes were recognized to belong to genus *Chaetoceros* of which 10 to subgenus *Chaetoceros*, 32 to subgenus *Hyalochaete* and one to subgenus *Bacteriastroides*, whereas 6 morphotypes were affiliated with the genus *Bacteriastrum*. Four taxa from the subgenus *Hyalochaete* do not fit any of the descriptions of so far described species and are referred as *Chaetoceros* sp. "A", "B", "C" and "D". In the following morphological descriptions and a taxonomic affiliation are presented for each taxon. An emended species diagnosis based on new observations obtained within present study is proposed for the species *Chaetoceros vixvisibilis*, *Bacteriastrum jadranum* and *B. mediterraneum*.

Table 3.1. List of *Chaetoceros* and *Bacteriastrum* species identified in this study with the indicated source of material (C-culture; F-field samples) and observation performed: + denotes information obtained within this study. n.d.: no data available.

Taxa	Source	LM	TEM	SEM
genus *Chaetoceros*				
subgenus *Phaeoceros*				
C. borealis	F	+	n.d.	n.d.
C. coarctatus	F	+	n.d.	n.d.
C. dadayi	F	+	n.d.	n.d.
C. danicus	C	+	+	+
C. densus	F	+	+	n.d.
C. eibenii	C,F	+	+	+
C. peruvianus	F	+	n.d.	n.d.
C. rostratus	C,F	+	+	+
C. tetrastichon	F	+	n.d.	n.d.
C. pseudodichaeta	C,F	+	+	+
subgenus *Hyalochaete*				
C. affinis	C,F	+	+	+
C. amanita	C	+	+	+
C. anastomosans	C	+	+	+
C. brevis	C,F	+	+	+
C. circinalis	C,F	+	+	+
C. constrictus	F	+	n.d.	+
C. contortus	C,F	+	+	+
C. costatus	C,F	+	+	+
C. curvisetus	C,F	+	+	+
C. decipiens	C,F	+	+	+
C. didymus	F	+	+	n.d.
C. diversus	C,F	+	+	+
C. cf. *laciniosus*	F	+	n.d.	n.d.

Table 3.1. continued

Taxa	Source	LM	TEM	SEM
C. lauderi	C	+	+	+
C. messanensis	F	+	n.d.	n.d.
C. neocompactus	F	+	n.d.	n.d.
C. pseudocurvisetus	F	+	n.d.	n.d.
C. protuberans	F	+	n.d.	+
C. salsugineus	C	+	+	+
C. simplex	F	+	+	n.d.
C. socialis	C,F	+	+	+
C. subtilis	F	+	n.d.	n.d.
C. tenuissimus	C	+	+	n.d.
C. throndsenii var. *throndsenia*	F	+	n.d.	n.d.
C. throndsenii var. *trisetosa*	F	+	n.d.	n.d.
C. tortissimus	C,F	+	+	+
C. vixvisibilis	F	+	+	+
C. cf. *wighamii*	C	+	+	+
Chaetoceros sp. „A“	C	+	+	+
Chaetoceros sp. „B“	F	+	n.d.	+
Chaetoceros sp. „C“	F	n.d.	n.d.	+
Chaetoceros sp. „D“	F	+	n.d.	+
subgenus *Bacteriastroides*				
C. bacteriastroides	F	+	n.d.	+
genus *Bacteriastrum*				
Bacteriastrum biconicum	F	+	n.d.	n.d.
B. furcatum	C	+	+	+
B. hyalinum	C,F	+	+	+
B. jadranum	C,F	+	+	+
B. mediterraneum	C,F	+	+	+
B. paralellum	F	+	n.d.	+

Presented observations on the species *Bacteriastrum jadranum* include also results obtained by AFM and the description of novel type of colony formation found in this species, a unique case among marine planktonic diatoms published in the paper by Bosak et al. (2012).

3.1.1 Genus *Chaetoceros* Ehrenberg (1844)

Type species: *Chaetoceros dichaeta* Ehrenberg

Bipolar centric diatoms. Cells cylindrically shaped, in girdle view rectangular and in valve view elliptical or circular. The cells contain either one plate-like, two or numerous small plastids. Each valve generally has two setae originating from near each valve apex with few exceptions in solitary species which have just one seta on one or both valves or in *C. bacteriastroides* which has six setae per valve. Few species are solitary but more often cells are joined in inseparable chains by fusion/interlinking of the setae or different siliceous structures of the frustule such as fusion of protuberances and setae and fusion of linking spines. Valve ornamentation consists of more or less observable annulus from which radiate dichotomously branching ribs towards the valve margin often continuing on the valve mantle. The mantle edge is often constricted near the abvalvar edge with this feature discernible in LM as a slight notch near the suture between the mantle and the girdle. Valves and setae can additionally be perforated by small poroids. The terminal valves and setae are often morphologically different. The girdle is composed from numerous half-bands with the connecting band having marked undulations through which the setae of the newly formed valves project. Resting spores frequently observed.

3.1.2.1 Subgenus Chaetoceros *Hendey (1964) (*Phaeoceros *Gran (1897))*

Large, robust, heavily silicified species. The chloroplasts are present within the cell body and in the thick setae. Cells united in chains by setae fusion or by linking process between sibling valves. Setae thick and strong, with a species-specific ornamentation. In cross-section round at the base perforated by irregularly distributed poroids, and further becoming polygonal and ornamented with strong spines at the thick longitudinal ridges. Setae sides ornamented with transverse costae interspaced by small areolae arranged in various patterns. Valves have central annulus and branching ribs and additionally perforated with small poroids. All species except *C. pseudodichaeta* have centrally positioned or eccentric process on each valve. Resting spores are known in one species (*C. eibenii).*

3.1.2.1.1 Chaetoceros borealis Bailey*(1854)*

(Figure 3.1. A-B)

Bibliography: Hustedt (1930), Rines and Hargraves (1988), Jensen and Moestrup (1998), Evensen and Hasle (1975), Berard-Therriault et al. (1999)

Synonyms: *C. borealis* var. *brightwellii* Cleve, *C. borealis* f. *typica* Cleve-Euler, *C. borealis* f. *varians* Gran

Description: apical axis (a.a.): 15 - 26 µm (Rines and Hargraves: 20 µm; Hustedt: 12 - 46 µm; Berard-Therriault et al.: 19 - 39 µm); pervalvar axis (p.a.): 21 - 33 µm (Berard-Therriault et al.: 28 – 46 µm)

LM: Heavily silicified cells forming straight, short and robust chains. Cells elliptical to almost circular in the valve view, in the girdle view rectangular with the pervalvar axis is often longer than the apical axis. The corners of the valve are strongly diagonally cut. Numerous small chloroplasts are present in the cell body and within the setae (Figure 3.1.A). Valve mantle quite high and the girdle part often equidimensional with the mantle. The mantle edge with the distinct constriction near the abvalvar edge, discernible in LM as a slight notch near the junction between the mantle and the girdle (suture) (Figure 3.1.B). Thick setae originate well inside the valve margin and have a prominent basal part extending more or less parallel with the pervalvar axis forming wide and hexagonally shaped apertures which are markedly shorter in length from the apical axis of the cell. Valve face is flat to slightly concave but very reduced in size due to the large and thick basal parts of the setae. The sibling setae cross each other or fuse for a short distance near the chain edge, afterwards diverging at the acute a ngle (Brunel group II or IV) extending straight and perpendicular to the apical axis (Figure 3.1.B). Terminal setae do not differ in structure or thickness from intercalary ones, only in their orientation diverging from the terminal valve towards the chain axis in a wide U-shaped curve (not shown).

Distinctive features: Wide hexagonal apertures distinctively shorter than the cell apical axis.

Comments: *C. borealis* is reported to be often confused with the *C. concavicornis* Mangin in EM due to the fact that they apparently share the same ultrastructural features of the valves and setae. However, in the latter species the origin of the setae is in the very centre of the valve often forming an interlocking tooth - like structure similar as in *C. peruvianus* and all setae are directed towards the same end of the cell. In LM *C. borealis* can appear similar to *C. densus* Cleve but the origin of the setae is much closer to the valve centre and the apertures are much shorter in first species.

3.1.2.1.2 Chaetoceros coarctatus Lauder *(1864)*

(Figure 3.1. C-D)

Bibliography: Hustedt (1930), Cupp (1943), Hernández-Becerril (1991a), Nagasawa and Warren (1996)

Synonyms: *C. borealis* var. *rudis* Cleve, *C. rudis* Cleve, *Chaetoceros validum* Grunow in Cleve and Möller

Description: a.a.: 26 - 36 µm (Cupp, Hustedt: 30 - 44 µm; Hernández - Becerril: 42 - 50 µm); p.a.: 42 - 63 µm (Hernández - Becerril: 40 - 45 µm)

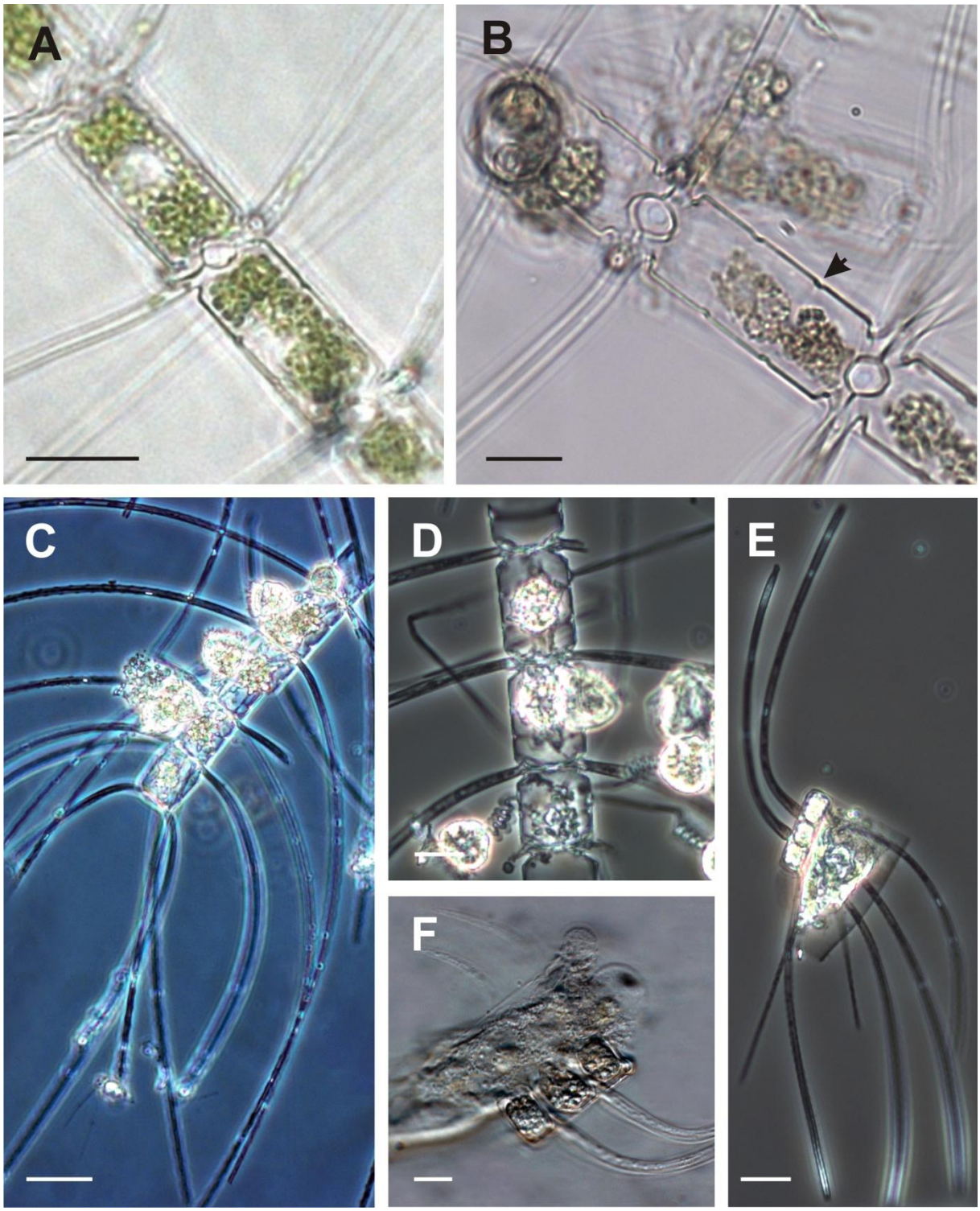

Figure 3.1. LM micrographs. of *Chaetoceros* spp from field samples. **A-B** *Chaetoceros borealis.* **A)** Middle part of the chain. Cells with small numerous chloroplasts present also in the setae. **B)** Intercalary cells with the constriction near the mantle abvalvar edge visible as a notch near the suture (arrow) Note the short hexagonal aperture between sibling cells; **C-D** *C. coarctatus.* **C)** Terminal part of the chain showing the orientation of the setae. **D)** Middle part of the chain, note the narrow apertures and attached symbiotic ciliates*;* **E-F** *C. dadayi*. **E)** Complete chain with the symbiotic tininnid. Note the orientation of two intercalary setae. **F)** Complete chain. Scale bars: A-B,D-E=20 µm; C=50 µm, F=10 µm.

LM: The cells are forming heteropolar, straight, robust and usually long chains. Heavily silicified cells are elliptical in the valve view and rectangular in girdle view with the diagonally cut valve corners. Numerous small chloroplasts are present in the cell body and the setae. There is a distinct groove on the mantle near the suture, mantle is high and equidimensional with the girdle. Valve surface is flat, setae arise within the valve margin with very short, and practically non-existent basal part therefore the apertures are extremely narrow and often the valve faces of sibling cells are touching each other (Figure 3.1.C-D). The sibling setae cross each other near the chain margin and after crossing point diverge at an angle of about 30-45° from the apical plane (Brunel group II). All setae are thick, coarse and curved towards the posterior end of the chain. Terminal setae morphologically similar to intercalary ones (Figure 3.1.C).

Distinctive features: Large cells, very narrow apertures. All setae curved towards one side of the chain. Attached numerous ciliates.

Comments: The species is commonly found with epizoic ciliate *Vorticella oceanica* Zacharias attached to the cells, sometimes in large numbers.

3.1.2.1.3 Chaetoceros dadayi Pavillard *(1913)*

(Figure 3.1. E-F)

Bibliography: Hustedt (1930), Cupp (1943), Hernández - Becerril (1992)

Description: a.a.: 7 - 17 µm (Cupp, Hustedt: 10 - 15 µm; Hernández - Becerril: 10 - 25 µm); p.a.: 7 - 26 µm (Hernández - Becerril: 9 - 16 µm)

LM: Chains are heteropolar, straight and short, composed of only three cells (Figure 3.1.E-F). In girdle view cells rectangular with round valve corners and in valve view elliptical. Numerous chloroplasts are present in the cell body and the setae. The mantle is high without visible notch near the suture. Thick setae are originating at the valve edge and immediately cross each other without a basal part hence the apertures are either very narrow or they do not exist and the sibling valve faces are closely pressed on each other. After the crossing point the setae run shortly almost perpendicular to the pervalvar axis but soon strongly curve towards it becoming almost parallel with the same axis. The setae are morphologically different as some of them are shorter and attach to a symbiotic tintinnid, e.g. one of the anterior terminal seta is shorter than the other of the same valve and curved strongly towards the posterior end of the chain. Two intercalary setae on the same side of the chain as the curved anterior seta are directed to the anterior end while the rest of the setae are directed toward the posterior side of the chain (Figure 3.1.E,F).

Distinctive features: Two setae of the neighbouring cells on the same side are directed towards the anterior side of the chain while rest of the setae are oriented towards posterior side. Attached tintinnid.

Comments: Very similar to *C. tetrastichon,* clearly differentiated in LM only in orientation of two intercalary setae towards the anterior chain end in *C. dadayi*. Both species are found with single *Tintinnus inquilinius* Dadayi cell attached to chain.

3.1.2.1.4 Chaetoceros danicus Cleve *(1889)*

(Figures 3.2.-3.3.)

Bibliography: Hustedt (1930), Cupp (1943), Rines and Hargraves (1988), Hernández - Becerril (1996), Jensen and Moestrup (1998), Sunesen et al. (2008), Kooistra et al. (2010)

Description: a.a.: 12 - 40 µm (Cupp: 7 - 15 µm; Hustedt: 8 - 20 µm; Sunesen et al.: 16 - 24 µm; Hernández-Becerril: 15 - 22 µm); p.a.: 13 - 23 µm (Hernández - Becerril: 16 - 28 µm)

LM: Cells are usually solitary but occasionally can be found in short chains composed of two to three cells. Cells are elliptical in valve view (Figure 3.2.A) and rectangular in girdle view (Figure 3.2.B). Cells contain numerous small chloroplasts located in the central body and in the setae. The valve face is flat or slightly concave, the mantle is moderately high, girdle low. Setae long and thick, originate from the valve corners and extend perpendicular to pervalvar axis. They are usually straight, but can also be slightly curved in the apical plane. When forming chains the sibling setae can diverge ca. 15 ° from the apical axis belonging to Brunel group I or II. The setae on different valves on the same cell are positioned at ca. 45° angle between each other hence they form a cross in valve view (Figure 3.2.A). When the cells are forming chains the setae are fused at the valve corners for a short distance without a basal part but the narrow apertures can still be observed due to the slight concave surface of the valves (Figure 3.2.C). The central process is present in every valve and it is possible to observe it in LM in cleaned material (Figure 3.2.D). Resting spores not observed.

EM: The valve is perforated by poroids irregularly scattered over the valve surface and mantle, lacking in the central part (Figures 3.2.F and 3.3.A). The small round annulus is visible in the valve centre with numerous branching costae extending from it towards the valve edge. On the valve mantle surface there are often observed irregularly shaped siliceous thickenings (Figure 3.2.E). The mantle is constricted near the advalvar edge. Every valve possesses a centrally located process in the form of a simple oval to comma-shaped hole on the internal and sometimes with a very small protrusion on the external side of the valve (Figures 3.2.F-G and 3.3.A-B). All setae are round at the bases in cross-section and later become four to six-sided, with rows of strong and long spines on the thickened ridges. The spines extend all the way to the setae tip (Figure 3.3.F). The basal parts of the setae are perforated by the poroids which similar to the ones on the valve surface. Further on the proximal part start longitudinal rows of areolae which extend parallel with the seta axis. In the more distal part of the seta when it becomes quadrangular, the ornamentation pattern of the sides consists of not particularly thick transverse costae alternating with the single transverse row of relatively large poroid areolae with 3-5 areolae in each row (Figures 3.3.C-E). Girdle bands are narrow and ornamented with alternating transverse striae and costae as well as the irregularly scattered small poroids between costae (Figure 3.3.G).

Distinctive features: Usually single cells, straight and thick setae perpendicular to the pervalvar axis. Setae are four-sided in cross section with long spines on the ridges and sides pattern consisting of transverse single row of 3-5 larger areolae between thin costae.

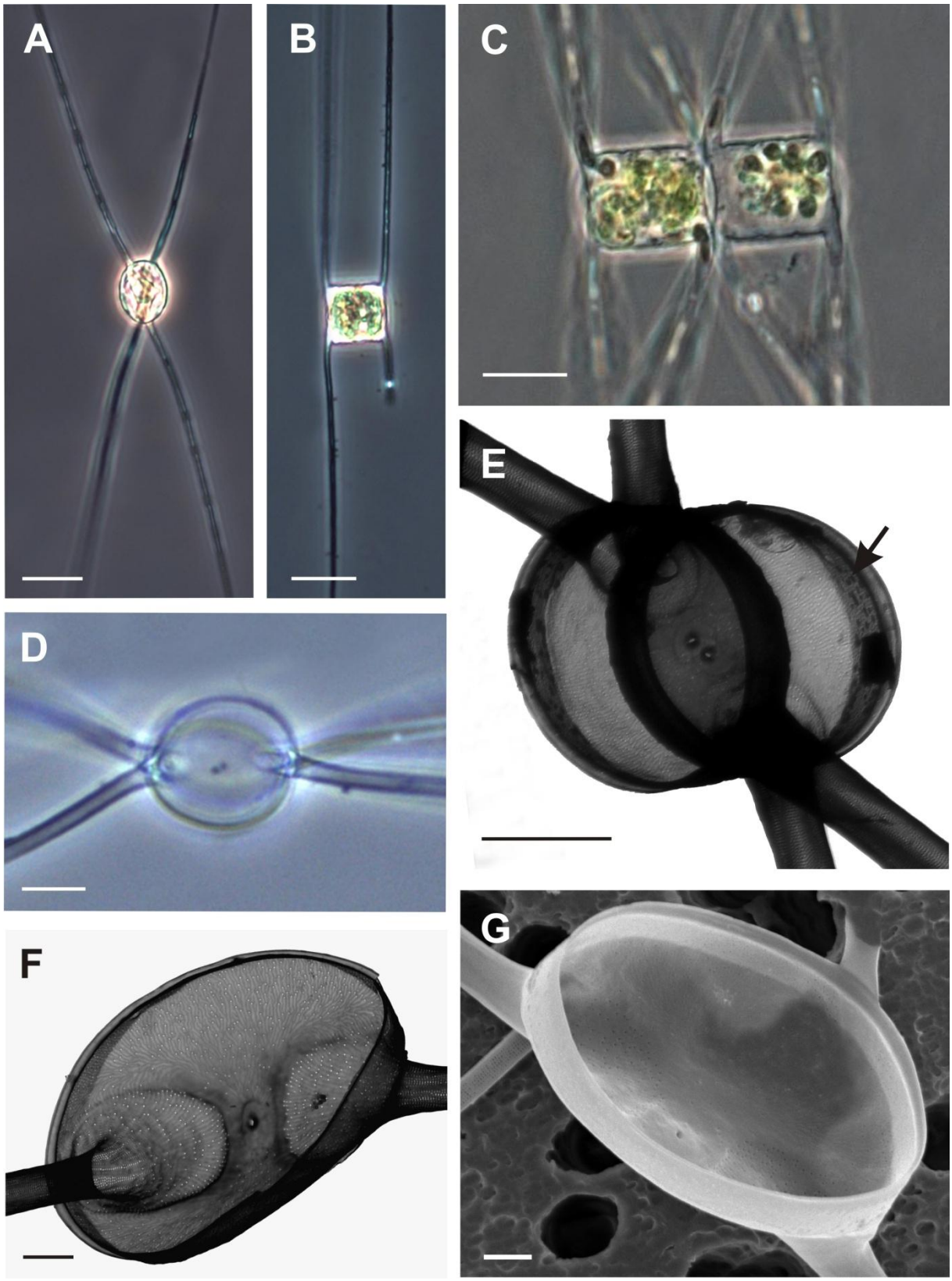

Figure 3.2. LM **(A-D)**, TEM **(E,F)** and SEM **(G)** micrographs of *Chaetoceros danicus* from culture material, strain PMFDA1. **A)** Cell in valve view, note the orientation of the setae on different valves on the same cell. **B)** Cell in girdle view. **C)** Chain of two cells in girdle view. **D)** Cell in valve view showing the central process. **E)** Fine structure of the two overlaid valves with the siliceous thickenings on the valve margin (arrow). **F)** and **G)** Internal view of the valve. Scale bars: A-B = 20 µm; C-D = 10 µm; E = 5 µm; F-G = 2 µm.

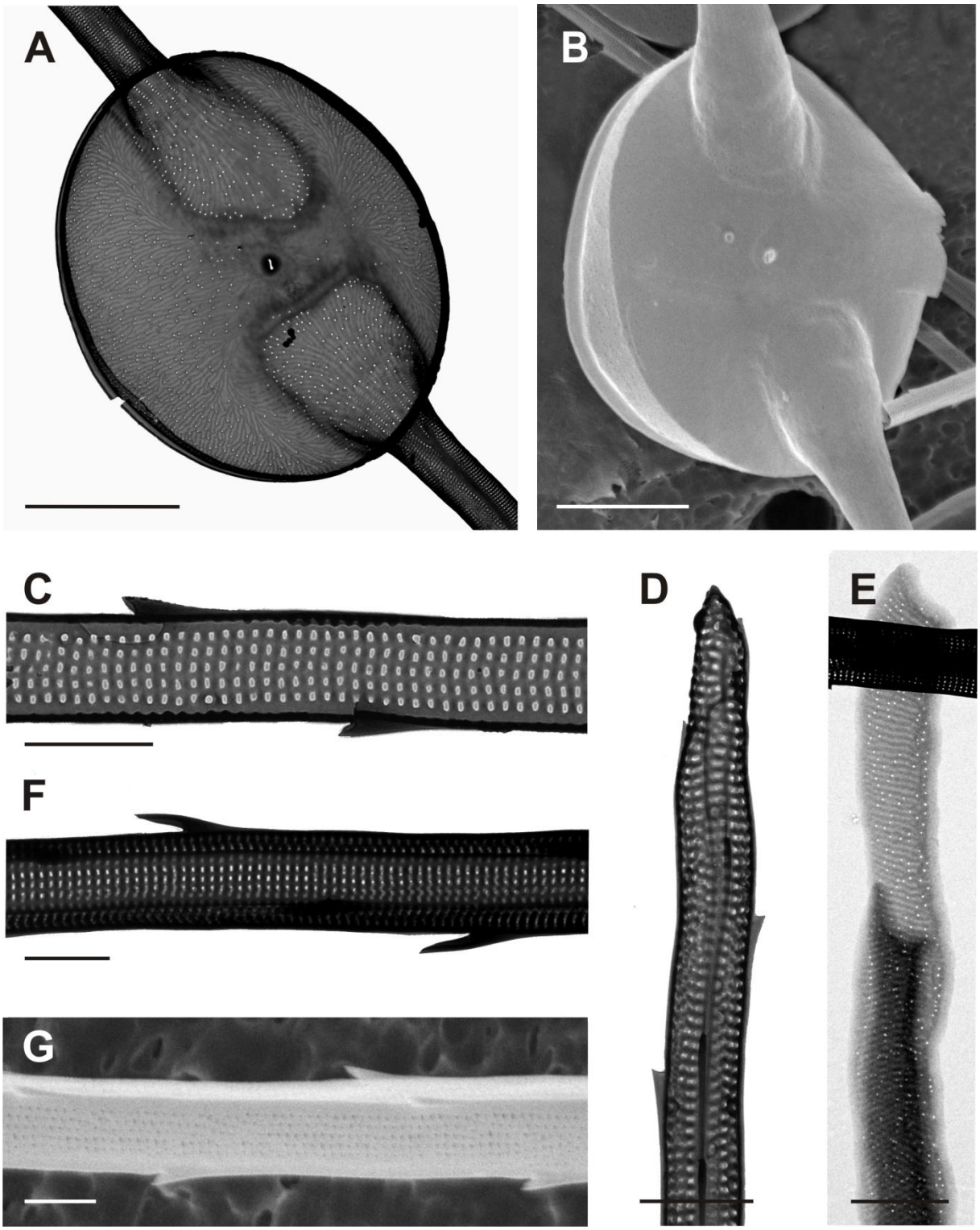

Figure 3.3. TEM **(A,C,D,F)** and SEM **(B,G)** micrographs of *Chaetoceros danicus* from culture material, strain PMFDA1. **A)** View on the valve showing the fine structure. **B)** External view on the valve showing the small protrusion of the central process (arrow). **C)** Single side of the seta with pointed spines on the edge and alternating transverse rows of 5 areolae and costae. **D)** and **E)** Detail of a seta. **F)** Tip of the seta. **G)** Detail of a girdle band. Scale bars: A,B = 5 µm; C-F = 1 µm; G = 2 µm.

3.1.2.1.5 Chaetoceros densus Cleve (1901)

(Figure 3.4. A-E)

Bibliography: Hustedt (1930), Rines and Hargraves (1988), Hernández-Becerril (1996), Jensen and Moestrup (1998)

Synonyms: *C. borealis* var. *densa* Cleve, *Chaetoceros borealis var. brigthwellii* Cleve, *C. brightwellii* (Cleve) Mills

Description: a.a.: 17 - 38 µm (Hustedt: 10 - 40 µm; Hernández-Becerril: 38 - 45 µm; Rines and Hargraves:35 -55 µm); p.a.: 13 - 63 µm (Hernández-Becerril: 32 - 48 µm)

LM: Cells united into robust, straight and usually long chains. Cells in valve view elliptical and in girdle view rectangular with diagonally cut valve corners (Figure 3.4.A,B). Cells and setae contain numerous small chloroplasts. The valve face is flat or slightly concave, the mantle is high and equidimensional with the girdle with the visible notch near the suture (Figure 3.4.B). Setae long, thick and straight, originating inside the valve margin with the sibling setae crossing over each other at the chain margin with no distinct basal part. Apertures variable in size, usually in form of very narrow slits and barely visible (Figure 3.4.A) but also can be slightly wider in which case they are hexagonally shaped (Figure 3.4.B). Terminal setae are different from intercalary ones in orientation, intercalary are slightly curved towards the posterior end of the chain or are perpendicular to the pervalvar axis and terminal are almost parallel to the chain axis (Figure 3.4.B). In valve view, the setae diverge from the apical plane at approximately equal angles (ca. 30 - 45°) belonging to the Brunel Group II (Figure 3.4.C).

EM: The valves are heavily silicified and densely perforated by poroids with the oblong annulus and a feeble costae pattern (Figure 3.4.E). The central process is in a form of a simple oval hole from the inside and found in each valve, possible to see it also in LM in cleaned material. From the inside view of the valve there is visible a mesh of small areolae ornamenting the bases of the setae (arrows in Figure 3.4.E). The setae are circular in cross-section at the bases but later become four-sided with the rows of strong spines on the ridges (Figure 3.4.D). The sides are ornamented with not particularly thick transverse costae alternating with the single row of 12 - 15 very small areolae per row (Figure 3.4.D).

Distinctive features: Very narrow apertures. Setae Brunel type II, in cross section four-sided with sides ornamented with single transverse rows of 12-15 small areolae between thin costae.

Comments: *C. densus* is easily confused in LM with *C. eibenii* (Grunow) Meunier especially when the apertures between adjacent cells are wider. However, the difference between two species can be observed in valve view due to the different divergence of the setae from the apical axis with *C. densus* belonging to Brunel Group II and *C. eibenii* generally to Brunel Group III. In the girdle view the difference is in the spine-like central process which is visible on each *C. eibenii* valve and lacking in C. *densus*. In EM these two species are easily distinguished due to completely different ultrastructure of the setae.

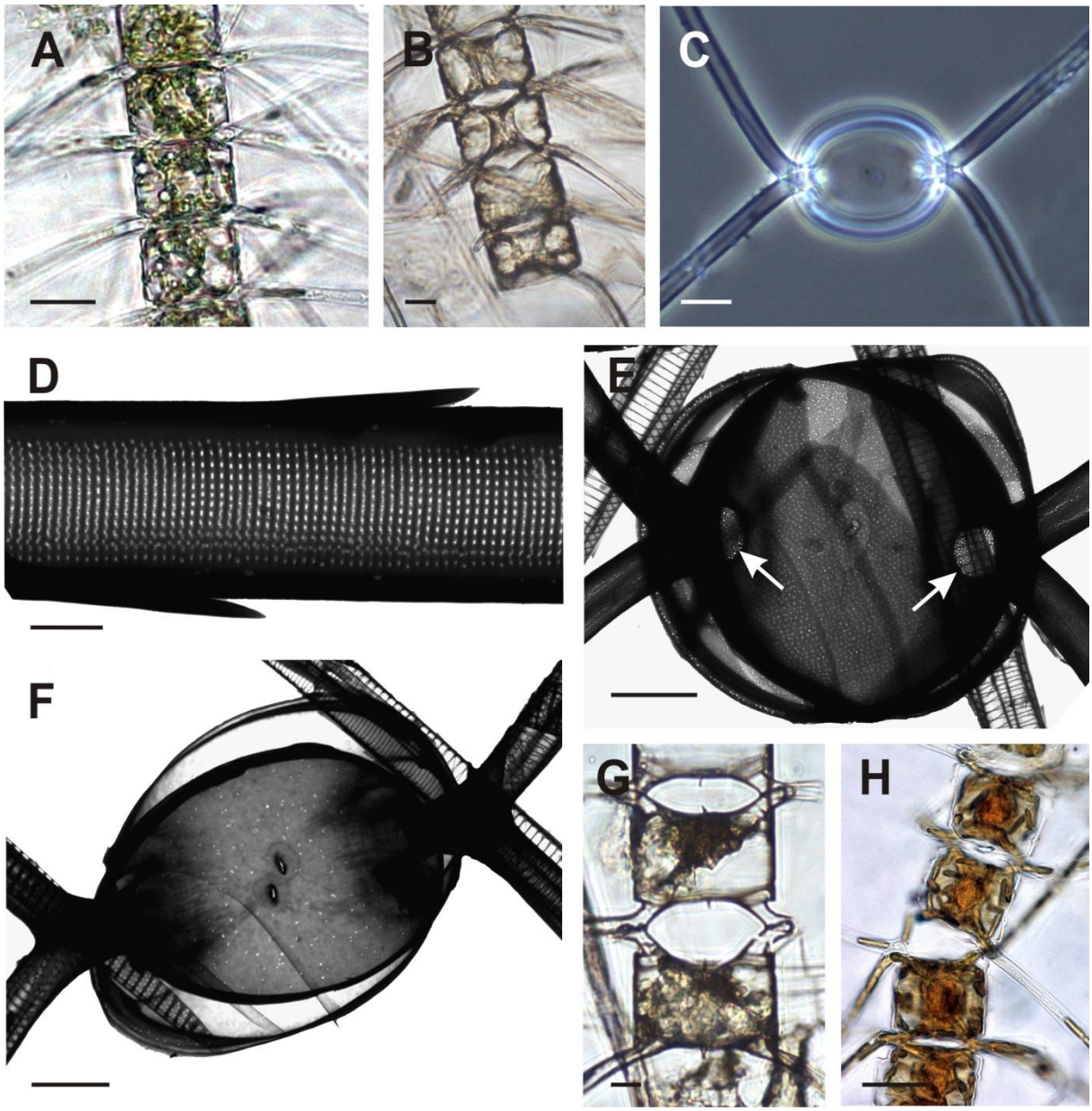

Figure 3.4. LM **(A-C, G-H)** and TEM **(D-F)** micrographs of *Chaetoceros* spp from field samples. **A-E** *C. densus.* **A)** Middle part of the chain with very narrow apertures and variable direction of the setae. **B)** Terminal part of the chain. **C)** Sibling valves in valve view. **D)** Detail of a seta. **E)** Fine structure of the two overlaid valves with the fine mesh of poroids at the bases of setae (arrows). **F-H** *C. eibenii.* **F)** Fine structure of the two overlaid valves with poroids. **G)** Terminal part of the chain showing wide hexagonal apertures and visible central processes on every valve. **H)** Middle part of the chain showing numerous small elongated plastids in cells and setae. Scale bars: A,H = 20 µm; B-C, G = 10 µm; D = 1 µm, E-F = 5 µm.

*3.1.2.1.6 Chaetoceros eibenii (*Grunow in Van Heurck (1882)) Meunier (1913)

(Figures 3.4.F-H, 3.5. - 3.6.)

Bibliography: Hustedt (1930), Cupp (1943), von Stosch et al. (1973), Koch and Rivera (1984), Rines and Hargraves (1988), Jensen and Moestrup (1998)

Synonyms: *C. paradoxus* var. *eibenii* Grunow

Description: a.a.: 13 - 42 µm (Hustedt: 25 - 78 µm; Cupp: 25–50 µm; Rines and Hargraves: 35 - 55 µm); p.a.: 11 - 38 µm

LM: Cells united into robust, straight and usually long chains. Cells in valve view broadly elliptical and in girdle view rectangular with sharp valve corners (Figure 3.4.G, 3.5 A-B). Cells and the setae contain numerous small elongated chloroplasts (Figure 3.4.H). The valve surface is slightly concave with a spine-like central process visible on every valve (Figure 3.4.G, 3.5.B). Valve mantle is low to moderate, girdle is broad and sometimes there is visible slight notch near the suture. Setae originate inside the valve margin and have a relatively short basal part, in girdle view generally diverging at ca. 30° from the apical axis hence forming distinct hexagonal apertures (Figures 3.4.G, 3.5.A-B). The setae are long, coarse and thick, after crossing point at the chain edge they diverge from each other at a wide angle and extend either straight perpendicularly to chain axis or more often they are bent towards the nearest end of the chain (Figure 3.5.A). In valve view their orientation appears often as belonging to Brunel Group III with the one seta lying parallel to the apical plane and the other diverging from it at approximately 90° angle (Figures 3.5.C-D). However, the divergence angle can be quite variable character hence in some valves it can appear that the two setae diverge at approximately equal angles (Figure 3.5.E). Terminal setae are of similar thickness and appearance as the intercalary ones but different in their orientation, being slightly curved and widely diverging from the chain (Figures 3.5. A-B).

EM: The valves are very heavily silicified and perforated with relatively small number of poroids irregularly scattered over the valve face, setae bases and mantle (Figures 3.4.F, 3.5.K). On the valve face, feeble costae diverge from a round central annulus. The marginal ridge is often ornamented with a strongly silicified low hyaline rim with an uneven edge (Figure 3.6.A) which is sometimes extended in the pervalvar direction into irregular siliceous projections (Figure 3.5.I). The central process is present in every valve and in the cultured material sometimes two processes per each valve were observed (Figure 3.5.J). The process appears to be an elliptical to comma-shaped hole from the inside, and either flattened or round tube with a tapering tip on the outside of the valve (Figures 3.5.K). The setae are circular in cross-section close to the bases but later become six-sided with the rows of very strong spines on the ridges. The spines extend all the way to the pointed tip of the setae (Figures 3.6.F,H). The bases of the setae are perforated by the scarce poroids which are the same as on the valve surface (Figures 3.6.B) and distally the ornamentation pattern of the setae sides consists of relatively thick and distinct transverse costae between which are scattered very small poroid areolae (Figures 3.6.C,E,G). After each 4 - 8 costae, one larger round poroid is found positioned near to the ridge and close to the costae on either sides of the side-wall.

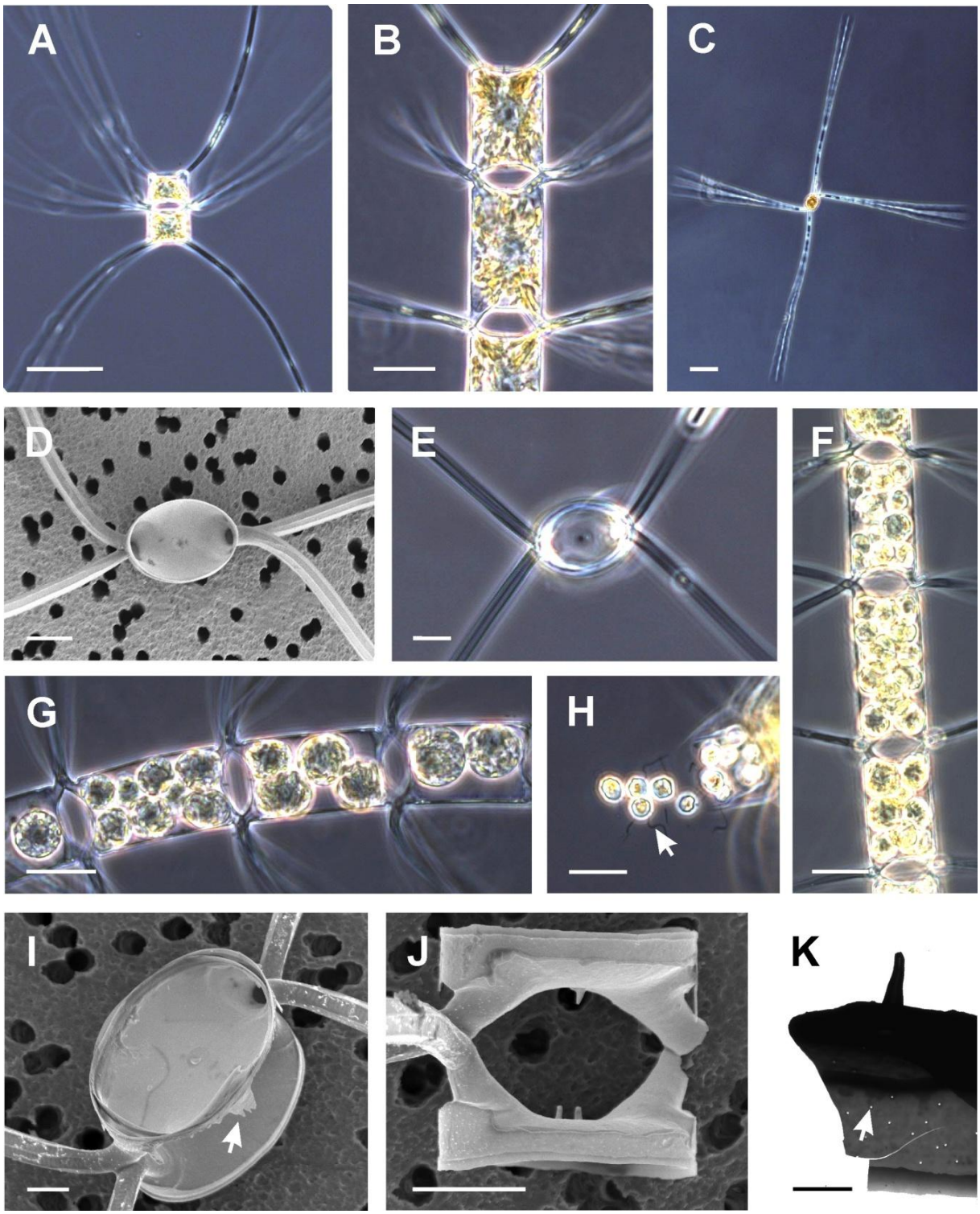

Figure 3.5. LM **(A-C,E-H)**, SEM **(D,I,J)** and TEM **(K)** micrographs of *Chaetoceros eibenii* from culture material, strain PMFH1. **A)** Complete chain of two cells. **B)** Terminal part of the chain. **C)** Cell in valve view. **D)** Valve view of the sibling valves with the setae divergence belonging to Brunel Group III. **E)** Valve view of the sibling valves with the setae divergence belonging to Brunel Group II. **F)** and **G)** Spermatogoniums with spermatocytes in different stages of development. **H)** Sperm cells released from the spermatogonium. Arrow indicates the sperm flagellum. **I)** Sibling valves in valve view with siliceous extensions projecting from the hyaline rim on the marginal ridge (arrow). **J)** Sibling valves in girdle view. Note the two central processes on the lower valve. **K)** Detail of a broken valve in girdle view with the spine-like central process and pores perforating the valve mantle (arrow). Scale bars: A, C = 50 µm; B, F-H = 20 µm; D-E = 10 µm; I-J = 5 µm; K = 2 µm.

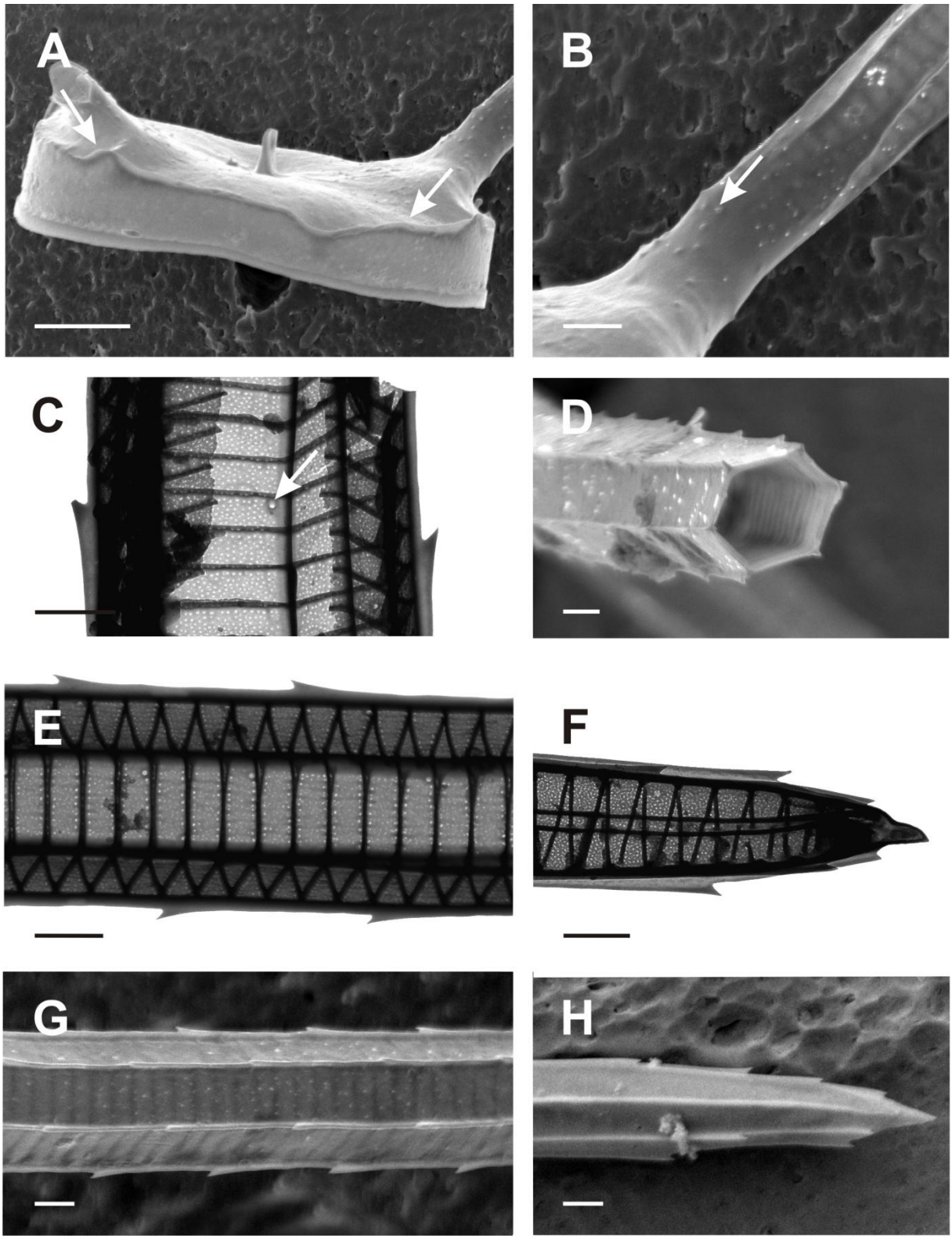

Figure 3.6. SEM **(A-B, D,G-H)** and TEM **(C, E-F)** micrographs of *Chaetoceros eibenii* from culture material, strain PMFH1. **A)** External view of the valve with central process and hyaline rim on the marginal ridge (arrows). **B)** Basis of the setae and the part proximal to the valve, showing the poroids (arrow) and the transition of the circular to four-sided cross-section of the setae. **C)** Detail of a broken seta showing the ornamentation pattern on the sides. The larger round poroid is indicated by an arrow. **D)** Hexagonal cross-section through seta. **E)** and **G)** Detail of the seta. **F)** and **H)** Seta tip. Scale bars: A = 5 µm; B-H = 1 µm.

Distinctive features: Hexagonal apertures, a spine-like central process visible in every valve. Setae Brunel group II/III, in cross section six-sided with sides ornamented with thick costae interspaced with the area perforated by numerous very small areolae.

Comments: For similar species see comments in *C. densus.*

In this particular species von Stoch et al. (1973) described a peculiar life cycle with the resting spores forming from the initial cell inside the lateral auxospores during the sexual phase and not from the vegetative cells. The spores are reported to have an evenly vaulted primary valve, a distinct mantle region and a flat to slightly vaulted secondary valve with the both valves having smooth surfaces. This is the only species belonging to the subgenus *Chaetoceros* for which is known to form resting spores. Whether the resting spore is the obligatory part of the life cycle it is yet not known. Unfortunately, in spite of the observed formation of spermatogoniums with spermatocytes in various stages of development (Figures 3.5.F-H), released flagellated sperm in the cultured material (Figure 3.5.H), and unfertilized egg cells laterally attached to the oogonium (not shown), neither auxospores nor the resting spores were observed in this study.

3.1.2.1.7 Chaetoceros peruvianus Brightwell (1856)

(Figure 3.7.A-D)

Bibliography: Hustedt (1930), Cupp (1943), Rines and Hargraves (1988), Hernández - Becerril (1996), Shevchenko et al. (2006), Sunesen et al. (2008), Kooistra et al. (2010)

Synonyms: *C. convexicornis* Mangin, *C. peruvianus* var. *currens* Peragallo, *C. peruvioatlanticus* Karsten, *C. chilensis* Krasske

Description: a.a.: 15 - 39 µm (Hustedt: 10 - 30 µm; Cupp: 16 - 32 µm; Rines and Hargraves: 20 µm; Hernández - Becerril: 13 - 22 µm; Shevchenko et al.: 15 - 35 µm; Sunesen et al.: 10 - 44 µm); p.a.: 16 - 33 µm (Hernández - Becerril: 20 - 36 µm, Shevchenko et al.: 15 - 40 µm)

LM: Cells are solitary, robust; in girdle view appear rectangular with rounded corners and in valve view elliptical. Cells contain numerous small plastids located in the cell body and in the setae. The frustules are heterovalvate with the convex anterior valve and the concave posterior valve. The mantles of both valves are usually high with a distinct constriction near the margin and the girdle low. Setae thick, coarse, long, ornamented with spines which are visible in LM (Figure 3.7 D). All setae lie in the apical plane and are oriented towards the same (posterior) end of the cell. The setae of the anterior valve emerge very close to the valve centre and are drawn up in the pervalvar direction, touching each other with a groove between them. The fusion occurs in the valve centre forming a characteristic tooth - like structure (Figure 3.7.B,C). From the fusion point onwards they sharply bend back in a curve toward the posterior end of the cell. The posterior setae originate close to the valve margins and then curve from the cell in the same direction as the anterior ones becoming almost parallel to the pervalvar axis.

Distinctive features: Solitary, heterovalvar cells, all setae curved towards the posterior cell end. The basal parts of anterior setae locked in a tooth-like structure.

Comments: In the Adriatic material there were observed some slender, more delicate cells with high valve mantle which exceeds the length of apical axis and relatively thin setae. Cupp (1943) and Hustedt (1930) ascribe this morphotype to *C. peruvianus* f. *gracilis* however, considering the high size variability of the diatom cells depending on their age, and as the size is the main character described to distinguish the forma *gracilis* from the original species these specimens are here referred to as *C. peruvianus*. The species *C. pendulus* Karsten (synonym *C. aequatorialis)* which is characterized by lacking the tooth-like structure formed by anterior setae was not observed in the investigated material.

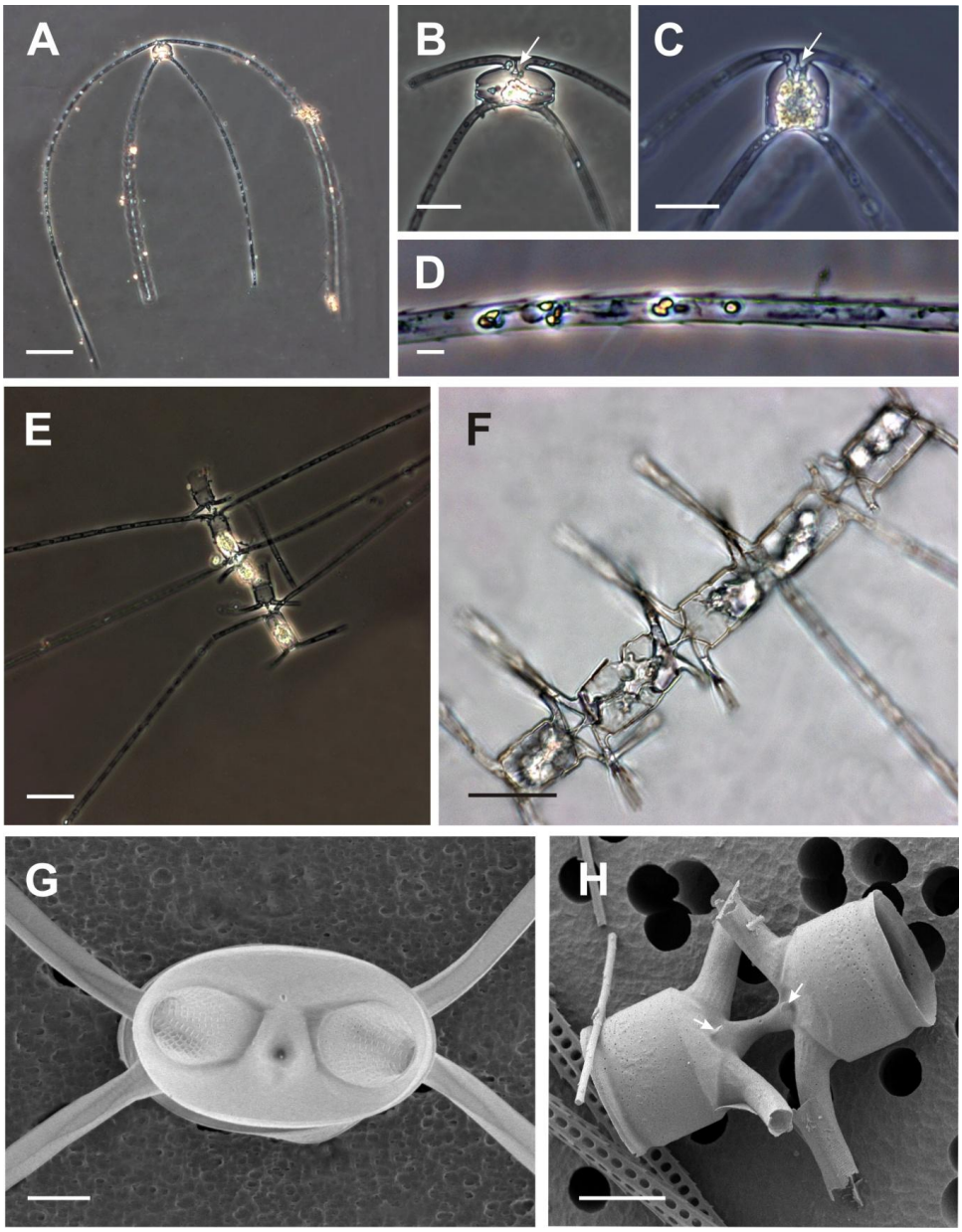

Figure 3.7. LM **(A-F)** and SEM **(G-H)** micrographs of *Chaetoceros* spp from field material. **A-D** – *C. peruvianus.* **A-C)** The cell in girdle view. Note the tooth-like structure between the setae on the anterior valve (arrow in B and C). **D)** Detail of setae with spines and chloroplasts. **E-H** – *C. rostratus* **E)** and **F)** Terminal part of a chain in the girdle view. Note the absence of the linking spine in the terminal valves. **G)** Intercalary sibling valves in valve view showing the setae divergence in the apical plane belonging to Brunel group II. **H)** Intercalary sibling valves in girdle view connected with the linking spine and visible tube-like processes on their side (arrows). Scale bars: A,E = 50 µm; B-C,F = 20 µm; G-H= 5 µm; D= 1 µm.

3.1.2.1.8 Chaetoceros pseudodichaeta Ikari (1926)

(Figures 3.8. - 3.11.)

Bibliography: Ikari (1926), Hernández-Becerril (2000)

Description: a.a.: 5.2 - 8 µm (culture); 4.1 - 13.2 µm (field samples); (Hernández - Becerril: 10 - 13 µm); p.a.: 12.3 - 25.0 µm (culture); 8.6 - 28.4 µm (field samples); (Hernández - Becerril: 15 - 20 µm); aperture: 8.6 - 15.8 µm (culture); 10.2 - 18.7 µm (field samples); (Hernández - Becerril: 8 - 9 µm)

LM: Short, straight and robust chains composed of 3-7 cells (Figure 3.8.A-B). Cells in girdle view appear rectangular with round corners and usually with the pervalvar axis longer than the apical axis (Figure 3.8.C). In valve view cells are in most cases circular (Figure 3.8.F) but can also be elliptical. Multiple spherical chloroplasts present in the cell body as well as inside the long and thick setae. Valves slightly concave or flat, mantle high with no distinct constriction near the suture, the girdle often higher than the mantle. The setae originate inside the valve margin and they have the prominent basal part, 6-10 µm long, which extends parallel with the pervalvar axis. The sibling setae fuse at a single point often crossing each other at the chain margin forming wide and rectangular aperture (Figure 3.8.C,E). After setae junction they diverge almost equally at an angle of ca. 30-45° from the apical plane belonging to the Brunel Group II. At first, the setae lie almost in the valvar plane and further they curve to the pervalvar axis toward either end of the chain thus the chains appear to develop in three-dimensional space (Figure 3.8.A-B). Setae up to 260 µm long, 2.0–2.4 µm wide in diameter at the base and tapering towards the end to width of 1–1.5 µm. All intercalary setae ornamented consecutively from the fusion point towards the distal part with the conspicuous long silica capilli (filamentous spines), scissor-like spines with the tip extended to a capillus (Figure 3.10.A), simple scissor-like spines and strong common spines (not shown). Terminal setae differ in morphology and orientation from the intercalary ones. They originate within the valve margin with their proximal part first extending parallel to the pervalvar axis then slightly bent outward but soon recurve back and becoming again almost parallel with the chain axis (Figures 3.8 A-B) and are ornamented only with the common spines. The long central tubular process is present on terminal valves and it is lacking on all intercalary valves (Figure 3.8.A). Resting spores not observed.

EM: The valves heavily silicified, the smooth valve face has pattern of relatively thick dichotomously branching costae radiating from a round central annulus, extending parallel on the valve mantle and ending before the mantle abvalvar edge (Figure 3.9.B-C). The valve face is often ornamented with several short siliceous thin capilli irregularly distributed across the surface (Figure 3.9.B-C,E). Marginal ridge (advalvar mantle edge) is adorned with a strongly silicified low hyaline rim which often extends in the pervalvar direction to one or several projections of variable shape and length (Figure 3.9.A). The mantle high 2.1–3.7 µm, smooth with a single ring of siliceous irregularly shaped thickenings on the abvalvar mantle edge (Figure 3.9.B,D) and without any constriction near the edge. On the mantle of some valves an elliptically shaped marking with thickened edge was observed

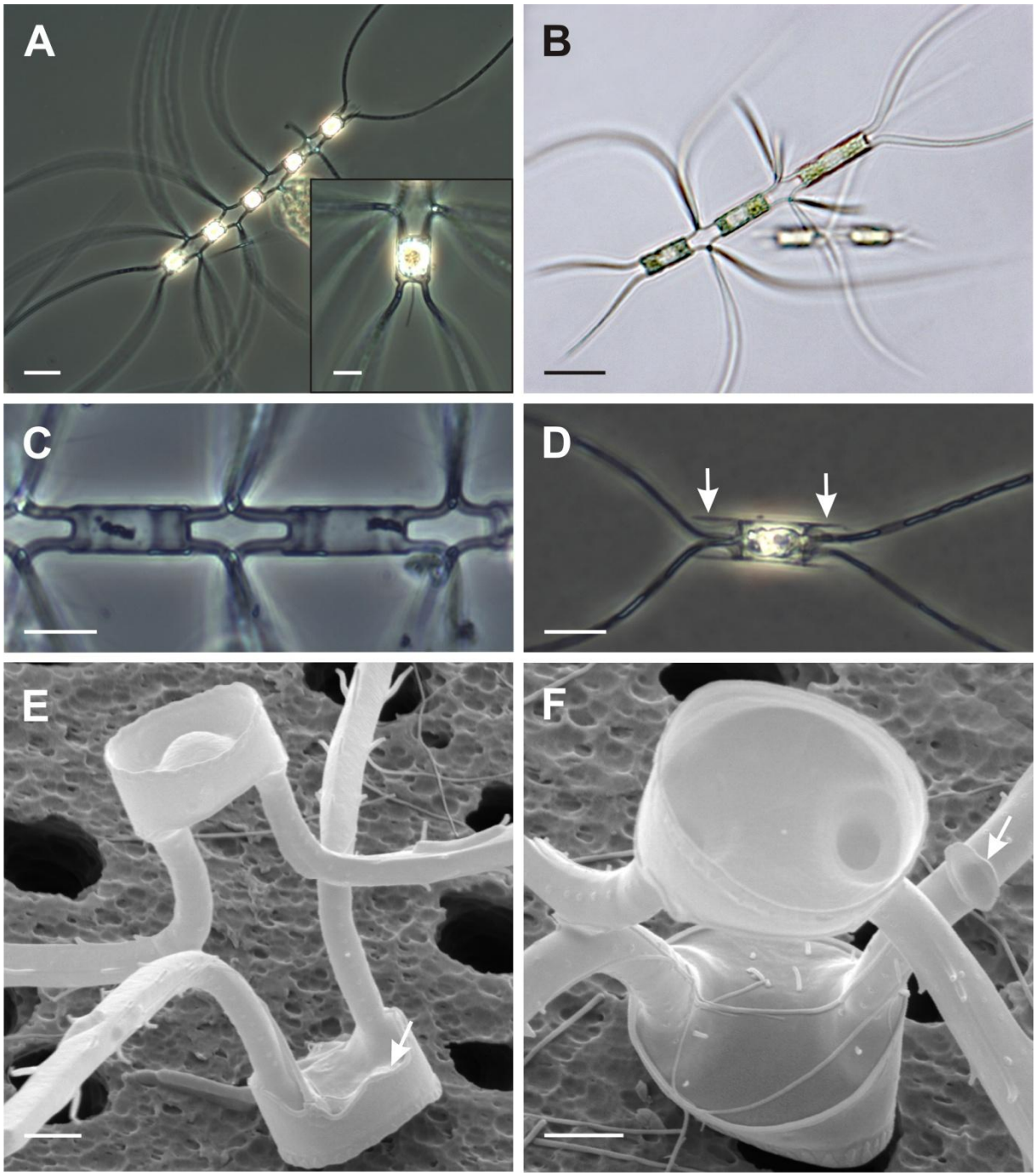

Figure 3.8. LM **(A-D)** and SEM **(E-F)** micrographs of *Chaetoceros pseudodichaeta* from natural sample **(A,C)** and cultured material, strain PMFED1 **(B,D-F)**. **A)** Complete chain showing the typical orientation of the setae. Note the orientation of the terminal setae. Insert showing the terminal cell of the same chain with the long tubular process. **B)** Complete chain of three cells. **C)** Middle part of the chain showing the large rectangular aperture. **D)** Single cell with the remains of the girdle bands from the maternal cell (arrows). **E)** Two sibling valves showing the fusion point of the setae which afterwards diverge in various directions. Note the hyaline rim on the valve edge (arrow). **F)** Intercalary valves from an internal (upper valve) and external (lower valve) view. Note the broken piece of silica from the fusion point between sibling setae (arrow). Scale bars: A = 20 µm; B-D = 10 µm; E-F = 2 µm.

(Figure 3.9.H). The girdle consists of half bands of various shapes arranged to form a zig-zag pattern. The bands are ornamented with very thin and densely distributed transverse costae and perforated by very small irregularly scattered poroids (Figure 3.9.I-J). The single connecting band possess two marked undulations through newly formed setae of the daughter cell protrude (Figure 3.9.K). In specimens from cultures the maternal girdle bands were frequently present surrounding the valves at the level of the aperture or covering the whole valve including the basal part of the setae (Figures 3.8.D, 3.9.L). The terminal valves posses the central process with an externally simple long tube and an internally round hole (Figure 3.9.F,G). The setae are circular in cross-section at the bases with the surface of the basal part perforated with scattered larger round pores with thickened (callous) edges, ca. 0.1 µm in diameter (Figure 3.10.B). Distally after the junction setae are becoming four-sided in cross section with the sides adorned with transverse thickened costae interspaced by two transverse rows of areolae (Figure 3.10.B-C,F). On one side there are 6-8 areolae per transverse row in the middle part of the setae with the number decreasing to 4 per row close to the tip. Longitudinally on the seta side, at each 10–12 areolae or ca. every 1–1.36 µm, one round and slightly larger poroid is found, situated at either end of the areolae row near the seta ridge. After the fusion, the seta ridges are ornamented in succession by 4 different types of projections: 1) 10–21 µm long siliceous capilli (Figure 3.11.A-C) followed by 2) conspicuous 2–7.5 µm long spines denticulate on the inner side of the spine as well as on the ridge, with 12–14 teeth like structures. The tips of these proximal scissor-like spines are extended into capilli measuring to 9–11 µm in length (Figure 3.11.D-G). Further on, 3) the scissor-like spines are the strong dentate ones which are identical to the type 2) in shape and size but without the capilli at their tip (Figure 3.10.A,C) and lastly, distally towards the setae tips, 4) the simple 0.6–0.8 µm long spines are found, the type common for other *Chaetoceros* species (Figure 3.10.D,F). The last three types of spines, except capilli are regularly arranged along the setae edge with the density 12–13 spines in 10 µm. The terminal setae are spineless and perforated with round pores in the part proximal to the valve, and further on the middle and distal part ornamented with the simple spines of type 4) (Figures 3.9.D,3.10.E).

Distinctive features: The orientation of setae in a three-dimensional space. Long tubular process present only on terminal valves and lacking on the intercalary ones. Heavily silicified frustules with many siliceous projections and thickenings. Intercalary setae ornamented with four different conspicuous types of spines: long siliceous capilli, two types of unique scissor-like spines with inner dentate margin of which one extends to a capillus at the tip and strong pointed spines Terminal setae ornamented only with simple spines.

Comments: *C. pseudodichaeta* is easy to be distinguished from the similar species *C. atlanticus* var. *neapolitanus* (Schröder) Hustedt previously recorded from the Adriatic Sea (although not observed in this study). In the latter species all setae are lying in the apical plane, the tubular central process is present on all valves and there is only one type of spine on the setae.

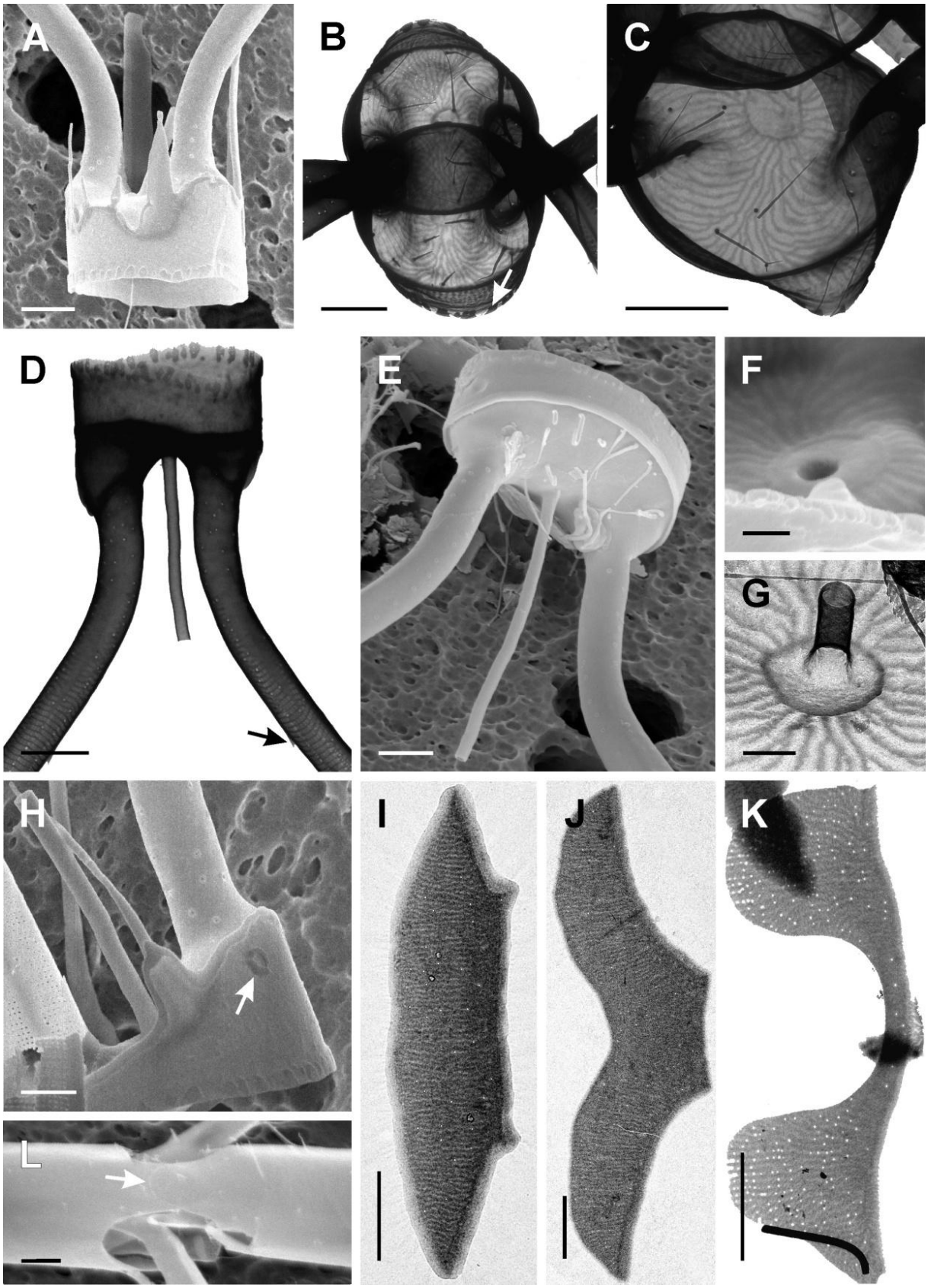
A
B
C
D
E
F
G
H
I
J
K
L

Figure 3.9. SEM **(A,E-F,H,L)** and TEM **(B-D,G,I-K)** micrographs of *Chaetoceros pseudodichaeta* from natural sample **(E)** and cultured material, strain PMFED1 **(A-D, F-L)**. **A)** Valve with silica projections. **B)** Fine structure of two overlaid valves with capilli and thickenings on the valve mantle edge (arrow). **C)** Valve face with the annulus, branching costae and few capilli. **D)** Terminal valve with a long hyaline tubular process. Note the small spines on setae (arrow). **E)** Terminal valve with long tubular process and valve face adorned with capilli. **F)** Detail of an internal view of the terminal valve with the hole-shaped central process. **G)** Detail of an external view of the valve with possibly broken tubular process in central annulus. **H)** Detail of the terminal valve with ellipsoid thickening on the mantle (arrow). **I)** and **J)** Complete girdle bands. **K)** Detail of a connecting band with marked indentation. **L)** Newly formed sibling cells with setae protruding from the indentations on overlapping connecting bands (arrow). Scale bars: A –E, I-K = 2 µm; F-G = 0.5 µm; H = 1 µm.

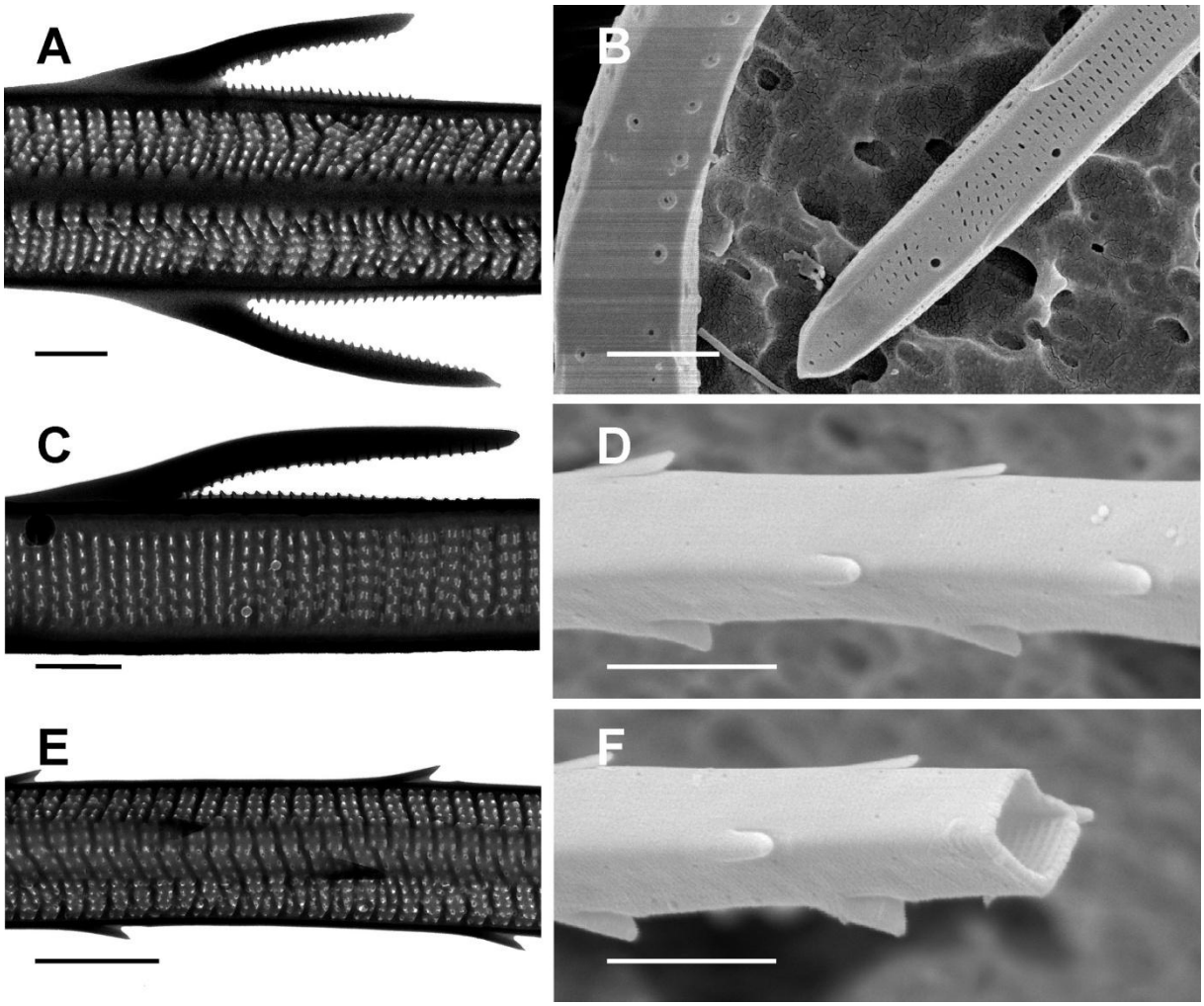

Figure 3.10. TEM **(A,C,E)** and SEM **(B,D,F)** micrographs of *Chaetoceros pseudodichaeta* cultured material, strain PMFED1. **A)** Detail of the seta with type 2) scissor-like spines **B)** Details of two setae, left is the basal part perforated with round poroids with thickened edge and right is the setae tip with transverse rows of areolae and costae, larger poroids and type 4) spines. **C)** Detail of a seta with type 3) scissor-like spine. **D)** Detail of a seta with type 4) spines **E)** Detail of the terminal seta with common spines. **F)** Quadragonal cross-section of a seta. Scale bars: A-B,E= 1 µm; D,F = 2 µm, C= 0.5 µm.

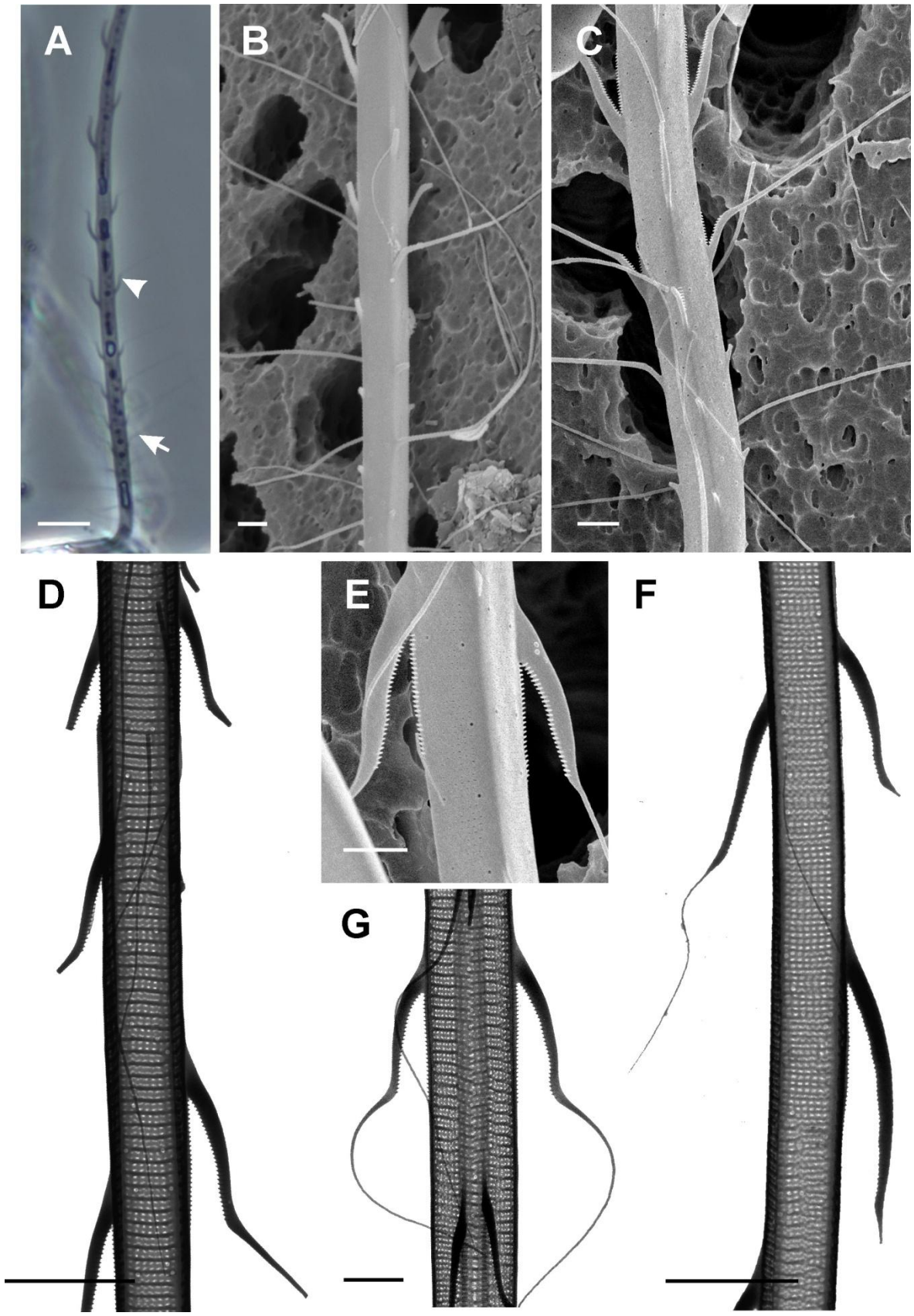

Figure 3.11. LM **(A)**, SEM **(B-C,E)** and TEM **(D,F-G)** micrographs of *Chaetoceros pseudodichaeta* from natural sample **(A)** and cultured material, strain PMFED1 **(B-G)**. **A-C)** Part of the seta proximal to the valve with type 1) spines-capilli (arrow) and type 2) dentate spines with tips extended to capilli (arrowhead). **D)** Detail of the seta with type 2) scissor-like spines. Scale bars: A = 10 µm; B-C, E, G = 1 µm; D,F = 2 µm.

3.1.2.1.9 Chaetoceros rostratus Lauder (1864)

(Figures 3.7.E-H, 3.12. - 3.13.)

Bibliography: Hustedt (1930), Giuffrè and Ragusa (1988), Rines and Hargraves (1988), Hernández - Becerril (1996), Hernández - Becerril and Flores Granados (1998), Shevchenko et al. (2006), Sunesen et al. (2008)

Synonyms: *C. glandazi* Mangin

Description: a.a.: 10 - 22 µm (Hustedt: 10 - 35 µm; Rines and Hargraves: 12 - 37 µm; Hernández - Becerril: 9 - 20 µm; Shevchenko et al.: 15 - 25 µm; Sunesen et al.: 14.5 - 17 µm); p.a.: 16–48 µm (Hernández - Becerril: 22 - 34 µm; Shevchenko et al.: 10 - 35 µm)

LM: The chains are robust, straight and short, usually composed of two to five cells or the species occasionally can be seen as single cells. Cells in valve view elliptical to round and in girdle view rectangular with more or less rounded corners. Cells and setae contain numerous plastids (Figure 3.12.B). Valve face slightly to strongly convex, mantle high with a visible constriction near the margin, girdle low to equidimensional with the mantle (Figure 3.7.F) The unique character in this species is that the cells are held together by a fusion of particular central linkage process (linking spine) between sibling valves and not by the setae crossing (Figures 3.7.E,F,H). Very long, straight and thick setae originate close to the valve margin and diverge perpendicular to the chain axis (Figure 3.12.A). In the same intercalary cell the two valves are twisted about 60° between them so the setae arise without touching the corresponding sibling setae on the neighbouring valve. In valve view, the sibling setae belong to the Brunel Group II (Figure 3.7.G). Resting spores not observed.

EM: Highly silicified valves are perforated by round poroids irregularly scattered across the valve face, mantle and setae bases (Figure 3.12.D-E). The valve face is ornamented with a dense branching costae pattern radiating from the eccentrically positioned annulus and when reaching the mantle edge running parallel to the pervalvar axis until the abvalvar mantle margin (Figures 3.12.E, 3.13.C). The linking spines are hollow, conically shaped with the pointed end (Figure 3.12.D). The spines are of variable length and can become very short and wide in culture but in natural material they are usually long and narrow. Their surface is completely smooth and may be perforated with a few poroids at the base (Figure 3.12.D). The terminal valve lacks the linking spine. The process is present in each valve and it is positioned slightly eccentric to one side of the spine (Figures 3.7.H and 3.13.A-B). The process is the simple slit on the internal side (Figure 3.12.E,F) and on the external side there is a small protuberance (Figure 3.13.A) or a short flat tube (Figure 3.7.H) sometimes very prominent especially at terminal valves (Figure 3.13.B). The setae are circular in cross-section at the bases but later become four-sided with rows of spines along each edge (Figure 3.13.F,G). The ornamentation pattern on the setae at their bases consists of the clusters of areolae separated by short narrow but thick transverse ribs and by larger longitudinal ribs that further away fuse into the setae edges (Figure 3.13.C). Distally, when the setae become quadrangular, the pattern on the side wall is composed of five transverse rows of areolae between two transverse thickened costae. After each 4 - 9 costae there is

often one larger round poroid located near to the ridge and close to the costae on either side of the areolae rows (Figure 3.13.E).

Distinctive features: Sibling cells interconnected with central linking spine of variable length. Setae four-sided with side-wall ornamented with thick transverse costae interspaced with five areolae rows.

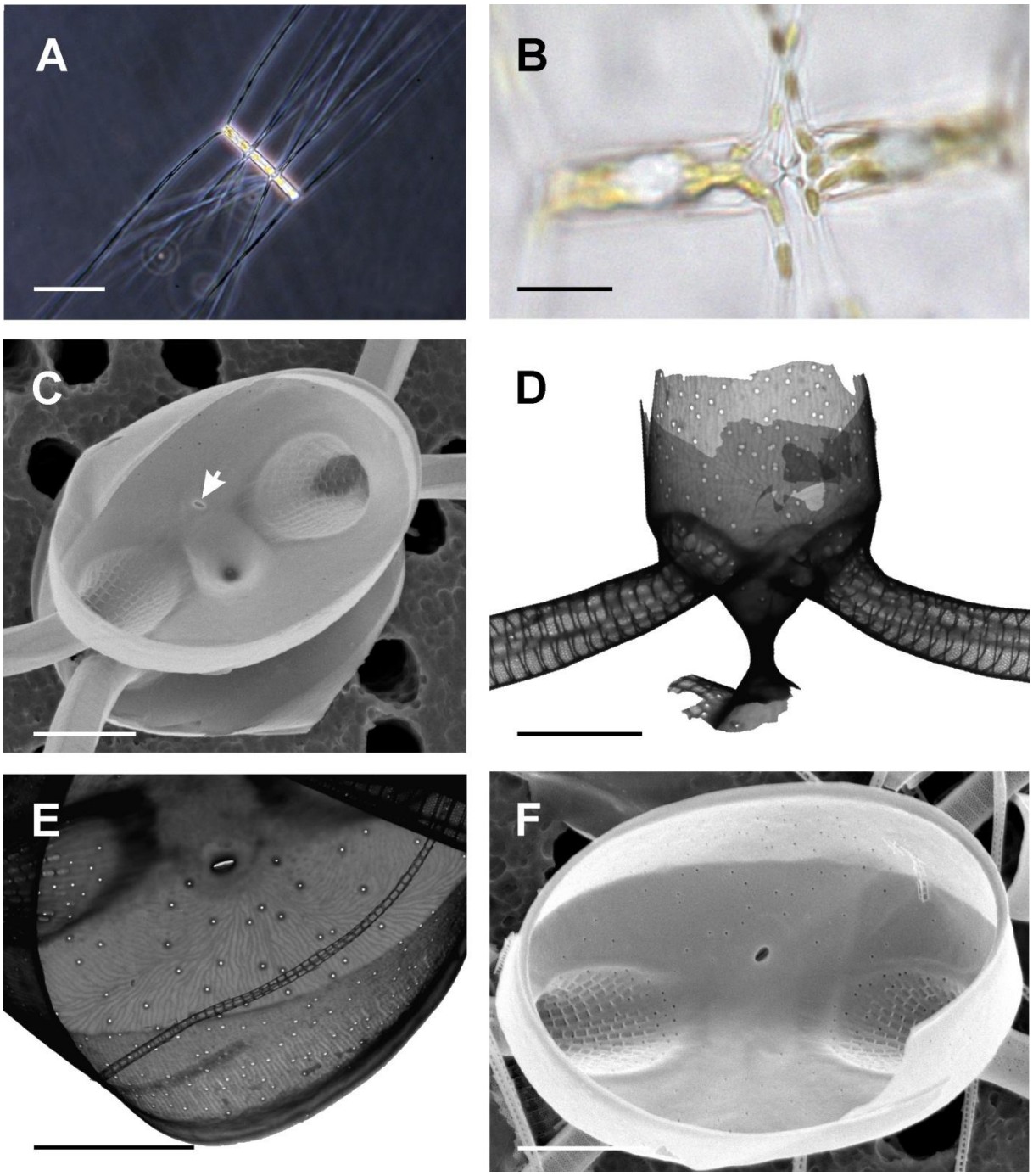

Figure 3.12. LM **(A-B)**, SEM **(C,F)** and TEM **(D-E)** micrographs of *Chaetoceros rostratus* from culture material, strain PMFR4. **A)** The complete chain. **B)** Two intercalary cells in the girdle view, showing the presence of the chloroplasts in the cell body and setae. **C)** Internal view of the intercalary valve showing the conical hole of the linking spine and the slit-like eccentric process. **D)** Intercalary valve in girdle view showing its fine structure with the mantle perforated with poroids and smooth surface of the linking spine. **E)** and **F)** Internal view of the terminal valve showing the slit-like eccentric process and the ornamentation of the valve face, mantle and setae bases. Scale bars: A = 20 µm; B = 10 µm; C-F = 5 µm.

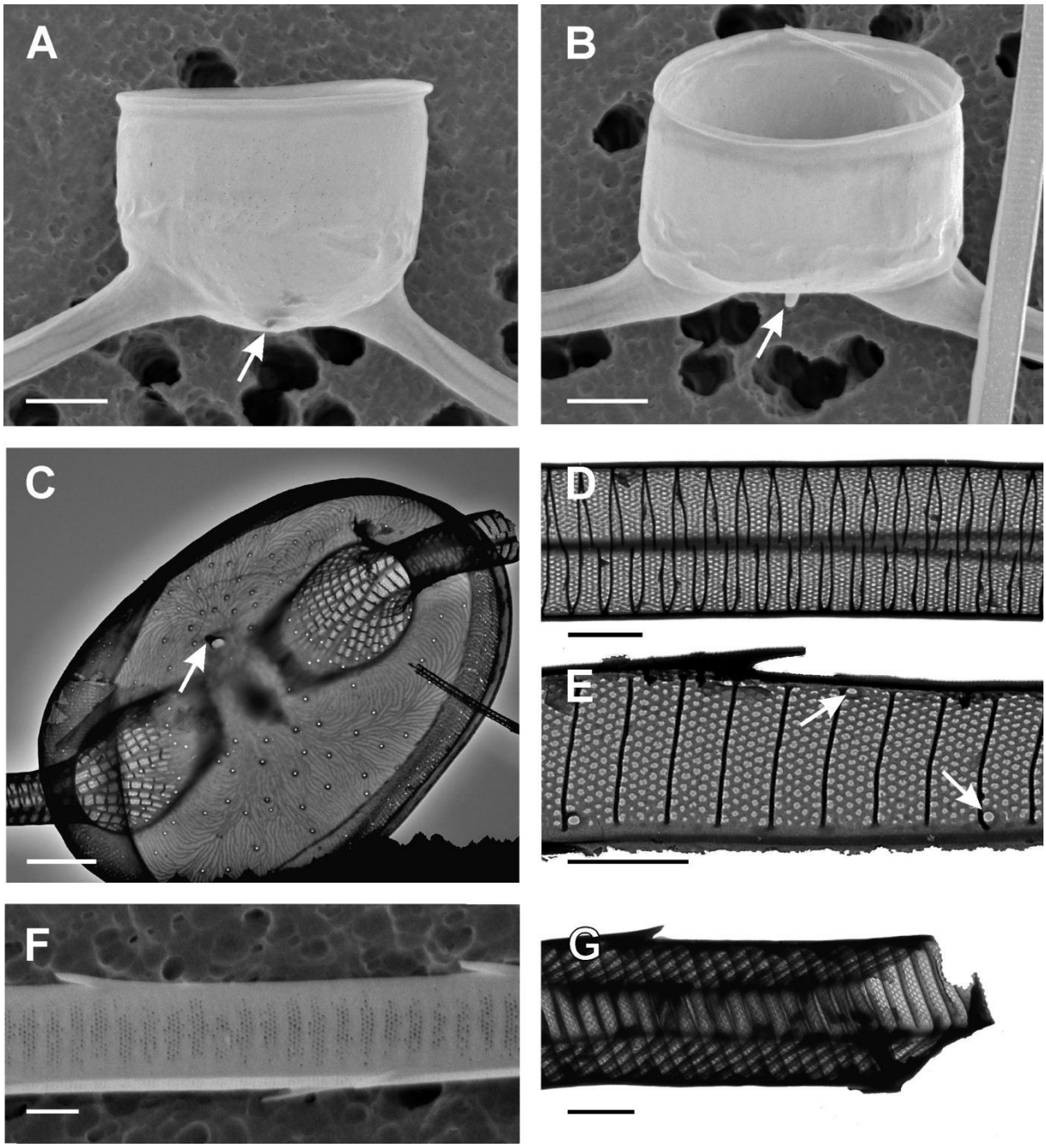

Figure 3.13. SEM **(A-B, F)** and TEM **(C-E,G)** micrographs of *Chaetoceros rostratus* from culture material, strain PMFR4. **A)** External view of the terminal valve with the process visible as a small prominence (arrow). **B)** External view of the terminal valve with the short tube-like process (arrow). **C)** External view of the terminal valve showing the small tube-like eccentric process (arrow) and the fine structure of the valve face, mantle and the bases of the setae. **D)** Detail of the spineless part of the setae proximal to the valve. **E)** Detail of a seta showing the ornamentation of the side wall with larger poroids on either side of the areolae rows (arrows). **F)** Detail of the seta. **G)** Quadragonal section through seta. Scale bars: A- B = 5 µm; C = 2 µm; D-G = 1 µm.

3.1.2.1.10 Chaetoceros tetrastichon Cleve (1897)

(Figure 3.14.)
Bibliography: Hustedt (1930), Cupp (1943), Hernández - Becerril (1992)
Description: a.a.: 14 – 18 µm (Hustedt: 10 µm; Cupp: 18 – 20; Hernández - Becerril: 15 - 38 µm); p.a.: 7 – 20 µm (Hernández - Becerril: 12 - 28 µm)

LM: Chains are heteropolar, straight and short, usually composed of two to three cells (Figure 3.14). Numerous chloroplasts are present in the cell body and the setae. Cells in girdle view rectangular and in valve view elliptical. Long and thick setae are originating at the valve corners and immediately cross each other without a basal part hence the apertures are either extremely narrow. The valve face is flat, the mantle is high with sometimes a visible constriction near the suture. After the crossing point the setae run shortly almost perpendicular to the pervalvar axis but soon strongly curve towards it becoming almost parallel with the chain axis. One pair of setae generally curves more strongly and may be attached to a tintinnid (Figure 3.14.A). All setae are curved in the same direction, towards the posterior end of the chain (Figure 3.14.).

Distinctive features: All setae are curved towards the posterior end of the chain.

Comments: *Tintinnus inquilinius* attached to a chain. On similar species see comments on *C. dadayi.*

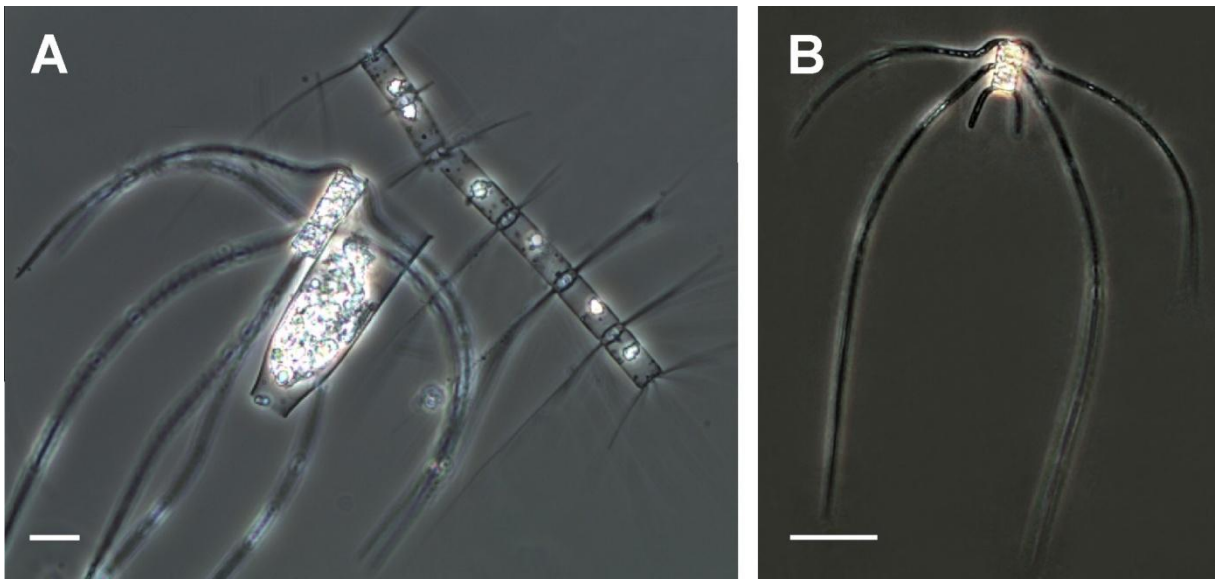

Figure 3.14. LM micrographs of *Chaetoceros tetrastichon* from field material. **A)** Chain with a tintinnid *Tintinnus inquilinius*. On the image is also the chain of *Bacteriastrum furcatum.* **B)** Chain of two cells with the broken terminal setae without the tintinnid. Scale bars: A = 20 µm; B = 50 µm.

3.1.2.2 Subgenus Hyalochaete *Gran (1897)*

Generally not heavily silicified species, variable in size, many delicate and fragile forms. One, two or more chloroplasts present only in the cell body. Cells solitary or united in chains by holding of setae, fusion of the protuberances of the valve and setae, by a siliceous bridge between setae and the most common, by a true setae fusion. Setae usually relatively thin and fragile, lacking true plastids, mostly circular in cross-section and in few cases polygonal, in all species observed within this study ornamented with spines except in *C. vixvisibilis*. Terminal setae often differentiated in structure and orientation with respect to intercalary ones, in few species also present special intercalary setae. The valve face has an annulus from which radiates a pattern of weak or strong costae and it is often perforated by poroids. One or more processes are generally present only on terminal valves, lacking in all intercalary valves and in some species (*C. amanita*) in all valves. The process is central or eccentric, circular, slit-like or a hole with a true labiate structure inside. The resting spores present in the majority of the species.

3.1.2.2.1 Chaetoceros affinis Lauder (1864)

(Figures 3. 15. - 3.17.)

Bibliography: Hustedt (1930), Cupp (1943), Evensen and Hasle (1975), Rines and Hargraves (1988), Hernández - Becerril (1996), Jensen and Moestrup (1998), Berard-Therriault et al. (1999), Shevchenko et al. (2006), Sunesen et al. (2008), Kooistra et al. (2010), Ishii et al. (2011)

Synonyms: *Chaetoceros javanicus* Cleve, *Chaetoceros ralfsii* Cleve, *Chaetoceros schüttii* Cleve, *Chaetoceros angulatus* Schütt, *Chaetoceros distichus* Schütt, *Chaetoceros procerus* Schütt, *Chaetoceros paradoxus* var. *schüttii* Schütt, *Chaetoceros clevei* Peragallo, *Chaetoceros raflsii* Karsten, *Chaetoceros schüttii var. genuina* Meunier, *Chaetoceros najadianus* Schussnig; *Chaetoceros adriaticus* Schussnig

Description: a.a.: 9 - 42 µm (Hustedt: 9 – 30 µm; Cupp: 7 - 27 µm; Rines and Hargraves: 20 µm; Hernández-Becerril: 18 - 25 µm; Shevchenko et al.: 10 - 30 µm; Sunesen et al.: 16 - 27 µm); p.a.: 8 - 16 µm (Hernández - Becerril: 10 - 22 µm; Shevchenko et al.: 20 - 30 µm)

LM: The cells united in usually short and straight chains (Figure 3.15.A-B). Each cell contains a single large chloroplast in a shape of a parietal plate around the girdle (Figure 3.15.B). The valve surface is concave and the valve corners are sharp and slightly drawn up. Valve mantle is high and often with a visible constriction near the margin (Figure 3.15.D-E), girdle low. Intercalary setae are thin, originating from the valve apices and almost immediately cross each other at the chain margin. Apertures are rather narrow but usually distinct in LM, slit-shaped to elliptical. Setae are very straight, in girdle view directed perpendicular to the chain axis and in valve view belonging to Brunel group I/II. Terminal setae can be similar or can differ very strongly from the intercalary ones, in both orientation and morphology. When different, they are much thicker and taper towards the end, strongly diverging in a broad V-or U-shaped curve towards the end of the chain, lying in the apical plane (Figure 3.15.A-B). The resting spores have unevenly vaulted valves with a broad distinct mantle. Primary valve is dome-shaped, ornamented with numerous short spines whereas in secondary valve

the central inflated part is somewhat higher and more strongly curved with the distinct edge, also it is ornamented with few longer spines (Figure 3.17.A,C,E).

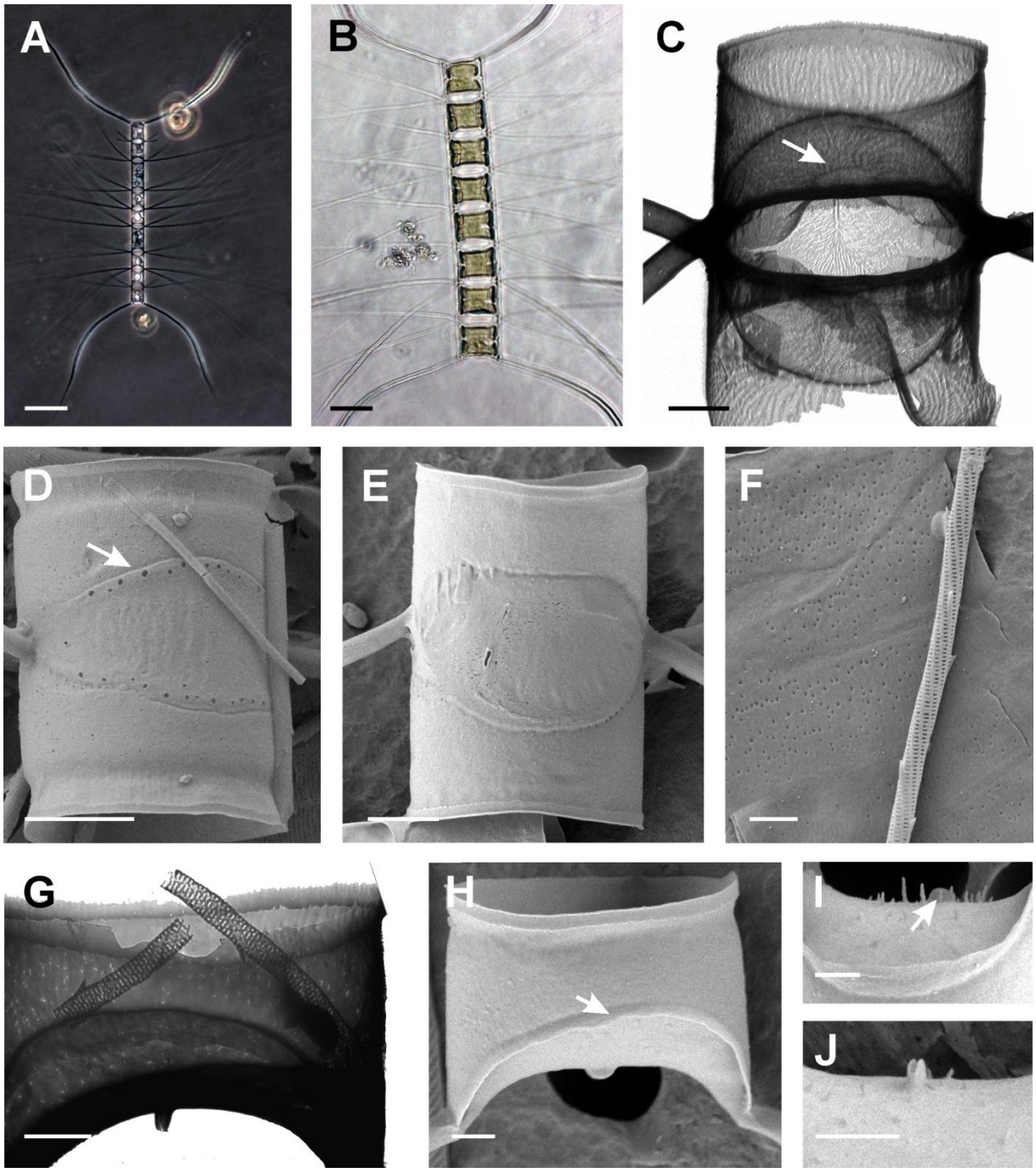

Figure 3.15. LM **(A-B)**, TEM **(C,G)** and SEM **(D-F, H-J)** micrographs of *Chaetoceros affinis* from natural samples **(A,B,D)** and culture material, strains PMFE1 **(C,E-H)** and PMFC2 **(I,J)**. **A)** The complete chain. **B)** The complete chain. Note one parietal chloroplast per cell positioned around the girdle. **C)** Two sibling valves in girdle view showing the complete silica flap in the back and ruptured in the front side. Arrow indicates central annulus. **D)** Two sibling valves with silica flap covering the aperture. Note the row of pores on the point of fusion with the marginal ridge. **E)** Two sibling valves with silica flap covering the aperture. **F)** Girdle bands ornamented with transverse rows of costae and perforated with poroids. **G)** Terminal valve perforated with poroids and beak-like labiates central process **H)** Terminal valve showing hyaline rim on the marginal ridge (arrow) with central process in the shape of flattened tube. I**)** Detail of the terminal valve with short capilli and tube-like process (arrow). J**)** Detail of the terminal valve with short capilli and beak-like process. Scale bars: A = 50 µm; B = 20 µm; C,G = 2 µm; D-E = 5 µm; F,H-J = 1 µm.

EM: The valves have pattern of dichotomously branching costae radiating from a round central annulus and are additionally perforated with numerous irregularly shaped very small poroids (Figure 3.15.C). The marginal ridge is ornamented with a hyaline rim (Figure 3.15.H). The aperture appears in the EM very often completely occluded by a thin silica wall with no distinct pattern (silica flap), except of the single row of pores on its edge where it fuses with the marginal ridge. It is not clear if it represents an extension of the hyaline rim, or the rim is enclosed within this structure (Figure 3.15.D-E). The silica flap is very fragile and may be ruptured, and it is not to be confused with the maternal girdle bands which can sometimes in *Chaetoceros* species cover the aperture between newly formed valves. The girdle bands have the fine structure of transverse costae and striae with small poroids (Figure 3.15.F) while the flap appears completely smooth. Terminal valves possess a central process and sometimes are ornamented with a few short capilli covering the valve face in the central part (Figure 3.15.I). The process is found to be very variable in morphology, even within the same clonal strain. In the internal view it is usually a slit-shaped opening with the external part ranging from beak-like labiate structure to a wide, short, flattened tube (Figure 3.15.G,J). Intercalary setae are circular in cross-section (Figure 3.16.G). They are composed of the longitudinal silica strings arranged in a helicoidal/spiral pattern along the setae length and interconnected with transverse silica bars (Figure 3.16.H). The longitudinal strings are ornamented along their length with small spines following the spiral arrangement around the setae. The width of the strings is very variable depending on the degree of the silification of the setae. The basic design is apparent in the weakly silicified setae (Figure 3.16.C) and where the strings and bars are thicker; the space between bars corresponds to usually described spiral row of small poroids/areolae. More heavily silicified setae have few additional elongated pores irregularly distributed along the seta length (Figure 3.16.C,D). Two types of terminal setae were observed: thin ones, structurally identical to the intercalary setae, and thicker ones which appear polygonal due to the longitudinal strings becoming very thick and fusing between each other. In this case the rows of small poroids disappear and only the elongated pores are present. The strings can either remain in spiral pattern (Figure 3.16.A,B) or extend parallel to the seta axis (Figure 3.16.C,D). The thick setae have stronger spines as well as elongated pores (Figure 3.16.A,B). The surface of the resting spores is covered with knobs and spines which are simple or with the dichotomously branching end (Figure 3.17.G). The mantle of secondary valve possess one single row of puncta (Figure 3.17.D,F).

Distinctive features: Narrow apertures, often completely occluded by a thin silica flap observable only in EM. Intercalary setae straight, all setae lie in the apical plane. Terminal setae often thicker and composed of longitudinal strings oriented parallel with seta axis, more curved than intercalary ones. Resting spores with numerous long spines. Process variable in shape but often a tube with beak-like end.

Comments: *C. affinis* appears to be a very variable species in terms of morphology, particularly in regards to ultrastructural features such as presence of capilli on terminal valve surface or shape of the

external part of the central process. It is possible that the observed Adriatic morphotypes actually represent several species within the *C. affinis* complex and further investigations are required to resolve this issue. The variety *C. affinis* var. *willei* is by some authors distinguished from the type on the basis of having thin terminal setae. However this character appears to be very variable in observed specimens, and robustness of terminal setae fast disappears when species is introduced in culture, therefore we did not this variety as a valid taxon.

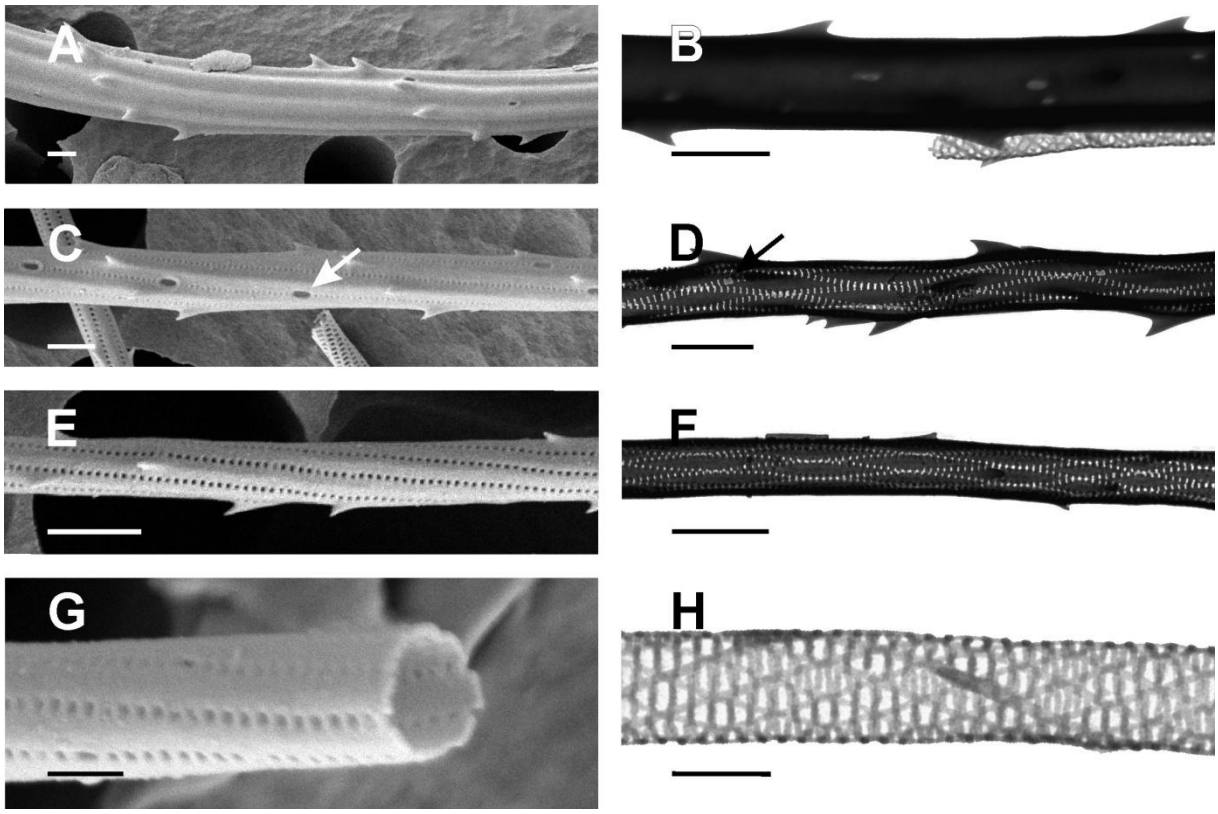

Figure 3.16. SEM **(A,C,E,G)** and TEM **(B,D,F,H)** micrographs of *Chaetoceros affinis* from culture material, strains PMFE1 **(B-H)** and PMFC2 **(A)**. **A)** and **B)** Detail of thick terminal seta with longitudinal strings parallel with the seta axis. **C)** and **D)** Detail of thick terminal seta with spiral arranegment of the strings. **E)** and **F)** Detail of intercalary seta. **G)** Circular cross-section of the intercalary seta. **H)** Detail of thin intercalary seta. Scale bars: A-F,H = 1 µm; G = 0.5 µm.

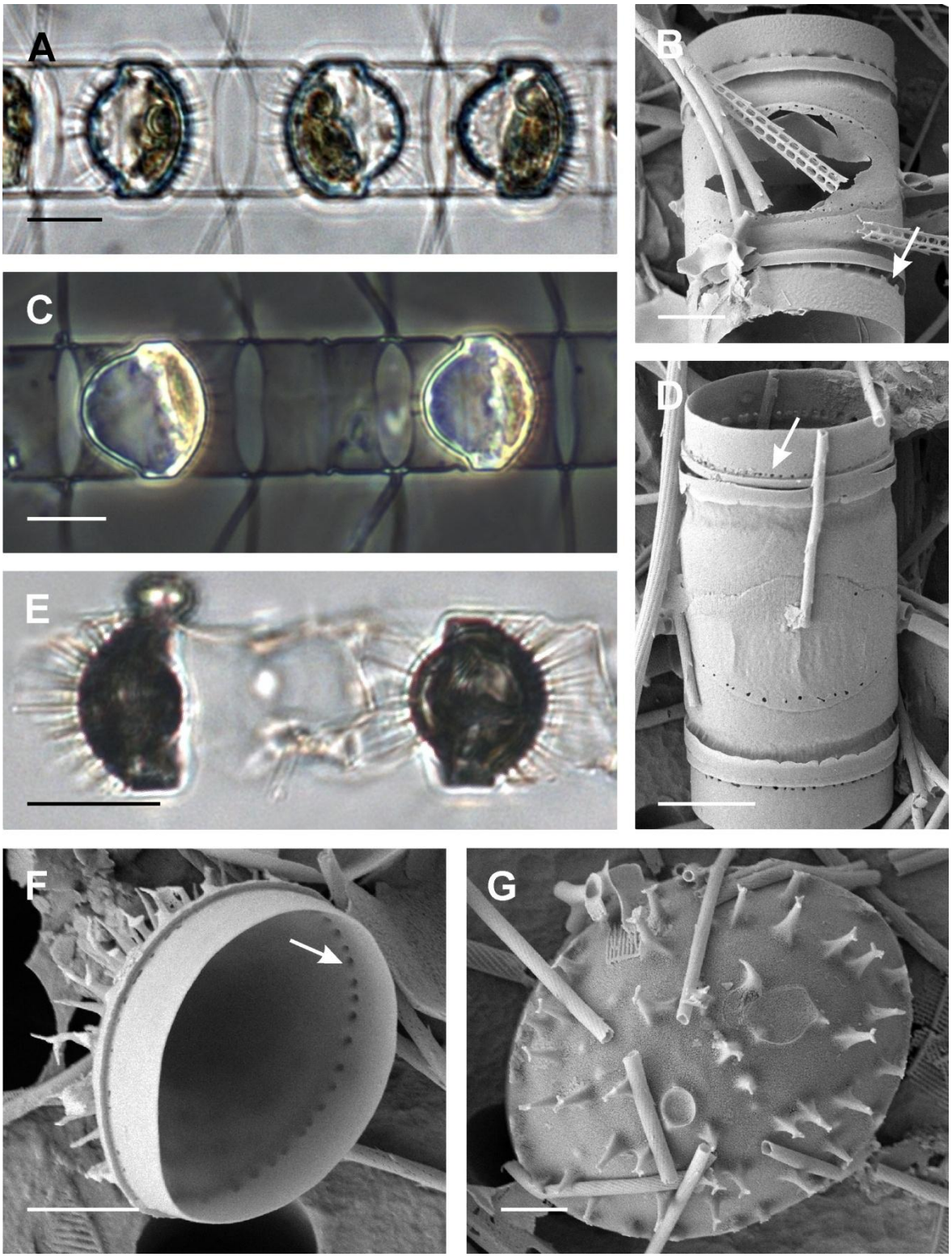

Figure 3.17. LM **(A,C,E)** and SEM **(B,D,F,G)** micrographs of *Chaetoceros affinis* resting spores from natural samples **(A,B,D)**. **A)**,**C)**,**E)** Resting spores within the parental cells. **B)** Sibling valves with the primary valve ofthe resting spore still remained attached within the valve. Note the spines on the valve surface (arrow). **D)** Sibling valves with the secondary valves of the resting spores. Note the single ring of puncta on the advalvar margin of the mantle (arrow). **F)** The secondary valve of the resting spore with the dichotomously branching and simple long spines on the surface. Arrow shows the single ring of puncta on the advalvar margin. **G)** Valve view on the resting spore (not certain if primary or secondary valve) showing surface covered with knobs and dichotomously branching spines. Scale bars: A = 20 µm; C,E = 10 µm; B,D = 5 µm; F,G = 2 µm.

3.1.2.2.2 Chaetoceros amanita Cleve – Euler (1915)

Figure 3.18.

Bibliography: Kaczmarska et al. (1985), Rushforth and Johansen (1986), Rines and Hargraves (1988), Castillo et al. (1992) (as *C. wighamii*)

Synonyms: *Chaetoceros wighamii* Brightwell

Description: a.a.: 14 - 26 µm (Kaczmarska et al.: 18-40 µm; Rushforth and Johansen: 10-15 µm; Rines and Hargraves: 15-20 µm); p.a.: 8 - 15 µm (Kaczmarska et al.: 10-20 µm; Rushforth and Johansen: 8-20 µm)

LM: Chains usually short and straight, composed of 4-7 cells (Figure 3.18.A-B). Cells cylindrical, in girdle view rectangular with sharp cell corners and pervalvar axis often shorter than the apical axis. In valve view cells are elliptical. Each cell contains a single large chloroplast in a shape of a parietal plate extending from valve to valve (Figure 3.18.C). The valve face is flat, sometimes with a central inflation which is usually more visible on the terminal valves. Valve corners sharp. Valve mantle is low with a very slight constriction near the margin. The girdle is usually equidimensional with the mantle. Intercalary setae are thin, originating from the valve apices and without the basal part (Figure 3.18.B-C). Apertures are slit-shaped and very narrow. Intercalary setae are very long and straight, diverging in various directions, some perpendicular but more often they extend at a certain angle to the chain axis (Figure 3.18.A). In most cases sibling setae diverge from each other at an angle of 90° belonging to Brunel Group III (Figure 3.18.D), but in the same chain they can also diverge equally from the apical plane at an angle 20-30° conforming to Brunel Group II. Terminal setae have the same morphology as intercalary ones but they are oriented more parallel to the chain axis, diverging in a broad V -shaped curve towards the end of the chain (Figure 3.18.A).

EM: The valve is ornamented with very densely distributed thick anastomosing ribs spreading from a irregularly shaped hyaline area positioned slightly eccentrically on the valve which does not seem to correspond to the annulus otherwise typical for *Chaetoceros* species (Figure 3.18.F-G). There is no process either on intercalary nor on terminal valve (Figure 3.18.E,H-I), and the outer surface of the terminal valve is ornamented with minute spines (Figure 3.18.I-J). In all valves the marginal ridge is ornamented with high hyaline rim. In intercalary valves, the aperture between sibling cells is partially occluded at the aperture margin by silica flaps appearing to project from a hyaline rim (Figure 3.18.E). The rim observed on the terminal valves appears ornamented with small round pores (Figure 3.18.J), however, we cannot exclude the possibility that the observed structure in this specimen were actually remains of the girdle band. The setae are circular in cross-section, composed of thick longitudinal strings arranged in spiral pattern and interconnected with very short transverse bars (Figure 3.18.K-L). The strings are ornamented with densely distributed somewhat strong spines following a helicoidal pattern.

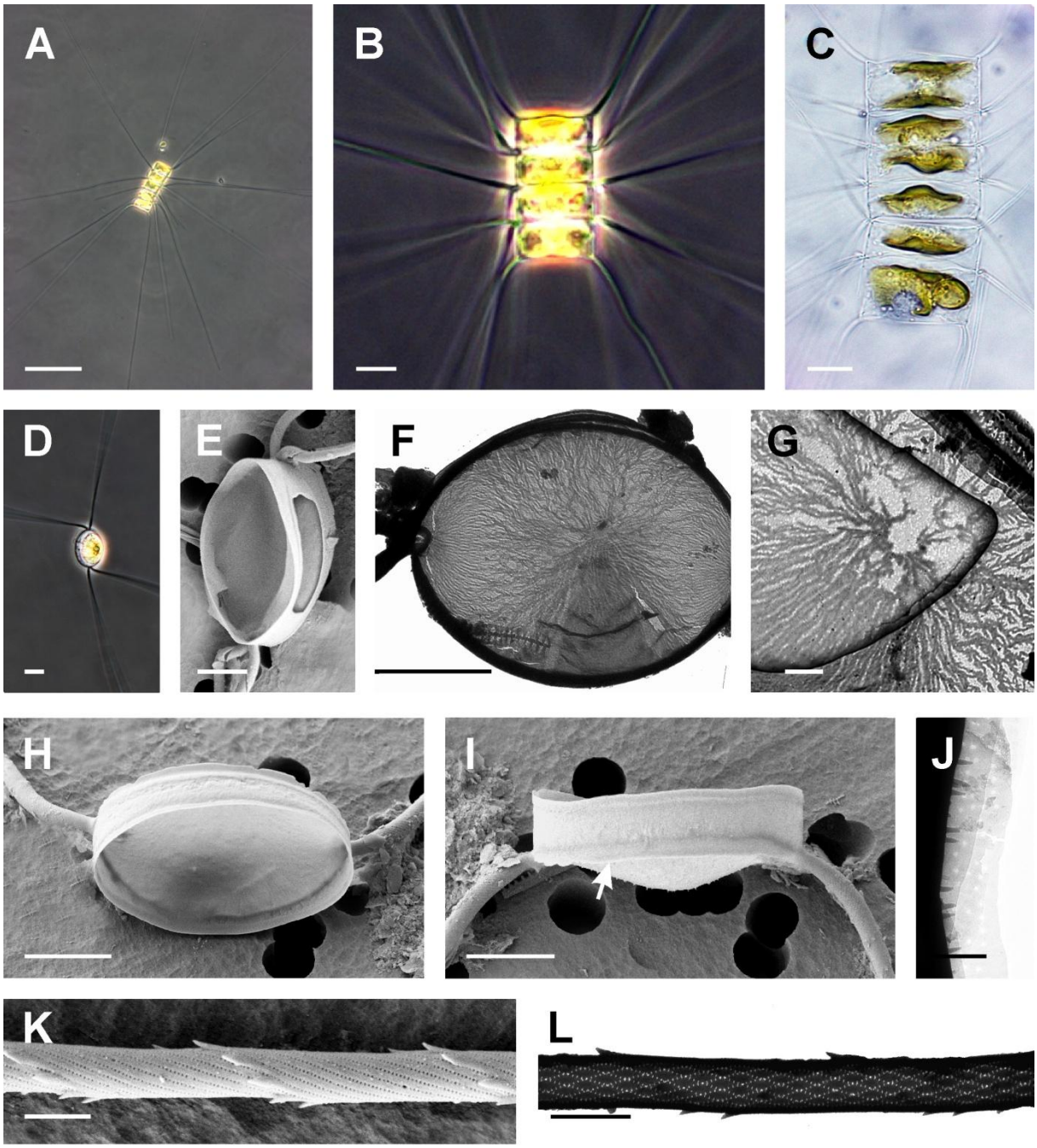

Figure 3.18. LM **(A-D),** SEM **(E,H,I,K)** and TEM **(F,G,J,L)** micrographs of *Chaetoceros amanita* from cultures, strain PMFM1. **A)** The complete chain showing orientation of the setae. **B)** The four-celled chain. **C)** Cells with one parietal chloroplast per cell extending from valve to valve. **D)** Sibling valves in valve view with setae diverging from each other at an angle of 90°, belonging to Brunel Group III. **E)** Two sibling valves with silica flap partially occluding the aperture. **F)** Two overlapped sibling intercalary valves showing the valve pattern with anastomosing ribs. **G)** Detail of the valve with the irregularly shaped hyaline eccentric area. **H)** Internal view of the terminal valve. **I)** Terminal valve in girdle view showing the minute spines on its surface and the hyaline rim extending from the marginal ridge (arrow). **J)** Detail of the terminal valve with minute spines and the structure corresponding to girdle band/rim. **K)** Detail of a seta with spirally positioned spines. **L)** Detail of a seta. Scale bars: A = 50 µm; B-D = 10 µm; E,F,H,I = 5 µm; G,K,L = 1 µm; J = 0.5 µm.

Distinctive features: Freshwater species. Long, stiff and straight setae projecting in various directions. Valve has a peculiar pattern with densely distributed anastomosing ribs without a distinct annulus. There is no process on either intercalary or terminal valves. Spines closely arranged in a helicoidal pattern around the seta.

Comments: *Chaetoceros amanita* is a very rarely reported taxon with disjunct geographical distribution, and it is a single freshwater species observed within this thesis with the cultured strain isolated from Vransko lake. The relationship with the taxon *C. wighamii*, an euryhaline species with very similar resting spore morphology, is controversial. *C. wighamii* is reported to be a eurihaline species with very variable morphology of both vegetative cells and resting spores which was described from the cold brackich waters. The morphotype observed within this study corresponds to the description of vegetative cells in Kaczmarska et al. (1985), though the isolated strain did not form resting spores they are found in the sediments from the same lake, and we refer to the observed morphotype as *C. amanita*. The resting spores of *C. amanita* have dissimilar valves with dome-shaped primary valve, surface covered with spines, high valve mantle and distinct marginal ridge. The secondary valve is shaped as a truncated cone which is considerably narrower in diameter than the primary valve (Kaczmarska et al. 1985).

3.1.2.2.3 Chaetoceros anastomosans Grunow in Van Heurck (1882)

Figure 3.19.

Bibliography: Hustedt (1930), Cupp (1943), Hernández-Becerril and Flores Granados (1998), Hernández-Becerril and Aké-Castillo (2001), Shevchenko et al. (2006)

Synonyms: *C. anastomosans* var. *speciosa* Schutt, *C. anastomosans* var. *genuina* Cleve-Euler, *C. externus* Gran, *C. anastomosans* var. *externa* (Gran) Hustedt

Description: a.a.: 8 – 10 µm (Hustedt: 9 - 30µm, Cupp: 8 - 10 µm, Hernández - Becerril and Flores Granados: 14 - 23 µm, Hernández-Becerril and Aké-Castillo: 9 - 15 µm Shevchenko et al.: 10 - 16 µm); p.a.: 5 – 14 µm (Hernández-Becerril and Aké-Castillo: 10 - 12 µm, Shevchenko et al.: 10 - 20 µm)

LM: The cells are united in usually long, straight to slightly curved chains (Figure 3.19.A). In girdle view cells are nearly squared to rectangular with the rounded valve corners (Figure 3.19.B), and in valve view elliptical (Figure 3.19.F). There are two chloroplasts per cell, positioned near the valves. The valve face is flat or slightly concave, sometimes slightly convex. Valve mantle is low with a very slight constriction near the margin. The mantle is equidimensional with the girdle (Figure 3.19.B). The thin and delicate setae originate from the valve corners. Intercalary setae can diverge in various directions, but in general they bend at right angles or extend perpendicular to the chain axis. In the valve view they belong to Brunel Group II (Figure 3.19.D). The mean of connection between sibling cells is by the siliceous cross-bridge of variable length which joins sibling setae at a short distance from the valves (Figure 3.19.B,D). Therefore, the sibling valves do not touch and the wide apertures have an unusual, octagonal shape, elongated in the apical direction (Figure 3.19.B). The terminal setae diverge obliquely towards the chain axis becoming almost parallel with it, forming U-shape. In cultures, the Alcian Blue stained material in form of the sheath surrounded the cells in chains with the setae protruding from the sheath borders (Figure 3.19.C). This are most likely the extracellular polymeric substances (mucus) produced by the cells which remained around the colonies but the actual structure of this material was not investigated in details in this study.

EM: The lightly silicified valves have a relatively large central annulus from which dichotomously branching costae radiate toward the valve margins, extending on the mantle (Figure 3.19.H). The marginal ridge is ornamented with a hyaline rim often extended in short projections in a pervalvar direction (Figure 3.19.E,I). The setae are circular in cross-section, composed of longitudinal silica strings arranged in a spiral pattern and interconnected with short transverse bars (Figure 3.19.L).The setae are additionally perforated with elongated poroids randomly distributed along their length (Figure 3.19.H). The setae also have minute spines running spirally throughout (Figure 3.19.L). The cross-bridge seems to be a hyaline structure fused on the setae surface (Figure 3.19.H). The central slit-shaped process is present only in terminal valves (Figure 3.19.K).

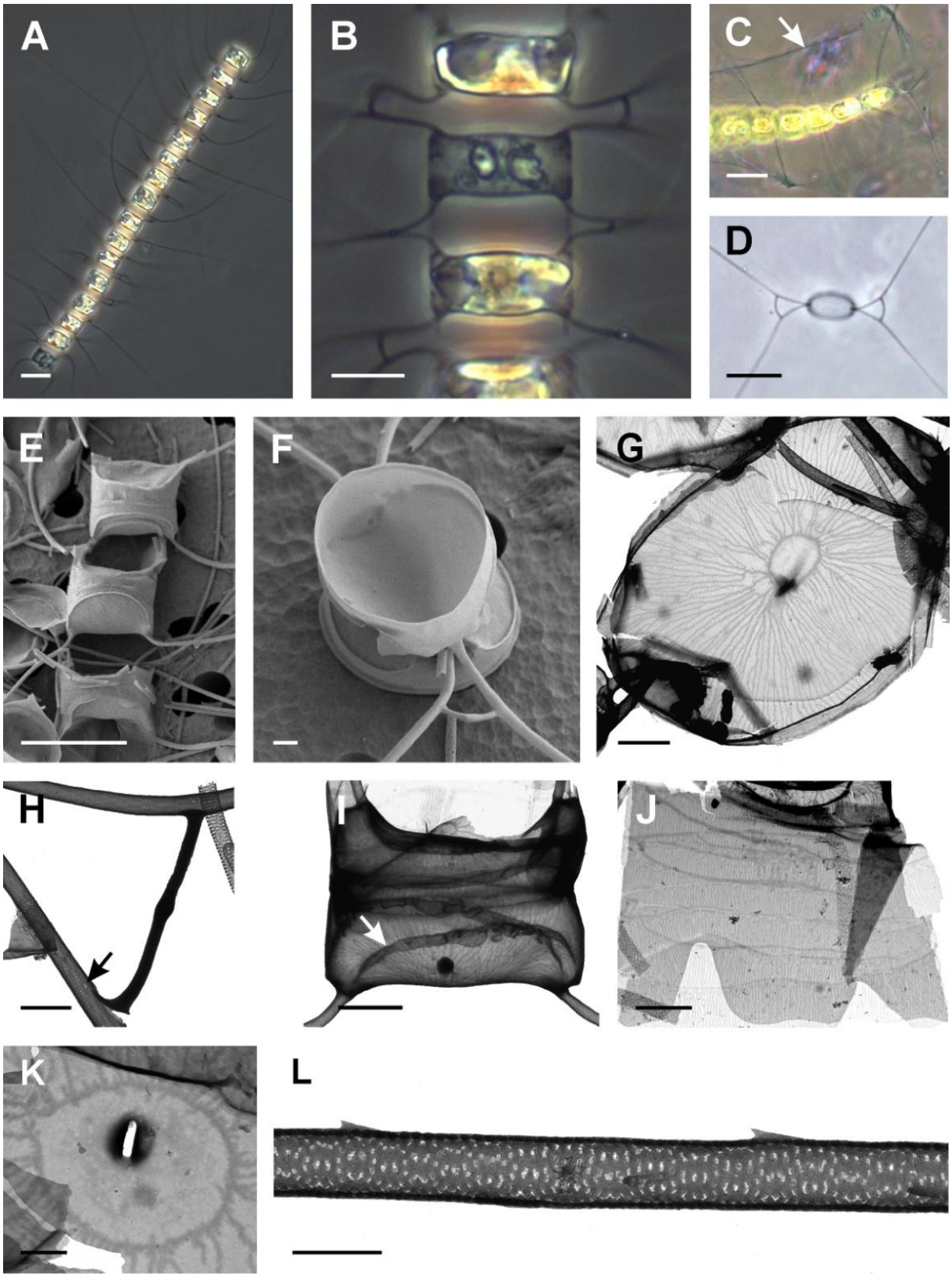

Figure 3.19. LM **(A-D),** SEM **(E,F)** and TEM **(G-L)** micrographs of *Chaetoceros anastomosans* from culture material, strains PMFAN1 **(E-G,I-L)** and PMF AN2 **(A-D,H). A)** Complete chain. **B)** Middle part of a chain showing a cross-bridge connection between sibling cells and the wide octagonal aperture. **C)** Alcian Blue stained mucus sheath extruded by the cells, with clearly defined borders (arrow) and setae protruding from it. **D)** Sibling valves in valve view showing divergence of the setae belonging to Brunel group II. **E)** Middle part of the chain **F)** Sibling valves in valve view.

Distinctive features: Cells connected in chains by a hyaline structured cross-bridge of variable length which joins sibling setae at a short distance from the valves.

Comments: Resting spores were not observed in this study; however they are reported to have equal convex valves and either with spines or smooth. Some authors such as Hustedt (1930) distinguish *C. anastomosans* var. *externa* from the type on the basis of length of the cross-bridge which is supposed to be shorter in this variety than in the type species. The results from this study show that the cross-bridge length within the same chain in cultured strains varied between 1 and 7 µm and we consider that there is no sufficient evidence to consider this character as important in recognizing the separate variety and therefore it is considered as a synonym of the species *C. anastomosans*.

Figure 3.19. continued

G) Valve face showing large central annulus and dichotomously branching costae. **H)** Cross-bridge between sibling setae, note its hyaline structure and the place where it is broken from setae wall. Arrow shows the elongated pore perforating the setae. **I)** Cell in a girdle view showing the hyaline rim at the mantle ridge (arrow). **J)** Part of a girdle with bands ornamented with transverse costae. Note the connecting band with marked undulation. **K)** Slit-shaped central process on a terminal valve. **L)** Detail of a seta showing minute spines and spirally arranged rows of areolae. Scale bars: A,C,D = 20 µm; B,E = 10 µm; F,G = 1 µm; H-J = 2 µm; K,L = 0.5 µm.

3.1.2.2.4 Chaetoceros brevis Schutt (1895)

Figure 3.20.

Bibliography: Hustedt (1930), Cupp (1943), Rines and Hargraves (1988) (as *C.* cf. *brevis*), Hernández - Becerril (1996), Jensen and Moestrup (1998), Bérard-Therriault et al. (1999), Sunesen et al. (2008)

Synonyms: *Chaetoceros hiemalis* (Cleve) Cleve, *C. dydimus* var. *hiemalis* Cleve, *C. pseudobrevis* Pavillard

Description: a.a.: 14-37 µm (Cupp: 8-17 µm, Rines and Hargraves: 17-23 µm, Hernández – Becerril: 15-28 µm, Jensen and Moestrup: 7-40 µm, Sunesen et al.: 9-26 µm,); p.a.: 9-40 µm (Hernández – Becerril: 22-29 µm)

LM: Cells united in straight, generally short chains (Figure 3.20.A) with longer colonies observed in the natural samples composed of up to 19 cells per chain. Cells cylindrical, rectangular in girdle view with sharp and drawn up corners, in valve view elliptical. Each cell has a single chloroplast often located close to one valve (Figure 3.20.B). Valve face concave, generally with a prominent central inflation. Mantle low or equidimensional with the girdle, with a slight constriction near its edge often visible as a notch near the suture. Setae originate from the drawn up valve corners and often cross immediately with the single point of crossing/fusion at the chain margin. Apertures wide with a slight constriction in the middle (peanut-shaped), due to the presence of central inflation on the sibling valves (Figure 3.20.B). Intercalary setae are extending almost parallel to the valvar plane and slightly symmetrically diverge from the apical plane of about 15° belonging to the Brunel Group II. Setae of the intercalary cells positioned in the centre of the chain are mostly oriented perpendicular to the chain axis while those near the chain end have setae curved towards that end. The terminal setae diverge obliquely towards the chain axis becoming almost parallel with it forming U-shape. All setae are thin and relatively delicate and very often contain some unknown plastid-like material, however this organic substance did not fluoresce under UV light therefore it probably has no photosynthetic function (Figure 3.20.C,D). In one culture the lateral auxospore was observed still attached to the parent cell (Figure 3.20.F).

Figure 3.20. LM **(A-F),** TEM **(G,H,J,N,O)** and SEM **(I,K-M)** micrographs of *Chaetoceros brevis* from field material **(C-E, K)** and cultures, strains PMFB1 **(A-B, G-J, L-O)** and PMFB2 **(F). A)** Complete chain. **B)** Middle part of a chain showing single plate-like chloroplast and peanut-shaped aperture. **C)** and **D)** Terminal part of the chain with plastid-like material within the setae. **E)** Chain with *Pseudo-nitzschia linea* epiphytes on the setae. **F)** Chain with lateral auxospore attached to the parent cell. **G)** Sibling valves in girdle view. **H)** Valve face showing central annulus and radially arranged parallel costae. Note the darker area in the central part of the valve. **I)** Terminal valve showin the internally slit- shaped central process (arrow) and silica flaps projecting from the marginal ridge (arrowheads). **J)** Detail of the valve with externally flattened tube of the central process. **K)** Resting spore still covered with the remains of the girdle bands from the parent cell. Primary valve ornamented with numerous thin filamentous spines. **L)** Terminal valve with externally flattened tube of the central process. **M)** and **O)** Detail of a seta. **N)** Part of a girdle with bands ornamented with transverse costae. Note the connecting band with marked undulation. Scale bars: A,D-F = 20 µm; B,C = 10 µm; G-I,K-L = 5 µm; J,M-O = 1 µm.

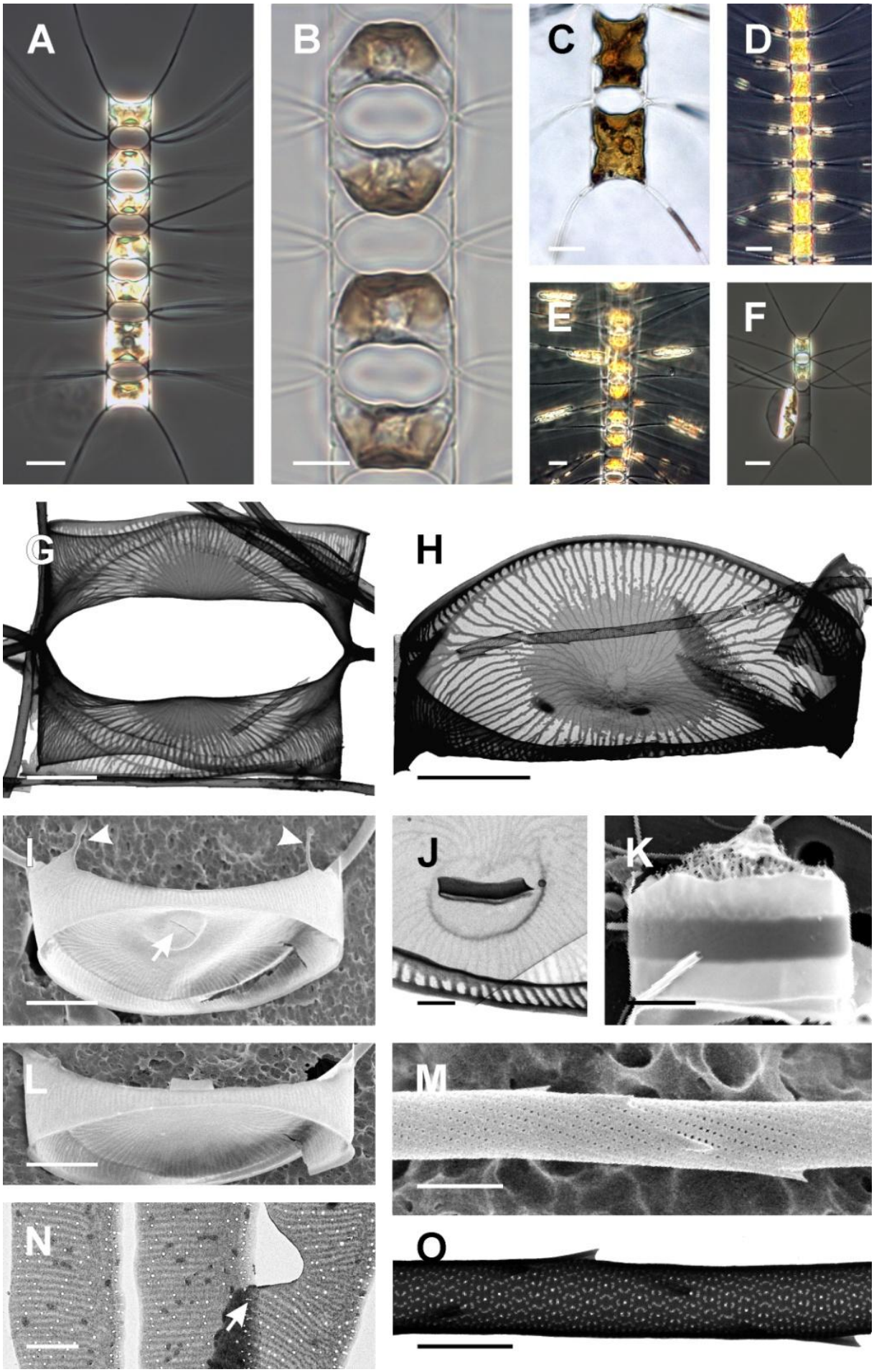
A
B
C
D
E
F
G
H
I
J
K
L
M
N
O

EM: The valve has a central annulus from which radiates the pattern of parallel and scarcely dichotomously branched costae, somewhat widely spaced, extending also parallel with each other on the valve mantle (Figure 3.20.G-H). The area between costae is hyaline and generally lightly silicified, however, in the centre of each valve and at the bases of the setae there is a large and irregularly shaped darker part of the surface, probably due to the slightly higher degree of silification (Figure 3.20.G-H). The marginal ridge possesses usually a very low hyaline rim from which sometimes in terminal valves project irregular silica flaps (Figure 3.20.I). Central process is present only in terminal valves and situated in the centre of the annulus. The process is externally shaped as a wide flattened tube (Figure 3.20.J,L) while internally is only a simple slit (Figure 3.20.I). The girdle bands are ornamented with transverse parallel costae and small round pores irregularly distributed in the hyaline area between them (Figure 3.20.N). The setae are circular in cross-section, composed of thick longitudinal strings arranged in helicoidal pattern and adorned with densely distributed spines while interconnected with very short transverse bars (Figure 3.20.M,O). Resting spores have unequally vaulted valves with the primary valve ornamented with numerous thin capilli and the distinct mantle region (Figure 3.20.K).

Distinctive features: Valve face with slight central inflation. Plastid-like material present in the setae. The valve ornamented with the pattern of parallel and scarcely dichotomously branched, widely spaced costae radiating from a central annulus. The surface of the valve central area appears much darker in TEM forming an irregularly shaped central patch. Primary valve of resting spore with numerous thin capilli.

Comments: Similar species is *C. pseudobrevis*, however as the main distinction between these two species is by Jensen and Moestrup (1998) considered to be more delicate chains with less regularly arranged setae, and no difference in ultrastructural characteristics therefore in this study it is not considered as a distinct species, although more investigations are necessary in order to establish a taxonomic validity.

Some epiphytic diatom species such as *Pseudo-nitzschia americana*, *P. linea* or *Nitzschia* spp. are often observed attached to the setae of *C. brevis* (Figure 20.E).

3.1.2.2.5 Chaetoceros circinalis (Meunier) Jensen and Moestrup (1998)

Figure 3.21.

Bibliography: Hustedt (1930) (as *C. affinis* var. *circinalis*), Cupp (1943) (as *C. affinis* var. *circinalis*), Jensen and Moestrup (1998)

Synonyms: *C. schüttii* var. *circinalis* Meunier, *C. affinis* var. *circinalis* (Meunier) Hustedt

Description: a.a.: 5-16 µm (Cupp: 12 µm, Jensen and Moestrup: 7-35 µm); p.a.: 10-28 µm

LM: The cells are usually united in short, straight chains but single cells are also common in field as well as in cultured material (Figure 3.21.A-B). Cells cylindrical, in valve view elliptical and in girdle view rectangular. Each cell contains a single chloroplast. The valve face is flat or slightly concave with sharp valve corners slightly drawn up and touching between sibling valves (Figure 3.21.A). Terminal valve face is sometimes flat but more often markedly convex. Valve mantle is high, sometimes with a slight notch near the suture. Girdle part is low or equidimensional with the mantle. Intercalary setae originate from the valve corners and almost immediately cross each other with very short basal part and fuse only at the point of crossing or for a short distance at the chain margin. Apertures are very narrow and slit-shaped. Intercalary setae characteristically curve backwards around the cell away from the apical axis, similar to Brunel Group IV with the difference that the setae are curved and not straight (Figure 3.21.C). In girdle view, setae curve strongly towards either side of the chain (Figure 3.21.B). Terminal setae are morphologically similar to the intercalary ones, but with different orientation, diverging in a broad U-shaped curve often lying in the apical plane or at a certain angle.

EM: The valve face and the advalvar part of the mantle are densely perforated by numerous irregularly shaped and relatively large poroids (Figure 3.21.D-G). The annulus and costae pattern exists but it is hardly observable due to the relatively high silification and perforations on the valve. The marginal ridge is ornamented with a distinct hyaline rim which extends in the pervalvar direction close to the valve apices and fuses between intercalary sibling valves (Figure 3.21.D). Terminal valves possess a central process and are often ornamented with short capilli covering the valve face (Figure 3.21.F-G). The process was not observed from the internal side of the valve but only from the external side where it appears as a more or less flattened wide tube (Figure 3.21.F-H). Intercalary setae are circular in cross-section (Figure 3.21.J-K). In the part proximal to the valve they appear completely smooth (Figure 3.21.I) and further on they seem to be composed of several relatively wide longitudinal silica strings extending parallel with the setae axis or with a slight torsion around it. The strings are interconnected with short transverse silica bars and ornamented with small spines arranged in a spiral pattern along their length (Figure 3.21.J,K). In the space between strings few elongated pores can be observed.

Distinctive features: Intercalary setae characteristically curved backwards around the cell away from the apical axis. The valve face and the advalvar part of the mantle are densely perforated by many irregular and relatively large poroids.

Comments: The resting spores were not observed within this study but they are reported by Jensen and Moestrup (1998) to have valves covered with knobs or very small spines.

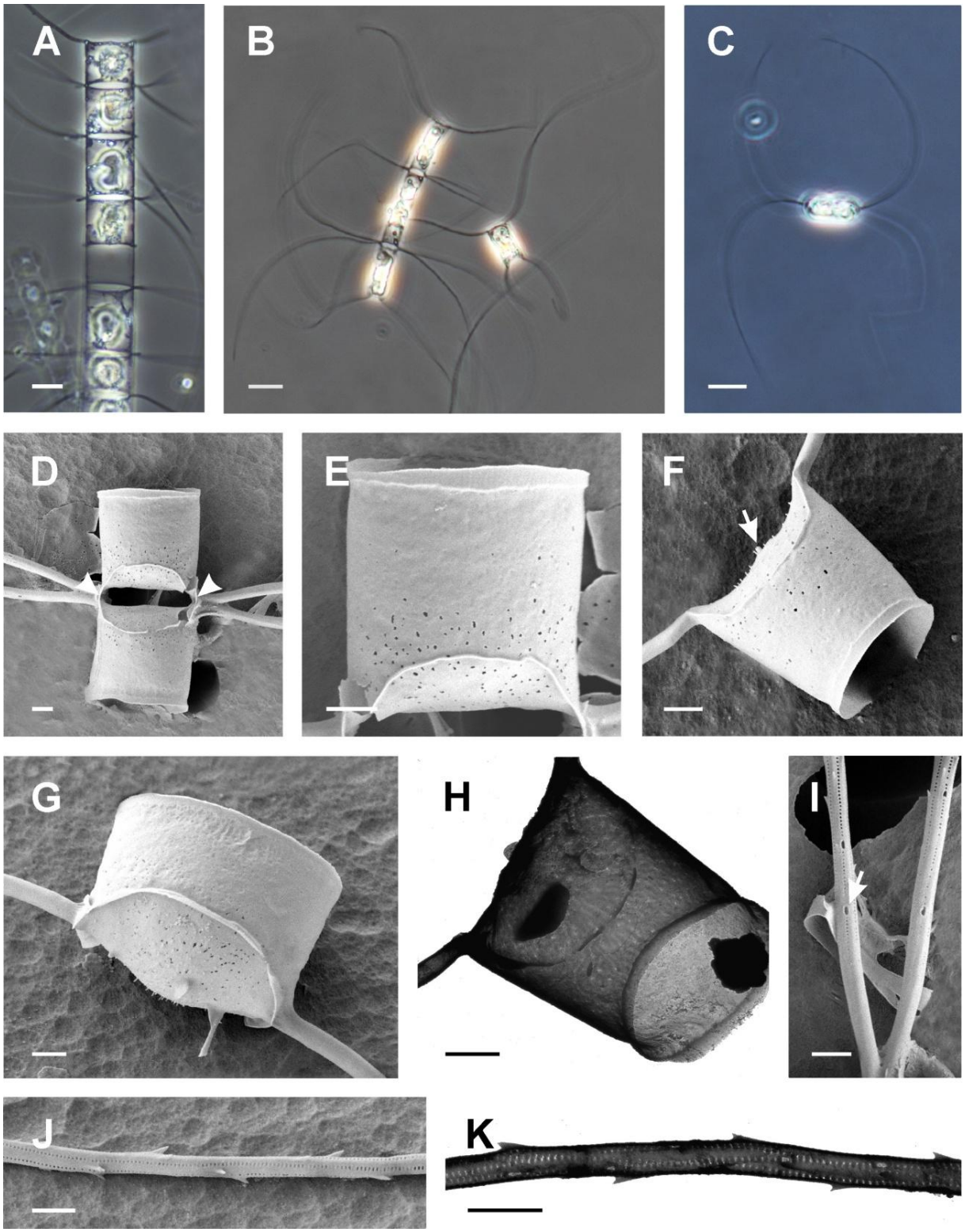

Figure 3.21. LM **(A-C)**, SEM **(D-G, I-J)** and TEM **(H,K)** micrographs of *Chaetoceros circinalis* from natural samples **(A)** and culture material, strain G4 **(B-K)**. **A)** The terminal part of the chain. Note the narrow. slt shaped apertures. **B)** The complete chain (left) and the single cell (right) showing the curvature of the setae. **C)** Cell from the valve view showing the characteristic curvature of the setae. **D)** Two sibling valves with partially fused hyaline rim at the aperture edge (arrowheads).

3.1.2.2.6 Chaetoceros constrictus Gran (1897)

Figure 3.22.

Bibliography: Hustedt (1930), Cupp (1943), Rines and Hargraves (1988), Hernández - Becerril (1996), Jensen and Moestrup (1998), Hernández-Becerril and Flores Granados (1998), Berard-Therriault et al. (1999), Shevchenko et al. (2006)

Description: a.a.: 5-18 µm (Hustedt: 14-35 µm, Cupp: 12-36 µm, Rines and Hargraves: 20 µm, Jensen and Moestrup: 7-30 µm, Hernández-Becerril and Flores Granados: 18-22 µm, Berard-Therriault et al.: 11-51 µm, Shevchenko et al.: 15-30 µm); p.a.: 7-17 µm (Berard-Therriault et al.: 25-32 µm, Shevchenko et al.: 15-30 µm)

LM: Cells united in very straight and usually short chains (Figure 3.22.B). Cells with two chloroplasts. The valve surface is concave and the valve corners are sharp and drawn up, touching between sibling valves (Figure 3.22.C-D). The aperture is quite large and markedly elliptical (Figure 3.22.D). Valve mantle is high with a distinct constriction near the margin (Figure 3.22.D). The girdle part is usually very low. Intercalary setae are quite long and rigid; originate from the valve apices and immediately cross each other at the chain margin without the basal part. In girdle view they are usually proximally perpendicular towards the chain axis and distally curved (Figure 3.22.A-B). In valve view they belong to Brunel group II. Terminal setae are usually characteristically oriented, long and straight, extending parallel to the chain axis with sometimes crossing each other distally (Figure 3.22.A-C). The resting spores have unevenly vaulted valves (Figure 3.22.E) and are reported to be covered with small spines, however, we could not confirm this notion because it was not possible to observe in details the valve ornamentation in available material.

EM: The valve face is ornamented with numerous small spines and the annulus and costae pattern were not observed due to the lack of TEM images. The marginal ridge is ornamented with a distinct hyaline rim which extends in the pervalvar direction close to the valve apices and fuses between intercalary sibling valves (Figure 3.22.G). Central process is present only in terminal valves, from the external side appearing as a short flattened wide tube (Figure 3.22.F-G). The terminal valve face is covered with numerous small spines which are more pronounced than in the intercalary valves, (Figure 3.22.F,G). Setae appear four sided in cross section, composed of relatively thick, straight longitudinal silica strings extending parallel with the setae axis and interconnected with parallel short silica bars (Figure 3.22.H). Strings are ornamented with small spines arranged in a spiral pattern.

←

Figure 3.21. continued

E) Close view on the intercalary valve showing the pore perforation pattern. **F)** Terminal valve with narrow tube-like central process (arrow) and short capilli on the valve surface. **G)** Terminal valve with wide flattened tube-like central process and short capilli on the valve surface. **H)** Terminal valve with wide flattened tube-like central process. **I)** Detail of setae in the part proximal to the valve showing elongated pores (arrow). **J)** and **K)** Detail of a seta. Scale bars: A-C =10 µm; D-K = 1 µm.

Distinctive features: Valve mantle markedly constricted near the advalvar margin, observable in LM as a large notch near the suture. Intercalary setae quite long, straight and rigid, terminal setae extending parallel to the chain axis sometimes distally crossing each other. The valve face ornamented with many small spines.

Comments: The vegetative cells of *C. vanheurckii* Gran are reported to be very similar to *C. constrictus*, and the former species appears to be distinguished only by the presence of long spines on the secondary valve of the resting spore. Within this study it was hard to observe even the small spines on the spores, therefore this morphotype was ascribed to *C. constrictus.* Moreover, *C. vanheurckii* has not been previously reported from the Meditteranean Sea.

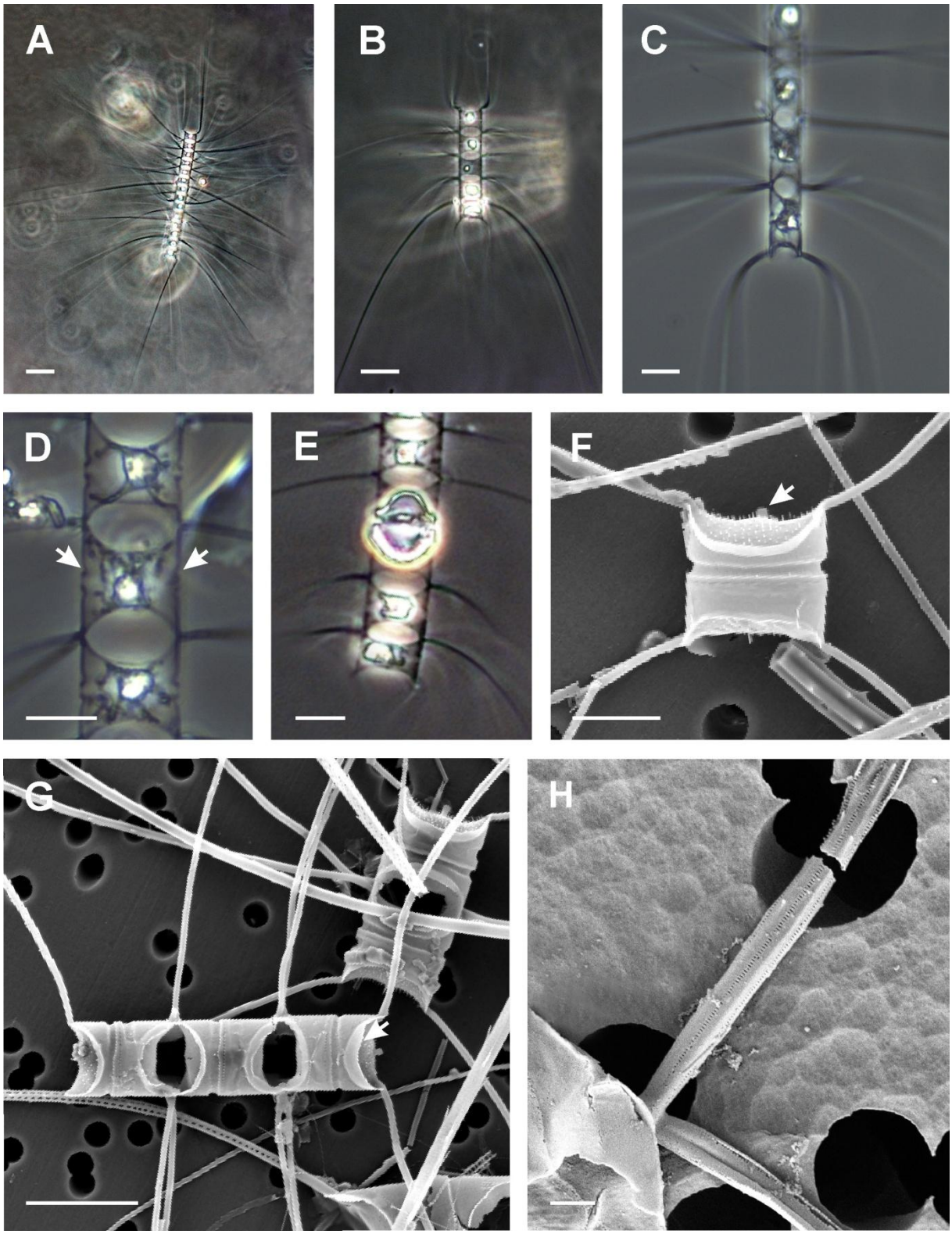

Figure 3.22. LM **(A-E)** and SEM **(F-H)** micrographs of *Chaetoceros constrictus* from field material. **A)** Complete long chain showing orientation of the setae. **B)** Complete short chain. **C)** Terminal part o the chain. **D)** Intercalary cells in girdle view showing the distinct constrictions near the mantle margin (arrows). **E)** Terminal part of the chain with a resting spore within the parent cell. **F)** Terminal cell showing external flattened tube of the central process (arrow), the small spines covering the valve surface and longitudinal groove near the mantle edge. **G)** Two short chains. The pronounced hyaline rim on the marginal ridge of the terminal valve is marked by an arrow. **H)** Detail of setae proximal to the valve. Scale bars: A-B =20 µm; C-G = 10 µm; H= 1 µm.

3.1.2.2.7 Chateoceros contortus Schütt (1895)

(Figure 3.23.)

Bibliography: Rines and Hargraves (1988) (as *C. compressus*), Jensen and Moestrup (1998), Bérard-Therriault et al. (1999), Rines (1999), Sunesen et al. (2008). Kooistra et al. (2010), Shevchenko and Orlova (2010), Lee and Lee (2011)

Description: a.a.: 6-23 µm (Rines and Hargraves; Rines: 6-22 µm, Jensen and Moestrup: 5-40 µm, Sunesen et al.: 10-17 µm, Shevchenko and Orlova: 20-35 µm); p.a.: 7-24 µm (Shevchenko and Orlova: 10-35 µm)

LM: Cells united in quite long (in culture often more than 30 cells) and straight chains, often twisted about the chain axis (Figure 3.23.A). Cells cylindrical, in girdle view rectangular with markedly rounded corners (Figure 3.23.B), in valve view elliptical to circular. Cells contain 5-12 small discoid-like chloroplasts (Figure 3.23.B). The valve face is slightly convex with a central inflation. Mantle more or less high with the girdle equidimensional or higher than the mantle. The setae originate within the valve margin with the basal part of moderate length which is slightly directed outwards before the single point of crossing/fusion at the chain margin (Figure 3.23.B). The apertures are relatively wide, hexagonal and often slightly constricted in the middle due to the central inflated part on valve face. There are two types of intercalary setae: common and special. Common setae are thin, generally oriented more or less perpendicularly to the chain axis or appear slightly curved due to their delicate structure (Figure 3.23.A,M,P,R). Special setae are thick and heavily silicified and curved in a bell-like curve towards the nearest extremity of the chain (Figure 3.23.C). The common type of setae belongs to Brunel Group II and III, and special to Brunel Group II (Figure 3.23.C) Special setae were observed only in specimens from natural samples and not in cultured material. They are always located on the intercalary cells near one end of the chain. The terminal setae resemble the normal intercalary setae but they are directed outwards from the terminal valve forming V-like shape. Resting spores were observed only in field samples, positioned centrally within the parent cell, with both valves smooth and dome-shaped (Figure 3.23.K). The primary valve is reported to have a silica collar perforated with a variable number of large holes, however due to the lack of EM observations this could not be confirmed. In field samples there was often a sheath of thick mucus surrounding the chain with the setae protruding from it, visible even without the Alcian Blue staining (Figure 3.23.E).

Figure 3.23. LM **(A-E,K),** SEM **(J,M)** and TEM **(F-I,L,N-R)** micrographs of *Chaetoceros contortus* from field samples **(C-E,K)** and from cultures, strains PMFCO1 **(B,M-O)** and PMFCO2 **(A,G-J,L,P,R). A)** Complete chain showing orientation of the setae. **B)** Middle part of a chain showing small chloroplasts. **C)** Specialized intercalary setae in the girdle view. **D)** Specialized intercalary setae in the valve view.
E) Mucus sheath extruded by the cells, with clearly defined borders (arrow) and setae protruding from it. **F)** Valve face and the mantle showing the reticulate area within the central annulus and small spirals on the end of some costae (arrow). Note the hyaline rim with a rectangular extension. **G)** Valve face with network of costae. **H)** Sibling valves in valve view showing the hyaline rim on the marginal ridge. **I)** Terminal valve with a club-like shaped external part of the central process. **J)** Detail of the terminal valve with hole of the terminal process from the internal view. **K)** Middle part of the chain with resting spores. **L)** Detail of a terminal valve with club-shaped central process. **M)** Detail of a common intercalary seta. **N)** Detail of a girdle band

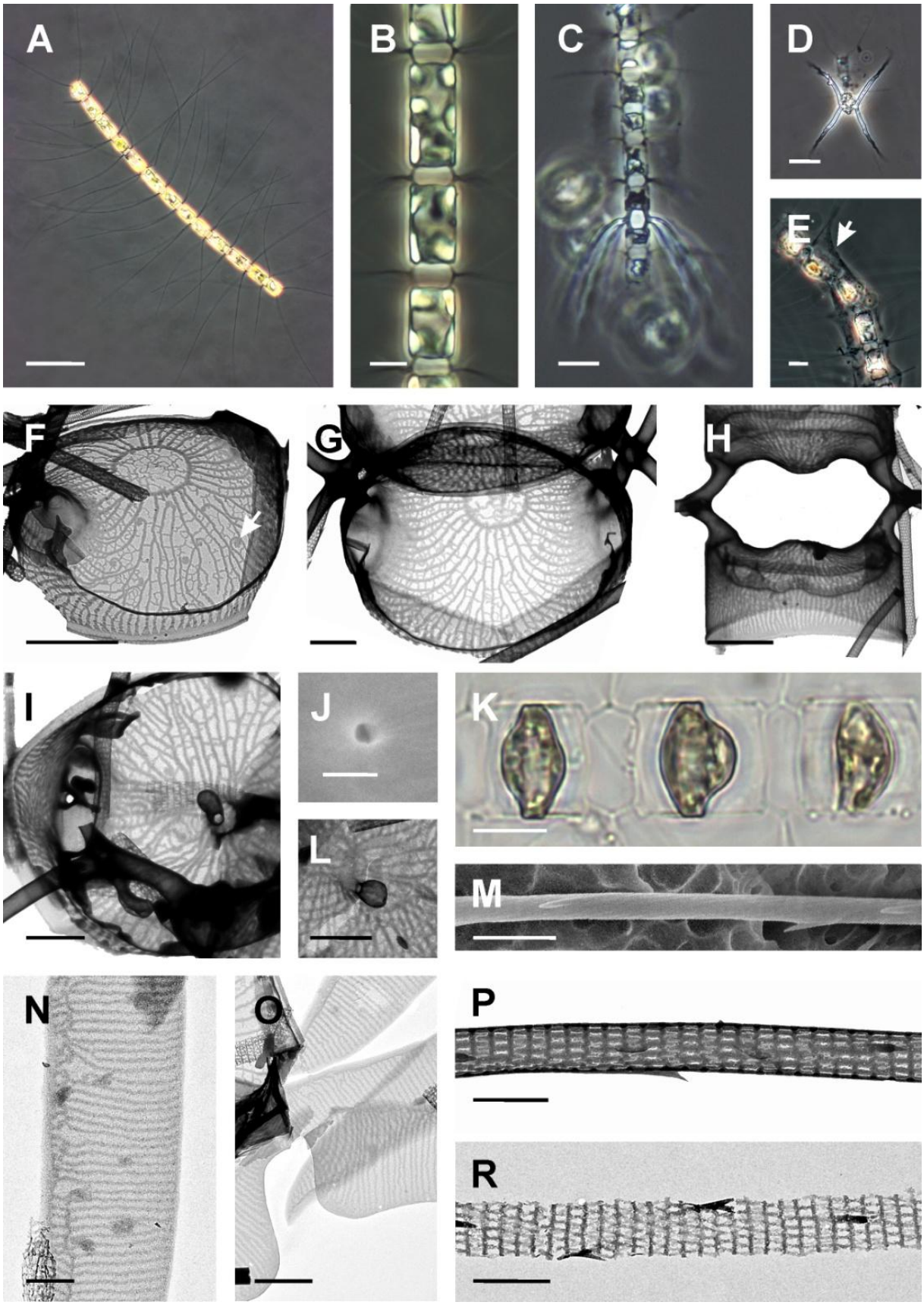

Figure 3.23. continued
O) Broken parts of girdle bands, with a part of connecting band showing marked indentation. **P)** Detail of a common intercalary seta. **R)** Detail of a common intercalary seta. Scale bars: A = 50 µm; B,C,K = 10 µm; D,E = 20 µm; F,H = 2 µm; G,I,J,L;M,O,P = 1 µm; N,R= 0.5 µm

EM: The valve has a central annulus from which extends a quite complex pattern of radiating costae, branching dichotomously towards the valve margin and becoming parallel on the valve mantle. The costae are often interconnected with transverse short connections and ends of some costae are twisted into small spirals. The central annulus is not hyaline but filled with an irregular reticulate pattern of costae, and the only hyaline area on the valve surface is observed around the bases of the setae (Figure 3.23.F-G). The marginal ridge possesses a hyaline rim, often extending into somewhat rectangular siliceous projections (Figure 3.23.F,H). A central process is present only in terminal valves. It is in form of a round hole from the internal view and externally appears as a short club-like tube with closed end (Figure 3.23.I-J,L). Setae are circular in cross-section and are composed of thin silica longitudinal strings extending mostly parallel with the seta axis but can also be arranged in a slight spiral pattern. The strings are interconnected with transverse bars which appear more strongly silicified than the strings, oriented perpendicularly to the seta axis and it seems that they are joined in regular parallel rings around the seta along its length. These composing elements appear in TEM to form a regular reticulate pattern on the setae (Figure 3.23.P-R). The strings are ornamented with spines which are sparsely arranged in a helicoidal pattern along the setae length lacking in the part proximal to the valve (Figure 3.23.M,P-R). Girdle bands are adorned with transverse fine striations and with a slightly thickened longitudinal rib near one edge (Figure 3.23.N-O).

Distinctive features: Cells usually circular in valve view united in very long chains with a slight torsion. Distinct hexagonal apertures. Special thick and short intercalary setae often present. Valves have a complex ornamentation pattern with reticulate area within the central annulus and transverse short connections between branching costae some of which have ends twisted into small spirals. Central process a short club-like tube with closed end. Setae appear in TEM composed of thin longitudinal strings parallel with seta axis and interconnected with transverse bars perpendicular to the same axis and joined in rings around the seta.

Comments: The very similar species is *C. compressus* Lauder which was for a long time considered as a synonym for *C. contortus* and many morphotypes were ascribed to it. The main difference between this two species is in the valve shape which is round in *C. contortus* and elliptical, strongly compressed in the transapical direction in *C. compressus*. The later species also often lacks torsion of the chain, the special setae are much longer and more curved with the valve bearing them heavily silicified and with the resting spore lacking lace-like sheath on the primary valve. In present study all examined specimens were more similar to *C. contortus* (except the EM confirmation of the silica collar on the resting spore primary valve) and are referred to this taxon.

3.1.2.2.8 Chaetoceros costatus Pavillard (1911)

Figure 3.24.

Bibliography: Hustedt (1930), Cupp (1943), Rines and Hargraves (1988), Jensen and Moestrup (1998), Hernández-Becerril and Flores Granados (1998), Hernández-Becerril and Aké-Castillo (2001), Kooistra et al. (2010), Ishii et al. (2011)

Synonyms: *C. adhaerens* Mangin

Description: a.a.: 11-15 µm (Hustedt: 12-40 µm; Rines and Hargraves: 8-24 µm; Jensen and Moestrup: 12-22 µm; Hernández-Becerril and Flores Granados: 15-24; Hernández-Becerril and Aké-Castillo: 9-24 µm); p.a.: 21-32 µm (Hernández-Becerril and Aké-Castillo: 9-19 µm)

LM: Cells arranged in straight chains which can sometimes be very long even reaching more than 50 cells per chain in cultured material. The cells are rectangular with rounded corners in girdle view, and elliptical in valve view. There is a single, plate-like chloroplast per cell (Figure 3.24.A). Valve face is flat to slightly concave and possesses four submarginal flattened protuberances, two on each side of the valve positioned close to the valve apices. The sibling cells join by fusion of these protuberances, but also by fusion of sibling setae (Figure 3.24.F). The aperture is very narrow, shaped as a linear thin slit, extending between the protuberances, shorter than the apical axis (Figure 3.24.B). The valve mantle is very low and the girdle often very high. The edges of the numerous girdle bands are readily visible in LM, even in water mounts (Figure 3.24.D). The thin and long intercalary setae originate at the valve margin, cross immediately without a basal part and extend mostly perpendicular to the chain axis or slightly curve towards the end of the chain, diverging variously from the apical plane (Brunel Group II and III). The terminal setae are morphologically similar to intercalary ones and curved obliquely towards the chain axis (Figure 3.24.A).

EM: The lightly silicified valve face has a distinct pattern of costae radiating from a central or slightly eccentric large hyaline annulus. In the central part of the valve face costae branch dichotomously towards the valve edge, whilst in part near the apices costae remain for a certain distance parallel with the apical axis converging towards the setae bases (Figure 3.24.G). Each valve, including the terminal ones has four protuberances which surface is not hyaline but adorned with parallel costae (Figure 3.24.G). The eccentrically positioned process is present only on terminal valves and it is slit-shaped from an internal view and a flattened tube from an external view (Figure 3.24.H-I). The marginal ridge is ornamented with a low siliceous hyaline rim (Figure 3.24.F). The girdle consists of half bands arranged to form a zig-zag pattern. The bands are ornamented with transverse costae interspaced with hyaline areas. The advalvar bands have distinct thickened longitudinal rib at one edge (Figure 3.24.J-L). Setae are circular in cross-section, smooth and hyaline in the basal part gradually becoming longitudinal thin strings which twist around the setae axis (Figure 3.24.M). The strings are interconnected with short silica bars of equal length. The strings bear loosely spaced, spirally arranged small spines (Figure 3.24.N).

Resting spores are oval or rounded in shape (Figure 3.24.O). The mantle of both valves is often elongated. Their primary valve is dome-shaped and covered with numerous hooked conical spines

sometimes joined at their basal part by siliceous vela. The edge of the valve and the mantle are covered with flaps of silica which appear to be remains of the girdle left from the parent cell (Figure 3.24.P). The secondary valve has fewer conical spines at the surface and possesses a single marginal ring of puncta on the advalvar margin of the mantle (Figure 3.24.R).

Distinctive features: Cells united in usually very long chains. The advalvar girdle bands have distinct thickened longitudinal rib at one edge which is visible in LM. On each valve, there are four submarginal flattened protuberances, two on each side. They are fused between sibling valves forming a short central aperture in addition to two small marginal apertures between protuberances and the setae. The valve ornamentation pattern has parallel costae in part close to the apices.

Figure 3.24. LM **(A-D),** SEM **(E,N-R)** and TEM **(F-M)** micrographs of *Chaetoceros costatus* field samples **(B,D)** and from cultures, strains PMFB6 **(N-R)**, PMFB8 **(E,F,G,L)** and PMFB7 **(A,C, H-K, M)**. **A)** Complete chain showing orientation of the setae. **B)** Middle part of the chain showing the short apertures. **C)** Part of the chain with two terminal cells indicating separation of the chain. **D)** Middle part of the chain showing the visible edges of the girdle bands (arrow) **E)** Sibling valves **F)** Sibling valves, note the fusion of protuberances and the sibling setae joining the cells. Arrow indicates hyaline rim on the marginal ridge. **G)** Valve face of the terminal valve showing eccentric annulus and costae pattern. **H)** External flattened tube of the process. **I)** Internal slit-shaped process. **J)** Girdle composed of half-bands with the thickened edges on advalvar bands. **K)** Detail of a girdle band with transverse costae and more silicified rib on the edge. **L)** Half girdle bands **M)** Part of the setae proximal to the valve. **N)** Detail of a seta. **O)** Complete resting spore. **P)** Primary valve with hooked spines. **R)** Secondary valve with conical spines and single marginal ring of poroids. Scale bars: A - D = 10 µm; E = 5 µm; F,G,L,O-R = 2 µm; J,K = 1 µm; H,I,M,N = 0.5 µm.

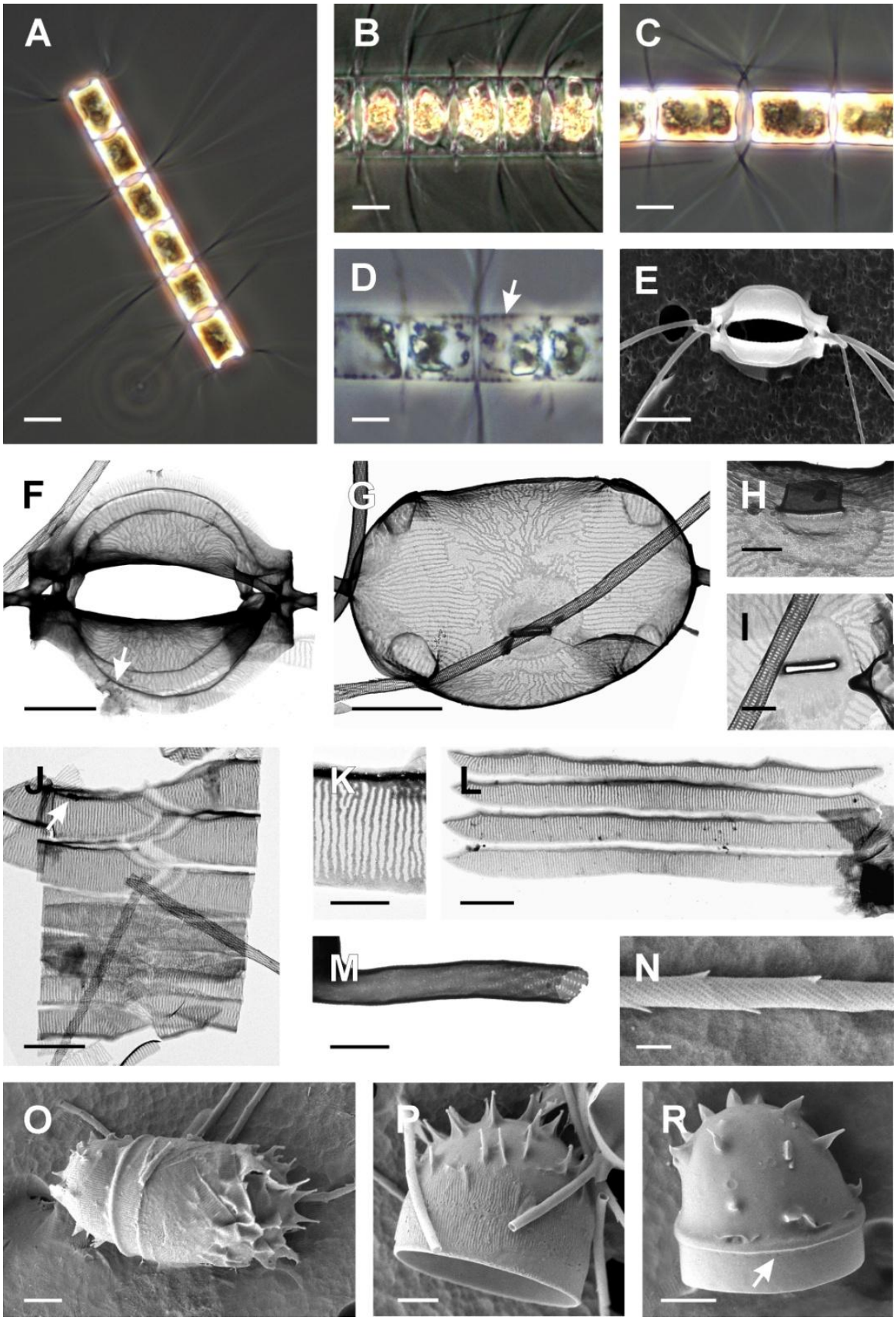
A
B
C
D
E
F
G
H
I
J
K
L
M
N
O
P
R

3.1.2.2.9 Chaetoceros curvisetus Cleve (1889)

(Figure 3.25.)

Bibliography: Hustedt (1930), Cupp (1943), Evensen and Hasle (1975), Hargraves (1979), Rines and Hargraves (1988), Hernández-Becerril (1996), Jensen and Moestrup (1998), Hernández-Becerril and Flores Granados (1998), Shevchenko et al. (2006), Sunesen et al. (2008), Kooistra et al. (2010)

Synonyms: *C. secundus* Schütt, *C. cochlea* Schütt

Description: a.a.: 11-34 µm (Hustedt: 10-30 µm, Cupp: 7-30 µm, Rines and Hargraves: 14-15 µm, Jensen and Moestrup: 15-20 µm, Hernández-Becerril and Flores Granados: 11-25 µm, Shevchenko: 10-30 µm, Sunesen: 8-24 µm); p.a.: 8-30 µm (Shevchenko: 12-35 µm)

LM: Cells united in usually long chains, in pervalvar plane curved and sometimes helical (Figure 3.25.A). Cells are broadly elliptical in valve view and rectangular in girdle view with the drawn up valve corners touching between sibling valves (Figure 3.25.B). In each cell there is a single large plate-like chloroplast (Figure 3.25.C). The valve face is markedly concave and the setae emerge from the valve corners immediately crossing each other at their point of origin without any or with only a short basal part. The apertures are large, elliptical to circular in shape (Figure 3.25.B). The girdle is usually high and the mantle is low with no observable notch near the suture. The setae are long and relatively thin. In girdle view they appear all curved towards the same, convex side of the chain (Figure 3.25.A) while in the valve view they are all bent to one side of the apical axis belonging to the Brunel Group V (Figure 3.25.D). The intercalary and terminal setae are not differentiated. Resting spores have unequally vaulted valves with the dome-shaped primary valve and less rounded to almost flat secondary valve. The surface of both valves is smooth (Figure 3.25.N).

Figure 3.25. LM **(A-C,N),** SEM **(D,G,L,O-P)** and TEM **(E-F,H-K,M)** micrographs of *Chaetoceros curvisetus* from field samples **(A-B,N-P)** and from cultures, strains PMFD2 **(E-F,H-K,M)**, PMFD6 **(D,G,L,O-P)** and PMFD8 **(C). A)** A complete chain in a narrow girdle view showing orientation of the setae **B)** Intercalary cells in a broad girdle view showing the aperture. **C)** Intercalary cells with a single plate-like chloroplast. **D)** Sibling valves from a valve view with setae curved towards one side of the apical axis (Brunel Group V). **E)** Sibling valves showing the valve ornamentation pattern. **F)** Detail of the valve. **G)** Outside view of the terminal valve with the hyaline rim on the marginal ridge and external flattened tube of the central process. **H)** Detail of the valve with external flattened tube of the central process. **I)** Detail of the girdle. **J)** Central annulus with the slit-like process. **K)** Detail of the girdle band with transverse ribs and the area between them perforated with poroids. **L)** and **M)** Detail of a seta. **N)** A cell with the resting spore. **O)** Internal view of the resting spore primary valve with the fissured collar. **P)** External view of the smooth surfaced resting spore perforated by poroids. Scale bars: A,B = 20 µm; C,N = 10 µm; D-E,G,O-P = 5 µm; F, H-M = 1 µm.

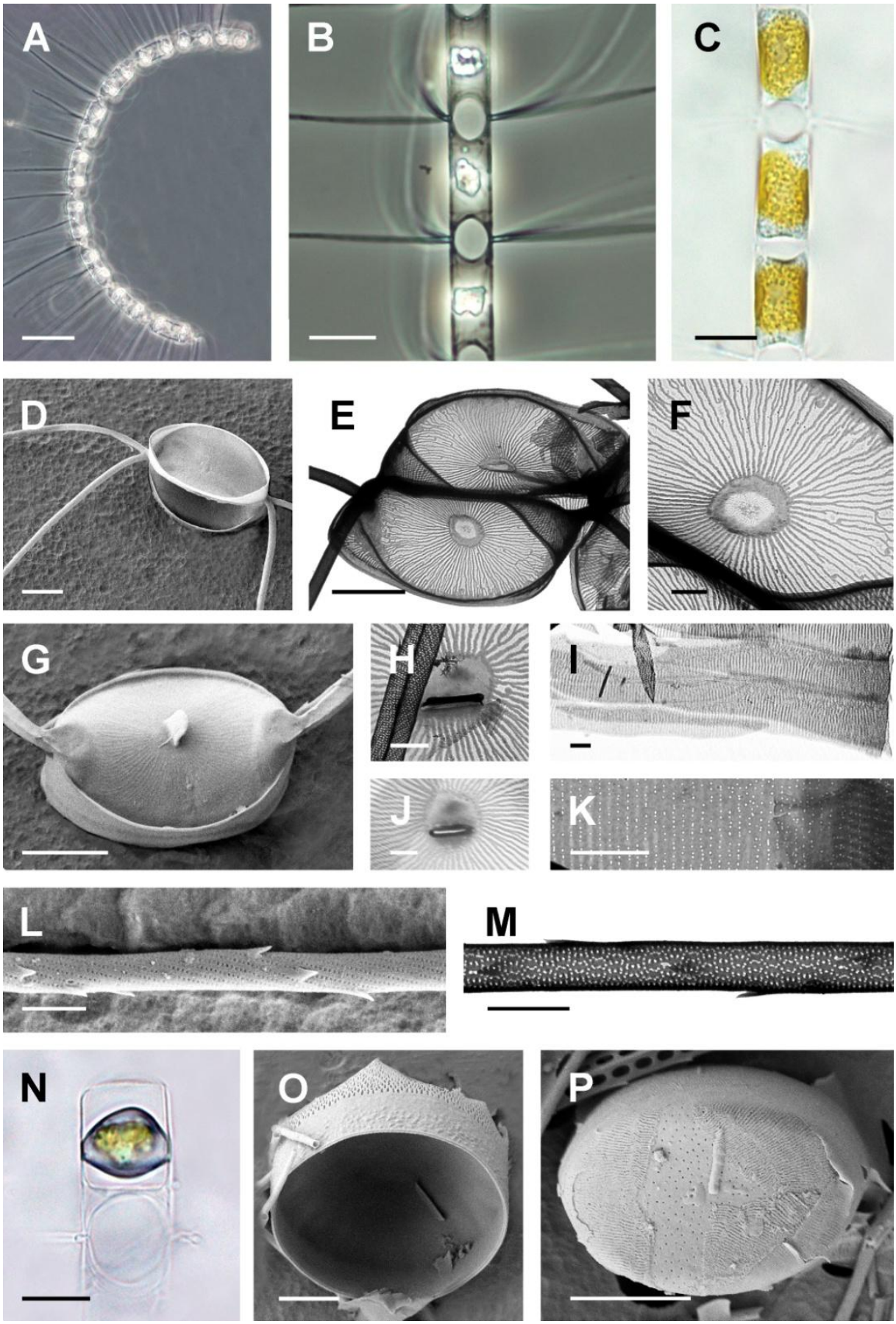
A
B
C
D
E
F
G
H
I
J
K
L
M
N
O
P

EM: The valve has a hyaline central annulus with lighter centre encircled with a slightly darker marginal area from which extends a pattern of relatively thick and rarely dichotomously branched costae (Figure 3.25.E-F). The costae pattern appears more complex towards the valve margin where sometimes ends of some costae are twisted into small spirals. The main radiating costae are also interconnected with transverse short connections sometimes fusing completely to the darker thickened hyaline surface in the area close to the bases of the setae and near the valve face margin (Figure 3.25.E). The low mantle appears hyaline in the advalvar part with parallel costae shortly extending towards the abvalvar margin (Figure 3.25.E). The marginal ridge posses a low hyaline rim. A central or slightly eccentric process is present only in terminal valves internally shaped as a simple slit and externally as a wide flattened tube (Figure 3.25.G-H,J). Girdle bands are adorned with transverse fine ribs and perforated with small round poroids in the area in between the striations (Figure 3.25.I,K). The setae are circular in cross-section, composed of thick longitudinal strings arranged in spiral pattern adorned with spines while interconnected with very short transverse bars (Figure 3.25.L,M). The surface of the valve of the resting spore appears to be perforated with small poroids (Figure 3.25.P). Both valves of the resting spore bear a silica collar that is in the primary valve perforated by a series of elongated simple fissures (Figure 3.25.O).

Distinctive features: Chains curved in pervalvar plane, sometimes helical. Large oval aperture. All setae curved towards the convex side of the chain. Smooth resting spores with a collar on both valves. In intercalary cells central annulus with lighter centre encircled with a slightly darker marginal area. The ends of some costae are twisted into small spirals.

Comments: The similar species is considered to be *C. debilis* Cleve. The distinctive characters of this species are the flat valve surface in *C. debilis* in comparison to *C. curvisetus* concave valve, hexagonal shape of the aperture and the morphology of the resting spore which in *C. debilis* has a marked undulation and two pronounced spines on the primary valve lacking the collar surrounding the valves.

3.1.2.2.10 Chaetoceros decipiens Cleve (1873)

(Figure 3.26.)

Bibliography: Hustedt (1930), Cupp (1943), Evensen and Hasle (1975), Rines and Hargraves (1988), Hernández-Becerril (1996), Jensen and Moestrup (1998), Berard-Therriault et al. (1999), Hernández-Becerril and Flores Granados (1998), Shevchenko et al. (2006), Sunesen et al. (2008), Kooistra et al. (2010) (as *C. lorenzianus*)

Synonyms: *C. grunowii* Schütt, *C. concretus* Engler

Description: a.a.: 7-51 µm (Hustedt: 10-80 µm, Cupp: 9-84 µm, Rines and Hargraves: 30-55 µm, Jensen and Moestrup: 27-34 µm, Hernández-Becerril and Flores Granados: 23-49, Shevchenko: 20-50 µm, Sunesen: 16-24 µm); p.a.: 8-43 µm (Shevchenko: 20-45 µm)

LM: Cells united in usually long and straight, sometimes slightly curved chains in the apical plane (Figure 3.26.A). Cells elliptical in valve view and rectangular in girdle view, often with the apical axis longer than the pervalvar axis (Figure 3.26.C,D). There are several (4-10) small discoid chloroplasts present in each cell (Figure 3.26.D). The valve face is flat to concave, sometimes with the central part slightly inflated. The valve corners are sharp and drawn up, touching those of the sibling cell. Apertures are usually wide and elliptical. The mantle is high, usually with a distinct constriction near the margin which is visible in most cases in LM as a notch at the suture. The girdle is usually lower than or equidimensional with the mantle. In specimens from the field samples there were often observed organic "wing" shaped structures projecting from the girdle region (Figure 3.26.C). The setae originate from the valve corners, fuse immediately at the chain margin and then diverge at an angle of ca 30° equally from the chain axis, all of them lying in the apical plane (Brunel Group I). The length of the fused part of the setae appears to be very variable character with the extent of fusion varying even within a single chain. In most cases setae can fuse for up to several times of their diameter (Figure 3.26.C), however, they can be also fused only at their point of cross over (Figure 3.26.B). The intercalary setae are very stiff, straight and variable in length. Terminal setae appear slightly thicker than intercalary ones, diverging from cell corners in a wide V- shaped curve. Resting spores were not observed in this study and they have been never described in the literature

EM: The valve has a central annulus from which extends a pattern of radiating costae branching dichotomously towards the valve margin and becoming parallel on the valve mantle (Figure 3.26.E). The hyaline areas between costae are densely perforated with poroids (Figure 3.26.E). The very small central process is found on terminal valves only, internally with a distinct labiate structure (Figure 3.26.I,J) and externally there is a small protrusion (Figure 3.26.H) or the external part is completely lacking (Figure 3.26.G). The marginal ridge is ornamented with a siliceous hyaline rim which is somewhat higher close to the valve apices on terminal valves (Figure 3.26.H) while in intercalary ones it extends further in the pervalvar direction in a siliceous projection which fuses with the corresponding structure of the sibling valve (Figure 3.26.E). This hyaline structure is located at the marginal border of the apertures sometimes partially occluding them (Figure 3.26.F).

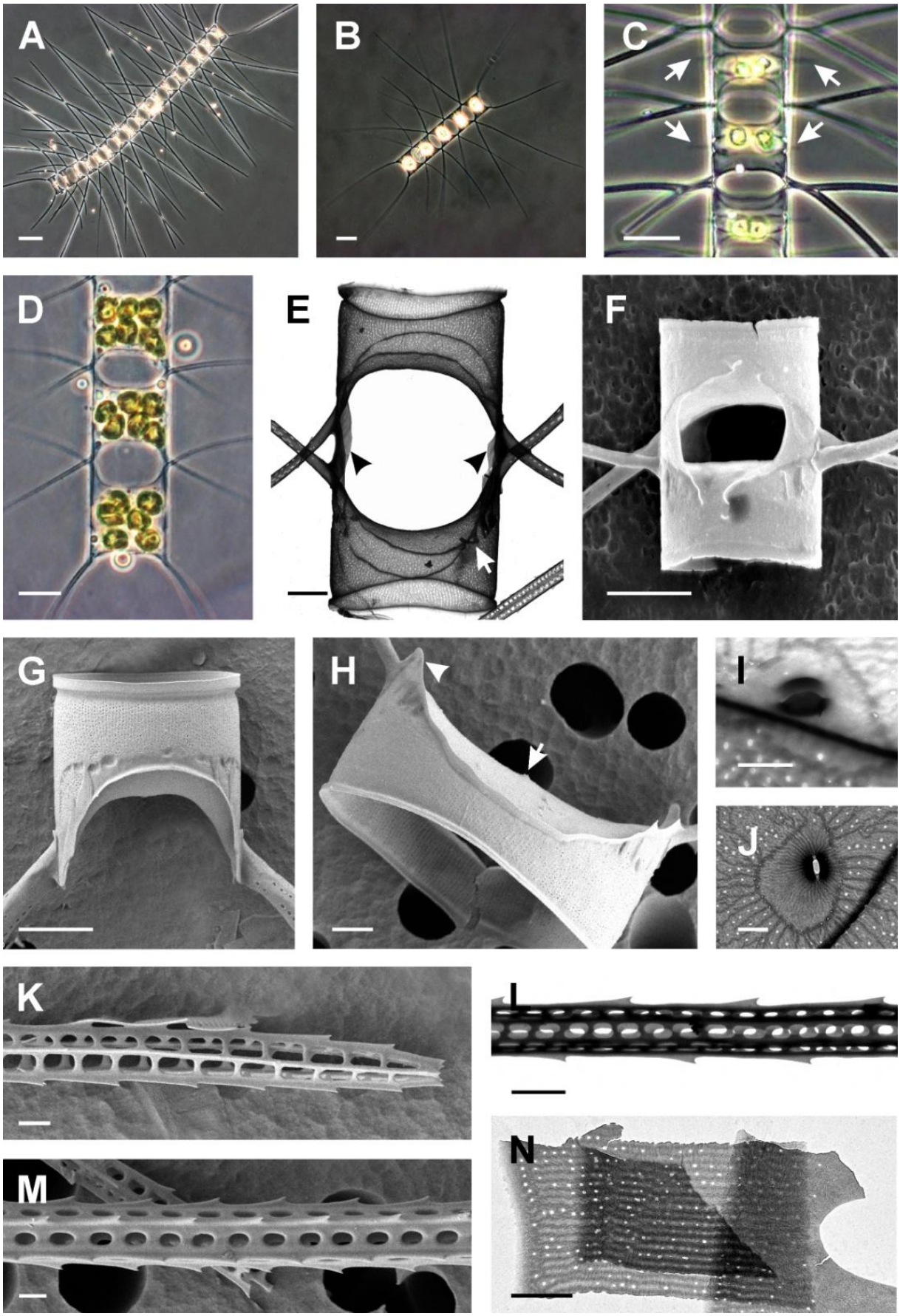
A
B
C
D
E
F
G
H
I
J
K
L
M
N

However, more often it is restricted to the seta bases and it appears that this junction between corners of sibling valves reinforces the intracellular connection in addition to the setae fusion. The area on the mantle near the valve corners and below the hyaline rim is often ornamented with short silica fringes (Figure 3.26.E). The setae are circular at the bases but soon becoming polygonal, predominantly four-sided. The setae structure can be described as the four thick longitudinal strings forming seta ridges which are ornamented with spines and interconnected with thick transverse bars (Figure 3.26.M,I). The ends of the strings are fused at the seta tip (Figure 3.26.K) where the architecture becomes more apparent due to the strings and bars being much thinner than in the part proximal to the valve. Girdle bands are ornamented with transverse ribs and irregularly scattered pores in the hyaline area between the ribs (Figure 3.26.N).

Distinctive features: Numerous chloroplasts. The corners of the sibling valves are touching forming large aperture with intercalary setae usually fused for a variable distance. Setae stiff, extended in the apical plane, polygonal in cross section, composed of four thick longitudinal strings forming seta ridges which are ornamented with spines and interconnected with thick transverse bars. Valve surface densely perforated with pores, valve mantle with silica fringes. Central process very small with an internally labiate structure.

Comments: The very similar species is *C. lorenzianus* Grunow which is often differentiated from *C. decipiens* on the basis of the fusion length between sibling cells, being short in the former and long in the latter species. However, this diagnostic character is found to be extremely variable. In addition, the ultrastructural characters are not a reliable identification tool to separate between these species due to the existence of many intermediate forms. Therefore, the identification of *C. lorenzianus* must be confirmed by the presence of the resting spores possessing two conical protuberances with a dichotomously branched process at their tip. In this study, the spores were never observed, neither in cultures nor in the field material therefore all investigated specimens were ascribed to the *C. decipiens sensu stricto*.

Figure 3.26. LM **(A-D),** TEM **(E,I,J,N)** and SEM **(F-H,K,M)** micrographs of *Chaetoceros decipiens* from field samples **(A,C,G)** and from cultures, strains PMFDE1 **(D,I,L)**, PMFDE3 **(E,F,G,L)** and PMFE1 **(B,H,J,K,M,N)**. **A)** Complete slightly curved chain. **B)** Complete chain showing orientation of the setae. **C)** Intercalary cells with the organic "wing" like structures projecting from the girdle (arrows). **D)** Cells with several chloroplasts. **E)** Sibling valves joined with setae fusion and hyaline projections from the rim on the marginal ridge (arrowhead) showing silica fringes below the mantle (arrow) **F)** Sibling valves with the fused projections from the hyaline rim partially occluding the aperture. **G)** Terminal valve with no visible external part of the central process. **H)** Terminal valve with slice-shaped extensions of the hyaline rim (arrowhead) and small external protrusion of the central process. **I)** Detail of the terminal valve with labiate process. **J)** Detail of the terminal valve with labiate process within the central annulus. **K)** Seta tip with longitudinal strings interconnected with the transverse bars. **L)** and **M)** Detail of a seta. **N)** Detail of broken girdle bands. Scale bars: A = 50 µm; B,C = 20 µm; D = 10 µm; E = 2 µm; F,G = 5 µm; H,K-N = 1 µm; I,J = 0.5 µm.

3.1.2.2.11 Chaetoceros didymus Ehrenberg (1845)

(Figure 3.27.)

Bibliography: Hustedt (1930), Cupp (1943), Rines and Hargraves (1988) (as *C. didymus* var. *dydimus*) Hernández-Becerril (1991b), Jensen and Moestrup (1998), Berard-Therriault et al. (1999), Hernández-Becerril and Flores Granados (1998), Shevchenko et al. (2006), Sunesen et al. (2008), Ishii (2011)

Synonyms: *Goniothecium gastridium* Ehrenberg, *C. gastridium* Ehrenberg, *C. mamillanum* Cleve, *C. didymus* var. *anglica* (Grunow) Gran, *C. didymus* var. *hiemalis* Tempere et Peragallo, *C. didymus* var. *genuina* Gran et Yendo, *C. didymus* f. *adriatica* Schussnig, *Chaetoceros didymus* f. *singularis* Takano.

Description: a.a.: 8-33 µm (Hustedt: 10-40 µm, Cupp: 12-34 µm, Rines and Hargraves: 18-34 µm, Jensen and Moestrup: 12-40 µm, Hernández-Becerril and Flores Granados: 16-22 µm, Shevchenko: 10-35 µm, Sunesen: 14-30 µm); p.a.: 9-26 µm (Shevchenko: 8-12 µm)

LM: The cells are united in short and straight chains (Figure 3.27.A). Cells elliptical in valve view and rectangular in girdle view with sharp and slightly drawn up corners. There are two large plastids per cell (Figure 3.27.B). Valve face is slightly concave with a prominent hemispherical protuberance in the centre, mantle low without any visible constriction near its edge (Figure 3.27.B-D). The setae originate at the valve corners and cross over each other usually at the point outside of the chain margin with a basal part of variable length (Figure 3.27.B-D). The apertures are wide and their shape can be described as panduriform (peanut-shaped) due to the presence of central protuberances on both sibling valves. The intercalary setae are perpendicular to the colony axis or sometimes slightly curve towards the terminal part of the chain (Figure 3.27.A). In valve view, the setae diverge at about 25-45° from the apical plane and they can be classified either as Brunel group II or III (Figure 3.27.E). Terminal setae extend almost parallel to the colony axis (Figure 3.27.A,D). There were often observed unidentified flagellates, possibly some heterotrophic species, in the vicinity of the cells and on the setae (Figure 3.27.D).

EM: The valve is ornamented with a weak pattern of costae radiating from the central annulus located on the protuberance (Figure 3.27.G). Between the costae valve surface is densely perforated with round small poroids with the exception of the central part around the protuberance (Figure 3.27.G). The valve edge and the setae bases are ornamented with capilli which can be observed also in LM (Figure 3.27.E). Some capilli can be very long and branched (Figure 3.27.F, G) and some short more like spines (Figure 3.27.H). The setae are in cross-section circular in their basal part and after the junction for a short distance ornamented with large elongated poroids (Figure 3.27.H). They become later generally four-sided, with evenly distributed spines on the ridges. Each side is perforated with a single longitudinal line of elliptically shaped small areolae and scarcely distributed larger elongated poroids (Figure 3.27.I).

Distinctive features: Valve face with a prominent hemispherical central protuberance. The valve edge and setae bases ornamented with long capilli. Setae four sided with evenly distributed spines on the ridges and each side perforated with a single longitudinal line of elliptically shaped small areolae and scarcely distributed larger elongated poroids.

Comments: Resting spores were not observed in this study, but they are reported to be paired, with smooth valves and held together by two short thick setae. The primary valve is dome- shaped or in some cases has a central high protuberance and the secondary valve is concave. In the literature there are two varieties recognized: *C. didymus* var. *didymus* Ehrenberg and *C. didymus* var. *aggregata* Mangin. These taxa are distinguishable by the aperture which is very narrow and much reduced central protuberances in the latter variety but the confirmation of their validity needs more careful and detailed investigations preferably observation of clonal cultured strains. See also comments in the description of *C. protuberans*.

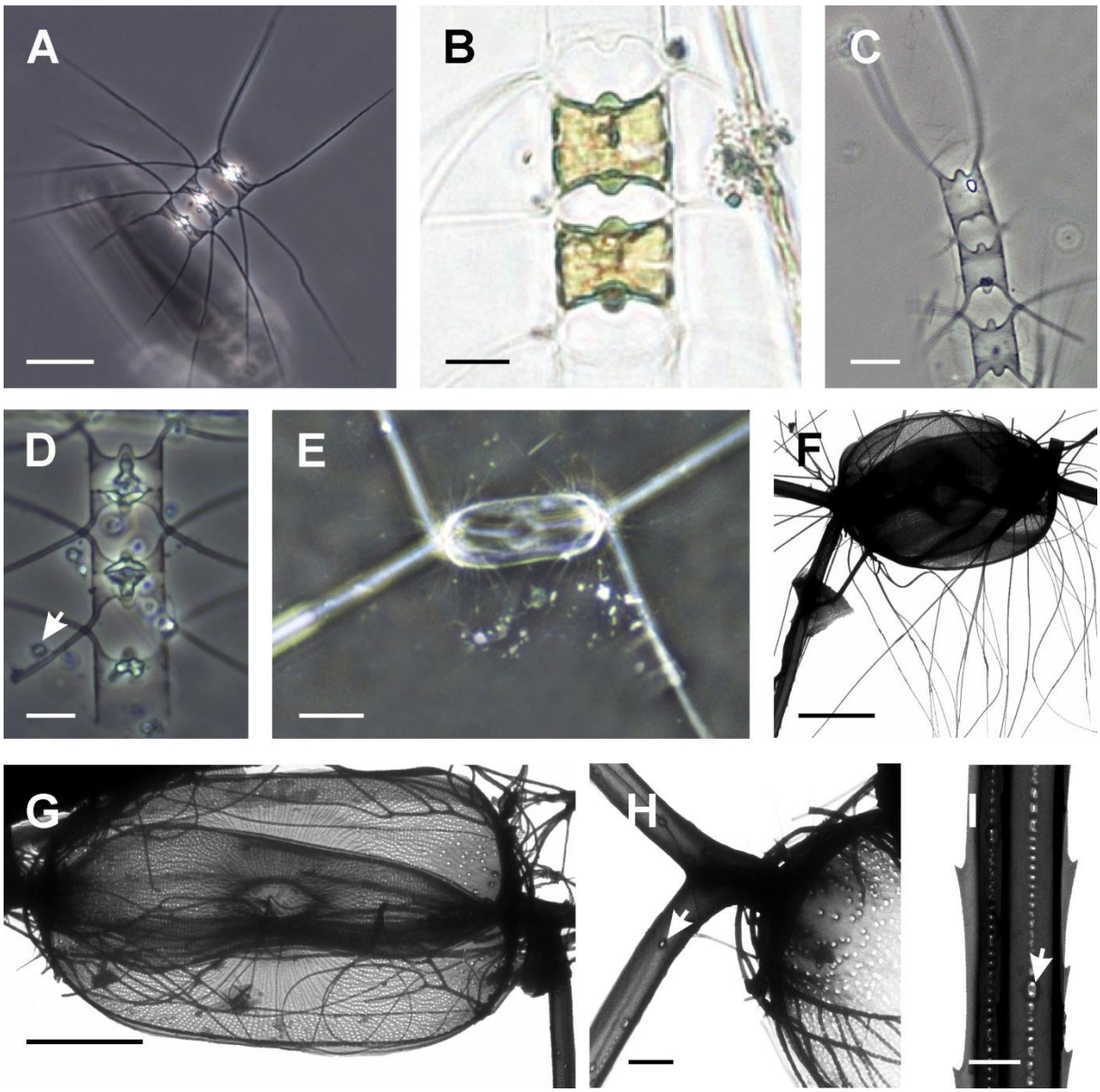

Figure 3.27. LM **(A-E),** TEM **(E,I)** and TEM **(F-I)** micrographs of *Chaetoceros didymus* from field material. **A)** Complete chain showing orientation of the setae. **B)** Intercalary cells with two chloroplasts. **C)** Terminal part of the chain. **D)** Middle part of the chain with flagellates attached to the cells and the setae (arrow). **E)** Valve view of the sibling valves showing setae orientation belonging to Brunel group III and capilli ornamenting the valve apices and setae bases. **F)** Two overlapped sibling valves with the long capilli. **G)** Intercalary valve showing valve ornamentation. **H)** Detail of the setae proximal to the valve, perforated by elongated pores (arrow). **I)** Detail of a seta. Scale bars: A = 20 µm; B-E = 10 µm; F,G = 5 µm; H = 1 µm; I = 0.5 µm.

3.1.2.2.12 Chaetoceros diversus Cleve (1873)

(Figure 3.28.)

Bibliography: Hustedt (1930), Cupp (1943), Hernández-Becerril (1996), Moreno Ruiz et al. (1993), Hernández-Becerril and Flores Granados (1998), Shevchenko et al. (2006)

Synonyms: *C. laevis* Leuduger-Fortmorel, *C. rudis* Leuduger-Fortmorel, *C. diversus* var. *tenuis* Cleve, *C. diversus* var. *mediterranea* Schröder

Description: a.a.: 7-14 µm (Hustedt: 8-12 µm, Cupp: 8-12 µm, Hernández-Becerril: 10-22 µm, Hernández-Becerril and Flores Granados: 12-19 µm, Shevchenko: 10-12 µm); p.a.: 6-11 µm (Hernández-Becerril: 7-19 µm Shevchenko: 6-18 µm)

LM: Cells united in short straight chains of 3-9 cells (Figure 3.28.A-C). In valve view cells generally circular, in girdle view rectangular with sharp corners. One chloroplast per cell (Figure 3.28.C). Valve face flat or slightly convex, mantle high with a slight constriction near the edge (Figure 3.28.C). The setae originate at the valve corners and fuse with the ones of the sibling valve immediately at the chain margin without a basal part. The fusion length varies between a single point of cross over to the length of several times of seta diameter. The apertures are slit shaped and very narrow or almost absent (Figure 3.28.C). Intercalary setae are diverging at an angle of 30-60° from the chain axis, proximally straight and distally curved strongly towards the terminal part of the chain. There are two morphological types of intercalary setae: the thin common ones and thick special ones (Figure 3.28.A). Special setae often become gradually thicker and tapering towards their ends. The setae lie in the apical plane and can be classified as Brunel Group I. Terminal setae extend almost parallel to the chain axis diverging in a U-shaped curve (Figure 3.28.A-B).

EM: The valve has a central annulus from which extends a weak pattern of radiating costae branching dichotomously towards the valve margin (Figure 3.28.D). The area between costae is irregularly perforated with densely scattered small pores (Figure 3.28.F). Between the valve face and the mantle in most cases there is no discernible marginal ridge, and only sometimes the extensions of the hyaline rim are fused between sibling cells at each edge of the aperture (Figure 3.28.E). Terminal cells have a central process with a small projection on the outside (Figure 3.28.G,H) and labiate structure from the inside of the valve (Figure 3.28.J). Girdle band ornamented with transverse parallel ribs (Figure 3.28.I). Common intercalary setae circular in cross-section with usually four longitudinal, relatively thick strings extending parallel with the seta axis and interconnected with very short parallel bars (Figure 3.28.L-N). The strings are ornamented with spines spirally arranged around the seta. Special setae are more silicified and have much thicker strings fused between each other and ornamented with stronger spines (Figure 3.28.K).

Distinctive features: Rectangular cells in girdle view with very sharp corners. Narrow apertures. Setae widely diverging in apical plane. Often present special intercalary setae which are thick and tapered towards ends.

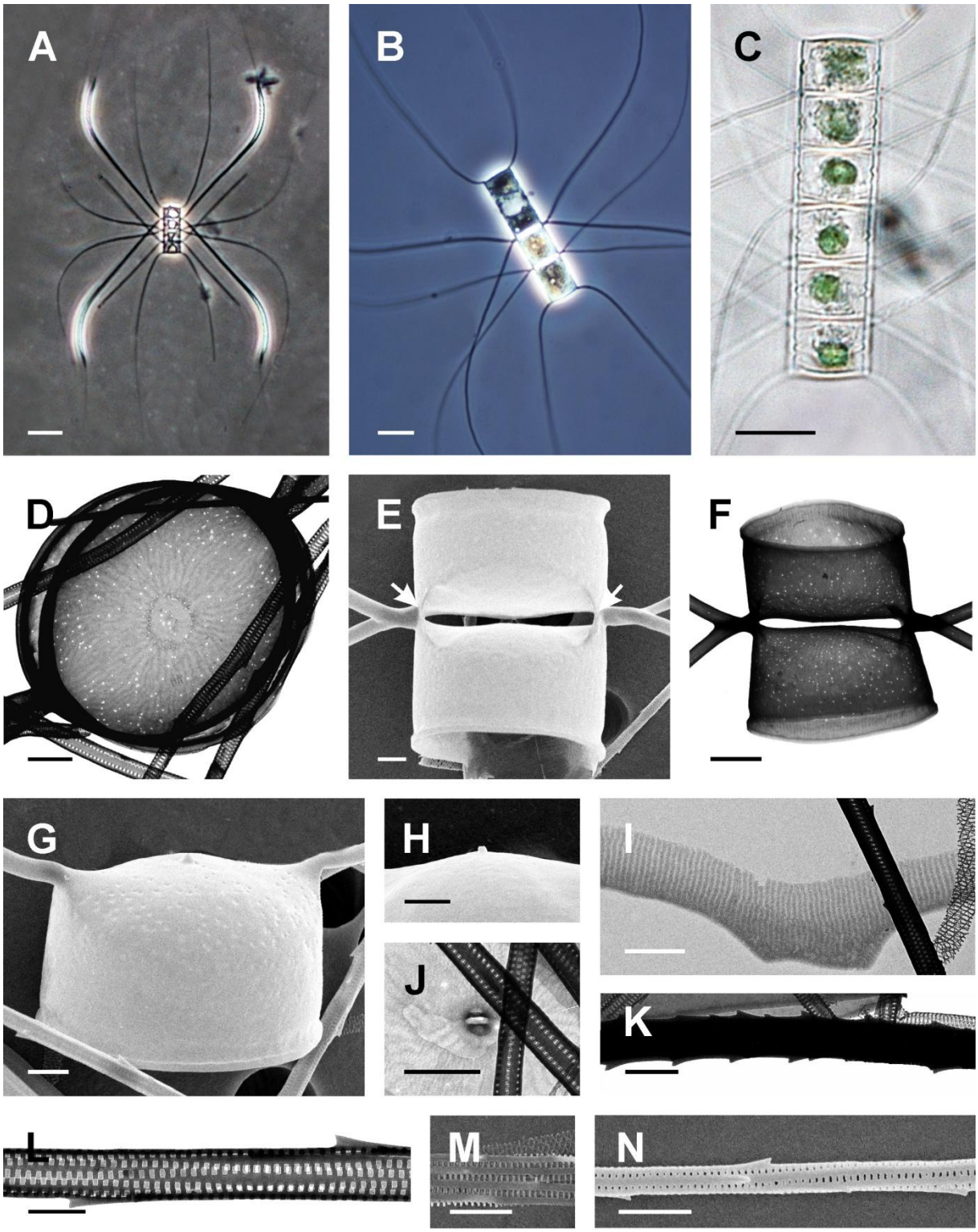

Figure 3.28. LM **(A-C),** TEM **(D,F,J-L)** and SEM **(E,G-H,M-N)** micrographs of *Chaetoceros diversus* from field samples **(A,C)** and from cultured strain PMFDIV1 **(B,D-N)**. **A)** Complete chain with special setae. **B)** Complete chain. **C)** Cells with single chloroplast. **D)** Two overlapped sibling valves showing valve ornamentation. **E)** Sibling valves with fused projections from the hyaline rim on the aperture edge (arrows). **F)** Sibling valves in girdle view. **G)** Terminal valve. **H)** External small projection of the central process. **I)** Detail of intercalary girdle band. **J)** Internal view on the labiate central process. **K)** Detail of special intercalary seta. **L), M)** and **N)** Detail of a seta. Scale bars: A = 20 µm; B-C = 10 µm; D-E,G,I-K, M-N = 1 µm; F = 1 µm; H,L = 0.5 µm.

3.1.2.2.13 Chaetoceros lauderi Ralfs in Lauder (1864)

(Figure 3.29. and 3.30.)

Bibliography: Hustedt (1930), Cupp (1943), Hargraves (1979), Rines and Hargraves (1988), Hernández-Becerril and Flores Granados (1998), Jensen and Moestrup (1998), Sunesen et al. (2008), Kooistra et al. (2010), Ishii (2011)

Synonyms: *C. weissflogii* Schütt

Description: a.a.: 15-39 µm (Cupp: 18-24 µm, Hernández-Becerril and Flores Granados: 23-30 µm, Sunesen et al.: 15-25 (38) µm); p.a.: 27-63 µm

LM: Cells are united into long straight chains which are slightly twisted around the chain axis (Figure 3.29.A). In valve view cells are circular to elliptical, in girdle view rectangular with sharp valve corners and often with the pervalvar axis longer than the apical axis (Figure 3.29.B-C). There are numerous (25-45) small chloroplasts present in each cell (Figure 3.29.B). The valve face is flat. The mantle is low without any constriction at its edge while the girdle is usually very high. Intercalary setae emerge from the corners of the valves and fuse immediately without basal part only at their point of crossing. Apertures are very narrow and slit-like (Figure 3.29.B-C). In girdle view, setae are generally straight, extending perpendicular to the chain axis, with some of them curving towards either end of the chain (Figure 3.29.A-B). Setae in valve view diverge from the apical plane at an angle of 30-40° or one seta parallel with the apical plane, the other more or less perpendicular to it hence the species can be classified as Brunel Group II or III (Figure 3.29.D). Terminal setae morphologically similar to intercalary ones, strongly diverging in a broad U-shaped curve towards the end of the chain (Figure 3.29.A). The resting spores are quite large, with the capitate primary valve constricted at its base and ornamented with long spines on its central part which are either completely straight or sharply bent near the tip (Figure 3.30.A-D). The mantle of both resting spore valves is quite high. Secondary valve is flat to vaulted, either with smooth surface or ornamented with few thin and very long hair-like spines (capilli) which are commonly present in a form of a single ring on the mantle advalvar margin. Further on the mantle, next to the capilli ring, there is a single ring of puncta (Figure 3.30.D).

EM: The valve face is ornamented with densely and irregularly distributed anastomosing ribs radiating from a relatively large central annulus (Figure 3.29.E-F) and becoming parallel on the valve mantle (Figure 3.29.H). The area between ribs is hyaline. The marginal ridge is often ornamented with a very low hyaline rim (Figure 3.29.I). Terminal valves possess a central process, in the internal view it is usually a slit-shaped opening (Figure 3.29.H,L) with the external part as a wide flattened tube (Figure 3.29.I,J). The girdle bands have the fine structure of parallel transverse ribs with small poroids irregularly distributed in the interrib area (Figure 3.29.K). Setae are circular in cross-section, composed of the longitudinal silica strings bearing spines and arranged in a helicoidal pattern while interconnected with transverse silica bars (Figure 3.29.M-N). The EM examination of the resting spores confirmed LM observations.

Distinctive features: Elongated cells, very narrow and almost non existent apertures. Chains slightly twisted around the axis. Characteristic resting spores with long spines on the capitate primary valve and ring of long capilli around the secondary valve mantle.

Comments: The vegetative cells of *C. teres* Cleve are reported to be very similar to *C. lauderi* with the only difference in the chain morphology being completely straight in the former opposed to slightly twisted in the latter species. However, the valves of the *C. teres* resting spore are evenly vaulted and have a completely smooth surface. On the secondary valve is sometimes present a marginal ring of fine capilli. The ultrastructural characteristics of *C. teres* are not reported in the available literature therefore they could not be compared with our findings. In this study, the cultured strain formed resting spores which morphology corresponded to *C. lauderi* and this spores were sometimes also found in the examined field material. For these reasons, we ascribe all the specimens examined in this study to *C. lauderi*.

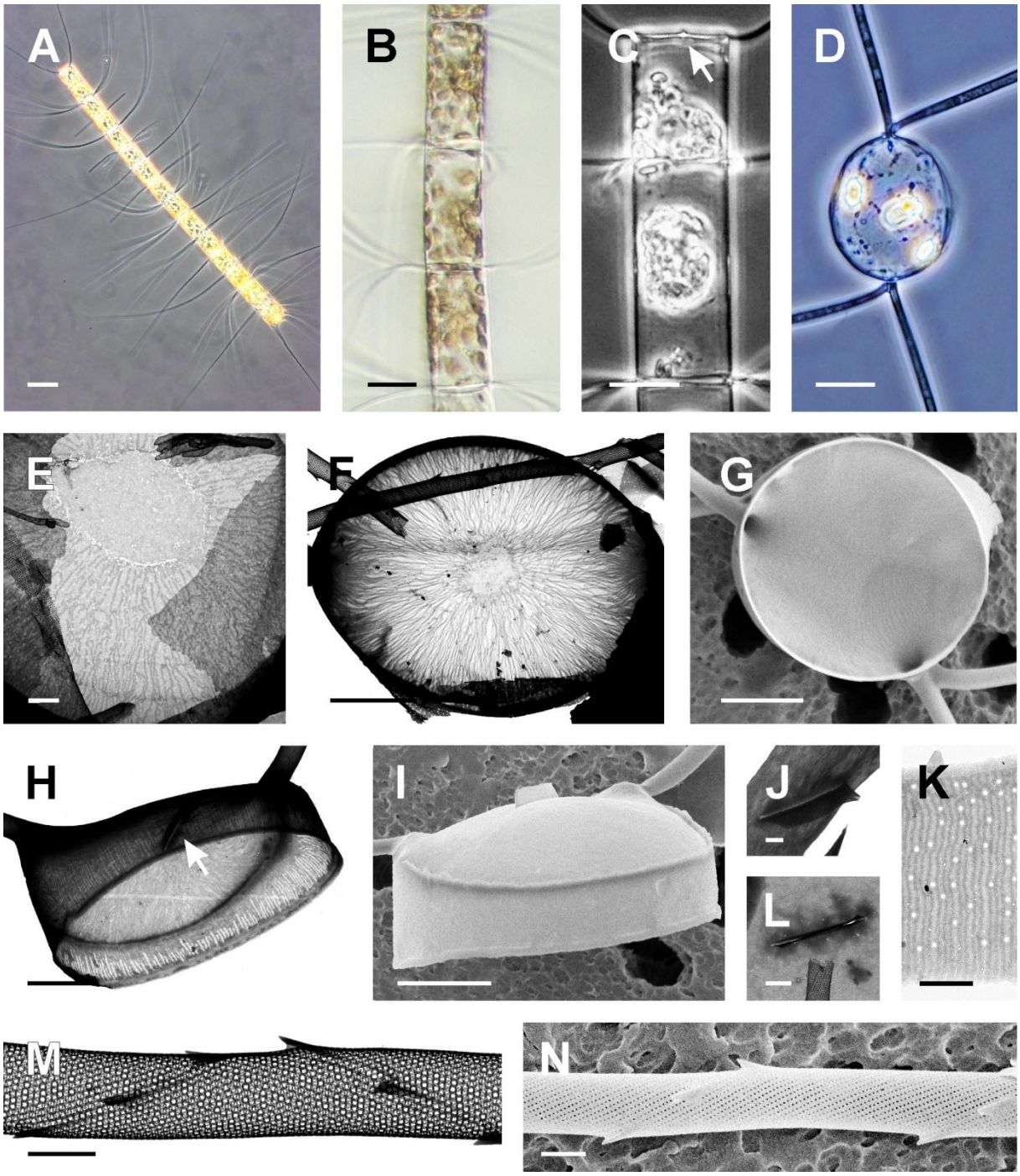

Figure 3.29. LM **(A-D),** TEM **(E,F,H,J-M)** and SEM **(G,I,N)** micrographs of *Chaetoceros lauderi* from cultured strain PMFL1. **A)** Complete chain showing setae orientation. **B)** Intercalary cells with numerous chloroplasts. **C)** Terminal part of the chain with external projection of the central process on the end valve (arrow). **D)** Valve view of the sibling valves showing setae orientation belonging to Brunel group III. **E)** Detail of the valve with central annulus and anastomosing ribs. **F)** Two overlapped sibling valves showing valve ornamentation. **G)** Sibling valves in valve view. **H)** Terminal valve with slit-like central process (arrow). Note the parallel ribs on the valve mantle. **I)** Terminal valve with external flattened tube of the central process. Note the low hyaline rim on the marginal ridge. **J)** Detail of the terminal valve with flattened tube of the central process. **K)** Detail of the girdle band. **L)** Detail of the terminal valve with the slit-like central process. **M)** and **N)** Detail of a seta. Scale bars: A = 50 µm; B-C = 20 µm; D = 10 µm; F-I =5 µm; E, K-N= 1 µm; J= 0.5 µm.

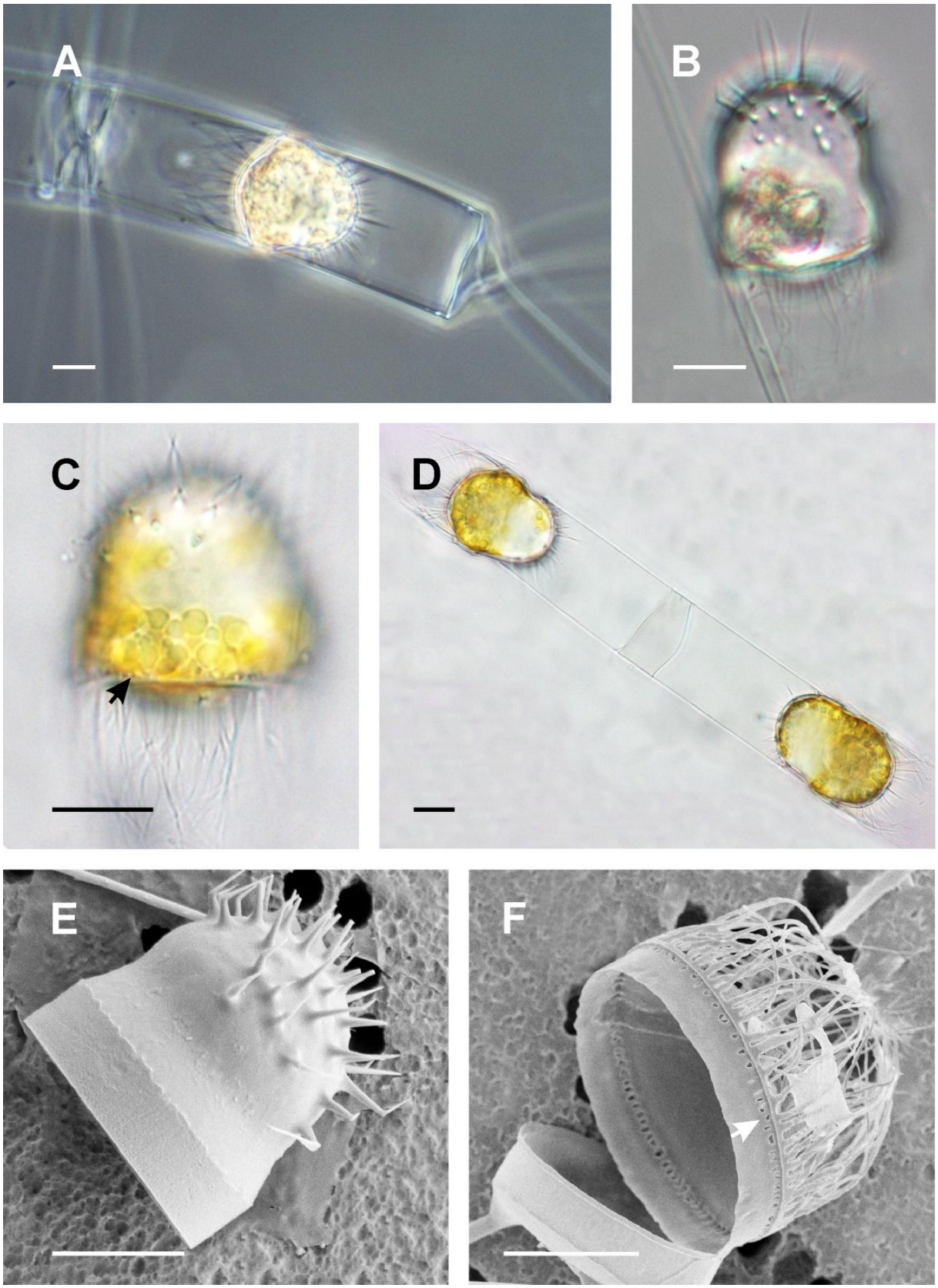

Figure 3.30. LM **(A-D),** SEM **(E,F)** micrographs of *Chaetoceros lauderi* from cultured strain PMFL1. **A)** Complete resting spore within the vegetative terminal cell. **B)** Complete resting spore. **C)** Resting spore. Note the single ring of puncta on the advalvar margin of the secondary valve mantle (arrow). **D)** Two resting spores in sibling cells. **E)** Primary valve of the resting spore. **F)** Secondary valve of the resting spore with the single ring of puncta on the advalvar mantle margin. Scale bars: A-F = 10 µm.

3.1.2.2.14 Chaetoceros cf. lacinious Schütt (1895)

(Figure 3.31. A-B)

Bibliography: Hustedt (1930), Cupp (1943), Evensen and Hasle (1975), Rines and Hargraves (1988), Hernández-Becerril (1996) (as *C. distans*), Jensen and Moestrup (1998), Hernández-Becerril and Flores Granados (1998), Shevchenko et al. (2006), Sunesen et al. (2008)

Synonyms: *C. commutatus* Cleve, and possibly: *C. distans* Cleve and *C. pelagicus* Cleve

Description: a.a.: 10-22 µm (Hustedt: 10-42 µm, Cupp: 10-28 µm, Rines and Hargraves: 9-31 µm, Jensen and Moestrup: 8-40 µm, Hernández-Becerril and Flores Granados: 13-18 µm, Shevchenko et al.: 10-25 µm, Sunesen et al.: 8-16 µm); p.a.: 16-35 µm (Shevchenko et al.: 15-25 µm)

LM: Cells united to form mostly long straight chains (Figure 3.31.A). Valve face flat to slightly concave with drawn up corners. Valve mantle low with a slight constriction near the edge, girdle high (Figure 3.31.B). Setae originate at the valve corners with a long basal part extending in the pervalvar direction and crossing at the chain margin. The aperture is very large and rectangular to hexagonal in shape (Figure 3.31.B). Setae are straight and mostly directed perpendicular to the chain axis. Terminal setae have their basal part extended in the pervalvar direction and further on diverged in a wide U-shaped curve (Figure 3.31.A) or bend towards the chain axis sometimes crossing each other.

Comments: Similar species are *C. diadema* which has characteristic spores with dichotomously branching spines on the primary valve and *C. brevis* which has a central inflation on the valve face and plastid-like material within setae. The relationship between several species: C. *laciniosus*, *C. distans* and *C. pelagicus* is currently unclear. If these species are in fact conspecific, then the name *C. distans* has a priority. To solve this problem, further morphological and molecular studies of the cultured strains are needed. In this study, the species is observed only with LM from the field samples without spores or ultrastructural observations therefore we tentatively ascribed this morphotype to *C.* cf. *laciniousus.*

3.1.2.2.15 Chaetoceros messanensis Castracane (1875)

(Figure 3.31. C-D)

Bibliography: Hustedt (1930), Cupp (1943), Evensen and Hasle (1975), Hernández-Becerril (1996), Hernández-Becerril and Flores Granados (1998), Shevchenko et al. (2006)

Synonyms: *C. furca* Cleve, *C. furca var. macroceros* Schröder, *C. cornutus* Leuduger-Fortmorel

Description: a.a.: 10-37 µm (Hustedt: 12-40 µm, Cupp: 9-33 µm, Hernández-Becerril: 20-32 µm, Hernández-Becerril and Flores Granados: 14-26 µm, Shevchenko: 12-35 µm); p.a.: 17-40 µm (Hernández-Becerril: 12-18 µm Shevchenko: 6-40 µm)

LM: Cells united in short, straight chains (Figure 3.31.C). Cells are elliptical in valve view and rectangular in girdle view with sharp, drawn up valve corners which are touching between sibling cells. There is one chloroplast per cell (Figure 3.31.C). The valve face is flat to slightly concave, the mantle low without any constriction at its edge and the girdle high or equidimensional with the mantle. Intercalary setae originate from the valve corners and fuse immediately without basal part. Apertures very wide and hexagonal. There are two morphological types of intercalary setae: the thin common ones and thick special ones (Figure 3.31.C-D). Special setae are long and thick, strongly silicified,

fused for about two thirds of their length and then strongly diverged opposite to each other appearing very thick and slightly undulated in the forked part probably due to the presence of the strong spines. They are usually present between the sibling cells close to either end of the chain. Common setae are thin and in the girdle view slightly equally diverged from the apical axis at an angle of 30–60°. All setae are mostly straight and lie in the apical plane therefore they can be classified as Brunel Group I. Terminal setae are thin, strongly bent outwards from their point of origin and further on widely diverged becoming almost perpendicular to the chain axis (Figure 3.31.C,D). The setae different in orientation, one is more strongly bent toward the chain.

Distinctive features: Intercalary special setae are long and thick, strongly silicified, fused for about two thirds of their length and forked at their ends.

3.1.2.2.16 Chaetoceros neocompactus VanLandingham (1968)

(Figure 3.31.E-I)

Bibliography: Ikari (1928) (as *C. compactum*)

Description: a.a.: 10-15 µm (Ikari 18-30 µm); p.a.: 8-9 µm

LM: Cells united in short, straight chains (Figure 3.31.G). Cells elliptical to round in valve view (Figure 3.31.H-I), rectangular in girdle view with longer apical than pervalvar axis and sharp valve corners (Figure 3.31.E-F). There is one chloroplast per cell. Intercalary valve face flat or convex, terminal valve face markedly convex (dome-shaped) (Figure 3.31.F). The setae originate at the cell corners and immediately cross each other at a single point. The sibling valves are positioned very close to each other so apparently there is no aperture between sibling cells. Setae are very long and possess conspicuous strong undulations (Figure 3.31.I). As there are no EM observations available we cannot conclude if the undulations visible in LM are the result of the setae ornamentation with strong spines or maybe some other specific ultrastructural feature. The setae are oriented perpendicularly to the chain axis or slightly curved towards either end of the chain. In valve view, sibling setae are obliquely curved from the apical axis, in most cases diverging from each other equally from the apical plane at an angle 20-30° conforming to Brunel Group II (Figure 3.31.H). Terminal setae extend almost parallel with the pervalvar axis (Figure 3.31.G).

Distinctive features: No visible apertures. Valves convex. Long setae appear strongly undulated.

Comments: This morphotype was described as *C. compactum* Ikari, however species under the name *C. compactus* described by Schütt is considered as a synonym of *C. atlanticus* Cleve, therefore VanLandingham changed the name to *C. neocompactus.*

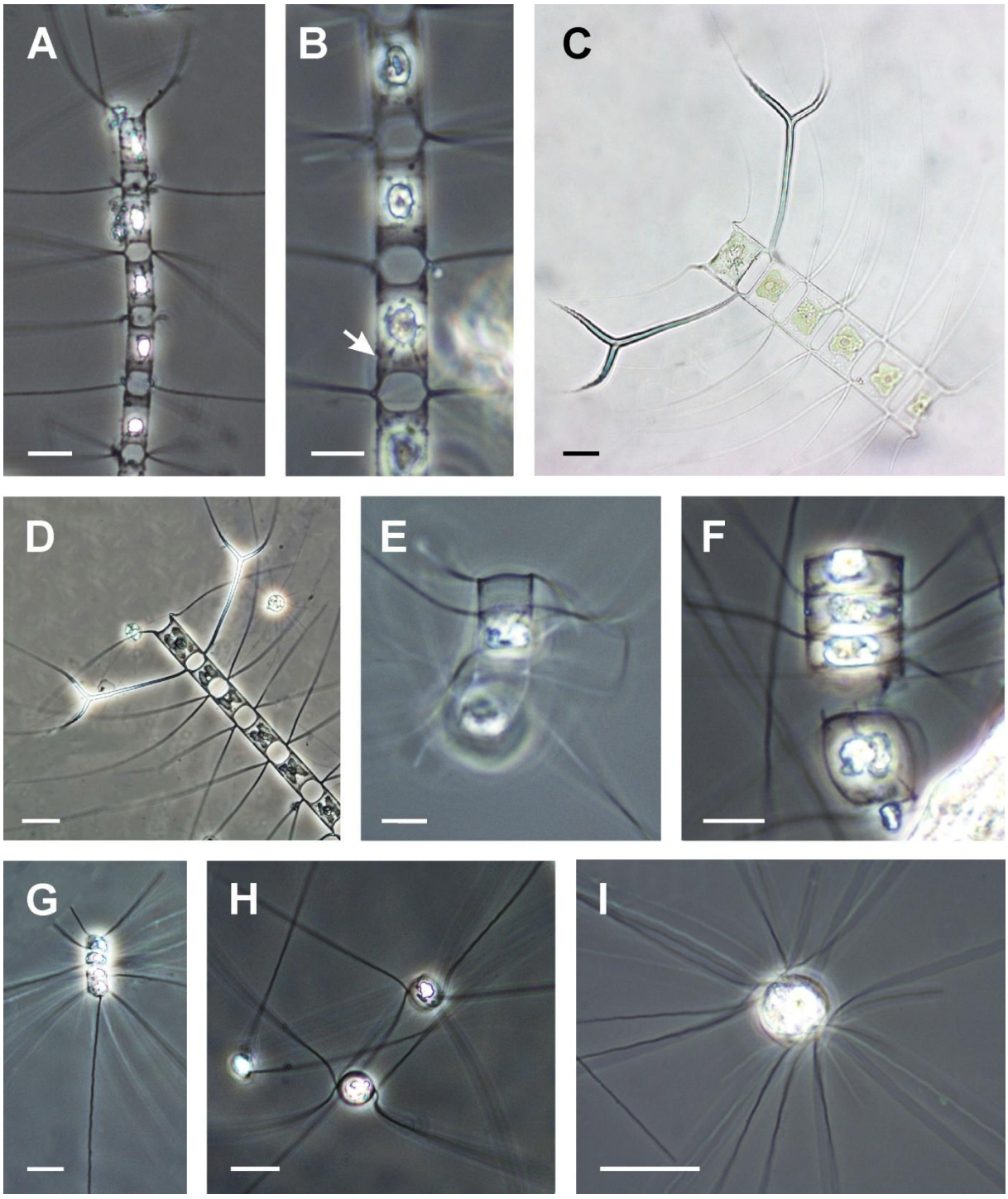

Figure 3.31. LM **(A-G)** and SEM **(H,I)** micrographs of *Chaetoceros* spp. from field material. **A-B** *Chaetoceros cf. laciniosus.* **A)** Terminal part of the chain showing the orientation of the setae. **B)** Middle part of the chain showing wide aperture and the constriction near the mantle edge on the valve(arrow); **C-D** *C. messanensis* **C)** Complete chain with special forked intercalary setae. **D)** Terminal part of the chain. **E-I** *C. neocompactus.* **E)** Terminal part of the chain, note the dome shaped terminal valve. **F)** Terminal part of the chain with no evident apertures between sibling cells. **G)** Complete chain showing orientation of the terminal setae parallel with the chain axis. **H)** Sibling valves in valve view. **I)** Intercalary cells in valve view. Note the strong undulations on the setae. Scale bars: A-B,E-F,I = 10 µm; C-D,G-H = 20 µm;

3.1.2.2.17 Chaetoceros pseudocurvisetus Mangin (1910)

(Figure 3.32.E-F)

Bibliography: Hustedt (1930), Cupp (1943), Fryxell (1978), Rines and Hargraves (1988), Hernández-Becerril (1996), Hernández-Becerril and Flores Granados (1998), Shevchenko et al. (2006), Kooistra et al. (2010).

Description: a.a.: µm (Hustedt: 15-50 µm, Cupp: 13-19 µm, Rines and Hargraves: 12-18 µm, Hernández-Becerril: 13-21 µm, Hernández-Becerril and Flores Granados: 11-22 µm, Shevchenko: 15-35 µm); p.a.: µm (Hernández-Becerril: 16-22 µm Shevchenko: 15-30 µm)

LM: Cells united in long, curved or helical chains (Figure 3.32.E). Cells elliptical in valve view and rectangular in girdle view. In each cell there is a single lobbed chloroplast (Figure 3.32.F). Valve face is concave with four protuberances situated along the valve margin, two per each side of the valve positioned close to the valve apices. Each pair of the protuberances fuses with the corresponding pair on the sibling valve thereby defining two small, lateral apertures (Figure 3.32.F). The fusion of the protuberances in addition to the setae fusion reinforces the connection of the cells in chain, similar as in *C. costatus* (Chapter 3.1.2.2.8.). The main aperture is oval and shorter than the apical axis. Valve mantle low without any constriction at its edge, girdle high. Intercalary setae originate from the valve corners between the projections and fuse immediately without basal part. In girdle view all setae are curved towards the same, convex side of the chain (Figure 3.32.E) while in the valve view they are all bent to one side of the apical axis belonging to the Brunel Group V.

Distinctive features: Chains curved in the pervalvar plane. On each valve four protuberances fused between sibling cells forming a characteristic aperture divided in three parts.

Comments: Easily confused with *C. curvisetus* with the main difference in the shape of the aperture as there are no protuberances in *C. curvisetus* valve.

3.1.2.2.18 Chaetoceros protuberans Lauder (1864)

(Figure 3.32.G-I)

Bibliography: Hustedt (1930) (as *C. didymus* var. *protuberans*), Cupp (1943) (as *C. didymus* var. *protuberans*), Rines and Hargraves (1988) (as *C. didymus* var. *protuberans*), Lechuga-Devéze and Hernandez-Becerril (1988), Hernández-Becerril (1991b), Jensen and Moestrup (1998) (as *C. didymus* var. *protuberans*), Hernández-Becerril and Flores Granados (1998), Shevchenko et al. (2006), Kooistra et al. (2010)

Synonyms: *C. dydimus* var. *protuberans* (Lauder) Gran & Yendo

Description: a.a.: 13-24 µm (Hustedt: 10-40 µm, Rines and Hargraves: 17-20 µm, Hernández-Becerril and Flores Granados: 16-22 µm, Shevchenko: 10-35 µm); p.a.: 22-26 µm (Shevchenko: 8-12 µm)

LM: The cells are united in short and straight chains. Cells elliptical in valve view and rectangular in girdle view with sharp and slightly drawn up corners. Valve face is slightly concave with a prominent hemispherical protuberance in the centre, mantle low with a slight constriction near its edge (Figure 3.32.G,H). The intercalary setae arise at the cell corners with a long basal part and cross over each other outside the chain margin. They diverge from the apical axis at a small angle (Brunel Group II) in valve view, and in girdle view they are generally straight or slightly bent towards the chain end. The apertures are wide and their shape can be described as panduriform (peanut-shaped) due to the presence of central protuberances on both sibling valves (Figure 3.32.G,H).

EM: The valve surface and the mantle are densely perforated with round small poroids distributed in rows lacking only in the part of the central protuberance (Figure 3.29.H). The hyaline rim is present along the marginal ridge of the valve. The setae are in cross-section circular in their basal part and after the junction they become four-sided, with evenly distributed spines on the ridges (Figure 3.29.H). Each side is perforated with a single longitudinal line of large elongated poroids (Figure 3.29.I).

Distinctive features: Valve face with a prominent hemispherical central protuberance without any capilli. Setae four sided with evenly distributed spines on the ridges and each side perforated with a single longitudinal line of elliptically shaped small areolae and scarcely distributed larger elongated poroids.

Remarks: Resting spores were not observed,but they are described to have smooth and unequally vaulted valves. The primary valve has a high marginal sheath, sometimes fissured, in most cases partially closed on the top but sometimes completely open. The morphology of *C. protuberans* is closely related to *C. didymus* with the distinctive characters being the lack of fine siliceous capilli present on the valves and the setae bases, the point of fusion between sibling setae which is further in *C. protuberans* and the morphology of the resting spores. *Chaetoceros didymus* var. *anglica* is considered to be very similar to *C. protuberans* with the difference only in more delicate appearance of the cells and very long basal part of the intercalary seta, but the confirmation of the taxonomic validity of this variety needs further investigations.

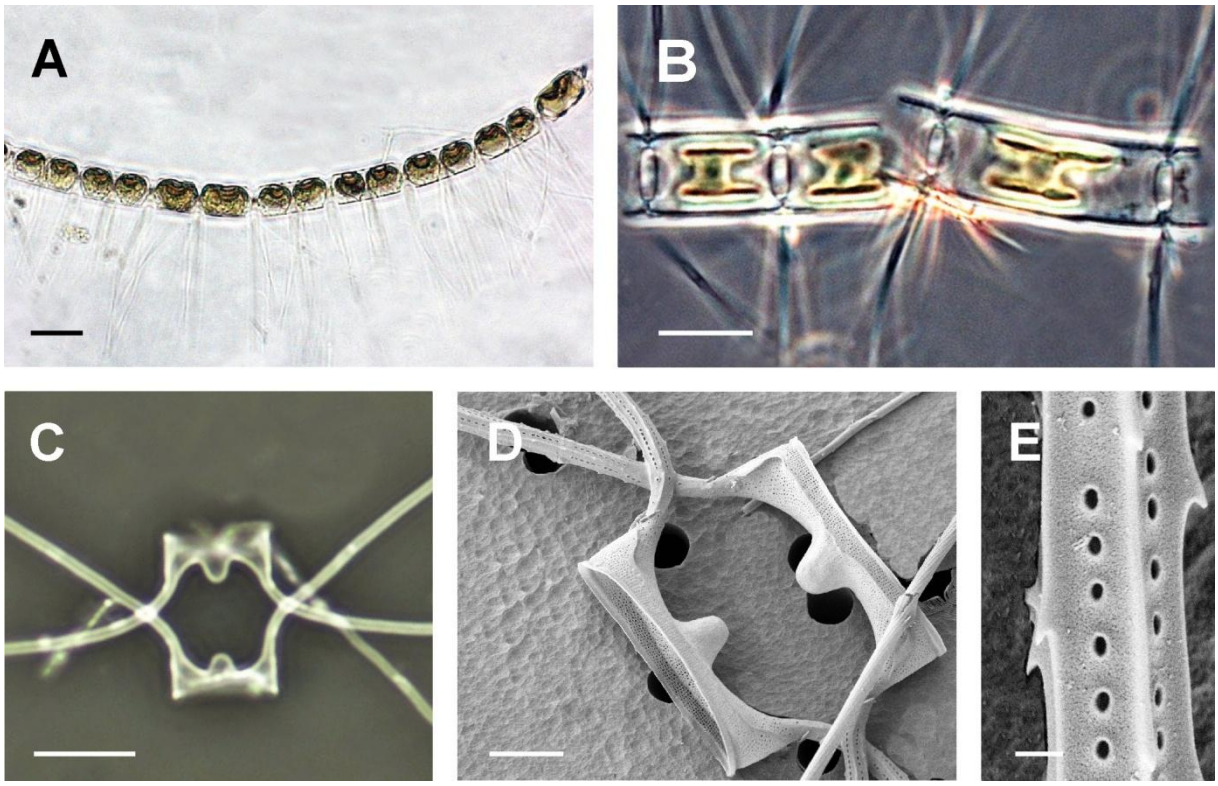

Figure 3.32. LM **(A-C)** and SEM **(D,E)** micrographs of *Chaetoceros* spp. from field material. **A-B** *C. pseudocurvisetus* **A)** Middle part of the chain showing orientation of the setae. **B)** Intercalary cells showing the short aperture. **C-E** *C: protuberans* **C)** Sibling valves. **D)** Sibling valves, note the poroids perforating the valve surface. **E)** Detail of a seta A= 20 µm; B-C = 10 µm; D = 5 µm; E = 0.5 µm.

3.1.2.2.19 Chaetoceros salsugineus Takano (1983)

(Figure 3.33.)

Bibliography: Orlova and Selina (1993), Orlova and Aizdaicher (2000), Trigueros et al. (2002), Shevchenko et al. (2006)

Description: a.a.: 4-10 µm (Orlova and Aizdaicher: 3-7 µm, Trigueros et al.: 4-9 µm, Shevchenko: 3-7 µm); p.a.: 5-13 µm (Trigueros et al.: 4-9 µm, Shevchenko: 4-9 µm)

LM: Cells united in short straight chains (Figure 3.33.A-B). In valve view cells elliptical, in girdle view rectangular with sharp valve edges. One large plate like chloroplast per cell (Figure 3.33.B). The valve face is flat or slightly concave. Valve mantle low without the constriction near the margin and the girdle is higher than the mantle or more often has the same dimensions. Setae are quite long and very thin, originating from the valve corners. Intercalary setae fuse immediately or after a short basal part with a single cross-over point at the chain margin (Figure 3.33.C). The apertures are very narrow and slit-like (Figure 3.33.C). In valve view the intercalary setae belong to Brunel Group II. In girdle view the setae extend very straight, diverging at an angle of 50-60° with the respect to the apical axis (Figure 3.33.A-B). Terminal setae are generally oriented parallel to the chain axis sometimes crossing each other in the distal part, but in few cases they can diverge more widely from the pervalvar axis forming a V-shape (Figure 3.33.A-B). The resting spores were not observed.

EM: The frustule appears to be weakly silicified. The valve is ornamented with the distinct pattern of relatively thick costae radiating from a central annulus and scarcely branching when reaching near the marginal ridge (Figure 3.33.D,G,I) becoming parallel on the mantle. All valves have a high rim projecting from the marginal ridge which is fissured with large oval perforations (Figure 3.33.G-I). The rim is often fused between sibling cells at the both side margins of the aperture (Figure 3.33.E-F). Central process is present only on the terminal valves, from the internal view it is a simple slit (Figure 3.33.H,J) and on the exterior it is a long, flattened and wide tube (Figure 3.33.I). The girdle bands striation pattern consists of numerous transverse parallel ribs (Figure 3.33.K). Setae are circular in cross section, the basal part is smooth and hyaline and gradually becomes six thin longitudinal strings twisted around the seta axis and interconnected with quite long transverse bars generating the helicoidal pattern (Figure 3.33.L). The strings bear small spines arranged in a helicoidal pattern. (Figure 3.33.M).

Distinctive features: Weakly silicified cells. Straight setae diverging at an angle of 50-60° with the respect to the apical axis. Terminal setae parallel to the chain axis sometimes crossing each other in the distal part, but in few cases they can form a V-shape. All valves have a high rim projecting from the marginal ridge which is fissured with large oval perforations and often fused between sibling valves.

Comments: The species appears inL M very similar to *C.* cf. *wighamii* but with a distinguishable ornamentation of the valve, structure of the setae and tube-like central process. It is possible also that this is a colonial form of *C. tenuissimus* but more investigations including molecular analyses are necessary.

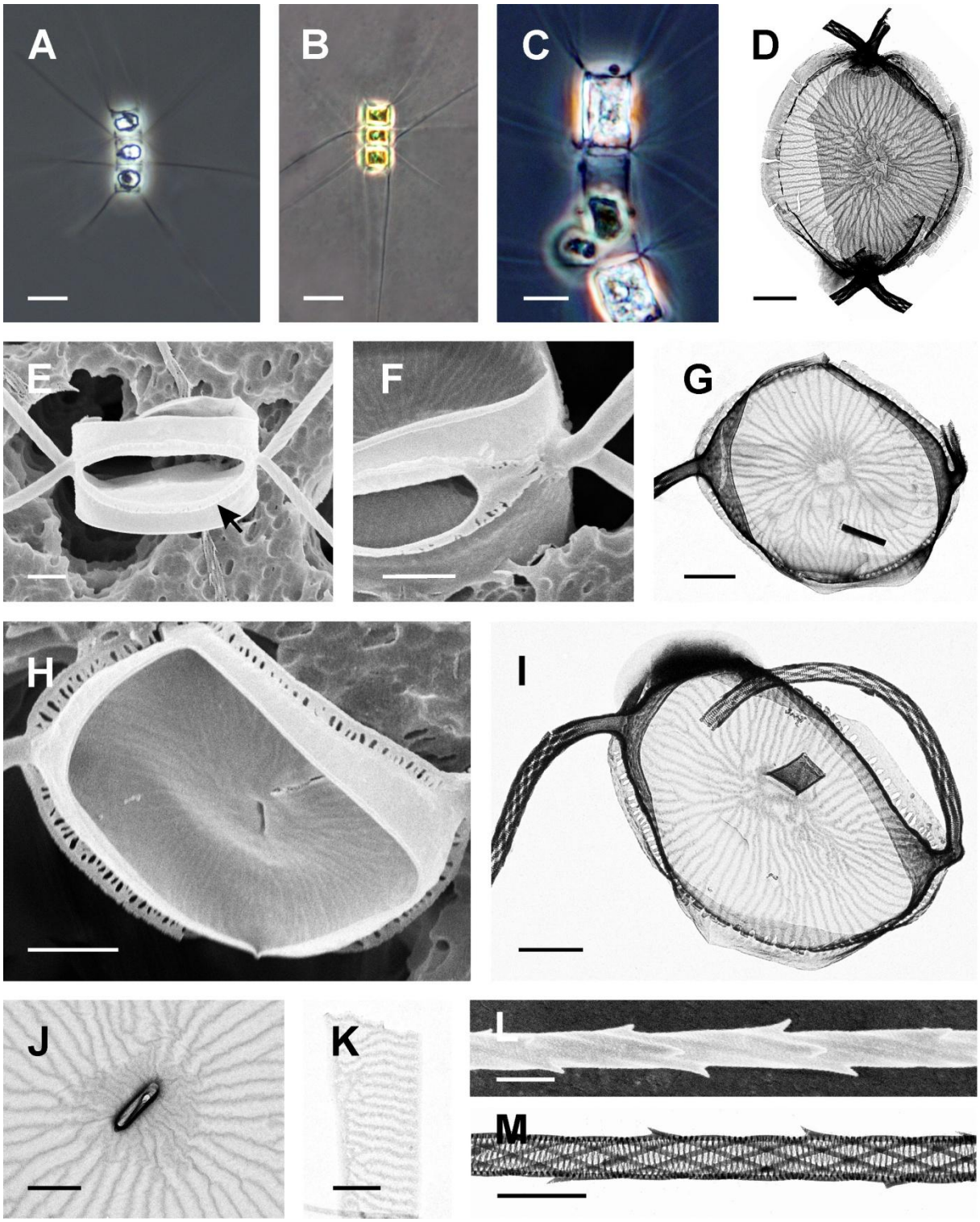

Figure 3.33. LM **(A-C),** TEM **(D,G,I-K,M)** and SEM **(E-F,H,L)** micrographs of *Chaetoceros salsugineus* from cultured strain PMFW1. **A)** and **B)** Complete chain showing setae orientation. **C)** Terminal part of the chain with narrow slit like apertures. **D)** Sibling valves in valve view. **E)** Sibling valves in girdle view. Note the fissured rim on the marginal ridge (arrow) **F)** Detail of the aperture marginally occluded with the fused rim between sibling valves. **G)** Intercalary valve in valve view showing the ornamentation pattern. **H)** Inside view of the terminal valve with slit-like central process. **I)** Terminal valve with external flattened tube of the central process. **J)** Detail of the terminal valve with internal hole of slit-like central process in the centre of the annulus. **K)** Detail of a girdle band. **L)** and **M)** Detail of a seta. Scale bars: A-B=10 µm; C=5 µm; D-I =1 µm; J-M=0.5 µm.

3.1.2.2.20 Chaetoceros simplex Ostenfeld (1901)

(Figure 3.34. A-C)

Bibliography: Hustedt (1930), Rines and Hargraves (1988), Jensen and Moestrup (1998), Berard-Therriault et al. (1999), Hoppenrath et al. (2009)

Description: a.a.: 5 – 7 µm (Hustedt: 4-30 µm, Jensen and Moestrup: 16-24 µm, Berard-Therriault et al.:6-15 µm, Hoppenrath et al.: 6-24 µm); p.a.: 7 - 9 µm

LM: Cells are solitary (Figure 3.34.A) with usually longer apical than the pervalvar axis. In valve view cells elliptical, in girdle view rectangular with sharp valve corners. There is a single chloroplast per cell. Valve face flat to slightly concave. Setae originate at the valve corners and extend straight, in the valve view lying in the apical plane. In the girdle view setae extend almost parallel with the apical axis (Figure 3.34.A) or are slightly diverged from it sometimes crossing over each other (Figure 3.34.C). Resting spores were not observed in this study, but they are described with vaulted valves and covered with spines.

EM: The valves are ornamented with annulus and radiating costae. On the marginal ridge there is a very low rim. Every valve possesses a long tube-like central process (Figure 3.34.B). Unfortunately, it was not possible to see details of the setae structure, except that they appear circular in cross section and are ornamented with spines.

Distinctive features: Solitary cells. Setae extend parallel with the apical axis, sometimes crossing each other distally. In valve view they lie in the apical plane.

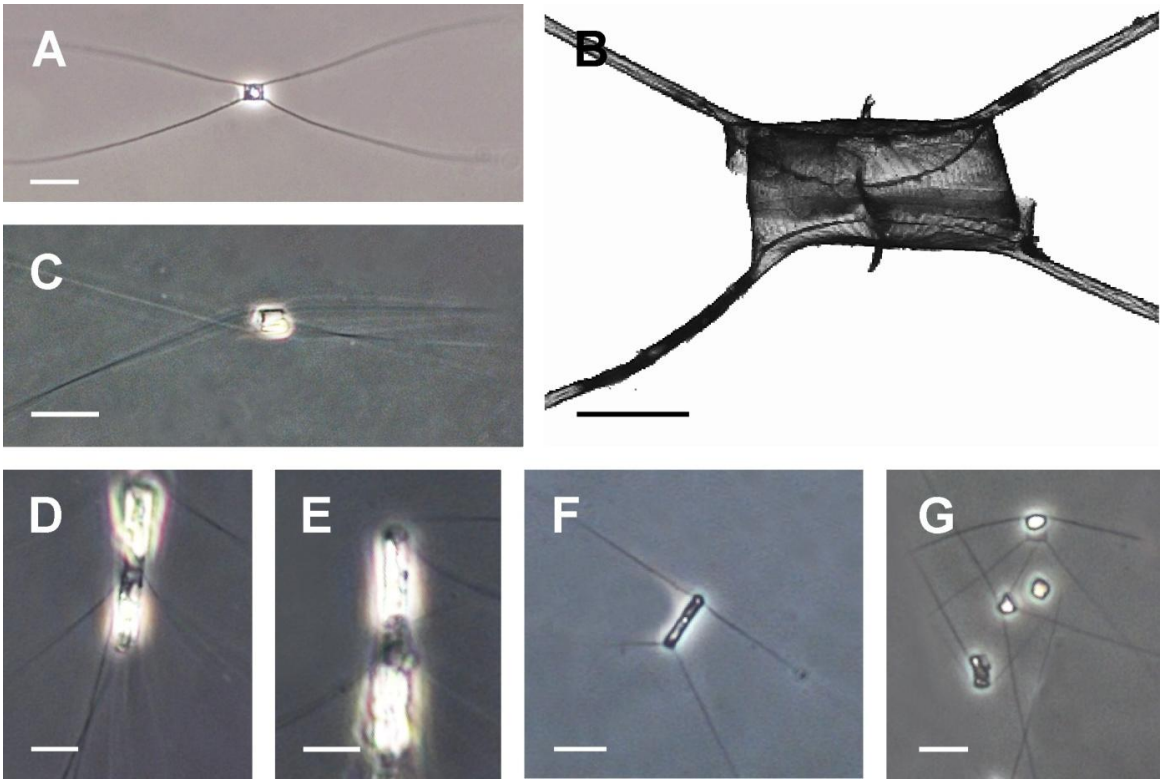

3.1.2.2.21 Chaetoceros subtilis Cleve (1896)

(Figure 3.34. D-G)

Bibliography: Hustedt (1930), Rines and Hargraves (1988), Jensen and Moestrup (1998), Berard-Therriault et al. (1999), Aké Castillo et al. (2004), Shevchenko et al. (2006), Hoppenrath et al. (2009)

Synonyms: *C. caspicus* Cleve, *C. knipowitschi* Henckel

Description: a.a.: 2-6 µm (Hustedt: 5-14 µm, Rines and Hargraves: 2-21 µm, Berard-Therriault et al.:3-13 µm, Shevchenko et al.: 4-12 µm, Hoppenrath et al.: 2-14 µm); p.a.: 3–17 µm (Shevchenko et al.: 8-20 µm).

LM: Cells usually united in short chains (Figure 3.34.D-E) or in some cases solitary (Figure 3.34.F-G). In valve view cells elliptical and in girdle view rectangular with sharp valve corners. There is one chloroplast per cell. Setae emerge at the valve corners and appear not to cross over between sibling valves. There is no aperture as the cells are joined in a chain by the valve faces fitting tightly together as the anterior valve is slightly convex and the posterior valve is slightly concave. Setae are delicate and all directed towards the same end of the cell and/or chain diverging at an angle of 30-70 ° to the pervalvar axis. The single cells and the chains appear to be heteropolar, with the anterior valve being convex and the posterior slightly concave (Figure 3.34.D-G).

Distinctive features: Delicate and straight setae are directed towards the same end of the cell/chain.

Comments: In the study *C. subtilis* var. *abnormis* Proschkina Lavrenko was also observed in the natural material, however without image documentation and therefore not separately listed. The conspicuous character for this variety is that the posterior valve carries only one thick seta instead of two as in the type. There is a possibility that the setae orientation is not enough distinctive character in *C. subtilis* to distinguish it from other single-celled species and more investigation on the cultured material is necessary.

Figure 3.34. LM **(A,C-G)** and TEM **(B)** micrographs of *Chaetoceros* spp. from field material. **A-C** *C. simplex* **A)** Cell in the girdle view. **B)** Cell with the central process on both valves. **C)** Cell in girdle view with crossed setae on the same side of the cell. **D-G** *C. subtilis* **D)** Posterior terminal part of the chain. **E)** Anterior terminal part of the same chain as in D). Note the convex valve face of the anterior valve. **F)** and **G)** Single cells. Scale bars: A,C, D-G= 10 µm; B= 2 µm

3.1.2.2.22 Chaetoceros socialis Lauder (1864)

(Figures 3.35-3.36.)

Bibliography: Hustedt (1930), Cupp (1943), Evensen and Hasle (1975), Hargraves (1979), Rines and Hargraves (1988), Hernández-Becerril (1996), Jensen and Moestrup (1998), Hernández-Becerril and Flores Granados (1998), Sieracki et al. (1998), Shevchenko et al. (2006), Sunesen et al. (2008), Shevchenko et al. (2008), Hoppenrath et al. (2009), Kooistra et al. (2010), Degerlund et al. (2012)

Synonyms: *C. lorenzianus* var. *parvula* Grunow, *C. furcellatus* Yendo, *C.socialis* var. *solitaria* Meunier, *C. socialis* var. *flabelliformis* Meunier, *C. socialis* var. *congesta* Meunier, *C. socialis* f. *socialis* Proschkina-Lavrenko, C. *socialis* f. *radians* Proschkina-Lavrenko, *C. radians* Schütt

Description: a.a.: 9-13 µm (Hustedt: 4-15 µm, Cupp: 6-12 µm, Rines and Hargraves: 7-9 µm, Jensen and Moestrup: 5-16 µm, Hernández-Becerril and Flores Granados: 10-17 µm, Shevchenko et al.: 5-10 µm, Sunesen et al.: 6-12.5 µm, Hoppenrath et al.: 4-15 µm); p.a.: 5-13 µm (Shevchenko et al.: 5-16 µm).

LM: Cells are united by joining of the sibling setae in short chains curved in a broad girdle view (first order colony). Each cell usually possesses one long and straight seta which is extending towards the concave part of the chain. By connection of the long setae tips short chains further form large spherical colonies (second order colony) with the interconnected tips being in the colony centre (Figure 3.35.A-B). The cells are elliptical in valve view and rectangular in girdle view with sharp corners. Each cell possesses a single large chloroplast (Figure 3.35.D). Valve face is flat to concave with an inflated central part, mantle low without a constriction near its edge, girdle usually equidimensional with the mantle. The delicate and thin setae originate inside the valve margins and direct outwards, with sibling setae crossing over each other after a long basal part thus forming wide hexagonal apertures (Figure 3.35.D). In valve view, the orientation of the setae classifies as a Brunel group VI with one pair of sibling setae diverging 30-50° from the apical plane and one member of the other pair curving back around the cell and continuing in the direction of the first pair, and the other being especially elongated and growing toward the colony centre. Resting spores round in shape, with both valves dome-shaped and covered with spines (Figure 3.36.A).

EM: The frustule is weakly silicified. The valve is ornamented with a weak pattern of scarcely distributed costae radiating from the central annulus and dichotomously branching in a somewhat curved fashion towards the valve margin (Figure 3.35.F). The setae are circular in cross-section composed of longitudinal quite wide strings bearing spines, arranged in a helicoidal pattern and interconnected with very short transverse bars (Figure 3.35.J-L). Between bars there are scarcely distributed elongated pores (Figure 3.35.K-L). Both valves of the resting spore are covered with spines over the whole surface with also a single ring of spines at the margin (Figure 3.36.B-F). The mantle of both valves is quite large with primary valve one somewhat higher than the secondary one (Figure 3.36.C). The spines appear to be conical in shape and occasionally the the longest spines have a minute bifurcation at the tip. The spines vary greatly in length with generally the primary valve spines being much longer than on the secondary valve. On the advalvar margin of the mantle of the secondary valve there is a single ring of puncta (Figure 3.36.C,E-F).

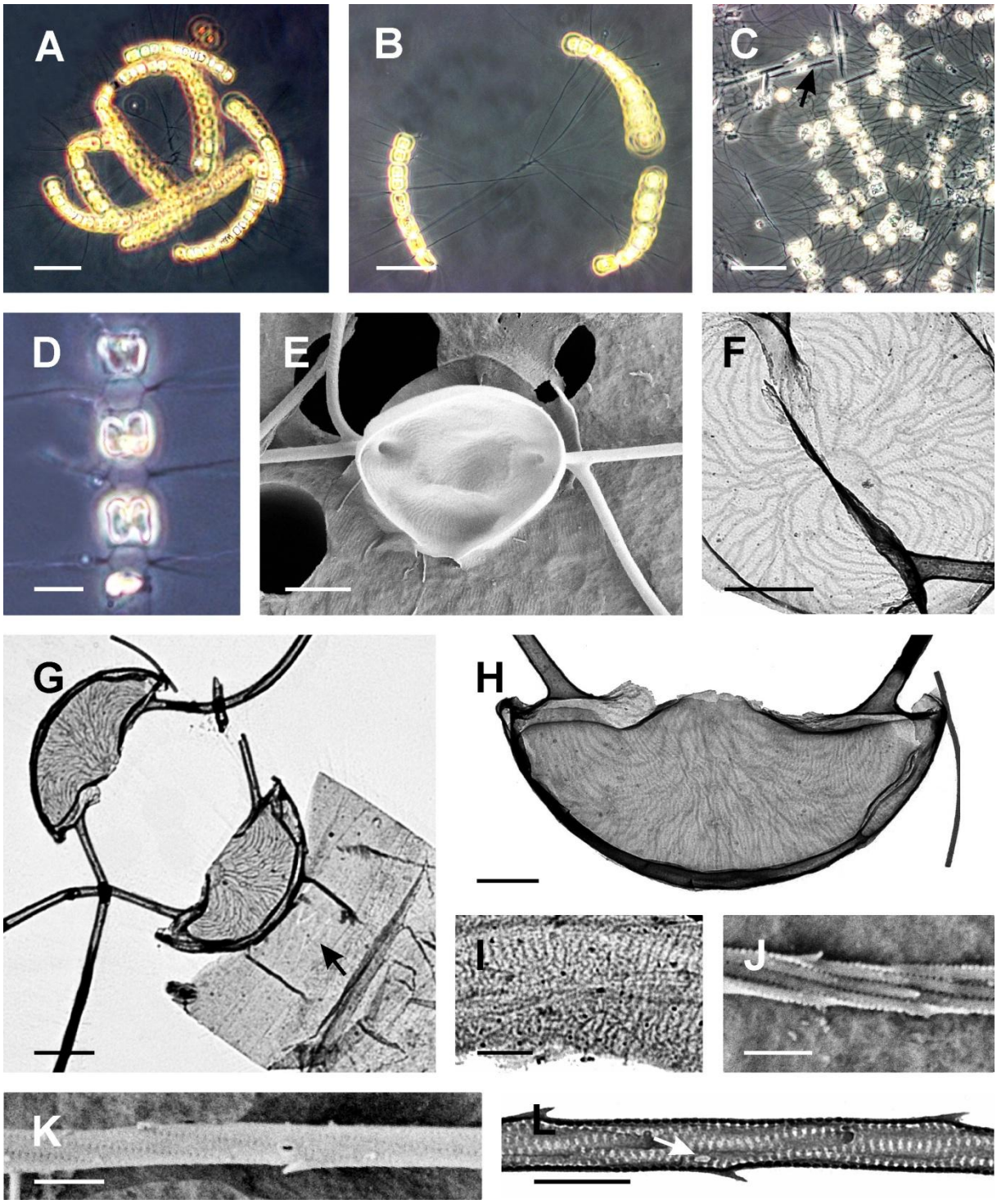

Figure 3.35. LM **(A-D),** SEM **(E,J-K)** and TEM **(F-I,L)** micrographs of *Chaetoceros socialis* from field samples **(C,D)** and cultured strains PMFA3 **(A,B)** and PMFA6 **(E-L)**. **A)** A spherical colony. **B)** Three chains connected with the long setae. **C)** Detail of a large spherical colony with epiphytic *Pseudo-nitzschia* species (arrow). **D)** Middle part of a chain showing the aperture. **E)** Sibling valves in valve view showing the orientation of the setae belonging to Brunel group VI. **F)** Detail of the valve with the ornamentation pattern. **G)** Sibling valves with the girdle of one valve. Note the point of girdle bands overlapping zone (arrow). **H)** Intercalary valve in the girdle view. **I)** Detail of the girdle. **J)** Detail of a seta. **K)** Detail of a seta. L) Detail of a seta. Note the elongated pore (arrow). Scale bars: A -- C = 50 µm; D = 10 µm; E-G =2 µm; H = 1 µm; I-L= 0.5 µm.

Distinctive features: Delicate and thin setae joined after a distinct basal part forming large hexagonal apertures. Three setae of two sibling valves short, fourth one straight and elongated. Short chains usually joined in large spherical colonies by connection of the tips of long setae. Setae Brunel type VI. Resting spores with both spiny surfaced valves.

Comments: The resting spore morphology observed in this study matches the spore description of *C. radians*/*C. socialis* var. *radians*, but due to the current unresolved taxonomic position of this taxon we refer here to the name *C. socialis.* The species in the natural as well as cultured material often produced copious amounts of mucilage material embedding the spherical colonies, however the staining with Alcian Blue did not reveal any definite shape of this material, only irregularly shaped aggregates. On the surface of large globular colonies there are often epiphytes present such as *Pseudo-nitzschia* spp. (Figure 3.35.C).

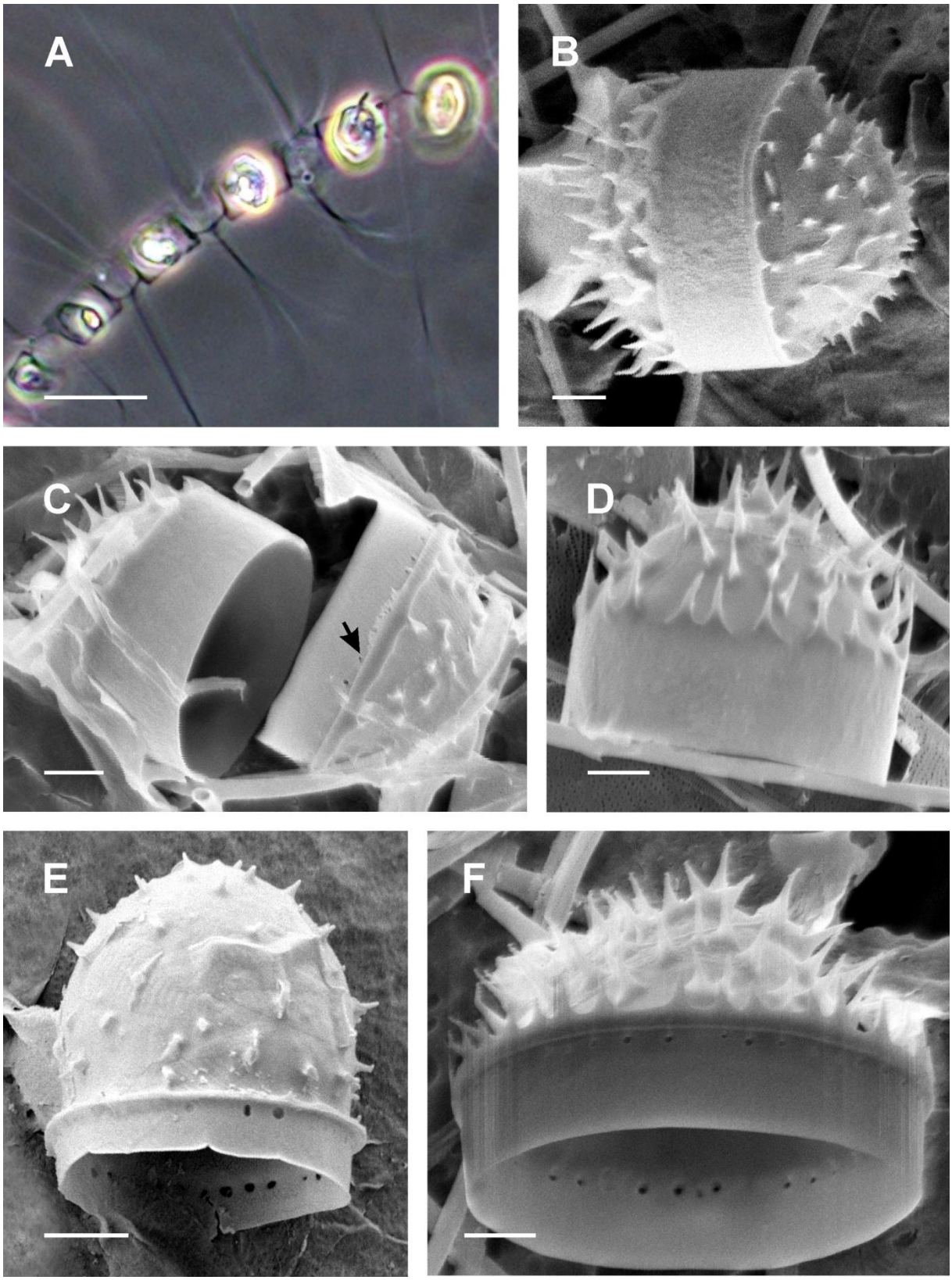

Figure 3.36. LM **(A)** and SEM **(B-F)** micrographs of *Chaetoceros socialis* resting spores from cultured strains PMFA6 **(A,E)** and PMFA7 **(B-D,F)**. **A)** Middle part of a chain with the resting spores within the parents cells. **B)** Complete resting spore. **C)** Open resting spore. Note the ring of puncta on the advalvar margin of the mantle of the secondary valve (arrow). **D)** Primary valve of the resting spore. **E)** Secondary valve of the resting spore with shorter spines. **F)** Secondary valve of the resting spore with longer spines. Scale bars: A = 20 µm; B-F = 1 µm.

3.1.2.2.23 Chaetoceros tenuissimus Meunier (1913)

(Figure 3.37.A-E)

Bibliography: Hustedt (1930) (as *C. simplex* var. *calcitrans*), Rines and Hargraves (1988), Berard-Therriault et al. (1999), Sar et al. (2002), Hoppenrath et al. (2009), Kooistra et al. (2010)

Synonyms: *C. simplex* var. *calcitrans* Paulsen, *C. calcitrans* (Paulsen) Takano, *C. calcitrans* f. *pumilus* (Paulsen) Takano; most likely *C. galvestonensis* Collier and Murphy, *C. minutissimus* Makarova and Proshkina-Lavrenko

Description: a.a.: 3-6 µm (Berard-Therriault et al. 3-5 µm, Hoppenrath et al.: 3-5 µm, Sar et al. 3.5-4 µm); p.a.: 6-8 µm (Sar et al. 4-11 µm)

LM: Solitary cells (Figure 3.37.A-B) or sometimes in culture material they can be found in pairs. Cells in valve view elliptical to circular and in girdle view square to rectangular with sharp and slightly drawn up corners. There is a single chloroplast per cell. The valve face is flat to slightly convex, mantle low and girdle usually high. Thin and straight setae emerge at the valve corners and are typically oriented at a 45 ° angle with the respect to both pervalvar and apical axes (Figure 3.37.A-B). In valve view they are lying in the apical plane. Resting spores were not observed in this study neither they are reported from the literature.

EM: Frustule is weakly silicified. The process is present in each valve within the more or less eccentric annulus from which relatively thick costae are radiating towards the mantle (Figure 3.37.C-D) sometimes extending parallel on the mantle. The process is a short flattened tube externally and internally a slit-like hole (Figure 3.37.C-D). The relatively low hyaline rim is present on the marginal ridge. The setae are circular in cross section and composed of relatively thin longitudinal strings arranged in a helicoidal pattern and connected with transverse bars which are perpendicular to the seta axis (Figure 3.37.E). The longitudinal strings are ornamented with small spines.

Distinctive features: Thin and straight setae emerge at the valve corners and are typically oriented at a 45 ° angle with the respect to both pervalvar and apical axes.

3.1.2.2.24 Chaetoceros throndsenii var. throndsenia (Marino, Montresor & Zingone) Marino, Montresor & Zingone (1991)

(Figure 3.37.F-G)

Bibliography: Marino et al. (1987), Marino et al. (1991), Aké Castillo et al. (2004)

Synonyms: *Miraltia throndsenii* Marino, Montresor and Zingone

Description: a.a.: 2-4 µm (Marino et al.: 1.5-5 µm, Aké Castillo et al.: 3-9 µm); p.a.: 6-13 µm (Marino et al.: 8-15 µm, Aké Castillo et al.: 9-20 µm)

LM: Cells single, rectangular in girdle view, one chloroplast. Cells heteropolar with reduced number of setae to one seta per valve. Anterior valve usually convex and posterior valve face flat. Anterior valve with a single seta originating at a valve corner and bending sharply back towards the posterior end of the cell forming a very acute angle with the pervalvar axis. The posterior valve has a seta arising almost perpendicularly from the margin of the valve face and running nearly parallel to the pervalvar axis (Figure 3.37.F-G).

Distinctive features: Cells heteropolar with reduced number of setae to one seta per valve.

3.1.2.2.25 Chaetoceros throndsenii var. trisetosa Zingone (1991)

(Figure 3.37.H-I)

Bibliography: Marino et al. (1991), Aké Castillo et al. (2004)

Description:a.a.: 3-4 µm (Marino et al.: 1.5-5 µm, Aké Castillo et al.: 4-5 µm); p.a.: 10-12 µm (Marino et al.: 8-15 µm, Aké Castillo et al.: 10-16 µm)

LM: Cells solitary, rectangular in girdle view, one chloroplast, heteropolar with three setae. Anterior valve with two long setae originating at valve corners and bending sharply back towards the posterior end of the cell forming a very acute angle with the pervalvar axis. The posterior valve has a seta arising at the valve corner and running nearly parallel to the pervalvar axis (Figure 3.37.H-I).

Comments: *C. throndsenii* var. *throndsenia* has only one seta on the anterior valve while *C. throndsenii* var. *trisetosa* has two setae.

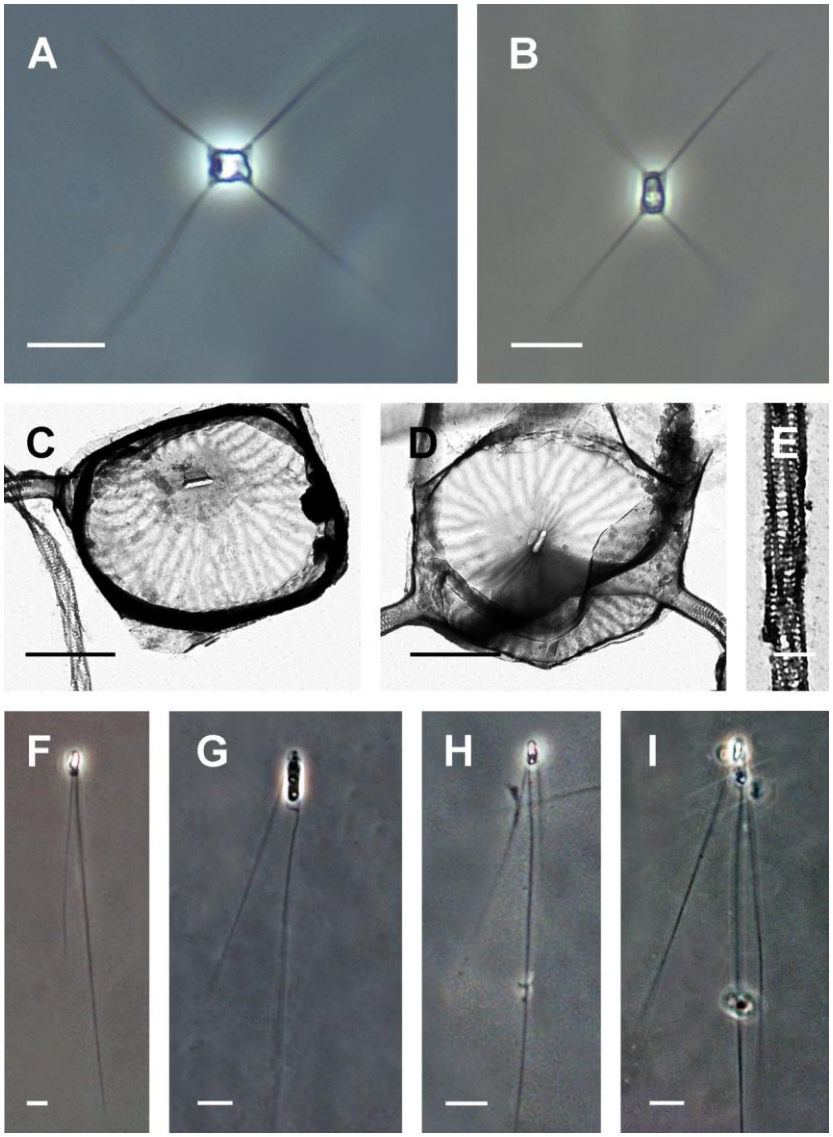

Figure 3.37. LM **(A,C-G)** and TEM **(B)** micrographs of *Chaetoceros* spp. from field material. **A-E** *C. tenuissimus*, cultured strain PMFF1 (A,C-E), and PMFF2 (B) **A)** and **B)** Cell in the girdle view showing the characteristic orientation of the setae. **C)** and **D)** Valves with a slit-shaped process. **E)** Detail of a seta. **F-G** *C. throndsenii* var. *throndsenia* cell in a girdle view with two setae. **H-I** *C. throndsenii* var. *trisetosa* cell in a girdle view with three setae. Scale bars: A,B= 10 µm; C,D= 1 µm; E= 0.25 µm; F-I= 5 µm.

3.1.2.2.26 Chaetoceros tortissimus Gran (1900)

(Figure 3.38.)

Bibliography: Ikari (1926), Hustedt (1930), Cupp (1943), Hoppenrath et al. (2009), Shevchenko et al. (2006)

Description: a.a.: 14-21 µm (Hustedt: 11-16 µm, Cupp: 14-20 µm,Hoppenrath et al: 11-20 µm, Shevchenko et al.: 14-25 µm); p.a.: 5-14 µm

LM: Cells united in usually long chains which are very strongly twisted along the chain axis in such way that some sibling valves are positioned perpendicular at each other (Figure 3.38.A-C). In valve view cells are broadly elliptical and compressed in the transapical direction, in girdle view rectangular with rounded valve corners. Each cell contains a single parietal plate-like chloroplast positioned around the girdle (Figure 3.38.D). The valve face is flat or slightly convex, mantle low sometimes constricted near the margin, girdle equidimensional or higher than the mantle. Long and thin setae originate within the valve margin with the more or less short basal part which is slightly directed outwards before the single point of fusion positioned slightly inside or at the chain margin (Figure 3.38.C-D). Apertures are usually narrow, hexagonal in shape. Intercalary setae are generally oriented more or less perpendicularly to the chain axis or appear slightly curved (Figure 3.38.A-C). In valve view they diverge at the equal angle (30-45°) from the apical plane thus belonging to Brunel group II (Figure 3.38.G,I). Terminal setae are the same thickness as the intercalary ones and extend almost parallel to the colony axis in a U-shaped curve (Figure 3.38.A). In cultures and in field samples there was often a sheath of thick mucus visible with or without Alcian Blue staining which was surrounding the chains with the setae protruding from it (Figure 3.38.E-F). Resting spores were not observed.

Figure 3.38. LM **(A-F),** SEM **(I,K,M)** and TEM **(G,H,J,L)** micrographs of *Chaetoceros tortissimus* from field samples **(B-C,E-G)** and from cultured strain PMFT1 **(A,D,H-M). A)** Complete chain with a slight torsion showing orientation of the setae. **B)** Complete chain strongly twisted around the chain axis. **C)** Middle part of a chain showing hexagonal apertures. **D)** Intercalary cells with one parietal plate-like chloroplast positioned around the girdle. **E)** Mucus sheath surrounding the chain. **F)** Cells in valve view surrounded by the mucus sheath with clearly defined borders (arrow) and setae protruding from it. **G)** Two overlapping sibling valves showing the valve ornamentation and the elongated pores near the bases of the setae (arrows). **H)** Detail of the valve face with network of costae and a round spots as a point origin for some costae (arrows). **I)** Sibling valves with the elongated pores (arrows). **J)** Detail of a girdle band. **K)** Detail of the basal part of the seta with the large elongated pore. **L)** and **M)** Detail of a seta. Scale bars: A-C,E-F=20 µm; D=10 µm; G,I=5 µm; H=2 µm; J-M=0.5 µm.

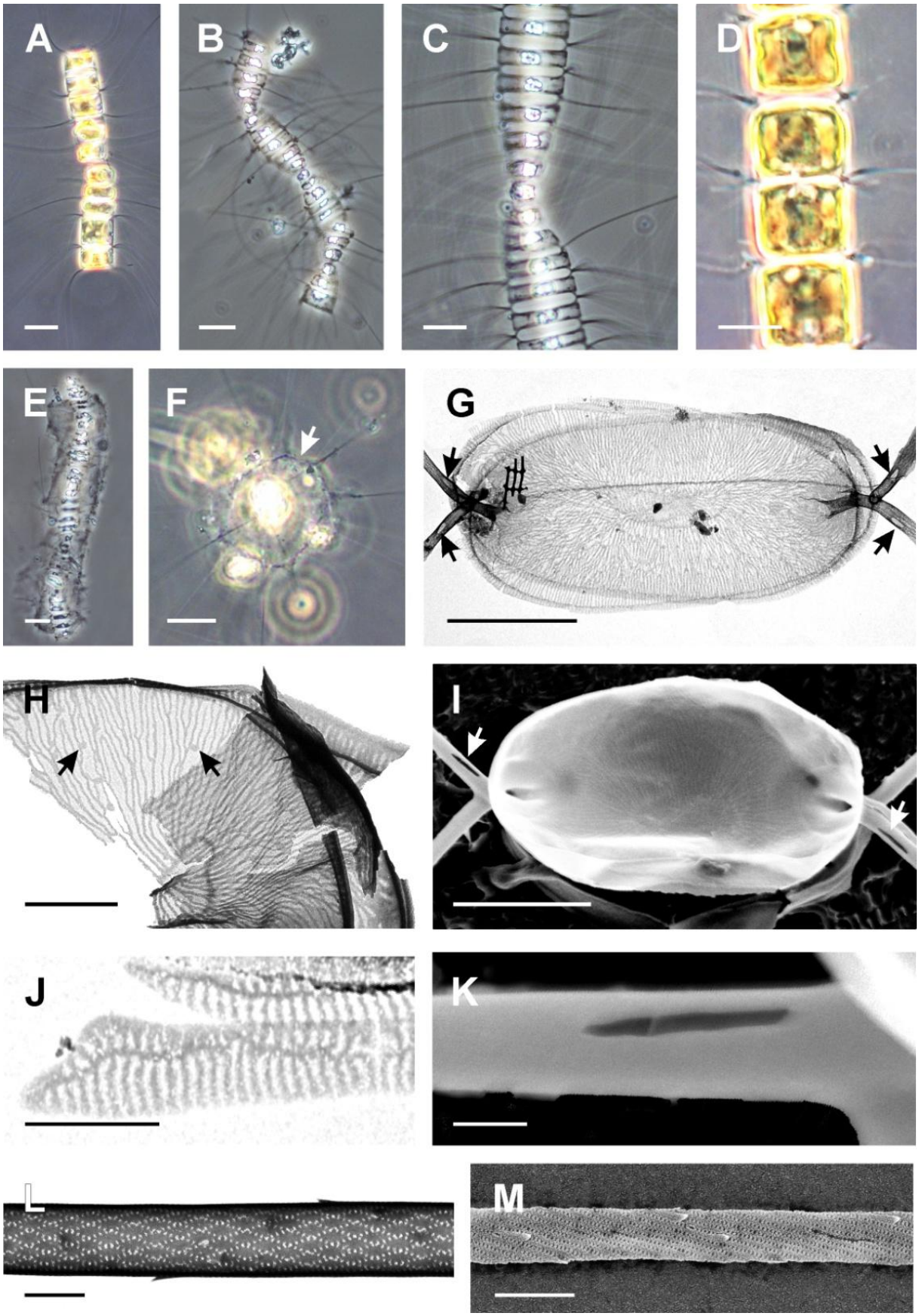
A
B
C
D
E
F
G
H
I
J
K
L
M

EM: The valve has a central hyaline annulus from which extends a complex pattern of radiating densely distributed costae, branching dichotomously towards the valve margin and becoming parallel on the valve mantle (Figure 3.38.G-H). For some costae it appears that their point of origin is not at the annulus but they seem to start from the single point in a form of a round spot between the centre of the valve and the valve margin (Figure 3.38.F). The marginal ridge does not have a rim, it is only observable as a thickened edge between the valve face and the mantle. There are no observations of the terminal valve therefore there are no information on the structure and shape of the process. Girdle bands are adorned with transverse fine striations and a slightly thickened longitudinal rib near one edge (Figure 3.38.J). Setae are circular in cross-section, hyaline and smooth in the basal part and further on composed of thin silica longitudinal strings interconnected with the small bars arranged in a helicoidal pattern similar as in *C. curvisetus* (Figure 3.38.L-M). The strings are ornamented with very small spines spirally positioned along the seta length, lacking in the part proximal to the valve. The conspicuous and unique character for this species is the presence of a quite large elongated pore on the proximal part of the seta, right after the crossing/fusion point between the sibling setae (Figure 3.38.G,I,K).

Distinctive features: Very strong torsion of the chain. Cells compressed in transapical direction. Valve ornamentation pattern has some costae originating from a single round point and not from the central annulus. There is a large elongated pore on the proximal part of the seta, right after the setae crossing/fusion point.

3.1.2.2.27 Chaetoceros vixvisibilis Schiller in Hustedt (1930) emend. Bosak

(Figure 3.39., 3.40.)
Species description: Holotype by Schiller in Hustedt (1930), p.727, Fig.417 a-d.
Bibliography: Hernández-Becerril (2010)
Type locality: Adriatic Sea
Epitype: Adriatic Sea, Croatia (fixed material and permanent slide sampled at N1 station in July 2007, labelled N1_7/2007 deposited in Division of Biology, Faculty of Science, University of Zagreb, Croatia)

Emended diagnosis: Straight and long chains, rectangular cells in girdle view with drawn up valve corners. Intercalary setae long and thin, fused without a basal part between sibling cells, generally oriented perpendicular to the chain axis. Setae circular in cross section, without spines. Apertures narrow, constricted in the middle due to the central inflation on the valve face. Conspicuous valve ornamentation pattern with the central or slightly eccentric annulus from which radiate dichotomously branching costae and with some costae originating as small spirals at a point distant from the annulus. Terminal valves have central process with a labiate structure, terminal setae similar to intercalary ones, sometimes different in orientation forming a wide U-curve. Resting spores with primary valve dome shaped with one to four dichotomously branching spines, secondary valve smooth, flat or with a convex central inflation.

Morphological description: a.a.: 8-17 µm (Hustedt: 8-15 µm, Hernández-Becerril: 11-28 µm); p.a.: 7-25 µm (Hernández-Becerril: 7-11 µm)

LM: Cells united in straight chains, sometimes slightly twisted around the chain axis (Figure 3.39.A,B). The chains are usually long with 10-14 cells but they can be composed of up to 45 cells per chain. The cells are elliptical in valve view and rectangular to square in girdle view with sharp, slightly drawn up valve corners. Each cell contains one large chloroplast, but it is difficult to observe it as the cell content often appears fragmented in several smaller parts (Figure 3.39.C,D). The valve face is flat with the slight central inflation, the valve mantle low with no observable constriction near the margin. The girdle moderately high. The setae originate at the valve corners and cross over immediately. Apertures are quite narrow and slightly constricted in the middle due to the presence of central inflation on the sibling valves (Figure 3.39.D). The setae are straight and usually very long and thin, however, they are very delicate and often found broken in the field samples (Figure 3.39.B-D). They are oriented generally perpendicular to the chain axis but can be bent more or less towards either chain end (Figure 3.39.A). Terminal setae not morphologically different from the intercalary ones and oriented either perpendicular to the chain axis or widely curved from the chain forming a U-shape. Resting spores are often found in the field samples (Figure 3.40.) displaying a very wide range of morphological variation in shape and size (see the description below).

EM: Valves have a very conspicuous pattern with a central or a slightly eccentric annulus from which costae radiate and mostly bifurcate towards the valve margin, becoming parallel on the valve mantle. The point of origin for some costae appears not to be at the annulus, but at the single point somewhere on the valve surface between the centre of the valve and the valve margin where the costae ends are twisted in small spirals. The valve margin has a very low hyaline rim. Terminal valves show the same basic features, but additionally, have a central process with the internally labiate structure (Figure 3.39.G). External part was not observed. Girdle bands are ornamented with transverse striation pattern (Figure 3.39.I). Setae are circular in cross-section and composed of longitudinal strings spirally arranged around the setae axis and interconnected with short parallel bars oriented perpendicular to the same axis. They appear smooth, without the ornamentation of any kind of spines or pores except the space between bars (Figure 3.39.J,K). The resting spores posses unequal valves. The primary valve is markedly dome-shaped, either with a smooth surface or more often with a variable number (1-4) of strong and long spines usually with many dichotomous branches at the tips (Figure 3.40.B-G). Secondary valve is smooth, either flat or with a more or less high round inflation in the centre. The mantle of both valves may be low to relatively high depending on the spore size. The advalvar margin of the secondary valve mantle is adorned with single ring of puncta (Figure 3.40.A-D).

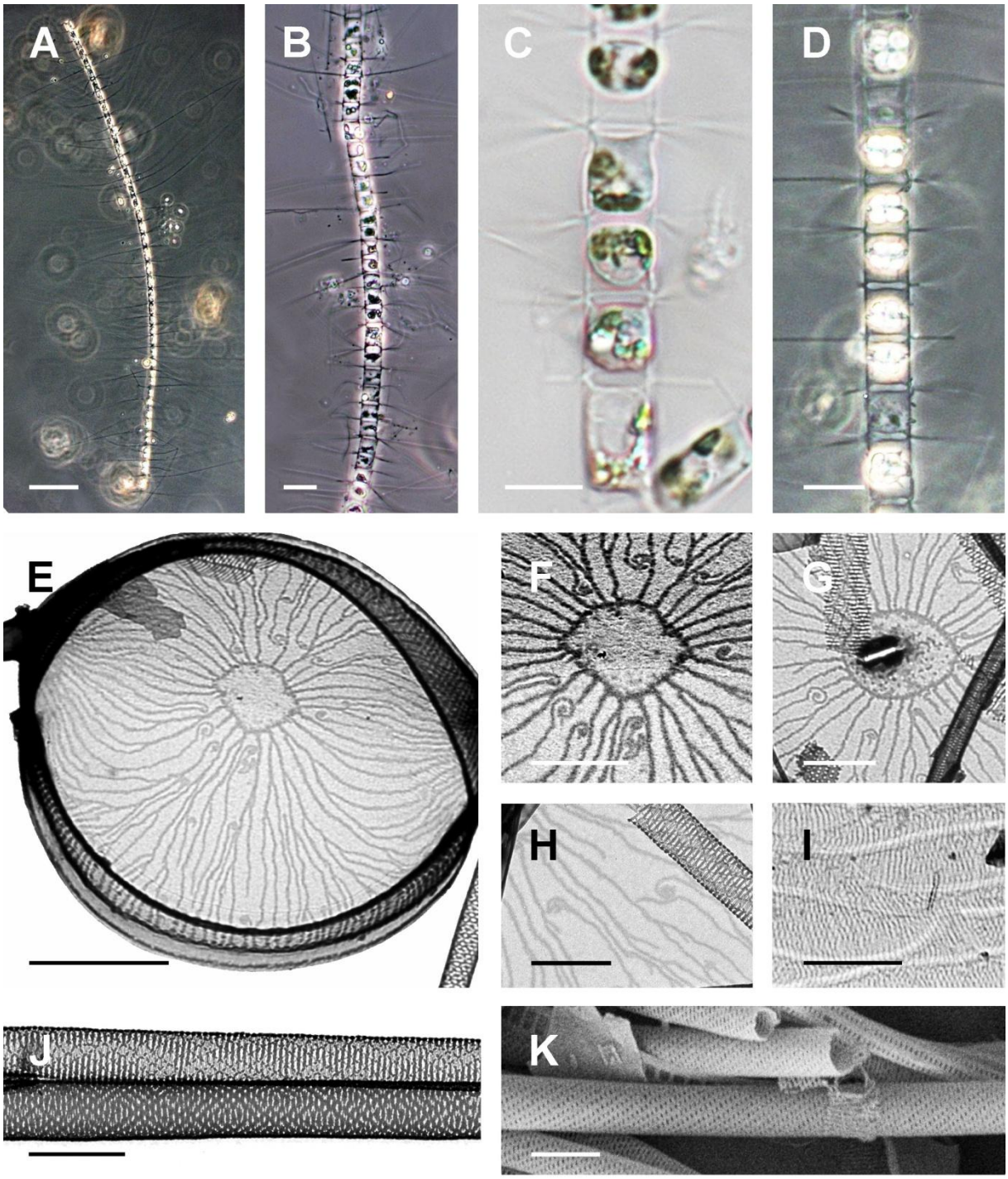

Figure 3.39. LM **(A-D),** TEM **(E-J)** and SEM **(G,H,J,L)** micrographs of *Chaetoceros vixvisibilis* from field samples. **A)** Middle part of a long broken chain showing orientation of the setae. **B)** Middle part of a chain with broken setae. **C)** and **D)** Intercalary cells showing the narrow aperture. **E)** Intercalary valve showing valve ornamentation. **F)** Detail of a valve with central annulus and ends of costae twisted in small spirals. **G)** Detail of a valve with labiate central process. **H)** Detail of a valve with ends of costae twisted in small spirals. **I)** Detail of the girdle. **J)** and **K)** Details of setae, note the absence of spines. Scale bars: A=100 µm, B=20 µm, C-D=10 µm; E=2 µm; F-K=1 µm.

Comments: *C. diadema* has very similar resting spores, also with dichotomously branching spines on the primary valve but the number in C. vixvisibilis is more often one to three and in *C. diadema* its more often four or more. The vegetative cells of the two species are markedly different with very narrow apertures in *C. vixvisibilis* while *C. diadema* they are rather wide. Ultrastructural characters are also different, such as spirals on the end of the costae and spineless setae in the former and polygonal setae in the latter species.

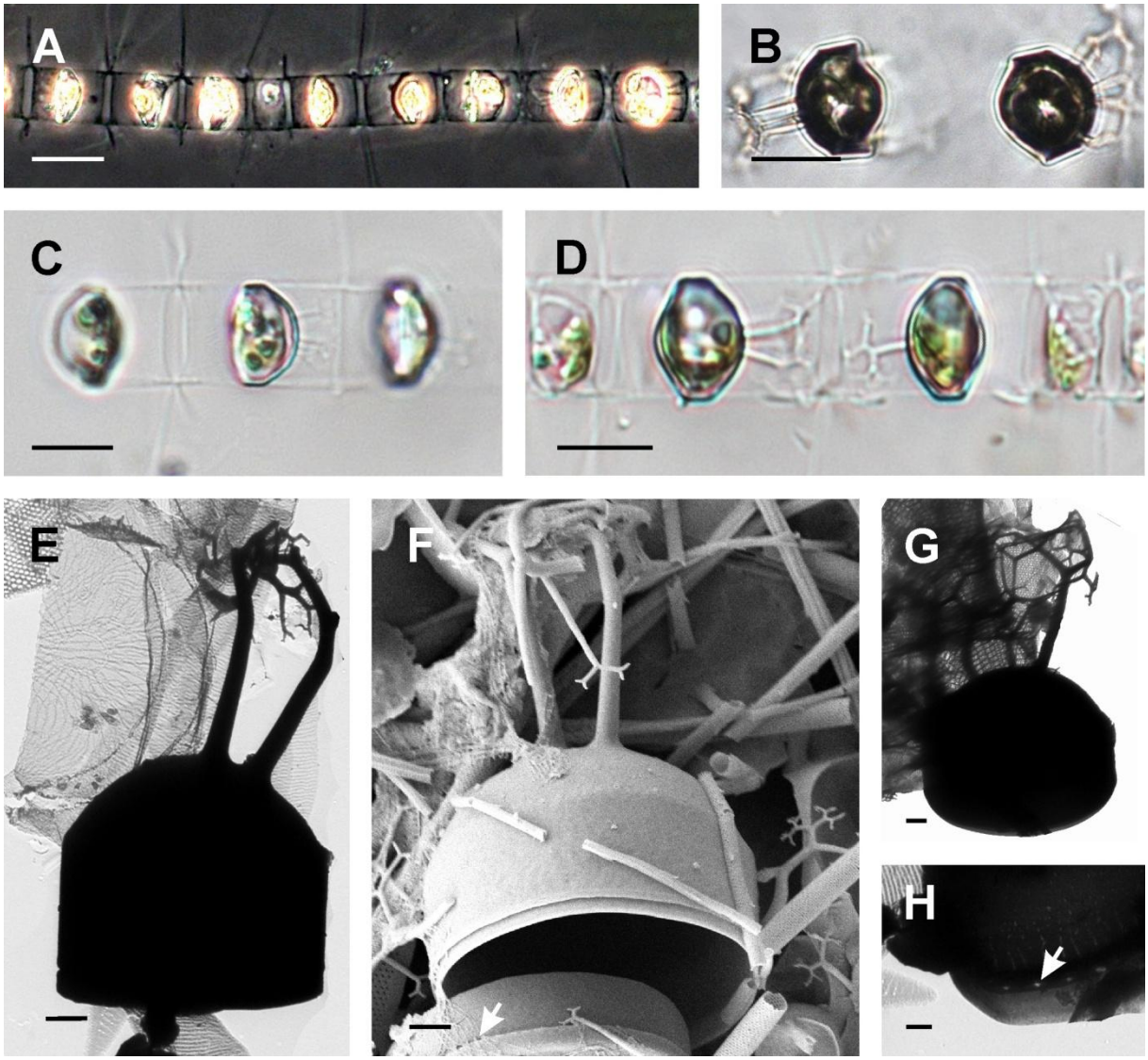

Figure 3.38. LM **(A-D),** TEM **(E,G,H)** and SEM **(F)** micrographs of *Chaetoceros vixvisibilis* resting spores from field samples. **A)** Middle part of a chain with resting spores. **B)** Complete resting spores, left with two and right with four dichotomously branched spines. **C)** and **D)** Complete resting spores within parent cells with variable number of branched spines on primary valves. **E)** Complete resting spore with two branched spines. **F)** Open resting spore, secondary valve has a single ring of puncta on the advalvar margin (arrow). **G)** Complete resting spore with four branched spines on the primary valve. **H)** Detail of secondary valve margin with a single ring of puncta (arrow). Scale bars: A=20 µm, B-D=10 µm, E-H=1 µm.

3.1.2.2.28 Chaetoceros cf. wighamii Brightwell (1856)

Figure 3.41.
Bibliography: Hustedt (1930), Cupp (1943), Hernández-Becerril (1996)
Synonyms: *Goniothecium barbatum* Grunow, *C. bottnicus* Cleve, *C. biconcavus* Gran, *C. caspicus* Ostenfeld, *C. perpusillus* Cleve (?)
Description: a.a.: 6-10 µm (Hustedt: 7-18 µm, Cupp: 7-14 µm, Hernández-Becerril: 6-8 µm); p.a.: 8-15 µm (Hernández-Becerril: 12-17 µm)

LM: Cells are united in short straight chains (Figure 3.41.A-C). In valve view cells elliptical, in girdle view rectangular with sharp and drawn up valve corners often touching between sibling cells. One large plate like chloroplast per cell (Figure 3.41.C). The valve face is usually concave but can be flat with the posterior terminal valve convex in few cases (Figure 3.41.B). Valve mantle is moderately high with the slight constriction near the margin and the girdle is low or more often equidimensional with the mantle. Setae are originating from the drawn up valve corners. Intercalary setae fuse immediately or after a short basal part with a single cross-over point at the chain margin (Figure 3.32.C). The shape of the apertures is very variable ranging from distinctively elliptically shaped in most of the cases (Figure 3.41. A) to very narrow and barely visible slits (Figure 3.39 B). In valve view the intercalary setae diverge either equally at an angle of 30-60° from the apical plane belonging to the Brunel Group II (Figure 3.41.E) or one seta lies in the apical plane while the other diverges at approximately 90° angle belonging to the Brunel Group III (Figure 3.41.D). In girdle view the setae are generally slightly curved towards either end of the chain or perpendicular to the chain axis. Terminal setae are oriented parallel to the chain axis with the posterior setae often crossing each other in the distal part (Figure 3.41.B).

Figure 3.41. LM **(A-D),** SEM **(D,E,K)** and TEM **(F-J,L-N)** micrographs of *Chaetoceros* cf. *wighamii* from cultured strain PMFW2. **A)** Complete chain showing orientation of the setae and the elliptical aperture between sibling cells. **B)** Complete chain with convex terminal cell, crossed terminal setae and very narrow apertures. **C)** Chain of three cells with plate like chloroplast. **D)** Sibling valves in valve view, Brunel group III. **E)** Sibling valves in valve view, Brunel group II, note the fissured rim (arrow) on the marginal ridge. **F)** Two overlapped sibling valves in valve view showing ornamentation. **G)** Two sibling valves in girdle view with fused fissured rim between them (arrow). **H)** Valve showing ornamentation with parts of the girdle bands around. **I)** Terminal valve. **J)** Detail of a terminal valve from an inside view with the slit-shaped process in the center of the irregular annulus. **K)** Detail of a terminal valve from an outside view with the small prominence of the process. **L)** Detail of the setae proximal to the valve. Note the small elongated pores (arrowheads). **M)** Detail of a seta with elongated pore (arrowhead). **N)** Partial view on the girdle bands. Scale bars: A-D=10 µm, E,H,I;K=1 µm, F,G=2 µm, E,H;K=1 µm; J,L,M=0.5 µm.

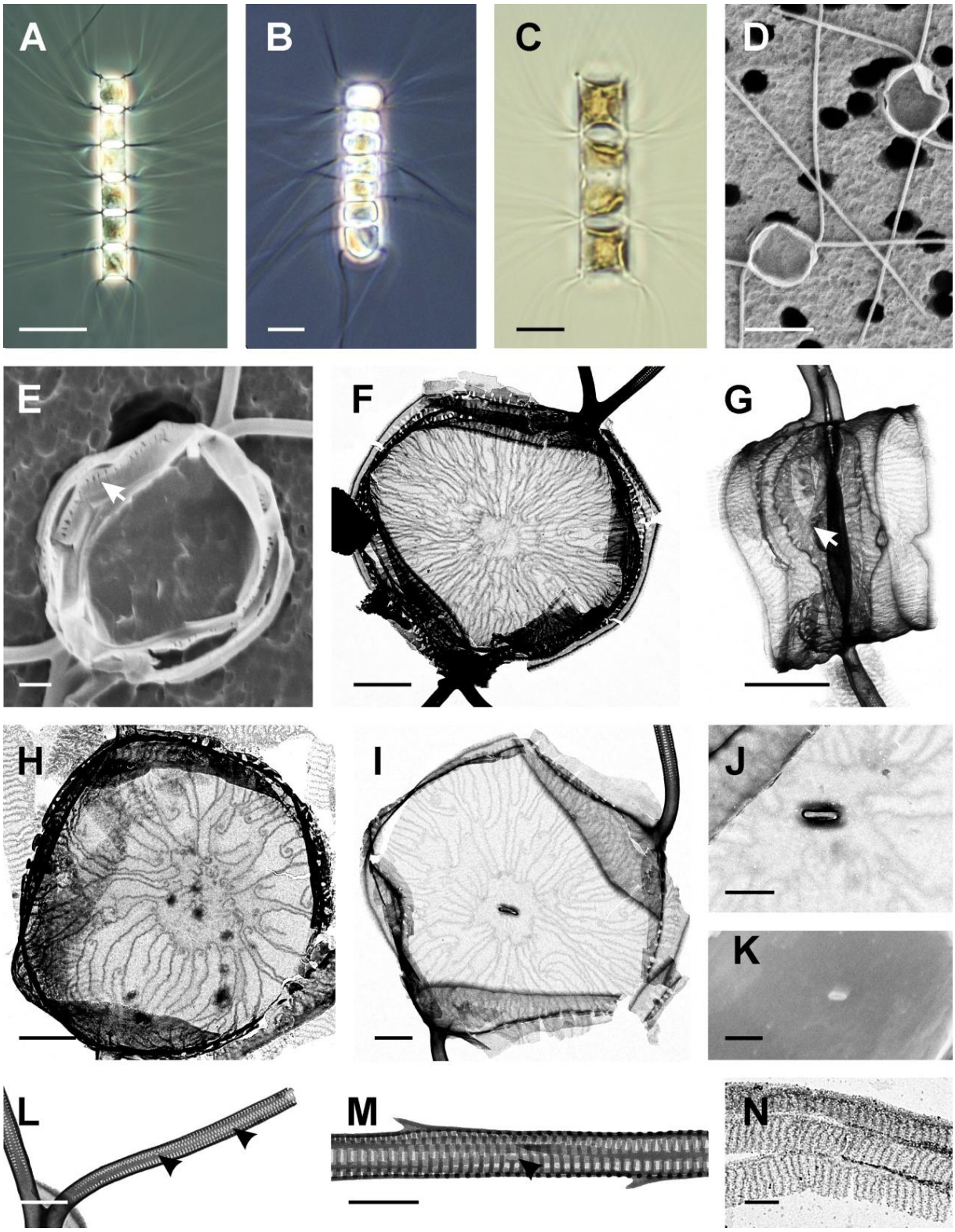
A
B
C
D
E
F
G
H
I
J
K
L
M
N

EM: The valve is ornamented with the distinct and unique irregular pattern of thin costae originating as more or less spiral curves and shaping an irregular central or slightly eccentric annulus. Frequently, the point of origin of some costae is appears not to be at the annulus, but at the spirals located between the centre of the valve and the valve margin (Figure 3.41.F,H,I). The costae are more or less dichotomously branching towards the marginal ridge and becoming parallel on the mantle (Figure 3.41.G). All valves have a high rim projecting from the marginal ridge which is fissured with large oval perforations (Figure 3.41.E-I) and sometimes fused between sibling cells closing the aperture (Figure 3.41.G). The process is present only on the terminal valves in the centre of the irregular annulus, from the inside of the valve it is a small simple slit (Figure 3.32.H,J) and on the outside it is a small prominence (Figure 3.41.G). The girdle bands striation pattern consists of numerous transverse parallel ribs (Figure 3.41.N). Setae are circular in cross section, the basal part is smooth and hyaline and gradually becomes variable number (4-7) longitudinal hyaline strings extending parallel with the seta axis (Figure 3.41.L). The strings are interconnected with transverse bars oriented perpendicular to the seta axis. Between bars there are often elongated pores (arrowheads in Figure 3.41.L-M) and the strings are ornamented with spines (Figure 3.41.M).

Distinctive features: Irregular orientation of the intercalary setae. Terminal setae are oriented parallel to the chain axis with the posterior setae often crossing each other in the distal part. Valve ornamented with irregular pattern of thin costae originating as more or less spiral curves and shaping an irregular central or slightly eccentric annulus. Setae are circular in cross section, composed of variable number (4-7) longitudinal hyaline strings extending parallel with the seta axis and interconnected with transverse bars oriented perpendicular to the seta axis.

Comments: *C. wighamii* is apparently a very problematic taxon with reported great morphological variability for which there is clear need for further investigations; hence we could not ascribe the morphotype obtained within this study with certainty to this name. The resting spores were not observed in this study and they are described to have unequal valves with convex primary valve convex ornamented with fine spines, and secondary valve constricted at base, in the middle blunt cone shaped, smooth or with spines. The species found in this study shows some similarity to *C. salsugineus* in some features, as having the fissured hyaline rim on the marginal ridge, but it is distinguished from it by its very conspicuous ultrastructure of the valve and setae, lack of the long tube-like central process and having elliptical shape of the apertures.

3.1.2.2.29 Chaetoceros sp. "A"

Figure.3.42.

Description: a.a.: 4-6 µm; p.a.: 10-20 µm

LM: Cells solitary, in girdle view rectangular with sharp and drawn up valve corners and in most cases longer pervalvar than the apical axis (Figure 3.42.A-B). The number and shape of plastids could not be determined with certainty due to the small size of the cells, but it appears as a single plate-like chloroplast is present in each cell. The valve face is flat to slightly concave and the mantle high, usually with a distinct constriction near the margin (Figure 3.42.C-D). Thin and straight setae originate at the valve corners and then either extend straight and parallel with the pervalvar axis or diverge at an angle of ca. 30° with the respect to the same axis (Figure 3.42.A-B). No resting spores were observed.

EM: The frustules are weakly silicified with valves having a pattern of a central annulus and the radiating branching costae which extend parallel on the valve mantle (Figure 3.42.D). The hyaline areas between costae are densely perforated with small poroids (Figure 3.42.C-E). The process is present in each valve and its external form is very variable, ranging from a small prominence to a short tube (Figure 3.42.E-G). The marginal ridge is discernible and ornamented either with a very low hyaline rim or completely lacking it. The setae are circular in cross-section with smooth surface at their bases but soon becoming four-sided. The setae are composed of four wide longitudinal strings which extend parallel with the seta axis and forming ridges ornamented with spines. The strings are interconnected with thick transverse bars with the space between bars corresponding to the oval-shaped pores (Figure 3.42.H-I).

Comments: It is possible that this species could represent a small, weakly silicified and unicellular form of *C. decipiens* due to the resemblance in the ultractructural characters such as the structure of the setae, poroid perforations on the valve and small central process. This morphotype is described from the culture, however it was often observed in the field samples where it can be confused in LM with *C. tenuissimus.* The difference is the specific orientation of the setae at a 45 ° angle with the respect to both pervalvar and apical axes in *C. tenuissimus* while this angle is very variable in *Chaetoceros* sp. "A".

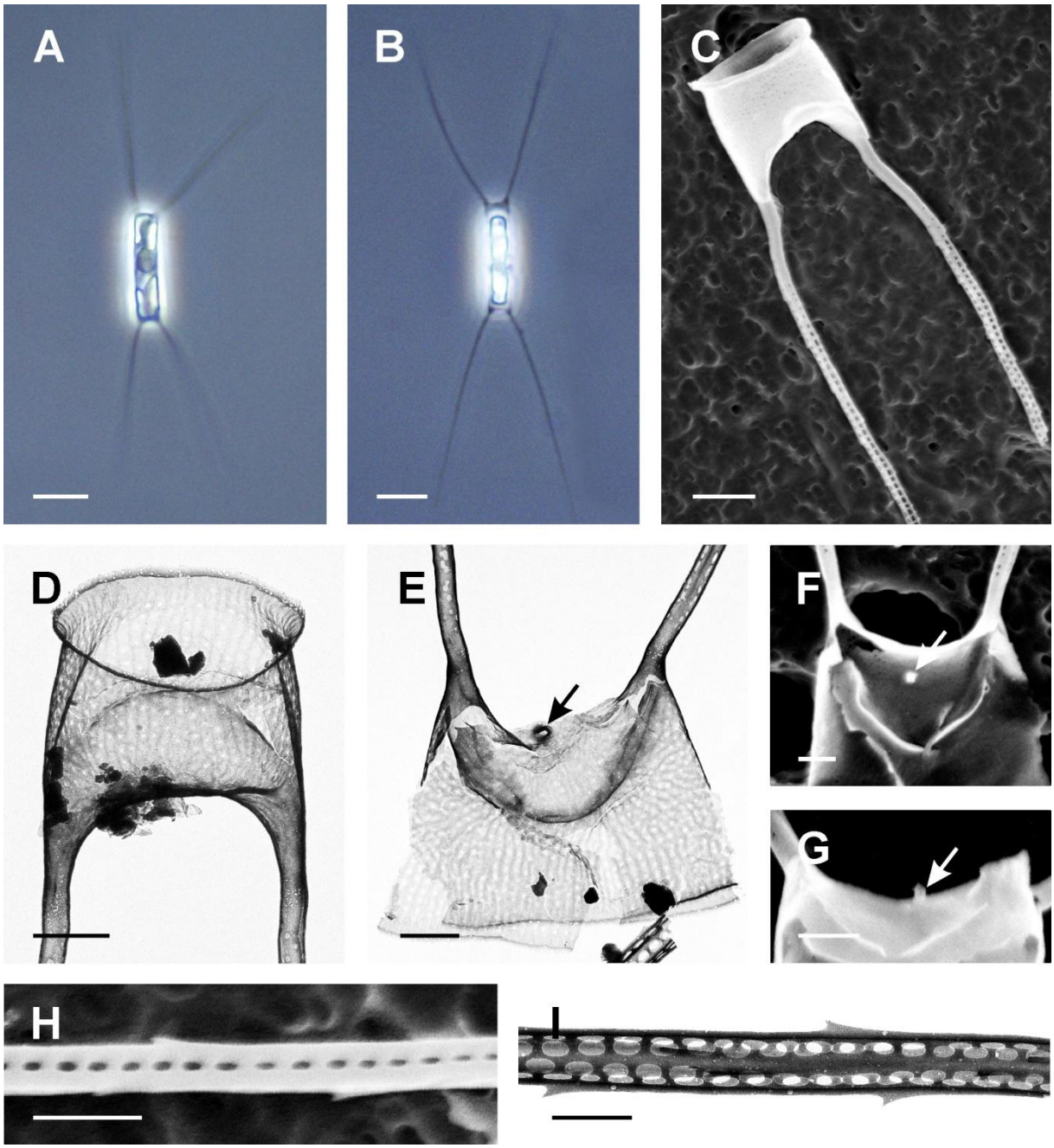

Figure 3.42. LM **(A-B),** SEM **(C,F-H)** and TEM **(D-E,I)** micrographs of *Chaetoceros* sp. "A" from cultured strain PMFS2. **A)** and **B)** Cell in the girdle view showing orientation of the setae. **C)** Valve with setae in the girdle view. **D)** Valve showing the striation pattern and pores on the mantle. Note the constriction near the mantle margin. **E)** and **F)** Valve with small external protuberance of the central process (arrow). **G)** Valve face with small tube-like central process (arrow). **H)** and **I)** Detail of a seta. Scale bars: A-B=10 µm, C=2 µm, D-G=1 µm, H-I=0.5 µm.

3.1.2.2.30 Chaetoceros sp. "B"

Figure.3.43.
Description: a.a.: 4-11 µm; p.a.: 5-12 µm

LM: Solitary cells, in girdle view rectangular with sharp and slightly drawn up valve corners (Figure 3.43.), in valve view elliptical. It appears as a single chloroplast is present in each cell. The mantle is high, girdle low. Valve face flat to slightly concave. Long setae originate at the valve corners and extend almost parallel to the pervalvar axis diverging in a distinct U-shaped curve. (Figure 3.43. A-C).
EM: No ornamentation pattern could be distinguished in SEM, except the small pores perforating the valves (Figure 3.43.G). The valve mantle is markedly constricted near its edge and there is no discernible rim on the marginal ridge. Every valve possesses a short tube-like central process (Figure 3.43.E-G). Setae are circular in cross-section, composed of longitudinal strings extending parallel with the seta axis and interconnected with parallel transverse bars. The strings are ornamented with spines spirally arranged around the seta (Figure 3.43.H-I).
Comments: This morphotype is regularly observed in the Adriatic natural samples and it is recognized by the characteristic orientation of the setae in U-shaped curve which is different from all other described unicellular *Chaetoceros* taxa. It shows resemblance to *C. diversus* in ultractructural characters such as the structure of the setae and valve and it could easily represent an unicellular form of this species. However, more detailed studies of this taxon are necessary before making any conclusions.

3.1.2.2.31 Chaetoceros sp. "C"

Figure 3.44.
Bibliography: Berard-Therriault et al. (1999) as *C. fallax* Proschkina Lavrenko
Description: a.a.: 4-5 µm; p.a.: 3-5 µm

EM: Solitary cells with quite long tubular central process present on each valve (Figure 3.44.A). In girdle view cells are rectangular with slightly drawn up valve corners, in valve view elliptical. The valve is ornamented with a pattern of apparently relatively thick costae radiating from the central annulus (Figure 3.44.B). The valve mantle is low without any constriction near its margin, the girdle is high. The marginal ridge is ornamented with low, but discernible hyaline rim (Figure 3.44.D). Thin setae originate at the corners of the valve and are oriented at 30-45 ° angle with the respect to apical axis (Figure 3.44.A). They are usually straight but also can be curved in various directions in both apical and valvar plane. The setae are circular in cross-section, structured from relatively thick longitudinal strings strongly twisted around the seta axis and bearing small spines. The strings are interconnected with very small transverse bars (Figure 3.44.E).
Comments: This morphotype is observed in the Adriatic natural samples and it shows resemblance to *C.fallax* due to the presence of quite long tubular central process. *C. fallax* is apparently not well known species, with lack of information on the ultrastructure, reported usually as forming short chains of 2-4 cells with the tubular process on each cell. As in this study LM observations are lacking and it

could not be established if this species forms chains, we did not affiliate this morphotype with taxon *C. fallax* but describe it as a separate morphotype.

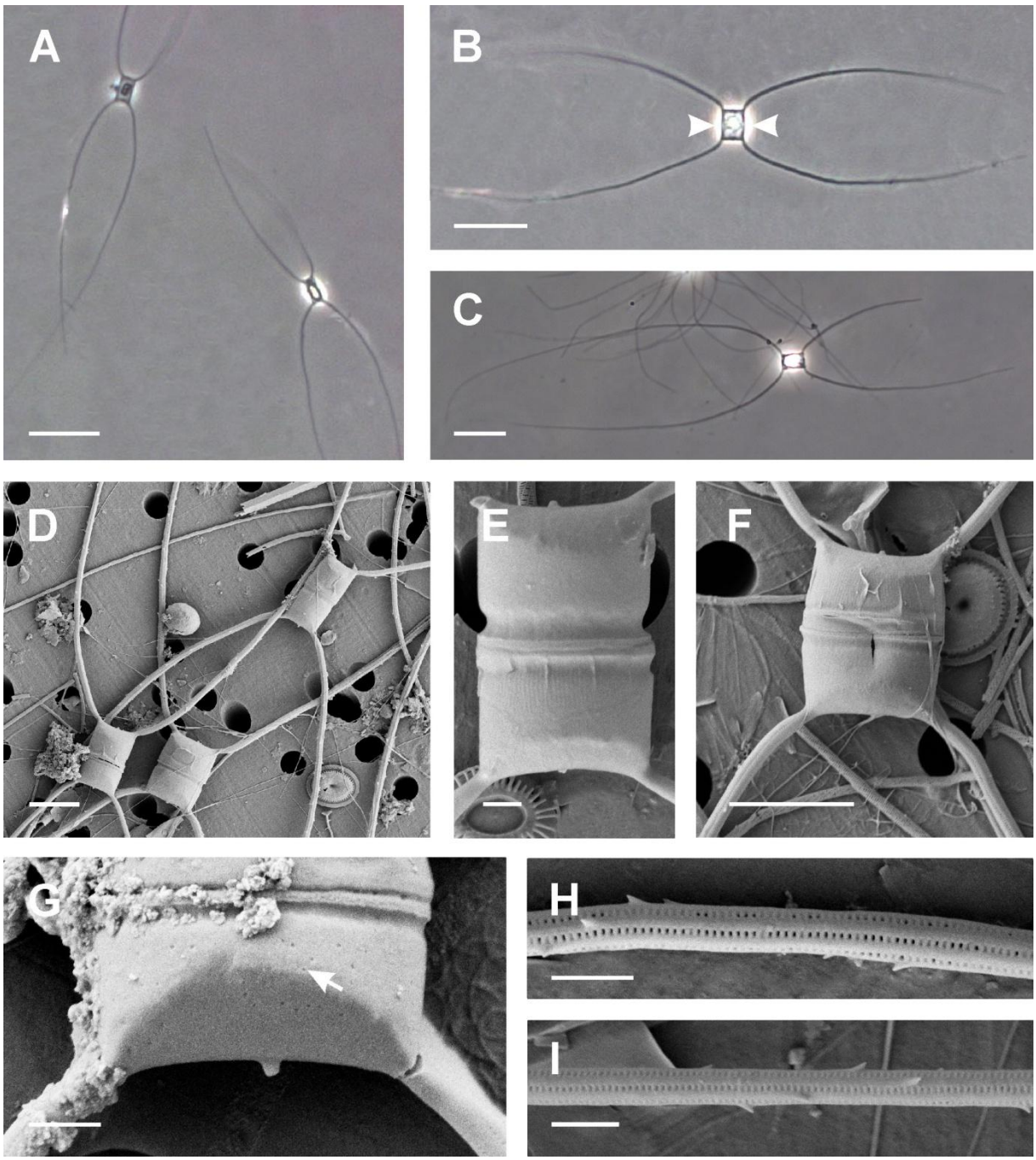

Figure 3.43. LM **(A-C)** and SEM **(D-I)** micrographs of *Chaetoceros* sp. "B" from field material. **A)** Two cells in the girdle view showing orientation of the setae. **B)** Cell in the girdle view, arrowheads are showing the position of the valves. **C)** Cell in the girdle view. **D)** Three cells in the girdle view. **E)** and **F)** Close view on the cell, note the marked constriction near the mantle margin on both valves. **G)** Close view on one valve, note the tube-like external process and pores perforating the valve (arrow). **H)** and **I)** Detail of a seta. Scale bars: A-C=10 µm, D,F=5 µm, E,G,H=1 µm.

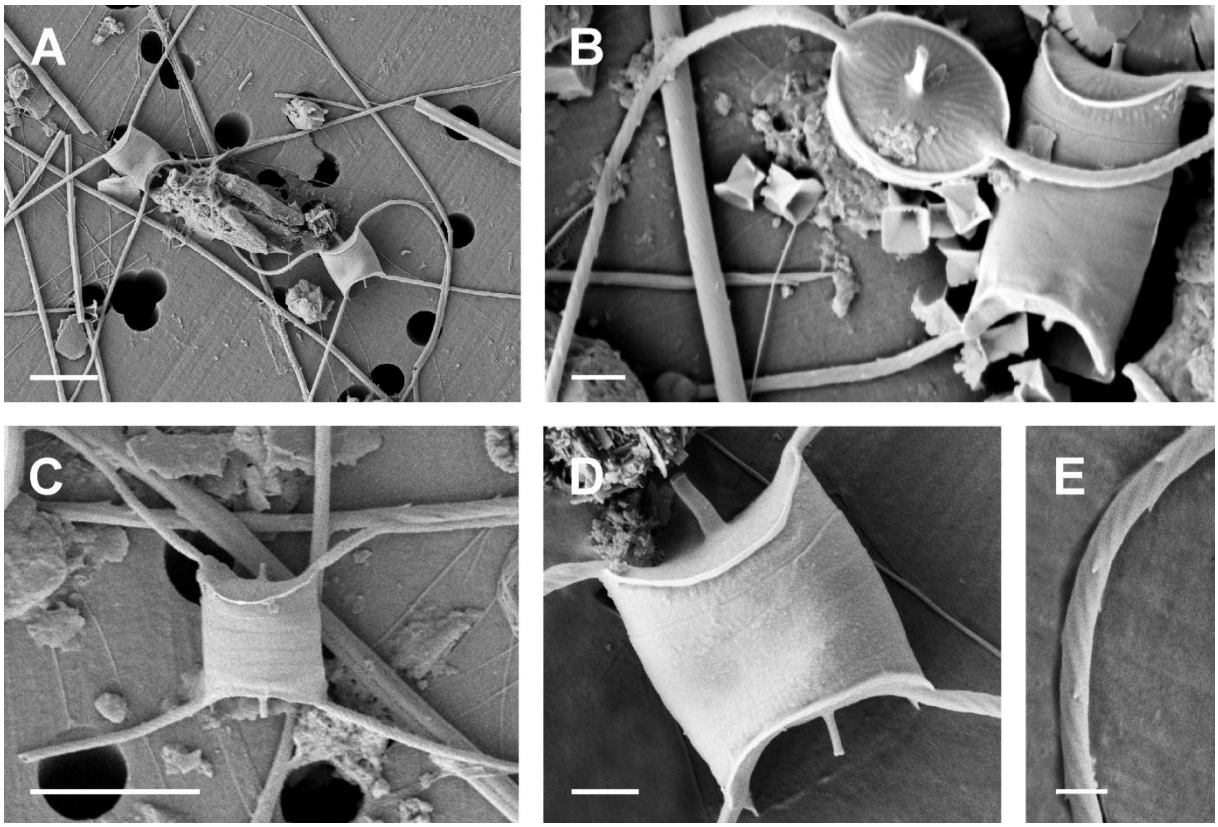

Figure 3.44. SEM micrographs of *Chaetoceros* sp. "C" from field material. **A)** Two cells in the girdle view showing orientation of the setae. **B)** Two cells, left one in valve view showing ornamentation of the valve and curved setae, right one in girdle view **C)** Cell in the girdle view. **D)** Detailed view on the cell in girdle view, note the long tubular processes on both valves and the hyaline rim on the marginal ridge (arrow). **E)** Detail of a seta. Scale bars: A,C=5 µm, B,C,D=1 µm, E =0.5 µm.

3.1.2.2.32 Chaetoceros sp. "D"

Figure 3.45.

Description: a.a.:7-20 µm; p.a.: 6-18 µm

LM: Cells united in straight and short chains (Figure 3.45.A-B). Cells cylindrical, in valve view elliptical and in girdle view rectangular. The number of chloroplasts could not be determined. The valve surface is slightly concave and the valve corners are sharp and drawn up, touching between sibling valves (Figure 3.45. C,D). Valve mantle is somewhat high with a slight constriction near the margin and the girdle low. Intercalary setae are very long, straight and rigid, originating from the valve apices and immediately cross each other at the chain margin without the basal part forming elliptical apertures (Figure 3.45.C,D). In girdle view the setae extend perpendicular to the chain axis (Figure 3.45.D). In valve view the sibling setae equally diverge from the apical plane at a 30-80° angle belonging to Brunel group II. The setae divergence angle differs greatly between adjacent cells therefore the setae extend in very variable directions. The terminal setae in girdle view are oriented as intercalary ones perpendicular to the pervalvar axis, and in the valve view each seta extend in the opposite direction diverging at approximately 90° angle from the apical plane (Figure 3.45.D,G).

EM: Due to the lack of TEM observations it was not possible to determine the valve ornamentation pattern. The marginal ridge is ornamented with a low hyaline rim which extends in the pervalvar direction close to the valve apices and fuses between intercalary sibling valves occluding the aperture edges (Figure 3.45.F). Central process is present only in terminal valves from the internal side it appears as a simple slit and from the external side it is a short flattened wide tube (Figure 3.45.G,H). Setae are circular in cross section at their bases but later becoming polygonal, with straight longitudinal strings extending parallel with the setae axis and forming ridges while interconnected with transverse short bars. The strings are ornamented with small spines arranged in a spiral pattern (Figure 3.45.I,J).

Comments: Due to the very long and straight setae the cells are very difficult to observe in the girdle view. This morphotype shows some resemblance to *C. constrictus* in the structure of the setae but all other features observed apparently are unique therefore more investigations are necessary to establish its identity.

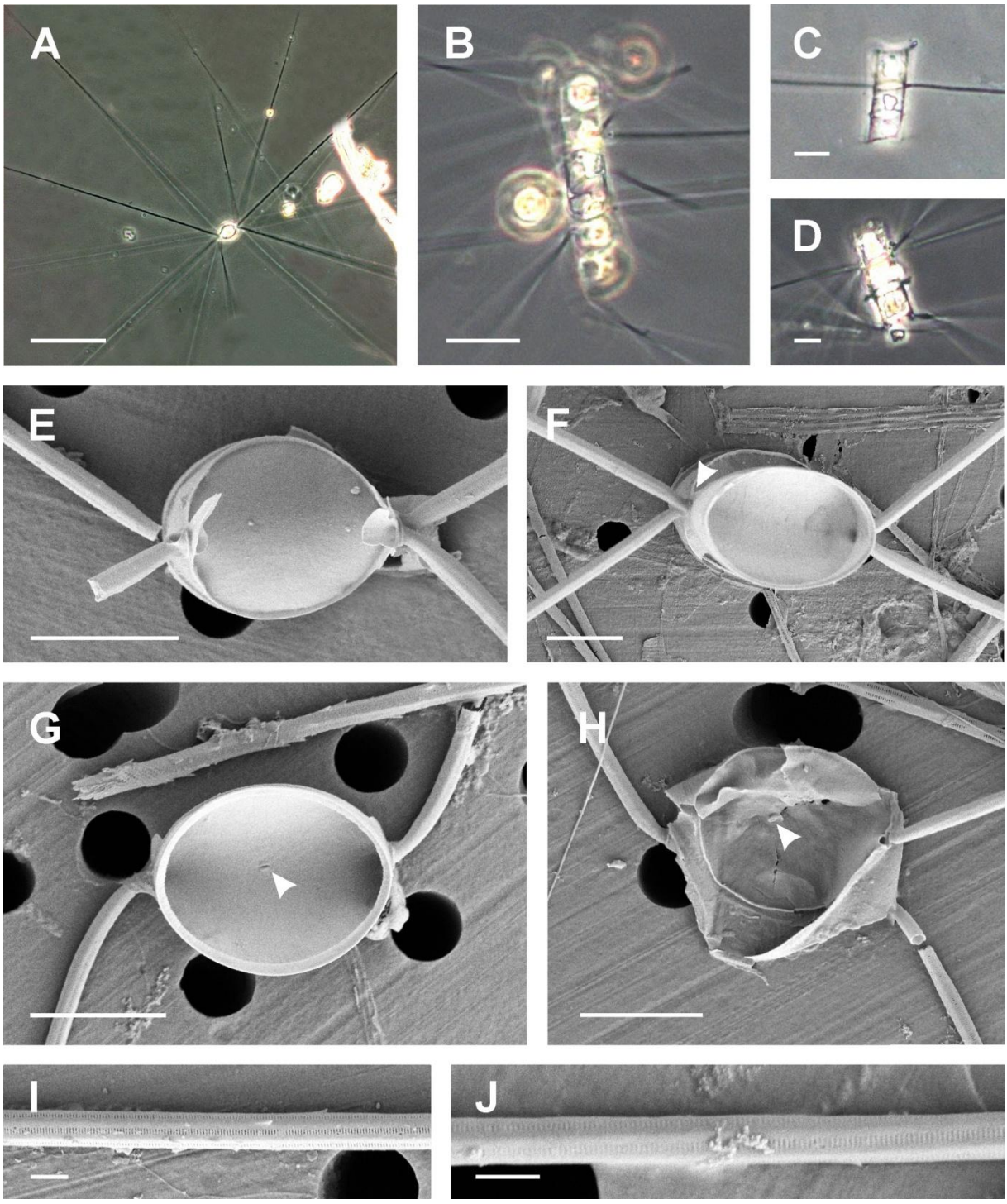

Figure 3.45. LM **(A-D)** and SEM **(E-J)** micrographs of *Chaetoceros* sp. "D" from field material. **A)** Chain in the valve view showing orientation of the long and straight setae. **B)** Complete short chain. **C)** Middle part of the broken chain showing the apertures **D)** Terminal part of the chain. **E)** Valve face in outside view with the upper broken sibling valve. **F)** Sibling intercalary valves in valve view showing setae orientation corresponding to Brunel group II. Note the fused hyaline rim on the aperture margin (arrow). **G)** Terminal valve from the inside view with internally slit-like central process (arrow) and typical terminal setae orientation. **H)** Terminal cell with the externally short flattened tube-like central process. **I)** and **J)** Detail of a seta. Scale bars: A= 50 µm, B=20 µm; C,D= 10 µm; E-H= 5 µm; I,J=1 µm.

3.1.2.3 Subgenus Bacteriastroidea Hernández-Becerril (1993)

Type species (monotypic genus): *Chaetoceros bacteriastroides* Karsten

Robust and fairly heavily silicified chain forming species. Numerous chloroplasts are present in each cell (only two according to Hernández-Becerril (1993)). Each intercalary valve has six setae arranged around the valve margin and fused between sibling cells. Two setae are long and thick, four are reduced in size and spirally twisted. There are regular shoehorn outgrowths between setae on the edge of the intercalary valves. Central process present only on terminal valves. Resting spores unknown.

3.1.2.3.1 Chaetoceros bacteriastroides Karsten (1907)

Figure 3.46.
Bibliography: Fryxell (1978), Hernández-Becerril (1993)
Description: a.a.: 9-10µm (Hernández-Becerril: 10-14 µm); p.a.: 22-30 µm (Hernández-Becerril: 19-25 µm)

LM: Cells united in short, straight and robust chains (Figure 3.46.A). In valve view cells are nearly circular, in girdle view rectangular with pervalvar axis longer than apical axis. Each cell contains numerous small chloroplasts (Figure 3.46.C). The setae appear to contain some plastid-like material in few of the observed specimens, but it was not possible to determine if these granules indeed contain chlorophyll. The valve face is flat to slightly concave and the mantle is quite high without a constriction near the margin. Each intercalary valve possesses six setae of which two are long and robust and they can be described as common as they resemble the setae in other *Chaetoceros* species while four are shorter and very strongly spirally undulated (Figure 3.46.A,C). Common setae originate at the valve margin on two opposite sides of each valve, and join between sibling cells remaining fused for somewhat longer distance (ca. half of the valve diameter) after a short basal part. After fusion they diverge equally at an angle of ca.30° from the apical axis, lying in the apical plane and thus can be classified as Brunel Group I. Spirally undulated short setae also connect the adjacent cells but they are fused only at a single point of their cross-over with a short basal part and then extend perpendicular to the chain axis lying in the valvar plane (Figure 3.46. A). The aperture between adjacent cells is distinct, and appears to be elliptical in shape due to the most visible connection between two long sibling setae. The terminal valve possesses only two long common setae extended in the direction of the chain. Two terminal setae slightly differentiate in the curvature, one of the pair is more parallel to the chain axis while the other is more widely curved and only later becomes parallel with the same axis. It appears that the more curved setae are situated both on the same side of the chain. There are often some flagellates attached in the vicinity of the apertures (Figure 3.46.B).

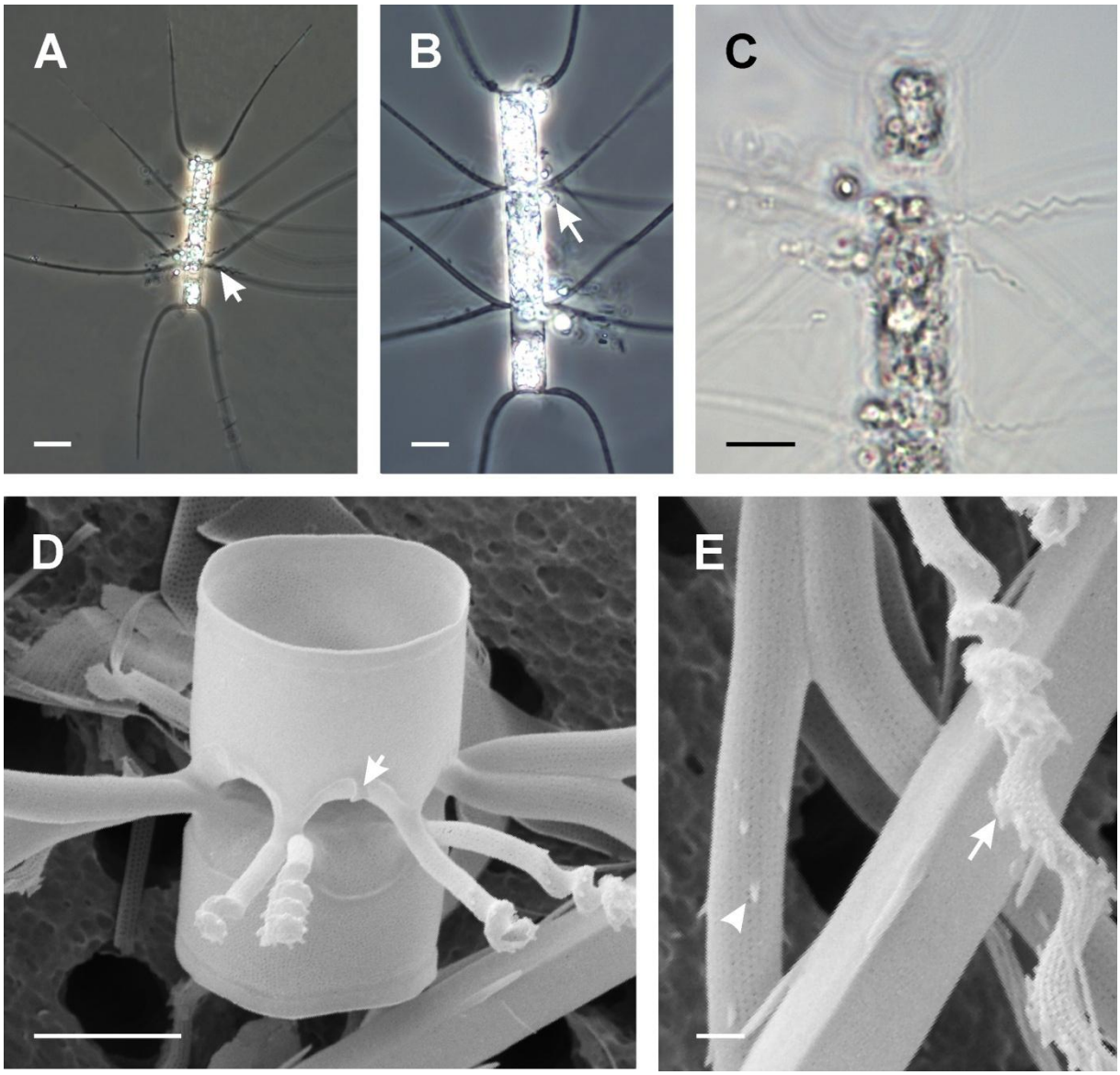

Figure 3.46. LM **(A-C)** and SEM **(D-E)** micrographs. of *Chaetoceros bacteriastroides* from field samples. **A)** Complete chain showing orientation of the setae. Arrow is showing the reduced undulated setae. **B)** Chain in a close view, showing shape of the cells and attached flagellates at the apertures (arrow). **C)** Close view on the terminal part of the chain with cells containing numerous chloroplasts. **D)** Sibling valves in girdle view showing two pairs of reduced spirally undulated setae and two fused parts of common intercalary setae. Arrow points to the shoehorn shaped outgrowth on the valve edge. **E)** Detail of the intercalary common setae with small spines (arrowhead) and spirally undulated setae with T-shaped spines (arrow). Scale bars: A=20 µm; B,C=10 µm; D= 5 µm; E=1 µm.

EM: The valve face and the mantle are densely perforated with small pores in an irregular pattern, lacking on the mantle edge whose surface is smooth (Figure 3.46.D). The annulus and costae were not observed in this study due to the lack of TEM observations. Two sibling intercalary valves were observed with shoehorn-shaped outgrowths arising from the valve margin between setae (Figure 3.46.D). Common setae are circular in cross-section. They appear to be perforated with longitudinal rows of very small poroids running parallel with the seta axis from their basal part throughout the whole length of the seta. The structure of the seta can also be interpreted as composed of numerous thin and flat longitudinal strings arranged in a spiral pattern and interconnected with short transverse bars. After the fused part small spines are found arranged in a spiral pattern around the seta (Figure 3.46.E). Each of the reduced setae is straight at their proximal part to the valve and then distally first the small spines appear and soon the whole seta becomes strongly spirally undulated with the T-shaped spines and small silicate nodules covering the surface of the strings in the coiled part following the seta undulated shape (Figure 3.46.E). These setae are only at the beginning very strongly spirally twisted and later the coils are being less intensive and the undulation more smooth.

Distinctive features: Cell circular in valve view. Two large, curved setae and four strongly spirally undulated setae.

3.1.3 *Bacteriastrum* Shadbolt (1854)

Type species: *Bacteriastrum furcatum* Shadbolt

Generally not heavily silicified species, sometimes only setae strongly silicified. Numerous small chloroplasts present only in cell body. *Bacteriastrum* species are showing multipolar/radial symmetry with numerous (6-20) setae regularly arranged around the circular valve margin. One species solitary (*B. parallelum*), other united in inseparable chains by fusion of the setae or in loose chain colony by embedding the cells within the organic matrix (*B. jadranum*). Setae usually relatively thin and fragile, circular in cross-section all ornamented with spines except in *B. jadranum*. Terminal cells differentiated from the intercalary ones by the orientation of the setae which can be identical (section *Isomorpha*) or differ between two poles of the chain (section *Sagittata*). The valve face has an annulus from which radiates a pattern of weak costae. Valve mantle low with no constriction near the advalvar margin. Central process is present only on terminal valves in form of a slit from the inside and small projection from the outside. The resting spores known in one species (*B. hyalinum*).

3.1.3.1 Bacteriastrum biconicum Pavillard (1916)

Section *Isomorpha*
Figure 3.47.A-C
Bibliography: Hustedt (1930)
Description: a.a.: 10 – 16 µm (Hustedt: 10 µm); p.a.: 30 - 55 µm

LM: Strongly silicified cells united in short and straight chains. The cells rectangular in girdle view, usually very elongated with much longer pervalvar than the apical axis, in valve view circular. Numerous small chloroplasts in each cell. The valve face is flat to slightly concave and the valve corners are strongly diagonally cut giving the whole valve conical appearance which is particularly noticeable in the terminal valve (Figure 3.47.A-B). The valve mantle is high, without any constriction near the abvalvar margin and there is no visible notch at the suture between the valve and valvocopula. The girdle usually occupies larger part of the cell and in some specimens where the two thecae were separated, the lobbed connecting band of each sibling theca was observed (Figure 3.47.C). 5-7 intercalary setae originate well inside the valve margin with the long basal part extending parallel to the pervalvar axis forming large apertures (Figure 3.47.A,C). The sibling setae sharply bend at a 90° angle at the fusion point, remaining fused for ca. 2x the cell diameter and afterwards bifurcate with often spiral undulations in their distal part (Figure 3.47.C). Both fused and bifurcated part of the setae lie in the valvar plane (Figure 3.47.A,C). There are usually five terminal setae which are long and thick, emerging well inside the valve margin and extending firstly for a short distance parallel to the pervalvar axis then directing strongly obliquely outwards from the chain axis forming a cone outline (Figure 3.47.B).

Distinctive features: Valve corners are strongly diagonally cut giving the conical appearance to the valve. 5-7 intercalary setae originate well inside the valve margin with the long basal part forming

large apertures before the fusion. Setae bifurcate in the valvar plane. Five long and thick terminal setae form a conical outline.

Comments: *B. biconicum* can be confused with *B. elongatum* Cleve which has been previously reported from the Adriatic but not confirmed in this study. These two species have a similar general appearance, strongly silicified cells with low number of setae, large apertures and cone-like outline of the terminal seta, however, in *B. elongatum* setae bifurcate in apical and in *B. biconicum* in the valvar plane.

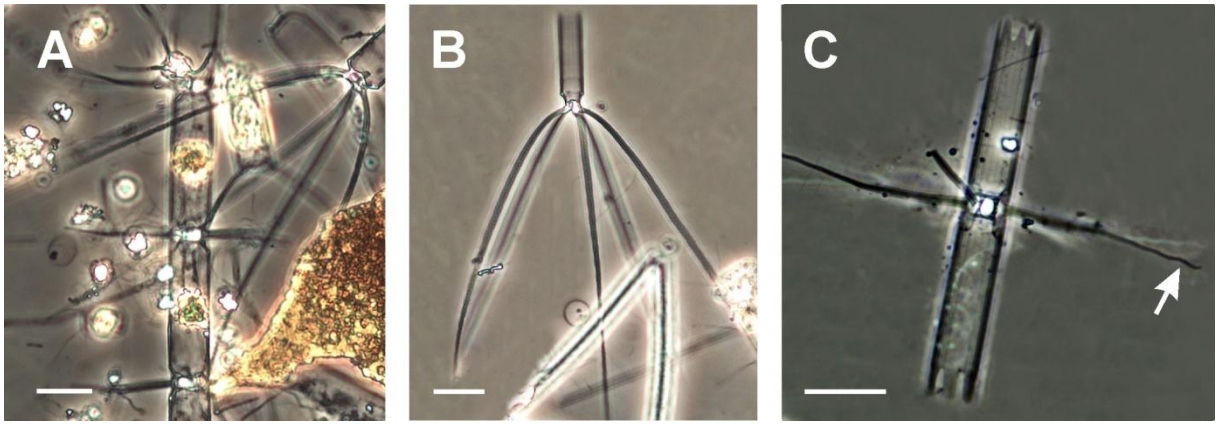

Figure 3.47. LM micrographs. of *Bacteriastrum biconicum* from field samples. **A)** Middle part of the chain with the partial view on a terminal valve in the top right corner. **B)** Terminal valve with the characteristic orientation of the setae. **C)** Sibling valves in girdle view showing the setae bifurcation in valvar plane and slightly undulated distal parts of the setae (arrow). Note the connecting girdle bands on each valve with the deep lobes on their abvalvar margin. Scale bars: A-C=20 µm

3.1.3.2 Bacteriastrum furcatum Shadbolt (1854)

Section *Sagittata*

Figure 3.48. and 3.49.

Bibliography: Boalch (1974), Fryxell (1978), Sarno et al. (1997)

Synonyms: *B. curvatum* Shadbolt, *B. nodulosum* Shadbolt

Species description: Shadbolt (1854) p. 14, pl. 1: fig. 1.; Lectotype: Slide B.M. no. 293. British Museum, London typified by {Boalch, 1974); Type locality: Port Natal (Durban), South Africa

Morphological description:

Morphometric values are reported in the Table 3.2.

LM: The cylindrical cells are united in long, straight and rigid chains which are formed by the fusion of setae of adjacent valves (Figure 3.48.A) with the tendency to be longer in cultures than in field samples (up to 17 cells and up to 11 cells, respectively). The cells are circular in valve view with slightly larger apical axis in cultured material (11.5 - 15 µm) than in specimens from natural samples (8.5 - 14.6 µm). The opposite was found for the pervalvar axis which was in generally shorter in cultures (12.6 - 31.2 µm) than in field specimens (11.5 - 44.9 µm). In girdle view cells are rectangular with slightly diagonally cut valve corners. Each cell contains 7-15 small chloroplasts (Figure 3.48.B). Valve face is flat or slightly convex. The valve mantle is rather low and the suture between the valve and girdle is not distinct hence the lines of the mantle and girdle appear straight and in most cases in LM it is not possible to determine the girdle height. The setae originate slightly inside the valve

margin with the long basal part (length in Table 3.2.) directed outwards and fusion point at or slightly outside the chain margin forming distinct apertures. The length of the fused part was found to be longer in natural samples than in cultures (Table 3.2.). After the fusion, intercalary setae bifurcate with the diverging parts lying in a valvar plane (Figure 3.48.F). The terminal setae of the anterior valve and those of the posterior valve have a different orientation and shape and this feature results in the formation of heteropolar chain colonies (Figure 3.48.A). The anterior setae are somewhat longer than the posterior ones (Table 3.2.) forming a wide and regular strong curve in the valve view (Figure 3.48.E) and lying almost parallel with the valve or with the proximal part bent slightly toward the inside of the chain in the girdle view (Figure 3.48.C). The posterior setae appear completely straight in the valve view (Figure 3.48.G) and in the girdle view their base is slightly arched toward the chain, then running outward from the posterior end forming a wide umbrella- like shape (Figure 3.48.D). Resting spores were not observed either in the cultures or in field material.

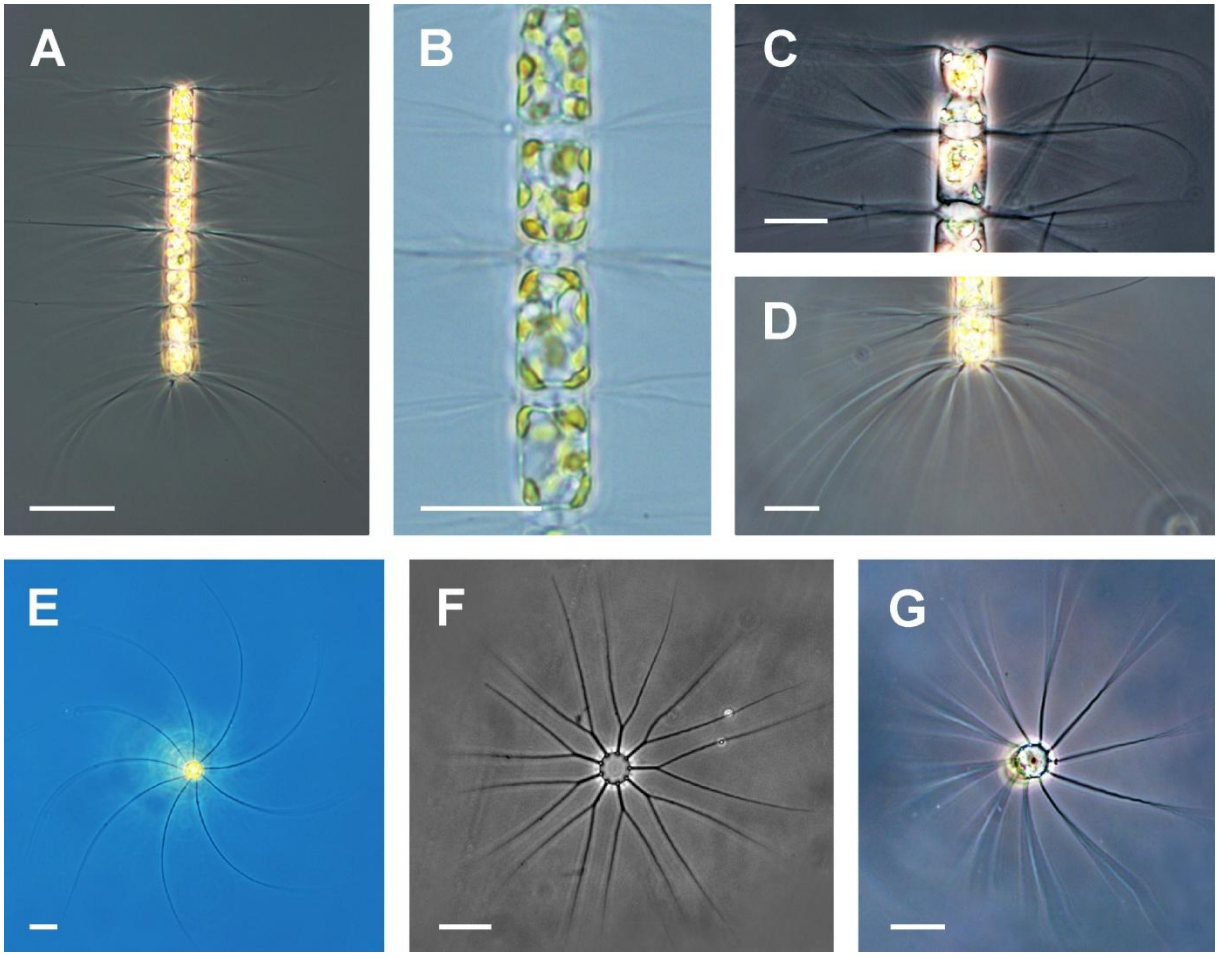

Figure 3.48. LM micrographs. of *Bacteriastrum furcatum* from cultured strain PMFBA4. **A)** Complete heteropolar chain with different shape and orientation of the terminal setae. **B)** Intercalary cells with numerous chloroplasts. **C)** Anterior part of the chain in girdle view showing the setae orientation. **D)** Posterior part of the chain in girdle view showing the setae orientation. **E)** Anterior terminal valve in valve view showing setae widely curved in the valvar plane. **F)** Intercalary valve in valve view showing fusion and bifurcation of sibling setae. **G)** Posterior terminal valve with setae extending straight in valvar plane. Scale bars: A=50 µm; B, E-G=20 µm; C,D=10 µm.

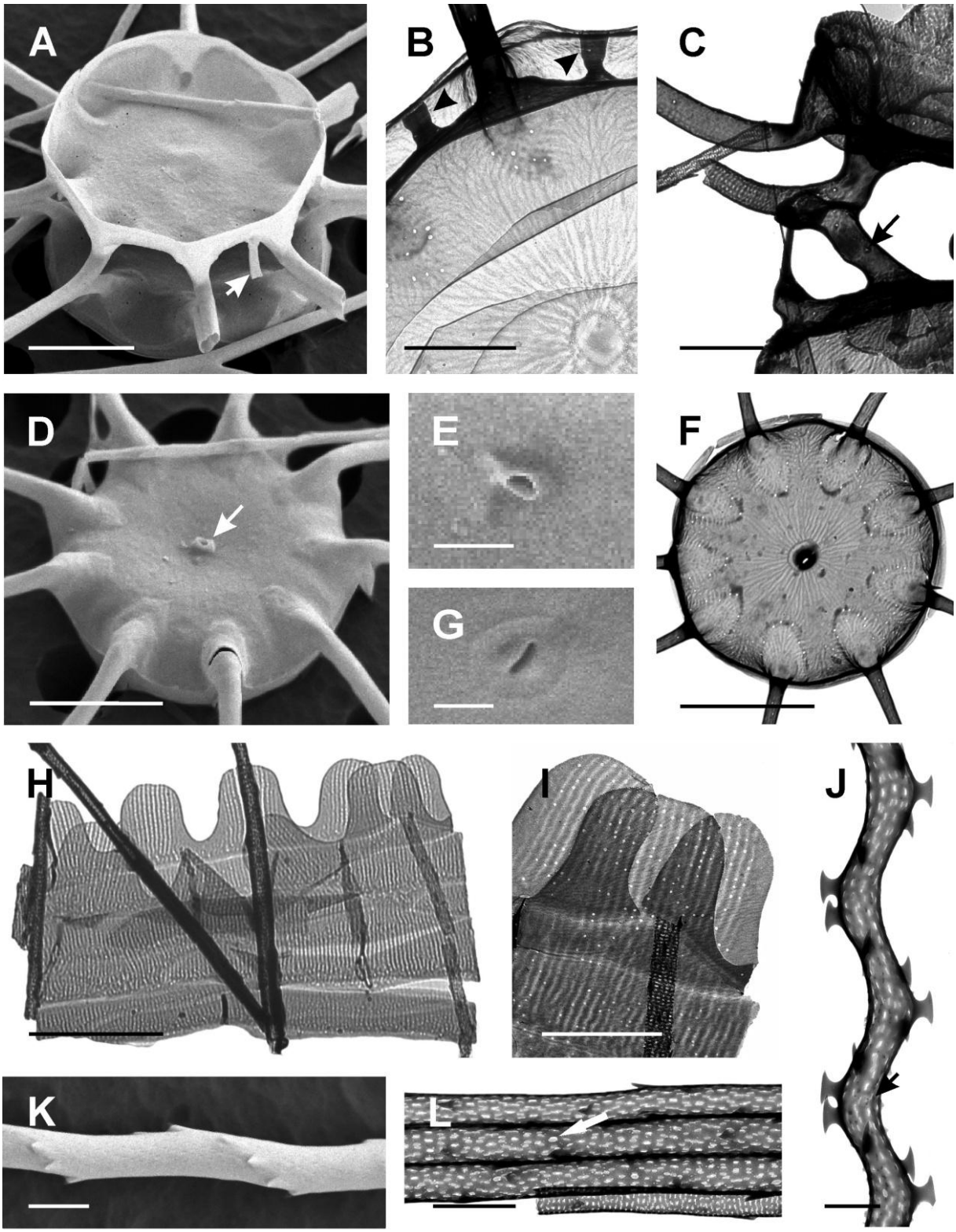

Figure 3.49. SEM **(A,D,E,G,K)** and TEM **(B,C,F,H-J,L)** micrographs of *Bacteriastrum furcatum* from cultured strain PMFBA4. **A)** Sibling intercalary valves with a showhorn-shaped outgrowth projecting from a valve margin (arrow). **B)** Fine structure of the two overlaid intercalary valves. Note the central annuli, the small pores scattered on the basis of the setae and the two outgrowths projecting from the upper valve (arrowheads). **C)** Sibling valves in girdle view showing setae fusion and basal part perforated by small pores (arrow). **D)** External view of the posterior terminal valve with the tube-like central process (arrow). **E)** Detail of the valve showing the external short tube-like process. **F)** External view of the posterior terminal valve showing the fine structure.

EM: The valve face is ornamented with the round to oval-shaped central annulus from which the parallel fine costae (6-7 per 1 μm) are radiating and branching out dichotomously towards the valve margin (Figure 3.49.B). The valve diameter measured in EM ranged between 10.7-13.5 μm. The size of the annulus varied among specimens (0.9-1.6 μm; 8-15 % of the valve diameter) but not depending on the size of the valve. The valve mantle, the marginal part of the valve face around the setae openings and basal part of the setae are perforated with irregularly scattered round to elongated ca. 0.1 μm sized pores (Figure 3.49.B-C). The end cells are heterovalvate, i.e. the terminal valve have a central process located in the annulus. On the outer side of the valve the process is a short and relatively narrow tube-like projection (Figure 3.49.D-E) and on the inner side it appears as a slit on a bulge. The anterior and the posterior valve share the identical ultrastructural characteristics, these two being different only in the shape and orientation of the setae. In intercalary as well as in terminal valves one or more silica outgrowths, 1.4-1.9 μm in length, are frequently found growing from the part of the margin separating two contiguous setae. These outgrowths appear as the flattened hollow elongated tubes, narrower in the base and wider towards the end, resulting in a shoehorn-shape. The girdle is composed of several intercalary and one connecting band per valve. The intercalary bands are open, more or less narrow (1.0–2.5 μm wide) with straight margins and pointed ends. Their ornamentation consists of parallel transverse ribs (7-8 per 1 μm) between which are irregularly distributed small, round pores. The advalvar margin of the connecting band is straight and the abvalvar margin is undulated with several deep lobes. The structure is the same as in intercalary bands. The setae are circular in the cross-section, composed of the longitudinal strings arranged in a spiral pattern and interconnected with transverse parallel bars. All setae are perforated with elliptically shaped pores, ca. 0.1 μm long, continuing in irregular distribution from the valve surface along the whole length of the setae. Besides elongated pores, the setae are after the fusion ornamented with small, 0.1–0.4 μm long, spines which are spirally arranged around the setae, commonly 6 spines in one turn with the distance of 0.3–0.9 μm between two adjacent spines. In both cultured and natural material, a few intercalary valves were observed with the setae having two morphologically different bifurcated parts with one strongly spirally twisted in the distal portion and the other one straight. The spirally undulated seta parts are ornamented with particular T-shaped spines with the 0.2–0.5 μm gap and small silicate nodules covering the surface of the strings in the coiled part following the seta undulated shape. The length of T-shaped spines varies between 0.2 – 0.3 μm and width in the terminal part of the spine is 0.3–0.5 μm.

←

Figure 3.49. continued

G) Detail of the valve showing the internal slit-shaped process on a bulge. **H)** Girdle with intercalary and connecting bands. **I)** Detail of the connecting and intercalary girdle bands. **J)** Detail of an undulating seta with T-shaped spines and silicate nodules (arrow). **K)** Detail of a seta. **L)** Detail of the setae with elongated pore (arrow). Scale bars: A-C,I = 2 μm; D,F,H = 5 μm; E,G= 1 μm; J-L= 0.5 μm.

Distinctive features: Setae bifurcate in valvar plane. Chains heteropolar. Anterior setae in valve view form a strong curve and in girdle view slightly bent towards the chain. Posterior setae radiate straight in valve view, and in girdle view form wide umbrella-like shape. Shoehorn-shaped outdgrowths between contiguous setae.

Comments: *B. furcatum* can be misidentified as *B.delicatulum* as apparently distinguishing characteristics between two species are the degree of silification of the cells and chain polarity. *B. furcatum* colonies are more robust and heteropolar and those belonging to *B. delicatulum* more delicate and isopolar. In this study, the careful examination of specimens similar to *B. delicatulum* and their examination in enrichment cultures and monoclonal strains showed the development of heteropolarity in all of the observed chains, hence we ascribe all of the specimens to *B. furcatum*. Further investigations of *B. delicatulum* are clearly necessary to establish its taxonomic validity and relationship with other species.

3.1.3.4 Bacteriastrum hyalinum Lauder (1864)

Section *Isomorpha*

Figure 3.50. and 3.51.

Bibliography: Ikari (1927), Hustedt (1930), Cupp (1943),Okuno (1962), Drebes (1972), Boalch (1975), Round et al. (1990), Hoppenrath et al. (2009), Kooistra et al. (2010).

Synonyms: *B. spirillum* Castracane, *Chaetoceros spirillum* (Castracane) De Toni, *B. hyalinum var. princeps* (Castracane) Ikari

Species description: Lectotype: Lauder (1864) p. 8, pl. 3: fig. 7 a & b typified by (Boalch, 1975); Type locality: Hong Kong Harbour, China

Morphological description:

Morphometric values are reported in the Table 3.2.

LM: The cylindrical cells are joined in long and straight chains through the fusion of the setae with the length of the fused part found to be longer in natural samples than in culture (Table 3.2). The chains were slightly shorter in nature being composed of up to 18 cells compared with up to 49 cells per chain found in cultures. The cells are rectangular in girdle view with round valve corners and circular in valve view. Both apical and pervalvar axis show a considerable range of variability in culture, being 29-46 µm and 13-56 µm long, respectively. Comparing with natural samples the measurement values of pervalvar axis were similar but the apical axis was slightly smaller (19-39 µm). Each cell contains very large number (21-55) of small chloroplasts (Figure 3.50.B). Valve face is flat or slightly convex. Valve mantle is very low and the suture is not distinct. The setae originate slightly inside the valve margin and due to their short basal part (Table 3.2.) and slightly convex valves the aperture is usually very narrow or in some cases sibling valve faces appear to be apressed to each other. The sibling setae fuse at the valve margin and after a certain distance bifurcate (Figure 3.50.C) with the forked parts extending in the pervalvar plane (Figure 3.50.A). The chain colonies are isopolar because the terminal setae on both ends are of similar shape and orientation (Figure 3.50.A). The terminal setae are found to be shorter than the intercalary ones (Table 3.2.). In the valve view they

form a wide curve (Figure 3.50.D) and in the girdle view at first they extend in the valvar plane and then slightly curve backwards toward the chain and continuing running outward from the posterior end of the chain (Figure 3.50.A). In specimens from natural samples some of the intercalary setae had strongly spirally undulated bifurcated ends, usually with both branches of the fork twisted. Resting spores were found both in the field samples and in cultures. They are round, with both valves dome-shaped and with the primary valve bearing a marginal silica collar of variable length which appears slightly bent inwards at its end (Figure 3.51.A).

EM: The valve ornamentation consists of fine ribs (6-7 in 1 μm) radially branching out from a central annulus to numerous anastomosing minor ribs that reach the valve margin (Figure 3.50.E). The valve diameter measured in EM varied between 8.3 and 30.5 μm. Annulus is a hyaline area, round to oval shaped with a diameter of 1.4-3.6 μm and its size does not vary proportional to valve diameter (10-17 %). The whole surface of the valve is perforated with irregularly scattered round ca. 0.1 μm sized pores. The terminal valves have a relatively large process located in the annulus centre (Figure 3.50.F). This central process appears as a short flattened tube from the outside of the valve (Figure 3.50.H) and a simple slit from the inner side(Figure 3.50.G). Intercalary valves are often adorned with outgrowths of a variable length (0.8-1.0 μm), arising from the valve margin between two setae (Figure 3.50.I). They are shaped similarly to a letter T, narrower at the base and ending with a perpendicularly oriented wide bar. The girdle is composed of several intercalary and connecting bands. The intercalary bands are open, with straight margins; narrow (1.1–3.4 μm wide) with overlapping pointed ends. They are ornamented with regularly oriented parallel 6-7 ribs per 1 μm between which are irregularly distributed small round ca. 0.1 μm sized pores (Figure 3.50.K). One margin of the connecting band is straight and the other is deeply lobed (Figure 3.50.J). The setae are circular in the cross section, composed of the longitudinal strings arranged in a helicoidal pattern and interconnected with transverse parallel bars. The setae are ornamented with elongated 0.1-0.2 μm long pores irregularly distributed along the whole seta length (Figure 3.50.L). The proximal, fused part of the intercalary setae is smooth and bears 0.2-0.8 μm long spinules with bifurcated ends appearing similar to a letter Y and not arranged in any specific pattern (Figure 3.50.N). Further on, after the fusion, the setae are ornamented with small common spines, 0.3-0.5 μm long, arranged in a spiral pattern positioned on the longitudinal strings (Figure 3.50.M). There are commonly 6 spines in one turn around the seta, 0.3-0.7 μm apart. In some intercalary setae that have strongly undulated distal bifurcated parts, these are adorned with spirally arranged T-shaped spines, positioned 0.5-0.7 μm apart. The T-spines are 0.2-0.3 μm long and 0.5-0.7 μm wide in their end part. The undulated part of the seta does not have a smooth surface but it is covered with very small silicate nodules (Figure 3.50.O). The primary valve of the resting spore bears marginal collar which usually collapses upon drying and observation with EM (Figure 3.51.B-D). The collar is perforated with a few rows of small irregular pores near to its advalvar margin (Figure 3.51.C) and in some cases the whole surface of the collar is fissured and appearing lace-like (Figure 3.51.B). The surface of the outer part of the primary valve mantle appears

granulated (Figure 3.51.B-D) while the surface of the primary valve face is covered with numerous spines, often branching dichotomously at their end (Figure 3.51.C,D). The surface of the secondary valve is smooth with the margin of the valve face bearing the single marginal ring of poroids (Figure 3.51.B,F). The poroid ring seems to be different from the single ring of puncta which is present on the inner side of the advalvar mantle margin (Figure 3.51.C), but this could not be confirmed with certainty. In the centre of a single primary valve from a resting spore obtained in culture, we observed a thick external protuberance similar to a flattened tube with a lip like structure in its end, probably representing a spore formed from the terminal cell.

Distinctive features: Numerous setae bifurcate in the apical plane. Chains isopolar. Terminal setae in valve view form a wide curve, in girdle view slightly bend towards the chain in the proximal part. Resting spore with both valves smooth and with a marginal collar on the primary valve. Y-shaped spines on the fused part of the setae. T-shaped outgrowths between contingous setae on the valve margin.

Comments: *B. hyalinum* var. *princeps* (Cactracane) Ikari differs from the type in the spirally twisted bifurcations on some of the intercalary setae. This morphological type was often observed in the field samples, however it is not considered in this thesis to be distinct from the type as the only different character is the undulation of some setae. The spirally twisted setae apparently are not a pertinent taxonomic character which appeared also in *B. furcatum* cultures therefore we considered these *B. hyalinum* specimens to belong to the type.

Figure 3.50. LM **(A-D)**, TEM **(E,G,J-L)** and SEM **(F,H,M-O)** micrographs. of *Bacteriastrum hyalinum* from cultured strain PMFBA2. **A)** Complete isoopolar chain with identical shape and orientation of the terminal setae. **B)** Terminal part of the chain showing numerous chloroplasts in each cell. **C)** Intercalary valve in valve view showing fused and bifurcated sibling setae. D**)** Terminal valve with setae slightly curved in valvar plane. **E)** Fine structure of two overlaid intercalary valves. **F)** Internal view of the terminal valve with a central slit-shaped process. Note the pores scattered on the valve surface (arrow). **G)** Detail of the valve with the slit-shaped process within the central annulus. **H)** Detail of the valve with the external wide flattened tube of the central process. **I)** Detail of the sibling valves with T-shaped ougrowths projecting from the upper valve. **J)** Detail of the connecting band. **K)** Detail of the intercalary bands. **L)** Detail of a seta. Note the elongated pore (arrow). **M)** Detail of a seta. **N)** Detail of the fused part of the setae with Y-shaped spinules. **O)** Detail of an undulating seta ornamented with T-shaped spines (arrow) and silicate nodules (arrowhead). Scale bars: A=50 µm; B = 10 µm; C-D= 20 µm; E,F=5 µm; H-O=1 µm; G= 0.5 µm.

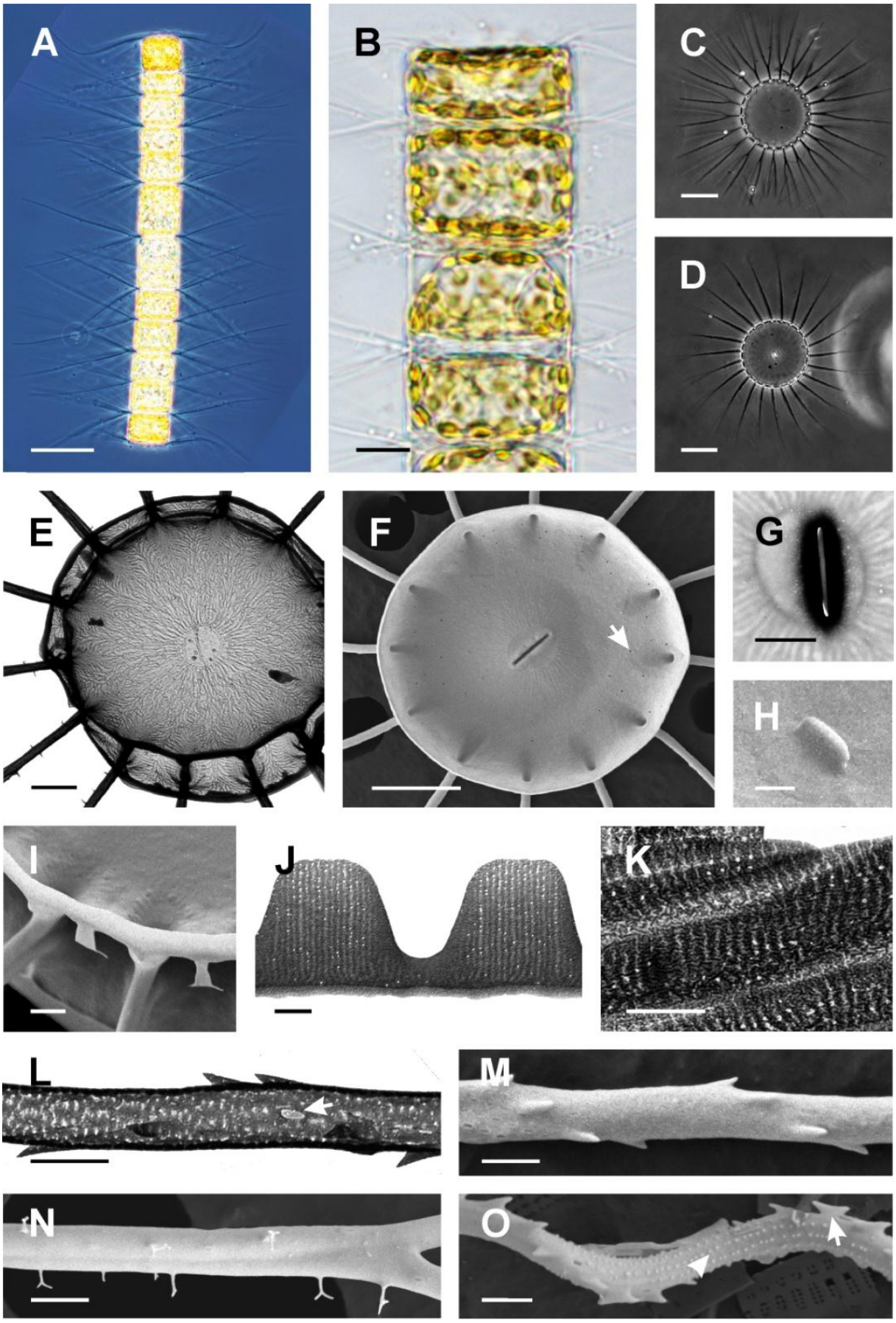
A
B
C
D
E
F
G
H
I
J
K
L
M
N
O

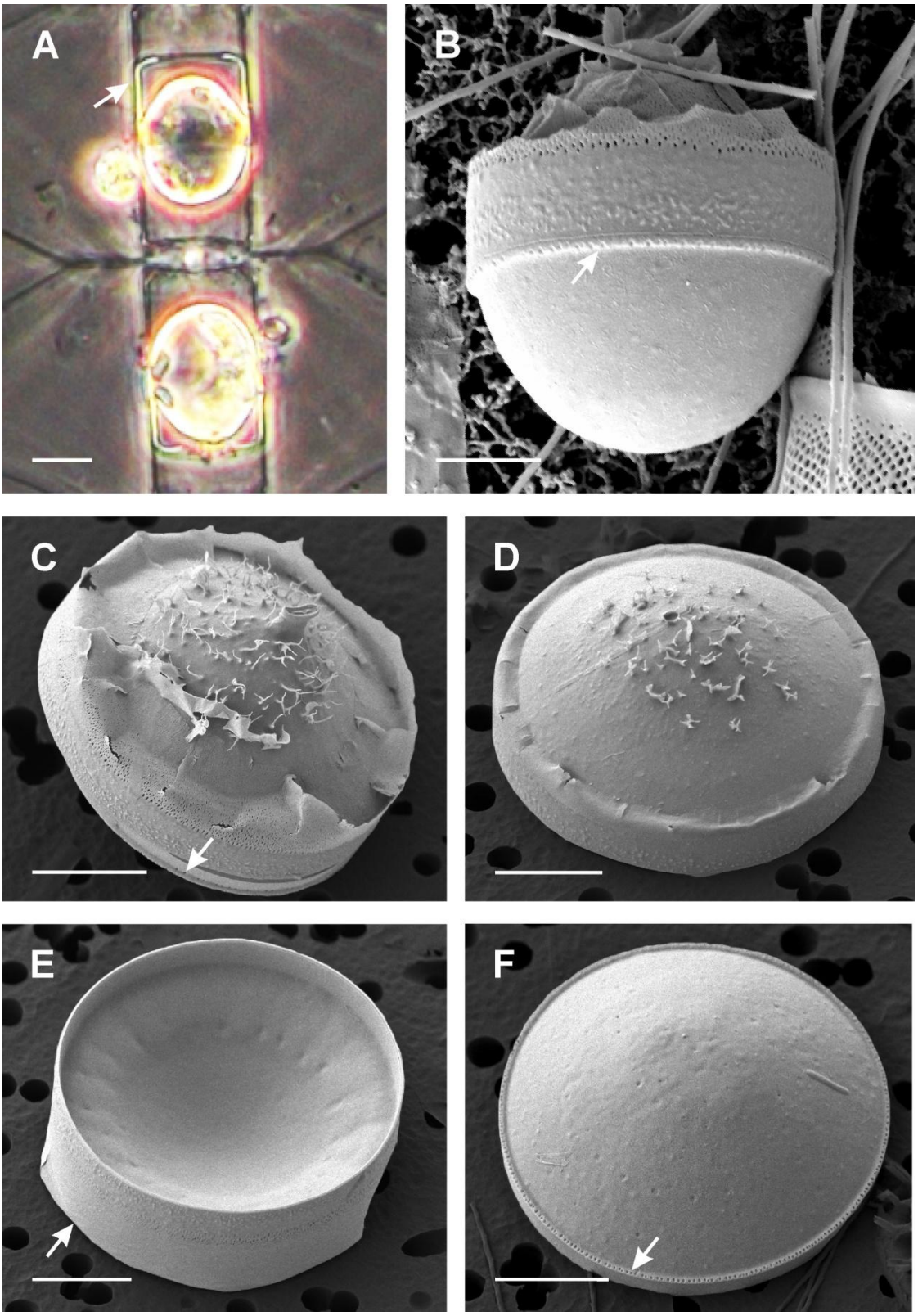

Figure 3.51. LM **(A)** and SEM **(B-F)** micrographs. of *Bacteriastrum hyalinum* resting spores from field samples **(A-B)** and cultured strain PMFBA2 **(C-F)**. **(A)** Two intercalary cells with resting spores, marginal collar surrounding the primary valve is marked with an arrow. **(B)** Complete resting spore Note the single ring of poroids on the secondary valve margin (arrow). **(C)** Partially open resting spore. Note the row of puncta (arrow) on the advalvar margin of the mantle of secondary valve. **(D)** Primary valve with the short collapsed collar. **(E)** Primary valve from an inside view showing marginal collar (arrow). **(F)** Secondary valve from an outside view. Note the single ring of poroids on the valve margin (arrow). Scale bars: A, C-D=10 µm; B=5 µm.

Table 3.2.: Morphological characters and morphometric data of four *Bacteriastrum* species obtained from LM, TEM and SEM examination from field samples and culture material; measurements given as a mean ± SD, minimum - maximum value, *n* = number of specimens/measurements, ND not determined.

	B. furcatum	*B. hyalinum*	*B. jadranum*	*B. mediterraneum*
Plane of bifurcation	valvar	pervalvar	–	valvar
Cells per colony	8 ± 3	21 ± 10	14 ± 8	10 ± 7
	3–17	6–49	4–41	1–29
	n = 35	*n* = 39	*n* = 40	*n* = 30
Apical axis (µm)	12.1 ± 1.6	30.7 ± 5.6	10.4 ± 2.1	15.6 ± 7.2
	8.5–14.9	18.9–46.1	7.2–16.6	10.2–38.5
	n = 131	*n* = 155	*n* = 150	*n* = 97
Pervalvar axis (µm)	23.0 ± 6.6	27.9 ± 9.8	12.2 ± 3.8	17.5 ± 5.0
	11.5–44.9	10.8–56.4	6.1–23.4	9.0–29.9
	n = 106	*n* = 157	*n* = 146	*n* = 92
Chloroplasts per cell	10 ± 2	32 ± 9	10 ± 2	24 ± 7
	7–15	21–55	7–15	11–34
	n = 40	*n* = 17	*n* = 38	*n* = 11
Setae per valve	9 ± 1	19 ± 4	9 ± 1	16 ± 2
	7–11	12–25	7–12	13–22
	n = 104	n = 88	n = 53	n = 69
Intercalary setae length (µm)	101.9 ± 26.0	80.0 ± 17.1	75.3 ± 24.9	72.7 ± 14.6
	31.3–180.6	39.8–141.2	23.1–120.0	22.6–108.8
	n = 119	*n* = 142	*n* = 168	*n* = 125
Terminal/anterior setae length (µm)	86.3 ± 28.2	55.9 ± 10.2	35.2 ± 14.4	34.9 ± 7.7
	32.1–153.9	36.3–76.9	19.9–65.0	20.8–47.2
	n = 30	*n* = 34	*n* = 11	*n* = 20
Posterior setae length (µm)	83.1 ± 23.8			39.4 ± 9.9
	30.6–127.3	–	–	21.5–62.0
	n = 34			*n* = 22
Fusion length in natural samples (µm)	22.3 ± 1.7	15.4 ± 1.2		17.4 ± 3.9
	19.0–25.3	11.2–17.5	–	10.2–24.0
	n = 40	n = 53		n = 25
Fusion length in culture (µm)	14.0 ± 2.9	6.7 ± 1.8		10.3 ± 3.0
	10.0–28.6	1.5–12.6	–	3.0–15.7
	n = 120	n = 105		n = 81
Basal part length (µm)	1.9 ± 0.4	2.9 ± 1.8		1.1 ± 0.2
	1.3–3.3	0.9–4.9	–	0.9–1.4
	n = 24	*n* = 9		*n* = 8
Girdle band width (µm)	1.6 ± 0.6	2.6 ± 1.3	0.8 ± 0.2	1.1 ± 0.1
	1.0–2.5	1.1–3.4	0.6–1.1	1.0–1.1
	n = 8	*n* = 3	*n* = 5	*n* = 3
Setae diameter (µm)	0.6 ± 0.1	0.5 ± 0.1	0.4 ± 0.1	0.3 ± 0.1
	0.4–0.8	0.4–0.9	0.3–0.7	0.3–0.4
	n = 39	*n* = 17	*n* = 26	*n* = 16

3.1.3.5 Bacteriastrum jadranum Godrijan, Maric et Pfannkuchen (2012) emend. Bosak

Section *Isomorpha*

Figures 3.52.-3.57.

Species description: Holotype: Slide B 40 0040730, Botanischer Garten und Botanisches Museum Berlin, Germany (Godrijan et al., 2012), Type locality: Adriatic Sea, Croatia

Epitype: Adriatic Sea, Croatia (fixed material and permanent slide labelled as PMFBA1 are deposited in in Division of Biology, Faculty of Science, University of Zagreb, Croatia; the LSU gene sequence is registered under accession number KC914885 with GenBank)

Emended diagnosis

Weakly silicified cells, round in valve view and rectangular in girdle view with diagonally cut corners. 7-15 small chloroplasts per cell. Apical axis 9-17 µm, pervalvar axis 6-23 µm. Valve face flat or slightly convex, mantle high, suture not distinct. 7-11 long and thin setae originate ca. 2 µm within the valve margin and to not touch at any point with the setae of the adjacent valve, running almost parallel to the valvar plane. Long, loose and very flexible chain–like colonies are assembled by enclosing the cells together with their setae within the cell jacket, optically transparent organic matrix of predominately polysaccharide composition. Intercalary cells isovalvate. Valve face ornamented with round central annulus (1.2-2.2 µm in diameter) from which the fine costae (6-7 per 1 µm) are radiating and branching out dichotomously towards the valve margin. End cells of the colony heterovalvate. Terminal valves have slit-shaped central process with a slightly thickened edge on the external side of the valve and simple slit on the valve interior. Terminal setae structurally identical to intercalary ones, but shorter, curved backwards toward the chain in their initial part and then curving forwards. Isopolar colonies. Setae diameter 0.3-0.7 µm, length span between 23 and 120 µm, composed of thin silica strings arranged in helicoidal pattern and interconnected with transverse bars. Setae surface smooth, lacking spines, ornamented with elongated pores.

Morphological description:

Morphometric values are reported in the Table 3.2.

LM: Weakly silicified cylindrical cells are assembled in regular but loose and very flexible chain–like colonies (Figure 3.52.A-C) composed of 4 to 23 cells in natural samples and up to 41 cells in cultures. Cells are circular in valve view (Figure 3.52.F) with the apical axis showing a slight difference in range of variability between specimens from natural samples and culture, being 9-14 µm and 7-17 µm, respectively. Moreover, this applies also to the pervalvar axis, being slightly larger in the field samples (6-21 µm vs. 7-23 µm). Cells appear rectangular in girdle view with strongly diagonally cut valve corners, valve mantle is high and suture not distinct (Figure 3.52.A-E). Each cell contains 7-15 small and usually spherical chloroplasts (Figure 3.52.F). Valve face is flat or slightly convex. The distance between individual neighbouring cells in natural samples can extend up to 4 times of the cell diameter (>40 µm) (Figure 3.52.A,B) while in the culture conditions it reduces to a level at which the sibling valves are almost touching (Figure 3.52.I) but without any actual contact between valves. Cells in the process of vegetative mitotic division were commonly observed in both natural and cultured samples

as it is shown in Figure 3.52. B,D and E where recently divided daughter cells can be recognized by the small distance between cells and the presence of very short setae growing out from the newly formed valves. The long and delicate intercalary setae do not cross or fuse at any point with the setae of the adjacent valve, running almost parallel to the valvar plane or are slightly irregularly curved (Figure 3.52.A-D). The terminal setae appear straight in the valve view and cannot be distinguished from the intercalary ones. However, in the girdle view it is visible that they are shorter (Table 3.2.) and differently curved, first bending slightly backwards in their initial part toward the chain and then curving forwards in their final part forming W-like shape (Figure 3.52.A,C,E). There is no observable difference in the morphology of the terminal setae of anterior and posterior valve hence the species forms isopolar colonies.

The colony formation in this species is achieved by embedding the cells within the organic matrix formed by the extracellular polymeric substances (EPS) extruded by the diatom cells. The matrix is optically transparent in the water mounts and visible with the LM only with Alcian Blue staining which detects the existence of acidic polysaccharide material (Figure 3.52.G-I). We termed the blue stained structure with a well-defined border toward the surrounding media as the cell jacket. A closer look at the colonies showed that the long and delicate setae were completely enclosed within the jacket domain. The cell jacket was observed in both cultured (Figure 3.52.H,I) and field samples (Figure 3.52.G), indicating that it represents a stable component of the cellular organisation of the species and not an artefact due to culture conditions. A parallel staining experiment with amino acid specific dye Comassie Brilliant Blue G (insert in Figure 3.52.H) showed that substantial amounts of proteins are not present in the structure. The dye stained only cells' interior contents and the bacteria presumably growing on the jacket organic matrix, but the material itself was not stained. The spores were not observed in cultures neither in natural samples.

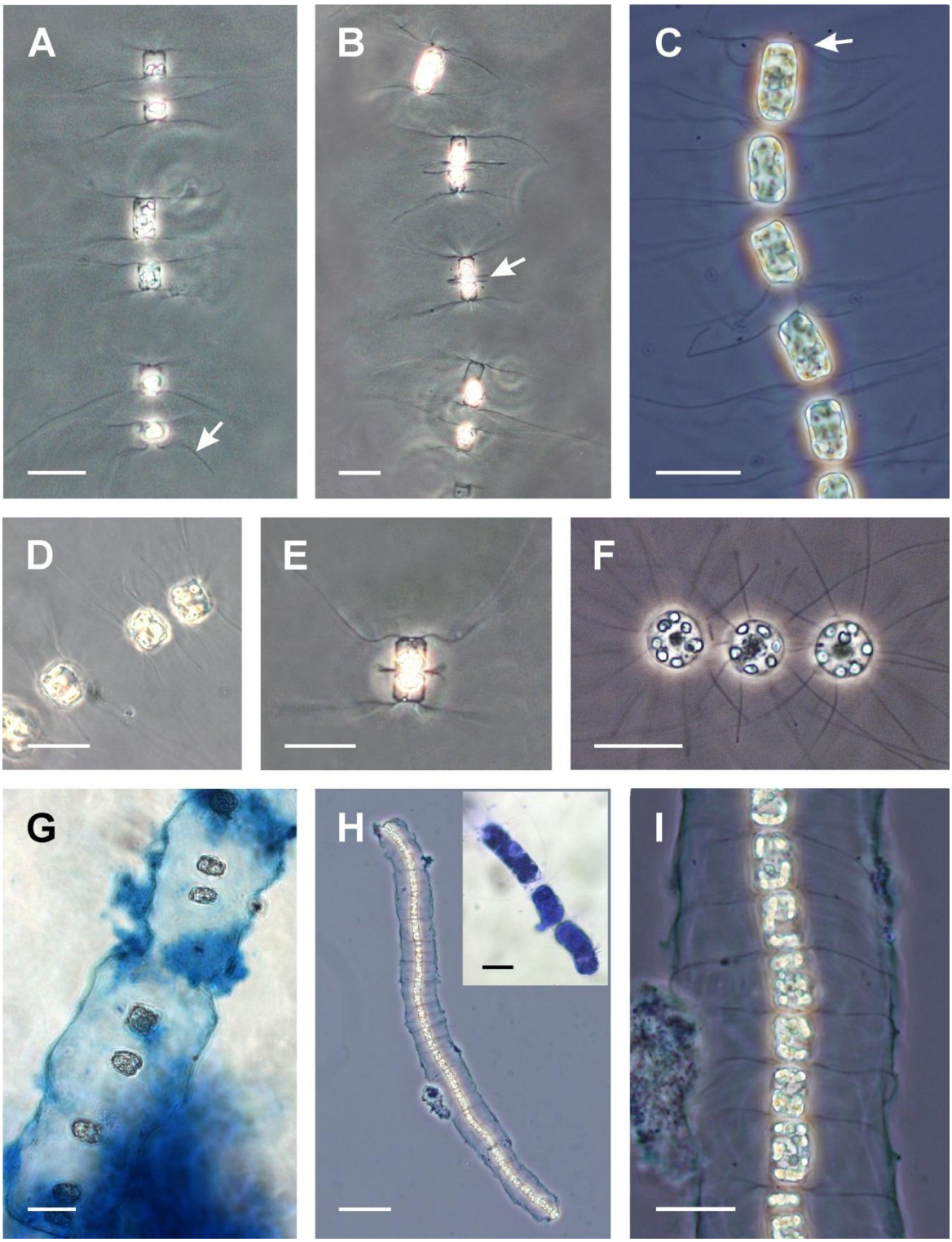

Figure 3.52. LM micrographs. of *Bacteriastrum jadranum* from field samples **(A,D-G)** and cultured strain PMFBA1 **(B,C,H,I)**. **A)** Terminal part of a colony in a girdle view showing the shape of terminal setae (arrow). **B)** Middle part of a colony showing cells in division (arrow). **C)** Terminal part of a colony in a girdle view showing the setae orientation, terminal setae are marked with an arrow. **D)** Two pairs of recently divided cells in girdle view. **E)** A pair of recently divided cells in a girdle view, the upper is a terminal cell recognisable by the shape of the setae. **F)** Cells in valve view with numerous chloroplasts. **G)** Cell jacket embedding the colony, stained by Alcian Blue. **H)** Chain-like colony with Alcian Blue cell jacket. Insert is showing Commassie Blue G-stained cells interior contents. **I)** Detail of a colony showing the setae completely enclosed within the structure domain. Scale bars: A-C,E-G,I=20 µm; D=10 µm; H=100 µm; insert in H=5 µm.

EM: The intercalary cells are isovalvate. The surface of the valve face and mantle is completely smooth without perforations and the ornamentation consists of very fine costae (6-7 in 1 μm) radially arranged around the central hyaline annulus branching dichotomously to numerous minor ribs reaching the valve margin (Figure 3.53.A-C). The annulus is circular in shape with diameter 1.2-2.2 μm, and occupies between 13-24 % of the valve diameter which ranges between 8-17 μm, however the size of the annulus is not proportional to the size of the valve. The terminal cells are heterovalvate. The ornamentation of the terminal valves is similar to the intercalary ones except they possess a central slit-shaped process (Figure 3.53.D-E). The slit is surrounded by a slightly thickened edge on the external side of the valve (Figure 3.53.G) and it is flat on the valve interior. The setae on both terminal and intercalary valves originate well inside the valve, ca. 2 μm within the valve margin (Figure 3.53.A-D). The setae are circular in cross section, with delicate structure composed of very thin siliceous longitudinal strings arranged in a spiral pattern and interconnected with somewhat long and parallel transverse bars. The setae are smooth, completely lacking any type of spines, but scarcely perforated with irregularly distributed elongated pores (0.1–0.2 μm long) (Figure 3.53.B,K-L). Smaller pores which represent the interspace between silica bars are sometimes visible (figure 3.53.K). There are no observed differences in the structure of proximal and distal part of the setae. The girdle is composed of intercalary and connecting bands (Figure 3.53.J). No discernible specialized valvocopula was observed. Proximal side of the connecting band is straight, and distal one has an undulate margin. Intercalary bands are narrow (Table 3.2.), open bands with pointed ends. The bands are ornamented with numerous weakly silicified transverse parallel ribs with the density of 6-8 in 1 μm. Small pores are irregularly scattered between the ribs.

The SEM observations of the air dried samples not subjected to acid-cleaning, showed the clumped organic matter covering the cells and the setae (Figure 3.53.F). The samples treated with dehydration procedure using HDMS revealed that this organic matter is in fact fibrillous organic network tightly associated with the valves and setae (Figure 3.53.H,I). This structure corresponds to the cell jacket, the Alcian blue stained structure enclosing the chain colonies visible with the LM.

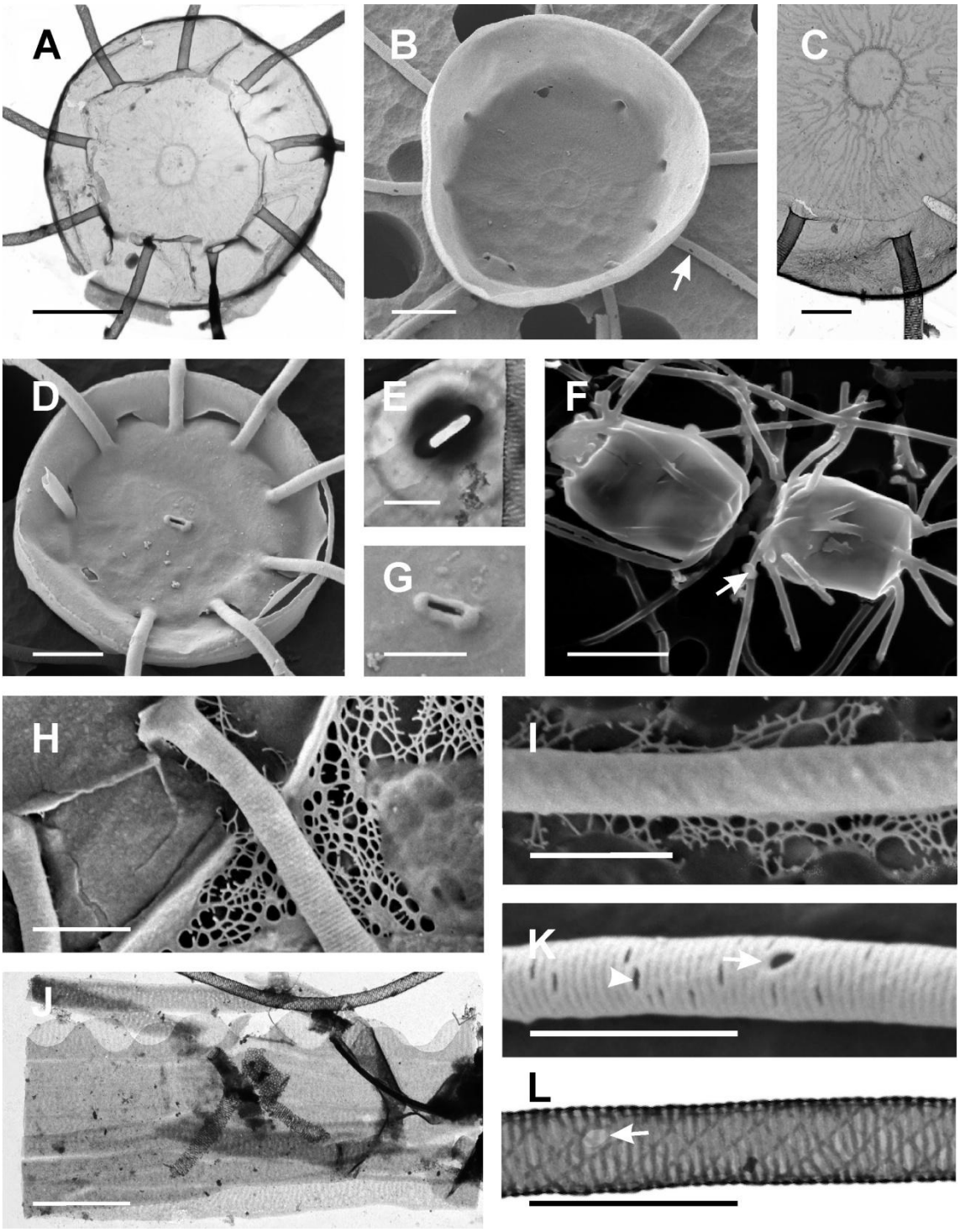

Figure 3.53. TEM **(A,C,E,J,L)** and SEM **(B,D,G-I,K)** micrographs. of *Bacteriastrum jadranum* from field samples **(A,C,F,H-J)** and cultured strain PMFBA1 **(B,D-G,K,L)**. **A)** Intercalary valve from an outside view showing the fine structure of the valve face. **B)** Intercalary valve from the internal view. Note the elongated pore on the setae (arrow). **C)** Detail of the valve with central annulus, radiating costae and two setae. **D)** Outside view on the terminal valve with central slit-shaped process. **E)** Detail of the valve with the slit-shaped central process. **F)** Two cells in girdle view with clumped organic matter attached to the cells (arrow). **G)** Detail of the valve with outside view on the slit-shaped process with thickened edges. **H)** Detail of the valve with two setae and the fibrillous network attached to the valve. **I)** Detail of a seta. Note the attached polysaccharide fibrils. **J)** Girdle with intercalary and connecting bands. **K)** and **L)** Detail of a seta. Note the difference between elongated pore (arrows) and interspace between parallel silica bars (arrowhead). Scale bars: A,B,D=2 µm; C,G,H,J=1 µm; E,I,K,L=0.5 µm;F=10 µm.

AFM: In order to investigate the mechanism of the *B.jadranum* colony formation the culture material was observed with AFM. This was done before the Alcian Blue experiments. We started with low magnification to identify the *Bacteriastrum* colony – the cells overlaid with a polysaccharide cell jacket and to relate the AFM image to the light micrograph of the cell colony. In AFM image, individual cells, polysaccharide jacket and setae are clearly identified (Figure 3.54.). The cell jacket extends up to 35 μm from the cell centre (30 μm in Figure 5.54.A). White areas on the central part of individual cells in Figure 3.54.B are the highest zones (700–900 nm) representing cell content and plastids. The cell jacket is more clearly recognised at higher magnifications and it is a continuous, bulk material reaching the span of seta (Figure 3.54.C). The directly measured jacket height in a dry state is only 20–30 nm. Further on, in order to reveal the fine structure of the cell jacket, AFM images of the cell jacket material were captured several hundred nm beyond the observed jacket border. This is the region where the jacket material is spread on the mica substrate as a thin layer. The cell jacket imaged at 8 μm with a 20 nm vertical scale appeared as a cross-linked fibrillar network (Figure 3.54.). The observed difference is caused by the extent of spreading over the mica substrate: a collapsed 3D network (Figure 3.54.A) and a 2D stretched network (Figure 3.54.B). By imaging at higher resolution (4 μm and a vertical scale of 10 nm), we detect the specific patterns of the cell jacket network. Frequently encountered 2D fibrillar network patterns are presented in Figure 3.56. together with height profiles along indicated lines. High-density domains (further called patches) are surrounded and interconnected by thicker fibrils in a continuous network and are taken as the basic structural motive (encircled in white in Figure 3.56.). Pores inside the patch are of the same hexagonal shape. Their size is continuously smaller from the patch edge towards the centre. The cell jacket network is reinforced by the fibrils branching into patches (Figure 3.57.A). Such fibrils are considerably wider but not higher than the fibrils that form large pore openings (height profile in Figure 3.56.). The branching fibrils are obviously the backbone of the network and critical for assuring its integrity. We succeeded in visualising the interconnected patches, both as a 2D stretched network and as a 3D collapsed network. The self-repeating pattern in 2D network is obvious (Figure 3.57.B). The spatial arrangement is also discerned as upper and lower layers of 3D network are remarkably well resolved (Figure 3.57.C). The collected AFM data, as those presented in Figure 3.56, were analysed in terms of fibril heights and pore openings using automatic pore detection image software. The results are presented in Table 3.3. The pore surface area was converted in pore diameter assuming the pores are circular in shape. The size of the pores may be overestimated due to a stretching of the network upon the deposition on the mica. Higher values reflect the association of two or more monomolecular fibrils.

Table 3.3. *Bacteriastrum jadranum* cell jacket network: pore openings diameter and corresponding fibril heights analysed over a surface area of 4x4 mm^2.

Pore forming fibrils height (nm)	Pore openings diameter (nm)	Number of pores
0.6 - 1.6	8 - 100	900
2.0 - 2.8	100 – 160	200
2.5 – 4.0	500 -1000	10

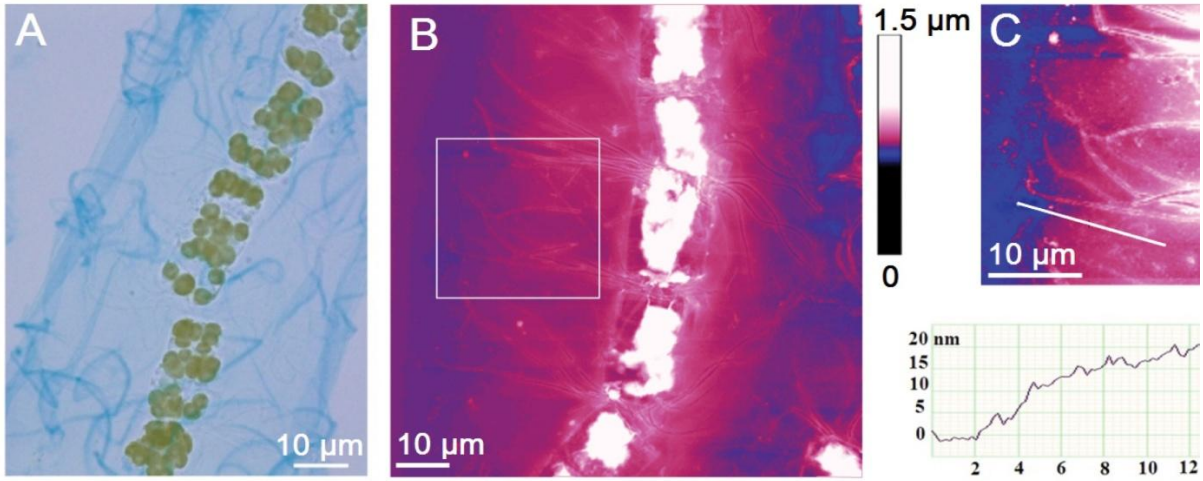

Figure 3.54. *Bacteriastrum jadranum* from cultured strain PMFBA1. **A)** LM micrograph of a Alcian Blue stained colony. **B)** AFM image of similar chain as in **A)** presented as height data with vertical scale of 1.5 µm, **C)** zoomed view (white box in **B)**) of cell jacket after maximizing the contrast and with height analyses along indicating line (height data, vertical scale 200 nm). Images are acquired in contact mode using mica as a substrate. Scan sizes of AFM images are 85 x 85 µm **B)** and 30.5 x 30.5 µm **C)**.

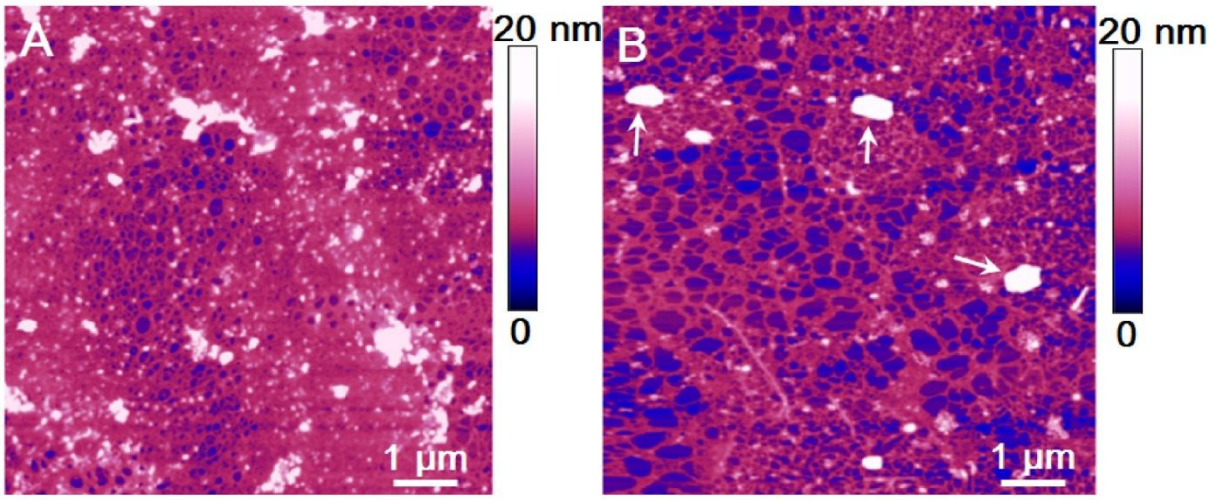

Figure 3.55. AFM images of the cell jacket with high and low density regions. **A)** collapsed 3D network and **B)** stretched 2D network. The arrows indicate salt crystallites. Scan size 8 x 8 µm with vertical scale of 20 nm.

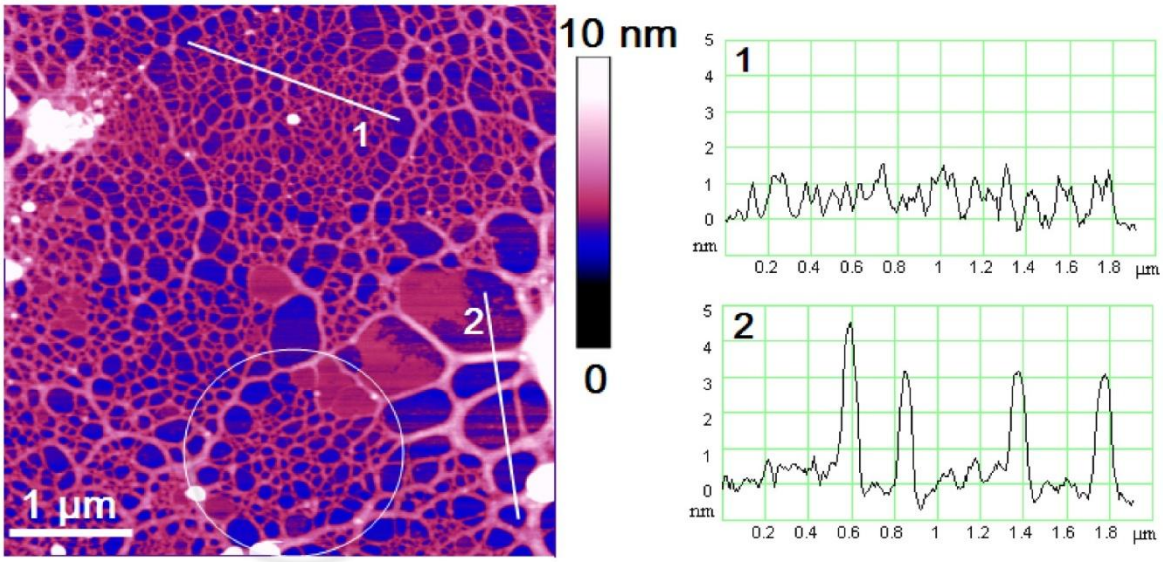

Figure 3.56. Specific patterns of the cell jacket revealed by high resolution AFM imaging. A high density domain (patch) is encircled in white. Scan size 4.5 x 4.5 µm with vertical scale of 10 nm. The vertical profiles present the fibrils heights along indicated lines. The white coloured regions (up to 20 nm high) could represent inorganic or organic nanoparticles entrapped from the surrounding media.

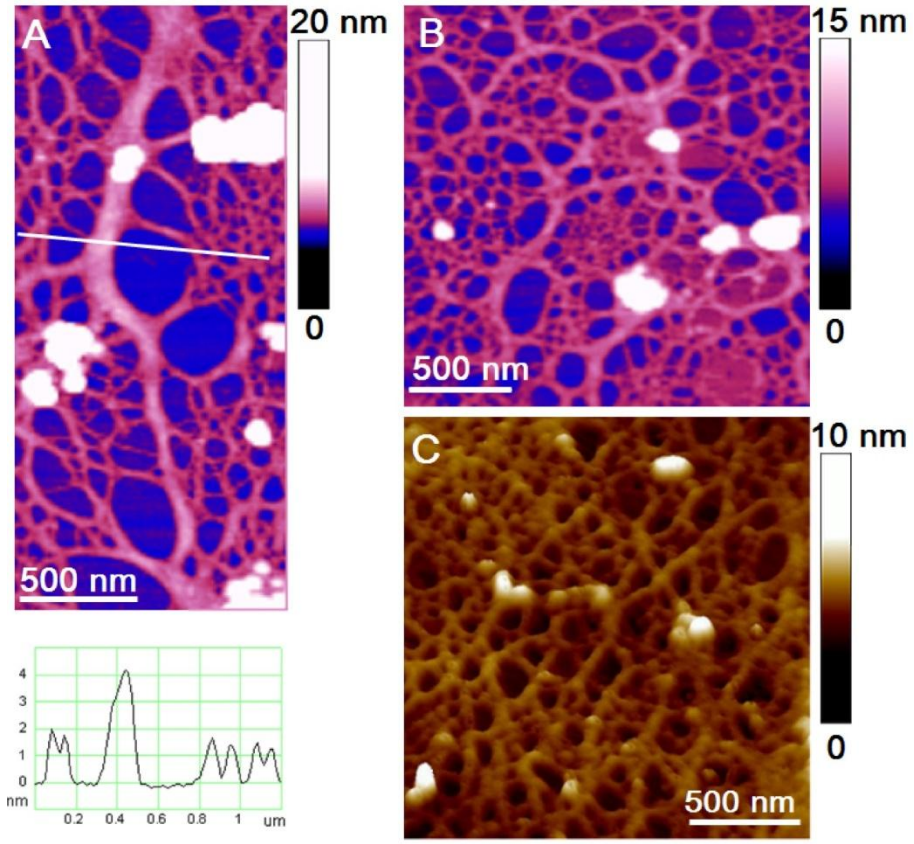

Figure 3.57. Structural details of the cell jacket network: **A)** branching fibril with height analysis along indicating line; **B)** 2D network of interconnect patches; **C)** spatial arrangement of interconnect patches in the 3D collapsed network (3D view).

3.1.3.6 Bacteriastrum mediterraneum Pavillard (1916) emend. Bosak

Section *Sagittata*
Figure 3.58. and 3.59.
Bibliography: Ikari (1927), Hustedt (1930)
Species description: Holotype by Pavillard (1916) p. 29, pl. 2: fig. 1 a-b.; Type locality: Gulf of Lyon, France
Epitype: Adriatic Sea, Croatia (fixed material and permanent slide labelled as PMFBA3 are deposited in Division of Biology, Faculty of Science, University of Zagreb, Croatia; the LSU gene sequence is registered under accession number KC914888 with GenBank)

Emended diagnosis Cells united in straight and long chains with more than 10 cells per chain. The cylindrical cells circular in valve view with apical axis ranging between 12-39 µm and rectangular in girdle view with pervalvar axis between 9-39 µm. 11 -34 chloroplasts per cell. The valve corners are sharp and valve face is flat or slightly convex. The valve mantle is rather low and the suture is not distinct. 13-22 setae originate within the valve margin, fuse at the chain margin and after a certain distance bifurcate diverging in the valvar plane. The aperture is very narrow. The shape and direction of the setae of terminal valves dissimilar. Anterior setae widely curved in the valvar plane and in girdle view at first curved posteriorly then afterwards recurving toward the front. Posterior setae straight in the valve view and in the girdle view strongly curved apart from the chain and then continuing parallel to the chain axis. The valve face ornamented with numerous fine ribs (6-8 in 1 µm) dichotomously branching out from the central annulus. The interrib space, the mantle and the proximal part of the setae irregularly perforated by round 0.05-0.1 µm wide pores. In terminal valves central process is present in shape of the simple slit from the inner and slit with the thickened edges from the outer side. In some valves there are shoehorn-shaped outgrowths between the setae. The girdle is composed of open intercalary bands, with straight margins and pointed ends and of connecting band with one straight and other undulating margin. Bands are ornamented with 6-8 per 1 µm transverse ribs, and between small pores. The setae are circular in the cross-section and composed of the silicate strings arranged in a helicoidal pattern interconnected with parallel silica bars, perforated with irregularly distributed elogated 0.05-0.1 µm long pores and ornamented with 0.1-0.2 µm long spines arranged in a spiral pattern around the setae.

Morphological description:

Morphometric values are reported in the Table 3.2.

LM: In natural samples, species occurred in long, straight and rigid chains composed of 10-16 cells. In culture conditions (Figure 3.58.A) the maximum recorded chain length was 29 cells; however, single cells were also commonly observed as having the two types of terminal valves (not shown). The cells are circular in valve view with slightly smaller apical axis observed in cultures (12-15 µm) than in specimens from the natural samples (13-39 µm). Each cell contains 11 -34 small chloroplasts (Figure 3.58.A insert). In girdle view cells are rectangular with sharp valve corners. Valve face is flat or slightly convex. The valve mantle is rather low and the suture is not distinct. The setae originate

slightly inside the valve margin and have a relatively short basal part (Table 3.2.) thus the apertures are very narrow (Figure 3.58.A-C). The basal part was found to be longer in natural samples than in culture. The sibling setae fuse at the chain margin and after a certain distance bifurcate with the furcated parts of the setae diverging in the valvar plane (Figure 3.58.A-C, E) and slightly curved towards the more proximal end of the chain in the girdle view (Figure 3.58.C). The terminal setae of the anterior valve and those of the posterior valve have a different orientation and shape and this feature results in the formation of heteropolar colonies (Figure 3.58.A). The anterior setae form a wide and regular curve when seen from the valve view (Figure 3.58.D) and in girdle view are at first curved posteriorly then afterwards recurving toward the front (Figure 3.58.B). The posterior setae appear completely straight in the valve view (Figure 3.58.F). In the girdle view they are strongly curved apart from the chain and then run parallel to the chain axis forming a characteristic bell-shape (Figure 3.58.C). In cultures, there was often a sheath of mucus (EPS) surrounding the chain with tips of setae protruding from it, visible even without the Alcian Blue staining (not shown). Resting spores were not observed in the cultures neither in the field material.

EM: The valve is ornamented with numerous fine ribs (6-8 in 1 μm) dichotomously branching out from the central annulus (Figure 3.59.A). The annulus is round to oval shaped with diameter of 0.9-2.3 μm and its size varies but not proportionally to valve diameter (10-20 %) which size varies between 9 and 11 μm measured in EM. The whole surface of the valve, with the exception of the hyaline central annulus, is perforated with numerous small round pores scattered between the ribs (Figure 3.59.C). The anterior and posterior valves share the same ultrastructural characteristics, being different only in shape and direction of the setae. Both terminal valves possess a process situated in the annulus centre (Figure 3.59.E). On both sides of the valve, outer and inner, the process appears as a slit-shaped opening, with the single difference that from the outer side the slit is surrounded by a slightly thickened edge and it is flat on the valve interior. (Figure 3.59.G). Some intercalary valves are adorned with shoehorn-shaped outgrowths of a variable length (0.5-0.8 μm), arising from the valve margin between two setae (Figure 3.59.A). These are narrower at the base with the wider end part. In some terminal valves small round outgrowths are found growing from the outer part of the valve margin (Figure 3.59.D). The girdle is composed of intercalary and connecting bands (Figure 3.59.H). The intercalary bands are open and narrow (Table 2.) with pointed ends, ornamented with transverse parallel ribs, 6-8 in 1 μm, with small round pores distributed between them. The connecting band has the same type of ornamentation as the intercalary ones with one straight and one undulating margin (Figure 3.59.I). The setae are circular in the cross-section (Figure 3.59.B) and composed of the silicate strings arranged in a helicoidal pattern interconnected with parallel silica bars (Figure 3.59.K). The proximal part of the setae is smooth and perforated with irregularly distributed small 0.05-0.1 μm long pores which are the same as on the valve face (Figure 3.59.B). These pores can be found further on the setae (Figure 3.59.K) together with 0.1-0.2 μm long spines arranged in a spiral pattern around the setae, commonly 6 of spines in one turn, 0.8 – 1.6 μm apart (Figure 3.59.J).

Comments: *B. elegans* Pavillard *and B. comosum* Pavillard are also heteropolar species which are previously recorded in the Adriatic. *B. comosum* has apparently low number of posterior setae, and differently curved anterior setae, but as in *B. mediterraneum*, the setae are directed towards the posterior end of the chain, although more strongly. *B. elegans* intercalary setae extend straight in the valvar plane, but the terminal setae are very strongly silicified. The anterior setae characteristically curve in the valvar plane, first extending straight and with the last third of the seta diverging in almost right corner. Posterior setae are bell-curved same as in *B. mediterraneum*, and can be mistaken if they are not strongly silicified.

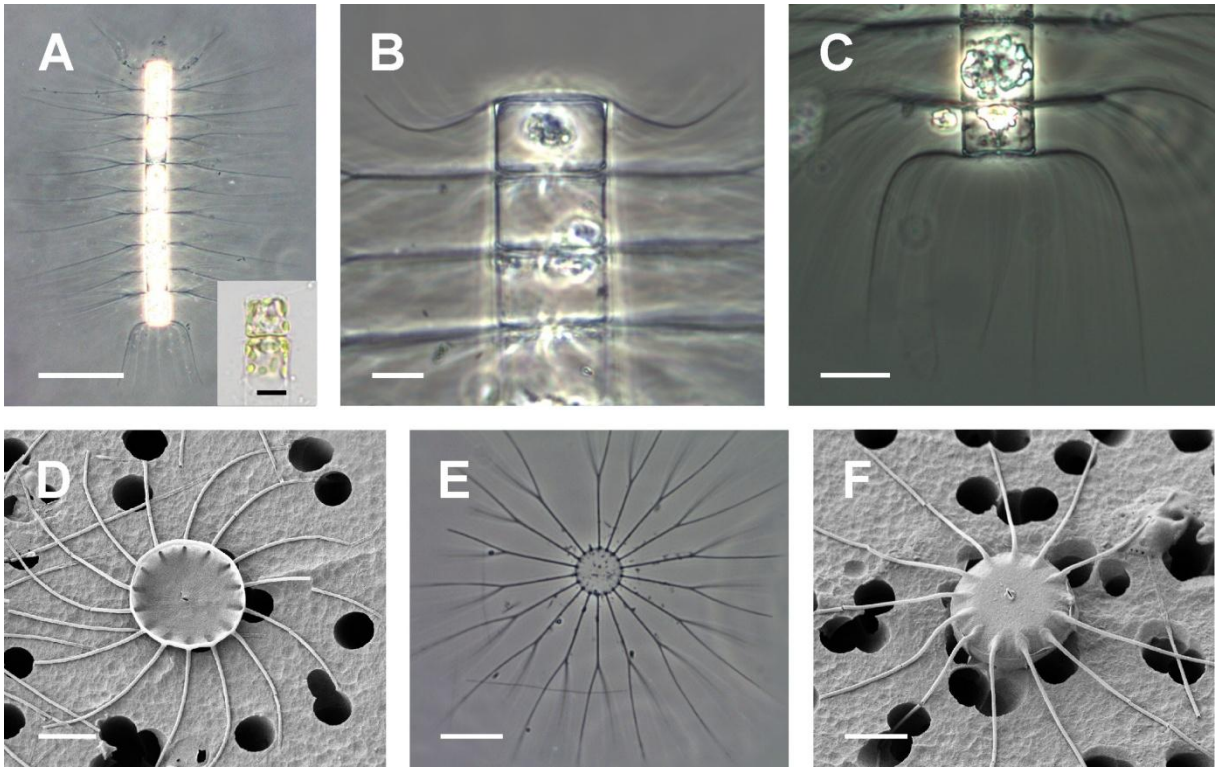

Figure 3.58. LM **(A-C,E)** and SEM **(D,F)** micrographs of *Bacteriastrum mediterraneum* from field samples **(B,C,E)** and cultured strain PMFBA4 **(A,D-F)**. **A)** Complete heteropolar chain with different shape and orientation of the terminal setae. Insert shows two cells with numerous small chloroplasts. **B)** Anterior part of the chain in girdle view showing the setae orientation. **C)** Posterior part of the chain in girdle view showing the setae orientation. **D)** Anterior terminal valve in valve view showing widely curved setae in the valvar plane. **E)** Intercalary valve in valve view showing fused and bifurcated sibling setae. **F)** Posterior terminal valve with setae extending straight in valvar plane. Scale bars: A=50 µm; B=10 µm; C,E=20 µm;D,F=5 µm.

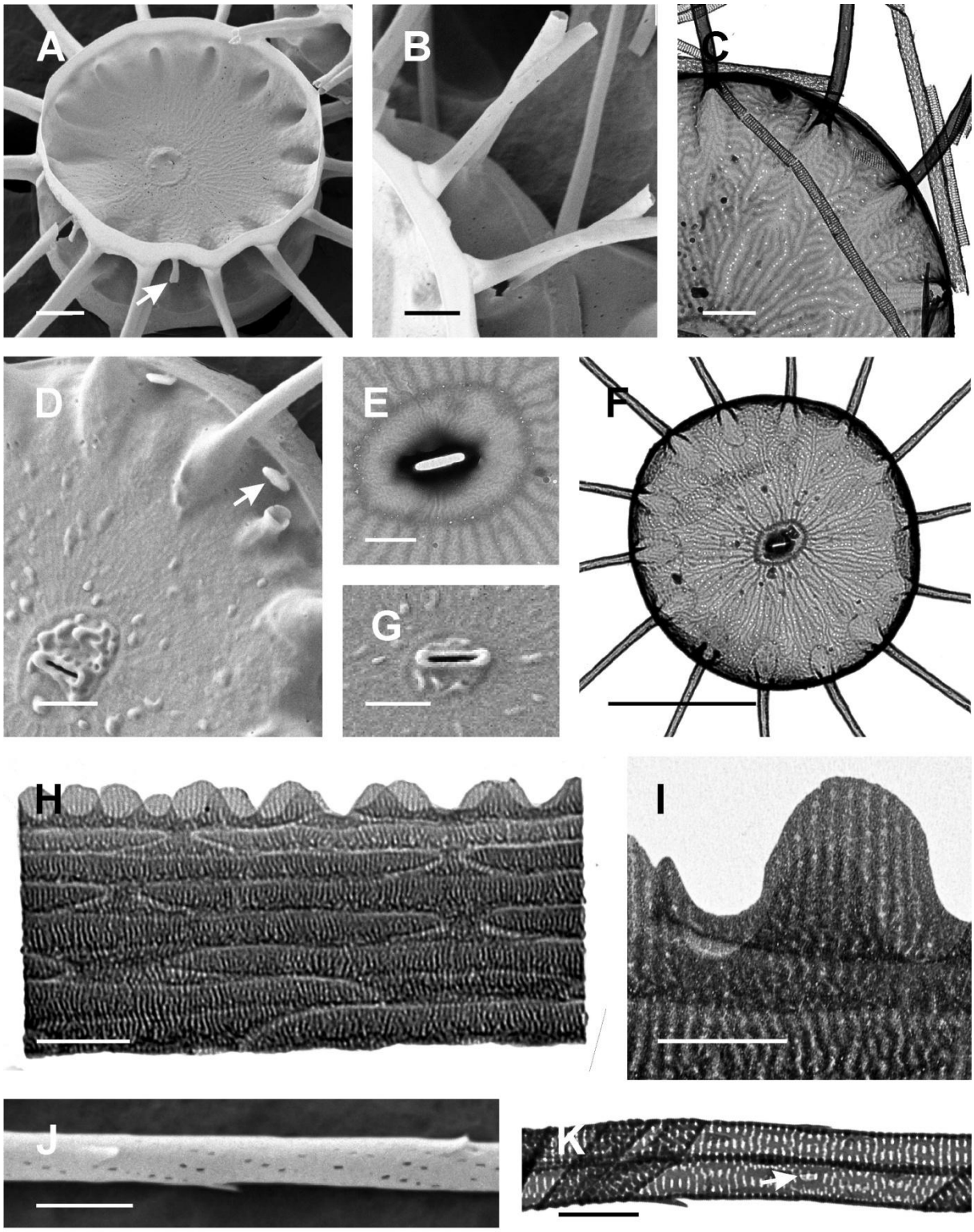

Figure 3.59. SEM **(A,B,D,G,J)** and TEM **(C,E,F,H,I,K)** micrographs of *Bacteriastrum mediterraneum* from cultured strain PMFBA3. **A)** Sibling intercalary valves with a shoehorn-shaped outgrowth projecting from a valve margin (arrow). **B)** Sibling valves in girdle view showing setae fusion and surface of the valve and setae proximal part perforated by small pores. **C)** Fine structure of the terminal valve, note the small pores scattered in the interrib space. **D)** Detail of the terminal valve from an outside view with small outgrowths (arrow). **E)** Detail of the valve showing the internal slit-shaped process. **F)** Fine structure of the posterior terminal valve with central slit-shaped process. **G)** Detail of the valve showing the external slit-shaped process. **H)** Girdle with intercalary and connecting bands. **I)** Detail of the connecting and intercalary girdle bands. **J)** Detail of a seta. **K)** Detail of the setae with elongated pore (arrow). Scale bars: A-D,G,I=1 µm; H=2 µm; E,J,K= 0.5 µm.

3.1.3.7 Bacteriastrum paralellum Sarno, Zingone & Marino (1997)

Section *Sagittata*
Figure 3.60.
Bibliography: Sarno et al. (1997)
Description: a.a.: 6-10 µm (Sarno et al.: 3-10 µm); p.a.: 10-16 µm (Sarno et al.: 4 - 16 µm)

LM: Weakly silicified solitary cells. The cells rectangular in girdle view, circular in valve view. Valve face concave,mantle quite high, suture not distinct. Cells heterovalvate, differing in the shape and orientation of the setae on each valve. Setae of the anterior valve bent sharply towards, and of the posterior setae outwards from the cell, both setae being parallel with each other and forming an acute angle with the pervalvar axis (Figure 3.60.A). In valve view, setae appear straight (Figure 3.60.B).

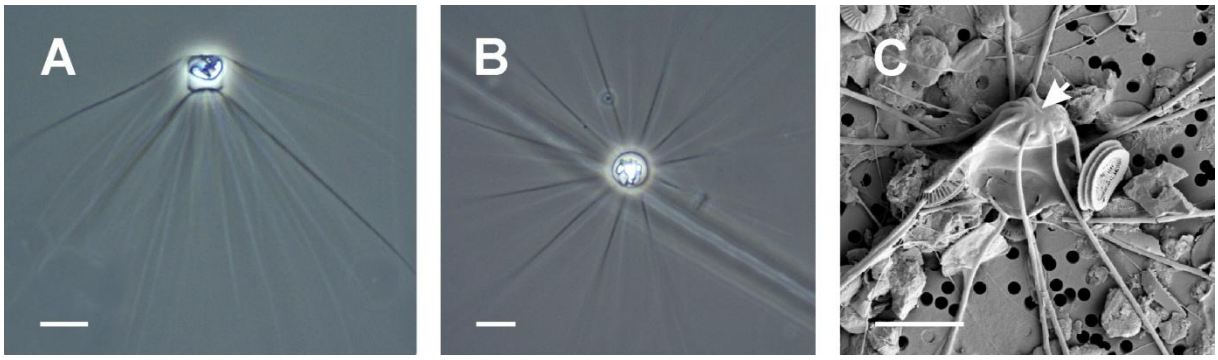

Figure 3.60. LM **(A,B)** and SEM **(C)** micrographs of *Bacteriastrum paralellum* from field samples. **A)** Cell in the girdle view showing the orientation of the setae. **B)** Cell in the valve view. **C)** Cell in the girdle view with the central process (arrow). Scale bars: A-B=10 µm; C=5 µm.

3.2 Phylogenetic analysis

The ML tree illustrating the phylogenetic relationships among the *Bacteriastrum furcatum, B. hyalinum, B. jadranum* and *B. mediterraneum* along with the other species of the *Chaetoceros* genera and outgroups is shown in Figure 3.61. The sequence of the strain *C. affinis* from the Adriatic Sea obtained within this study differed markedly from that of the strain of *C. affinis* from the Gulf of Naples. All the species of *Bacteriastrum* were recovered in a sister clade to the clade with *C. affinis*, *C. lorenzianus* and *C. diadema*. The *Bacteriastrum* clade formed two subclades, first with *B. mediterraneum* and *B. jadranum* and the second clade included *B. hyalinum* and *B. furcatum*. The species *B. jadranum* form a well-supported single branch outside of which *B. mediterraneum* forms a separate branch. *Bacteriastrum hyalinum* and *B. furcatum* stay as a single branch in which *B. furcatum* form a slightly longer branch to that of *B. hyalinum.*

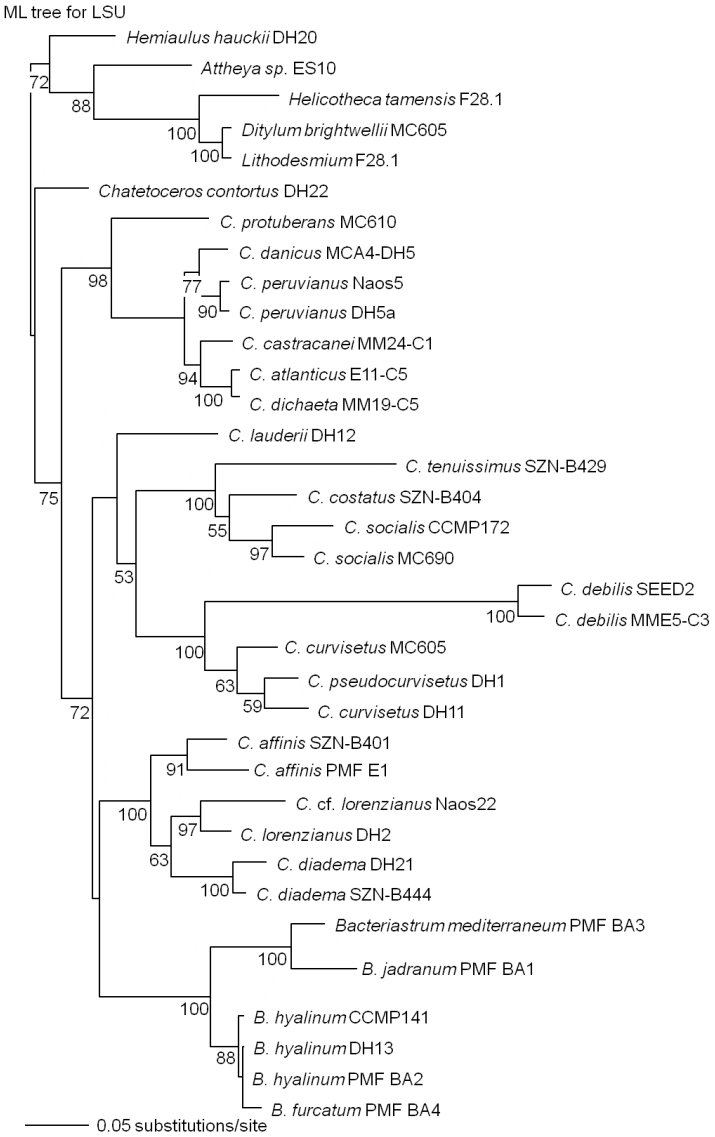

Figure 3.61. ML phylogenetic tree inferred from LSU rDNA sequences

3.3 Checklists of diatom species from family *Chaetocerotaceae* from eastern Adriatic Sea

Table 3.4. gives the list of planktonic diatom species belonging to the genera *Bacteriastrum* and *Chaetoceros* identified along the eastern coast of the Adriatic Sea. The list counts 42 *Chaetoceros* and 6 *Bacteriastrum* species, altogether 49 Chaetocerotacean taxa.

Table 3.4. Checklist of Chaetocerotacean species found along the eastern coast of the Adriatic Sea. NA – Northern Adriatic; CA-Central Adriatic; SA-Southern Adriatic.

Species	NA	CA	SA
Bacteriastrum biconicum Pavillard	+	+	
B. furcatum Shadbolt	+	+	+
B. hyalinum Lauder	+	+	+
B. jadranum	+	+	
B. mediterraneum Pavillard	+	+	+
B. paralellum Sarno, Zingone & Marino			+
Chaetoceros affinis Lauder	+	+	+
C. anastomosans Grunow	+	+	+
C. bacteriastroides Karsten		+	
C. borealis Bailey	+	+	
C. brevis Schütt	+	+	+
C. circinalis (Meunier) Jensen and Moestrup			+
C. coarctatus Lauder	+	+	+
C. constrictus Gran	+	+	+
C. contortus Schütt	+	+	+
C. costatus Pavillard	+	+	+
C. curvisetus Cleve	+	+	+
C. dadayi Pavillard	+	+	+
C. danicus Cleve	+	+	+
C. decipiens Cleve	+	+	+
C. densus Cleve	+	+	+
C. didymus Ehrenberg	+		
C. diversus Cleve	+	+	+
C. eibenii (Grunow in Van Heurck) Meunier	+	+	+
C. cf. *lacinious* Schütt	+	+	+
C. lauderi Ralfs in Lauder	+	+	+
C. neocompactus VanLandigham		+	+
C. messanensis Castracane	+	+	
C. peruvianus Brightwell	+	+	+
C. protuberans Lauder	+	+	
C. pseudocurvisetus Mangin	+	+	
C. pseudodichaeta Ikari		+	
C. rostratus Lauder	+	+	+
C. salsugineus Takano		+	+

Table 3.4. continued

Species	NA	CA	SA
C. simplex Ostenfeld	+	+	+
C. socialis Lauder	+	+	+
C. subtilis Cleve		+	
C. tenuissimus Meunier	+	+	+
C. tetrastichon Cleve	+	+	+
C. throndsenii var. *throndsenia* (Marino, Montresor & Zingone) Marino, Montresor & Zingone	+	+	+
C. throndsenii var. t*risetosa* Zingone	+	+	
C. tortissimus Gran	+	+	+
C. vixvisibilis Schiller	+	+	+
C. cf. *wighamii* Brightwell	+	+	+
Chaetoceros sp. "A"	+		
Chaetoceros sp. "B″	+	+	+
Chaetoceros sp. "C"			+
Chaetoceros sp. "D"	+		

Table 3.5. shows the distribution of chateocerotacean species found at each investigated station, at 8 locations along the eastern Adriatic coast.

Northern Adriatic

The study in Lim Bay in the period from 2006 to 2011 counts 5 *Bacteriastrum* and 26 *Chaetoceros* species, in total 31 species from the family Chaetocerotaceae. The number of species identified at the north-eastern coastal station RV001 during one year (2008/2009) was slightly higher and counts 36 taxa from the family Chaetocerotaceae; 32 *Chaetoceros* and 4 *Bacteriastrum* species. Checklist of species for Pag and Velebit Channel includes 28 *Chaetoceros* and 5 *Bacteriastrum* taxa, altogether 33 Chaetocerotacean species.

Central Adriatic

In Telašćica Bay during 2011-2012 5 *Bacteriastrum* and 26 *Chaetoceros* species were identified, 30 species from the family Chaetocerotaceae. Checklist of species for Krka Estuary in 2010-2011 lists 4 species of *Bacteriastrum* and 37 species of *Chaetoceros*, altogether 41 Chaetocerotacean species, the highest number found from all the investigated locations

Southern Adriatic

Checklist of species for island of Mljet in 2010-2011 counts 3 species of *Bacteriastrum* and 23 species of *Chaetoceros*, altogether 26 Chaetocerotacean species and list of species for Boka Kotorska Bay includes 21 *Chaetoceros* and 2 *Bacteriastrum* taxa, altogether 21 Chaetocerotacean species. In Albanian coastal zone 5 species of *Bacteriastrum* and 24 species of *Chaetoceros* was found, in total 29 taxa from the family Chaetocerotaceae.

Table 3.5. Checklist of *Chaetoceros* and *Bacteriastrum* species identified at 8 locations in the Adriatic Sea in the period 2006-2011. The position of stations is indicated in Table 2.2. North Adriatic: LM- Lim Bay (stations LIM1-LIM3); RV- coastal area in front of the city of Rovinj; PV- Pag and Velebit Channel system including Novigrad Sea (P1-P3,V1-V4, N1); Central Adriatic: TL- Telašćica Bay (T0-T3); KR- Krka River estuary(C1,E5,E4a,E3); South Adriatic: MT- island of Mljet (G); BK- Boka Kotorska Bay(BK1-BK3); AL- Albanian coastal zone(A50-A1000).

Location	LM			RV	PV								TL				KR					MT	BK			AL					
Species /Station	LIM 1	LIM2	LIM3	RV 001	P3	P2	P1	V4	V3	V2	V1	N1	T0	T1	T2	T3	C1	E5	M	E4a	E3	G	BK1	BK2	BK3	A 50	A150	A200	A300	A 900	A 1000
Bacteriastrum biconicum Pavillard	+				+	+			+	+				+																	
B. furcatum Shadbolt	+	+	+	+	+	+	+	+	+	+	+	+	+	+	+	+	+	+	+	+	+	+	+		+	+		+	+	+	+
B. hyalinum Lauder	+	+	+	+		+				+	+	+		+			+	+	+	+	+		+	+	+	+					
B. jadranum	+	+	+	+	+	+	+	+	+	+	+	+		+	+	+				+	+										
B. mediterraneum Pavillard	+	+	+	+	+	+	+	+	+	+	+	+		+	+	+	+	+	+	+	+	+				+	+	+			+
B. paralellum Sarno, Zingone & Marino																						+				+					
Chaetoceros affinis Lauder	+	+	+	+	+	+	+	+	+	+	+	+	+	+	+	+	+	+	+	+	+	+	+	+	+	+	+	+	+		
C. anastomosans Grunow	+	+	+	+	+	+	+	+	+	+			+	+	+	+	+	+	+	+	+	+									
C. bacteriastroides Karsten													+				+														
*C. borealis*Bailey				+					+			+								+											
C. brevis Schütt	+	+	+	+	+		+				+		+	+				+	+							+	+	+		+	+
C. circinalis (Meunier) Jensen and Moestrup																						+				+	+	+	+	+	+
C. coarctatus Lauder	+			+	+	+	+	+	+	+				+					+	+		+	+								
C. constrictus Gran	+	+	+	+	+	+	+	+					+	+	+		+	+				+				+		+	+	+	+
C. contortus Schütt	+	+	+	+	+	+	+	+	+	+	+	+	+	+	+	+	+	+	+	+	+	+	+	+	+	+		+		+	+
C. costatus Pavillard	+	+		+									+	+	+	+	+	+		+	+			+		+					
C. curvisetus Cleve	+	+	+	+	+	+	+	+	+	+	+	+	+	+	+	+	+	+	+	+	+	+	+	+	+	+	+	+	+	+	+
C. dadayi Pavillard	+	+	+	+				+	+	+	+	+		+			+		+	+	+	+			+						+

Table 3.5. continued

Location	LM			RV	PV								TL				KR					MT	BK			AL					
Species /Station	LIM 1	LIM2	LIM3	RV 001	P3	P2	P1	V4	V3	V2	V1	N1	T0	T1	T2	T3	C1	E5	M	E4a	E3	G	BK1	BK2	BK3	A 50	A150	A200	A300	A 900	A 1000
C. danicus Cleve	+	+	+	+	+	+	+		+	+	+	+		+		+	+	+	+	+	+	+	+	+	+	+	+	+	+		
C. decipiens Cleve	+	+	+	+	+	+	+	+	+	+	+	+	+	+	+	+	+	+	+	+	+	+	+	+	+	+	+	+	+	+	+
C. densus Cleve	+	+	+	+													+	+		+	+		+	+	+	+					
C. didymus Ehrenberg	+	+	+	+	+	+	+					+	+	+	+																
C. diversus Cleve	+	+	+	+		+	+	+	+	+	+	+	+	+		+	+	+	+	+	+	+	+	+	+	+	+	+	+	+	+
C. eibenii (Grunow in Van Heurck) Meunier	+	+		+													+			+	+		+	+	+						
C. cf. *lacinious* Schütt					+					+	+	+	+	+								+			+	+			+	
C. lauderi Ralfs in Lauder	+	+	+	+	+	+		+	+	+	+		+	+	+		+	+	+	+		+				+	+				+
C. neocompactus VanLandigham													+	+								+									
C. messanensis Castracane						+											+														
C. peruvianus Brightwell	+	+	+	+	+	+	+	+	+		+	+	+	+			+	+	+	+	+	+	+	+	+	+	+	+	+	+	+
C. protuberans Lauder					+	+	+	+		+							+				+										
C. pseudocurvisetus Mangin				+													+	+		+											
C. pseudodichaeta Ikari													+	+			+	+	+	+	+										
C. rostratus Lauder	+	+	+	+	+	+	+	+	+		+	+	+	+		+	+	+	+	+	+	+	+			+		+			
C. salsugineus Takano													+	+	+	+		+	+	+	+	+			+						
C. simplex Ostenfeld	+	+	+	+	+	+	+	+	+	+	+	+					+	+	+	+	+	+	+	+	+	+	+	+	+	+	+
C. socialis Lauder	+	+	+	+	+	+	+	+	+	+	+	+	+	+		+	+	+	+	+			+								
C. subtilis Cleve																	+	+		+	+										
C. tenuissimus Meunier	+	+	+	+					+								+	+	+	+	+		+	+	+				+		
C. tetrastichon Cleve	+			+				+	+	+	+	+	+	+			+	+				+				+				+	

Table 3.5. continued

Location	LM			RV	PV								TL					KR				MT	BK			AL					
Species /Station	LIM 1	LIM2	LIM3	RV 001	P3	P2	P1	V4	V3	V2	V1	N1	T0	T1	T2	T3	C1	E5	M	E4a	E3	G	BK1	BK2	BK3	A 50	A150	A200	A300	A 900	A 1000
C. throndsenii var. *throndsenia* (Marino, Montresor, & Zingone) Marino, Montresor & Zingone	+	+	+	+	+	+	+	+	+							+	+	+	+	+	+		+	+	+	+	+	+	+		
C. throndsenii var. t*risetosa* Zingone				+														+	+	+	+										
C. tortissimus Gran	+	+	+	+	+	+		+	+	+	+	+	+	+			+		+	+	+	+				+				+	+
C. vixvisibilis Schiller	+	+	+	+	+	+	+	+	+	+	+	+	+	+	+	+	+		+			+								+	
C. cf. *wighamii* Brightwell	+	+	+	+	+								+	+	+	+	+	+	+	+	+	+	+	+								
Chaetoceros sp. "A"				+														+	+	+	+										
Chaetoceros sp. "B″				+	+	+	+	+	+	+	+	+	+	+	+	+		+	+	+	+	+	+	+	+	+	+	+	+	+	+
Chaetoceros sp. "C"																														+	+
Chaetoceros sp. "D"				+														+		+											

3.4 Species succession and ecological relationships

3.4.1 Seasonal dynamics and succession of *Chaetoceros* and *Bacteriastrum* species in the northeastern Adriatic coastal zone (station RV001)

3.4.1.1 Environmental characterization of the station RV001

Over the study period, temperatures varied between 9.28 and 27.48°C in surface waters and between 9.56 and 18.02 °C in the bottom layer, at 30 m depth (Figure 3.62.A). The water column was homotherm down to the bottom from the beginning of October until April, while thermal stratification due to the heating of the sea surface started to develop in May and disrupted by the October 2009 (Figure 3.62.A). Salinity was found to be significantly negatively correlated with temperature (Table 3.6.) and decreased in the upper layer of the water column in late spring/summer period with the minimum values measured in June at the surface (Figure 3.62.B).

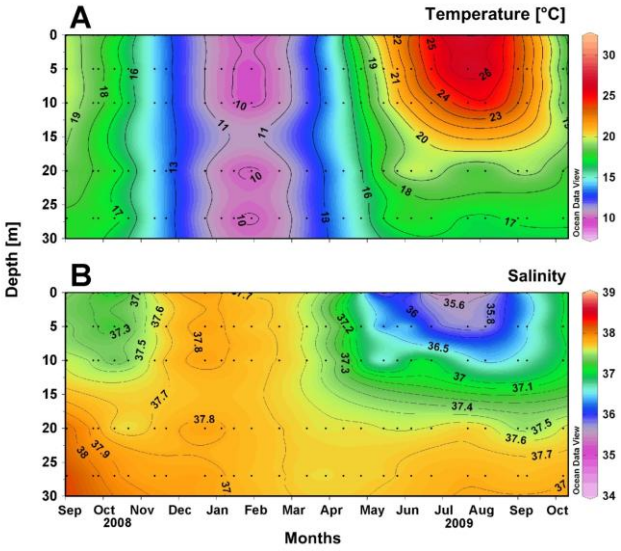

Figure 3.62. Temporal distribution of temperature **(A)** and salinity **(B)** at station RV001 from September 2008 to October 2009.

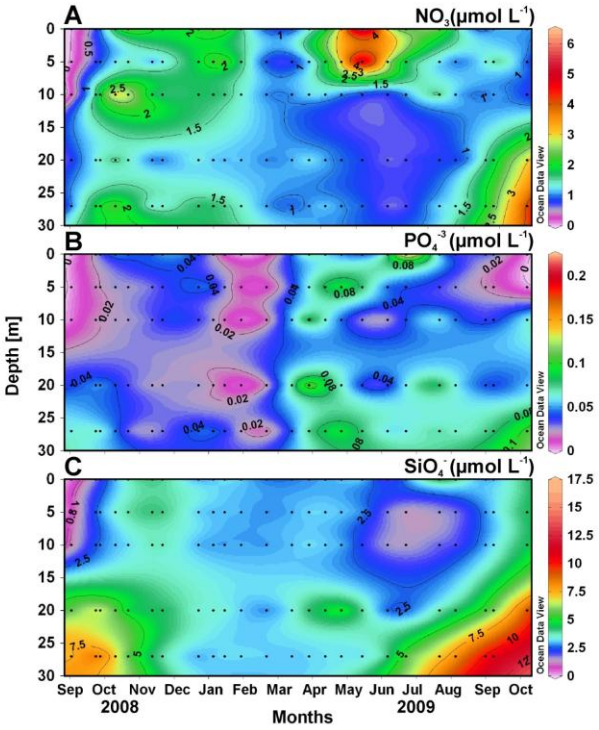

Figure 3.63. Temporal distribution of nitrate **(A)** phosphate **(B)** and silicate **(C)** at station RV001 from September 2008 to October.

Nutrient stocks markedly varied during the year (Figure 3.63., Table 3.6.). Nitrate concentration was highest in the upper layer of the water column in May, and lowest in August at the surface and it was found to be significantly negatively correlated with salinity. The phosphate concentrations were generally very low, particularly in February and March when their concentrations were below detection limit (< 0.01 µmol L^{-1}) throughout the entire water column. Silicate concentrations were generally higher in the bottom layer reaching their maximum in October 2009 and with minimum in September 2008 in the upper layer of the water column (Table 3.6.). Generally, concentrations of all nutrients were found to be significantly positively correlated with each other (Table 3.7.).

Table 3.6. Physical and chemical parameters during the study period (September 2008-October 2009) at RV001 sampling station. recorded at the surface (S) and integrated over the whole water column (Int. 0-30 m). min – minimum; max – maximum; st.dev.- standard deviation; N- number of samples, Lower Qu. – lower quartile, Upper Qu.- upper quartile; NO_3^- - nitrate; NO_2^- - nitrite; NH_4^+ - ammonium; PO_4^{-3} – phosphate; SiO_4^- - silicate.

	Temperature (°C)		Salinity		NO_3^- (µmol L^{-1})		NO_2^- (µmol L^{-1})		NH_4^+ (µmol L^{-1})		PO_4^{3-} (µmol L^{-1})		SiO_4^{4-} (µmol L^{-1})	
	S	Int. (0-30 m)	S	Int. (0-30 m)	S	Int. (0-30 m)	S	Int. (0-30 m)	S	Int. (0-30 m)	S	Int. (0-30 m)	S	Int. (0-30 m)
Min.	9.28	9.26	34.22	34.22	0.07	0.03	0.01	0.01	0.12	0.12	<0.01	<0.01	0.47	0.38
Lower Qu.	13.36	13.36	36.52	37.32	0.98	0.69	0.07	0.05	0.32	0.36	0.01	0.01	2.50	2.48
Median	18.09	17.17	37.33	37.61	1.55	1.28	0.10	0.12	0.61	0.55	0.03	0.03	2.95	3.12
Mean	17.59	16.55	36.95	37.35	1.84	1.50	0.24	0.32	0.62	0.68	0.04	0.04	2.96	3.72
St.dev.	5.48	4.60	0.97	0.75	0.05	1.46	1.79	0.42	0.32	0.59	0.37	0.04	1.19	2.18
Upper Qu.	22.16	19.45	37.60	37.76	0.04	1.80	2.14	0.43	0.26	0.80	0.81	0.05	3.98	4.22
Max.	27.48	27.48	37.89	38.18	9.12	10.34	1.16	2.07	1.35	5.1	0.24	0.26	4.99	11.75
N	25	125	25	125	24	120	24	120	24	120	24	120	24	120

Table 3.7. Correlation matrix for physical and chemical parameters. (N=120) Marked Spearman correlation coefficients are significant at p<0.05.

	Temperature	Salinity	PO_4^{3-}	NO_3^-	NO_2^-	NH_4^+	SiO_4^{4-}
Temperature	1.0000	**-0.6664**	0.1105	0.0632	**-0.2399**	0.0947	-0.0370
Salinity		1.0000	-0.0998	**-0.3880**	**0.3405**	-0.0138	**0.2524**
PO_4^{3-}			1.0000	0.2059	-0.0084	**0.4098**	**0.3307**
NO_3^-				1.0000	0.0364	**0.2078**	**0.2455**
NO_2^-					1.0000	0.0130	**0.4639**
NH_4^+						1.0000	**0.4356**
SiO_4^{4-}							1.0000

The Principal Component Analysis (PCA) ordination of the samples based on their physical and chemical characteristics is shown in Figure 3.64. The percentages of variance explained and the correlations between the first two components (PCA 1 and PCA 2) of the input variables are expressed in Table 3.8. The first PCA component is mostly positively correlated with silicate and nitrate so that the different sampling dates characterised by different concentrations of these nutrients are separated along the first component. The second component is mostly negatively correlated with temperature with summer/autumn sampling dates distributed in the lower two quadrants of the plot.

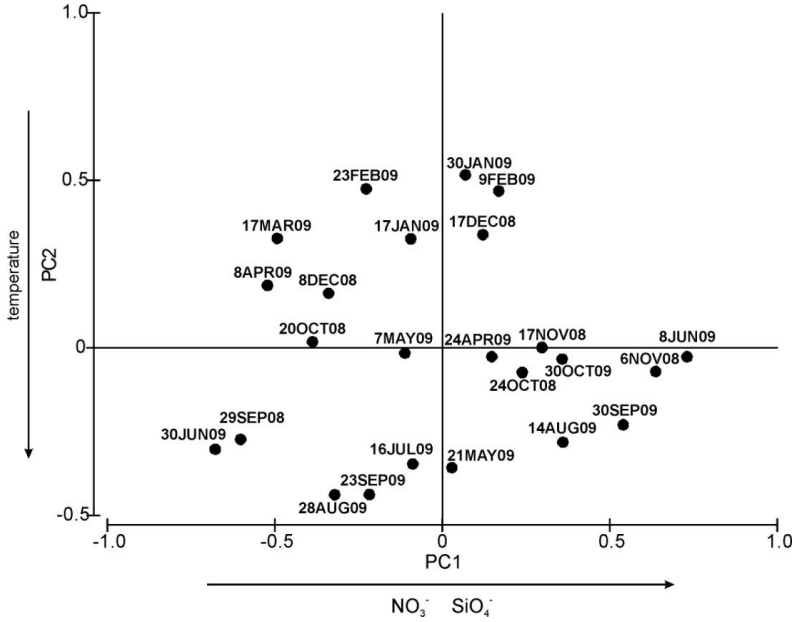

Figure 3.64. Principal Component Analysis (PCA) of the physical-chemical parameters of the study area. The data represent averaged values on the water column per each sampling date.

Table 3.8. Relative variance explained and factor coordinates of the variables of the first two components (PC 1 and PC 2) of the Principal Component Analysis. The factors ≥ 0.40 were considered to be mostly significantly correlated with the PCA axis and shown in bold.

	PC 1	**PC 2**
Variance explained	42.1%	24.3%
Temperature (°C)	0.13	**-0.82**
Salinity	-0.02	0.03
NO_3^- (µmol L^{-1})	**0.85**	0.28
NO_2^- (µmol L^{-1})	0.05	0.37
NH_4^+ (µmol L^{-1})	0.32	-0.33
PO_4^{-3} (µmol L^{-1})	0.03	-0.04
SiO_4^- (µmol L^{-1})	**0.40**	-0.11

3.4.1.1 Phytoplankton

Total Chl *a* concentration was quite low during the investigated period, generally below 1 μg L^{-1}, with the depth-averaged values ranging between 0.2 and 0.7 μg L^{-1} (Figure 3.65.A). The most pronounced peak was observed in September and October 2008 due to the high contribution of the micro size-class (Figure 3.65.B). The similar increase in the Chl *a* biomass was not observed in the same period of 2009 but occurred after the end of this study in November (not shown) and therefore not taken into consideration within this thesis. Figure 3.65.B shows that during the rest of the investigated period, the phytoplankton was generally predominated by the pico size-class, but also with slightly higher contribution of the micro size-class again during the period from April until July.

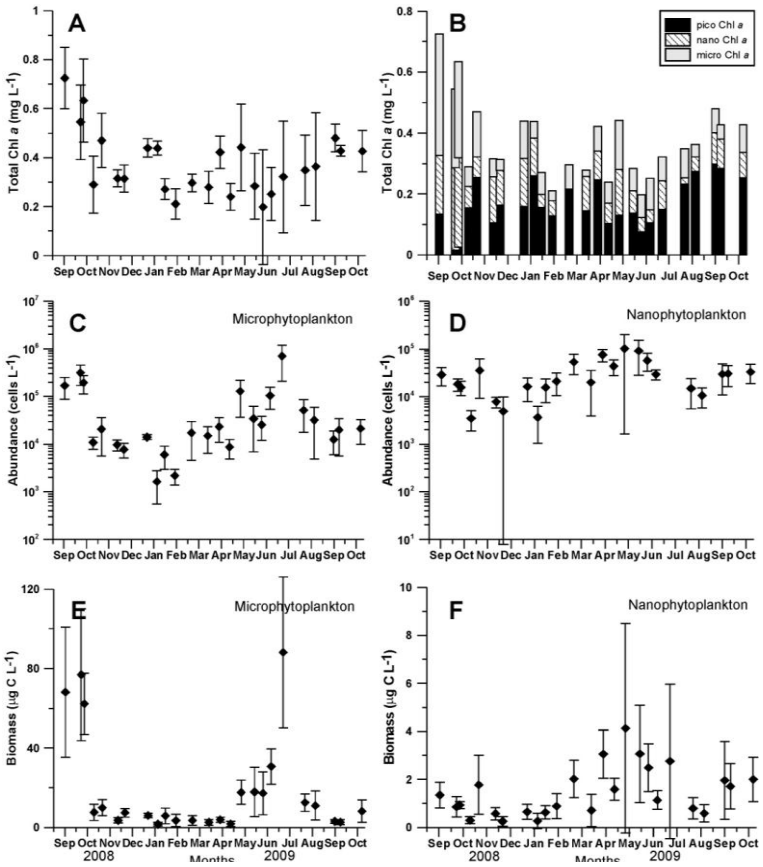

Figure 3.65. Temporal distribution of **A)** total Chl *a*, **B)** size-fractionated Chl *a*, **C)** microphytoplankton abundance, **D)** Nanophytoplankton abundance, **E)** Microphytoplankton carbon biomass, **F)** Nanophytoplankton carbon biomass at station RV001 from September 2008 to October 2009. Data are presented as averaged values with standard deviations (except in B) where only average is shown), obtained from each sampling and clustered for the whole water column. Note the log scale in **C)** and **D)**.

Both microphytoplankton abundance and carbon biomass showed the similar trend in the distribution as Chl *a* micro size-class with high values recorded in autumn 2008. The difference was observed in the high microphytoplankton abundance (>10^6) observed also in July 2009, which was not visible as the increase in Chl *a* concentration (Figure 3.65.C,E). Generally the contribution of the nano size-class according to the Chl *a* values was highest in October 2008 (Figure 3.65.B), but it did not correspond to the nanophytoplankton abundance and biomass values which both showed a slight increase during late spring/early summer months (Figure 3.65.D,F).

3.4.1.2 Diatom diversity

Throughout the study period, from end of September 2008 to the end of October 2009, 89 diatom taxa were enumerated at station RV001. Among all taxa, 67 were identified to the species level and the remaining to the genus or group level. The additional 24 species were identified from net samples which adds up to 113 diatom taxa. The list of all recognized phytoplankton taxa found in this study, diatoms included, together with their biovolume and carbon content per cell is presented in the Appendix III of this thesis.

24 diatom taxa were considered dominant in the phytoplankton assemblage (Table 3.9.). Most frequently found (>70%) were *Nitzschia longissima* and species from *Pseudo-nitzschia pseudodelicatissima* complex. Subsequent TEM analysis of the net samples revealed that the complex was comprised from two species, *P. calliantha* Lundholm, Moestrup & Hasle and *P.* cf. *pseudodelicatissima* (Hasle) Hasle, both simultaneously present in all of the examined samples. The same analysis identified the species constituting *P. seriata* group as *P. subfraudulenta* (Hasle) Hasle, *P. fraudulenta* (Cleve) Hasle and *P. pungens* var. *pungens* (Grunow) Hasle with first two species dominating the group from October to December 2008 and March to May 2009, and the last species in January/February 2009. The small centric diatoms belonging to *Cyclotella* genus were enumerated as a supra-specific group and not examined in detail, however it appears that the large proportion of the observed specimens may be affiliated to chain-forming *C. choctawhatcheeana* Prasad.

Table 3.9. Dominant diatom taxa with frequency of appearance (Freq.)>10% and maximum abundance (Max.) >10 000 cells L^{-1} enumerated in plankton samples at station RV001 between September 2008 and October 2009. Avg. – average abundance (cells L^{-1}). St. dev. – standard deviation. Number of samples =125. Chaetocerotacean species are marked in bold.

Species	Freq. (%)	Max.	Avg.	St.dev.
Asterionellopsis glacialis (Castracane) Round	16	82 080	2 671	9 802
***Bacteriastrum furcatum* Shadbolt**	**19**	**118 560**	**1 685**	**12 241**
***B. mediterraneum* Pavillard**	**12**	**50 540**	**1 541**	**6 308**
B. jadranum	**13**	**52 060**	**901**	**5 033**
Cerataulina pelagica (Cleve) Hendey	58	16 340	1 209	3 035
***Chaetoceros affinis* Lauder**	**21**	**18 240**	**638**	**2 241**
***C. brevis* Schütt**	**17**	**10 260**	**344**	**1 361**
***C. contortus* Schütt**	**34**	**175180**	**8 054**	**24 503**
***C. decipiens* Cleve**	**23**	**12 920**	**629**	**2 243**
***C. socialis* Lauder**	**22**	**28 380**	**1 508**	**4 464**
***C. throndsenii* var. *throndsenia* (Marino, Montresor & Zingone) Marino, Montresor & Zingone**	**26**	**24 140**	**1 259**	**3 669**
***C. vixvisibilis* Schiller**	**17**	**1 349 679**	**29 447**	**159 486**
Cyclotella spp.	34	127 800	3537	14 251
Cylindrotheca closterium (Ehrenberg) Reihmann et Lewin	26	11 352	694	1 902
Dactyliosolen fragilissimus (Bergon) Hasle	38	12 920	720	1 815
Guinardia striata (Stolterfoth) Hasle	40	12 540	816	2 128
Leptocylindrus danicus Cleve	56	39 520	2722	6 532

Table 3.9. continued

Species	Freq. (%)	Max.	Avg.	St.dev.
L. mediterraneus (Peragallo) Hasle	20	30 210	621	3 237
Nitzschia longissima (Brébisson) Ralfs	74	29 260	1 465	3 503
Proboscia alata (Brightwell) Sundström	54	13 680	755	1 643
Pseudo-nitzschia pseudodelicatissima (Hasle) Hasle species complex	72	126 920	12 234	26 087
Pseudo-nitzschia seriata group	40	14 060	901	2 030
Skeletonema marinoi Sarno et Zingone	28	25 460	1 417	4 139
Thalassionema nitzschioides (Grunow) Mereschkowsky	63	11 400	963	1 984

Diatoms were the most abundant group in the phytoplankton dominating in terms of both abundance and biomass in micro size-class. Diatom cell concentrations varied considerably over time, ranging between 6×10^2 cells L^{-1} in January 2009 and 1.4×10^6 cells L^{-1} in July 2009. The maximum abundance observed in the summer can be recognized as the second major peak during the study period, while the first peak occurred in autumn 2008 (Figure 3.66.A-B). Diatoms belonging to the nano size-class were the most abundant in May, reaching also the peak in their biomass in same period (Figure 3.66.C-D).

The first major diatom peak lasted through three sampling dates in September/October 2008 (Figure 3.66.A-B) and it was composed of 52 identified diatom taxa with species *Chaetoceros contortus*, *Pseudo-nitzschia pseudodelicatissima* (both *P. calliantha* and *P.* cf. *pseudodelicatissima*), *Chaetoceros vixvisibilis* and *Asterionellopsis glacialis* constituting together between 43 % and 69 % of the total diatom population in terms of abundance. *C. contortus* was the most abundant with the contribution of up to 50 % in the individual sample, followed by *P. pseudodelicatissima* with 47%, *C. vixvisibilis* with 24% and *A. glacialis* with 23%. in the second diatom peak in July 2009 31 taxa were identified in samples, however the bloom itself was constituted almost exclusively from a single species, *Chaetoceros vixvisibilis*, responsible for up to 99% and averaging 90 % of the total diatom abundance.

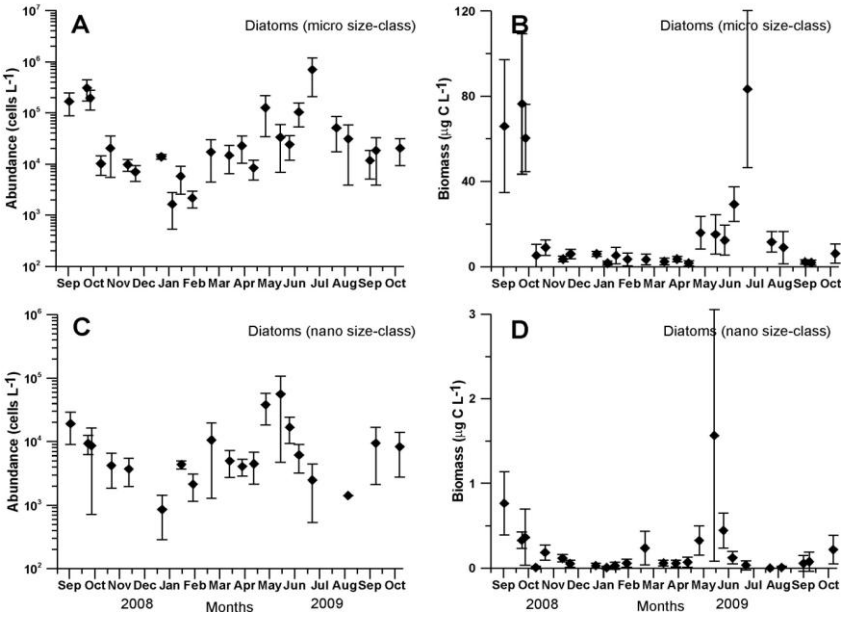

Figure 3.66. Temporal distribution of **A)** and **D)** diatom abundance with **A)** micro size-class and **D)** nano size-class. **B)** and **D)** diatom carbon biomass with **B)** micro size-class and **D)** nano size-class. Data are presented as averaged values with standard deviations obtained from each sampling and clustered for the whole water column. Note the log scale in **A)** and **B)**.

3.4.1.2 Chaetoceros and Bacteriastrum species composition, succession and ecology

Chaetoceros and *Bacteriastrum* species were as previously stated above, among the dominant diatoms in the phytoplankton assemblage during the study period (Table 3.9.). Therefore, their temporal distribution followed the similar trend as the overall diatom community with two distinct peaks in both terms of abundance and carbon biomass, while their numbers during the rest of the period were markedly lower (Figure 3.67.). The first peak in autumn 2008 was characterized with the high abundances reaching $>10^5$ cells L^{-1} and developing predominately in the surface layer (autumn bloom), while the second peak was more evenly distributed throughout the water column with high abundance observed from surface to 5m as well as at 20 m of depth (summer bloom) (Figure 3.67.A).

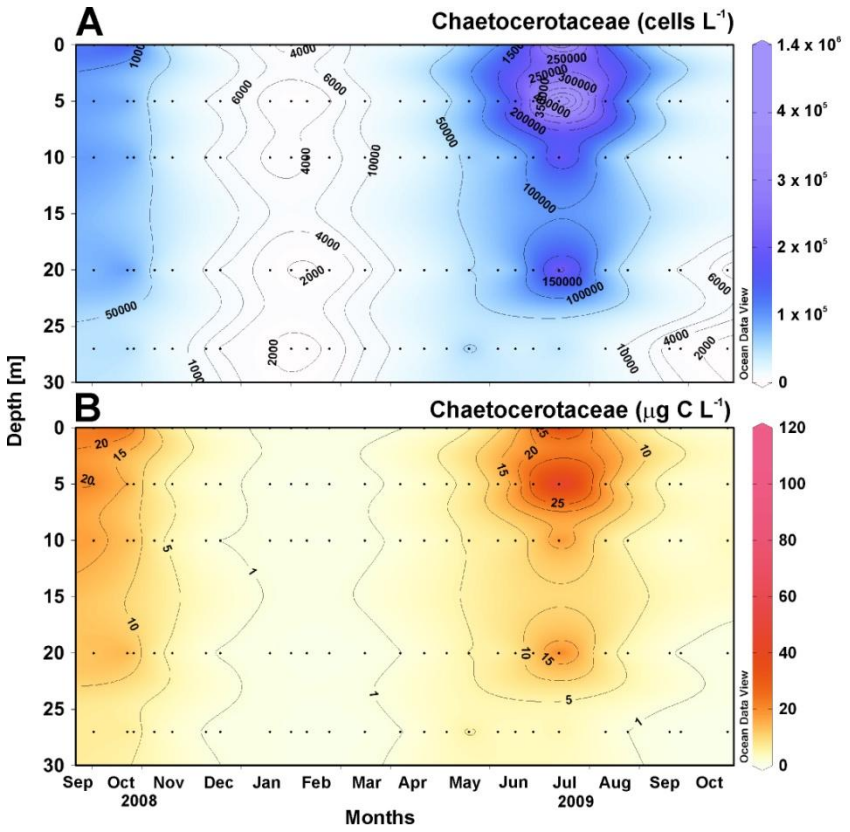

Figure 3.67. Temporal distribution of Chaetocerotacean species (both *Chaetoceros* spp. and *Bacteriastrum* spp.) at station RV001 from September 2008 until October 2009. **A)** abundance and **B)** carbon biomass.

Taxonomic list from the investigated period at the station RV001 counts altogether 36 species from the family Chaetocerotaceae; 32 *Chaetoceros* and 4 *Bacteriastrum* species (Table 3.10.). Of these species, 10 are commonly found in the water column almost throughout all study period with frequency of appearance between 12% and 36 % and belong to the list of dominant species reaching abundances above 10^5 cells L^{-1} (marked bold in Tables 3.9.- 3.10.). Seven species such as *C. curvisetus* and *C. danicus* were frequently present in samples, with frequency 17 % and 28%, but their abundances were lower than it was considered as a threshold for dominate species, reaching 7.6×10^3 and 4.2×10^3 cells L^{-1}, respectively. The rest of the species were considered as rare.

Table 3.10. Taxonomic list of *Chaetoceros* and *Bacteriastrum* species identified at the station RV001 in the period 2008-2009. Max- maximal abundance; Freq. - frequency of appearance. Number of samples= 125; + indicates species observed only in net samples. D - dominant species with Freq. ≥ 10% and Max. >10 000 cells L^{-1} (marked in bold); F – species with Freq. ≥ 10% and Max. <10 000 cells L^{-1}; R – rare and not abundant species.

	Species	Max (cells L^{-1})	Freq. (%)
D	***Bacteriastrum furcatum* Shadbolt**	**118 560**	**19**
R	*B. hyalinum* Lauder	640	2
D	***B. jadranum***	**52 060**	**13**
D	***B. mediterraneum* Pavillard**	**50 540**	**12**
D	***Chaetoceros affinis* Lauder**	**18 240**	**21**
R	*C. anastomosans* Grunow	7 030	6
D	***C. brevis* Schütt**	**10 260**	**17**
R	*C. borealis* Bailey	680	1
R	*C. coarctatus* Lauder	+	+
D	***C. contortus* Schütt**	**175 180**	**36**
R	*C. constrictus* Gran	+	+
R	*C. costatus* Pavillard	3 420	2
F	*C. curvisetus* Cleve	7 600	17
R	*C. dadayi* Pavillard	120	1
F	*C. danicus* Cleve	4 180	28
D	***C. decipiens* Cleve**	**12 920**	**29**
F	*C. densus* Cleve	5 320	12
F	*C. didymus* Ehrenberg	4 560	10
F	*C. diversus* Cleve	6 080	12
R	*C. eibenii* (Grunow in Van Heurck) Meunier	1 520	6
R	*C. lauderi* Ralfs in Lauder	1 520	6
R	*C. peruvianus* Brightwell	1 140	7
R	*C. pseudocurvisetus* Mangin	+	+
F	*C. rostratus* Lauder	6 840	14
F	*C. simplex* Ostenfeld	5 680	12
D	***C. socialis* Lauder**	**28 380**	**22**
R	*C. tenuissimus* Meunier	4 820	4
R	*C. tetrastichon* Cleve	+	+
D	***C. throndsenii* var. *throndsenia* (Marino, Montresor & Zingone) Marino, Montresor & Zingone**	**24 140**	**21**
R	*C. throndsenii* var. t*risetosa* Zingone	8 360	5
R	*C. tortissimus* Gran	9 120	5
D	***C. vixvisibilis* Schiller**	**1 349 679**	**17**
R	*C.* cf. *wighamii* Brightwell	2 660	3
R	*Chaetoceros* sp. "A"	8 360	6
R	*Chaetoceros* sp. "*B*"	49 700	9
R	*Chaetoceros* sp. "*D*"	40 280	7

The total number of Chaetocerotacean species simultaneously present in the water column at the individual sampling date ranged from only 5 in September 2009 up to 20 during the autumn bloom 2008. The highest number of species enumerated from the water samples was 15 occurring during the autumn bloom in 2008, but also in end of June, before the summer bloom (Figure 3.68.). In few occasions, such as in December 2009, the number of identified species from the net samples counted up to 13, while only 2 species were recorded from water samples, indicating their presence in the water column at the time, but in negligible numbers therefore non-detectable by Ütermohl method.

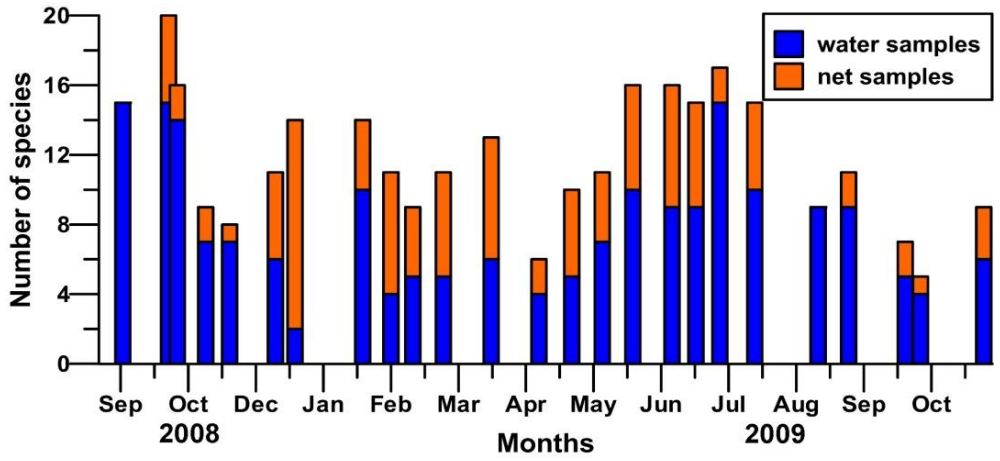

Figure 3.68. Temporal distribution of number of species from genera *Chaetoceros* and *Bacteriastrum* recorded for each sampling date at the station RV001 in water samples and additionally identified in net samples.

The contribution of individual species to the Chaetocerotaceae community was investigated in details on selected dates (Figures 3.69. and 3.70). During September and November 2008, the species composition was very similar, however the contribution of the dominant species markedly varied between different sampling dates (Figure 3.69.A-C). On 29th September 2008, the community was composed from 15 species, with 5 species contributing over 5% to the chaetocerotacean abundance. Of these species, *B. furcatum* and *C. socialis* were the most significant with 27% and 21% of contribution, respectively. *C. contortus* contributed only with 14% (Figure 3.69.A) which changed three weeks later, when this species was dominant over other species with 63% of contribution (Figure 3.69.B). Only six days later, its contribution fell to just 18% and other species, *C. vixvisibilis* took over the dominant position with 45% of contribution (Figure 3.69.C). The end of the bloom was recorded after 10 more days when chaetocerotacean populations markedly decreased in numbers (Figure 3.67.A) accompanied with obvious change in species composition. On 6th November 2008, the community was composed only from 7 taxa, with dominant *B. mediterraneum*, *C. curvisetus* and *C. densus* (Figure 3.69.D). In summer 2009, on 30th June when also 15 species was recorded present simultaneously in the water column, the dominant species were *B. furcatum* with 47% and *C. contortus* with 33% of contribution (Figure 3.70.A).

The summer bloom which was recorded after 16 days was 99% composed of one species, *C. vixvisibilis* which was not recorded at all on the previous date. Nine other species contributed together only to 1% of overall Chaetocerotaceae numbers (Figure 3.70.B).

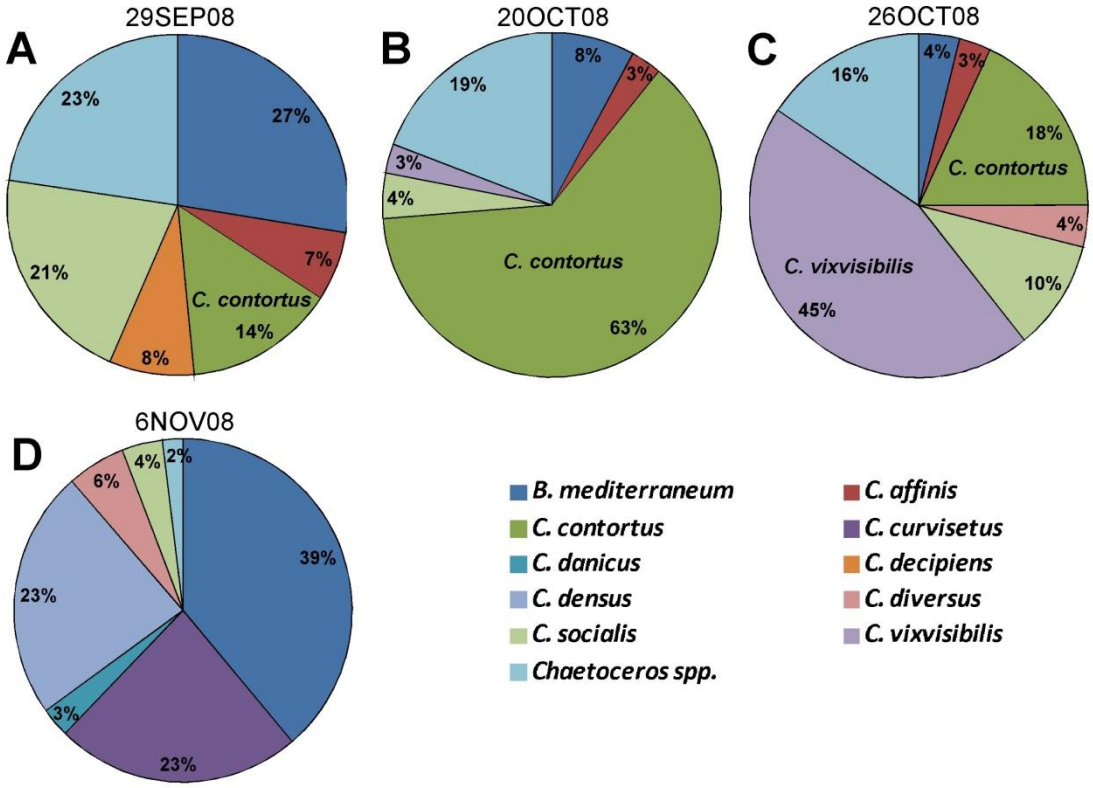

Figure 3.69. Relative percentage contribution of individual species to the Chaetocerotaceae community during the dates of autumn 2008 bloom **A)** 29th September, **B)** 20th October, **C)** 26th October and after the bloom on **D)** 6th November. Species with more than 3% contribution are listed, others are combined in group *Chaetoceros* spp.

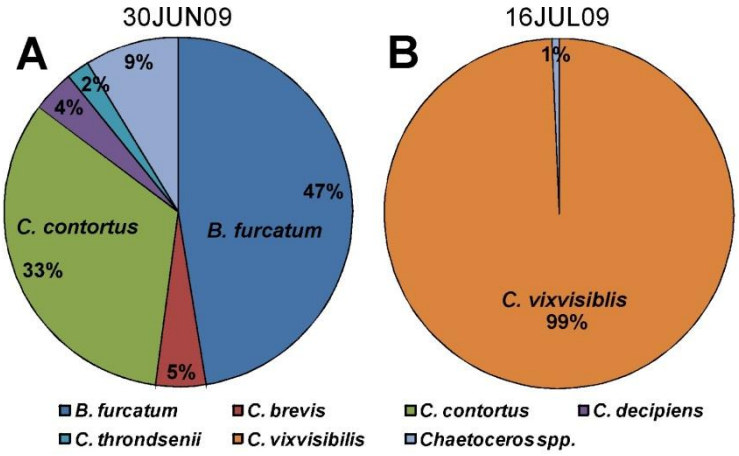

Figure 3.70. Relative percentage contribution of individual species to the Chaetocerotaceae community in summer 2008 **A)** 30th June, **B)** summer bloom on 16th July.

The distribution of dominant species abundances over time showed that the majority of these species except *B. furcatum, B. jadranum* and *C. throndsenii* reached high abundance during the dates of the autumn bloom in 2008. *C contortus* had two other distinct peaks, first in late May and second in the end of June 2009. *C. vixvisibilis* had three peaks in total as well, each of these one sampling date after *C. contortus* (Figure 3.71.A-B). According to Pearson correlation coefficient, *C. vixvisibilis* abundance was significantly positively correlated with temperature (r=0.2902; p=0.001) and phosphate (r=0.2610; p=0.004) while with salinity it showed negative correlation (r=-0.3471; p=0.000). On the other hand, *C. contortus* did not show any significant correlation with environmental parameters. Other dominant species reached high abundances during different dates in the summer/autumn period 2009 (Figure 3.70. C-E).

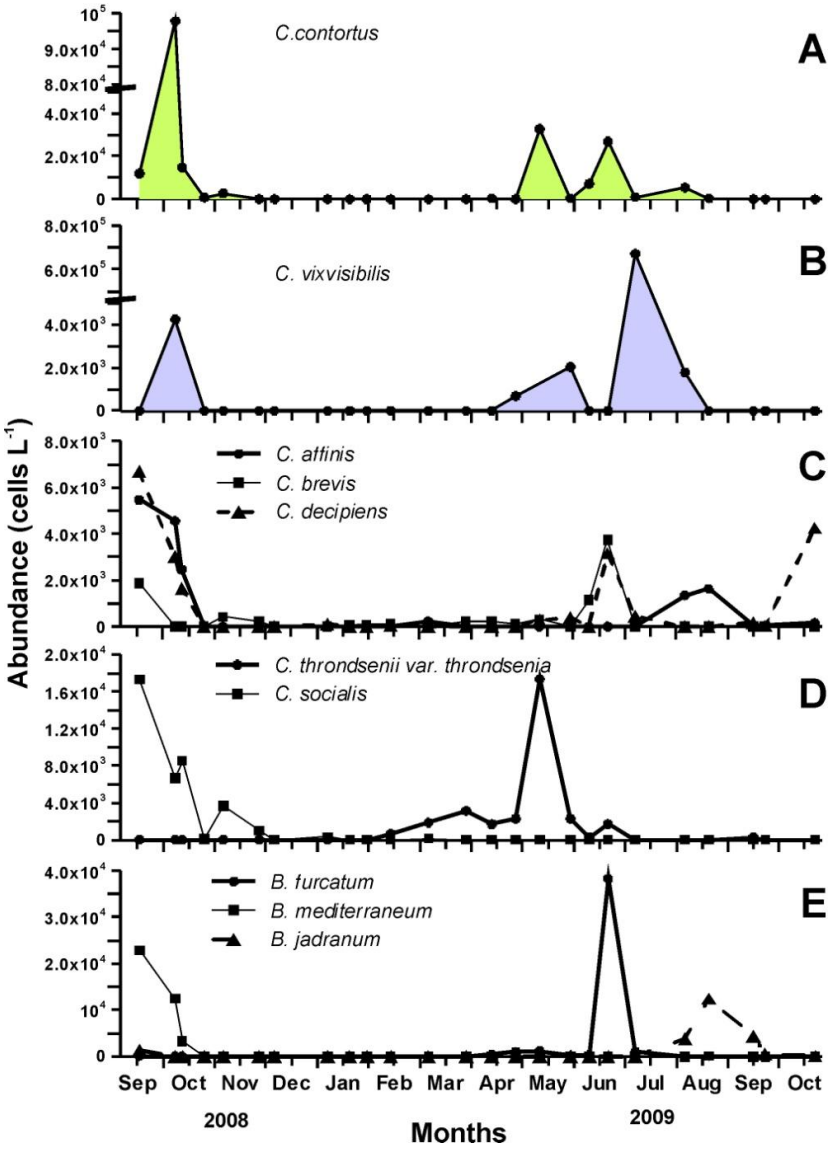

Figure 3.71. Temporal distribution of dominant *Chaetoceros* **(A-D)** and *Bacteriastrum* **(E)** species abundances at the station RV001 from September 2008 to October 2009.

Non-metric multi-dimensional scaling (MDS) analysis of dominant species based on their log-transformed abundances distinguished 4 groups of species at the level of 50% similarity resolved by the corresponding group- averaging cluster analysis (CA plot not shown, except superimposed results on the MDS plot in Figure 3.72.). First group is comprised of *B. furcatum*, *C. throndsenii* and *C. brevis*, species which showed only one distinct abundance peak, although in the different period of spring/summer 2009. Second group is comprised of the most dominant taxa *C. contortus* and *C. vixvisibilis* with *C. decipiens*, all of them showing three peaks in their abundances during the investigated period. Third group has two members, *C. socialis* and *B. mediterraneum* each showing a single peak in the autumn 2008. Fourth group has also two members: *C. affinis* and *B. jadranum* which had their abundance peaks in late summer/autumn 2009.

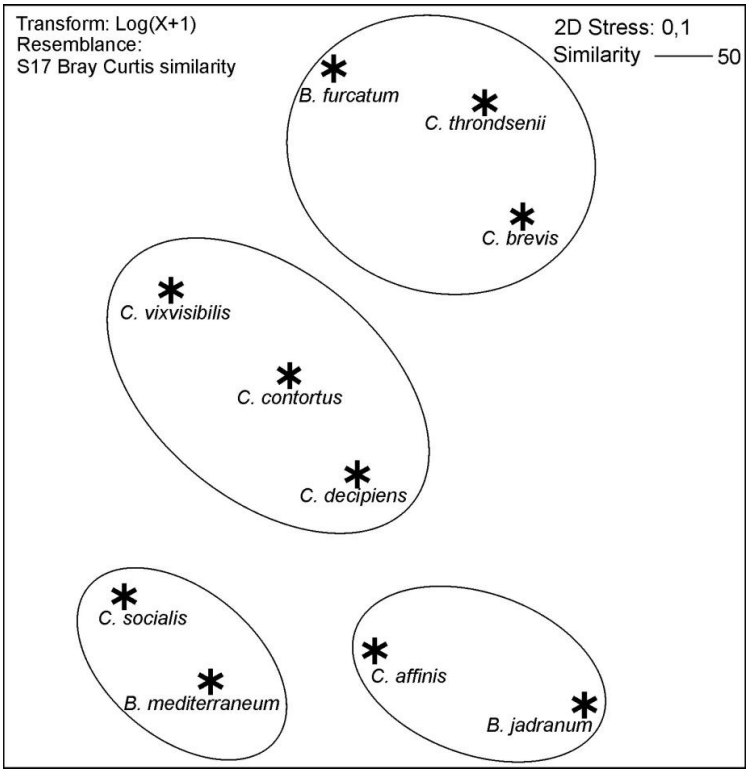

Figure 3.72.MDS ordination plot of dominant Chaetocerotaceae species with the superimposed results of the cluster analysis showing 4 groups at similarity level of 50%

The distribution of abundances of the rest of the *Chaetoceros* and *Bacteriastrum* taxa recorded frequently or rarely during the study period, is shown in Figure 3.73. The majority of the species had their peaks in abundances in autumn 2008 or summer/autumn 2009, with exception of several species such as *C. tenuissimus*, *C. eibenii* or *B. hyalinum* which presence was detected in low numbers in the water column during winter months (Figure 3.73.D,E).

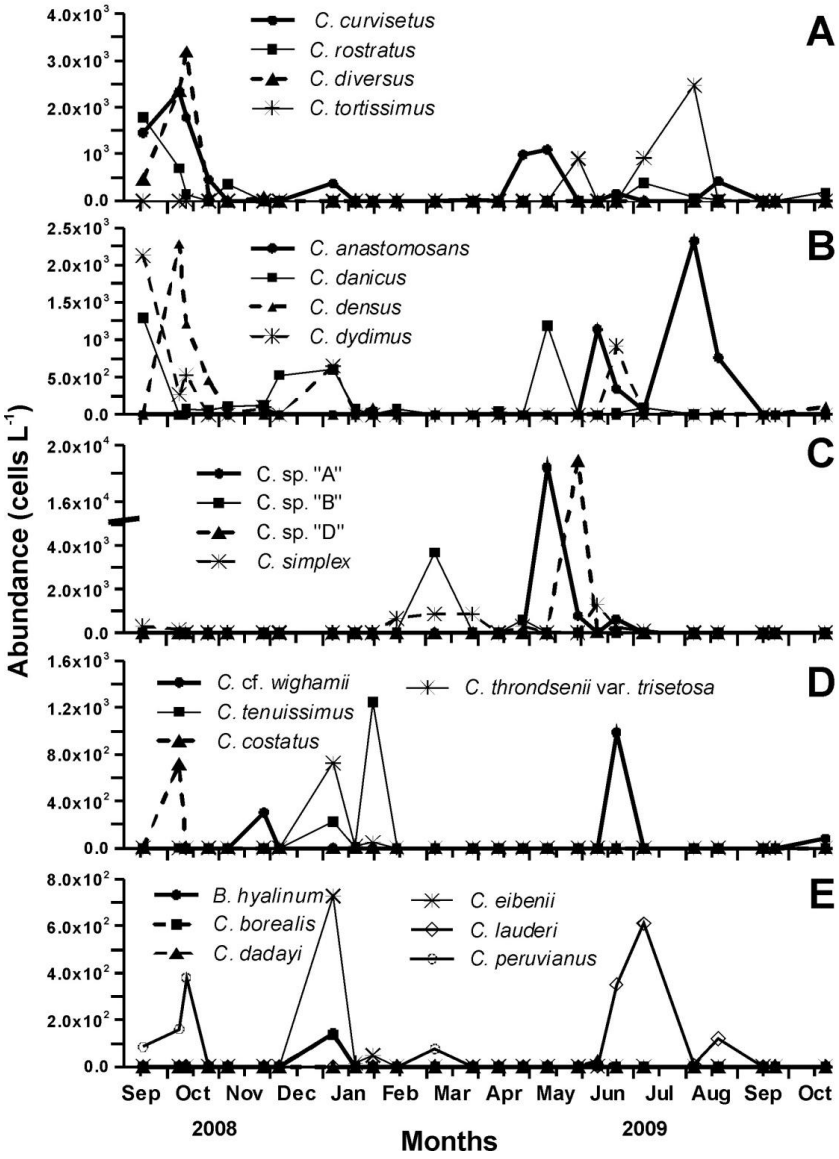

Figure 3.73. Temporal distribution of frequent and rare *Chaetoceros* **(A-E)** and *Bacteriastrum* **(E)** species abundances recorded at the station RV001 from September 2008 to October 2009.

MDS analysis of samples with log-transformed Chaetocerotacean species abundances showed separation of 5 distinct groups at the 30% level of similarity resolved by the corresponding group-averaging cluster analysis on the same resemblance matrix (Figure 3.74.). The MDS plot showed that the distinct species composition was present at the certain point of time in the water column and indicated temporal succession of Chaetocerotaceae community changing from the beginning to end of sampling period. The group A was composed from samples collected in the first part of the study, from September until the beginning of December 2008. In the second B group there is a single winter sample from the middle of December, which is followed by the third C group representing a winter assemblage from January /February 2009. Third group D is the largest, describing the community that was apparently similar in composition from end of February and ending in July with the date corresponding to summer *C. vixvisibilis* bloom. E group is the last including samples describing the community of late summer/autumn 2009.

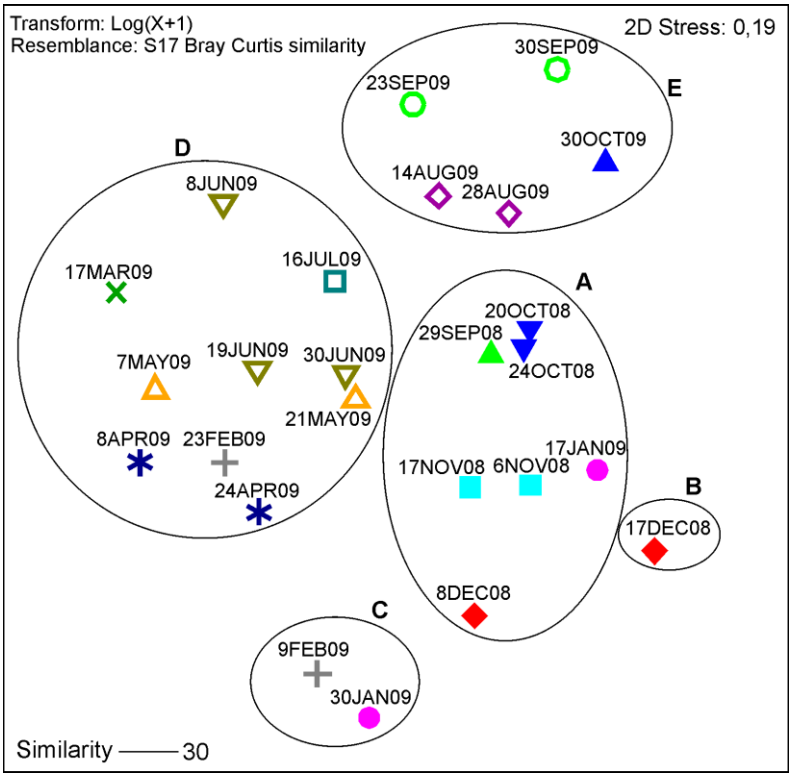

Figure 3.74. MDS plot for Chaetocerotaceae species abundances from different sampling dates at the station RV001 from September 2008 until October 2009. 5 distinct groups of samples are separated at the similarity level 30%, and superimposed on the MDS ordination. A- autumn/early winter 2008 ; B – winter 2008; C – winter 2009; D – spring/summer 2009; E – late summer/autumn 2009.

BIO-ENV analysis showed that the main environmental factors describing the Chaetocerotaceae abundances dataset were temperature, nitrite (NO_2^-) and silicate (SiO_4^+) with Rho 0.428 and significance level of sample statistic of 0.1% (number of permutations performed is 999).

CAP (canonical analysis of principal coordinates) procedure applied to the same dataset in order to test correlations with environmental factors, showed some similarity but did not completely confirm those results. The CAP analysis showed that there were some strong and significant correlations between the chaetocerotacean abundances and the environmental variables. The permutation test statistics (number of permutations used is 999) were both significant with p = 0.001 and resulting with tr(Q m'HQ m)= 2,42 and delta 1^2 = 0.93. First canonical analysis correlation was 0.96 and second one 0.84. In Figure 3.75. the environmental data vectors are overlaid on the sample data ordination showing their correlation with CAP axes. CAP axis 1 was mostly correlated with temperature (correlation coefficient 0.789) and silicate (0.343) and CAP axis 2 positively with salinity (0.542) and negatively with phosphate (-0.610).

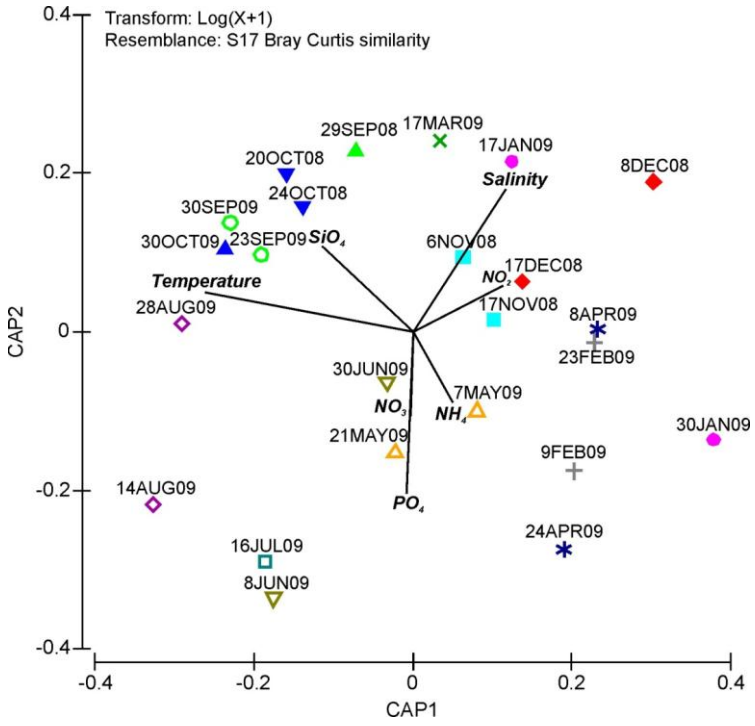

Figure 3.75. CAP analysis of samples with chaetocerotacean species abundances showing separation of sampling dates according to the physiochemical parameters describing the axes.

3.4.2 Summer diurnal succession pattern of *Chaetoceros* and *Bacteriastrum* species in the Krka River estuary

3.4.2.1 Temperature and salinity profiles at station Martinska (M)

Over the research period of six days from 19 to 24 July 2010, temperature and salinity profile did not significantly varied between sampling occasions, which was confirmed with one-way ANOVA test; F=1.182, p=0.305 for temperature and F=0.332, p=0.964 for salinity. The temperature ranged between 18.1 °C in the layer below 8.5 m depth and 27.9 °C in the surface layer (0.1-0.5 m depth) with the average value of 23.4 ± 2.8 °C. Mean salinity was 33.1 ± 6.7, ranging between 19.7 in the surface layer and up to 39.6 below 6 m depth. On Figure 3.76. the depth profiles of the average values of both parameters are shown and a water column stratification due to the combined effects of extensive heating of the surface layer and surface freshwater influence can be clearly observed.

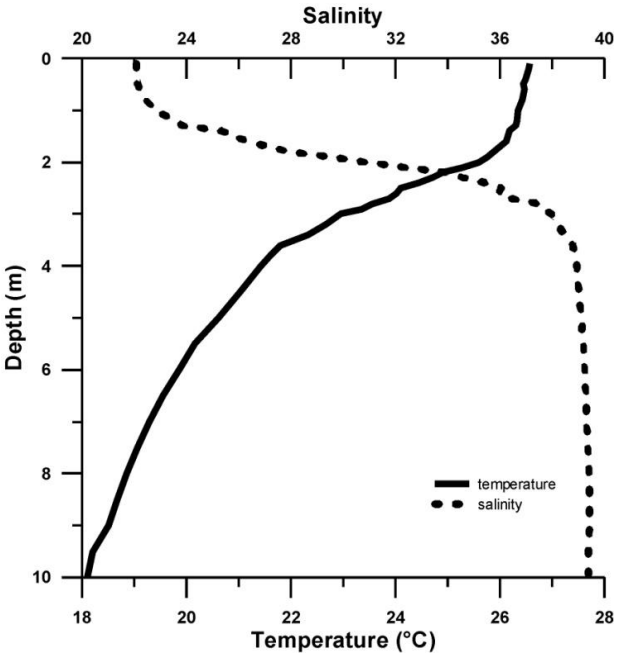

Figure 3.76. Vertical profiles of temperature and salinity in July 2010 at the station M in Krka Estuary. Data are averaged per depth for all sampling occasions.

3.4.2.2 Phytoplankton

The Chl *a* concentrations were quite low, generally below 1 μg L^{-1}, except in the first day of sampling when the values were up to 1.1 μg L^{-1} measured at 1.8 m of depth (Figure 3.77.A). The levels of fucoxanthin were also slightly increased below the surface layer, generally at 1.3 m of depth. Microphytoplankton carbon biomass distribution corresponded to the distribution of diatoms from micro-size-class as the diatoms constituted between 66% and 99% of microphytoplankton carbon. Two distinct peaks can be distinguished, first at 1.3 m of depth in the afternoon of sampling day 2, and second also in the afternoon but at 1.8 m of depth. In nanophytoplankton size fraction, the contribution of diatoms ranged from 3% to 38%, and for the peak in Figure 3.77.D, responsible group were coccolithophorids, not diatoms. Small diatoms followed similar distribution as the larger ones belonging to micro size-class, with the corresponding peaks in biomass (Figure 3.77.D).

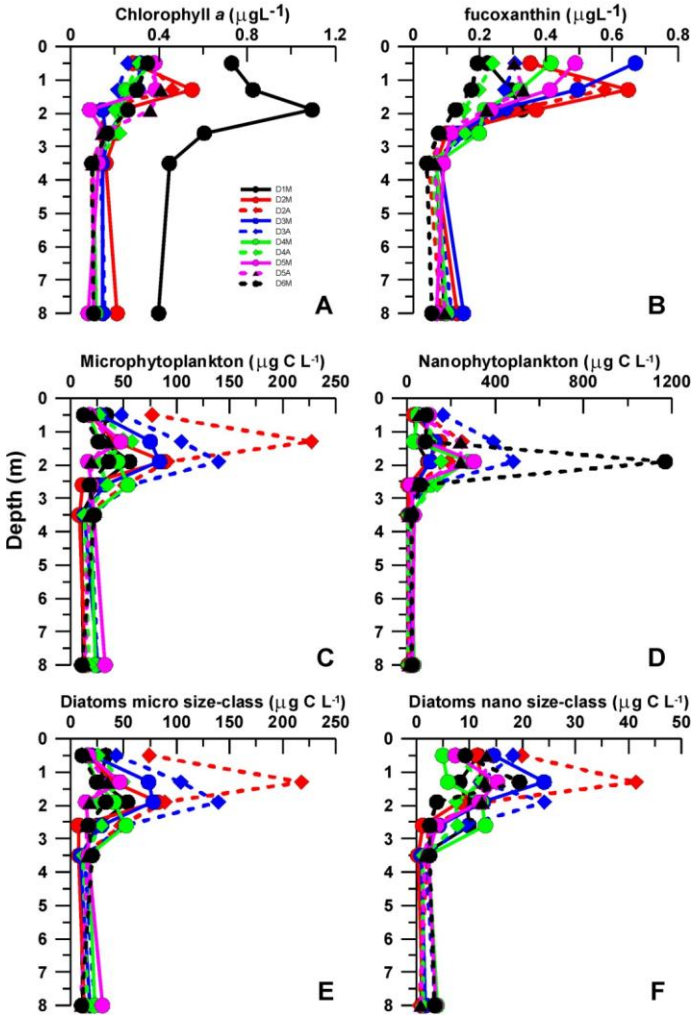

Figure 3.77. Vertical distribution of phytoplankton pigments and carbon biomass in 10 sampling occasions from 19 to 24 July at station M in Krka Estuary. **A)** chlorophyll *a*, **B)** fucoxanthin, **C)** microphytoplankton, **D)** nanophytoplankton, **E)** Diatoms belonging to micro size-class, **F)** Diatoms belonging to nano size-class. Legend in **A)** can be applied to all figures. D1M – day 1, morning; D2M – day2 morning; D2A – day 2 afternoon etc...

Abundances were quite high at all sampling times during the study period, with the micro-diatom abundance ranging from 3.93 x 10^5 to 2.7 x 10^6 cells L^{-1} (averaged for first 2.6 m of water column), and nano-diatom abundance in similar range from 5.7 x 10^5 to 2.2 x 10^6 cells L^{-1} (Table 3.11).

Table 3.11. Abundances of diatom and total phytoplankton size-groups at 10 sampling occasions from 19 to 24 July at station M in Krka Estuary. Values are presented as mean ± standard deviation per first 4 sampling depths (0-2.6 m). D1M- sampling day 1, morning; D2A – day 2, afternoon.

	D1M	**D2M**	**D2A**	**D3M**	**D3A**	**D4M**	**D4A**	**D5M**	**D5A**	**D6M**
Diatoms micro size-class (10^3 cells L^{-1})	863 ± 320	873 ± 859	2688 ± 2038	1204 ± 776	2182 ± 1233	669 ± 445	716 ± 313	567 ± 402	393 ± 184	455 ± 279
Diatoms nano size-class (10^3 cells L^{-1})	1029 ± 321	569 ± 377	2215 ± 2673	812 ± 559	983 ± 542	506 ± 221	526 ± 188	671 ± 474	649 ± 367	747 ± 811
Microphytoplankton (10^3 cells L^{-1})	881 ± 335	877 ± 862	2696 ± 2041	1215 ± 780	2189 ± 1230	672 ± 445	722 ± 315	569 ± 401	399 ± 183	459 ± 281
Nanophytoplankton (10^3 cells L^{-1})	1458 ± 364	1271 ± 1086	3331 ± 3414	1736 ± 921	3032 ± 1312	1435 ± 797	1682 ± 423	1983 ± 1013	1875 ± 913	2882 ± 2067

3.4.2.3 Diatom diversity

At station M in Krka estuary, during the study period, 82 diatom taxa were enumerated in samples from station RV001; of these 53 were identified to the species level and the remaining to the genus or group level. 10 diatom taxa were considered dominant in the phytoplankton assemblage (Table 3.12.).

Table 3.12. Dominant diatom taxa with frequency of appearance (Freq.) > 50% and maximum abundance (Max.) > 10^5 cells L^{-1} enumerated in plankton samples at station M in Krka estuary in July 2010 Avg. – average abundance (10^3 cells L^{-1}). St. dev. – standard deviation. Number of samples =60. Chaetocerotacean species are marked in bold.

	Freq. (%)	Max.	Avg.	St.dev.
Cerataulina pelagica (Cleve) Hendey	98.3	71	9	10
***Chaetoceros* cf. *salsugineus* Takano**	65.0	355	56	74
***Chaetoceros socialis* Lauder**	75.0	312	47	68
***Chaetoceros throndsenii* var. *throndsenia* (Marino, Montresor & Zingone) Marino, Montresor & Zingone**	100.0	5397	408	755
***Chaetoceros throndsenii* var. *throndsenia* Zingone**	100.0	1079	82	151
Cylindrotheca closterium (Ehrenberg) Reihmann et Lewin	76.7	99	17	22
Cyclotella spp.	100.0	488	156	138
Pseudo-nitzschia galaxiae Lundholm et Moestrup	95.0	144	21	25
Skeletonema marinoi Sarno et Zingone	100.0	5311	637	881
Thalassionema nitzschioides (Grunow) Mereschkowsky	100.0	112	28	25

3.4.2.4 Chaetoceros and *Bacteriastrum* species

Taxonomic list from the study period at the station M counts altogether 27 species from the family Chaetocerotaceae; 24 *Chaetoceros* and 3 *Bacteriastrum* species (Table 3.13.). Of these species, 15 species were present in more than 45% of examined samples with the maximum abundance > 50 000 cels L^{-1}, marked bold in Table 3.13.

Table 3.13. Taxonomic list of *Chaetoceros* and *Bacteriastrum* species identified at the station M in July 2010. Max- maximal number of cells counted in the water samples; Freq. - frequency of appearance. Number of samples= 60.

Species	Max (10^3cells L^{-1})	Freq. (%)
Bacteriastrum furcatum Shadbolt	4.18	28
Bacteriastrum hyalinum Lauder	0.56	2
Bacteriastrum mediterraneum Pavillard	2.28	10
***Chaetoceros affinis* Lauder**	**6.65**	**72**
Chaetoceros anastomosans Grunow	0.57	3
Chaetoceros brevis Schutt	0.24	2
Chaetoceros coarctatus Lauder	0.32	2
Chateoceros contortus Schütt	9.50	43
***Chaetoceros curvisetus* Cleve**	**32.30**	**60**
Chaetoceros dadayi Pavillard	0.12	3
Chaetoceros danicus Cleve	1.14	35
Chaetoceros decipiens Cleve	3.80	43

Table 3.13. continued

Species	Max (10^3cells L^{-1})	Freq. (%)
***Chaetoceros diversus* Cleve**	**13.30**	**83**
Chaetoceros lauderi Ralfs in Lauder	1.14	2
Chaetoceros pseudodichaeta Ikari	0.76	2
Chaetoceros peruvianus Brightwell	0.38	5
Chaetoceros rostratus Lauder	0.76	7
***Chaetoceros* cf. *salsugineus* Takano**	**354.75**	**65**
Chaetoceros simplex Ostenfeld	8.51	13
***Chaetoceros socialis* Lauder**	**312.18**	**75**
Chaetoceros tenuissimus Meunier	6.70	22
***Chaetoceros throndsenii* var. *throndsenia* (Marino, Montresor, & Zingone) Marino, Montresor & Zingone**	**5396.94**	**100**
***Chaetoceros throndsenii var. trisetosa* Zingone**	**1079.39**	**100**
Chaetoceros tortissimus Gran	24.38	8
Chaetoceros vixvisibilis Schiller	14.82	22
***Chaetoceros* cf. *wighamii* Brightwell**	**36.10**	**48**
***Chaetoceros* sp. "B"**	**14.19**	**75**

The dominant species were generally most abundant at the pycnocline depth, although not all species in the same sampling occasion. *C. affinis, C. curvisetus, C.* cf. *salsugineus* and *C. socialis* abundances were highest on the third day of sampling in the morning, while *C: diversus, C. throndsenii* var. *throndsenia* and *C. throndsenii* var. *trisetosa* were most abundant at the second day of sampling in the afternoon. *Chaetoceros* sp. "B" showed several peaks in three distinct sampling occasions (Figure 3.78.).

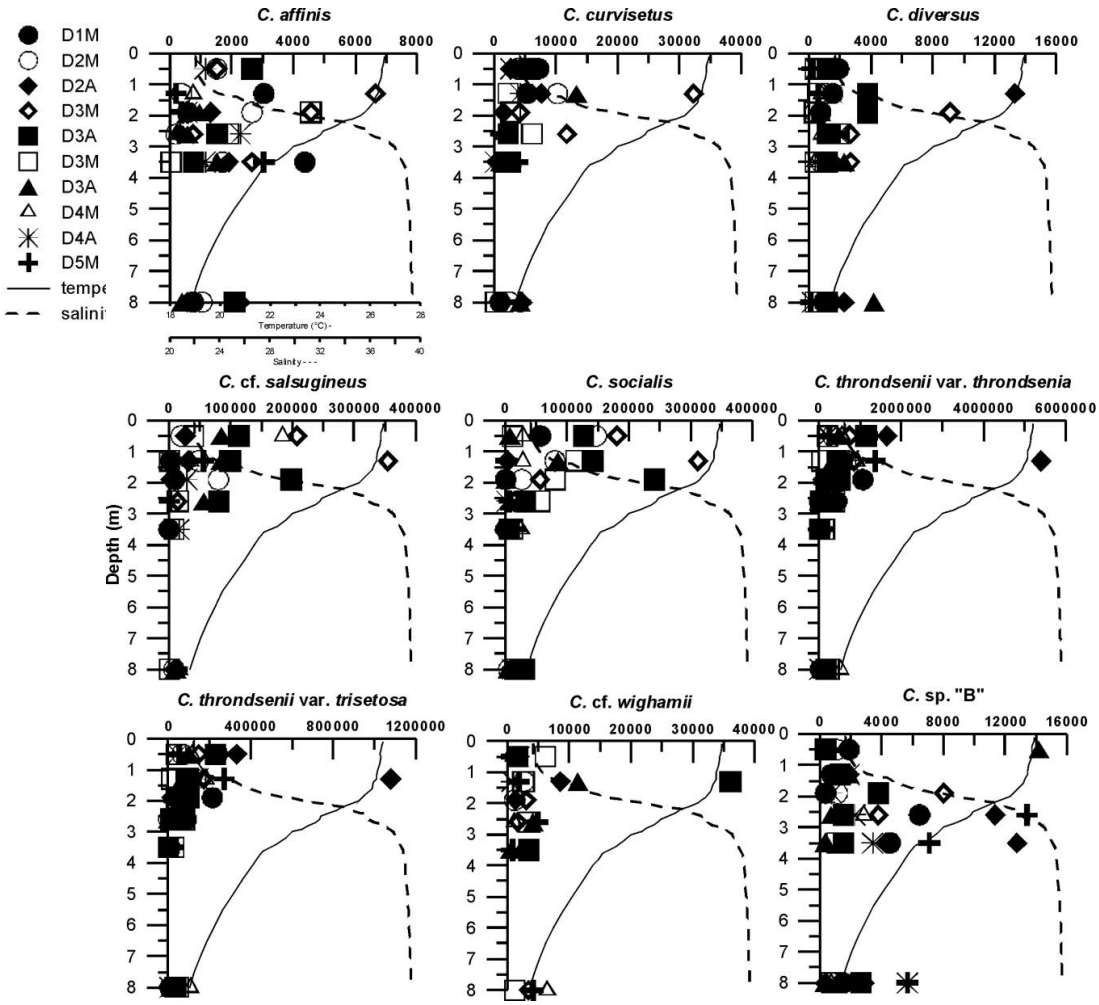

Figure 3.78. Vertical distribution of dominant *Chaetoceros* species overlayed on the salinity and temperature profile in the water column collected in 10 sampling occasions during July 2010. The timing of sampling is explained by symbols, where D1M corresponds to sampling day 1, morning, D2A – sampling day 2 afternoon, etc.

CHAPTER 4

DISCUSSION

"Socrates: The second principle is that of division into species according to the natural formation, where the joint is, not breaking any part as a bad carver might."

Plato (ca. 428-347 BC) from "Phaedrus, 265d-266a"

4.1. Morphology and taxonomy of Chaetocerotaceae

4.1.1 Evaluation of the taxonomic characters in species identification

The species identification in the genera *Bacteriastrum* and *Chaetoceros* has been traditionally based on general shape of the frustule and morphological characters visible by light microscopy (Cupp, 1943, Hasle and Syvertsen, 1997) which appears more informative than ultrastructural details available for several taxa (e.g. Evensen and Hasle, 1975, Hernández-Becerril, 1996). This is different from the majority of extant diatom genera and species for which EM studies have significantly redefined their circumscriptions (Round et al., 1990). For instance, the information on the number, location and shape of the processes and the structure of areolae is essential for the identification of *Thalassiosira* species where cell and colony shape are scarcely variable (Hasle, 1968). A similar case is the highly diverse *Pseudo-nitzschia* genus where species are distinguished by subtle ultrastructural differences observable only with TEM, such as the fine striation pattern of the frustule (Hasle et al., 1996). It appears to be due to the fact that the general shape of the *Chaetoceros* and *Bacteriastrum* frustule as seen on the LM appears more informative than ultrastructural details. The results obtained from this thesis partially support this view, as the main delineating features, e.g. the mode of joining the cells in colonies, orientation of the setae, chloroplasts were visible in LM. However, the examination of ultrastructural features allowed us to obtain further information on morphological details of the silica frustule and to recognize/identify some species-specific traits e.g. the valve ornamentation pattern or setae structure which enables the recognition of species in EM as well. Results of molecular studies have demonstrated that these fine ultrastructural differences are taxonomically informative and useful to circumscribe different species, and also that genetically distinct groups might exist within morpho-species (cryptic species) such as shown in genus *Skeletonema* (Sarno et al., 2005) and *Pseudo-nitzschia* (Amato and Montresor, 2008, Lundholm et al., 2002, Lundholm et al., 2003, Lundholm et al., 2006).

Generally, the morphology of chaetocerotacean species is quite variable and it is additionally complicated by a wide range of morphological diversity found within individual taxa. Even 65 variable morphological features were used in the phylogenetic study by Rines and Theriot (2003) for constructing a cladogram, but majority of them were excluded or merged in the subsequent study by Kooistra et al. (2010) which used only 20 characters. In this thesis the morphological characters visible in LM, e.g. the mode of joining the cells in colonies, the orientation of the setae, the number and shape of chloroplasts have been considered as main delineating features in species identification. However, the detailed information of ultrastructural features of the silica frustule has been acquired for all the studied species, with the aim of recognizing/identifying species-specific traits e.g. the valve ornamentation pattern or setae structure which enables the recognition of species in EM as well. The morphological characters observed for all the species have apparently different diagnostic value and have been tentatively rated according to their importance in the taxa recognition. These data, although restricted to a limited number of Adriatic morphotypes, can be useful to trace the evolutionary

relationships among species in future studies on the morphological cladistic and phylogeny of the *Chaetoceros* genus.

SHAPE OF THE CELLS

Cell size –generally not important

Cell size and the ratio of the pervalvar to apical axis which tells us about the cell shape, being more or less elongated, are very unreliable characters. The reason is that they are dependent on the stage in the life cycle of the population because the cells become smaller and more elongated following mitotic divisions. This phenomenon was observed regularly in all cultures but also often in field samples of e.g. *Chaetoceros decipiens, C. costatus* or *Bacteriastrum hyalinum*. However, we emphasize here that it is important to report this parameter within the species descriptions because it is useful to group the species according to their mean size in different categories.

i) Small cells with average apical axis (a.a.) 5-10 µm: solitary species such as *Chaetoceros tenuissimus, C. simplex, Bacteriastrum paralellum,* colonial weakly silicified forms such as *C. salsugineus,* distinct colonial forms *C. diversus, C. socialis.*

ii) Middle sized cells with average a.a. 12-20 µm: majority of *Hyalochaete* taxa such as *C. curvisetus, C. contortus, C. costatus, C. affinis.*

iii) Large cells with average a.a. 20-35 µm: large *Hyalochaete* taxa such as *C. lauderi* and *C. brevis* or *B. hyalinum.*

iv) Very large cells: with mean a.a. 25-50 µm: robust *Chaetoceros* species such as *C. eibenii, C. densus, C. coarctatus.*

The ratio of valve mantle height to girdle height – not important

A feature of the cells which depends on the cell cycle stage but for some species it is characteristic to have very elongated cells due to the high girdle consisting of large number of girdle bands as is in *C. lauderi* while for some other species such as *C. tortissimus* this ratio is almost always low and cells appear more squared. However, in any of the species this character should be used as a delineating one.

GENERAL MORPHOLOGY/OVERALL ASPECT OF THE COLONY

Usual growth form (solitary/colonies) – moderately important

Most of *Chaetocreos* species are colonial and a limited number of species has been reported as solitary. Some solitary forms such as *C. danicus* can occasionally form short chains of two to three cells but under which circumstances, it is not quite clear as some other species such as *C. peruvianus* were never observed to form chains. The common way of distinguishing the *Hyalochaete* or *Bacteriastrum* solitary species from the intercalary ones is the existence of the process on each valve, as in these species the process is present only on the terminal valves of the chain colony (Evensen and Hasle, 1975). On the other hand, in addition to colonies many species have single celled forms and this present significant identification problems because none of the colony features can be used for the species identification. These have often been given a separate taxonomical status, but they may simply

represent a stage in the life cycle of the population such as the initial cell in *Bacteriastrum hyalinum* previously called *B. solitarium* (Drebes, 1967). In this study the morphotype *Chaetoceros* sp. "B" showed resemblance to species *C. diversus* in ultractructural characters such as the structure of the setae and valve and it could easily represent a unicellular form of this species. It seems that this morphotype is well distributed along the Adriatic coast, and its appearance sometimes corresponds, but not always with the appearance of *C. diversus*. However, more detailed studies of the life cycle of this taxon including the molecular information are necessary before making any significant conclusions.

Mode of colony formation – very important

The way of connecting the individual cells in the colonies appears to be a very stabile and species-specific characteristic in the culture and natural conditions, unlike the coloniality itself. Several species have a very distinctive way of connecting sibling cells which enables an easy recognition, as, for instance, the unique polysaccharide cell jacket in *B. jadranum*, the linking process in *C. rostratus*, the bridge joining setae in *C. anastomosans*, the prehensors on the posterior valve in *C. convolutus* (Hernández-Becerril, 1996), or the fusion of the marginal protuberances on the sibling valves in *C. costatus* and *C. pseudocurvisetus.*

Length of the chain – moderately important

Different species have a tendency to form colonies of a certain length. In this study chains are considered long if they have more than 10 cells or short if they have less than 10. The *Chaetoceros* (*Phaeoceros*) species such as *C. dadayi* are rarely observed in chains longer more than 3 cells while *C. diversus* chains are always composed of three cells or multiple of three. *Chaetoceros costatus* and *C. contortus* form very long chains consisting of up to 50 cells. In *Hyalochaete* and *Bacteriastrum* colonies the end cells are heterovalvate, with terminal valve bearing setae with a very distinct shape therefore we may know if we are observing the complete colony or a broken one. The coloniality and chain formation is probably under some specific combination of the genetic control and the environmental cues, and this issue is in need for a more thorough research. The commonly observed feature of the majority of the colonial chaetocerotacean taxa is that when they grow in cultures for a longer period of time they partially/completely lose their coloniality and form very short chains or become single celled.

Shape of the chain – very important

The majority of *Chaetoceros* species forms straight chains. In some speciesthe chain shape is very characteristic as in the case of the chains curved in a narrow girdle view of *C. pseudocurvisetus* and *C. curvisetus*, curved in broad girdle view of *C. socialis* or twisted around the chain axis of *C. tortissimus.*

Polarity of the chain/cells - very important

Heteropolar cells such as *C. peruvianus* have different valves and heteropolar chains such as *C. dadayi* have different end valves which often differ only in the setae orientation. The case of the

heteropolarity of the colonies in *Bacteriastrum* species from the section *Sagitatta* implies some kind of genetic control of the shape of the terminal setae. It was observed in this study that when chains of *B. mediterraneum* split in two shorter chains the newly formed terminal cells have always the opposite shape from the previously existent one.

CHLOROPLASTS

Number per cell and shape– very important

The number and shape of chloroplasts was confirmed to be a species-specific feature. The species may have one chloroplast which is usually plate-like and extends from valve to valve as in *C. amanita* or around the girdle as in *C. affinis.* Two chloroplasts are present in *C. anastomosans* and numerous small ones in *C. decipiens* or *C. contortus.* The possible problem is that in preserved samples or generally in the field material from the Adriatic Sea, cell content seems often destroyed or granulated and the chloroplasts are very difficult to observe.

Presence/absence in setae - very important

All of the members from the subgenus *Chaetoceros (Phaeoceros)* contain chloroplasts within the setae whereas *C. bacteriastroides* contains them only in long fused setae but not in short spiral ones. Some members of *Hyalochaete*, such as *C. brevis* have chloroplast-like material within the setae but these granules do not contain chlorophyll and therefore do not have the photosynthetic function.

APERTURE

Shape and size of the aperture –moderately important

A character which depends on several other important characters: the way how sibling cells connect with each other, the presence of protuberances on the valve face, the point of setae crossing/fusion hence on the length of the basal part, the shape of the valve face and the shape of the valve edges. In several species it can vary such as in *C. affinis,* between very narrow to lanceolate in LM which is probably depending on the silica flap. However, in most of the species the feature is generally constant and considered important, such as for the identification of *C. curvisetus* especially when the chain is observed in a broad girdle view.

RESTING SPORE MORPHOLOGY - very important

The importance of the morphology of the resting spores was shown previously in a number of studies as presented in Ishii et al (2011). For a great number of species valid taxonomic identity can only be confirmed in presence of spores, such as in *C. lorenzianus* or *C. teres/C. lauderi* in the Adriatic Sea. There are also opposite cases of species having the same types of spore but clearly different vegetative cells, as in the case of *C. pseudocurvisetus* and *C. curvisetus* (Rines and Hargraves, 1988).

DEGREE OF SILIFICATION – moderately important

On infrageneric level this can be considered as an important character in the differentiation between *Chaetoceros* (*Phaeoceros*) which species are generally more robust and *Hyalochaete* species which are usually weakly silicified. However, on the species level the degree of silification is generally variable as it is dependent on the concentration of the silicate in the surrounding medium and on the uptake ability of individual cells, although there are more silicified taxa such as *C. decipiens*.

VALVE FACE

Shape from girdle view – moderately important

It can be flat/concave/convex. Most of the species have flat or slightly concave valves but in some species it can represent an important characteristic e.g. the anterior valve is convex in *C. peruvianus.*

Shape from valve view-moderately important

Generally, most of the cells are elliptical, but in several species the circular shape of the valve is very pronounced and it is considered as one of the delineating characters such as for the distinction between *C. contortus* and *C. compressus.* However, with the cell age the cells become smaller the shape gets more rounded, and the recommendation here is that this character should be considered as distinguishing only if the post-auxospore cells could be observed.

Presence of protuberance – very important

Distinguishing character for *C. dydimus* and *C. protuberans* (single large central protuberance), *C. costatus* and *C. pseudocurvisetus* (four marginal protuberances).

Ornamentation pattern –very important in several cases

All of the observed chaetocerotacean species have the same basic ornamentation pattern. It consists of the annulus which is circular to slightly oval with the dichotomously branching ribs extending towards the valve margin. Previously some *Chaetoceros* (*Phaeoceros*) species were described as not having a costae and annulus pattern (Hernández-Becerril, 1996) but most probably they were only very hard to observe due to the high degree of silification in these cells. For several species it can represent an important delineating feature. *C. amanita* is the only species with very specific ornamentation with dense anastomosing costae but without annulus. *C. contortus* has reticulate annulus and transverse ribs between the main ones, but this feature is shared with *C. compressus* (Rines, 1999). *C. costatus* has the pattern on the valve which has costae close to the valve apices becoming parallel with the apical axis. *C. tortissimus* has dots as an origin of costae, and C. *vixvisibilis* has spirals. Most of the species have additionally perforated valves by pores, and they are generally present in more silicified species of subgenus *Chaetoceros* and *Hyalochaete* such as *C. decipiens*, *C. protuberans*. In *Bacteriastrum furcatum* the pore distribution around the setae bases and mantle may be considered as a possible delineating character, same as the smooth surface in *B. jadranum*.

VALVE MANTLE

Presence of the constriction near the advalvar mantle edge – moderately important

The constriction is usually interpreted as a notch at the suture between the girdle and the mantle and it is readily visible in LM. Rines and Hargraves (1988) pointed out that the shape of the suture is among the significant taxonomic characters and they distinguish that the junction may be barely discernible, a slight notch or a distinctively incised furrow or groove. In this study the EM observations confirm that this is actually a constriction around the valve mantle, near its advalvar margin which can vary in depth of the indentation, and it is present in majority of the species, with only in *C. constrictus* considered as a significant feature.

Siliceous hyaline rim on the marginal ridge – moderately important

Most of the species have some extension of the hyaline rim except *C. diversus* or *C. rostratus* where the rim is completely lacking and the edge between valve mantle and face is smoothly curved. In *C. salsugineus* and *C.* cf. *wighamii* the rim is fissured which is the characteristic most probably shared by some other small colonial morphotypes. The rim height varies in the culture conditions.

SILICA PROJECTIONS

Capilli presence/length – very important

The presence of short capilli was observed on all valves of *C. constrictus* in this study which agrees with the observations of the morphotype from Danish Sea (Jensen and Moestrup, 1998). *C. affinis* has also short capilli on the terminal valves. For *C. dydimus* important distinguishing character are the long capilli ornamenting the valves which are lacking in *C. protuberans* (Hernández-Becerril, 1991b). In *C: pseudodichaeta* there are two types of capilli, short on the valve face and long on the proximal part of the setae.

Silica flap/projections from the marginal ridge – moderately important

Most of the species have distinct rim on a marginal ridge which is often extended into projections of variable shape and length but it is not present in each valve therefore we do not consider it as a crucial delineating feature except in *C. affinis*. In this species there is a characteristic silica flap fused between the marginal ridges of two sibling cells which is completely occluding the aperture. In *C. pseudodichaeta* the projections are usually irregularly shaped, long and found several per each valve. In *C. decipiens* as firstly observed by Evensen and Hasle (1975) the rim is extended only at the edges of the aperture and fused between sibling cells, similar feature was observed in *C. diversus* (Hernández-Becerril, 1996) and *C. amanita*.

PROCESS

The presence of the process on all valves is generally characteristic for *Phaeoceros* species, all except *C. pseudodichaeta.* In *Hyalochaete* the process is present only in terminal valve, or as in *C. amanita* is lacking. The importance of the process as a taxonomically important character was first proposed by Evensen and Hasle (1975)

Number of processes - very important

It can vary between one per valve as in majority of species and numerous such in *C. phuketensis* or *C. buceros* (Rines et al., 2000). In Adriatic species there are no observations on the species which posses

this characteristic, except *C. coarcatus* which was reported in (Hernández-Becerril, 1991a) to have numerous (18-22) small, slit-like processes occurring at each valve. Unfortunately, in this study this species has been observed only with LM and we could not confirm this feature.

Location – not important

The eccentric/central location of the annulus and the process is previously considered as very important (Hernández-Becerril, 1996, Evensen and Hasle, 1975). In this study it is found not to be as important and almost all species have central position, with exceptions of e.g. *C. rostratus* due to the presence of the linking spine.

Shape- moderately important

Generally, the shape can be very variable characteristic, but it is still not clear if this is due to the morphological variation within species. In *C. dichaeta* it is generally a long tube but the length can vary considerably dependent on the cell size and age (Assmy et al., 2008). The same was observed in this study for *C. pseudodichaeta*. On the other hand the morphology of the *C. affinis* process was found here to be very variable in a single strain. Generally it can be considered as important distinction between slit-shape and round hole from the internal side of the valve.

SETAE

Number per valve –very important

Several *Chaetoceros* species have one seta per valve, all of *Bacteriastrum* species have more than two.

Orientation and direction– very important

In *C. dadayi* and *C. tetrastichon* the main delineating character is the direction of two intercalary setae.

Brunel groups (arrangement) – sometimes variable, but generally important

For some species as *C. circinalis* or *C. socialis*, it is very characteristic. In other species can vary such as in *C. eibenii* which is generally considered to belong to group III but in cultures the group II was found as well.

Thickness – very important

Some species have special intercalary setae which are thicker than the common ones (*C. diversus*) and some have thicker terminal setae (*C. affinis*), the basic design is the same as the common ones, but the higher amount of silica can change their cross section from circular that they appear polygonal.

Length – not important

The length of the setae depends on the age of the cells as they are short while they grow, and often they can be broken in field samples.

Length of the basal part –moderately important

Basic character which depends on the mode of the chain formation in certain species, determines the size and shape of the aperture in addition to the setae fusion point. In several species there is variability in length of the basal part and it is very subjective to define it as long or short, but generally when it is absent than the aperture is narrow and this is a stabile feature.

Length of the fusion – not important

Species *C. decipiens/C.lorenzianus* were previously distinguished by this character but it was rejected as it was shown to be very variable and not important. It is also not recommended as a delineating character in *Bacteriastrum* species.

Setae ultrastructural design and ornamentation – very important

The idea that the form and fine structure of the setae can be used as useful taxonomic characters was first proposed by (Evensen and Hasle, 1975) who examined the ultrastructure of limited number of species. The usual interpretation of the setae design is that they are perforated by poroids in a straight or spiral pattern. Here, we claim that these poroids are in fact the space between siliceous longitudinal strings and bars which are the main building elements. The more detailed descriptions of the classification on the basis of setae design are found in the following subchapters and they are considered separately for *Chaetoceros* (*Phaeoceros*) taxa where 9 designs were recognized, in *Hyalochaete* 9, *Bacteriastroides* 1, and in genus *Bacteriastrum* 3.

GIRDLE BANDS - in majority of cases not important

All of the observed girdle bands have the same structure. They are narrow and ornamented with alternating transverse striae and costae as well as the irregularly scattered small poroids between costae. *C. costatus* is the only species which has distinct advalvar girdle bands with one thickened edge.

4.1.2 Specific comments on morphology of taxa from the genus *Chaetoceros*

4.1.2.1 Subgenus *Chaetoceros (Phaeoceros)*

The species belonging to the subgenus *Chaetoceros* (*Phaeoceros*) appear to be very morphologically diverse. In the first definition of the subgenus Gran (1897) mentioned as the important delineating character the thick setae, often filled with protoplasm and plastids which escape when setae are broken. In his work Gran included only four species in the subgenus, *C. danicus*, *C. borealis*, *C. atlanticus* and *C. brightwellii* (synonym of *C. densus*) mentioning from other characters only the lack of resting spores in the members of the subgenus. Afterwards, a hundred years later, Hernandez Beccerril (1996) added other characters such as presence of at least one process, central or positioned to one side of every valve as it was suggested also earlier by Evensen and Hasle (1975) and the presence of resting spores in one species (*C. eibenii*). Hernandez Becerril (1996) also added ultrastructural features to the subgeneric specific characters such as the valves are perforated with poroids with thickenings or costae, the tubular, circular, oval, or slit-like shape of the process, and the polygonal cross section of the thick setae.

Here, we can conclude according to our findings that setae in subgenus *Chaetoceros* are all polygonal in cross-section, very robust and usually long. They contain small globular numerous chloroplasts within them, along their entire length, which is proposed to increase the photosynthetic capacity of the cells. Evolutionary there are indications that the acquisitions of plastids happened after

the development of the setae and that this ability may provided an adaptive advantage to the cells (Kooistra et al., 2010). The plastids migrate within the setae along the whole length and it was observed here when they were exposed to high UV-light in epifluorescent microscope in species *C. rostratus*, *C. pseudodichaeta* and *C. danicus* that they retracted towards and in the cell body.

The Adriatic species observed in this study can easily be distinguished not only in LM, but also in EM by the structure of the setae. In 10 recorded species there were found 9 different structural designs. Five were determined within this study and for four species which were not observed with EM, the supplementary information on the description of seta structure was obtained from the literature. Therefore, for this particular cases as this species are observed from different geographical locations, there exists a slight possibility that the Adriatic morphotype described in this study possess a different ultrastructure than the one described from the literature. Five structural types are shown in Figure 4.1. and the description of all types is presented in Table 4.1.

Only the middle region of the setae was taken into consideration as the setae are in their basal part are circular in the cross-section and either smooth (*C. rostratus*) or perforated by round larger poroids (*C. pseudodichaeta*). Later they become polygonal and near the tips the six-sided setae often become quadrangular. The most common cross-section was found to be quadrangular. The types c and d are taken from the literature, but they appear to be very similar with the only differing feature being the cross-section. In two species *C. dadayi* and *C. tetrastichon*, which appear to be highly similar in a general morphology, the delineating character according to Hernández - Becerril (1992) was proposed to be eight sided setae in the former and four sided setae in the latter species. In this study this could not be confirmed due to the lack of EM observations. Apparently, the ornamentation of side wall is the same with three rows of small areolae between two thick costae. In setae which have thick costae it gives the impression of a ladder-like appearance. Apparently, in the majority of design types, except in 2, larger round poroid was observed situated near the ridge at either side of the side wall. The poroid seem to correspond to the ones which often perforate the setae basal part extending from the mantle.

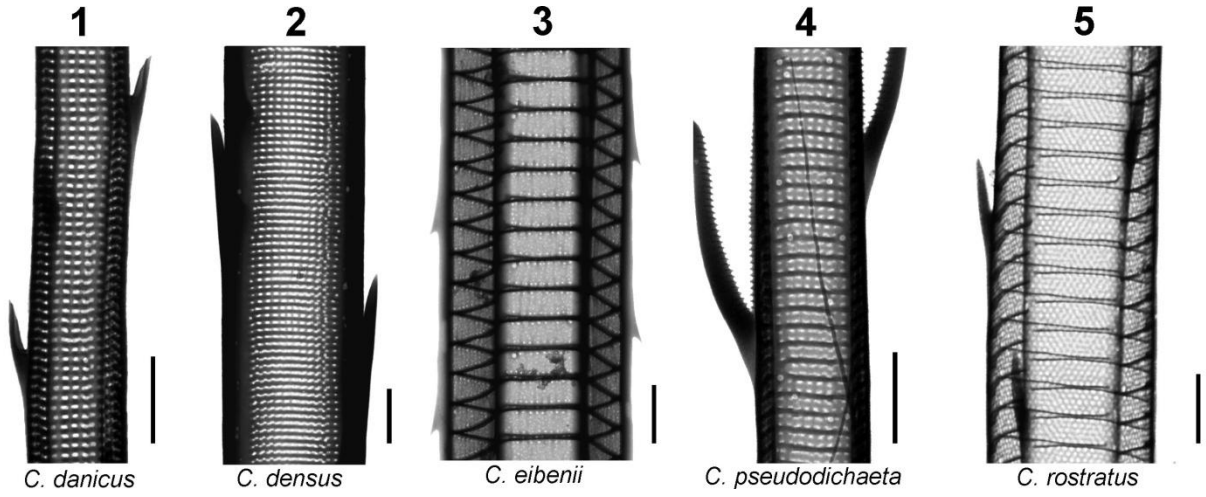

Figure 4.1. SEM micrographs of 5 structural types of setae in *Chaetoceros* subgenus observed within this study. The morphological characteristics of each type are described in Table 4.1. Scale bars 1 μm.

Table 4.1. Ultrastructural morphological characteristics of setae structural types found in species belonging to *Chaetoceros* subgenus. S – stria; C – costae.

Species	Type	Cross-section	Side-wall pattern	Areolae	Costae	Spines	Source
Chaetoceros borealis	a	4-5 sided	2S/2C	small	thick	strong, large	Evensen and Hasle (1975)
C. coarctatus	b	4-6 sided	1S/2C	small	thick	strong, large	Hernández-Becerril (1991a)
C. dadayi	c	up to 8 sides	3S/2C	small	thick	strong, large	Hernández - Becerril (1992)
C. danicus	1	4-6 sided	1S/2C	larger, 3-5 per stria	thin	strong, very long	this study
C. densus	2	4 sided	1S/2C	small, 12-15 per stria	thin	strong, large	this study
C. eibenii	3	6 sided	n/2C	very small, irregullarly scattered	thick	strong, small	this study
C. peruvianus, *C. tetrastichon*	d	4 sided	3S/2C	small	thick	strong, large	Kooistra et al. (2010); Hernández - Becerril (1992)
C. pseudo-dichaeta	4	4 sided	2S/2C	small, 6-8 per stria	thick	4 types: capilli, dentate with capilli, dentate, strong	this study
C. rostratus	5	4 sided	5S/2C	small, 13-15 per stria	thick	strong, very long	this study

The observations on the ultrastructure of the *Chaetoceros* (*Phaeoceros*) Adriatic morphotypes generally agree with the descriptions from the literature, in spite of the different geographic origin. There is a lot of cryptic diversity in phytoplankton, and in genus *Chaetoceros* in particular (Kooistra et al., 2010) so there is a great possibility of divergence between populations. However, the fine morphology of the specimens from tropical flora (Hernández-Becerril, 1996) appears very similar to the Adriatic specimens in the case of the *Phaeoceros* species but without the molecular information we do not have any way to evaluate if we are dealing with different or same species. Nevertheless in the following some of the remarks and additional information taken from the literature on the species-specific features are given.

C. coarctatus- The posterior setae are for this species described as large, strongly curved, heavily spined and shorter than others. In EM very coarse, polygonal with 10 or more sides, and heavily armoured with spines, which run in longitudinal rows with some thickenings and pores scattered between them.(Hernández-Becerril, 1991a). This is different than in the Adriatic specimens where no such difference of the terminal from the intercalary ones was observed.

C. danicus- The observations from this study of the Adriatic strain are in concordance with the ones reported from literature with valve perforated with poroids, thickenings on the mantle edge

(Hernández-Becerril, 1996) and the seta structure. The difference is the central process, which is in this study either an oval hole without any elevation or with a small protrusion on the external side of the valve as in the strains reported from Gulf of Naples (Kooistra et al., 2010) or from the tropical-subtropical Pacific Ocean of Mexico (Hernández-Becerril, 1996) while by Jensen and Moestrup (1998) it was reported as a externally flat short tube from the specimens in Danish waters.

C. densus- From the inside view of the valve there is visible a mesh of small areolae ornamenting the bases of the setae, which agrees with the observations from the tropical seas (Hernández-Becerril, 1996) and it was found common with *C. danicus* and *C. coarctatus* (Hernández-Becerril, 1991a).

C. eibenii - Previous reports (Koch and Rivera, 1984) show the EM structure of valves and setae but in this study it is clear that in comparison with *C. densus* with which is often confused, the ultrastructure is quite different. The setae sides in *C. densus* have regular pattern of single rows of small areolae between not particularly thick costae while *C. eibenii* has thick costae between which are even smaller areolae irregularly distributed.

C. peruvianus - The valves are heavily silicified and perforated by poroids with the pattern of weak costae visible in anterior valve and lacking in the posterior one (Hernández-Becerril, 1996). Both valves possess an eccentric annulus and process with a simple hole on the interior side and a flattened external tube (Kooistra et al., 2010).

C. rostratus - In literature there is a discussion about distinguishing another species *C. glandazii* on the basis of linking spine length which some authors recognize as a morphotype with longer spine. However, in our culture material this proved to be a very variable character varying within the clonal strain between very short to very long. Therefore we consider this two species to be synonymous. The more stabile taxonomic character proved to be the ultrastructure of the setae which consisted of setae sides with 5 rows of areolae between 2 thick costae which is species-specific character together with the ability to form chains linking cells through fusion of the central spine and not setae. The previously described pattern (Hernández-Becerril, 1996) is 2 rows of areolae between two costae which is clearly different from ours and also from observations of Giuffre and Ragusa (1988). Other characteristics agree, also in the field specimens from tropical seas the variability of the linking spine length was observed and considered not to be a valid character to distinguish *C. glandazii*.

C. pseudodichaeta - Characteristic spines, absence of tubular or any kind of process from intercalary valves. It is apparently very similar to two other previously well known species: *C. dichaeta* and C. *atlanticus* Cleve, including the varieties of the latter species: *C. atlanticus var. neapolitanus* (Schröder) Hustedt and *C. atlanticus var. skeleton* (Schütt) Hustedt. However, if we compare their morphology, a number of distinctive features between the five taxa can be distinguished (Table 4.1.). Species was described in LM by Ikari in (1926) from samples from the Indian ocean, there was only one more observation by (Hernández-Becerril, 2000) where some of EM images were shown but without the no particular description of the spines. The unique character found in this species is the complete absence of the process on the intercalary valves. In all other species belonging

to the subgenus the process occurs in each valve, being eccentrically or centrally positioned (Hernández-Becerril, 1996, Evensen and Hasle, 1975, Kooistra et al., 2010, Hernández-Becerril, 1992). In some species it is in the form of the small protuberance on the external side and in others a long simple tube. In *C. coarctatus* numerous small processes can be found (Hernández-Becerril, 1991a) and in all of the species the process is found on all valves. On the other hand, in nearly all species of the subgenus Hyalochaete so far studied as well as in *C. bacteriastroides* the process is confined to the terminal cells (Hernández-Becerril, 1993).

Table 4.2. Comparison of morphological characteristics among similar species and varieties: *C. pseudodichaeta., C. dichaeta*, C. *C. atlanticus var.atlanticus, C. atlanticus var. neapolitanus* and *C. atlanticus var. skeleton.*

Feature	*C. pseudodichaeta*	*C. dichaeta*	*C. atlanticus var. atlanticus*	*C. atlanticus var. neapolitanus*	*C. atlanticus var. skeleton*
Apical axis; Pervalvar axis (µm)	4–13; 8–28	6–44; 13–48	10–40; 25–40	7–13; 6–25	10–17; 8–11
Aperture - Size (µm)	9–19	n.d.	n.d.	24–30	8–10
- Shape	rectangular	Rectangular	hexagonal	rectangular	hexagonal
Setae - Orientation	Brunel II, 3D space	Brunel II, 3D space	Brunel I, apical plane	Brunel I, apical plane	Brunel I, apical plane
- Origin	inside the valve margin	inside the valve margin	at valve corners	at valve corners	at valve corners
- Basal part	long	Long	short	long	short
- Shape	basal part broad, tapering toward tips	basal part broad, tapering toward tips	basal part narrow, broader toward tips	n.d.	n.d.
- Cross-section	4 sided	5-9 sided	4 sided	4 sided	4 sided
- Side wall pattern	2S/2C	longitudinal rows of large poroids	longitudinal rows of large poroids	2S/2C	2S/2C
- Spines	4 types	strong, large	strong, large	strong, large	strong, large
Valve - Mantle	high	low, higher with size reduction	high	low	very low
- Capilli on valve face	scattered on valve surface	along the valvar margin	no	no	no
- Poroid distribution	setae bases	setae bases, valve face and mantle	setae bases, valve face and mantle	setae bases, valve face and mantle	setae bases
Distribution	temperate areas (Adriatic)	Antarctic circumpolar / temperate areas	temperate areas	temperate/ subtropical distribution	temperate/ subtropical distribution
Source	this study	Asmy (2008)	Evensen and Hasle (1975), Cupp (1943)	Shevchenko (2008), Hernandez Becerril (1996)	Hernandez Becerril (1996)

4.1.2.2 Subgenus *Hyalochaete*

According to our findings, we can agree with Hernandez-Becerril (1996) in his definition of the important features for the taxa belonging to the subgenus *Hyalochaete*. These are indeed less robust forms and silicified to the lesser degree with many forms being very delicate and fragile. The important distinction from the taxa belonging to the subgenus *Phaeoceros* are the presence of thin setae without chloroplasts as defined by Gran (1897). The granules of some unknown chloroplast like-material are found in setae of several species (e.g. *C. brevis*) however, these do not have a photosynthetic capabilities and their function is unknown. Another difference is that only terminal valve in the chain possesses a process, which is lacking on all intercalary ones. The shape of the process is very variable, ranging from circular, slit-like to a flattened hollow with a true labiate structure inside. The valve is ornamented with the annulus from which a pattern of weak or strong costae radiates and rows of poroids run in between the costae. The resting spores are found in the majority of taxa.

In *Hyalochaete* among 32 analysed species, nine different structural design types were recognized with the subtypes in I, two in II and VIII type. All structural types belonging to the subgenus *Hyalochaete* and *Bacteriastroides* as well as to genus *Bacteriastrum* are shown in Figures 4.2. and 4.3. and the description of all types is presented in Table 4.2.

Chaetoceros cf. l*acinious* and *C. messanensis,* belong probably to group II, the most common type, according to the micrographs reported in Evensen and Hasle (1975) as well as *C. pseudocurvisetus* according to Hernadez Becerril (1996). *C. messanensis* common setae have apparently the same structure, with the special intercalary setae more strongly silicified and the spirally arranged spines more pronounced on the forked part. *C. subtilis* Shevchenko et al. (2006), and *C. throndsenii* var. *throndsenia* Marino et al. (1987) belong to type VIII, same as *C. cf. wighamii.*

Chaetoceros neocompactus, C. simplex, B. biconicum, C. throndsenii var. *trisetosa* were not determined, and no images were found available in the literature.

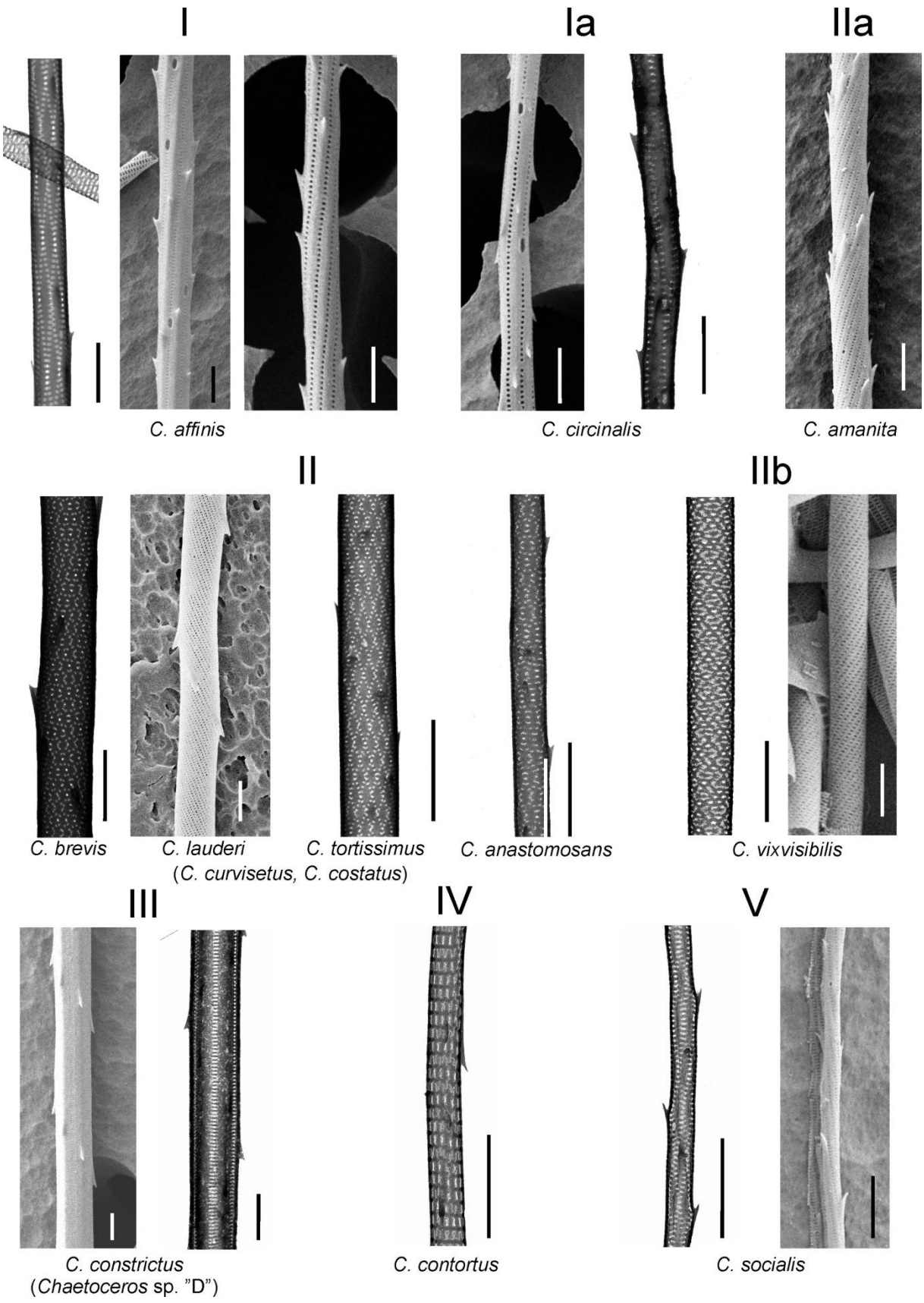

Figure 4.2. SEM micrographs of 8 structural types of setae in *Hyalochaete* subgenus observed within this study. The morphological characteristics of each type are described in Table 4.3. Scale bars 1 µm.

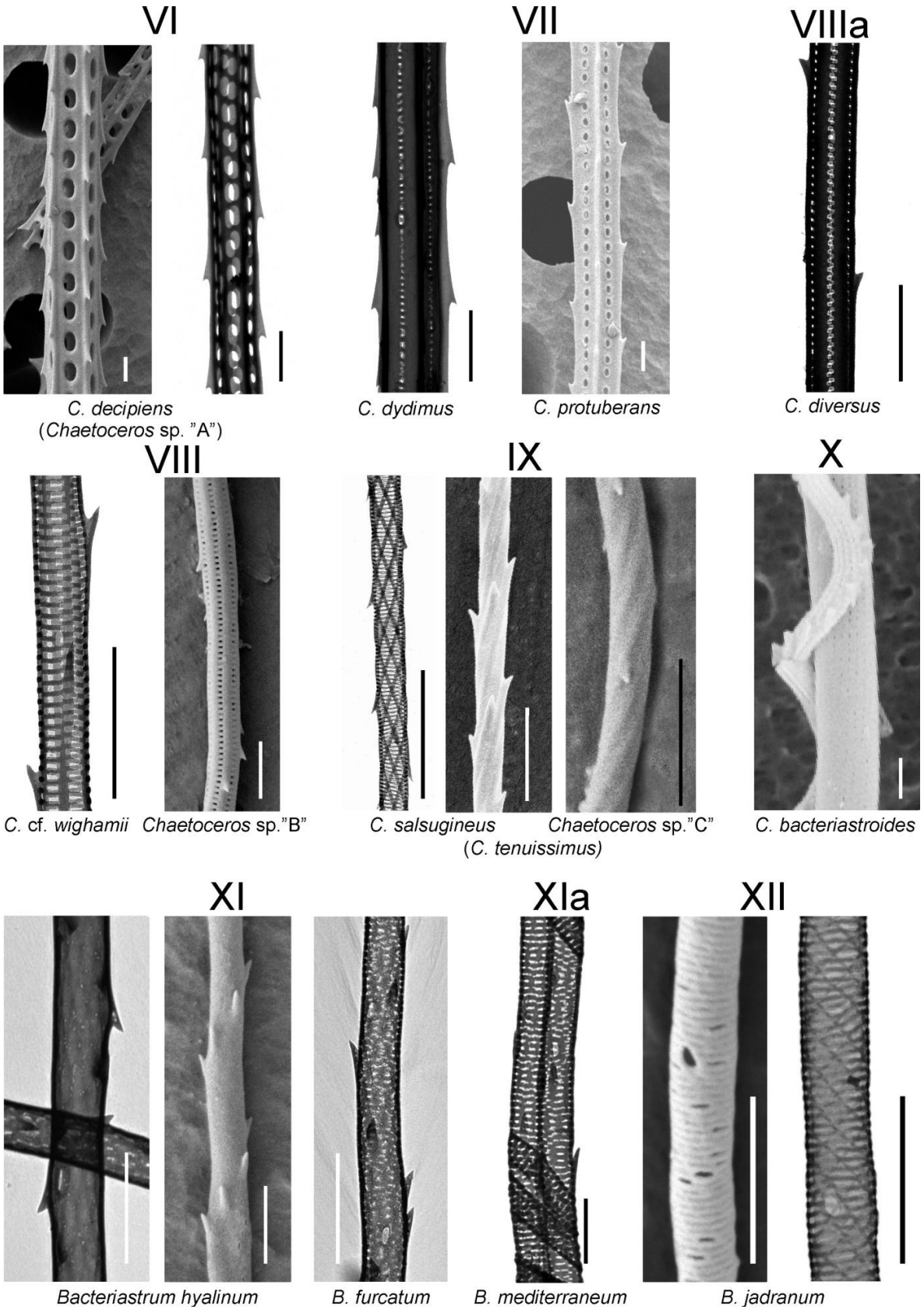

Figure 4.3. SEM micrographs of 5 structural types of setae in *Hyalochaete* subgenus (VI-IX), 1 in *Bacteriastroidea* (X) and 3 in *Bacteriastrum* (XI-XII) observed within this study. The morphological characteristics of each type are described in Table 4.3. Scale bars 1 µm.

Table 4.3. Ultrastructural morphological characteristics of setae structural types found in species belonging to subgenera *Hyalochaete* (I-IX) and *Bacteriastroides* (X) and genus *Bacteriastrum* (XI-XII). S – stria; C – costae.

Species	Type	Cross-section	Longitudinal strings	Transverse bars	Spines	Large oval pores	Remark
C. affinis	**I**	circular	wide, weak spiral pattern	very short, perpendicular/tilted to seta axis	small, spiral pattern	yes	terminal setae polygonal due to the fusion of straight strings
C. circinalis	**Ia**	circular	wide, straight	very short, perpendicular to seta axis	small, spiral pattern	yes	less number of strings than I, no specialized setae
C. anastomosans, *C. brevis*, *C. costatus*, *C. curvisetus*, *C. lauderi*, *C. tortissimus*	**II**	circular	numerous, thin, strong spiral pattern	short, perpendicular/tilted to seta axis	small, widely arranged in spiral pattern	no	the most common type
C. amanita	**IIa**	circular	numerous, wider than II, strong spiral pattern	very short, perpendicular to seta axis	small, closely arranged in spiral pattern	no	larger spines and more closely positioned than in II
C. vixvisibilis	**IIb**	circular	numerous, thin, strong spiral pattern	short, perpendicular/tilted to seta axis	no	no	same as II, spineless
C. constrictus, *Chaetoceros* sp. "D"	**III**	4 sided	wide, straight	thin, longer, perpendicular to seta axis	spiral pattern, situated on the ridges	no	
C. contortus	**IV**	circular	thin, same thickness as bars	long appear as rings around seta, perpendicular to seta axis	small, loosely arranged in spiral pattern	no	right angle between bars and strings forming reticulate pattern
C. socialis	**V**	circular	relatively thin	longer, perpendicular/tilted in relation to seta axis	small, loosely arranged in spiral pattern	yes	
C. decipiens, *Chaetoceros* sp. "A"	**VI**	4-6 sided	straight, bulged in a ridge in the middle	thin/thick, widely spaced, concave on both sides	strong, longitudinally on the ridges	no	space between bars forming large elliptical pores

Species	Type	Cross-section	Longitudinal strings	Transverse bars	Spines	Large oval pores	Remark
C. didymus, *C. protuberans*	**VII**	4 sided	straight, bulged in a ridge in the middle	thick, short, concave on both sides	small, longitudinally on the ridges	yes	larger pore corresponds to wider space between bars
C. diversus	**VIIIa**	circular	thick, straight/slightly twisted around the axis	thin, short, perpendicular to seta axis	small, spiral pattern	no	strings thicker than VIII, special setae have fused strings and more closely aranged spines
C. cf. *wighamii*, *Chaetoceros* sp. "B"	**VIII**	circular	not particularly thick, straight	short, perpendicular to seta axis	small/longer spiral pattern	no	
C. salsugineus, *Chaetoceros* sp. "C", *C. tenuissimus*	**IX**	circular	very thin, strongly twisted in a spiral pattern	long, thin, perpendicular to the axis	small, loosely in a spiral pattern	no	seta with uneven surface, strings thick
C. bacteriastroides	**X**	circular	straight, wide	extremely short, perpendicular/tilted in relation to seta axis	very small, spirall pattern	no	2 types of setae, spirally coiled with T spines, and common straight ones
B. furcatum, *B. hyalinum*	**XI**	circular	wide, spiral pattern	short, perpendicular/tilted in relation to seta axis	small, dense spiral pattern	yes	both straight and spirally twisted setae present. Often strings and bars fused in a smooth surface
B. mediterraneum, *B. parallelum*	**XIa**	circular	wide, spiral pattern	short, perpendicular/tilted in relation to seta axis	small, dense spiral pattern	yes	
B. jadranum	**XII**	circular	very thin, twisted in a spiral pattern	long, widely spaced, perpendicular to seta axis	no	yes	

The observations on the ultrastructure of the *Hyalochaete* Adriatic morphotypes generally agree with the descriptions from the literature, in spite of the different geographic origin. The discussion on the some of the questionable taxa and their species-specific features is presented in the following.

Chaetoceros affinis was found to be very morphologically variable taxon, particularly in regards to ultrastructural features such as presence of capilli on terminal valve surface or shape of the external part of the central process. The great variability was also observed and pointed out by other authors that investigated specimens of various geographic origin (Jensen and Moestrup, 1998, Rines and Hargraves, 1988). PMF E1 strain which was molecularly analysed within this study was found distinct from the strain isolated from the gulf of Naples (Kooistra et al., 2010), but the ultrastructure was very similar with the only difference in the possession of silica flap in the Adriatic strain. Interestingly, within the same clonal strain there were found two types of terminal valves, smooth as well as ornamented with capilli, and both types of processes, beak-like and flattened tube with the round end. General morphology of the taxon is very recognizable with very narrow slit-like aperture, long and straight setae belonging to Brunel Group I/II and common presence of the very thick and differently curved terminal setae. This morphotype is by some authors (Hustedt, 1930) regarded as a separate variety *C. affinis* var. *affinis.* It was a very commonly observed morphotype in the field samples from all investigated Adriatic locations. Three cultured strains, PMFC1, PMFC2 and PMFE1, showed in the time of their initial isolation the same characteristics; however this character was quickly lost in the culture and after several days there were observed chains with all setae of the same thickness. A distinct variety, *C. affinis* var. *willei* is by some authors (Hustedt, 1930) recognized by the same thickness of the terminal and the intercalary setae, shorter and more delicate colonies and narrower aperture. This variety is was described from the northern Atlantic Ocean by Gran (1897) as a separate species *Chaetoceros willei*, but proclaimed as a variety by Hustedt (1930). The ultrastructure of this morphotype is unfortunately not available in the literature neither is the information on the resting spores, so clearly more thorough investigation which includes the molecular information on this species complex is necessary. However, due to the fact that I observed wide range of morphologies in clonal cultures of isolated *C. affinis* var. *affinis* - like cells of which some specimens corresponded to the description of variation *willei*, here it is considered as a morphological variation of the type, agreeing with the conclusion of Jensen and Moestrup (1998).

Another variety, *C.* affinis var. *circinalis* was also distinguished by Hustedt (1930) by having characteristic intercalary setae that curve to form a semicircle, which in some cases surrounds the colony. The variety was raised to a species level by Jensen and Moestrup (1998). In this study, the fine structure of the Adriatic strain somewhat differed from the Danish one, in terms of the different structure of the setae. The micrographs from the Danish strain show setae belonging to the II type, similar to *C. curvisetus* and in this study setae were classified as type Ia with longitudinal strings and more similar to *C. affinis*. The corresponding character was the dense irregularly shaped perforations of the valves and shape of the process, as well as the distinct curvature of the setae and here it is also

considered as a separate species and not the variety level. Silica flaps were not observed, but hyaline rim was extended and fused between sibling cells at the edge of the apertures. Unfortunately, the resting spores were not observed

Chaetoceros brevis is another controversial taxon for which was pointed out by Rines and Hargraves (1988) that it is probably a "collecting ground" containing atypical forms of other taxa as the name is often assigned to differing material. There is a similar species *C. pseudobrevis* which is recognized as valid by Jensen and Moestrup (1998) and by Rines and Hargraves (1988) described as *Chaetoceros* sp. A. Both Hustedt (1930) and VanLandingham (1968) considered these two species as synonyms, and we did as well in this study for some smaller observed chains. *C. pseudobrevis* has also chloroplast like material in the setae but it is distinguished by smaller size, more delicate chains and less regularly arranged setae and no information on ultrastructural characters or resting spores is available. In this study, we found characteristic ornamentation of the valve, with darkened central area in the shape of the irregular patch on the valve face which can be considered as a species- specific characteristic. In Jensen and Moestrup (1998) the patch is not visible on the micrographs, but other morphological characteristics seem to correspond to the Adriatic strain.

Chaetoceros contortus is a species very similar to *C. compressus* in terms of both general morphology and ultrastructure (Rines, 1999). Both taxa share the same valve ornamentation with reticulate annulus and transverse ribs connecting costae as well as the structural design of the setae belonging to the type IV, but they differ in the shape and length of the special setae as well as more circular shape of the valve in *C. contortus*. In the present study, the feature emphasized by Rines (1999) and Jensen and Moestrup (1998) of the terminal setae being bent outwards with the large oval pore on their bases was not observed. The large elliptical pore on the part of the setae proximal to the valve was here found characteristic for *C. tortissimus*, and it was present in all setae, intercalary as well terminal ones. Another peculiar characteristics found in both analysed Adriatic strains (PMFCO1, PMFCO2) was the shape of the process. The previous EM observations (Jensen and Moestrup, 1998, Kooistra et al., 2010, Rines, 1999) show the process as a flattened and wide tube from the outside of the valve while a simple slit is present from the inside. In our study, the process was found to be a simple round hole which extends on the outside of the valve to a peculiar club-like tube, widened at its end. Another difference is in the morphology of the resting spores which in our LM observations corresponds to the one presented in figs 7 and 8 by Rines (1999). The both valves are rounded, or nearly flat and smooth. The siliceous sheath fissured at its end extending from the primary valve margin, reported by Kooistra et al. (2010) from SEM observations, but also mentioned by Rines (1999) is probably hard to observe in LM, therefore we cannot confirm this character. On the other hand, Ishii et al. (2011) describe a *C. contortus* spore from Japanese waters with a primary valve bearing very short spines which are also hard to observe in LM and lacking a siliceous collar. We can conclude that it is definitely necessary to observe spores of the Adriatic species in EM to be sure of their morphology. The same is necessary for the resting spore of *Chaetoceros curvisetus*, for which

only primary valve is found in our study, bearing a siliceous collar and it is not clear if the morphology is more similar to the one reported by Kooistra et al. (2010) which shows both valves with a collar, or only a primary one as in the paper by Ishii et al. (2011). Kooistra et al. (2010) discussed the possible cryptic diversity within this species but our observations here can indicate also possible pseudocryptic diversity as the observed strains from the Adriatic Sea showed the costae pattern which appears more complex and some costae ends are twisted into small spirals and these features were not observed in species from other geographic areas (Hernández-Becerril, 1996, Kooistra et al., 2010).

Chaetoceros decipiens is another species which has very complicated taxonomic relationships with similar taxa, such as *C. lorenzianus.* The criteria used until now for the differentiation of this two species, either in LM (Hasle and Syvertsen, 1997) or in EM (Hernández-Becerril, 1996) proved to be very variable and shared between the taxa, with the main delineating feature being the length of the fusion between sibling setae. Some recent studies (Kownacka et al., 2013) emphasize the importance of the presence of the resting spore, which formation is not known at all for *C. decipiens,* and very characteristic for *C. lorenzianus* with two elevations extended into branching spines on the primary valve (Ishii et al., 2011). Until more clearly defined taxonomic criteria are set up, here we consider all specimens to belong to *C. decipiens* sensu lato. The peculiar single celled morphotype isolated in cultures was designated as *Chaetoceros* sp "A". It was observed in short chains of two to three cells or solitary, and it was at first affiliated with *C. tenuissimus* according to the general appearance and the orientation of the setae. However, the EM observations revealed the ultrastructure corresponding to *C. decipiens*-like species. As no molecular data is available, we cannot know for sure if this strain represents the unicellular form of *C. decipiens*. In the time of initial isolation it had the same morphology which was not similar at all to *C. decipiens*, but there is a chance that we isolated the specimen which belonged to an old population and had the smaller cell size.

The morphology of *Chaetoceros diversus* agrees with the descriptions from the literature in terms of general appearance of the cells and setae, however there are differences in descriptions of the ultrastructure. In the Adriatic strain the valve pattern of annulus and costae is visible, which is different than observations of Hernandez Becerril (1996) who points out that no annulus can be observed. Another difference is in the setae design. Here it is visible that they are circular in cross section and not polygonal with 4-6 sides as it was previously described (Hernández-Becerril, 1996). The narrow apertures between sibling cells in our study are seen sometimes to be connected at their edges with the fusion of the silica extensions from the marginal ridge, but in study by Hernandez Becerril (1996) the apertures are partially occluded with very similar silica flap to the one observed in this study for *C. affinis* with the row of pores encircling the mantle edge. The morphotype *Chaetoceros* sp. "B" is very similar to *C. diversus* in terms of ultrastructure of the valve and setae, and it is clearly a solitary form as the process is present on each valve. There is a possibility that this type represents a solitary form of *C. diversus*, but the characteristically curved setae in U-shape were not

observed in the culture PMFDIV1, and this form was found present in the samples when *C. diversus* was not detected, therefore we designated it as a separate taxon.

In the case of two very similar species, *C. protuberans* and *C. dydimus* they were both found in the field samples and not isolated in cultures, therefore we do not have the observations on the terminal valve and the process. It is reported in both species to be located in the centre of the protuberance, externally appearing as a short tube-like projection in *C. protuberans* (Kooistra et al., 2010) and in *C. dydimus* as the slit-like structure encircled with small spines (Hernández-Becerril, 1996). The resting spores were not observed either. They are paired in *C. dydimus* with the attached setae and in *C.protuberans* single, with the primary valve bearing a long sheath. Nevertheless, the distinction between these two taxa was made on the basis of the long capilli present on the valves of *C. dydimus*, while valves of *C. protuberans* were smooth.

Chaetoceros vixvisibilis was originally described by Schiller from the Adriatic Sea and it was published in Hustedt (1930). It was decades later until the next report together with the remarks on the ecology of the species were published by Hernandez Becerril et al. (2010), with the author of this thesis as one of the co-authors. The conclusions and morphological description from this publication are confirmed in this thesis and added some additional information which contributes to the emended diagnosis of the species. The absence of spines on the setae can be considered a remarkable morphological feature: most species belonging to the family Chaetocerotaceae, which have been studied by EM so far, show the presence of, at least, minute spines, with an exception of *Bacteriastrum jadranum* and one long and straight setae in *C. socialis* (Hernández-Becerril, 1996). The basic setae design is the same as in all species belonging to the type II. The ornamentation of the valve was found to be quite specific. The pattern consists of the common annulus from which radiate bifurcating costae but the point of origin for some costae appears not to be at the annulus, but at the single point somewhere on the valve surface between the centre of the valve and the valve margin where the costae ends are twisted in small spirals. Similar feature was found in *C. tortissimus* but with the dots as origin instead of spirals. The process seems to have internally a labiate structure, which is found also for *C. decipiens*, *C: diversus* and in some specimens of *C. affinis*. The most distinctive feature of this very common Adriatic species is, however, the resting spores which are commonly present within the cells. Showing morphological variability, solitary spores have both valves convex to domed with a smooth surface or a surface with small granules, and one to four strong spines often branching dichotomically projecting from the primary valve. These resting spores appear unique among other members of the subgenus Hyalochaete, only superficially comparable to those occurring in *C. diadema* where the number of branching processes is more often between four to eight (Ishii et al., 2011, Sunesen et al., 2008). However, the spores of *C. diadema* can also have one or two branching processes as reported in (Kooistra et al., 2010) therefore, one should be careful and check carefully other features of the vegetative cells e.g. setae in *C. diadema* are polygonal/foursided (Kooistra et al., 2010) where in *C. vixvisibilis* they are circular and spineless. Another similar spore is

found in *C. lorenzianus* and *C. mitra* (Hasle, 1978): they have two large arms or branches with various smaller branches, although the number of large arms is always two which project from two conical elevations on the primary valve and the vegetative cells are quite different**.**

Surely, the largest taxonomic confusion exists among the various thin single celled species as well as among the thinly silicified "featureless" colonial morphotypes. The taxonomic status of quite a few species of *Chaetoceros* is still unclear, and further studies are needed to clarify this issue. The task is even harder as many of the species first descriptions are only drawings (iconotypes) and often without an indicated location of the holotype. Until now there have been some attempts to clear up this situation (Sar et al., 2002, Aké Castillo et al., 2004, Castillo et al., 1992), however the molecular information is crucial in the resolving the taxonomic and phylogenetic relationships and help in establishing clear delineation criteria. In this thesis, several of these species were isolated in culture, while some were observed in field samples and identified according to the currently valid taxonomic criteria. Some solitary, or short chain-forming species found in this study include *C. simplex*, *C. subtilis*, *C. throndsenii* with its two varieties var. *trisetosa* and var. *throndsenia* and are identified according to their setae orientation. The relationships between these and some similar taxa (*C. gracilis*, *C. vistulae*) we would not discuss here as they were observed only from field material and we do not have enough own data. The extensive discussion is available in Rines and Hargraves (1988) and Sar et al. (2002), and we did not found in this study no significant new information that would contribute to resolve their taxonomic position. Single celled species also include *C. tenuissimus* which was identified by the setae orientation at a 45 ° angle with the respect to both pervalvar and apical axes. This species was studied by Sar et al. (2002) and the results correspond to the morphology of the Adriatic species. However, its ultrastructure appears to be very similar to the morphotype identified as *C. salsugineus* in or study as well as to the one described in publication by Trigueros et al. (2002). These two species share the same ultrastructure of the valve as well as the design of the setae, with the single difference in the fissured hyaline rim present in *C. salsugineus*, therefore there is a possibility that this species in fact represents a colonial form of *C. tenuissimus*. The same setae structure is observed in the morphotype identified here as *Chaetoceros* sp. "C". It shows some resemblance with the description of *C. fallax* due to the presence of quite long tubular central process (Bérard-Therriault et al., 1999). The taxonomic position of *C. fallax* is also very controversial and it was considered as a synonym of *C. wighamii* (Jensen and Moestrup, 1998). *C. fallax* is apparently not well known species, with lack of information on the ultrastructure, reported usually as forming short chains of 2-4 cells with the tubular process on each cell. However, the presence of the processes in intercalary valves is actually the indication that division of the chain is in progress, as all investigated *Hyalochaete* species have the process only on terminal valves. Therefore, Jensen and Moestrup (1998) considered this species not to be valid. To conclude, in this study we considered these three morphotypes as distinct taxa: *C: salsugineus, C. tenuissimus* and *Chaetoceros* sp. "C", but we allow the possibility that these represent different morphological forms of the same species.

On the other hand, the species which was here designated as *Chaetoceros* cf. *wighamii* shows in LM the same general morphology of the vegetative cells as species described as *C. wighamii* (Jensen and Moestrup, 1998, Cupp, 1943, Hasle, 1978, Bérard-Therriault et al., 1999, Rines and Hargraves, 1988) with drawn up poles on the rectangular cells and irregularly oriented setae. However, the ultrastructure of the cultured strain PMFW2 observed here is very much different. It shares with *C: salsugineus* the strongly fissured rim on the marginal ridge, but it differs in the ornamentation of the valve with very irregular branching costae which sometimes start in spirally twisted ends. Moreover, the setae structure is similar to *C. diversus* with longitudinal strings and the external part of the process is a small prominence. In Jensen and Moestrup (1998) the presented morphotype has a hyaline rim, spiral pattern of the setae and external part of the process shaped as a flattened tube. Unfortunately, the resting spore was not observed here, but it is described to have a spiny primary valve, and smooth/spiny secondary valve constricted at its base. The cone-shaped secondary valve is usually characteristic for freshwater species (Rushforth and Johansen, 1986), and indeed *C. wighamii* is described as a species from brackish waters from the Baltic Sea. Castillo et al. (1992) concluded in their publication that the species originally described by Brightwell (1856) is actually what here is considered as *C. amanita*, and *C: bottnicus* Cleve, a synonym of *C. wighamii*, is a valid marine species. The authors presented the original iconotype from the Brightwell's publication and indeed it shows very high variability in spore morphology of which some drawings can correspond to *C. amanita* spore. *Chaetoceros perpusillus* Cleve is another species which was previously considered (Cupp, 1943, Rines and Hargraves, 1988) as a possible thinly silicified form of *C. wighamii*, but as its delineation characters are not clearly defined, and no ultrastructural information is available in the literature, we did not affiliate any of the observed specimens with this name.

Chaetoceros amanita was isolated from Vransko lake as a single freshwater species listed in thesis. There are apparently some twenty taxa described to live in low salinity waters (Kaczmarska et al., 1985) but only in several species morphology is thoroughly investigated. The isolated strain did not form resting spores, however the spores are found in the sediments from the same lake (Galović, personal communication). *C. amanita* observed in this study has peculiar characteristics of lacking any type of the process on all valves. It was also noted by (Kaczmarska et al., 1985) who observed field specimens and therefore the authors could not be sure if they indeed observed terminal valves. This peculiar feature is apparently shared with other freshwater species as it was noted by (Reinke, 1984) for *C. muelleri*. The same author proposed proposes that there is a general trend within the genus towards the progressive simplification of morphology from marine to freshwater.

In summary, a great taxonomic confusion between the aforementioned taxa and some other *C. wighamii* –like species present in the literature would deserve a dedicated extensive study including cultivation and molecular analyses of several strains isolated from different geographical area covering the locations where these species have been originally found, and this is beyond the scope of this thesis. Especially, there is in an urgent need for redefinition of *C. wighamii* circumscription as this

taxon is reported to be widespread in temperate/tropical environments as well as in the colder seas. In this thesis, the isolated morphotype is tentatively ascribed to *C. wighamii*, and the freshwater species to *C. amanita* according to Rines and Hargraves (1988) who considered these as a separate taxa and similar only in terms of the orientation of the setae.

4.1.2.3 Genus *Bacteriastrum*

The six *Bacteriastrum* species examined in this study can be clearly identified by the morphological characters observable by the light microscope, which coincides with the conclusions provided in the early works of Pavillard (Pavillard, 1924, Pavillard, 1925). The detailed comparison of the morphological features of Adriatic *Bacteriastrum* taxa found here with included three species previously reported from the area (Cupp, 1943) is presented in Table 4.4. Unfortunately, for this three species: *Bacteriastrum comosum, B. elongatum* and *B. elegans*, as well as for *B. biconicum* do not exist published EM observations on the ultrastructure and there is a clear need for it in the future studies. For solitary species *B. paralellum* a detailed morphological study has been published by (Hasle and Syvertsen, 1997) which includes both LM and EM observations. We observed here the fine morphology of only four species, and some discrepancies do exist between our results and those from other studies, which may have different explanations. In the following we will discuss the morphological characteristics of *Bacteriastrum furcatum, B. hyalinum, B. jadranum* and *B. mediterraneum* in a comparative way, attempting to extract those that are typical or apparently unique to the particular species.

The most informative characters in species delineation were found to be the ones associated with the general appearance of the colonies, particularly the mode of linkage between sibling cells and the setae orientation. Of all *Bacteriastrum* species, *B. parallelum* is until now the only known solitary form and it is very easy to identify due to the characteristic parallel orientation of the setae on both valves directed towards the posterior part of the cell. In field samples there are often present solitary forms of chain forming species, especially when species are in a bloom, or near bloom state of their cell cycle. They are often difficult to identify as the shape of setae can be somewhat distorted, but from *B. parallelum* they can be easily distinguished as in these species setae are always nearly parallel with the valvar plane, and not bend at an angle.

The pattern in vegetative growth of the colonial *Bacteriastrum furcatum* is illustrated by Fryxell (1930) and confirmed by observations of cultures within this study. After cell division the daughter cells detach from each other although they are held firmly together in straight and rigid chains by the fused setae. The fusion between two sibling intercalary setae is so strong that the individual valves when the frustules are separated still remain joined with sibling valve by the bifurcated setae. Therefore, the valves of colonial taxa could also be easily identified in LM if the dichotomously branching setae were observed. This, however, does not apply to terminal valves, which setae do not fuse, and to solitary forms. These valves posses the central process which can be observed in cleaned

material. The exception are the intercalary valves of *Bacteriastrum jadranum* where after the cell division, daughter cells detach and the distance between them increases without any observable contact between setae but the cells are held together in the loose chain-like colony by embedding them in the transparent organic material. The intercalary valves have no bifurcated setae and the process is present only on terminal valves.

Some other *Bacteriastrum* species also extrude organic matter, but unlike *B. jadranum* do not use it in a colony formation as their cells are connected via setae. The mucilage material around the *B. mediterraneum* chains was often observed in this study in cultured material and according to Ikari (1924) Cleve and Schroder mention gelatinous envelope around the chains of *B. hyalinum* but the author mentions that it is not always observable in a living condition. Another species which had in the original description illustration of an organic envelope-like structure is *Bacteriastrum minus* Karsten described from the Southern Ocean (Karsten, 1907). Together with *Bacteriastrum tenue* Steemann Nielsen which was described from the Indian Ocean (VanLandingham, 1968), these species were reported to form colonies only by crossing and not by fusion of the sibling setae at a certain distance from the cells, which is reported for *B. tenue* to be very large (½ to 2 of cell diameter). The original description of *Bacteriastrum jadranum* (Godrijan et al., 2012) described substantial apertures between the adjacent cells due to the point of crossing of sibling setae at distance of 2 – 3 times of the cell diameter. However this is not a valid observation, as the cells are completely detached from one to another and setae touch only by accident. Godrijan et al. (2012) failure to recognize the mode of colony formation in this species is by enclosing the cells in the cell jacket can be appreciated since the authors investigated the material without the staining methods as it was shown by Bosak et al. (2012a). Other two species *B. minus* and especially *B. tenue*, deserve certainly more attention because it is possible that they form colonies in the same way, but the obtaining of the fresh samples and its examination is probably very difficult as they are rarely reported in the literature (Fourtanier and Kociolek, 2011, Reinecke, 1969) and certainly were not observed in the Adriatic Sea.

The combination of setae bifurcation plane and shape and orientation of the terminal setae are proved to be reliable characters for the separation of other colonial species (Table 4.4.). Therefore, for an accurate identification, the chains should be observed in a complete form as it was emphasized before by Drebes (1967). It applies especially to the species from the section *Sagitatta* where the posterior setae are oriented completely different than the anterior ones, usually in a bell/umbrella shape. Both terminal setae of isopolar species are similar to the anterior setae in heteropolar species, and they are easily confused if only one part of the chain is observed, as it is probably in the case of *Bacteriastrum furcatum* and *B. delicatulum*. Observations by Sarno et al. (1997) clarified the asymmetric structure of *B. furcatum* colonies and included it in the section Sagitatta, which is confirmed here. In the case of *B. delicatulum* there is still a need for proper investigation which would include the examination of the cultivated strains to establish if this species is really isopolar, and defined some other species-specific delineating characters. Isopolar *B. hyalinum* may also be confused

with anterior part of the chain of *B. mediterraneum*, as both species have large number of setae per valve, and the same shape of the terminal and anterior setae, respectively. However, in this particular case, the clear distinction between two species is in the bifurcation plane which is parallel with the apical plane in the former, and with valvar in the latter species. Also, in *B. mediterraneum* the intercalary setae when observed in girdle view are curved in their forked part towards the posterior end, same as in *B. comosum.* In the case of *B. jadranum* description of the terminal setae morphology, here we propose a change from the original description by (Godrijan et al., 2012), where they are reported to be directed toward the chain at both ends. Here it is observed that they are also shorter from the intercalary ones, and more curved with the inner part bent inwards, but the outer part extended outwards from the chain forming a W-like shape in a girdle view.

Cell size and the ratio of the pervalvar to apical axis which tells us about the cell shape, being more or less elongated, are very unreliable characters as they are dependent on the stage in the life cycle of the individual species and with age the cells become smaller and more elongated. However, certain difference between generally smaller cell size of *B. furcatum* on one side and larger cell size of *B. hyalinum* and *B. mediterraneum* on the other side can be observed. It is also possible to differentiate that in *B. biconicum* and probably *B. elongatum* the cells are more elongated than in other species, with the p.a./a.a. ratio ranging between 0.3 and 0.5. The length of both basal and fused part of the intercalary setae proved not to be stabile characters as in the cultivated material were generally shorter than in natural samples and sometimes only crossed setae without any fusion were observed. On the other hand, if we compare for instance *B. hyalinum* and *B. furcatum,* it is visible that in the former, the fused part is indeed in most of the cases shorter than in the latter species, but the recommendation here is that it should not be used as a delineating feature.

Bacteriastrum hyalinum is distinguished from all other species in the genus as this is apparently the only taxon capable to produce resting spores which morphology and formation were described in details by Drebes (1972). The spore morphology is very similar to some *Hyalochaete* species, with the spiny primary valve bearing high sheath (collar) bent inwards at its end, similar to the spore of *C. protuberans* and *C. curvisetus* (Kooistra et al., 2010) and with secondary valve having the single ring of puncta at the advalvar margin, characteristic for all *Chaetoceros* spores (Ishii et al., 2011) . Our SEM observations confirmed the spore morphology previously described with LM in all aspects, and added the information about the ring of puncta and a granular surface of the primary valve mantle. Hargraves (1978) reported a description of the resting spore belonging to the species identified as *B. delicatulum* based on SEM observations. The closer look reveals that morphology actually corresponds to the *B. hyalinum* spore, except the surface of the primary valve is described as granulated and not spiny. There is a high probability that the author misidentified the vegetative cells as the micrographs (Figures 1 and 8) show the bifurcation of the sibling setae that could be in the apical plane and not in the valvar as it was described in the results. The source of the material was the preserved net sample from the North Atlantic Ocean and it is visible that in Fig.1. there are two

species present, one more similar to *B. hyalinum*, and other to *B. delicatulum*/*B. furcatum*. Another report of the *Bacteriastrum* resting spore is for *B. varians* in Ikari (1997) who described with the highly vaulted primary valve ornamented with minute spines, and the secondary one almost flat and smooth. Boalch (Okuno, 1962) examined the Lauder's type material and original descriptions, and apparently he described both *B. hyalinum* and *B. varians* from the same field material collected in Hong Kong, so there is a possibility that the *B. varians* spore reported by (Round et al., 1990) actually belongs to *B. hyalinum*. Moreover, the species *B. varians* was by Boalch observations indicated as a synonym of *B. furcatum*, which is the view also accepted by the author of this thesis, and here *B. furcatum* spores were not observed, neither in the study by Sarno et al. (1997).

Table 4.4. Main morphological characters useful for differentiating *Bacteriastrum* species reported from the Adriatic Sea. n.a. not applicable, n.d. not determined.

Character	*B. furcatum*	*B. hyalinum*	*B. jadranum*	*B. mediterraneum*	*B. paralellum*	*B. biconicum*	*B. elegans*	*B. elongatum*	*B. comosum*
Cell size									
- Apical axis (µm)	9–15	19–46	7–17	10–39	3-10	10–16	15-28	10-27	5-22
- Apical to pervalvar axis ratio	0.5	1	0.8	1	0.6-0.8	0.3	0.5	0.3-0.5	0.5
Colony									
- Cell linkage	setae fusion	setae fusion	cell jacket	setae fusion	solitary	setae fusion	setae fusion	setae fusion	setae fusion
- Chain length	3–17	6–49	4–41	1–29	n.a.	short	long	short	long
- Polarity	heteropolar	isopolar	isopolar	heteropolar	heteropolar cell	isopolar	heteropolar	isopolar	heteropolar
- Bifurcation plane	valvar	apical	n.a.	valvar	n.a.	valvar	valvar	apical	valvar
Setae									
- No. per valve	7-11	12-25	7-12	13-25	7-12	5-7	8-10	7-9	8
- Spirally twisted ends	yes	yes	no	no	no	yes	no	yes	no
- Basal part length	1.3–3.3	0.9–4.9	n.a.	0.9–1.4	n.a.	Long	Long	Short	Short
- Fusion length	19.0–25.3	11.2–17.5	n.a.	10.2–24.0	n.a.	long (>2 a.a.)	long (>2 a.a.)	Short	1-2 a.a.
- Origin	near valve margin	near valve margin	well inside valve margin	near valve margin	inside valve margin	inside valve margin	near valve margin	near valve margin	near valve margin
- Curved towards the posterior end	no	no	no	yes	yes, at an acute angle	no	yes	no	Yes
- Anterior /terminal shape in valve view	wide and strong curve	wide curve	straight	wide curve	-	straight	wide curve with strongly bent ends, strongly silicified	straight with hook- like ends, strongly silicified	wide curve with strongly bent ends
- Anterior /terminal shape in girdle view	parallel with valve/ proximally slightly bent inwards	inner part bent inwards	inner part bent inwards	inner part bent inwards	-	cone-like	parallel with valve/proximally slightly bent inwards	parallel with valve/proximally bent inwards	arched back towards the chain
- Posterior shape in valve view	straight	-	-	straight	-	-	straight, strongly silicified	-	straight, strongly silicified
- Posterior shape in girdle view	umbrella-like	-	-	bell-like	-	-	bell-like	-	long, bell-like

Table 4.4. continued

Character	*B. furcatum*	*B. hyalinum*	*B. jadranum*	*B. mediterraneum*	*B. paralellum*	*B. biconicum*	*B. elegans*	*B. elongatum*	*B. comosum*
Spine types	common on all setae, T-shaped on spirally twisted setae	common; Y shaped capilli on fused part ; T shaped	none	common	common	common	n.d.	n.d.	n.d.
Valve - Shape of central process	external short tube, internal round hole	external flattened tube, internal slit	external small prominence, internal slit	external small prominence, internal slit	external small prominence, internal round hole	n.d.	n.d.	n.d.	n.d.
- Distribution of pores	around the setae bases	all over the valve surface	none/smooth surface	all over the valve surface	around the setae bases	n.d.	n.d	n.d.	n.d
- Outgrowths	shoehorn-shape	T-shape	no	shoehorn-shape	shoehorn-shape	n.d.	n.d	n.d.	n.d
Resting spore	no	yes	no	no	no	no	no	no	no
Source	this study, Sarno et al. (1997), Fryxell (1978)	this study, Ikari (1927), Okuno (1962), Round et al. (1990)	this study	this study, Pavillard (1916)	this study & Sarno et al. (1997)	this study, Ikari (1927), Pavillard (1916)	Pavillard (1916)	Pavillard (1916), Ikari (1927)	Pavillard (1916), Ikari (1927)

Early TEM and SEM observations on the genus (Okuno, 1962, Rampen et al., 2009) revealed the basic structure of the valves looking remarkably similar to the species from the *Chaetoceros* section *Hyalochaet*e and here we agree with that notion. Observations of *B. furcatum* cultivated strain allowed the confirmation of the stability of most morphological characters which were considered important when the species was redefined by Sarno et al. (1997) and Fryxell (1978). The structure of the valves follows the general pattern of the costae radially branching dichotomously from the central annulus towards the valve margin. The surface of the valves is perforated by simple, small irregularly distributed pores and their distribution pattern differs among investigated species indicating a potential delineation feature. In *B. hyalinum* and *B. mediterraneum* the pores are distributed all over the valve surface and in *B. furcatum* they are restricted to the area around the setae bases similarly as shown for in *B. parallelum* in image 7 in the publication by Sarno et al. (1997). In the same paper, the pore pattern on the *B. furcatum* valves was not emphasized as important, but it was Fryxell (1978) who described similar pattern to the one found in this study with the pores distributed only on the mantle and around seta openings. The valve surface of *B. jadranum* is apparently completely smooth, without any perforations, which is again contrary with the original description by Godrijan et al. (2012) who report areolae perforating the valve surface.

The morphology of the central process was similar among all examined species, except in *B. furcatum* which had a process shaped externally as a short circular tube. In other species the process was shaped as a slit from the inner side of the valve with the external part ranging from only thickened edges of the slit in *B. mediterraneum* to a flattened tube in *B. hyalinum.* Generally, the shape of the central process in *Bacteriastrum* is very similar to other *Chaetoceros* species from the subgenus *Hyalochaete*, as first observed by Evensen and Hasle (1975) and confirmed here. The species from the subgenus *Bacteriastroidea, Chaetoceros bacteriastroides* has also a single process only on terminal valves, and it is reported to be a slit-like structure from the inside and a short protrusion to the outside (Fryxell, 1978, Hernández-Becerril, 1993). Another similar feature shared between *C. bacteriastroides* and other *Bacteriastrum* species are the short outgrowths projecting from the valve margin between two contiguous setae. These structures have not been observed in other *Chaetoceros* species, and they are common for all *Bacteriastrum* species examined here except for *B. jadranum*. Their function is unknown, but they are not characteristic only for the chain forming species as they are reported to appear also in the valves of solitary *B. parallelum* (Sarno et al., 1996). Usually there is only one outgrowth present between the setae, but according to Fryxell (Fryxell, 1978) there can be two as well. Their shape is narrower in the bases while it becomes wider near the end. In *B. hyalinum* they are differently shaped, with the wider and thinner end bar therefore it is similar to letter T while in other species the outgrowths can be better described as shoehorn-shaped. Unlike setae, they appear not as hollow structures but this is not confirmed with certainty as their cross-section is not possible to observe due to their closed ends.

The ornamentation of the girdle bands, same as the basic design of the valves, appears almost identical in all investigated species which makes it is impossible to morphologically distinguish the bands between taxa. The same conclusion is valid for all other previously examined *Chaetoceros* species (Evensen and Hasle, 1975) as well to the ones observed in this study. The intercalary bands are open with pointed ends which are ornamented with transverse parallel ribs, with small pores scattered in the interrib area. The only difference between species is in the number of indentations on the undulating margin of the connecting bands as this character depends on the number of setae in particular species.

The basic design of the setae is also very similar to the type II of the *Hyalochaete* group being composed of longitudinal strings in a helicoidal pattern interconnected with the short transverse bars. The observation put forward by Round et al (1990) that the *Bacteriastrum* setae differ from *Chaetoceros* setae because the first lack any type of fenestration is obviously wrong after the examination of four species in this study. The *Bacteriastrum* setae are in this study grouped in two distinct major types and one subtype due to few particular ultrastructural details. The setae in the majority of examined species are ornamented with small spines arranged in a helicoidal pattern around the setae, and perforated with irregularly distributed oval pores. In the part of the setae proximal to the valve the strings are often fused between each other and the surface of the setae in SEM appears smooth only perforated with oval pores. In *B. hyalinum* intercalary setae, the fused part is ornamented with short spinules with dichotomously bifurcated ends, the so-called Y-spines. These spinules were first observed and described by Round et al. (2010) and here they are considered to be a species-specific character. Similar capilli-like projections are found in the setae of *C. radicans* (Shevchenko et al., 2006) but they are much longer, often simple without dichotomously branched ends and distributed along the entire seta length. The ornamentation and the fine structure of the undulated part of the setae found in *B. hyalinum* and *B. furcatum* is remarkably similar to the ornamentation of the coiled small setae present in *Chaetoceros bacteriastroides* sharing the T- shaped spines and the surface covered with small silicate nodules. The undulated parts in other *Bacteriastrum* species e. g. *B. biconicum* unfortunately have not been investigated with the EM. *Bacteriastrum jadranum* setae are grouped separately in type XII due to the complete absence of spines. They are similar to *Chaetoceros vixvisibilis* grouped in type IIb which are spineless as well, but with a larger number of strings and much longer transverse bars. The *B. jadranum* setae also have oval pores which were not observed in *C. vixvisibilis*. The origin of the setae is in *B. jadranum* well inside the valve margin, much closer to the centre than in other examined species, therefore the valves of this species are very easy to recognize in cleaned material in LM as well as in EM. The original description of *B. jadranum* describes the setae composed of helicoidal and ring like costae (Godrijan et al., 2012), which is apparently a fail description due to the wrong interpretation of the structure of the setae visible in TEM micrographs.

The presented findings of the ML phylogenetic tree grouping of four molecularly investigated Adriatic strains confirms the separation of the genetically distinct species on the basis of a single marker, 28S (LSU) sequence. The sequences obtained in this study were included with several LSU sequences from other *Chaetoceros* species obtained in the study by Kooistra et al. (2010) in the phylogenetic analysis and it resulted in the confirmation of the conclusion that *Bacteriastrum* species form a lineage within the genus *Chaetoceros* which corroborates the view proposed in the same publication. However, for the drastic changes in the taxonomy there is still a need for a more thorough investigation which would encompass a larger number of strains and include also some other molecular markers. All four strains were recovered as a sister clade to the clade containing several *Hyalochaete* species but they were both recovered in a group distinct from species belonging to *Chaetoceros (Phaeoceros).* The relationships within the *Bacteriastrum* species revealed some unexpected relations. As shown previously, these four species can be clearly distinguished on the basis of their morphology. The only available LSU sequences in GenBank database were the ones belonging to *B. hyalinum*. The strains from both Gulf of Naples and Gulf of Mexico were found to be almost genetically identical to the strain from the Adriatic Sea, but all three strains were grouped with the Adriatic strain of *Bacteriastrum furcatum*. Morphologically, these species are very distinct, not only that each belongs to the different section, *B. hyalinum* to *Isomorpha* and *B. furcatum* to *Sagitatta*, but the plane of bifurcation is different and the *B. hyalinum* has an ability to form resting spores while *B. furcatum* does not. The ultrastructural characters are different as well, with some species-specific characteristics such as Y-spines on the setae of *B. hyalinum* and pore pattern on the *B. furcatum* valves. The common feature found for this two species is the setae design. In both species there are common intercalary setae as well as the setae with spirally twisted ends which are ornamented with T-spines, but this is also shared by *Chaetoceros bacteriastroides*. In conclusion, although there is a clear distinction between these two species based on a series of morphological features but these differences are not reflected in a clear differentiation of the LSU gene sequences. Hence, for the further clarification of the phylogenetic relationships and taxonomic status of these two species, other molecular markers such as ITS (internal transcribed spacer rDNA region) should be used such as in the case of distinguishing between *Pseudo-nitzschia pseudodelicatissima* and *P. cuspidata* which share LSU sequence but differ in ITS region (Amato et al., 2007). On the other hand, *Bacteriastrum jadranum* and *B. mediterraneum* both are very well recovered as separate species in the molecular tree which confirms their morphological differences. The resolution of species that belong to different sections (*Isomorpha* and *Sagitatta*) in a common clade suggests again the provisional use of these terms which seems not supported by the molecular data. However, the use of the sections in the genus *Bacteriastrum*, has unlike the section within *Chaetoceros* genus, more consistent assignment to each group and they are based on only single well established character, the polarity of the chain colony, while in *Chaetoceros* the morphological characters defining each section are very much doubtful (Rines and Hargraves, 1988). To conclude, further analyses on more *Bacteriastrum* strains should

clarify whether these and the other discrepancies mentioned above have an impact on the taxonomy of the whole family and that the taxonomic validity of two genera should be reappraised as it was indicated from the results obtained within this study.

4.1.3 The novel type of colony formation in marine planktonic diatoms, the case of *Bacteriastrum jadranum*

The diatoms from the family Chaetocerotaceae are known to produce large amounts of EPS with polysaccharides as the dominant component usually releasing them in the ambient water (Myklestad et al., 1989, Myklestad, 1995, Myklestad et al., 1972) and these substances are sometimes visible as a mucus sheath around the chain colonies with an optical microscope with water mounts in C. anastomosans and in *C. contortus* which they described as "pallium" around the chain bit it is clearly EPS mucus sheath (Jensen and Moestrup, 1998). Lot of species in this study were observed to produce EPS - and it is also noted by different authors such as (Rines and Hargraves, 1988) *C. costatus* cultures produce copious amounts of mucose material that can noticeably change the viscosity of the medium. They also noted for *C. cinctus* and *C. radicans* that these species secrete mucus which often contains debris. However, the primary means of association of adjacent cells in these species are always by interlocking or fusion of the siliceous setae and not by cell exudates. The presence of setae in members of the family *Chaetoceraceae* may act as a defence against grazing (Hamm and Smetacek, 2007) by injuring or hurting the digestive structures in some grazers, such as the filter-feeding apparatus in appendicularians (Troedsson et al., 2007). However, the *B. jadranum* setae are very delicate and completely enclosed within the polysaccharide jacket; therefore, we argue that their function is not defensive; rather, they represent the mechanical support and stabilisation of the colonial polysaccharide matrix. The *B. jadranum* chain colonies can be compared with the gelatinous colonies of some marine centric diatom species from the genus *Thalassiosira*, the cells of which are embedded in thick mucilage and extrude many chitin threads with the assumed role of reinforcing the organic matrix (Fryxell et al., 1984). The main difference between these *Thalassiosira* and *Bacteriastrum* colonies is that in the former, the colonies appear to be irregular clusters of the morphologically identical cells (Elbrächter and Boje, 1978) while in the latter; cells are regularly arranged in chains. Although there are a few *Cyclotella* species in which cells are united in ordered chain colonies without evident contact among valves (Prasad et al., 1990), the essential distinct feature of the *Bacteriastrum* chains remains the existence of the morphologically different end cells of the chain.

After carefully analyzing the structural details of jacket polysaccharide network we propose the model of network organization with patches and leading fibrils as basic structural elements. Such organization of the network would be stable enough to keep the integrity of the cell colony but porous enough to ensure nutrient transport and to allow flexibility of chain of singular diatom cells. To our knowledge, an ordered mosaic-like network of polysaccharide fibrils has not yet been reported in the literature. Similar structures were not found nor in marine gel networks collected from Northern Adriatic (Mišić Radić et al., 2011) nor in polymer networks produced by *Cylindrotheca closterium*

(Svetličić et al., 2011, Pletikapić et al., 2011b) or other diatoms such as *Navicula* spp. and *Nitschia* spp. species (unpublished data). Our results led us to the conclusion that the *Bacteriastrum* sp. polysaccharide jacket represents an essential part of the cell and not a random web like structure produced by self-assembly of extruded extracellular polysaccharides. The lack of studies focused on the structural aspect and not on the chemical composition of EPS released by the diatoms from the family Chaetoceraceae does not allow us to compare the ultrastructural features of the *Bacteriastrum* sp. network with the ones produced by the organisms of the similar taxonomic affiliation. Nevertheless, this study opens up some interesting, but neglected questions. Its worth of recalling that diatoms are able to synthesize a very large variety of species-specific highly ordered 3D silica structures designing their frustules (Hildebrand et al., 2009) so can we then assume that this also applies to the organization or production of the produced extracellular polymer networks? Knowing chemical heterogeneity of diatom EPS (Underwood and Paterson, 2003), are the driving forces and basic types of fibrils association characteristic for particular diatom species as could be hypothesized from our results? Do high density patches found in this study, represent specificity on microscale and if so, what are the differences in chemical composition leading to such self assembly and implication of this diversity for formation of marine gel particles? Clearly, in order to answer these questions more carefully designed experiments and observations from natural environment are needed in the future.

The unique way of *Bacteriastrum* sp. colony formation probably represents a very effective evolutionary strategy adapted in this diatom species as it uses EPS, the relatively energetically inexpensive by-product of photosynthesis (Decho, 1990) acquiring numerous additional important ecological advantages. By virtue of their physical properties (fibrillar nature), exopolymers are highly absorptive substances and can readily sequester and concentrate nutrients from the surrounding water (Decho, 1990). Hence they can allow efficient uptake of nutrients when concentration in nearby water is low acting as an active nutrient trap as suggested for the gel structure of the tube dwelling diatom *Berkleya rutilans* (Drum, 1969). The EPS matrix can also act as a chelator to complex chemical substances so it can trap trace metals otherwise hardly accessible to the cells or to provide protection against heavy metals and other toxins (Decho, 1990, Bhaskar and Bhosle, 2005). For example, recent studies proposed extrusion of greater amounts of polysaccharide-rich EPS as one of the detoxification mechanisms for the Cd^{+} , Cu^{+} (Pistocchi et al., 2000) and Ag^{+} (Miao et al., 2009) ions. Moreover, the EPS produced by *Cylindrotheca closterium* can have a protective role against silver nano-particles proven to be harmful for diatom cells (Pletikapić et al. submitted). Our observations of *Bacteriastrum* sp. material showed the bacteria commonly inhabit the *Bacteriastrum* sp. jacket polysaccharide matrix. The interactions between bacteria and planktonic diatom cells appear to be very important for both organisms in the marine environment (Grossart et al., 2005). Bacteria are using the polymer substances released by the diatoms thus providing the remineralized inorganic nutrients back to the cells. Furthermore, the bacteria or their extracellular substances can actively influence on the diatom secretion of extracellular carbohydrates and proteins (Bruckner et al., 2011).

The availability to grazers may have a substantial autoecological role as well. A coat of mucilage around the colony is probably an easiest way of defense, as it can ward of various attack systems from viruses to predators (Hamm and Smetacek, 2007). The grazers often feed more on single phytoplankton cells than the ones included in some form of mucus as found in *Phaeocystis* (Nejstgaard et al., 2007) or *Thalassiosira partheneia* (Schnack, 1983) so the embedding the cells in polysaccharide gel-like matrix in this species of *Bacteriastrum* may additionally provide a form of protection against predators. The presence of setae in members of the family *Chaetoceraceae* may act as a defence against grazing (Hamm and Smetacek, 2007) by injuring or hurting the digestive structures in some grazers, like filter feeding apparatus in appendicularians (Troedsson et al., 2007). However, the *Bacteriastrum* sp. setae are very delicate and completely enclosed within the polysaccharide jacket therefore we argue that their function is not defensive but they rather represent the mechanical support and stabilization of the colonial polysaccharide matrix. It can be compared to the gelatinous colonies of marine diatoms *Thalassiosiraceae* whose cells extrude many chitin threads with the assumed role of reinforcing the gel structure (Fryxell et al., 1984). The essential differences between *Thalassiosira* and *Bacteriastrum* sp. colonies are that in the former the colonies represent irregular clusters of the morphologically identical cells while in the latter in addition to the regular cell arrangement, the specialized heterovalvate end cells of the chain exist as well. This imposes the hypothesis that in *Bacteriastrum* sp. chain length is regulated by strict internal molecular control of the species itself and not by accidental clustering. Furthermore, the cells genetics and metabolism probably have some control over the regulation of the structure and extension of the polysaccharide gel network enclosing the colony as it is implied from the specific organization of the polysaccharide jacket network observed in this study.

4.2 *Bacteriastrum* and *Chaetoceros* species spatial distribution and previous misidentifications

The genus *Chaetoceros* is characterized by a large species diversity with reported ca. 170 valid taxa (VanLandingham, 1968). Although this number is probably largely overestimated this group is considered together with *Thalassiossira* to be the one of the most speciose, widespread and most common among the planktonic diatom genera (Rines and Hargraves, 1988). The published *Chaetoceros* floras from different marine environments which include micrographs and detailed morphological descriptions count from 20 taxa recognized in south-western Atlantic waters of Buenos Aires coastal area (Sunesen et al., 2008) to 46 taxa from tropical/subtropical Pacific ocean (Hernández-Becerril, 1996). Other areas include the Gulf of Mexico with recorded 42 taxa (Hernández-Becerril and Flores Granados, 1998), north-western Atlantic, Narrangasett Bay with 40 taxa (Rines and Hargraves, 1988), north-western Sea of Japan with 33 taxa (Shevchenko et al., 2006) and 35 taxa from inner Danish coastal waters, North/Baltic Sea (Jensen and Moestrup, 1998). The available checklists count similar number of species, as for example 26 taxa in the list from North Sea

around Helgoland (Hoppenrath, 2004) and 30 taxa from Western English Channel near Roscoff (Guilloux et al., 2013).

The Mediterranean Sea *Chaetoceros* species lists are much shorter than expected although the phytoplankton in this area is considered to be highly diversified and species-rich (Siokou-Frangou et al., 2010). The study which included only cultured strains from Gulf of Naples listed 13 species (Kooistra et al., 2010) while checklists from the north-western (Percopo et al., 2011), and south-western (Bouza and Aboal, 2008) Mediterranean report 19 and 27 species, respectively. In the context of these data, the Adriatic Sea flora counts 49 taxa found on the eastern (Viličić et al., 2002) and 78 taxa (varieties and forms included) on the western coast (Cabrini et al., 2010) although the closer look brings out the suspicion on the correct identification of some not so common morphotypes. In this thesis altogether 42 morphologically distinct taxa were recognized in the study period 2006-2012 of which 34 species, two varieties, two tentatively identified and four unknown morphotypes. The majority of the taxa found in this study are considered to be rather widespread in the temperate regions, such as *C. affinis* or *C. curvisetus* and reported in all of the previously mentioned taxonomic surveys. However, there are some taxa distributed in the tropical/subtropical regions which are often found in the Mediterranean such as *C. coarctatus*, *C. dadayi* or *C. diversus* (Hernández-Becerril, 1996). In this thesis, the Adriatic Sea checklist is supplemented by 5 species for the first time found in the area. *Chaetoceros bacteriastroides*, *C. neocompactus*, *C. pseudodichaeta* are taxa which are until now recorded only from the tropical/subtropical Pacific Ocean (Ikari, 1926, Ikari, 1928, Hernández-Becerril, 2000, Hernández-Becerril, 1993). C. *circinalis* and *C. salsugineus* are also previously not recorded from the Adriatic, with the former species reported from the North/Baltic Sea (Jensen and Moestrup, 1998) and the second with a disjunctive distribution from an estuary situated on the Atlantic coast of Spain (Trigueros et al., 2002) and from the Sea of Japan (Orlova and Selina, 1993).

The marine planktonic diatom checklists are susceptible to many corrections as the constant changes and discoveries in the taxonomy force the adjustment of names as it was the recent case of ex. *Skeletonema costatum* (Greville) Cleve (Sarno et al., 2005). The formerly identified as one cosmopolitan species it was recognized to be in fact, a complex of several species of which in the Adriatic there are only *Skeletonema marinoi* and *S. dohrnii* present (Kooistra et al., 2008). Another example is the potentially toxic marine genus *Pseudo-nitzschia* where the improved taxonomical resolution in recent years has brought several new descriptions of cryptic and pseudocryptic species (Amato and Montresor, 2008, Lundholm et al., 2002, Lundholm et al., 2003, Lundholm et al., 2006). In other phytoplankton groups, even the most familiar names to the phytoplankton taxonomists are recently changed such as the recent proposal in the change of marine genus *Ceratium* to *Neoceratium* (Gómez et al., 2010). Within such large and cosmopolitan genus as *Chaetoceros*, it is reasonable to suspect that there exists a huge undiscovered taxonomical diversity. In fact, some of the species are notoriously variable in their morphology, such as *C. contortus* (Rines, 1999) and probably represent a complex of cryptic/pseudocryptic species. The indications are found also in the study from Gulf of

Naples (Kooistra et al., 2010) where morphospecies such as *C. curvisetus* and *C. diadema* include several distinct genotypes. For *C. socialis* there is an evidence on physiological separation between two varieties from the cold-water and temperate region (Degerlund et al., 2012) Until now, there are no significant large changes in the taxonomy, however, this can be expected to happen in this genus in the following years.

Several doubts on the possible previous misidentifications of some Adriatic morphotypes will be presented here. The problematic identification of *C. decipiens/lorenzianus* is currently resolved with the presence of resting spores which are known only in the latter species (Kownacka et al., 2013). The previously considered important character for the differentiation of these two species was the length of the fusion between two sibling setae being longer in *C. decipiens* and shorter in *C. lorenzianus* (Jensen and Moestrup, 1998). In the Adriatic lists there are both species listed, with addition of *C. mitra* in the western coast (Cabrini et al., 2010). This species has similar spore morphology to *C. lorenzianus* but it is distributed mainly in cold waters (Tomas, 1997), so this record could in fact easily represent *C. lorenzianus sensu stricto.* The *C. decipiens/lorenzianus* in all the examined samples within this thesis did not form resting spores although in some occasions it was quite abundant, therefore it is proposed to attribute all the Adriatic specimens to the name *C. decipiens* in the publications from northern Adriatic (Viličić et al., 2009a), Lim Bay (Bosak et al., 2009) and Velebit and Pag Channel (Šupraha et al., 2011, Viličić et al., 2009b).

Another problematic identification is the one of *C. compressus*/*contortus* species. The morphology of these two taxa is reported to be extremely variable with the main distinguishing characters being the strong transapical compression of the valve outline and longer special setae in *C. compressus* (Rines, 1999). In some of the most used taxonomical literature for the phytoplankton identification e.g. (Tomas, 1997, Cupp, 1943), only *C. compressus* is described with a note of its common occurrence in great abundances in temperate and warm seas and with no mention of similar species *C. contortus.* This is due to the fact that these two species were considered as synonymous before the detailed study performed by (Rines, 1999). These two taxa were shown to be morphologically separated and corrected the previous identification of *C. compressus* to *C. contortus* of the morphotype from Narrangasett Bay (Rines and Hargraves, 1988). In addition, according to the same authors the two taxa have different distribution as *C. compressus* can be found in Indo-Pacific tropical seas, and *C. contortus* is cosmopolitan. In the study from Gulf of Naples (Kooistra et al., 2010) three strains were molecularly/morphologically identified as *C. contortus* and their description corresponds to the specimens found in our study. Therefore, in this thesis it is proposed to affiliate all the specimens to *C. contortus* in distinction from previous published data (Viličić et al., 2009a, Bosak et al., 2009, Viličić et al., 2009b, Šupraha et al., 2011).

The third problematic pair of species is *C. lauderi/teres.* The vegetative cells of these species are very much alike, but the resting spores are completely different, smooth and round in *C. teres* and with very distinct hairs and spines in the capitate primary valve of *C. lauderi*. The distribution of two

species is apparently different as well with *C. teres* characterized as a more cold water winter/spring species and *C. lauderi* present in warmer seas in summer/autumn (Hoppenrath et al., 2009). The proposed change to the lists excludes *C. teres* as the observed specimens were all present in the late spring to autumn period in addition to the often findings of the resting spores: northern Adriatic (Viličić et al., 2009a) and Lim Bay (Bosak et al., 2009).

Furthermore, the differences between the published north-eastern Adriatic checklist (Viličić et al., 2009a) include records of *C. atlanticus, C. convolutus, C. pseudocrinitus* and *C subtilis* which were sporadically present in the samples before 2006 but not identified afterwards by the thesis author and therefore not present in the list given in this study. Additional species found in this study for the north-eastern Adriatic include *C. peruvianus, C. constrictus, C.* cf. *laciniousus* and the separation of two varieties *C. throndsenii* var. *trisetosa* and var. *throndsenia*. In Lim Bay the differences between the species lists presented in the thesis and the one published (Bosak et al., 2009) include in the latter the identification of *C. convolutus* which was present before 2006 and *C. perpusillus* which identification is uncertain as these lightly silicified colonial forms need more detailed investigation using cultured strains and possibly EM observations. The species list from the Kotor Bay published in (Bosak et al., 2012b) is supplemented by subsequent findings in net samples of 8 taxa: *C. coarcatatus, C. eibenii, C. dadayi, C. rostratus, C.* cf. *lacinious, C. socialis, C. salsugineus Chaetoceros* sp. ”B”.

In the Adriatic checklists (Viličić et al., 2002, Cabrini et al., 2010, Cabrini et al., 2012) there are several small and lightly silicified colonial or single celled taxa which are poorly described and reported in the literature often only from a single source (Hustedt, 1930). These taxa include for example *C. paulsenii, C. criophilus, C. insignis, C. fragilis, C. rigidus, C. delicatulus* and *C. gracilis* and their identification has to be taken with caution until more taxonomic investigation is carried out. Other differences include previous records of *C. atlanticus, C. criophilus, C. convolutus, C. concavicornis, C. furcellatus, C. radicans, C. diadema, C. pseudocrinitus, C. holsaticus, C. debilis.* In this study formerly recorded *C. pelagicus* and *C. distans* are considered as the synonym of *C. laciniosus* but this group needs further investigations in order to clear the actual relationships between species (Jensen and Moestrup, 1998, Hernández-Becerril, 1996). Moreover, other probable misidentifications include *C. dichaeta* reported by (Cabrini et al., 2010) which is the species with strictly circumpolar distribution (Assmy et al., 2008) and probably mistaken for *C. pseudodichaeta* or for *C. atlanticus.* Obviously, the *Chaetoceros* taxonomic composition in the neritic areas is changing with time, therefor the data collected in this thesis will serve as a basis for further investigations.

The number of recorded taxa for the Adriatic Sea from the genus *Bacteriastrum* was relatively small with only six species. Nevertheless, this was expected due to the fact that the whole genus includes only 16 species recognized in the literature of which at least 3 are insufficiently described (Sarno et al., 1997) and some such as *B. tenue* and *B. minus* very rarely reported (Reinecke, 1969, Karsten, 1907). The *Bacteriastrum* diversity found in this study is higher than from other taxonomic studies from the Mediterranean Sea. For example, from the northwestern part there are only two

species reported (*B. comosum* and *B. furcatum*) (Percopo et al., 2011) and from southwestern part (Bouza and Aboal, 2008) only four although with both *B. furcatum* and *B. delicatulum* included. In colder seas the diversity is even lower, hence in the North Sea around Helgoland only one species *B. hyalinum* is found (Hoppenrath, 2004).

Among seven species from the eastern Adriatic checklist (Viličić et al., 2002) three of them were not found in this study (*B. delicatulum*, *B. elongatum* and *B. elegans*). The checklist from the western side (Cabrini et al., 2010) includes nine taxa among which the three aforementioned species together with *B. comosum* and a variety *B. hyalinum* var. *princeps* were not found in this study. The spatial distribution of recorded *Bacteriastrum* species shows that three species are found in all three parts of the Adriatic coast and differently from (Viličić et al., 2002) *B. biconicum* was not found in southern Adriatic. *B. jadranum* was a recently described species therefore its records will probably be more frequent and the distribution will spread in time, it was recorded in the northern and central Adriatic. In the study of the autumnal phytoplankton composition in Velebit and Pag Channel (Šupraha et al., 2011) *Bacteriastrum* sp. is in fact the first record and published micrograph of the species *B. jadranum*. *B. parallelum* was in this study for the first time recorded in the eastern coast although it can be found in the taxonomic list from the western side of the Adriatic coast (Cabrini et al., 2010). As mentioned in the comments part of the species descriptions (Chapter 3.1.3.) *B. delicatulum* identification was not confirmed in spite of often findings of similar specimens that could be ascribed to this morphotype. In all of the examined samples, the observed complete chains were heteropolar and more similar to *B. delicatulum*, and in case of observations of broken chains or only individual valves, the proper identity cannot be confirmed with certainty. *B. delicatulum* is commonly reported dominant species in the previous ecological studies conducted in northern (Revelante and Gilmartin, 1976, Cabrini et al., 2012), central (Burić et al., 2007) and southern Adriatic. Therefore, instead of *B. delicatulum* determined by Viličić et al. (2009a, 2009b, 2011) and Bosak et al. (2009, 2012b) the correct name should be *B. furcatum*. We can also doubt in the taxonomic validity of *B. hyalinum* var. *princeps*, as the spirally twisted ends of the setae were not stabile delineating character in this study, but this variety was not reported in aforementioned publications by thesis author.

4.3 *Chaetoceros* and *Bacteriastrum* seasonal dynamics and ecological relationships in NE Adriatic coastal zone

The eastern coastal Northern Adriatic Sea is generally characterized as an oligotrophic area due to the large influence of EAC which brings highly saline and low-nutrient water from the southern Adriatic coast (Cushman-Roisin et al., 2001). However, the whole basin was for many years considered to be a highly productive area with episodes of intensive phytoplankton blooms which resulted in occurrences of massive accumulation of gelatinous aggregates known as “mucilage events” (Rinaldi et al., 1995) often observed also near the eastern coast (Degobbis et al., 1995). This situation apparently changed since the beginning of 21st century with the ongoing a trend of oligotrophication in the north-eastern Adriatic which is visible in chlorophyll *a* data (Mozetič et al., 2010) and

biogeochemical parameters (Solidoro et al., 2009). The trend is ascribed to the reduction of the anthropogenic impact, mainly due to a substantial decrease of the nutrient loads in the River Po, particularly phosphorus and ammonia, and climatic modifications, resulting in a decline of atmospheric precipitations and, consequently, of the runoff in the northern Adriatic Sea (Giani et al., 2012). Within the first decade of 21st century the occurrence of the south-easterly Istrian Coastal Countercurrent (ICCC) was also much less frequent and contributing the larger influence of EAC (Djakovac et al., 2012).

In the study period during 2008/2009 the mean annual discharge of river Po was relatively low (Godrijan et al., 2013) therefore the conditions in the whole basin were mainly oligotrophic. However, in the first days of May 2009 there was an exceptionally high flow rate peak of the freshened water (Djakovac et al., 2012) which reached the eastern part of NE Adriatic and was the probable trigger for the summer diatom bloom which occurred in July 2009 along the whole Istrian coast (Godrijan et al., 2013). This event is evident in the surface decrease of salinity from 36 to 34 observed within the summer of 2009 at the station RV001, which markedly enhanced the water column stratification in addition to the summer heating of the surface layer. These spring/summer freshwater spreading events of the Po River plume as a thin surface layer over the North Adriatic basin are apparently a common phenomenon (Viličić et al., 2013, Djakovac et al., 2012). At the station RV001 the lower salinity coincided only with the slightly increased concentrations of orthophosphate, but not with elevated levels of other nutrients. The PCA results show that the samples with the highest concentrations of nitrate and silicate were actually the sampling dates when the lowest phytoplankton abundances were detected, in the beginning of June and in the end of the 2008 autumn bloom. The surface peak of nitrate was observed earlier in May 2009, and silicate in bottom layer later in October 2009. The elevated nitrate concentration in May apparently stimulated the growth of various planktonic diatoms both belonging to micro (e.g. *Pseudo-nitzschia pseudodelicatissima* species complex, *Cerataulina pelagica*, *Proboscia alata*, *Leptocylindrus danicus* and nano size class (e.g. *Cyclotella* spp., single celled *Chaetoceros* spp.). Of all the nutrients, the phosphorous is the one which strongly limits phytoplankton growth in the whole Mediterranean Sea (Siokou-Frangou et al., 2010), including the Adriatic basin (Bernardi Aubry et al., 2004, Viličić et al., 2009a). The phytoplankton can exploit the dissolved organic phosphorous by increasing their enzymatic activity of alkaline phosphatase which happens during late spring/summer period in north-eastern Adriatic (Ivančić et al., 2010). Although, the enzymatic activity of particular species was not investigated we can speculate that the summer diatoms are among the most responsible for this activity. Regardless of reduced nitrate levels later in July, the monospecific *Chaetoceros vixvisibilis* bloom was probably stimulated by the increased availability of orthophosphate associated with the freshwater discharge, which was previously shown to correlate with the increased abundances of this species (Hernández-Becerril et al., 2010) and corroborated with the results obtained in this study. Generally, the concentration of silicate is not considered to be limiting in this part of the north-eastern coast (Viličić et al., 2009a) and its

concentration was apparently high enough to sustain the growth of diatoms as they were found to be the dominant group in the microphytoplankton throughout the entire study period. Low levels of silicate were recorded coinciding with intensive diatom blooms in surface layer in autumn 2008 and at 5-10m in July 2009 indicating its utilization by the diatom cells. However, it was quickly replenished either by regeneration processes (Schultes et al., 2010) or by upward flux from the bottom layer.

The autumn diatom bloom recorded in 2008 was probably triggered by the water column mixing event which happened at the end of September and enriched the upper layers with nutrients stimulating the growth of autumn diatoms (*Chaetoceros* spp., *Pseudo-nitzschia* spp., *Nitzschia longissima, Asterionelopsis glacialis*). In the following year the mixing event did not occur until the end of October. The autumn bloom in 2009 apparently shifted towards end of November as it is shown in the study conducted along the Istrian coast in the same period (Godrijan et al., 2013). Interestingly, the late winter/spring bloom, the first annual phytoplankton bloom which has been defined as a unifying feature for the phytoplankton for the whole Mediterranean Sea (Ribera d'Alcalà et al., 2004) and otherwise typical for the North Adriatic area (Viličić et al., 2009a, Cabrini et al., 2012, Bernardi Aubry et al., 2012) was not observed during this study. Apparently, there was a change in the timing and composition of this bloom in recent decade, as in Gulf Of Trieste typical intensive blooms of main species *Skeletonema marinoi* were from 2003 onwards replaced with the lower bloom intensities of *Chaetoceros* spp. (Cabrini et al., 2012) and generally shifted towards summer (Mozetič et al., 2012). Unfortunately, the authors did not specify which species from the genus *Chaetoceros*, indicating them only as group *Chaetoceros* spp. or *Chaetoceros* cf. single. According to these studies, we can possibly interpret the observed *C. vixvisibilis* summer bloom as a time delayed spring bloom and conclude that the diatom population still kept the bimodal distribution of maxima, classical cycle for the temperate seas although with a time- shift of the first bloom occurrence. Usually the spring and autumn blooms differ in both terms of abundance and biodiversity, spring peaks are higher and due only one-two taxa while the autumn peaks are lower but with higher biodiversity. The two blooms have the different implications on the carbon cycling in the ecosystem. In particular, the intense winter blooms are mostly exported to bottom and only partly grazed by zooplankton (Fonda Umani et al., 2012) so we can assume that this was the fate of the *C. vixvisibilis* summer bloom. This is corroborated with the observed state of teh cells and abundance of resting spores which presumabely sank to the sea floor. On the other hand the autumn bloom is mainly consumed by the intense grazing activities and the energy transported further in the food-web (Fonda Umani et al., 2012).

The values of the total Chl *a* concentration were lower than 1 μg L^{-1}, which is an indication of oligotrophic conditions (Mozetič et al., 2010). Due to the size-fractionated Chl *a* values the phytoplankton was generally predominated by picophytoplankton and markedly contribuded by micro size-class during the period of increased diatom abundances. Together with the low contribution of nanophytoplankton to the total phytoplankton biomass these results are in concordance with similar studies in north-eastern (Šilović et al., 2012b), north-western (Bernardi Aubry et al., 2006) and south-

eastern (Bosak et al., 2012b) Adriatic. The noted discrepancy in July 2009 between absence of peaks in total and micro Chl *a* values and pronounced peaks in both microphytoplankton abundances and biomasses can be possibly explained with the growth stage of the bloom-responsible species *Chaetoceros vixvisibilis*. The observed chains were mostly composed of relatively empty cells with reduced cell content, containing large number of endogenous resting spores and therefore with a low Chl *a* content. This appearance of the cells indicates the population stage at the termination of the bloom period. The population probably reached its peak some days before the sampling occasion and we caught the bloom at its end stage. This is corroborated by the observed accumulation of the cells at and below the pycnocline indicating the sinking of the chains together with the resting spores very characteristic for the species from this genus, which provides the seeding population for the next bloom (Montresor et al., 2013). The species was present in the samples in the preceding sampling dates in May and June, although in not such high numbers. Taking into consideration also the observations from the 2008 autumn bloom, it is likely that the population dynamics of this species is such that it responds to the favourable conditions very quickly developing mass dense populations which do not last long and quickly disappear from the phytoplankton assemblage.

Chaetoceros vixvisibilis is one of the most remarkable and significant diatom species for the phytoplankton assemblage of the whole Adriatic Sea, including northern (Viličić et al., 2009a) as well as the southern basin where it was identified as a significant component of the spring bloom (Viličić et al., 1995). The environmental preferences of this diatom are previously identified in the study by (Hernández-Becerril et al., 2010) as the temperature between 12 and 17 °C which does not completely agree with the results obtained within this study where this species was observed in the seawater temperature higher than 19°C indicating even a greater thermotolerance. The thermophylic preferences of this species are further confirmed by the positive correlation which the *C. vixvisibilis* abundances showed with the temperature. On the other hand, the salinity between 33 and 38.8 with the concentration of phosphate 0.02 - 0.05 µmol L^{-1} agrees well with the conditions found in this study. For the more precise results on the actual ecological preferences, it would be necessary to isolate this species in the laboratory culture and investigate it in well designed experiments as it was done for instance for salinity tolerance in *Skeletonema marinoi* (Balzano et al., 2011), which unfortunately was not possible within this thesis.

The interesting successional pattern of *C. contortus* and *C. vixvisibilis* was found which were characterized as the most dominant phytoplankton taxa in this study as well as among all the investigated species of Chaetocerotaceae. Together with *C. decipiens* they were grouped by MDS analysis as these species showed three distinct peaks in their abundances throughout the study period. It appears that each time *C. contortus* abundance peak precedes *C. vixvisibilis* peak exactly for one sampling date. This could be explained by the different timing of the germination of resting spores which both species produce and which probably provides the seeding population from the sediments for their next appearance in the water column (Hollibaugh et al., 1981). In this way these species

would not be co-dominant in the assemblage being able to compete for the similar resources in the different time. However, *C. contortus* was found in study from Gulf of Naples, in spite of recorded spore formation not to form high numbers of benthic resting stages and hypothetisized that for these species planktonic inoculum is more important than benthic (Montresor et al., 2013). Therefore, the north Adriatic case could possibly represent an example of combination of two successful strategies, first of *C. contortus* population developing from low number of cells present in the plankton and being followed by germination of the *C. vixvisibilis* spores from the sediment. The effect of the top down control in these two populations seems as a highly unlikely explanation as these species appear very similar with very long chains and thin setae hence the zooplankton preferences probably would not differ between these two species. The third possibility is that each of these two morphologically perceived species in fact represents three distinct genetically different populations or cryptic species each with their own different timing of the bloom. As most of the investigated chateocerotacean species actually showed only one distinct peak in their abundances during the whole study period, except *C. affinis* and *C. decipiens* which could also represent species-complexes, we can assume that we did not detect the true diversity during the study and that the taxonomic resolution still needs to improve including preferably the molecular markers. Although the recent study of *C. socialis* (Degerlund et al., 2012) which is considered to be a cosmopolite bloom-former low as well as high latitudes, indicated the existence of pseudo-cryptic species with different physiological preferences among the northern and southern strains. In the same study strains isolated from both spring and autumn samples from Gulf of Naples showed no significant differences in molecular sequences (LSU) or in the growth rate, therefore we can also speculate that this could apply for some other species which exhibit a bimodal maxima distribution found in this study.

The Chaetocerotaceae species composition identified in this study generally agrees with the taxonomic lists provided in other recent studies from this area (Viličić et al., 2009a, Cabrini et al., 2012, Godrijan et al., 2013) although with some slight modifications which especially tackle the list of dominant species. The species previously identified as *Bacteriastrum delicatulum* was considered in this study as *Bacteriastrum furcatum* as the all observed complete colonies were heteropolar with the morphological attributes more similar to *B. furcatum* description and the true *B. delicatulum* isopolar chains were not found in any of the investigated samples. Another proposed change is of the species *Chaetoceros compressus* which was in this thesis identified as *C. contortus.* Bernardi Aubry et al. (2012) in his study of the phytoplankton time series from 30 year period in North Adriatic identified *C. compressus* as a key species responsible for the summer peak in July together with *Proboscia alata*. As previously mentioned, in our study this species occurred also in summer, although in the end of the June and not in such high numbers as in autumn. *Chaetoceros socialis* is another dominant species, recorded in higher abundances in the northern than in southern part of the Adriatic coast (Viličić et al., 2009a), which was in our study grouped with *B. mediterraneum* as both diatoms were dominant in early point of autumn 2008 bloom. Although in the western part of Adriatic it is recognized as a

typical spring diatom (Bernardi Aubry et al., 2004), in 2003 it was recorded to form an autumn bloom in November in the central part of the basin (Viličić et al., 2009a) which agrees with the results of this study.

In the North Adriatic area there is previously recognized large interannual variability of phytoplankton successions (Revelante and Gilmartin, 1976). The authors detected the interannual difference between dominant species during 1972 and 1973 with e.g. *C. diversus* prevailing in the summer of the first year while during the following year *C. curvisetus.* Their conclusion is that this variability reflects the significance of Po River nutrient input as a main driving force in shaping the phytoplankton communities. However, they proposed that the grazing rate by microzooplankton could also be an important factor, and the observed population explosions are the signal of uncoupling the phytoplankton from grazer populations and becoming bottom up regulated. In spite that the magnitude of abundance peaks of the main species and their timing may vary from year to year, the annual cycles of a single phytoplankton species are recognisable with a high degree of reliability (Bernardi Aubry et al., 2012, Cabrini et al., 2012). These rather constant patterns in species occurrence can be possibly explained by the phenological traits of individual taxa (internal, endogenous clocks) (Ribera d'Alcalà et al., 2004, Siano, 2007) which drive the seasonal changes in community composition rather than by the spatial and temporal variations of abiotic parameters. As a bloom can be defined as a significant increase in the population of phytoplankton species (Smayda, 1997) and it differs intrinsically among species, we cannot know if we do know well enough the behaviour of the population of each species to recognize the true point when it reaches the state identified as bloom. At any given time or spatial location one or more species are in state of bloom even though they may not reach high biomass or high population density. Although in this study the investigated period was limited to one year, we can draw some important conclusions and provide the information on seasonal evolution pattern of principal *Chaetoceros* and *Bacteriastrum* species including the ones which were not dominant in the phytoplankton assemblage.

The MDS analysis of samples with chaetocerotacean abundances clearly showed the succession of the species composition pointing out five distinct groups. The succession pattern can be partially explained by the environmental parameters in CAP analysis, with the temperature, silicate, salinity and phosphate as most important factors driving the community succession. Higher seawater temperature was responsible for grouping communities present from the late May till end of October together with the availability of silicate which was found to be significant for September/October communities in both investigated years. The community in the period from late May to the middle of August was apparently associated with warmer waters, low salinity and increased orthophosphate values. The winter/spring communities (except in March) were related mostly with nitrogen availability, in form of ammonia and nitrite, and negatively with temperature.

First group encompassed the samples from autumn and beginning of winter 2008 with the three sampling dates from the previously mentioned autumn bloom period positioned much closer on the

plot than the rest of the group indicating their greater similarity. The great diversity of *Chaetoceros* species in autumn was previously found for the Lim Bay (Bosak et al., 2009). It is known from other temperate coastal seas that in autumn it can simultaneously appear up to 15-20 different *Chaetoceros* species of which typically one to three species dominate. The bloom may be established rapidly and it may vanish again in only a few days but also it can last for several weeks and during this period a succession of species usually takes place (Jensen and Moestrup, 1998, Rines and Hargraves, 1988). In the end of September, the most significant species were *B. mediterraneum* and *C. socialis*, of 15 species detected in the water column. However, on this date the highest abundance peaks of species *C. affinis*, *C. brevis*, *C. rostratus*, *C. danicus* and *C. dydimus* were also recorded. In the next sampling date at the end of October, 20 species were present with *C. contortus* clearly dominating with still high abundances of both *B. mediterraneum* and *C. socialis* although in a declining phase. Only six days afterwards *C. vixvisibilis* predominated while the recorded number of species fell to 16 but with taxa such as *C. diversus*, *C. densus*, *C. costatus* and *C. peruvianus* reaching also their highest peaks in the study period. The diatom species of *Chaetoceros* genus which develop mass populations apparently escape the grazing pressure possibly due to the presence of setae (Schultes et al., 2010) and due to their inherently high growth rates, as it is found for *Pseudo-nitzschia* spp. which domoic acid toxin apparently had no influence on the predation rates by microzooplankton (Olson and Lessard, 2010).

After the autumn bloom termination, the species composition somewhat changed and the main bloom-forming species disappeared from the water column. Interestingly, *B. mediterraneum* and *C. socialis* again were present in higher abundances than other chaetocerotacean species, accompanied with the appearance of *C. curvisetus*. The early winter composition at the beginning of December was still found to be similar to the autumn one although with markedly lower abundances as well as the number of species detected in the water samples. The species number was actually high as great number of species was additionally identified from the net samples. The composition somewhat changed at the middle of December which is separated from the rest of the period in MDS plot as well as from the January /February samples, when only two species *C. danicus* and *C. cf. wighamii* were recorded from the water samples. The winter period is characterized by low light, homogenous water column but in this case of the station RV001 not particularly high levels of nutrients. The end of January and beginning of February separated winter community with species such as *C. eibenii*, *C. danicus* and *B. hyalinum.* These robust species are regularly present in colder seas e. g. North Sea (Hoppenrath et al., 2009, Hoppenrath, 2004) where they reach maximum abundances often as leading forms usually in summer months August/September. Late February was apparently another changing point in chaetocerotacean community which remained similar until the end of July with all sampling dates grouped together. In the late February/March/April, the typical vernal diatom bloom was absent and the still homogenous water column had very low nutrient concentrations. In these conditions only small single celled *Chaetoceros* species such as *C. tenuissimus*, *C. simplex*, *C. throndsenii* var. *throndsenia* and *Chaetoceros* sp. “B” were present although in low numbers, possibly due to their high

surface to volume ratio they were able to use the limited amount of available nutrients, as in the same period small celled picophytoplankton was also found abundant. The late May was characterized by high level of nitrate in the surface layer, which stimulated the growth of species *C. contortus, C. curvisetus, C. danicus, C. throndsenii* var. *throndsenia,* and *Chaetoceros* sp. "A". In June the community was replaced by *C. anastomosans* and *Chaetoceros* sp. "D" and in the end of this month when the heating of the surface started, the community was composed of 16 species, with a similar composition as in autumn bloom, but with *Bacteriastrum furcatum*, *C. cf. wighamii*, and *C. lauderi* appearing as previously not present.

The *C. vixvisibilis* post-bloom period was again characterized with low nutrient levels in the upper layer and stability of the water column. The last MDS group encompassed late August community and all other sampling dates until the end of investigated period in the end of October 2009. Different species were present in the autumn 2009 than in the previous year, except of *C. decipiens* and *C. affinis*, and it included *B. jadranum, C. tortissimus, C. anastomosans, C. lauderi* and they were all present in low abundances. It would be very interesting to know the composition of the following bloom in 2009 and if these species predominated, but unfortunately these data are not available.

4.3 Summer diurnal succession of *Chaetoceros* and *Bacteriastrum* species in Krka River estuary

The hypothesis for this part of the thesis was that the higher temporal resolution in sampling effort would resolve the dynamics on a fine temporal scale of selected *Chaetoceros* species during the period of their presumed high abundances. From the previous studies (Svensen et al., 2007, Šupraha, 2012, Cetinić et al., 2006) it was known that diatoms dominate in Krka River estuary in the warm period of the year. The small *Chaetoceros* species such as single celled *C. simplex* or chain forming *C. socialis* are recorded in high densities together with *Skeletonema marinoi, Cerataulina pelagica*, and pennate genus *Pseudo-nitzschia*. The summer period in the estuary is characterized by intensive water column stratification due to the combined effect of the salinity and temperature. The heating of the surface layer results in a development of the seasonal thermocline, typical for temperate seas during summer. The salinity in surface layer is decreased due to the freshwater riverine input in the estuary with halocline depth often coinciding with the thermocline (Svensen et al., 2007). The position of pycnocline was at ca. 2 m of total 10 m of depth with a constant stability throughout the whole week of study period. Unfortunately, for this study there are no available nutrient data, hence it is not possible to draw some significant conclusions on the ecology of the phytoplankton species. However, the published studies (Svensen et al., 2007, Cetinić et al., 2006) describe the summer distribution of nutrient levels as follows. Generally, the source of nitrogen and silicate is the freshwater surface inflow from Krka River, with the levels of these nutrients usually being lower in summer than in other seasons, due to their utilization by the phytoplankton cells and low river-runoff. For the halocline layer significantly increased nutrient levels are characteristic due to the intensive remineralisation processes

at the brackish/marine interface. During summer, the investigated station is under the influence of higher phosphate concentrations from anthropogenic sources of the nearby town of Šibenik which is recorded to be up to 3 times higher in the surface layer and at halocline than in the rest of the estuary (Svensen et al., 2007).

The Chl *a* concentrations show the similar trend in all sampling occasions, with the increased phytoplankton biomass on the halocline. This is related to the higher concentration of nutrients in the halocline, due to the decaying freshwater phytoplankton in the halocline (Viličić et al., 1989). The fucoxantin, biomarker pigment characteristic for diatoms (Viličić et al., 2008), generally follows the same distribution as the microphytoplankton was largely dominated by diatoms. Nanophytoplankton biomass had slightly different trend, as the dominant group in this size-fraction were found to be coccolithophorids, and their peak was recorded slightly below the halocline, in the marine layer at 2m of depth.

The diurnal oscillations in diatom cell numbers showed generally lower values in the morning (10:30) than in the afternoon (16:30); however the observed period is too small to draw some significant conclusions. There are limited number of studies found to deal with the diurnal variations in phytoplankton abundances (Ferguson Wood and Corcoran, 1966, Yentsch and Scagel, 1958, Türkoglu and Erdogan, 2010) and they all recognize a difference between the cell numbers in the morning and afternoon. (Türkoglu and Erdogan, 2010) found in their study of summer phytoplankton community in the Dardanelles, diatom growth capacity is much higher early in the day (08:00-09:00) compared to afternoon (18:00- 19:00), and they correlated it with the increased nutrient influx in the morning period of the day. In this study, as already mentioned nutrient data are no available, we can only assume the similar driving force for the observed variations in phytoplankton/diatom densities.

The composition of dominant taxa agreed with the previously reported summer diatom species (Cetinić et al., 2006, Svensen et al., 2007) and all of them are known to prefer nutrient enriched conditions. The slight difference found in this study is the identification of *Chaetoceros* cf. *salsugineus* which is apparently very similar to *C. wighamii* in morphology. Although the true relationship between these two taxa is not well resolved, the former species is reported to form dense populations in other estuarine environments (Trigueros et al., 2002) and it corresponds well in morphology to the Adriatic species. Another modification is the recognized two distinct varieties of *C. throndsenii*, which were in former studies considered together as one taxon. The first record for this estuary is the *Pseudo-nitzschia galaxiae*, a potentially toxic diatom species which was present in relatively high abundances (Cerino et al., 2005).

The closer look on the list of *Chaetoceros* and *Bacteriastrum* species shows that most of these taxa are found in other locations in the Adriatic Sea (Chapter 3.3. of this thesis). Interestingly, 27 species were recorded simultaneously present in the water column. That is higher diversity than recorded in the summer/autumn period in the study done in north eastern coastal RV001 station (Chapter 3.4.1). The dominant species were generally most abundant at the pycnocline depth with *C:*

diversus, C. throndsenii var. *throndsenia* and *C. throndsenii* var. *trisetosa* as most abundant in the afternoon on the second day of sampling. The next peak followed the next sampling occasion, in the morning of the the third day, but with different species: *C. affinis*, *C. curvisetus*, *C.* cf. *salsugineus* and *C. socialis.* In the afternoon on the same day, *C. socialis* and *C.* cf. *salsugineus* were still highly abundant, but also *C. cf. wighamii* reached its peak.

CHAPTER 5

CONCLUSIONS

"I may not have gone where I intended to go, but I think I have ended up where I intended to be."

Douglas Adams (1951 – 2001)

Thus far the study of planktonic diatom taxa belonging to the genera *Bacteriastrum* and *Chaetoceros* from the Adriatic Sea has been included in the general studies on phytoplankton seasonal dynamics and spatial distribution. Overall, a little attention has been paid to the species from these genera although these diatoms are ecologically important in the area as they represent a constitutive component of the phytoplankton and often develop dense populations. Therefore, the aim of this study was to give a detailed overview of the morphology and taxonomy of chaetocerotacean species found along the eastern Adriatic coast and with the improved taxonomic resolution contribute to the information on their spatial distribution, seasonal dynamics and ecological relationships. Based on the findings in this dissertation we can make the following conclusions.

5.1 Morphology and taxonomy of Chaetocerotaceae

- The species descriptions accompanied by photographical illustrations were provided for 49 morphologically distinct taxa including 25 taxa identified from 48 cultivated strains. Six species were affiliated with genus *Bacteriastrum* and 43 with genus *Chaetoceros* of which 10 taxa belong to subgenus *Chaetoceros* (*Phaeoceros*), 32 to subgenus *Hyalochaete* and one to subgenus *Bacteriastroides*. The list includes 41 species, two varieties, two tentatively identified taxa and four unknown morphotypes designated as *Chaetoceros* sp. “A”, “B”, “C” and “D”. The emended diagnoses based on new morphological and/or molecular information on 3 species which had been originally described from Adriatic Sea, *Chaetoceros vixvisibilis*, *Bacteriastrum jadranum* and *B. mediterraneum*, are provided
- The morphological analysis helped to clarify previously common misidentifications in the dominant Adriatic species in cases of *Bacteriastrum furcatum/B. delicatulum, Chaetoceros contortus/C. compressus, C. decipiens/C. lorenzianus* and *C. lauderi/C. teres.* The analysis showed that in all analysed material only first species from the given pair could be identified.
- Majority of Adriatic *Chaetoceros* species can be identified using the morphological characters visible with light microscopy, but it was found that some species could be further recognized in electron microscope due to certain species-specific ultrastructural features. According to their importance in species identification we classified the individual morphological characters into 3 groups: not important, moderately important and very important.
    - Not important characters are generally recommended not to be used in the identification due to two main reasons: 1) The characters are not variable among the investigated species, as for example is the case of the girdle bands structure. 2) The characters are variable but not species-specific. These include features that vary depending on the cell age, such as the cell size or the girdle height, and features that vary even among cells of a single chain, as, for example, length of the fusion between sibling setae, length of the setae and position of the process on the valve face. These differences have been observed both in cultivated strains and in natural populations.

- Moderately important characters are considered the features which are quite stabile in the natural populations, but are susceptible to variations depending on environmental conditions (phenotypic plasticity). In cultures they should be determined as close as possible to the point of the initial isolation as they are prone to change during the prolonged period of cultivation. These features include: usual growth form (either solitary or colonial), length of the chain, shape and size of aperture, degree of silification, shape of the valve face, depth of the indentation of the constriction near the mantle edge, silica flap/projections from the marginal ridge, shape of the terminal process and finally the length of the setae basal part.
- Very important characters appear to be species-specific and are recommended to be used in the morphological taxa identification are: mode of colony formation, shape of the chain, polarity of the cells/chain colony, number of chloroplast per cell, their shape and their presence or absence in the setae, the presence of capilli or protuberances on the valve face, presence and number of processes, number of setae per valve, setae orientation, direction and thickness. Resting spore morphology was shown to be one of the most important features, especially in the subgenus *Hyalochaete.*

- The ornamentation pattern of the valve was found to be a very important character in several species, although all investigated specimens had the same basic design consisting of mostly central annulus from which the dichotomously branching ribs extend towards the valve margin. A unique valve design lacking any type of annulus but with very dense anastomosing costae was found in *Chaetoceros amanita*. *Chaetoceros contortus* has a complex network of reticulate annulus and transverse ribs between the main ones. *Chaetoceros costatus* shows a peculiar pattern with costae becoming parallel with the apical axis in proximity of the valve apices, *C. tortissimus* has dots in correspondence with the point of origin of some costae and *C. vixvisibilis* has spirals. *Chaetoceros brevis* has an irregularly shaped darkened patch in the central area of the valve.
- In addition to the presence of various projections and process on the valve face, the distribution of the pores perforating the valve surface was found to be significant in some species such as *Bacteriastrum furcatum* which has pore only around setae bases and on the mantle and *B. jadranum* which has a smooth surface.
- Particular attention was paid to the investigation of the structural design and ornamentation of the setae as these are the main morphological elements characteristic for this diatom group. This character was found to vary markedly among the members of subgenus *Chaetoceros* (*Phaeoceros*) with 9 different structural types in 10 investigated species. All *Chaetoceros* setae contain small chloroplasts, are polygonal in cross section, and are ornamented with strong spines. The design of non–containing chloroplasts setae in subgenus *Hyalochaete* was more uniform across species with a predominately circular cross-section. Among 32 analysed species 9 ultrastructural types were found with four additional subtypes. The setae of the species *Chaetoceros bacteriastroides* apparently belong to a separate type but more TEM investigations are necessary. In genus *Bacteriastrum* we distinguished

three different types of setae. Both *B. jadranum* and *C. vixvisibilis* have spineless setae, a remarkable characteristic until now found only in these two species.

- Some of the controversial features were clarified such as the presence of groove at the suture often mentioned in the previous species descriptions which was shown to represent rather the constriction near the edge of the valve mantle. Several terms were introduced for the description of newly discovered structures, such as cell jacket in *Bacteriastrum jadranum* or silica flap for the structure covering the aperture in *Chaetoceros affinis.*
- Several distinctive morphological characteristics were found for species *Chaetoceros pseudodichaeta* (subgenus *Phaeoceros*), originally described from the tropical/subtropical Pacific Ocean and recorded for the first time in the Adriatic Sea in this thesis. The species has four peculiar types of spines, some of them remarkably silicified, succeeding along the setae. In addition, differently from all the species belonging to the subgenus, a long tubular process is only present on the terminal valves and it is lacking on the intercalary valves.
- In the molecular phylogenies based on 28S (LSU) *Bacteriastrum furcatum* and *B. hyalinum* cluster in a well-supported clade sister to a clade comprising *B. jadranum* and *B. mediterraneum*.
- In the first pair, although there is a clear morphological distinction these differences are not reflected in a clear differentiation of the LSU gene sequences. Hence, for the further clarification of the phylogenetic relationships and taxonomic status of these two species, other molecular markers such as ITS should be investigated. The molecular data confirmed the separation of the morphologically distinct species *B. jadranum* and *B mediterraneum*. In relation to other *Chaetoceros* species all *Bacteriastrum* species were recovered as a sister clade to the clade containing several *Hyalochaete* taxa but they were both recovered in a group distinct from species belonging to *Chaetoceros (Phaeoceros).* These results imply that that *Bacteriastrum* species form a lineage within the genus *Chaetoceros*, but for the drastic changes in the taxonomy there is still a need for a more thorough investigation which would encompass a larger number of strains and include larger number of molecular markers.
- The novel mode of colony formation in marine planktonic diatoms was found and described within this thesis. *Bacteriastrum jadranum* forms chain colonies by enclosing the cells within an optically transparent organic matrix called “cell jacket” while all other members of the family link cells in inseparable chains by interlocking/fusion of the siliceous structures. Visualisation of the general layout of the structure with Alcian Blue staining showed the long setae completely enclosed within the jacket and indicated that the jacket’s principal components are acidic polysaccharides. Using AFM, we showed that at the nanoscale the optically transparent organic matrix appears as a cross-linked fibrillar network organised in recognisable structure. The circular patches of a self-repeating pattern composed of hexagonally shaped pores are connected through thicker surrounding fibrils and reinforced by branching fibrils. The well-defined and regular shape on the microscale, as well as the ordered structure on the nanoscale, indicate that the *B. jadranum* cell jacket represents an

extended, but nevertheless essential, part of the cell This is further supported by the facts that the conjunction of the polymer network with the frustule appears to be extremely tight and such specific and unique patterns have never been found in self-assembled polysaccharide gel networks usually encountered in the marine environment.

5.2 Species spatial distribution, seasonal dynamics and ecological relationships

- The Adriatic Sea checklist was supplemented by 5 species found for the first time in the area. *Chaetoceros bacteriastroides*, *C. neocompactus*, *C. pseudodichaeta* have been until now recorded only in the tropical/subtropical Pacific Ocean. *Chaetoceros circinalis* and *C. salsugineus* are also previously not recorded from the Adriatic. The former species has been reported from the North/Baltic Sea and the second with a disjunctive distribution from an estuary situated on the Atlantic coast of Spain and from the Sea of Japan. Additionally, the freshwater species *C. amanita* was recorded from Vransko lake.
- The ecological study in Adriatic eastern coastal area during 2008/2009 showed that, out of 36 dominant diatom taxa, 7 species belonged to *Chaetoceros* and 3 to *Bacteriastrum.* Different species were present in different periods of the year with a change in dominance and a clear annual succession pattern. Most of species showed only one peak in their abundance, while some had more than one (3 maximum).
- The 2008 autumn bloom was investigated in detail and the relationship between *C. contortus* alternating with *C. vixvisibilis.* Vernal bloom was lacking, and instead summer 2009 was characterized by a spreading of freshwater from river Po up to the eastern coast triggering the monospecific *C. vixvisibilis* bloom in correspondence with an increased availability of phosphate.
- The multivariate analysis done only with chaetocerotacean species showed the existence of five distinct groups of species pointing out a seasonal succession in phytoplankton composition. For autumn 2008 bloom *C. contortus* and *C. vixvisibilis* were most significant, but also *B. mediterraneum* and *C. socialis.* In winter 2008/2009 *C. danicus*, *C. eibenii*, *B. hyalinum* but also small chain-forming species *C.* cf. *wighamii*. Early spring 2009 was characterised by small single celled *C. tenuissimus*, *C. throndsenii* var. *throndsenia* and *Chaetoceros* sp. "B", *C. simplex*. In late spring intensive development of diverse community similar to autumn was observed with addition of *C. curvisetus*, *C. danicus* and *Bacteriastrum furcatum*. In July 2009 a monospecific bloom of *C. vixvisibilis* was observed while in autumn 2009 a diverse community composed of *C. decipiens* and *C. affinis* with *B. jadranum, C. tortissimus, C. anastomosans, C. lauderi* was recorded.
- The succession pattern can be partially explained by the environmental parameters, with the temperature, silicate, salinity and phosphate as most important factors driving the community succession.

5.3 Perspectives for future research

The perspectives and possibilities opened up by the results of this research are numerous. The subjects of this thesis were the crucial and omnipresent taxa in the coastal environments which deserve more attention in the future. The information gathered in this dissertation can represent a first step towards the clearing up of some of the taxonomic confusions existing in the family.

- As most problematic taxa were identified:
    - *Chaetoceros wighamii* and its relationship with *C. amanita* and *C. fallax*. *Chaetoceros salsugineus* and its interrelationships between *C. tenuissimus* and many other single celled and weakly silicified colonial morphotypes.
    - *Chaetoceros affinis* due to the great morphological and molecular variability which indicates the existence of possible pseudocryptic species within the taxon. Its relation with *C. willei* (*C. affinis* var. *willei*) needs also further investigation.
    - *C. brevis* and its relationship with *C. pseudobrevis.*
    - *C. laciniousus* and its relation to *C. pelagicus* and similar taxa.
    - *C. decipiens*, *C. lorenzianus* and morphotype *Chaetoceros* sp. "A to set up more clearly defined taxonomic criteria for identification of each species.
- More investigation of resting spores of greater number of species is necessary.
- Ultrastructural information should be supplemented for *Bacteriastrum biconicum, B. comosum, B. elongatum, B. elegans* and *Chaetoceros neocompactus.*
- Further studies on morphological variation through the life cycles in the cultivated material are highly recommended to elucidate valid species but also for *C. eibenii* to investigate the formation of resting spores.
- Molecular information should be supplemented on greater number of species with *C. vixvisibilis* as one of the priorities.
- More investigation on the taxonomic relationship among the *Bacteriastrum* and *Chaetoceros* genus.
- The issue on colony formation in diatoms in general, and in the whole family Chateocerotaceae. What are the environmental triggers and genetic foundation for determining the length of individual chains, the shape of the colony or the shift from solitary to colonial habit?
- More carefully designed experiments are needed on the exopolymeric substances extruded by the cells, and their autoecological role in chaetocerotacean species.
- The ecological role of setae and their evolutionary origin.
- The better resolution on autumn bloom in Adriatic. The results from this thesis showed that it is possible to distinguish a succession on a fine scale, but an investigation that would include more frequent sampling during the bloom should be conducted.

CHAPTER 6

BIBLIOGRAPHY

ADL, S. M., SIMPSON, A. G. B., LANE, C. E., LUKEŠ, J., BASS, D., BOWSER, S. S., BROWN, M. W., BURKI, F., et al. 2012. The Revised Classification of Eukaryotes. *Journal of Eukaryotic Microbiology*, 59**,** 429-514.

AKÉ CASTILLO, J. A., GUERRA-MARTÍNEZ, S. L. & ZAMUDIO-RESÉNDIZ, M. E. 2004. Observations on some species of *Chaetoceros* (Bacillariophyceae) with reduced number of setae from a tropical coastal lagoon. *Hydrobiologia*, 524**,** 203-213.

ALLDREDGE, A. L., PASSOW, U. & LOGAN, B. E. 1993. The abundance and significance of a class of large, transparent organic particles in the ocean. *Deep Sea Research Part I: Oceanographic Research Papers*, 40**,** 1131-1140.

AMATO, A., KOOISTRA, W. H. C. F., LEVIALDI GHIRON, J. H., MANN, D. G., PRÖSCHOLD, T. & MONTRESOR, M. 2007. Reproductive isolation among sympatric cryptic species in marine diatoms. *Protist*, 158**,** 193-207.

AMATO, A. & MONTRESOR, M. 2008. Morphology, phylogeny, and sexual cycle of *Pseudo-nitzschia mannii* sp. nov. (Bacillariophyceae): a pseudo-cryptic species within the *P. pseudodelicatissima* complex. *Phycologia*, 47**,** 487–497.

ANONYMOUS 1975. Proposals for a standardization of diatom terminology and diagnoses. *Nova Hedwigia Beiheft*, 53**,** 323-354.

ARMBRUST, E. V., BERGES, J. A., BOWLER, C., GREEN, B. R., MARTINEZ, D., PUTNAM, N. H., ZHOU, S., ALLEN, A. E., et al. 2004. The genome of the diatom *Thalassiosira pseudonana*: ecology, evolution, and metabolism. *Science*, 306**,** 79-86.

ARTEGIANI, A., BREGANT, D., PASCHINI, E., PINARDI, N., RAICICH, F. & RUSSO, A. 1997. The Adriatic Sea general circulation. Part I: Air-sea interactions and water mass structure. *Journal of Physical Oceanography* 27**,** 1492-1514.

ASSMY, P., HERNÁNDEZ-BECERRIL, D. U. & MONTRESOR, M. 2008. Morphological variability and life cycle traits of the type species of the diatom genus *Chaetoceros, C. dichaeta*. *Journal of Phycology*, 44**,** 152-163.

BAILEY, J. W. 1854. Notes on new species and localities of microscopical organisms. *Smithsonian Contributions to Knowledge*, 7**,** 1-15.

BALZANO, S., SARNO, D. & KOOISTRA, W. H. C. F. 2011. Effects of salinity on the growth rate and morphology of ten *Skeletonema* strains. *Journal of Plankton Research*, 33**,** 937-945.

BARLOW, R. G., CUMMINGS, D. G. & GIBB, S. W. 1997. Improved resolution of mono- and divinyl chlorophylls a and b and zeaxanthin and lutein in phytoplankton extracts using reverse phase C-8 HPLC. *Marine Ecology Progress Series*, 161**,** 303-307.

BECKER, B., HOEF-EMDEN, K. & MELKONIAN, M. 2008. Chlamydial genes shed light on the evolution of photoautotrophic eukaryotes. *BMC Evolutionary Biology*, 8**,** 203.

BENOVIĆ, A., LUCIĆ, D., ONOFRI, V., PEHARDA, M., CARIĆ, M., JASPRICA, N. & BOBANOVIĆ-ČOLIĆ, S. 2000. Ecological characteristics of the Mljet Islands seawater lakes (South Adriatic Sea) with special reference to their resident populations of medusae. *Scientia Marina*, 64**,** 197-206.

BÉRARD-THERRIAULT, L., POULIN, M. & BOSSÉ, L. 1999. *Guide d'identification du phytoplancton marin de l'estuarie et du golfe du Saint-Laurent incluant également certains protozoaires (Guide to the identifying marine phytoplankton of the estuary and gulf of St. Lawrence including certain protozoans)*, Ottawa, Publication spéciale canadienne des sciences halieutiques et aquatiques.

BERNARDI AUBRY, F., ACRI, F., BASTIANINI, M., PUGNETTI, A. & SOCAL, G. 2006. Picophytoplankton contribution to phytoplankton community structure in the Gulf of Venice (NW Adriatic Sea). *International Review of Hydrobiology*, 91**,** 51-70.

BERNARDI AUBRY, F., BERTON, A., BASTIANINI, M., SOCAL, G. & ACRI, F. 2004. Phytoplankton succession in a coastal area of the NW Adriatic, over a 10-year sampling period (1990-1999). *Continental Shelf Research*, 24**,** 97-115.

BERNARDI AUBRY, F. B., COSSARINI, G., ACRI, F., BASTIANINI, M., BIANCHI, F., CAMATTI, E., DE LAZZARI, A., PUGNETTI, A., et al. 2012. Plankton communities in the northern Adriatic Sea: Patterns and changes over the last 30 years. *Estuarine, Coastal and Shelf Science,* 115**,** 125-137.

BHASKAR, P. V. & BHOSLE, N. B. 2005. Microbial extracellular polymeric substances in marine biogeochemical processes. *Current Science,* 88**,** 45-53.

BOALCH, G. T. 1974. The type material of the diatom genus *Bacteriastrum* Shadbolt. *Nova Hedwigia, Beiheft,* 45**,** 159-163.

BOALCH, G. T. 1975. The Lauder species of the diatom genus *Bacteriastrum* Shadbolt. *Nova Hedwigia Beiheft,* 53**,** 185-189.

BOSAK, S., BURIĆ, Z., DJAKOVAC, T. & VILIČIĆ, D. 2009. Seasonal distribution of plankton diatoms in Lim Bay, northeastern Adriatic sea. *Acta Botanica Croatica,* 68**,** 351-365.

BOSAK, S., PLETIKAPIĆ, G., HOZIĆ, A., SVETLIČIĆ, V., SARNO, D. & VILIČIĆ, D. 2012a. A novel type of colony formation in marine planktonic diatoms revealed by atomic force microscopy. *PLoS ONE,* 7**,** e44851.

BOSAK, S., ŠILOVIĆ, T., LJUBEŠIĆ, Z., KUŠPILIĆ, G., PESTORIĆ, B., KRIVOKAPIĆ, S. & VILIČIĆ, D. 2012b. Phytoplankton size structure and species composition as an indicator of trophic status in transitional ecosystems: The case study of a Mediterranean fjord-like karstic bay. *Oceanologia,* 54**,** 255-286.

BOUZA, N. & ABOAL, M. 2008. Checklist of Phytoplankton on the South Coast of Murcia (SE Spain, SW Mediterranean Sea). *In:* EVANGELISTA, V., BARSANTI, L., FRASSANITO, A., PASSARELLI, V. & GUALTIERI, P. (eds.) *Algal Toxins: Nature, Occurrence, Effect and Detection.* Springer Netherlands.

BOWLER, C., ALLEN, A. E., BADGER, J. H., GRIMWOOD, J., JABBARI, K., KUO, A., MAHESWARI, U., MARTENS, C., et al. 2008. The *Phaeodactylum* genome reveals the evolutionary history of diatom genomes. *Nature,* 456**,** 239-244.

BRADBURY, J. 2004. Nature's Nanotechnologists: Unveiling the Secrets of Diatoms. *PLoS Biology,* 2**,** e306.

BRAY, D. F., BAGU, J. & KOEGLER, P. 1993. Comparison of hexamethyldisilazane (HMDS), Peldri II, and critical-point drying methods for scanning electron microscopy of biological specimens. *Microscopy Research and Technique,* 26**,** 489-495.

BRIGHTWELL, T. 1856. On the filamentous long-horned Diatomaceae, with a description of two new species. *Quarterly Journal of Microscopical Science,* 4**,** 105-109.

BRUCKNER, C. G., REHM, C., GROSSART, H.-P. & KROTH, P. G. 2011. Growth and release of extracellular organic compounds by benthic diatoms depend on interactions with bacteria. *Environmental Microbiology,* 13**,** 1052-1063.

BRUNEL, J. 1966. Normalisation de la terminologie des soies dans le genre *Chaetoceros*. *Naturaliste Canadien,* 93**,** 849-860.

BRUNEL, J. 1972. Orientation of setae in the genus *Chaetoceros,* in regard to the apical axis. *Journal of the Marine Biological Association of India,* 14**,** 315-327.

BURIĆ, Z., CETINIĆ, I., VILIČIĆ, D., CAPUT-MIHALIĆ, K., CARIĆ, M. & OLUJIĆ, G. 2007. Spatial and temporal distribution of phytoplankton in a highly stratified estuary (Zrmanja, Adriatic Sea). *Marine Ecology,* 28**,** 169-177.

CABRINI, M., BERNARDI AUBRY, F. & GUARDIANI, B. 2010. Microphytoplancton Le diatomee / diatoms. *Biologia Marina Mediterranea,* 17**,** 686-753.

CABRINI, M., FORNASARO, D., COSSARINI, G., LIPIZER, M. & VIRGILIO, D. 2012. Phytoplankton temporal changes in a coastal northern Adriatic site during the last 25 years. *Estuarine, Coastal and Shelf Science,* 115**,** 113-124.

CAMPANELLI, A., BULATOVIC, A., CABRINI, M., GRILLI, F., KLJAJIC, Z., MOSETTI, R., PASCHINI, E., PENNA, P., et al. 2009. Spatial distribution of physical, chemical and biological oceanographic properties, phytoplankton, nutrients and coloured dissolved organic matter (CDOM) in the Boka Kotorska

Bay (Adriatic Sea). *Geofizika,* 26**,** 215-228.

CASTILLO, P. M. S., LEON, M. A. U. & ROUND, F. E. 1992. Estudio de *Chaetoceros wighamii* Brightwell: un taxon mal interpretado. *Diatom Research,* 7**,** 127-136.

CASTRACANE, F. 1875. Contribuzione alla florulla delle Diatomee del Mediterraneo ossia esame del contenuto nello stomaco si un salpa pinnata pescata a Messina. *Atti dell'Accademia Pontificia de'Nuovi Lincei,* 28**,** 377-396.

CERINO, F., ORSINI, L., SARNO, D., DELL'AVERSANO, C., TARTAGLIONE, L. & ZINGONE, A. 2005. The alternation of different morphotypes in the seasonal cycle of the toxic diatom *Pseudo-nitzschia galaxiae*. *Harmful Algae,* 4**,** 33-48.

CETINIĆ, I., VILIČIĆ, D., BURIĆ, Z. & OLUJĆ, G. 2006. Phytoplankton seasonality in a highly stratified karstic estuary (Krka, Adriatic Sea). *In:* MARTENS, K., QUEIROGA, H., CUNHA, M. R., CUNHA, A., MOREIRA, M. H., QUINTINO, V., RODRIGUES, A. M., SEROÔDIO, J. & WARWICK, R. M. (eds.) *Marine Biodiversity.* Springer Netherlands.

CHEPURNOV, V. A., MANN, D. G., SABBE, K. & VYVERMAN, W. 2004. Experimental studies on sexual reproduction in diatoms. *International Review of Cytology,* 237**,** 91-154.

CLARKE, K. R. & GORLEY, R. N. 2006. *PRIMER v6: User Manual/Tutorial,* Plymouth, PRIMER-E.

CLARKE, K. R. & R.M., W. 2001. *Change in marine communities: an approach to statistical analysis and interpretation, 2nd edition.,* Plymouth, PRIMER-E.

CLEVE-EULER, A. 1915. New contributions to the diatomaceous flora of Finland. *Arkiv för Botanik,* 14**,** 1-81.

CLEVE, P. T. 1873. Examination of diatoms found on the surface of the sea of Java. *Bihang Till Konglica Svenska Vetenskaps-Akademiens Handlingar,* 11**,** 3-13.

CLEVE, P. T. 1889. Pelagisk Diatomeer från Kattegat. *In:* PETERSEN, C. G. J. (ed.) *Det Videnskabelige Udbytte af Kanonbaaden "Hauchs" Togter i de Danske Have Indefor Skagen, I. Aarene 1883-86.* Kjøbenhavn: Andr. Fred. Høst & Sons Forlag.

CLEVE, P. T. 1896. Redogörelse för de svenska hydrografiska undersökningarne februari 1896. V. Planktonundersökningar: Vegetabilskt plankton. *Bihang till Kungliga Svenska Vetenskapsakademiens Handlingar,* 22**,** 1-33.

CLEVE, P. T. 1897. *A treatise of the phytoplankton of the Atlantic and its tributaries and on the periodical changes of the plankton of Skagerak,* Uppsala, P.T.Cleve.

CLEVE, P. T. 1901. *The seasonal distribution of Atlantic plankton-organisms.,* Göteborg, Göteborgs Kongliga Vetenskaps- och Vitterhets-samhälle handlingar.

CRAWFORD, R. M., GARDNER, C. & MEDLIN, L. K. 1994. The genus *Attheya*. I. A description of four new taxa, and the transfer of *Gonioceros septentrionalis* and *G. armatus*. *Diatom Research,* 9**,** 27-51.

CULLAJ, A., HASKO, A., MIHO, A., SCHANZ, F., BRANDL, H. & BACHOFEN, R. 2005. The quality of Albanian natural waters and the human impact. *Environment International,* 31**,** 133–1446.

CUPP, E. E. 1943. Marine plankton diatoms of the west coast of north America. *Bulletin of the Scripps Institution of Oceanography Technical series,* 5**,** 1-237.

CUSHMAN-ROISIN, B., GACIC, M., POULAIN, P.-M. & ARTEGIANI, A. 2001. *Physical oceanography of the Adriatic Sea,* Kluwer Academic Publishers.

ČALIĆ, M., CARIĆ, M., KRŠINIĆ, F., JASPRICA, N. & PEĆAREVIĆ, M. 2013. Controlling factors of phytoplankton seasonal succession in oligotrophic Mali Ston Bay (south-eastern Adriatic). *Environmental Monitoring and Assessment,* 185**,** 7543-7563.

D'ALELIO, D., RIBERA D'ALCALÀ, M., DUBROCA, L., SARNO, D., ZINGONE, A. & MONTRESOR, M. 2010. The time for sex: a biennial life cycle in a marine planktonic diatom. *Limnology and Oceanography,* 55**,** 106-114.

DECHO, A. W. 1990. Microbial exopolymer secretions in ocean environments: their role(s) in food webs and marine

processes. *Oceanography and Marine Biology: an Annual Review*, 28**,** 75-153.

DEGERLUND, M., HUSEBY, S., ZINGONE, A., SARNO, D. & LANDFALD, B. 2012. Functional diversity in cryptic species of *Chaetoceros socialis* Lauder (Bacillariophyceae). *Journal of Plankton Research,* 34**,** 416-431.

DEGOBBIS, D., FONDA-UMANI, S., FRANCO, P., MALEJ, A., PRECALI, R. & SMODLAKA, N. 1995. Changes in the northern Adriatic ecosystem and the hypertrophic appearance of gelatinous aggregates. *Science of the Total Environment*, 165**,** 43-58.

DJAKOVAC, T., DEGOBBIS, D., SUPIĆ, N. & PRECALI, R. 2012. Marked reduction of eutrophication pressure in the northeastern Adriatic in the period 2000–2009. *Estuarine, Coastal and Shelf Science*, 115**,** 25-32.

DREBES, G. 1967. *Bacteriastrum solitarium* Mangin, a stage in the life history of the centric diatom *Bacteriastrum hyalinum*. *Marine Biology*, 1**,** 40-42.

DREBES, G. 1972. The life history of the centric diatom *Bacteriastrum hyalinum* Lauder. *Nova Hedwigia, Beiheft,* 39**,** 95-110.

DRUM, R. W. 1969. Light and electron microscope observations on the tube-dwelling diatom *Amphipleura rutilans* (Trentepohl) Cleve. *Journal of Phycology*, 5**,** 21-26.

EDGAR, R. K. 2013. *Diatoms: cleft confervas, or carved at the joints.* [Online]. Available: http://www.diatom.org/marginalia/1_Diatomes/dFS1.htm [Accessed 26. 2 .2013.].

EDLUND, M. B. & STOERMER, E. F. 1997. Ecological, evolutionary, and systematic significance of diatom life histories. *Journal of Phycology*, 33**,** 897-918.

EHRENBERG, C. G. 1844. Vorläufige Resultate seiner Untersuchungen der ihm von der Südpolreise des Capitain Ross, so wie von den Herren Schayer und Darwin zugekommenen Materialien über das Verhalten des kleinsten Lebens in den Oceanen und den grössten bisher zugänglichen Tiefen des Weltmeers vor. *Bericht über die zur Bekanntmachung geeigneten Verhandlungen der Königlichen Akademie der Wissenschaften zu Berlin***,** 182-207.

EHRENBERG, C. G. 1845. Neue Untersuchungen über das kleinste Leben als geologische Moment. *Bericht über die zur Bekanntmachung geeigneten Verhandlungen der Königlichen Akademie der Wissenschaften zu Berlin***,** 53-88.

ELBRÄCHTER, M. & BOJE, R. 1978. On the ecological significance of *Thalassiosira partheneia* in the northwest African upwelling area. *In:* BOJE, R. & TOMCZAK, M. (eds.) *Upwelling Ecosystems.* Berlin: Springer-Verlag.

EVENSEN, D. L. & HASLE, G. R. 1975. The morphology of some *Chaetoceros* (Bacillariophyceae) species as seen in electron microscopes. *Nova Hedwigia Beiheft*, 53**,** 153-184.

FALKOWSKI, P. G., BARBER, R. T. & SMETACEK, V. 1998. Biogeochemical controls and feedbacks on ocean primary production. *Science*, 281**,** 200-206.

FERGUSON WOOD, E. J. & CORCORAN, E. F. 1966. Diurnal variations in phytoplankton. *Bulletin of Marine Science*, 16(3)**,** 383-403.

FONDA UMANI, S., MALFATTI, F. & DEL NEGRO, P. 2012. Carbon fluxes in the pelagic ecosystem of the Gulf of Trieste (Northern Adriatic Sea). *Estuarine, Coastal and Shelf Science*, 115**,** 170-185.

FOURTANIER, E. & KOCIOLEK, J. P. 2011. *Catalogue of Diatom Names On-line Version updated 19 Sep 2011. Compiled by Elisabeth Fourtanier & J. Patrick Kociolek. Available online at http://research.calacademy.org/research/diatoms/names/index.asp* [Online]. California Academy of Sciences. [Accessed 2013].

FRANCIUS, G., TESSON, B., DAGUE, E., MARTIN-JEZEQUEL, V. & DUFRENE, Y. F. 2008. Nanostructure and nanomechanics of live Phaeodactylum tricornutum morphotypes. *Environmental Microbiology*, 10**,** 1344-1356.

FRENCH III, F. W. & HARGRAVES, P. E. 1986. Population dynamics of the spore-forming diatom *Leptocylindrus danicus* in Narragansett Bay, Rhode Island. *Journal of Phycology*, 22**,** 411-420.

FRYXELL, G. A. 1978. Chain-forming diatoms: three species of Chaetoceraceae. *Journal of Phycology*, 14**,** 62-71.

FRYXELL, G. A., GOULD, R. W. & WATKINS, T. P. 1984. Gelatinous colonies of the diatom *Thalassiosira* in Gulf Stream Warm Core Rings including *T. fragilis*, sp. nov. *British Phycological Journal*, 19**,** 141-156.

FRYXELL, G. A. & MEDLIN, L. K. 1981. Chain forming diatoms, evidence of parallel evolution in *Chaetoceros*. *Cryptogamie Algologie*, 2**,** 3-29.

GAČIĆ, M., LASCARATOS, A., MANCA, B. B. & MANTZIAFOU, A. 2001. Adriatic deep water and interaction with the Eastern Mediterranean Sea. *In:* CUSHMAN-ROISIN, B., GAČIĆ, M., POULAIN, P.-M. & ARTEGIANI, A. (eds.) *Physical oceanography of the Adriatic Sea: past, present and future*. Dordrecht: Kluwer Academic Publishers.

GIANI, M., DJAKOVAC, T., DEGOBBIS, D., COZZI, S., SOLIDORO, C. & UMANI, S. F. 2012. Recent changes in the marine ecosystems of the northern Adriatic Sea. *Estuarine, Coastal and Shelf Science*, 115**,** 1-13.

GIUFFRÈ, G. & RAGUSA, S. 1988. The morphology of *Chaetoceros rostratum* Lauder (Bacillariophyceae) using light and electron microscopy. *Botanica Marina*, 31**,** 503-510.

GODRIJAN, J., MARIĆ, D., IMEŠEK, M., JANEKOVIĆ, I., SCHWEIKERT, M. & PFANNKUCHEN, M. 2012. Diversity, occurrence, and habitats of the diatom genus *Bacteriastrum* (Bacillariophyta) in the northern Adriatic Sea, with the description of *B. jadranum* sp. nov. *Botanica Marina*, 55**,** 1-12.

GODRIJAN, J., MARIĆ, D., TOMAŽIĆ, I., PRECALI, R. & PFANNKUCHEN, M. 2013. Seasonal phytoplankton dynamics in the coastal waters of the north-eastern Adriatic Sea. *Journal of Sea Research*, 77**,** 32-44.

GÓMEZ, F., MOREIRA, D. & LÓPEZ-GARCÍA, P. 2010. *Neoceratium* gen. nov., a new genus for all marine species currently assigned to *Ceratium* (Dinophyceae). *Protist*, 161**,** 35-54.

GORDON, R., LOSIC, D., TIFFANY, M. A., NAGY, S. S. & STERRENBURG, F. A. S. 2009. The Glass Menagerie: diatoms for novel applications in nanotechnology. *Trends in Biotechnology*, 27**,** 116-127.

GOULD, S. B., WALLER, R. F. & MCFADDEN, G. I. 2008. Plastid Evolution. *Annual Review of Plant Biology*, 59**,** 491-517.

GRAN, H. H. 1897. *Botanik. Protophyta: Diatomaceae, Silicoflagellata og Cilioflagellata.*, Den Norske Nordhavs-Expedition 1876-1878.

GRAN, H. H. 1900. Bemerkungen über einige Planktondiatomeen. *Nytt Magasin for Naturvidenskapene*, 38**,** 102-128.

GROSSART, H.-P., LEVOLD, F., ALLGAIER, M., SIMON, M. & BRINKHOFF, T. 2005. Marine diatom species harbour distinct bacterial communities. *Environmental Microbiology*, 7**,** 860-873.

GUILLARD, R. R. L. 1975. Culture of phytoplankton for feeding marine invertebrates. *In:* SMITH, W. L. & CHANLEY, M. H. (eds.) *Culture of Marine Invertebrate Animals.* Plenum Press, New York, USA.

GUILLOUX, L., RIGAUT JALABERT, F., JOUENNE, F., RISTORI, S., VIPREY, M., NOT, F., VAULOT, D. & SIMON, N. 2013. An annotated checklist of Marine Phytoplankton taxa at the SOMLIT-Astan time series off Roscoff (Western English Channel, France): data collected from 2000 to 2010. *Cahiers de biologie marine*, 54**,** 247-256.

HAMM, C. & SMETACEK, V. 2007. Armour: why, when and how. *In:* FALKOWSKI, P. G. & KNOLL, A. H. (eds.) *Evolution of Primary Producers in the Sea*. Elsevier Academic Press.

HARGRAVES, P. E. 1976. Studies on marine plankton diatoms. II. Resting spores morphology. *Journal of Phycology*, 12**,** 118-128.

HARGRAVES, P. E. 1979. Studies on marine plankton diatoms. IV. Morphology of *Chaetoceros* resting spores. *Nova Hedwigia Beiheft*, 64**,** 99-120.

HASLE, G. R. 1968. The valve processes of the centric diatom genus *Thalassiosira*. *Nytt Magasin for Botanikk*, 15**,** 193-201.

HASLE, G. R. 1978. Diatoms. *In:* SOURNIA, A. (ed.) *Phytoplankton Manual*. UNESCO.

HASLE, G. R., LANGE, C. B. & SYVERTSEN, E. E. 1996. A review of *Pseudo-nitzschia*, with special reference to the Skagerrak, North Atlantic, and

adjacent waters. *Helgoländer Meeresuntersuchungen,* 50**,** 131-175.

HASLE, G. R. & SYVERTSEN, E. E. 1997. Marine diatoms. *In:* TOMAS, C. R. (ed.) *Identifying marine phytoplankton.* San Diego: Academic Press.

HENDEY, N. I. 1964. *An introductory account of the smaller algae of British coastal waters. V. Bacillariophyceae (Diatoms),* London, HMSO.

HERNÁNDEZ-BECERRIL, D. U. 1991a. The morphology and taxonomy of the planktonic diatom *Chaetoceros coarctatus* Lauder (Bacillariophyceae). *Diatom Research,* 6**,** 281-287.

HERNÁNDEZ-BECERRIL, D. U. 1991b. Note on the morphology of *Chaetoceros didymus* and *C. protuberans*, with some considerations on their taxonomy. *Diatom Research,* 6**,** 289-297.

HERNÁNDEZ-BECERRIL, D. U. 1992. Observations on two closely related species, *Chaetoceros tetrastichon* and *C. dadayi* (Bacillariophyceae). *Nordic Journal of Botany,* 12**,** 365-371.

HERNÁNDEZ-BECERRIL, D. U. 1993. Note on the morphology of two planktonic diatoms: *Chaetoceros bacteriastroides* and *C. seychellarus*, with comments on their taxonomy and distribution. *Botanical Journal of the Linnean Society,* 111**,** 117-128.

HERNÁNDEZ-BECERRIL, D. U. 1996. A morphological study of *Chaetoceros* species (Bacillariophyta) from the plankton of the Pacific Ocean of Mexico. *Bullettin of the Natural History Museum of London,* 26**,** 1-73.

HERNÁNDEZ-BECERRIL, D. U. 2000. Morphology and taxonomy of three little-known marine planktonic *Chaetoceros* species (Bacillariophyceae). *European Journal of Phycology,* 35**,** 183-188.

HERNÁNDEZ-BECERRIL, D. U. & AKÉ-CASTILLO, J. A. 2001. Morphological study of two marine planktonic diatoms of the genus *Chaetoceros*: *C. anastomosans* and *C. costatus*. *In:* JAHN, R., KOCIOLEK, J. P., WITKOWSKI, A. & COMPÈRE, P. (eds.) *Studies on Diatoms.* Gantner, Ruggell. Liechtenstein: Lange-Bertalot-Festschrift:.

HERNÁNDEZ-BECERRIL, D. U. & FLORES GRANADOS, C. 1998. Species of the diatom genus *Chaetoceros* (Bacilariophyceae) in the plankton from the southern Gulf of Mexico. *Botanica Marina,* 41**,** 505-519.

HERNÁNDEZ-BECERRIL, D. U., VILIČIĆ, D., BOSAK, S. & DJAKOVAC, T. 2010. Morphology and ecology of the diatom *Chaetoceros vixvisibilis* (Chaetocerotales, Bacillariophyceae) from the Adriatic Sea. *Journal of Plankton Research,* 32**,** 1513-1525.

HIGGINS, M. J. & WETHERBEE, R. 2011. The role of atomic force microscopy in advancing diatom research into the nanotechnology era. *In:* Y.F., D. (ed.) *Life at the Nanoscale: Atomic Force Microscopy of Live Cells.* Singapore: Pan Stanford Publishing.

HILDEBRAND, M., DAVIS, A. K., SMITH, S. R., TRALLER, J. C. & ABBRIANO, R. 2012. The place of diatoms in the biofuels industry. *Biofuels,* 3**,** 221-240.

HILDEBRAND, M., HOLTON, G., JOY, D. C., DOKTYCZ, M. J. & ALLISON, D. P. 2009. Diverse and conserved nano- and mesoscale structures of diatom silica revealed by atomic force microscopy. *Journal of Microscopy,* 235**,** 172-187.

HILLEBRAND, H., DURSELEN, C. D., KIRSCHTEL, D., POLLINGHER, U. & ZOHARY, T. 1999. Biovolume calculation for pelagic and benthic microalgae. *Journal of Phycology,* 35**,** 403-424.

HOLLIBAUGH, J. T., SEIBERT, D. H. L. & THOMAS, W. H. 1981. Observations on the survival and germination of resting spores of three *Chaetoceros* (Bacillariophyceae) species. *Journal of Phycology,* 17**,** 1-9.

HOPPENRATH, M. 2004. A revised checklist of planktonic diatoms and dinoflagellates from Helgoland (North Sea, German Bight). *Helgoland Marine Research,* 58**,** 243-251.

HOPPENRATH, M., ELBRÄCHTER, M. & DREBES, G. 2009. *Marine Phytoplankton: Selected microphytoplankton species from the North Sea around Helgoland and Sylt,* Stuttgart, Kleine Serckenerg - Reihe 49, Schweitzerbart Science Publishers.

HUSTEDT, F. 1930. *Die Kieselalgen Deutschlands, Österrreichs und der Schweiz under Berücksichtigung der übrigen Länder Europas sowie der*

angrenzenden Meeresgebiete. 1. Teil, Leipzig, Akademische Verlaggesellschaft.

IKARI, J. 1926. On some *Chaetoceras* of Japan. I. *Botanical Magazine, Tokyo.*, 40**,** 517-534.

IKARI, J. 1927. On *Bacteriastrum* of Japan. *The Botanical Magazine, Tokyo,* 41**,** 421-431.

IKARI, J. 1928. On some *Chaetoceras* of Japan. II. *Botanical Magazine, Tokyo,* 42**,** 247-262.

ISHII, K.-I., IWATAKI, M., MATSUOKA, K. & IMAI, I. 2011. Proposal of identification criteria for resting spores of *Chaetoceros* species (Bacillariophyceae) from a temperate coastal sea. *Phycologia*, 50**,** 351-362.

IVANČIĆ, I. & DEGOBBIS, D. 1984. An optimal manual procedure for ammonia analysis in natural waters by the indophenol blue method. *Water Research* 18**,** 1143-1147.

IVANČIĆ, I., FUKS, D., RADIĆ, T., LYONS, D. M., ŠILOVIĆ, T., KRAUS, R. & PRECALI, R. 2010. Phytoplankton and bacterial alkaline phosphatase activity in the northern Adriatic Sea. *Marine Environmental Research*, 69**,** 85-94.

JENSEN, K. G. & MOESTRUP, Ø. 1998. The genus *Chaetoceros* (Bacillariophyceae) in innner Danish coastal waters. *Opera Botanica*, 133**,** 1-68.

KACZMARSKA, I., POULÍČKOVÁ, A., SATO, S., EDLUND, M. B., IDEI, M., WATANABE, T. & MANN, D. G. 2013. Proposals for a terminology for diatom sexual reproduction, auxospores and resting stages. *Diatom Research***,** 1-32.

KACZMARSKA, I., RUSHFORTH, S. R. & JOHANSEN, J. R. 1985. *Chaetoceros amanita* Cleve-Euler (Bacillariophyceae) from Blue Lake Warm Spring, Utah, USA. *Phycologia,* 24**,** 103-109.

KARSTEN, G. 1907. Das Phytoplankton des Antarktischen Meeres nach dem Material der deutschen Tiefsee-Expedition 1898-1899. *Wissenschaftliche Ergebnisse der Deutschen Tiefsee-Expedition auf dein Dampfer 'Valdivia' 1898-1899*, 2**,** 221-544.

KOCH, P. & RIVERA, P. 1984. Contribution to the diatom flora of Chile. III. The genus *Chaetoceros* Ehr. (subgenus *Phaeoceros* Gran). *Gayana Botánica,* 41**,** 61-84.

KOOISTRA, W. H. C. F., GERSONDE, R., MEDLIN, L. K. & MANN, D. G. 2007. The Origin and Evolution of the Diatoms: Their Adaptation to a Planktonic Existence. *In:* FALKOWSKI, P. G. & KNOLL, A. H. (eds.) *Evolution of Primary Producers in the Sea* Burlington. MA: Elsevier Academic Press.

KOOISTRA, W. H. C. F. & MEDLIN, L. K. 2007. Species concepts in diatoms: a clarification. *Diatom Research,* 22**,** 227-228.

KOOISTRA, W. H. C. F., SARNO, D., BALZANO, S., GU, H., ANDERSEN, R. A. & ZINGONE, A. 2008. Global diversity and biogeography of *Skeletonema* species (Bacillariophyta). *Protist,* 159**,** 177—193.

KOOISTRA, W. H. C. F., SARNO, D., HERNANDEZ-BECERRIL, D. U., ASSMY, P., DI PRISCO, C. & MONTRESOR, M. 2010. Comparative molecular and morphological phylogenetic analyses of taxa in the Chaetocerotaceae (Bacillariophyta). *Phycologia*, 49**,** 471-500.

KOWNACKA, J., EDLER, L., GROMISZ, S., ŁOTOCKA, M., OLENINA, I., OSTROWSKA, M. & PIWOSZ, K. 2013. Non-indigenous species *Chaetoceros* cf. *lorenzianus* Grunow 1863 – A new, predominant component of autumn phytoplankton in the southern Baltic Sea. *Estuarine, Coastal and Shelf Science*, 119**,** 101-111.

KRABERG, A., BAUMANN, M. & DÜRSELEN, C. D. 2010. *Coastal Phytoplankton: Photo Guide for Northern European Seas*, Munchen, Pfeil Verlag.

KRIVOKAPIĆ, A., PESTORIĆ, B., BOSAK, S., KUŠPILIĆ, G. & RISER, C. W. 2011. Trophic state of Boka Kotorska bay (South-eastern adriatic sea). *Fresenius Environmental Bulletin*, 20**,** 1960-1969.

KRIVOKAPIĆ, S., STANKOVIĆ, Z. & VUKSANOVIĆ, N. 2009. Seasonal variations of phytoplankton biomass and environmental conditions in the inner Boka Kotorska Bay (Eastern Adriatic sea). *Acta Botanica Croatica*, 68**,** 45-55.

KRÖGER, N. & POULSEN, N. 2008. Diatoms—From Cell Wall Biogenesis to Nanotechnology. *Annual Review of Genetics,* 42**,** 83-107.

KUWATA, A., HAMA, T. & TAKAHASHI, M. 1993. Ecophysiological characterization of two life forms, resting spores and resting cells, of a marine planktonic diatom, *Chaetoceros pseudocurvisetus*, formed under nutrient depletion. *Marine Ecology Progress Series*, 102**,** 245-255.

LAUDER, H. S. 1864. On new diatoms. *Quarterly Journal of Microscopical Science,* 4**,** 6-8.

LECHUGA-DEVÉZE, C. H. & HERNÁNDEZ-BECERRIL, D. U. 1988. Life cycle of the diatom *Chaetoceros protuberans* Lauder (1864) (Bacillariophyceae). *Investigacion Pesquera,* 52**,** 77-83.

LEE, S.-D. & LEE, J.-H. 2011. Morphology and taxonomy of the planktonic diatom *Chaetoceros* species (Bacillariophyceae) with special intercalary setae in Korean coastal waters. *Algae,* 26**,** 153-165.

LEGOVIĆ, T., GRŽETIĆ, Z. & ŽUTIĆ, V. 1991. Subsurface temperature maximum in a stratified estuary. *Marine Chemistry,* 32**,** 163-170.

LONG, R. A. & AZAM, F. 1996. Abundant protein-containing particles in the sea. *Aquatic Microbial Ecology,* 10**,** 213-221.

LUND, J. W. G., KIPLING, C. & LE CREN, E. D. 1958. The inverted microscope method of estimating algal numbers and the statistical basis of estimations by counting. *Hydrobiologia,* 11**,** 143-170.

LUNDHOLM, N., HASLE, G. R., FRYXELL, G. A. & HARGRAVES, P. E. 2002. Morphology, phylogeny and taxonomy of species within the *Pseudo-nitzschia americana* complex (Bacillariophyceae) with descriptions of the two new species *P. brasiliana* and *P. linea*. *Phycologia,* 41**,** 480-497.

LUNDHOLM, N., MOESTRUP, Ø., HASLE, G. R. & HOEF-EMDEN, K. 2003. A study of the *Pseudo-nitzschia pseudodelicatissima/cuspidata* complex (Bacillariophyceae): what is *P. pseudodelicatissima*? *Journal of Phycology,* 39**,** 797-813.

LUNDHOLM, N., MOESTRUP, Ø., KOTAKI, Y., HOEF-EMDEN, K., SCHOLIN, C. & MILLER, P. 2006. Inter- and intraspecific variation of the *Pseudo-nitzschia delicatissima* complex (Bacillariophyceae) illustrated by rRNA probes, morphological data and phylogenetic analyses. *Journal of Phycology,* 42**,** 464-481.

LJUBEŠIĆ, Z., BOSAK, S., VILIČIĆ, D., BOROJEVIĆ, K. K., MARIĆ, D., GODRIJAN, J., UJEVIĆ, I., PEHAREC, P., et al. 2011. Ecology and taxonomy of potentially toxic Pseudo-nitzschia species in Lim Bay (north-eastern Adriatic Sea). *Harmful Algae,* 10**,** 713-722.

MANGIN, L. 1910. Sur quelques Algues nouvelles ou peu connues du Phytoplancton de l'Atlantique. *Bulletin de la Société Botanique de France.,* 57**,** 344-350.

MANN, D. G. 1993. Patterns of sexual reproduction in diatoms. *Hydrobiologia,* 269-270**,** 11-20.

MANN, D. G. 1999. The species concept in diatoms. *Phycologia,* 38**,** 437-495.

MANN, D. G. & DROOP, S. J. M. 1996. 3. Biodiversity, biogeography and conservation of diatoms. *Hydrobiologia,* 336**,** 19-32.

MARGALEF, R. 1978. Life-forms of phytoplankton as survival alternatives in an unstable environment. *Oceanologica Acta,* 1**,** 493-509.

MARINO, D., GIUFFÉ, G., MONTRESOR, M. & ZINGONE, A. 1991. An electron microscope investigation on *Chaetoceros minimus* (Levander) comb. nov. and new observations on *Chaetoceros throndsenii* (Marino, Montresor and Zingone) comb. nov. *Diatom Research,* 6**,** 317-326.

MARINO, D., MONTRESOR, M. & ZINGONE, A. 1987. *Miraltia throndsenii* gen. nov., sp. nov., a planctonic diatom from the Gulf of Naples. *Diatom Research,* 2**,** 205-211.

MEDLIN, L. K. & KACZMARSKA, I. 2004. Evolution of the diatoms: V. Morphological and cytological support for the major clades and a taxonomic revision. *Phycologia,* 43**,** 245-270.

MENDEN-DEUER, S. & LESSARD, E. J. 2000. Carbon to volume relationships for dinoflagellates, diatoms, and other protist plankton. *Limnology and Oceanography,* 45**,** 569-579.

MEUNIER, A. 1913. Microplankton de la Mer Flamande. 1ére partie: The genre *Chaetoceros* Ehrenberg. *Memoirs du Musée Royal d'Histoire Naturelle de Belgique,* 7**,** 1-49.

MIAO, A.-J., SCHWEHR, K. A., XU, C., ZHANG, S.-J., LUO, Z., QUIGG, A. & SANTSCHI, P. H. 2009. The algal toxicity of silver engineered nanoparticles and detoxification by exopolymeric substances. *Environmental Pollution,* 157**,** 3034-3041.

MILANOVIĆ, S. 2007. Hydrogeological characteristics of some deep siphonal springs in Serbia and Montenegro karst. *Environmental Geology,* 51**,** 755-759.

MIŠIĆ RADIĆ, T., SVETLIČIĆ, V., ŽUTIĆ, V. & BOULGAROPOULOS, B. 2011. Seawater at the nanoscale: marine gel imaged by atomic force microscopy. *Journal of Molecular Recognition,* 24**,** 397-405.

MONIZ, M. B. J. & KACZMARSKA, I. 2010. Barcoding of diatoms: nuclear encoded ITS revisited. *Protist,* 161**,** 7-34.

MONTRESOR, M., DI PRISCO, C., SARNO, D., MARGIOTTA, F. & ZINGONE, A. 2013. Diversity and germination patterns of diatom resting stages at a coastal Mediterranean site. *Marine Ecology Progress Series,* 484**,** 79-95.

MORENO RUIZ, J. L., SOTO, P. J., ZAMUDIO, M. E., HERNÁNDEZ-BECERRIL, D. U. & LICEA, S. D. 1993. Morphology and taxonomy of *Chaetoceros diversus* (Bacillariophyceae) based on material from the southern Gulf of Mexico. *Diatom Research,* 8**,** 419-428.

MOUSTAFA, A., BESZTERI, B., MAIER, U. G., BOWLER, C., VALENTIN, K. & BHATTACHARYA, D. 2009. Genomic footprints of a cryptic plastid endosymbiosis in diatoms. *Science,* 324**,** 1724-1726.

MOZETIČ, P., FRANCÉ, J., KOGOVŠEK, T., TALABER, I. & MALEJ, A. 2012. Plankton trends and community changes in a coastal sea (northern Adriatic): Bottom-up vs. top-down control in relation to environmental drivers. *Estuarine, Coastal and Shelf Science,* 115**,** 138-148.

MOZETIČ, P., SOLIDORO, C., COSSARINI, G., SOCAL, G., PRECALI, R., FRANCÉ, J., BIANCHI, F., DE VITTOR, C., et al. 2010. Recent trends towards oligotrophication of the northern Adriatic: Evidence from chlorophyll *a* time series. *Estuaries and Coasts,* 33**,** 362-375.

MYKLESTAD, S., HAUG, A. & LARSEN, B. 1972. Production of carbohydrates by the marine diatom *Chaetoceros affinis* var. *willei* (Gran) Hustedt. II. Preliminary investigation of the extracellular polysaccharide. *Journal of Experimental Marine Biology and Ecology,* 9**,** 137-144.

MYKLESTAD, S., HOLM-HANSEN, O., VARUM, K. M. & VOLCANI, B. E. 1989. Rate of release of extracellular amino acids and carbohydrates from the marine diatom *Chaetoceros affinis*. *Journal of Plankton Research,* 11**,** 763-773.

MYKLESTAD, S. M. 1995. Release of extracellular products by phytoplankton with special emphasis on polysaccharides. *Science of the Total Environment,* 165**,** 155-164.

NAGASAWA, S. & WARREN, A. 1996. Redescription of *Vorticella oceanica* Zacharias, 1906 (Ciliophora: Peritrichia) with notes on its host, the marine planktonic diatom *Chaetoceros coarctatum* Lauder, 1864. *Hydrobiologia,* 337**,** 27-36.

NANJAPPA, D. 2012. *Genetic, physiological and ecological diversity of the diatom genus Leptocylindrus* PhD thesis. Open University of London, Stazione Zoologica Anton Dohrn, Napoli, Italy.

NEJSTGAARD, J. C., TANG, K. W., STEINKE, M., DUTZ, J., KOSKI, M., ANTAJAN, E. & LONG, J. D. 2007. Zooplankton grazing on *Phaeocystis*: A quantitative review and future challenges. *Biogeochemistry,* 83**,** 147-172.

NOT, F., SIANO, R., KOOISTRA, W. H., SIMON, N., VAULOT, D., PROBERT, I., DE CLERCK, O., BOGAERT, K. A., et al. 2012. Diversity and ecology of eukaryotic marine phytoplankton. *Advances in Botanical Research,* 64**,** 1-53.

OKUNO, H. 1962. Electron-microscopical study on fine structures of diatom frustules. XIX. *The Botanical Magazine, Tokyo,* 75**,** 119-126.

OLSON, M. B. & LESSARD, E. J. 2010. The influence of the *Pseudo-nitzschia* toxin, domoic acid, on microzooplankton grazing and growth: A field and laboratory assessment. *Harmful Algae,* 9**,** 540-547.

ORLIĆ, M., LEDER, N., PASARIĆ, M. & SMIRČIĆ, A. 2000. Physical properties and currents recorded during September and October 1998 in the Velebit Channel (east Adriatic). *Periodicum Biologorum*, 31 - 37.

ORLOVA, T. Y. & AIZDAICHER, N. A. 2000. Development in culture of the diatom *Chaetoceros salsugineus* from the Sea of Japan. *Russian Journal of Marine Biology,* 26**,** 8-11.

ORLOVA, T. Y. & SELINA, M. S. 1993. Morphology and ecology of the bloom-forming planktonic diatom *Chaetoceros salsugineus* Takano in the Sea of Japan. *Botanica Marina,* 36**,** 123-130.

ORSINI, L., SARNO, D., PROCACCINI, G., POLETTI, R., DAHLMANN, J. & MONTRESOR, M. 2002. Toxic *Pseudo-nitzschia multistriata* (Bacillariophyceae) from the Gulf of Naples: morphology, toxin analysis and phylogenetic relationships with other *Pseudo-nitzschia* species. *European Journal of Phycology,* 37**,** 247-257.

OSTENFELD, C. H. 1903. Plankton from the sea around the Færöes. *In:* WARMING, E. (ed.) *Botany of the Færöes.* Copenhagen: Nordisk Forlag.

OSTENFELD, C. H. & SCHMIDT, J. 1901. Plankton fra det Røde Hav of Adenbugten. *Videnskabelige meddelelser fra Dansk Naturhistorisk Forening***,** 141-182.

PARSONS, T. R., MAITA, Y. & LALLI, C. M. 1984. *Manual of chemical and biological methods for seawater analysis,* Oxford, Pergamon Press.

PAVILLARD, J. 1911. Observations sur les Diatomées. *Bulletin de la Société Botanique de France,* 58**,** 21-29.

PAVILLARD, J. 1913. Observations sur les diatomees. - 2e. ser. *Bull. Soc. Bot. France,* 60**,** 126-133.

PAVILLARD, J. 1916. Recherches sur le diatomées pélagiques du Golfe du Lion. *Travail de l'Institut de Botanique de l'Université de Montpellier et de la Station Zoologique de Cette,* 5**,** 7-62.

PAVILLARD, J. 1924. Observations sur les Diatomées, 4ème série. Le genre *Bacteriastrum*. *Bulletin de la Société Botanique de France,* 71**,** 1084-1090.

PAVILLARD, J. 1925. Bacillariales. *Rep Danish Oceanogr Exp 1908-1910 to the Mediterranean and Adjacent Seas,* 2**,** 1-72.

PERCOPO, I., SIANO, R., CERINO, F., SARNO, D. & ZINGONE, A. 2011. Phytoplankton diversity during the spring bloom in the northwestern Mediterranean Sea. *Botanica Marina,* 54**,** 243.

PISTOCCHI, R., MORMILE, M. A., GUERRINI, F., ISANI, G. & BONI, L. 2000. Increased production of extra- and intracellular metal-ligands in phytoplankton exposed to copper and cadmium. *Journal of Applied Phycology,* 12**,** 469-477.

PITCHER, G. C. 1990. Phytoplankton seed populations of the Cape Peninsula upwelling plume, with particular reference to resting spores of *Chaetoceros* (Bacillariophyceae) and their role in seeding upwelling waters. *Estuarine Coastal and Shelf Science,* 31**,** 283-301.

PLETIKAPIĆ, G., MIŠIĆ RADIĆ, T., HOZIĆ ZIMMERMANN, A., SVETLIČIĆ, V., PFANNKUCHEN, M., MARIĆ, D., GODRIJAN, J. & ŽUTIĆ, V. 2011a. AFM imaging of extracellular polymer release by marine diatom *Cylindrotheca closterium* (Ehrenberg) Reiman & J.C. Lewin. *Journal of Molecular Recognition,* 24**,** 436-445.

PLETIKAPIĆ, G., RADIĆ, T. M., ZIMMERMANN, A. H., SVETLIČIĆ, V., PFANNKUCHEN, M., MARIĆ, D., GODRIJAN, J. & ŽUTIĆ, V. 2011b. AFM imaging of extracellular polymer release by marine diatom *Cylindrotheca closterium* (Ehrenberg) Reiman & J.C. Lewin. *Journal of Molecular Recognition,* 24**,** 436-445.

POLIMENE, L., PINARDI, N., ZAVATARELLI, M. & COLELLA, S. 2007. The Adriatic Sea ecosystem seasonal cycle: Validation of a three-dimensional numerical model. *Journal of Geophysical Research C: Oceans,* 112.

POLOVIĆ, D. 2013. *Raznolikost fitoplanktona u Parku prirode Telašćica (Diversity of phytoplankton in Nature park Telašćica),* MSc.Thesis. University of Zagreb, Faculty of Science, Division of Biology (in croatian).

POULAIN, P.-M. & CUSHMAN-ROISIN, B. 2001. Circulation. *In:* CUSHMAN-ROISIN, B., GACIC, M., POULAIN, P.-M. & ARTEGIANI, A. (eds.) *Physical*

oceanography of the Adriatic Sea. Dordrecht: Kluwer Academic Publishers.

POULAIN, P. M. 2001. Adriatic sea surface circulation as derived from drifter data between 1990 and 1999. *Journal of Marine Systems*, 29**,** 3-32.

PRASAD, A. K. S. K., NIENOW, J. A. & LIVINGSTON, R. J. 1990. The genus *Cyclotella* (Bacillariophyta) in Choctawhatchee Bay, Florida, with special reference to *C. striata* and *C. choctawhatcheeana* sp. nov. *Phycologia*, 29**,** 418-436.

RAMBAUT, A. 1996-2002. Sequence Alignment Editor v2.0a11. *available at http://evolve.zoo.ox.ac.uk/ accessed 18/01/05*.

RAMPEN, S. W., SCHOUTEN, S., ELDA PANOTO, F., BRINK, M., ANDERSEN, R. A., MUYZER, G., ABBAS, B. & SINNINGHE DAMSTÉ, J. S. 2009. Phylogenetic position of *Attheya longicornis* and *Attheya septentrionalis* (Bacillariophyta). *Journal of Phycology*, 45**,** 444-453.

RAMUS, J. 1977. Alcian blue: a quantitative aqueous assay for algal acid and sulfated polysaccharides. *Journal of Phycology*, 13**,** 345-348.

REINECKE, P. 1969. A note on the *Bacteriastrum tenue* Steemann Nielsen. *The Journal of South African Botany*, 35**,** 207-210.

REINKE, D. C. 1984. Ultrastructure of *Chaetoceros muelleri* (Bacillariophyceae): auxospore, resting spore and vegetative cell morphology. *Journal of Phycology*, 20**,** 153-155.

REVELANTE, N. & GILMARTIN, M. 1976. Temporal succession of phytoplankton in the Northern Adriatic. *Netherlands Journal of Sea Research*, 10**,** 377-396.

RIBERA D'ALCALÀ, M., CONVERSANO, F., CORATO, F., LICANDRO, P., MANGONI, O., MARINO, D., MAZZOCCHI, M. G., MODIGH, M., et al. 2004. Seasonal patterns in plankton communities in a pluriannual time series at a coastal Mediterranean site (Gulf of Naples): an attempt to discern recurrences and trends. *Scientia Marina*, 68 (Suppl. 1)**,** 65-83.

RINALDI, A., VOLLENWEIDER, R. A., MONTANARI, G., FERRARI, C. R. & GHETTI, A. 1995. Mucilages in Italian seas: the Adriatic and Tyrrhenian Seas, 1988–1991. *Science of The Total Environment*, 165**,** 165-183.

RINES, J. E. B. 1999. Morphology and taxonomy of *Chaetoceros contortus* Schütt 1895, with preliminary observations on *Chaetoceros compressus* Lauder 1864 (Subgenus Hyalochaete, Section Compressa). *Botanica Marina*, 42**,** 539-551.

RINES, J. E. B., BOONRUANG, P. & THERIOT, E. C. 2000. *Chaetoceros phuketensis* sp. nov. (Bacillariophyceae): a new species from the Andaman Sea. *Phycological Research*, 48**,** 161-168.

RINES, J. E. B. & HARGRAVES, P. E. 1988. *The Chaetoceros Ehrenberg (Bacillariophyceae) Flora of Narragansett Bay, Rhode Island, U.S.A.*, Berlin, Bibliotheca Phycologica, Band 79, J. Cramer.

RINES, J. E. B. & THERIOT, E. C. 2003. Systematics of Chaetocerotaceae (Bacillariophyceae). I. A phylogenetic analysis of the family. *Phycological Research*, 51**,** 83-98.

ROSS, R., COX, E. J., KARAYEVA, N. I., MANN, D. G., PADDOCK, T. B. B., SIMONSEN, R. & SIMS, P. A. 1979. An amended terminology for the siliceous components of the diatom cell. *Nova Hedwigia Beiheft*, 64**,** 513-533.

ROUND, F. E., CRAWFORD, R. M. & MANN, D. G. 1990. *The diatoms: biology & morphology of the genera*, Cambridge, UK, Cambridge University Press.

ROUSSEAU, V., CHRÉTIENNOT-DINET, M.-J., JACOBSEN, A., VERITY, P. & WHIPPLE, S. 2007. The life cycle of Phaeocystis: state of knowledge and presumptive role in ecology. *In:* LEEUWE, M. A., STEFELS, J., BELVISO, S., LANCELOT, C., VERITY, P. G. & GIESKES, W. W. C. (eds.) *Phaeocystis, major link in the biogeochemical cycling of climate-relevant elements.* Springer Netherlands.

RUSHFORTH, S. R. & JOHANSEN, J. R. 1986. The inland *Chaetoceros* (Bacillariophyceae) species of North America. *Journal of Phycology*, 22**,** 441-448.

SAR, E. A., HERNÁNDEZ-BECERRIL, D. U. & SUNESEN, I. 2002. A morphological study of *Chaetoceros tenuissimus*

Meunier, a little-known planktonic diatom, with a discussion of the section Simplicia, subgenus Hyalochaete. *Diatom Research,* 17**,** 327-335.

SARACINO, O. D. & RUBINO, F. 2006. Phytoplankton composition and distribution along the Albanian coast, South Adriatic Sea. *Nova Hedwigia,* 83**,** 253-266.

SARNO, D., KOOISTRA, W. C. H. F., MEDLIN, L. K., PERCOPO, I. & ZINGONE, A. 2005. Diversity in the genus *Skeletonema* (Bacillariophyceae). II. An assessment of the taxonomy of *S. costatum*-like species, with the description of four new species. *Journal of Phycology,* 41**,** 151-176.

SARNO, D., ZINGONE, A. & MARINO, D. 1996. General shape and ultrastructure as taxonomic characters in diatoms: the case of the genus *Bacteriastrum*. *Giornale Botanico Italiano,* 130**,** 1069-1071.

SARNO, D., ZINGONE, A. & MARINO, D. 1997. *Bacteriastrum parallelum* sp. nov., a new diatom from the Gulf of Naples, and new observations on *B. furcatum* (Chaetocerotaceae, Bacillariophyta). *Phycologia,* 36**,** 257-266.

SCALCO, E. 2012. *Factors regulating transitions among life cycle phases in the marine pennate diatom Pseudo-nitzschia multistriata*, PhD thesis. Open University of London, Stazione Zoologica Anton Dohrn, Napoli, Italy.

SCHLITZER, R. 2011. *Ocean Data View* [Online]. Available: http://odv.awi.de [Accessed 2013].

SCHNACK, S. B. 1983. On the feeding of copepods on *Thalassiosira partheneia* from the northwest African upwelling area. *Marine Ecology Progress Series,* 11**,** 49-53.

SCHULTES, S., LAMBERT, C., PONDAVEN, P., CORVAISIER, R., JANSEN, S. & RAGUENEAU, O. 2010. Recycling and uptake of Si(OH)4 when protozoan grazers feed on diatoms. *Protist,* 161**,** 288-303.

SCHÜTT, F. 1895. Arten von *Chaetoceras* und *Peragallia*.Ein Beitrag zur Hochseeflora. *Berichte der Deutsche Botanisch Gesellschaft,* 13**,** 35-50.

SHADBOLT, G. 1854. A short description of some new forms of Diatomaceae from Port Natal. *Transactions of the Microscopical Society of London,* 2**,** 13-18.

SHEVCHENKO, O. & ORLOVA, T. 2010. Morphology and ecology of the bloom-forming diatom *Chaetoceros contortus* from Peter the Great Bay, Sea of Japan. *Russian Journal of Marine Biology,* 36**,** 243-251.

SHEVCHENKO, O., ORLOVA, T. & AIZDAICHER, N. 2008. Development of the diatom Chaetoceros socialis f. radians (Schütt) Proschkina-Lavrenko 1963 in laboratory culture. *Russian Journal of Marine Biology,* 34**,** 224-229.

SHEVCHENKO, O. G., ORLOVA, T. Y. & HERNÁNDEZ-BECERRIL, D. U. 2006. The genus *Chaetoceros* (Bacillariophyta) from Peter the Great Bay, Sea of Japan. *Botanica Marina,* 49**,** 236-258.

SIANO, R. 2007. *The phytoplankton of the Campania coast: an ecological and taxonomic study,* Naples, PhD thesis. University of Messina/ Stazione Zoologica Anton Dohrn, Napoli, Italy.

SICKO-GOAD, L., STOERMER, E. F. & KOCIOLEK, J. P. 1989. Diatom resting cell rejuvenation and formation: time course, species records and distribution. *Journal of Plankton Research,* 11**,** 375-389.

SIEBURTH, J. N., SMETACEK, V. & LENZ, J. 1978. Pelagic ecosystem structure: Heterotrophic compartments of the plankton and their relationship to size fractions. *Limnology and Oceanography,* 23**,** 1256-1263.

SIERACKI, M. E., GIFFORD, D. J., GALLAGER, S. M. & DAVIS, C. S. 1998. Ecology of a *Chaetoceros socialis* Lauder patch on Georges Bank: distribution, microbial associations and grazing losses. *Oceanography,* 11**,** 30-35.

SIMONSEN, R. 1972. Ideas for a more natural system of the centric diatoms. *Nova Hedwigia, Beiheft,* 39**,** 37-54.

SIMONSEN, R. 1974. The diatom plankton of the Indian Ocean expedition of r.v. 'Meteor' 1964,65. *"Meteor" Forsch.-Ergebnisse D,* 19**,** 1-66.

SIOKOU-FRANGOU, I., CHRISTAKI, U., MAZZOCCHI, M. G., MONTRESOR, M., RIBERA D'ALCALÀ, M., VAQUÉ, D. & ZINGONE, A. 2010. Plankton in the open Mediterranean Sea: a review. *Biogeosciences,* 7**,** 1-44.

SMAYDA, T. J. 1997. What is a bloom? A commentary. *Limnology and Oceanography,* 42**,** 1132-1136.

SMAYDA, T. J. 2006. *Diatom Blooms and fish mortality.* [Online]. In: Scottish Executive Environment Group, Harmful Algal Bloom Communities in Scottish Coastal Waters: Relationship to Fish Farming and Regional Comparisons - A Review. Available: http//www.scotland.gov.uk/Publications [Accessed 6.3.2013.].

SOCAL, G., ACRI, F., BASTIANINI, M., BERNARDI AUBRY, F., BIANCHI, F., CASSIN, D., COPPOLA, J., DE LAZZARI, A., et al. 2008. Hydrological and biogeochemical features of the Northern Adriatic Sea in the period 2003-2006. *Marine Ecology,* 29**,** 449-468.

SOCAL, G., BOLDRIN, A., BIANCHI, F., CIVITARESE, G., DE LAZZARI, A., RABITTI, S., TOTTI, C. & TURCHETTO, M. M. 1999. Nutrient, particulate matter and phytoplankton variability in the photic layer of the Otranto strait. *Journal of Marine Systems,* 20**,** 381-398.

SOLIDORO, C., BASTIANINI, M., BANDELJ, V., CODERMATZ, R., COSSARINI, G., MELAKU CANU, D., RAVAGNAN, E., SALON, S., et al. 2009. Current state, scales of variability, and trends of biogeochemical properties in the northern Adriatic Sea. *Journal of Geophysical Research: Oceans,* 114**,** C07S91.

SORHANNUS, U. & FOX, M. G. 2012. Phylogenetic analyses of a combined data set suggest that the *Attheya* lineage is the closest living relative of the pennate diatoms (Bacillariophyceae). *Protist,* 163**,** 252-262.

SOURNIA, A., CHRETIENNOT-DINET, M. J. & RICARD, M. 1991. Marine phytoplankton:how many species in the world ocean? *Journal of Plankton Research,* 13(5)**,** 1093-1099.

SUNESEN, I., HERNÀNDEZ-BECERRIL, D. U. & SAR, E. A. 2008. Marine diatoms from Buenos Aires coastal waters (Argentina). V. Species of the genus *Chaetoceros*. *Revista de Biologia Marina y Oceanografia,* 43**,** 303-326.

SUPIĆ, N., ORLIĆ, M. & DEGOBBIS, D. 2000. Istrian Coastal Countercurrent and its year-to-year variability. *Estuarine, Coastal and Shelf Science,* 51**,** 385-397.

SUTO, I. 2006. *Truncatulus* gen. nov., a new fossil resting spore morphogenus related to the marine diatom genus *Chaetoceros* (Bacillariophyceae). *Phycologia,* 45**,** 585-601.

SVENSEN, C., VILIČIĆ, D., WASSMANN, P., ARASHKEVICH, E. & RATKOVA, T. 2007. Plankton distribution and vertical flux of biogenic matter during high summer stratification in the Krka estuary (Eastern Adriatic). *Estuarine, Coastal and Shelf Science,* 71**,** 381-390.

SVETLIČIĆ, V., ŽUTIĆ, V., MIŠIĆ RADIĆ, T., PLETIKAPIĆ, G., HOZIĆ ZIMMERMAN, A. & URBANI, R. 2011. Polymer networks produced by marine diatoms in the northern Adriatic Sea. *Marine Drugs,* 9**,** 666-679.

SWOFFORD, D. L. 1998. *PAUP*. Phylogenetic analysis using Parimony (* and other methods). Version 4,* Sunderland, Massachusetts, Sinauer Associates.

ŠILOVIĆ, T., BALAGUÉ, V., ORLIĆ, S. & PEDRÓS-ALIÓ, C. 2012a. Picoplankton seasonal variation and community structure in the northeast Adriatic coastal zone. *FEMS Microbiology Ecology,* 82**,** 678-691.

ŠILOVIĆ, T., BOSAK, S., JAKŠIĆ, Ž. & FUKS, D. 2012b. Seasonal dynamics of the autotrophic community in the Lim Bay (NE Adriatic Sea). *Acta Adriatica,* 53**,** 41-56.

ŠILOVIĆ, T., LJUBEŠIĆ, Z., MIHANOVIĆ, H., OLUJIĆ, G., TERZIĆ, S., JAKŠIĆ, Ž. & VILIČIĆ, D. 2011. Picoplankton composition related to thermohaline circulation: The Albanian boundary zone (southern Adriatic) in late spring. *Estuarine, Coastal and Shelf Science,* 91**,** 519-525.

ŠUPRAHA, L. 2012. *Ekologija i taksonomija kriptofita u visokostratificiranom estuariju Krke (Taxonomy and ecology of cryptophytes in highly stratified Krka estuary),* MSc.Thesis. University of Zagreb, Faculty of Science, Division of Biology (in croatian).

ŠUPRAHA, L., BOSAK, S., LJUBEŠIĆ, Z., OLUJIĆ, G., HORVAT, L. & VILIČIĆ, D. 2011. The phytoplankton composition and spatial distribution in the north-

eastern Adriatic Channel in autumn 2008. *Acta Adriatica,* 52**,** 29-44.

TAKANO, H. 1983. New and rare diatoms from Japanese marine waters. X. A new *Chaetoceros* common in estuaries. *Bulletin of Tokai Regional Fisheries Research Laboratory,* 110**,** 1-11.

TOMAS, C. R. (ed.) 1997. *Identifying marine phytoplankton,* San Diego: Academic Press.

TOTTI, C., CIVITARESE, G., ACRI, F., BARLETTA, D., CANDELARI, G., PASCHINI, E. & SOLAZZI, A. 2000. Seasonal variability of phytoplankton populations in the middle Adriatic sub-basin. *Journal of Plankton Research,* 22**,** 1735-1756.

TRIGUEROS, J. M., ORIVE, E. & ARRILUZEA, J. 2002. Observations on *Chaetoceros salsugineus* (Chaetocerotales, Bacillariophyceae): first record of this bloom-forming diatom in a European estuary. *European Journal of Phycology,* 37**,** 571-578.

TROEDSSON, C., FRISCHER, M. E., NEJSTGAARD, J. C. & THOMPSON, E. M. 2007. Molecular quantification of differential ingestion and particle trapping rates by the appendicularian *Oikopleura dioica* as a function of prey size and shape. *Limnology and Oceanography,* 52**,** 416-427.

TÜRKOGLU, M. & ERDOGAN, Y. 2010. Diurnal variations of summer phytoplankton and interactions with some physicochemical characteristics under eutrophication in the Dardanelles. *Turkish Journal of Biology,* 34**,** 211-225.

UTERMÖHL, H. 1958. Zur Vervollkommnung der quantitativen Phytoplankton Methodik. *Mitteilungen der Internationale Vereinigung für theoretische und angewandte Limnologie,* 9**,** 1-38.

VAN HEURCK, H. 1882. *Synopsis des diatomees de Belgique. Atlas pls. LXXVIII-CIII.,* Anvers, Ducaju et Cie.

VANLANDINGHAM, S. L. 1968. *Catalogue of the fossil and recent genera and species of diatoms and their synonyms. Part II. Bacteriastrum through Coscinodiscus,* Lehre, J. Cramer.

VERITY, P. G., WHIPPLE, S. J., NEJSTGAARD, J. C. & ALDERKAMP, A.-C. 2007. Colony size, cell number, carbon and nitrogen contents of Phaeocystis pouchetii from western Norway. *Journal of Plankton Research,* 29**,** 359-367.

VILIČIĆ, D., BOSAK, S., BURIĆ, Z. & CAPUT-MIHALIĆ, K. 2007. Phytoplankton seasonality and composition along the coastal NE Adriatic Sea during the extremely low Po River discharge in 2006. *Acta Botanica Croatica,* 66**,** 101-115.

VILIČIĆ, D., DJAKOVAC, T., BURIĆ, Z. & BOSAK, S. 2009a. Composition and annual cycle of phytoplankton assemblages in the northeastern Adriatic Sea. *Botanica Marina,* 52**,** 291-305.

VILIČIĆ, D., KUZMIĆ, M., BOSAK, S., ŠILOVIĆ, T., HRUSTIĆ, E. & BURIĆ, Z. 2009b. Distribution of phytoplankton along the thermohaline gradient in the north-eastern Adriatic channel; winter aspect. *Oceanologia,* 51**,** 495-513.

VILIČIĆ, D., KUZMIĆ, M., TOMAŽIĆ, I., LJUBEŠIĆ, Z., BOSAK, S., PRECALI, R., DJAKOVAC, T., MARIĆ, D., et al. 2013. Northern Adriatic phytoplankton response to short Po River discharge pulses during summer stratified conditions. *Marine Ecology***,** n/a-n/a.

VILIČIĆ, D., LEDER, N., GRŽETIC, Z. & JASPRICA, N. 1995. Microphytoplankton in the Strait of Otranto (eastern Mediterranean). *Marine Biology,* 123**,** 619-630.

VILIČIĆ, D., LEGOVIĆ, T. & ŽUTIĆ, V. 1989. Vertical distribution of phytoplankton in a stratified estuary. *Aquatic Sciences,* 51**,** 31-46.

VILIČIĆ, D., MARASOVIĆ, I. & MIOKOVIĆ, D. 2002. Checklist of phytoplankton in the eastern Adriatic Sea. *Acta Botanica Croatica,* 61**,** 57-91.

VILIČIĆ, D., ŠILOVIĆ, T., KUZMIĆ, M., MIHANOVIĆ, H., BOSAK, S., TOMAŽIĆ, I. & OLUJIĆ, G. 2011. Phytoplankton distribution across the southeast Adriatic continental and shelf slope to the west of Albania (spring aspect). *Environmental Monitoring and Assessment,* 177**,** 593-607.

VILIČIĆ, D., TERZIĆ, S., AHEL, M., BURIĆ, Z., JASPRICA, N., CARIĆ, M., CAPUT MIHALIĆ, K. & OLUJIĆ, G. 2008. Phytoplankton abundance and pigment biomarkers in the oligotrophic,

eastern Adriatic estuary. *Environmental Monitoring and Assessment,* 142**,** 199-218.

VON DASSOW, P. & MONTRESOR, M. 2011. Unveiling the mysteries of phytoplankton life cycles: patterns and opportunities behind complexity. *Journal of Plankton Research,* 33**,** 3-12.

VON STOSCH, H. A., THEIL, G. & KOWALLIK, K. 1973. Entwicklungsgeschichtiliche Untersuchungen an zentrischen Diatomeen. V. Bau und Lebenszyklus von *Chaetoceros didymum*, mit beobachtungen über einige andere Arten der Gattung. *Helgoländer wissenschaftilche Meeresuntersuchungen,* 25**,** 384-445.

YENTSCH, C. S. & SCAGEL, R. F. 1958. Diurnal study of phytoplankton pigments. An in situ study in East Sound, Washington. *Journal of Marine Research,* 17**,** 567-583.

ZAVATARELLI, M., PINARDI, N., KOURAFALOU, V. H. & MAGGIORE, A. 2002. Diagnostic and prognostic model studies of the Adriatic Sea general circulation: Seasonal variability. *Journal of Geophysical Research: Oceans,* 107**,** 2-1-2-20.

APPENDICES

APPENDIX I

Glossary of Chaetocerotaceae terminology

The terminology used to describe *Chaetoceros* and *Bacteriastrum* is ambiguous as it contains many synonyms and contradictory terms for the same structures. The following terms listed here and used in this thesis have been adopted from Rines and Hragraves (1988), Hernadez Becerril (1996), Evensen and Hasle (1975) and Ishii et al. (2011), modified and supplemented with novel terms based on the observations on Adriatic material. The glossary covers various structures observable with both light and electron microscopy. The synonyms for particular terms are given in brackets.

Annulus – [central field] circular/elliptical and usually hyaline area positioned in the valve centre or slightly shifted towards the one side of the valve. It is apparently lacking in *Chaetoceros amanita* and in *C. contortus* it is ornamented with reticulate costae network.

Aperture – [foramen, window] the space between adjacent cells in a chain. Its size and shape is determined by the length of the basal part of setae, shape of the valves and type of fusion. It can be less or more than 5 μm and it is described as narrow or wide, respecively. Some species show a very wide range of variation in the aperture size within the same chain. The term aperture is chosen in preference to foramen following Hernandez Becerril (1996) because the latter represents rather the structure in the valve itself, and not the space between cells.

Apical axis – long axis extending through the valve centre and in elliptically shaped valves between the two valve apices, parallel with the valve face.

Apical plane – plane extending from the apical axis, perpendicular on the valve face.

Basal part – the portion of the seta proximal to the valve between its point of origin and its point of fusion with the sibling seta. The basal part on the terminal seta or where the setae are not fused is the portion closest to the valve face and of not determined length.

Capillus – a long, or short hairlike/filamentous siliceous spine of a simple solid construction, found either on spores or on parts of vegetative cells e.g. setae, valve face.

Cell jacket – organic fibrillar network which embeds individual cells of *Bacteriastrum jadranum* connecting them in a loose-chain colony formation.

Central process – [rimoportula] the process found more or less in the centre of only terminal or of all valves, dependent on the particular species. It varies from a simple round/elliptical hole through the valve or long external tube to reduced labiate process. The term process is rather used instead of rimoportula because a typical rimoportular structure is rarely evident in *Chaetoceros* and *Bacteriastrum*.

Chain – [chain colony] colony formed of a number of cells with sibling valves oriented facing one another and generally held together by interconnection/fusion of setae. Chains are arbitrarily

considered short if they are composed of less than ten cells and long if composed of ten cells or more. In shape they may be straight, twisted about chain axis or helically coiled.

Chain axis – the long axis through the chain, runs parallel to the pervalvar axis.

Chain margin – the line parallel to the chain axis which runs along the edge of the chain at its widest dimension, usually refers to broad girdle view.

Connecting band – [pleura] the band in the middle of the girdle, usually having marked indentations (2 in *Chaetoceros*, more in *Bacteriastrum*) through which newly formed setae protrude.

Costa - [rib] unornamented thickening of silica on the surface of either par tof the frustule.

Cross-bridge – [siliceous cross piece, silica rod, bridge], the hyaline silica structure connecting the sibling setae in *Chaetoceros anastomosans.*

Divergence angle – the angle by which a seta departs from the apical axis/apical plane, used in description of three dimensional structure of a chain or Brunel groups. Sometimes, the angle is also measured with respect to the valvar plane.

Girdle – [cingulum] the part of the frustule connecting the valves in the same cell. The girdle is composed of numerous intercalary half bands and a distinct connecting band. There is no morphologically different valvocopula in any of the examined species so far.

Girdle view – front view obtained when cell/chain is oriented that one looks at the girdle. In *Chaetoceros* species which have oval valves when viewed in the apical plane it is termed broad/wide girdle view and the frustule is viewed from the broad side. When in transapical plane perspective it is termed narrow girdle view and the elipsoid shaped frustule seen from the narrow side.

Granule – a small rounded protuberance on the valve, giving the surface the granulated appearance. The same term is used to describe the chloroplast-like material in setae of some *Hyalochaete* species such as *C. brevis*.

Heteropolar - two ends of a chain or two valves of a cell are markedly different from each other. To distinguish each end the terms anterior and posterior are used, the anterior having setae curved towards the chain or cell, and posterior end with setae curved away from the chain or cell.

Heterovalvate – when the two valves of a same cell are dissimilar.

Hyaline rim – the rim of the variable height and hyaline structure or fissured, extending from the marginal ridge.

Intercalary setae – [inner setae] those setae which arise on the intercalary valves of a chain, includes the setae on the internal valve of the terminal cell as that is intercalary valve as well.

Intercalary valve – the valves on the inside of the chain, bearing intercalary setae.

Intercalary bands – [copulae] the girdle bands close to the valves, usually half bands in Chaetocerotaceae.

Isovalvate – the two valves of the frustule have similar morphology.

Linking spine – [linkage process] spine-like process in *Chaetoceros rostratus* which links sibling valves in a chain.

Marginal ridge – [advalvar mantle edge, valve edge] a ridge between the valve face and the valve mantle.

Mantle edge – [abvalvar mantle edge] an edge between the valve mantle and the girdle, usually just before the very edge the mantle is more or less constricted, depending on the particular species.

Outgrowth- the shoehorn- or T- shaped structure projecting from the valve margin between two contiguous setae in *Chaetoceros bacteriastroides* and several *Bacteriastrum* species. Unlike setae, they do not appear hollow but this is not confirmed as their cross-section is not possible to observe due to their closed ends.

Palisade spines – a straight and rigid spines projecting from the marginal ridge in some resting spores.

Pervalvar axis - long axis through the centre of the valve, perpendicular to the valve face.

Primary valve – [epivalve] the initially formed valve of a resting spore

Projection – strongly silicified structure often extending from the edge of the marginal ridge, an irregular extension of the hyaline rim, very distinct in e.g. *Chaetoceros pseudodichaeta* valves. The same term is used to describe the external part of the central process.

Protuberance – a protrusion, bulge on the valve face.

Resting spore – cell produced by mitotic division, morphologically different from the vegetative cells; it can withstand a broader range of environmental conditions and/or undergo quienescence period. Its morphology is a very important taxonomic character.

Secondary valve – [hypovalve] the secondly formed valve of a resting spore.

Silica flap - a thin silica wall with no distinct pattern covering the aperture in *Chaetoceros affinis*

Spermatogonium – a cell that subsequently produces the sperm.

Sperm – the anteriorly uniflagellate microgametes of oogamus diatoms (all Chaetocerotaceae species)

Seta – a hollow spine-like outgrowth of the valve projecting outside the valve margin, with a very different structure from that of the valve. The hallmark of the members of family Chaetocerotaceae. In cross-section, setae may be round, four sided or polygonal. The setae are usually ornamented with various spines which spiral around the round setae or are positioned in rows along the ridges of polygonal seta. They are also often perforated by pores, or areolae. The setae structural design represents an useful taxonomic identification character, especially in *Phaetoceros* species.

Sheath – [collar] a sleeve-like siliceous membrane which is attached to the resting spore mantle. The sheath can extend in the pervalvar direction further than the spore valve itself does and partially obscure the spore. Either one or both valves may be sheathed. The term collar is defined as a projection of the valve face and not the valve mantle which originates as a vertical extension of the wall of a loculate areola by Crawford (1975) but in literature both terms are used (e.g. Kooistra et al. 2010).

Sibling setae – The setae on the same side of adjacent/sibling valves of the neighbouring cells in a chain, commonly fused/interconnected.

Single ring of puncta - A single row of pores at the advalvar margin of the secondary valve mantle of the resting spore. When the complete and closed spore is observed, the row is hardly visible because it is covered by the primary valve.

Special setae - morphologically different intercalary setae, usually thicker than ordinary ones.

Spine – a closed or solid structure projecting out from the cell wall, occurs on the setae or on the valves of resting spores.

Spinule – a very small spine, arbitrary difference between spine and spinule. Used in describing spines usually occurring on the vegetative valves but also including the Y-shaped spines found on the *Bacteriastrum hyalinum* setae.

Stria – one or more rows of pores/poroids/areolae.

Suture – the junction between the mantle and the girdle.

Terminal setae – setae on the terminal/end valve of a chain. Often different in morphology and direction with respect to the intercalary ones.

Terminal valve – the end valves of a colony, chain terminating valves (separation valves) because their setae do not join with corresponding sibling setae resulting in separation of a parent colony into two daughter colonies. In *Bacteriastrum* spp., in the subgenus Hyalochaete and *Chaetoceros pseudodichaeta* only terminal valves possesses central process, which is lacking in intercalary valves.

Transapical axis - short axis extending through the valve centre, perpendicular on the apical axis, does not exist in round shaped valves.

Transapical plane - – plane extending from the apical axis, perpendicular both on the valve face and apical plane.

Valvar plane – the plane parallel with the valve face, plane of cell division.

Valve apex – [pole of the apical axis] the point where the apical axis comes in contact with the edge of the valve, commonly the point of origin of the setae.

Valve corner – in girdle view, the point at which the valve face, valve apex and valve mantle meet. They may be sharp, rounded or diagonally cut.

Valve face- the central, surface portion of the valve which lies in the valvar plane, surrounded by the valve mantle.

Valve mantle – the marginal part of the valve differentiated by slope and sometimes by structure. Perpendicular to the valve face and together with the girdle composing the pervalvar dimension of the cell. It may be defined as high or low with the respect to the length of the girdle.

Valve view – a view on a cell such that the valve face is seen.

APPENDIX II

Brunel groups

Brunel (1972) defined six categories in order to describe the divergence angles formed by the setae of two intercalary sibling valves when observed in valve/apical view (Appendix II - Figure.1.). Rines and Hargraves (1988) added one more group where all setae curve back around the cell, away from the apical axis, similar to Brunel group IV but curved and not straight with the representative species *C. circinalis*.

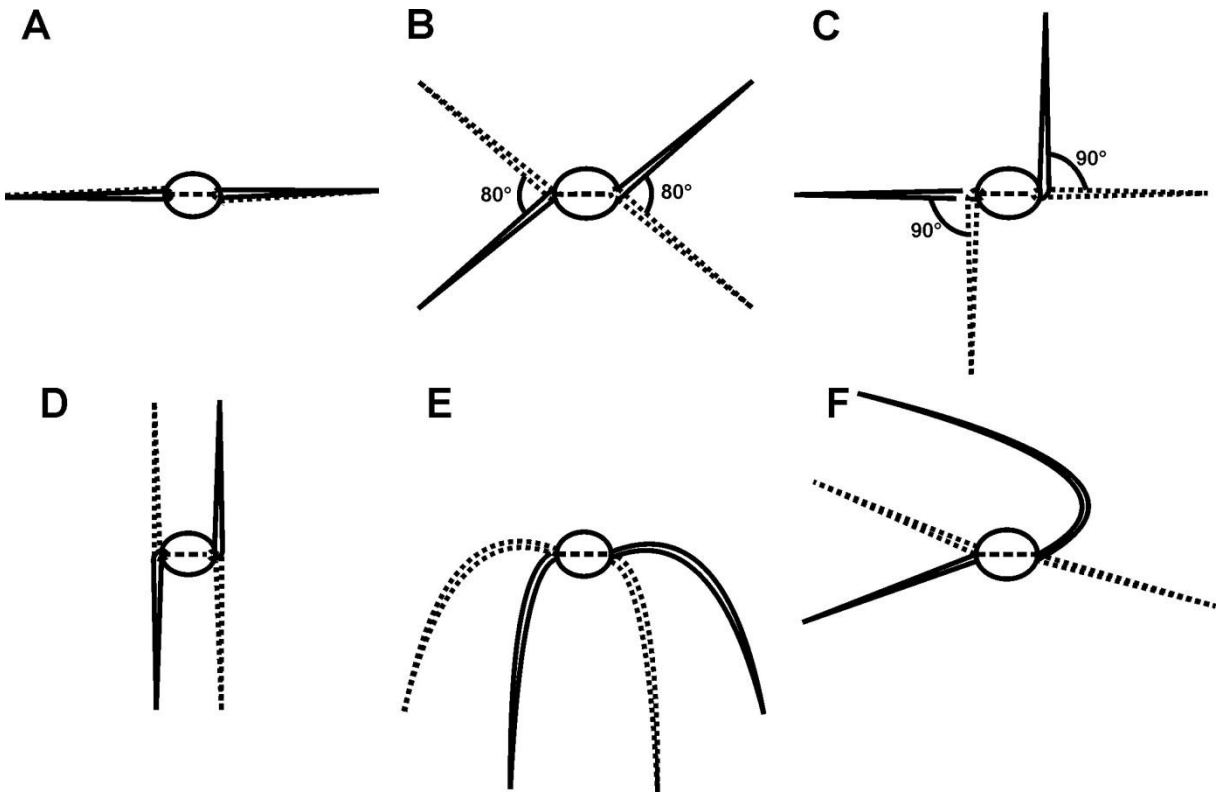

Appendix II - Figure 1. *Chaetoceros* cells in apical view with a pair of superimposed setae of sibling valves. Upper setae - full line, lower setae- dotted line. **A)** Brunel group I: all setae parallel to apical plane, divergence 0°. **B)** Brunel group II: setae diverge at an angle of 30°-80° from each other, and about 15°-45° equally from the apical plane. **C)** Brunel group III: one seta parallel with the apical plane, the other more or less perpendicular to it, setae diverge by 90° from each other. **D)** Brunel group IV: all setae diverging 180° from each other, all four being perpendicular to the apical axis. **E)** Brunel group V: all setae diverging from each other at base at an angle of 40°-50° but all curved toward the same side of the apical axis. **F)** Brunel group VI: one pair of sibling setae diverge 30-50° from the apical plane. One member of the other pair curves back around the cell and continues in the direction of the first pair, the other is especially elongated and grows toward the colony center (adapted from Brunel (1978)).

APPENDIX III

List of phytoplankton species and supra-specific taxa recorded at station RV001 between September 2008 and October 2009 with mean cellular volumes; ESD – equivalent spherical diameter, MLD – maximum linear dimension and carbon content; N – nanophytoplankton; M – microphytoplankton; n.d. – not determined. * - taxa identified only from net samples, [1] – heterotrophic taxa. Chaetocerotacean species are marked in bold.

Species	Size-class	Volume (μm^3)	ESD (µm)	MLD (µm)	Carbon (pg)
Diatoms					
Achnanthes sp.	N	703.74	11.04	16.09	58.70
*Actinocyclus sp.**	M	5 928.80	22.46	19.62	330.57
Actinoptychus splendens (Shadbolt) Ralfs ex Pritchard*	M	395 952.78	91.12	89.05	9978.87
Amphora sp.	M	10 396.30	27.08	53.85	521.29
Asterionellopsis glacialis (Castracane) Round	M	2 229.33	16.21	70.96	149.54
Asteromphalus heptactis (Brébisson) Ralfs	M	31 641.24	39.25	44.06	1 285.58
Asterolampra marylandica Ehrenberg*	M	216 314.60	74.49	83.00	6 111.49
Bacillaria paxillifera (Müller) Hendey *	M	13 389.77	29.47	156.83	640.04
***Bacteriastrum furcatum* Shadbolt**	M	2 483.44	16.80	24.11	163.22
***Bacteriastrum hyalinum* Lauder**	M	18 241.65	32.67	28.55	822.46
Bacteriastrum jadranum	M	895.34	11.96	21.28	71.36
***Bacteriastrum mediterraneum* Pavillard**	M	6 202.97	22.80	23.78	342.92
***Bacteriastrum* sp.**	M	8 311.33	25.14	11.20	434.76
Corataulina pelagica (Cleve) Hendey	M	37 671.76	41.60	100.10	1 480.95
***Chaetoceros affinis* Lauder**	M	1 792.74	15.07	19.23	125.31
***Chaetoceros anastomosans* Grunow**	M	393.29	9.09	9.01	36.62
***Chaetoceros brevis* Schutt**	M	3 163.82	18.22	17.22	198.64
***Chaetoceros borealis* Bailey**	M	10 498.92	27.17	24.56	525.46
Chaetoceros coarctatus* Lauder		n.d.	n.d.	n.d.	n.d.
***Chateoceros contortus* Schütt**	M	1 690.54	14.78	23.85	119.49
Chaetoceros constrictus* Gran		n.d.	n.d.	n.d.	n.d.
***Chaetoceros costatus* Pavillard**	M	3 923.72	19.57	22.81	236.53
***Chaetoceros curvisetus* Cleve**	M	2 929.53	17.76	20.59	186.62
***Chaetoceros dadayi* Pavillard**	M	2 371.48	16.55	12.92	157.23
***Chaetoceros danicus* Cleve**	M	5 545.88	21.96	18.37	313.15
***Chaetoceros decipiens* Cleve**	M	5 918.82	22.45	23.02	330.12
***Chaetoceros densus* (Cleve) Cleve**	M	21 841.82	34.69	30.25	951.82
***Chaetoceros didymus* Ehrenberg**	M	2 403.31	16.62	19.75	158.94
***Chaetoceros diversus* Cleve**	M	375.25	8.95	8.57	35.25
***Chaetoceros eibenii* (Grunow in Van Heurck) Meunier**	M	12 719.01	28.97	30.42	613.91
***Chaetoceros lauderi* Ralfs in Lauder**	M	21 168.82	34.33	41.12	927.97
***Chaetoceros peruvianus* Brightwell**	M	22 861.31	35.22	26.57	987.70
***Chaetoceros rostratus* Lauder**	M	8 923.71	25.74	22.79	460.56
***Chaetoceros simplex* Ostenfeld**	N	164.09	6.79	7.31	18.02
***Chaetoceros socialis* Lauder**	M	464.90	9.61	10.62	41.94
***Chaetoceros tenuissimus* Meunier**	N	148.81	6.58	6.73	16.65
Chaetoceros tetrastichon* Cleve		n.d.	n.d.	n.d.	n.d.
***Chaetoceros throndsenii* var. *throndsenia* (Marino, Montresor & Zingone) Marino, Montresor & Zingone**	N	45.28	4.42	8.66	6.34
***Chaetoceros throndsenii* var. *trisetosa* Zingone**	N	45.28	4.42	8.66	6.34
***Chaetoceros tortissimus* Gran**	M	1 158.60	13.03	17.52	87.95
***Chaetoceros vixvisibilis* Schiller**	M	1 159.70	13.04	12.24	88.02
***Chaetoceros* cf. *wighamii* Brightwell**	M	416.06	9.26	11.14	38.33
***Chaetoceros* sp. "A"**	M	859.75	11.80	13.00	69.05
***Chaetoceros* sp. "B"**	N	185.97	7.08	7.91	19.95
***Chaetoceros* sp. "C"**	N	49.44	4.55	5.92	6.81
***Chaetoceros* spp.**	M	2 413.51	16.65	20.79	159.49
Cocconeis scutellum Ehrenberg	M	1 070.27	12.69	21.53	82.47

Species	Size-class	Volume (μm^3)	ESD (µm)	MLD (µm)	Carbon (pg)
Coscinodiscus sp.	M	264 667.82	79.67	100.08	7 197.86
Cyclotella sp.	N	292.94	8.24	7.81	28.84
Cylindrotheca closterium (Ehrenberg) Reihmann et Lewin	M	290.69	8.22	26.21	28.66
Dactyliosolen blavyanus (Peragallo) Hasle	M	106 360.23	58.79	187.48	3 436.45
Dactyliosolen fragilissimus (Bergon) Hasle	M	7 281.20	24.05	73.64	390.52
Dactyliosolen phuketensis (Sundström) Hasle	M	13 331.21	29.42	116.78	637.77
Detonula pumila (Castracane) Gran*	M	23 348.28	35.47	44.86	1 004.73
Diploneis bombus Ehrenberg	M	3 836.11	19.43	33.90	232.24
Diploneis sp.	M	5 969.23	22.51	35.25	332.40
Ditylum brightwellii (West) Grunow	M	73 617.61	52.01	162.93	2 549.85
Entomoneis sp.	M	51 337.40	46.12	89.27	1 903.51
Eucampia cornuta (Cleve) Grunow	M	7 085.21	23.83	52.10	381.97
Eucampia zodiacus Ehrenberg*	M	9 796.99	26.55	32.40	496.79
Guinardia flaccida (Castracane) Peragallo	M	169 192.73	68.63	170.56	5 007.37
Guinardia striata (Stolterfoth) Hasle	M	96 682.83	56.95	168.37	3 180.61
Gyrosigma sp.	M	47 976.38	45.09	173.51	1 801.80
Haslea wawrikae (Hustedt) Simonsen	M	10 713.24	27.36	525.26	534.14
Hemiaulus hauckii Grunow	M	21 563.05	34.54	64.33	941.96
Hemiaulus sinensis Greville	M	33 115.78	39.85	50.53	1 333.95
Lauderia annulata Cleve	M	32 961.58	39.79	48.96	1 328.91
Leptocylindrus danicus Cleve	M	2 833.18	17.56	60.36	181.63
Leptocylindrus mediterraneus (Peragallo) Hasle	M	9 420.82	26.21	69.18	481.26
Leptocylindrus minimus Gran*	M	1 133.82	12.94	44.38	86.42
Licmophora sp.	M	21 005.92	34.24	93.25	922.17
Lioloma pacificum (Cupp) Hasle	M	5 501.33	21.91	390.54	311.11
Lyrella sp.	M	1 492.86	14.18	22.11	108.02
Melosira nummuloides Agardh*	M	3 899.86	19.53	22.15	235.36
Melosira sp.*	M	3 899.86	19.53	22.15	235.36
Navicula sp.	M	3 084.48	18.06	45.27	194.59
Neocalyptrella robusta (Norman) Hernández–Becerril et Meave	M	7 543 474.85	243.37	758.45	108 918.82
Nitzschia incerta (Grunow) Peragallo	M	4 271.41	20.13	108.77	253.39
Nitzschia longissima (Brébisson) Ralfs	M	573.41	10.31	102.63	49.72
Nitzschia sp.	M	2 091.04	15.87	73.53	141.97
Paralia sulcata (Ehrenberg) Cleve	M	2 928.48	17.75	19.55	186.57
Pleurosigma sp.	M	28 799.59	38.04	118.58	1 191.12
Podocystis sp.*	M	n.d.	n.d.	n.d.	n.d.
Podosira stelligera (Bailey) Mann*	M	47 202.28	44.85	44.08	1 778.18
Psammodictyon panduriforme (Gregory) Mann	N	1 080.67	12.73	24.19	83.12
Proboscia alata (Brightwell) Sundström	M	26 177.21	36.85	566.23	1 102.37
Proboscia indica (Peragallo) Hernández–Becerril	M	1 269 497.34	134.36	992.37	25 670.71
Pseudo-nitzschia linea Lundholm, Hasle & Fryxell*	M	883.47	11.91	32.19	70.59
Pseudo-nitzschia delicatissima (Cleve) Heiden	M	347.08	8.72	57.74	33.09
Pseudo-nitzschia fraudulenta (Cleve) Hasle*	M	2 937.49	17.77	79.32	187.03
Pseudo-nitzschia galaxiae Lundholm et Moestrup	M	32.04	3.94	28.36	4.79
Pseudo-nitzschia pseudodelicatissima complex	M	485.39	9.75	87.41	43.43
Pseudo-nitzschia cf. *pseudodelicatissima* (Hasle) Hasle*		n.d.	n.d.	n.d.	n.d.
Pseudo-nitzschia calliantha Lundholm, Moestrup & Hasle*		n.d.	n.d.	n.d.	n.d.
Pseudo-nitzschia pungens (Grunow ex Cleve) Hasle*	M	1 382.11	13.82	97.59	101.48
Pseudo-nitzschia seriata group	M	2 134.66	15.98	90.00	144.37
Pseudo-nitzschia subfraudulenta (Hasle) Hasle*	M	2 725.36	17.33	99.14	176.00
Pseudosolenia calcar-avis (Schultze) Sundström	M	1 447 835.53	140.38	714.88	28 558.53
Raphoneis sp.	N	501.08	9.86	14.76	44.57

Species	Size-class	Volume (μm^3)	ESD (µm)	MLD (µm)	Carbon (pg)
Rhizosolenia castracanei Cleve*	M	15 513 371.74	309.49	693.49	195 458.79
Rhizosolenia decipiens Sundström*	M	113 069.95	60.01	386.69	3 611.25
Rhizosolenia imbricata Brightwell	M	104 511.60	58.45	495.03	3 387.93
Rhizosolenia sp.	M	9 533.00	26.31	426.07	485.90
Rhizosolenia styliformis Brightwell*	M	134 149.91	63.52	458.52	4 148.28
Skeletonema marinoi Sarno & Zingone	M	398.00	9.13	12.91	36.97
Striatella unipunctata (Lyngbye) Agardh	M	75 515.77	52.45	121.66	2603.04
Thalassionema nitzschioides (Grunow) Mereschkowsky	M	2 063.45	15.80	78.59	140.45
Thalassiosira rotula Meunier	M	12 333.87	28.67	33.09	598.79
Thalassiosira spp.	M	27 970.57	37.67	40.67	1 163.23
Thalassiothrix longissima Cleve et Grunow*	M	8 000.00	24.82	500.00	421.50
Toxarium undulatum Bailey*	M	19 922.20	33.64	297.63	883.40
Other pennate diatoms (>20 µm)	M	2 318.07	16.42	48.73	154.35
Other pennate diatoms (<20 µm)	N	137.91	6.41	15.47	15.65
Dinoflagellates					
Actiniscus pentasterias (Ehrenberg) Ehrenberg*	M	n.d.	n.d.	n.d.	n.d.
Ceratocorys gourettii Paulsen*	M	n.d.	n.d.	n.d.	n.d.
Dinophysis acuminata Claparéde et Lachmann	M	28 704.12	37.99	56.00	3 314.85
Dinophysis caudata Seville-Kent	M	39 596.97	42.30	83.89	4 483.92
Dinophysis fortii Pavillard	M	38 732.81	41.99	60.66	4 391.98
Dinophysis infundibulus Schiller*	M	2 952.39	17.80	31.62	391.69
Dinophysis sacculus Stein*	M	18 417.04	32.77	51.18	2 185.22
Diplopsalis - complex[1]	M	118 526.27	60.96	60.96	12 553.52
Dissodinium pseudolunula Swift ex Elbrächter & Drebes[1]	M	32 500.00	39.60	22.72	3 724.88
Gonyaulax spp.	M	67 882.22	50.62	55.72	7 438.28
Gymnodinium spp.	M	2 832.37	17.56	22.56	376.72
Gyrodinium fusiforme Kofoid & Swezy	M	23 887.91	35.74	72.29	2 789.74
Gyrodinium spp.	M	4 438.98	20.39	46.02	574.45

Species	Size-class	Volume (μm^3)	ESD (µm)	MLD (µm)	Carbon (pg)
Kofoidinium velelloides Pavillard[1]	M	6 471 043.55	231.24	231.24	536 980.65
Lingulodinium polyedrum (Stein) Dodge	M	75 662.49	52.48	56.53	8 236.12
Mesoporos perforatus (Gran) Lillick	N	2 910.24	17.72	18.35	386.44
Neoceratium azoricum (Cleve) Gómez, Moreira et López-Garcia*	M	42 163.35	43.19	51.01	4 756.28
Neoceratium candelabrum (Ehrenberg) Gómez, Moreira et López-Garcia	M	157 491.86	67.01	81.19	16 393.78
Neoceratium carriense (Gourret) Gómez, Moreira et López-Garcia*	M	100 678.38	57.73	63.41	10 769.88
Neoceratium extensum (Gourret) Gómez, Moreira et López-Garcia	M	19 935.47	33.65	27.37	2 353.98
Neoceratium falcatum (Kofoid) Gómez, Moreira et López-Garcia*	M	5 862.37	22.38	14.45	745.89
Neoceratium furca (Ehrenberg) Gómez, Moreira et López-Garcia	M	34 136.75	40.25	44.38	3 900.76
Neoceratium fusus (Ehrenberg) (Gómez, Moreira et López-Garcia	M	12 196.68	28.56	21.17	1 484.00
Neoceratium hexacanthum (Gourret) Gómez, Moreira et López-Garcia	M	201 305.41	72.73	79.60	20 643.06
Neoceratium longirostrum (Gourret) Gómez, Moreira et López-Garcia *	M	15 306.85	30.81	23.84	1 836.80
Neoceratium horridum (Cleve) Gómez, Moreira et López-Garcia *	M	57 416.24	47.87	52.74	6 356.05
Neoceratium macroceros (Ehrenberg) Gómez, Moreira et López-Garcia*	M	91 234.96	55.86	61.39	9 818.50
Neoceratium massiliense (Gourret) Gómez, Moreira et López-Garcia	M	76 546.44	52.69	57.96	8 326.44
Neoceratium pentagonum (Gourret) Gómez, Moreira et López-Garcia	M	71 188.89	51.43	67.84	7 778.02
Neoceratium pulchellum (Schröder) Gómez, Moreira et López-Garcia *	M	113 279.89	60.04	70.95	12 031.04
Neoceratium sp.	M	71 806.49	51.58	56.75	7 841.36
Neoceratium symmetricum	M	43 325.11	43.58	51.48	4 879.24

Species	Size-class	Volume (μm^3)	ESD (µm)	MLD (µm)	Carbon (pg)
(Pavillard) Gómez, Moreira et López-Garcia *					
Neoceratium trichoceros (Ehrenberg) Gómez, Moreira et López-Garcia	M	26 535.86	37.01	40.94	3 079.17
Neoceratium tripos (Müller) Gómez, Moreira et López-Garcia	M	97 034.56	57.02	67.38	10 403.46
Noctiluca scintillans (Macartney) Kofoid et Swezy[1]	M	37 964 998.43	417.06	417.06	2 828 099.93
*Ornithocercus sp.**	M	415 82.86	42.99	42.99	4 694.77
Ornithocercus magnificus Stein*	M	415 82.86	42.99	42.99	4 694.77
Oxytoxum adriaticum Schiller*	M	4 386.63	20.31	30.59	568.09
Oxytoxum caudatum Schiller*	M	756.80	11.31	40.65	109.10
Oxytoxum sceptrum (Stein) Schröder	M	5 145.69	21.42	68.92	659.93
Oxytoxum spp.	M	523.33	10.00	20.00	77.16
Oxytoxum sphaeroideum Stein*	M	4 386.63	20.31	30.59	568.09
Oxytoxum variabile Schiller	N	254.59	7.86	19.80	39.22
Phalacroma rotundatum (Claparéde & Lachmann) Kofoid & Michener[1]	M	12 677.10	28.93	49.63	1 538.83
Podolampas bipes Stein*	M	111 228.13	59.68	85.45	11 826.31
Podolampas palmipes Stein	M	18 382.12	32.75	78.03	2 181.33
Prorocentrum compressum (Bailey) Abé	M	18 872.83	33.04	34.22	2 235.96
Prorocentrum micans Ehrenberg	M	13 149.86	29.29	49.77	1 592.65
Prorocentrum minimum (Pavillard) Schiller	N	1 000.29	12.41	17.29	141.77
Prorocentrum sp.	M	9 768.46	26.53	36.81	1 204.76
Prorocentrum triestinum Schiller	N	1 004.34	12.43	19.16	142.31
Protoperidinium conicum (Gran) Balech[1]	M	136 312.81	63.86	72.02	14 314.75
Protoperidinium depressum (Bailey) Balech[1]	M	442 806.96	94.58	126.70	43 276.20
Protoperidinium diabolum (Cleve) Balech[1]	M	27 925.01	37.65	59.58	3 230.29
Protoperidinium divergens (Ehrenberg) Balech[1]	M	149 691.35	65.89	78.96	15 630.16
Protoperidinium globulum (Stein) Balech*[1]	M	10 674.16	27.32	30.22	1 309.36
Protoperidinium oblongum (Aurivillius) Parke & Dodge[1]	M	384 719.26	90.25	139.82	37 923.11
Protoperidinium oceanicum (VanHöffen) Balech[1]	M	155 689.90	66.76	99.79	16 217.59
Protoperidinium cf. *ovatum* Pouchet*[1]		n.d.	n.d.	n.d.	n.d.
Protoperidinium pellucidum Bergh ex Loeblich & Loeblich III[1]	M	62 29.30	22.83	32.94	789.65
Protoperidinium cf. pentagonum (Gran) Balech*[1]		n.d.	n.d.	n.d.	n.d.
Protoperidinium sp.[1]	M	95 012.54	56.62	74.27	101 99.76
Protoperidinium steinii (Joergensen) Balech[1]	M	17 302.70	32.10	47.65	2 060.83
Pseliodinium vaubanii Sournia	M	10 637.89	27.29	27.29	1 305.18
Pyrophacus steinii (Schiller) Wall & Dale*	M	118 868.49	61.01	87.76	12 587.56
Scrippsiella sp.	M	8 861.10	25.68	32.46	1 099.37
Undetermined dinoflagellates (>20 µm)	M	35 250.41	40.69	40.69	4 020.14
Undetermined dinoflagellates (<20 µm)	N	802.98	11.53	11.53	115.34
Incertae sedis					
Hermesinum adriaticum Zacharias[1]	M	5 022.91	21.25	30.16	645.14
Meringosphaera mediterranea Lohmann	N	211.04	7.39	7.39	32.89
Dictyochophyceans					
Dictyocha fibula Ehrenberg	M	9 095.97	25.90	32.64	1126.71
Dictyocha speculum Ehrenberg	M	4 502.33	20.49	25.82	582.14
Octactis octonaria (Ehrenberg) Hovasse	M	3 997.84	19.69	24.81	520.68
Chrysophyceans					
Dinobryon faculiferum (Willén) Willén	N	77.59	5.29	8.35	12.85
Dinobryon sp.	N	95.17	5.67	8.41	15.57
Cryptophyceans					
Undetermined cryptophytes (5-20	N	230.20	7.61	13.33	35.68

Species	Size-class	Volume (μm^3)	ESD (µm)	MLD (µm)	Carbon (pg)
µm)					
Hemiselmis sp.*	N	597.78	10.45	20.68	87.42
Plagioselmis sp.*	N	208.56	7.36	12.78	32.53
*Teleaulax sp.**	N	580.96	10.35	16.17	85.11
Chlorophyceae					
phytoflagellates (<20 µm) - green flagellates	N	225.81	7.56	7.59	35.04
*Halosphaera sp.**	M	847 308.59	117.42	117.42	79 594.82
Pachysphaera sp.	N	125.36	6.21	6.69	20.17
Prasinophyceae					
Pseudoscourfieldia marina (Throndsen) Manton	N	9.88	2.66	3.57	1.86
Pyramimonas sp.*	N	340.94	8.67	9.76	51.60
Euglenophyceae					
Eutreptia sp.	M	499.32	9.84	28.51	73.83
Prymnesiophyceans					
Chrysocromulina parkerae Green et Leadbeater	N	145.01	6.52	8.99	23.12
Chrysocromulina sp.	N	1 316.94	13.60	19.56	183.54
Phaeocystis sp.*	N	250.98	7.83	7.83	38.70
Calyptrosphaera oblonga Lohmann*	N	923.67	12.09	12.09	131.55
Emiliania huxleyi (Lohmann) Hay et Mohler*	N	128.81	6.27	6.27	20.69
Syracosphaera pulchra Lohman*	N	2 961.49	17.82	16.05	392.83

APPENDIX IV

Partial list of phytoplankton species and supra-specific taxa enumerated at station Martinska (M) between 19 and 24 July 2010 with mean cellular volumes; ESD – equivalent spherical diameter, MLD – maximum linear dimension and carbon content; N – nanophytoplankton; M – microphytoplankton. [1] – heterotrophic taxa. Chaetocerotacean species are marked in bold. Species recored in this part of the study but having the same dimensions as in Appendix III are not repeated.

Species	Size	Volume (μm^3)	ESD (µm)	MLD (µm)	Carbon (pg)
Diatoms					
Achnanthes spp.	M	7797.02	24.61	38.36	412.81
Amphora spp.	M	10272.20	26.98	54.53	516.24
Asteromphalus heptactis (Brébisson) Ralfs	M	7651.51	24.45	27.45	406.55
***Bacteriastrum furcatum* Shadbolt**	**M**	**1203.96**	**13.20**	**21.26**	**90.73**
***Bacteriastrum* sp.**	M	892.41	11.95	15.45	71.17
Cerataulina pelagica (Cleve) Hendey	M	2478.35	16.79	69.32	162.95
***Chaetoceros affinis* Lauder**	**M**	**1384.37**	**13.83**	**14.81**	**101.61**
***Chaetoceros coarctatus* Lauder**	**M**	**60605.97**	**48.74**	**54.46**	**2177.77**
***Chaetoceros curvisetus* Cleve**	**M**	**1545.21**	**14.35**	**16.74**	**111.09**
***Chaetoceros pseudodichaeta* Ikari**	**M**	**390.88**	**9.07**	**13.62**	**36.44**
Chaetoceros salsugineus	**M**	**108.29**	**5.91**	**6.28**	**12.87**
***Chaetoceros simplex* Ostenfeld**	**N**	**57.31**	**4.78**	**5.24**	**7.68**
***Chaetoceros tenuissimus* Meunier**	**N**	**813.24**	**11.58**	**11.53**	**66.01**
***Chaetoceros throndsenii* var. *throndsenia* (Marino, Montresor & Zingone) Marino, Montresor & Zingone**	**N**	**33.83**	**4.01**	**5.36**	**5.01**
***Chaetoceros* cf. *wighamii* Brightwell**	**M**	**396.38**	**9.12**	**8.81**	**36.85**
***Chaetoceros* sp. "B"**	**N**	**164.09**	**6.79**	**7.31**	**18.02**
***Chaetoceros* spp.**	**M**	**859.75**	**11.80**	**13.00**	**69.05**
Coscinodiscus spp.	M	20388.29	33.90	50.64	900.12
Cymbella spp.	N	250.00	7.82	20.00	25.36
Dactyliosolen blavyanus (Peragallo) Hasle	M	7659.62	24.46	51.46	406.90
Diatoma vulgare Bory	M	300.00	8.31	50.00	29.40
Entomoneis sp.	M	17666.95	32.32	74.98	801.38
*Fragilaria crotonensis*Kitton	M	1067.23	12.68	55.05	82.28
Leptocylindrus danicus Cleve	M	2706.32	17.29	81.46	175.01
Leptocylindrus mediterraneus (Peragallo) Hasle	M	11110.19	27.69	140.97	550.14
Licmophora sp.	M	1744.26	14.94	41.79	122.56
Lithodesmium undulatum Ehrenberg	M	10121.00	26.84	25.43	510.07
Melosira sp.*	M	3899.86	19.53	22.15	235.36
Navicula sp. A	N	3084.48	18.06	10.00	6.65
Navicula sp. B	N	135.00	6.37	15.00	15.38
Navicula sp. C	N	180.00	7.01	20.00	19.43
Navicula sp. D	M	270.00	8.02	30.00	26.99
Navicula sp. E	N	9.00	2.58	5.00	1.71
Navicula sp. F	M	3000.00	17.90	50.00	190.26
Nitzschia sp. A	M	1976.44	15.57	84.08	135.63
Nitzschia sp. B	M	100.00	5.76	50.00	12.06
Pleurosigma spp.	M	53965.17	46.89	165.46	1982.15
Proboscia alata (Brightwell) Sundström	M	5444.96	21.83	566.23	308.52
*Pseudo-nitzschia multistriata (*Takano) Takano	M	489.17	9.78	63.68	43.71
*Pseudo-nitzschia galaxiae*Lundholm et Moestrup	M	41.67	4.30	32.69	5.93

Species	Size	Volume (μm^3)	ESD (µm)	MLD (µm)	Carbon (pg)
Rhizosolenia imbricata Brightwell	M	9595.31	26.37	472.54	488.48
Synedra ulna (Nitzsc) Ehrenberg	M	642.35	10.71	124.21	54.51
Synedra sp.	M	12359.90	28.69	426.48	599.81
Thalassionema frauenfeldii (Grunow) Tempère & Peragallo	M	9813.94	26.57	167.61	497.48
Thalassionema nitzschioides (Grunow) Mereschkowsky	M	1265.62	13.42	65.95	94.48
Thalassiosira sp. A	M	4710.00	20.80	20.00	274.29
Thalassiosira spp.	M	150.00	6.59	50.00	16.76
Other pennate diatoms A	M	90.00	5.56	30.00	11.07
Other pennate diatoms B	M	60.00	4.86	20.00	7.97
Other pennate diatoms C	M	30.00	3.86	10.00	4.54
Other pennate diatoms (<20 µm)	N	7.50	2.43	5.00	1.48
Dinoflagellates					
Dinophysis acuminata Claparéde et Lachmann	M	9398.08	26.19	45.10	1161.82
Gonyaulax spp.	M	5673.77	22.13	24.36	723.33
Gymnodinium spp. A	M	2950.38	17.80	23.50	391.44
Gymnodinium spp. B	N	25.64	3.66	7.00	4.54
Gyrodinium spp.	M	1131.19	12.93	31.10	159.12
Mesoporos perforatus (Gran) Lillick	N	1929.22	15.45	16.00	262.68
Neoceratium breve (Ostenfeld et Schmidt) Gómez, Moreira et López-Garcia	M	91216.84	55.86	66.00	9816.67
Oxytoxum spp.	M	402.71	9.16	19.00	60.33
Oxytoxum sceptrum (Stein) Schröder	M	5128.67	21.40	100.00	657.88
Oxytoxum variabile Schiller	M	890.19	11.94	42.00	127.06
Peridinium sp.	M	30144.00	38.62	40.00	3470.75
Protoperidinium bipes (Paulsen) Balech [1]	M	2852.80	17.60	29.35	379.27
Protoperidinium steinii (Joergensen) Balech[1]	M	8831.25	25.65	35.00	1095.89
Scrippsiella sp.	M	49.06	4.54	5.00	8.36
Torodinium sp.	M	9274.35	26.07	61.85	1147.45
Chrysophyceans					
Dinobryon faculiferum (Willén) Willén	N	48.40	4.52	8.76	8.25
Cryptophyceans					
Undetermined cryptophytes (5-20 µm)	N	184.99	7.07	10.00	29.06
Chlorophyceae					
Chlamydomonas sp.	N	143.60	6.50	7.00	22.91
Scenedesmus sp.	N	162.41	6.77	6.70	27.99
Prymnesiophyceans					
Calciosolenia brasiliensis (Lohmann) Young	M	1201.77	13.19	105.30	168.42
Calciosolenia murrayi Gran	M	219.58	7.49	32.29	34.14
Calyptrosphaera oblonga Lohmann* (*S. pulchra* HOL *oblonga* type)	N	1436.03	14.00	14.00	199.08
Ophiaster sp.	N	99.00	5.74	5.75	16.23
Rhabdosphaera clavigera var. *stylifer* Lohmann	N	696.56	11.00	11.00	100.92
Syracosphaera pulchra Lohman	N	2245.69	16.25	18.92	302.95
Undetermined coccolitophorids A	N	65.42	5.00	5.00	10.95
Undetermined coccolitophorids B	N	1766.25	15.00	15.00	241.79
Ciliates					
Myrionecta rubra (Lohmann) Jankowski	N	2207.81	16.16	15.00	298.15

CURRICULUM VITAE

Sunčica Bosak was born on 7th of June 1982 in Zagreb, Croatia where she completed primary and high school education (II Gymnasium). In 2000 she enrolled the undergraduate engineering degree program of Biology, Ecology at the Division of Biology, Faculty of Science, University of Zagreb where she graduated in 2006 with an average grade of 4.76. Research for her diploma thesis entitled "Investigation of *slr0192* gene function in cyanobacterium *Synechocystis* sp. PCC 6803" was focused on elucidation of regulation mechanisms of photosynthesis and conducted at Laboratory for Electron Microscopy, Department for Molecular Biology, Ruđer Bošković Institute, Zagreb under the supervision of Prof. Hrvoje Fulgosi.

From 2006 until 2008 she worked as an associate teaching assistant engaged in student practical courses in Microbial Ecology, Microbiology and General Microbiology at the Department of Botany, Division of Biology, Faculty of Science. In 2007 she enrolled the Interdisciplinary Doctoral study in Oceanology at the Faculty of Science, University of Zagreb with the research interest focused on taxonomy and ecology of marine phytoplankton. Since January 2008 she has been employed as a junior researcher at the project no. 119-1191189-1228 "Structure and development of microalgae communities along the trophic gradient" lead by Prof. Damir Viličić, funded by the Ministry of Science, Education and Sports of the Republic of Croatia. She has been also actively engaged as a teaching assistant in several undergraduate courses at the Division of Biology, Faculty of Science, Zagreb including: "Microbial Ecology", "Protists" and "Biological Oceanography".

During her work she participated in eight different national and international scientific projects of which in two funded by the European FP7 project ASSEMBLE was the main applicant and carried it during her research visits to Stazione Zoologica Anton Dohrn in Naples, Italy. She completed eight international training courses, participated at 11 international and nine national conferences as a first author and co-author of 34 presentations. She has until now published 14 scientific papers in journals cited by *Web of Science* of which nine are in the journals cited in the *Current Content* base.

Since 2007 she has been working as a managing editor of the scientific journal Acta Botanica Croatica. She is also a member of various professional associations/societies including Croatian Biological Society 1885, Croatian Botanical Society, International Society for Diatom Research and International Phycological Society, Australasian Society for Phycology & Aquatic Botany and British Phycological Society. In the period of 2007 – 2010 she was the treasurer of Croatian Society for Plant Biology and 2008 – 2009 head of the "Young Researchers", section of the Croatian Society of Natural Sciences.

Identification number of scientist: 301434

SCIENTIFIC RESEARCH PROJECTS:

1. The project funded by the Ministry of Science, Education and Sports of the Republic of Croatia no. 119-1191189-1228 "Structure and development of microalgae communities along the trophic gradient" lead by Prof. Damir Viličić, PMF, Zagreb, Croatia (2008 – current)
2. The Croatian National Monitoring Programme: "Project Adriatic", lead by Dr. Nenad Smodlaka, IRB, Zagreb, Croatia funded by the Ministry of Science, Education and Sports of the Republic of Croatia (2006 – 2012)
3. „Norwegian Cooperation Program on Research and Higher Education with the countries on the Western Balkans: Marine Science and Coastal Management in the Adriatic, Western Balkan, An Educational and Research Network 2006-2009", headed by Dr. Božena Ćosović IRB, Zagreb, Croatia and Prof. Paul Wassman NCFS, Tromso, Norway (2006-2009).
4. "Plankton food webs in the future ocean: effects of temperature, CO_2 and bloom structure" headed by Dr. Sam Dupont, University of Göteborg, Sweden, funded by the European FP7 Capacities project MESOAQUA (Network of leading MESOcosm facilities that are working together to advance studies in AQUAtic ecosystems from the Arctic to the Mediterranean) (September 2009).
5. BIOMARDI (Biodiversity of the marine diatoms: morphological and molecular characterization), headed by Sunčica Bosak, PMF, Zagreb, Croatia funded by FP7 project ASSEMBLE (Association of European Marine Biological Laboratories) (June/July 2011).
6. „ An impact of antifouling paints as a source of contamination by ecotoxic metals in the coastal marine environment " (French/Croatian bilateral COGITO project) headed by Dr. Dario Omanović, IRB, Zagreb, Croatia and Prof. Cedric Garnier, University of Toulon (USTV), France (2010-2012).
7. „Phytoplankton biodiversity in relation to environmental conditions in Nature Park Telašćica" funded by Ministry of Culture, Republic of Croatia lead by Dr. Zrinka Ljubešić, PMF, Zagreb, Croatia (2010-2013)
8. NOTCH (New insights on morphology and taxonomy of the planktonic diatom genus *Chaetoceros*) headed by Sunčica Bosak, PMF, Zagreb, Croatia funded by FP7 project ASSEMBLE (February-May 2013).

SCIENTIFIC TRAINING COURSES:

1. FP7 MIDTAL (Microarrays for the Detection of Toxic Algae) workshop. Stazione Zoologica Anton Dohrn, Naples, Italy, 16-17 April 2012.
2. Workshop on Effective Grant Writing. University of Zagreb, Faculty of Science Division of Biology, Zagreb, Croatia, 1-3 February 2011.
3. Workshop on Speaking Effectively on Your Research, University of Zagreb, Faculty of Science, Division of Biology, Zagreb, Croatia, 14-17 December 2010.
4. Taxonomy of Recent Dinophyceae. Alfred-Wegener-Instituts für Polar- und Meeresforschung (AWI), Wattenmeerstation Sylt, List, Sylt, Germany, 1-9 November 2010.
5. SAHFOS and MBA Marine Phytoplankton Taxonomy Workshop. Plymouth, UK, 6-17 July 2009.
6. Course 4: English writing course. Belgrade, Serbia, 16-20 February, 2009.
7. Course 3: Marine Chemistry – Analytical methods, trace elements and organic matter in marine environment. Zagreb, Croatia, 12-17 November, 2007.
8. Course 2: Marine Ecology, Kotor, Montenegro, 21-27 October, 2007.

Courses 2,3 and 4. were organized as part of the project Marine Science and Coastal Management in the Adriatic, Western Balkan, An Educational and Research Network 2006-2009.

RESEARCH VISITS

1. 1 February 2013 – 1 May 2013: Stazione Zoologica Anthon Dohrn, Naples, Italy, ASSEMBLE funded project NOTCH (PhD research).
2. 26 September – 2 October 2011: Université du Sud Toulon – Var (USTV), COGITO project.
3. 10 June – 12 July 2011: Stazione Zoologica Anthon Dohrn, Naples, Italy, ASSEMBLE funded project BIOMARDI (PhD research).
4. 22 August – 12 September 2009: Norwegian National Mesocosm Center Espegrend, University of Bergen, Norway. MESOAQUA funded project „Plankton food webs in the future ocean: effects of temperature, CO_2 and bloom structure" (participated in mesocosm experiment).
5. 12 – 26 April 2008: study visit to Department of Biology, University of Bergen, Norway funded by Norwegian Cooperation Program on Research and Education „Marine science and coastal management in the Adriatic region, Western Balkans".
6. 24 – 28 March 2008: Hungarian Danube Research Station at the Institute of Ecology and Botany Hungarian Academy of Science, Göd, Hungary.

LIST OF PUBLICATIONS (WoS)

1. Viličić, D., Kuzmić, M., Tomažić, I., Ljubešić, Z., **Bosak, S.**, Precali, R., Djakovac, T., Marić, D. and Godrijan, J. (2013) Northern Adriatic phytoplankton response to short Po River discharge pulses during summer stratified conditions. Marine Ecology. doi:10.1111/maec.12046
2. Troedsson C., Bouquet J-M., Lobon C. M., Novac A., Nejstgaard J. C., Dupont S., **Bosak S.,** Jakobsen H.H., Romanova N., Pankoke L. M., Isla A., Dutz J., Sazhin A. F., Thompson E.M. (2013) Effects of ocean acidification, temperature and nutrient regimes on the appendicularian *Oikopleura dioica*: A mesocosm study. Marine Biology, 160 (8), 2175-2187. doi:10.1007/s00227-012-2137-9.
3. **Bosak, S.**, Pletikapić, G., Hozić, A., Svetličić, V., Sarno, D., Viličić, D. (2012) A novel type of colony formation in marine planktonic diatoms revealed by atomic force microscopy. PLoS ONE, 7, 9, e44851; doi: 10.1371/journal.pone.0044851
4. **Bosak, S.**, Šilović, T., Ljubešić, Z., Kušpilić, G., Pestorić, B., Krivokapić, S., Viličić, D. (2012) Phytoplankton size structure and species composition as an indicator of trophic status in transitional ecosystems: the case study of a Mediterranean fjord-like karstic bay. Oceanologia 54 (2), 255-286.
5. Šilović, T., **Bosak, S.,** Jakšić, Ž., Fuks, D. (2012) Seasonal dynamics of the autotrophic community in the Lim Bay (NE Adriatic Sea). Acta Adriatica. 53 (1): 41 - 56.
6. Šupraha, L., **Bosak, S.**, Ljubešić, Z., Olujić, G., Horvat, L., Viličić, D. (2011) The phytoplankton composition and spatial distribution in the north-eastern Adriatic Channel in autumn 2008. Acta Adriatica. 52 (1) 29-44.
7. Krivokapić, S., Pestorić, B., **Bosak, S.**, Kušpilić, G., Wexels Riser, C. (2011) Trophic state of Boka Kotorska Bay (south-eastern Adriatic Sea). Fresenius Environmental Bulletin. 20 (8), 1960-1969.
8. Ljubešić, Z., **Bosak, S.**, Viličić, D., Kralj Borojević, K., Marić, D., Godrijan, J., Ujević, I., Peharec, P., Đakovac, T. (2011) Ecology and taxonomy of potentially toxic *Pseudo-nitzschia* species in Lim Bay (north-eastern Adriatic Sea). Harmful algae. 10, 713-722. doi: 10.1016/j.hal.2011.06.002.
9. Viličić, D., Šilović, T., Kuzmić, M., Mihanović, H., **Bosak, S.**, Tomažić, I., Olujić, G. (2011) Phytoplankton distribution across the southeast Adriatic continental and shelf slope to the west of Albania (spring aspect). Environmental Monitoring and Assessment. 177 (1/4), 593-607. doi: 10.1007/s10661-010-1659-1.
10. Hernández-Becerril D., Viličić D., **Bosak S.**, Đakovac T. (2010) Morphology and ecology of the diatom *Chaetoceros vixvisibilis* (Chaetocerotales, Bacillariophyceae) from the Adriatic Sea. Journal of Plankton Research. 32 (11), 1513-1525. doi: 10.1093/plankt/fbq080.
11. Viličić D., Đakovac T., Burić Z., **Bosak S.** (2009) Composition and annual cycle of phytoplankton assemblages in the northeastern Adriatic Sea. Botanica Marina, 52 (4), 291-305. doi: 10.1515/bot.2009.004
12. **Bosak S.**, Burić Z., Djakovac T., Viličić D. (2009) Seasonal distribution of plankton diatoms in Lim Bay, northeastern Adriatic Sea. Acta Botanica Croatica 68 (2), 351-365.
13. Viličić D., Kuzmić M., **Bosak S.**, Šilović T., Hrustić E., Burić Z. (2009) Distribution of phytoplankton along the thermohaline gradient in the north-eastern Adriatic channel; winter aspect. Oceanologia, 51 (4), 495-513.
14. Viličić D., **Bosak S.**, Burić Z., Caput Mihalić, K. (2007) Phytoplankton seasonality and composition along the coastal NE Adriatic Sea during the extremely low Po River discharge in 2006. Acta Botanica Croatica, 66 (2), 101-117.

SCIENTIFIC MEETINGS

Proceedings

1. **Bosak S.**, Horvat L., Pestorić B., Krivokapić S., (2010) Observations on *Pseudo-nitzschia* species in the Bay of Kotor, SE Adriatic Sea. Rapport du Commission Internationale pour l' Exploration Scientifique de la Mer Mediterranee 39, 721. (poster presentation)
2. Krivokapić S., Pestorić B., **Bosak S**., Kušpilić G. (2010) Trophic condition in the Boka Kotorska Bay Rapport du Commission Internationale pour l' Exploration Scientifique de la Mer Mediterranee 39, 767.

Proceedings (in Croatian)

1. Viličić D., Ivančić I., **Bosak S.** (2012) Sezonska raspodjela i ekološki značaj kriptofita u Riječkom zaljevu i u Vinodolskom kanalu. Prirodoslovna istraživanja Riječkog područja 2, Prirodoslovni muzej Rijeka, Rijeka, Hrvatska, 205-216.
2. **Bosak S.,** Hrestak S., Burić Z., Caput-Mihalić K., Viličić D., Terzić S., Carić M. (2007) Raspodjela fitoplanktona u uvjetima limitiranosti dušikom u estuariju Zrmanje. Zbornik radova 4. Hrvatske konferencije o vodama, 17. – 19. svibnja 2007., Opatija, Hrvatska, 75-83. (poster presentation)
3. Viličić D., Ivančić I., **Bosak S.** (2007) Toksični dinoflagelati u Limskom kanalu. Zbornik radova 4. Hrvatske konferencije o vodama, 17. – 19. svibnja 2007. Opatija, Hrvatska, 241-252.

Proceedings of Abstracts

1. **Bosak S.**, Sarno D. (2012) Biodiversity of marine diatoms: morphological and molecular characterization. ASSEMBLE conference: Access to Marine Resources Generating Knowledge for Science and Society Programme and Abstract Book. Olhao, Portugal. 16-17 (invited oral presentation).
2. **Bosak, S.**, Pletikapić, G., Hozić, A., Svetličić, V., Sarno, D., Viličić, D. (2012) A novel type of colony formation in marine planktonic diatoms revealed by atomic force microscopy. Twentysecond International Diatom Symposium, Aula Academica, Ghent, Belgium, 26-31 August 2012. Abstracts. VLIZ Special Publication 58, 135 (poster presentation)
3. **Bosak, S.,** Sarno, D., Šupraha, L., Nanjappa, D., Kooistra, W., Viličić, D. (2012) Morphology and taxonomy of four species of the marine planktonic diatom genus *Bacteriastrum* (Bacillariophyta) from the Adriatic Sea. Twentysecond International Diatom Symposium, Aula Academica, Ghent, Belgium, 26-31 August 2012. Abstracts. VLIZ Special Publication 58, 29 (oral presentation)
4. **Bosak, S.**, Godrijan, J., Šilović, T., Viličić, D. (2011) Seasonal dynamics of potentially harmful microalgae in the coastal area of Rovinj, NE Adriatic Sea. 46th European Marine Biology Symposium Book of Abstracts. Rovinj, Croatia. 11 (oral presentation).
5. Godrijan, J., **Bosak, S**., Šilović, T., Marić, D., Pfannkuchen, M., Precali, R. (2011) Phytoplankton community dynamics in the coastal north-eastern Adriatic Sea. 46th European Marine Biology Symposium Book of Abstracts. Rovinj, Croatia. 27.
6. Ljubešić, Z., Cetinić, I., **Bosak, S.**, Viličić, D., Jones, B., Olujić, G., Carić, M., Marini, M. (2011) Phytoplankton biodiversity in the Adriatic deep chlorophyll maxima. 46th European Marine Biology Symposium, Book of Abstracts. Rovinj, Hrvatska. 36.
7. **Bosak S.**, Šilović T., Horvat L., Viličić D., (2010) Taxonomical study of phytoplankton in the Bay of Kotor, SE Adriatic Sea.Final Conference of the Project Marine science and coastal management in the Adriatic region, Western Balkans, Cavtat, Croatia. 13 (oral presentation).
8. Viličić D., Šilović T., Kuzmić M., Mihanović H., **Bosak S.**, Tomažić I., Olujić G. (2010) Plankton distribution and hydrography above the Albanian shelf and continental slope, May 2009 aspect. Challenge for future research. Final Conference of the Project Marine science and coastal management in the Adriatic region, Western Balkans. Cavtat, Croatia. 2.
9. Thompson E., Bouquet J-M., Dupont S., Lobon C., Novac A., Nejstgaard J.C., **Bosak S.**, Isla A., Dutz J., Romanova N., Sahzin A., Troedsson C., (2010) Effects of ocean acidification and temperature increase on planktonic tunicate, *Oikopleura*, population dynamics at laboratory and mesocosm scales. ASLO/NABS Joint Summer Meeting - Aquatic sciences: global changes from the center to the edge, Abstract Book. Santa Fe, New Mexico, USA. 70-71.
10. **Bosak S.**, Šilović T., Krivokapić S., Kušpilić G., Wexels Riser C., Horvat L., Viličić D. (2009) Phytoplankton composition in relation to physico-chemical drivers in the Bay of Kotor, SE Adriatic Sea. Abstracts of papers presented at the 9th International Phycological Congress Tokyo, Japan 2-8 August 2009. Phycologia 48 (sp. 4), 11-12 (poster presentation).
11. Burić Z., **Bosak S.**, Viličić D., Kralj K., Marić D., Peharec P., Đakovac T. (2009) Ecology and taxonomy of *Pseudo-nitzschia* in Lim Bay (northeastern Adriatic Sea). Diatom Taxonomy in the 21st Century, Programme and Abstracts, Meise, Belgium. Scripta Botanica Belgica 45, 23.
12. Šupraha L., **Bosak S.**, Burić Z., Olujić G., Viličić D. (2009) New species of *Bacteriastrum* (Chaetocerotaceae, Bacillariophyta) in the Adriatic Sea? Diatom Taxonomy in the 21st Century, Programme and Abstracts, Meise, Belgium. Scripta Botanica Belgica 45, 61.
13. Šilović T., **Bosak S.**, Jakšić Ž., Fuks D. (2009) Pico- and nano autotrophic community in the Lim bay (NE Adriatic Sea) SAME11-2009 Abstract book, Piran, Slovenia, 48.
14. **Bosak S.**, Burić Z., Đakovac T., Viličić D. (2008) Marine planktonic diatoms in the Lim Bay (NE Adriatic Sea). 20th International Diatom Symposium Abstract Book, Dubrovnik, Croatia, 112 (poster presentation).
15. Burić Z., **Bosak S**., Marić D., Godrijan J., Viličić D., Kralj K., Peharec P. (2008) Taxonomical study of *Pseudo-nitzschia* species in the eastern Adriatic Sea. 20th International Diatom Symposium Abstract Book, Dubrovnik, Croatia, 115.
16. Godrijan J., Burić Z., Marić D., **Bosak S.**, Peharec P., Đakovac T. (2008) *Pseudo-nitzschia* and *Chaetoceros* bloom in the coastal waters of Istrian penninsula, Northern Adriatic Sea. 20th International Diatom Symposium Abstract Book, Dubrovnik, Croatia, 137.
17. Marić D., Burić Z., Godrijan J., **Bosak S.**, Đakovac T., Peharec P. (2008) The occurrence of potentially toxic *Pseudo-nitzschia calliantha* in the costal waters of the Northern Adriatic Sea. 20th International Diatom Symposium Abstract Book, Dubrovnik, Croatia, 182.

18. **Bosak S.**, Burić Z., Viličić D. (2007) Temporal distribution of phytoplankton at one station in the northern Adriatic Sea. American Geophysical Union: Chapman conference on long time-series observations in coastal ecosystems: comparative analyses of phytoplankton dynamics on regional to global scales, Rovinj, Croatia, 23-24 (poster presentation).
19. Fulgosi H., Jurić S., Hazler-Pilepić K., Bionda T., **Bosak S.** (2005) TROL - from sulfur metabolism to a regulatory function in oxygenic photosynthesis? Book of Abstracts Advanced Course - Origin and Evolution of Mitochondria and Chloroplast". FEBS (Federation Of European Biochemical Societies), Wildbad Kreuth, Germany. 25.

Proceedings of Abstracts (Croatian conferences with international participation)

1. **Bosak S.,** Sarno D., Viličić D. (2013) Morphology and taxonomy of the planktonic diatom genus *Chaetoceros* Ehrenberg (Bacillariophyta) from the Adriatic Sea. 4th Botanical Symposium with international participation, Split 2013, Book of Abstracts, Split, Croatia, 35-36 (oral presentation).
2. **Bosak S.**, Ljubešić Z., Viličić D. (2012) SEM examination of fine structure of *Meringosphaera mediterranea*, a microalga of enigmatic taxonomic position. Proceedings of Abstracts of Croatian microscopical symposium, Pula, Croatia, 42-43 (poster presentation).
3. **Bosak S.**, Omanović D., Dautović J., Mihanović H., Olujić G., Šupraha L., Ahel M., Viličić D. (2010) Distribution of phytoplankton, organic matter and trace metals in the Krka river estuary. Proceedings of Abstracts of 3rd Croatian Botanical Congress with international participation, Jezera, Murter, Croatia, 46-47 (poster presentation)
4. **Bosak S.**, Šilović T., Viličić D., (2010) Seasonal variability of size fractionated phytoplankton biomass: a comparative study in two eastern Adriatic Sea coastal systems. Proceedings of Abstracts of 3rd Croatian Botanical Congress with international participation, Jezera, Murter, Croatia, 48-49 (oral presentation).
5. **Bosak S.**, Šilović T., Burić Z., Đakovac T., Viličić, D. (2009) Phytoplankton in Lim Bay (Northern Adriatic): taxonomy and ecology. Proceeding of Abstracts of 10th Croatian Biological Congress with international participation, Osijek, Croatia, 114-115 (oral presentation).
6. Godrijan J., Marić D., Pfannkuchen M., **Bosak S.**, Đakovac T., Degobbis D., Precali R. (2009) Coccolithophorid observations in the coastal north eastern Adriatic Sea. Proceeding of Abstracts of 10th Croatian Biological Congress with international participation, Osijek, Croatia, 218-219.
7. Šupraha L., **Bosak S.**, Burić Z., Olujić G., Horvat L., Viličić D. (2009) Jesenski sastav fitoplanktona u Velebitskom i Paškom kanalu (Jadransko more). Proceeding of Abstracts of 10th Croatian Biological Congress with international participation, Osijek, Croatia, 122-123.
8. **Bosak S.**, Viličić D., Đakovac T. (2007) Spatial and temporal distribution of phytoplankton in the Lim Channel (the Northern Adriatic). Proceedings of Abstracts of 2nd Croatian Botanical Congress, Zagreb, Croatia, 149-150 (poster presentation).
9. **Bosak S.**, Grgić M., Viljetić B., Fulgosi H. (2006) The function of a rhodanese under sulfur limitation conditions in cyanobacterium *Synechocystis* sp. PCC 6803. Proceeding of Abstracts of 9th Croatian Biological Congress with international participation, Rovinj, Croatia, 178-180 (oral presentation).
10. Fulgosi H., Jurić S., **Bosak S.**, Bionda T., Hazler-Pilepić K. (2005) Dissecting chloroplast regulatory pathways. Book of Abstracts of Second congress of croatian geneticists, Zagreb, Croatia, 27.